

## **Pergamon Titles of Related Interest**

**BANHIDI**

Radiant Heating Systems: Design and Applications

**BOWEN & YANNAS**

Passive and Low Energy Ecotechniques

**CARTER & DE VILLIERS**

Principles of Passive Solar Heating Systems

**GRANQVIST**

Materials Science for Solar Energy Conversion Systems

**HARRISON**

Geothermal Heating

**HORIGOME**

Clean and Safe Energy Forever

**McVEIGH**

Sun Power, 2nd Edition

**SAITO**

Heat Pumps

**SAYIGH**

Energy and the Environment: into the 1990s, 5-vol set

**SAYIGH & McVEIGH**

Solar Air Conditioning and Refrigeration

**STECCO & MORAN**

A Future For Energy

**TREBLE**

Generating Electricity from the Sun

## **Pergamon Related Journals\***

Energy

Energy Conservation and Management

Geothermics

Heat Recovery Systems and CHP

International Journal of Heat and Mass Transfer

International Journal of Hydrogen Energy

Progress in Energy and Combustion Science

Renewable Energy

Solar Energy

*\*Free Specimen Copy Gladly Sent on Request*

## **Pergamon Titles of Related Interest**

**BANHIDI**

Radiant Heating Systems: Design and Applications

**BOWEN & YANNAS**

Passive and Low Energy Ecotechniques

**CARTER & DE VILLIERS**

Principles of Passive Solar Heating Systems

**GRANQVIST**

Materials Science for Solar Energy Conversion Systems

**HARRISON**

Geothermal Heating

**HORIGOME**

Clean and Safe Energy Forever

**McVEIGH**

Sun Power, 2nd Edition

**SAITO**

Heat Pumps

**SAYIGH**

Energy and the Environment: into the 1990s, 5-vol set

**SAYIGH & McVEIGH**

Solar Air Conditioning and Refrigeration

**STECCO & MORAN**

A Future For Energy

**TREBLE**

Generating Electricity from the Sun

## **Pergamon Related Journals\***

Energy

Energy Conservation and Management

Geothermics

Heat Recovery Systems and CHP

International Journal of Heat and Mass Transfer

International Journal of Hydrogen Energy

Progress in Energy and Combustion Science

Renewable Energy

Solar Energy

*\*Free Specimen Copy Gladly Sent on Request*

# ENERGY CONSERVATION IN BUILDINGS

The Achievement of 50% Energy Saving:  
An Environmental Challenge?

*Proceedings of NORTHSUN 90, an International Conference,  
University of Reading, UK, 18–21 September 1990*

Edited by

**A. A. M. SAYIGH**  
*University of Reading, UK*

Organized by

World Renewable Energy Congress Company Limited

Sponsored by

*Institute of Energy  
UK Solar Energy Society  
Building Research Establishment  
Pergamon Press  
World Renewable Energy Congress*



**PERGAMON PRESS**

Member of Maxwell Macmillan Pergamon Publishing Corporation  
OXFORD . NEW YORK . BEIJING . FRANKFURT  
SÃO PAULO . SYDNEY . TOKYO . TORONTO

U.K.	Pergamon Press plc, Headington Hill Hall, Oxford OX3 0BW, England
U.S.A.	Pergamon Press, Inc., Maxwell House, Fairview Park, Elmsford, New York 10523, U.S.A.
PEOPLE'S REPUBLIC OF CHINA	Pergamon Press, Room 4037, Qianmen Hotel, Beijing, People's Republic of China
FEDERAL REPUBLIC OF GERMANY	Pergamon Press GmbH, Hammerweg 6, D-6242 Kronberg, Federal Republic of Germany
BRAZIL	Pergamon Editora Ltda, Rua Eça de Queiros, 346, CEP 04011, Paraiso, São Paulo, Brazil
AUSTRALIA	Pergamon Press (Australia) Pty Ltd., P.O. Box 544, Potts Point, NSW 2011, Australia
JAPAN	Pergamon Press, 5th Floor, Matsuoka Central Building, 1-7-1 Nishishinjuku, Shinjuku-ku, Tokyo 160, Japan
CANADA	Pergamon Press Canada Ltd, Suite No. 271, 253 College Street, Toronto, Ontario, Canada M5T 1R5

---

Copyright © 1991 Pergamon Press Plc

*All Rights Reserved. No part of this publication may be reproduced, stored in a retrieval system or transmitted in any form or by any means: electronic, electrostatic, magnetic tape, mechanical, photocopying, recording or otherwise, without permission in writing from the publisher.*

First edition 1991

**Library of Congress Cataloging in Publication Data**  
Applied for

**British Library Cataloguing in Publication Data**

NORTHSUN 90 (*University of Reading*)

Energy conservation in buildings.

1. Solar energy

I. Title II. Sayigh, A. A. M.

621.47

ISBN 0-08-037215-5

## Organising Committee

Prof A A M Sayigh Chairman	University of Reading
Prof B Norton	University of Ulster
Prof D J Croome	University of Reading
Dr G Saluja	University of Ulster
Prof N Lipman	Rutherford Laboratory
Mr R Perks	BP Solar
Dr J Twidell	University of Strathclyde
Dr L Duckers	Coventry Polytechnic
Mrs J Aley	University of Reading
Mr S Winkworth	UK-ISES
Dr V H C Crisp	Building Research Establishment

## International Committee

Prof L Broman	Sweden
Prof R L Datta	India
Prof K G T Hollands	Canada
Dr L Jesch	UK
Prof V Korsgaard	Denmark
Mr T E Loxley	USA
Prof P D Lund	Finland
Mr L Michalicka	Czechoslovakia
Prof F Peterson	Sweden
Judit Pinter	Hungary
Prof F Salvesen	Norway
Prof S de Schiller	Argentina
Prof E Shpilrain	USSR
Prof C Spassov	Bulgaria
Dr T Stapinski	Poland
Dr V Wittwer	West Germany

## International Standing Committee

Dr. K. MacGregor	UK
Mr. A. Boysen	Sweden
Mr. T. Esbensen	Denmark
Prof. A.A.M. Sayigh	UK

## Organising Committee

Prof A A M Sayigh Chairman	University of Reading
Prof B Norton	University of Ulster
Prof D J Croome	University of Reading
Dr G Saluja	University of Ulster
Prof N Lipman	Rutherford Laboratory
Mr R Perks	BP Solar
Dr J Twidell	University of Strathclyde
Dr L Duckers	Coventry Polytechnic
Mrs J Aley	University of Reading
Mr S Winkworth	UK-ISES
Dr V H C Crisp	Building Research Establishment

## International Committee

Prof L Broman	Sweden
Prof R L Datta	India
Prof K G T Hollands	Canada
Dr L Jesch	UK
Prof V Korsgaard	Denmark
Mr T E Loxley	USA
Prof P D Lund	Finland
Mr L Michalicka	Czechoslovakia
Prof F Peterson	Sweden
Judit Pinter	Hungary
Prof F Salvesen	Norway
Prof S de Schiller	Argentina
Prof E Shpilrain	USSR
Prof C Spassov	Bulgaria
Dr T Stapinski	Poland
Dr V Wittwer	West Germany

## International Standing Committee

Dr. K. MacGregor	UK
Mr. A. Boysen	Sweden
Mr. T. Esbensen	Denmark
Prof. A.A.M. Sayigh	UK

## Organising Committee

Prof A A M Sayigh Chairman	University of Reading
Prof B Norton	University of Ulster
Prof D J Croome	University of Reading
Dr G Saluja	University of Ulster
Prof N Lipman	Rutherford Laboratory
Mr R Perks	BP Solar
Dr J Twidell	University of Strathclyde
Dr L Duckers	Coventry Polytechnic
Mrs J Aley	University of Reading
Mr S Winkworth	UK-ISES
Dr V H C Crisp	Building Research Establishment

## International Committee

Prof L Broman	Sweden
Prof R L Datta	India
Prof K G T Hollands	Canada
Dr L Jesch	UK
Prof V Korsgaard	Denmark
Mr T E Loxley	USA
Prof P D Lund	Finland
Mr L Michalicka	Czechoslovakia
Prof F Peterson	Sweden
Judit Pinter	Hungary
Prof F Salvesen	Norway
Prof S de Schiller	Argentina
Prof E Shpilrain	USSR
Prof C Spassov	Bulgaria
Dr T Stapinski	Poland
Dr V Wittwer	West Germany

## International Standing Committee

Dr. K. MacGregor	UK
Mr. A. Boysen	Sweden
Mr. T. Esbensen	Denmark
Prof. A.A.M. Sayigh	UK

## Preface

**NORTHSUN 90** is a biannual conference of those countries situated at latitudes greater than 45 degrees north and south of the Equator. It first started in Scotland in 1984 with a small number of participants, and has grown into a successful assembly in 1988 in Sweden, following the second meeting in 1986 in Denmark.

The main aim of this conference is to provide a unique opportunity for the participants from different countries of high latitudes to exchange their ideas, to share their results and to promote together the best use of solar energy.

The emphasis is towards building and energy conservation as well as design orientation and comfort. Also discussed are the realisation and utilisation of solar heating devices with special consideration for the cooling needs in hot climates.

This year, the UK meeting has attracted 150 abstracts from 60 countries. Over 130 people attended the meeting, and 79 papers were selected, representing 44 countries; namely, Australia, Bulgaria, Belgium, Botswana, China, Colombia, Cyprus, Czechoslovakia, Denmark, Egypt, Finland, France, Germany, Ghana, Greece, Hungary, India, Iran, Iraq, Israel, Italy, Japan, Jordan, Kuwait, Libya, Morocco, Netherlands, New Zealand, Norway, Poland, Romania, Somalia, Spain, Sudan, Sweden, Tanzania, Turkey, UK, USA, USSR, Venezuela, Yemen, Yugoslavia and Zimbabwe.

It is well proven that in northern latitudes, energy savings in buildings of up to 50% can be achieved if energy conservation methods such as natural lighting, ventilation, greenhouse heating and orientation in buildings are used. They are the main elements of passive heating in the northern levels. However, well stated also in many papers is that passive solar cooling could lead to a reduction in energy if energy conservation is used in hot climates.

The proceedings is divided into two parts. Part One includes 25 papers, dealing with energy conservation and management in buildings as well as solar and low energy architecture. Part Two, which consists of 54 papers, covers all aspects of renewable energy; material science and photovoltaic conversion, weather data, heating and cooling of buildings, hot water systems, wave energy, geothermal energy, energy storage, country programmes and other related topics.

**NORTHSUN 90's** main message is to encourage countries in the high latitudes to implement all aspects of energy conservation in buildings, to promote the use of solar energy in heating, and to work collectively on solar projects of direct benefit to the region.

I should like to thank all the sponsoring agents for their generous help, all my fellow colleagues of various committees, and all the contributors and participants who made **NORTHSUN 90** another successful conference.

Prof. A.A.M. Sayigh  
Conference Chairman



# A TOTAL ENERGY DESIGN FOR 92 HOUSES WITH COMBINED USE OF SOLAR HEATING AND ENERGY CONSERVATION

P. VEJSIG PEDERSEN

Thermal Insulation Laboratory, Technical University of  
Denmark, DK-2800 Lyngby, Denmark

O. MØRCK

Cenergia Aps., Stationsvej 3, DK-2760 Måløv, Denmark

## ABSTRACT

A 80% saving compared to normal gas consumption for heating and DHW is expected in the community, Tubberupvænge with 92 houses near Copenhagen in Denmark. This is the most ambitious energy saving building project in Denmark until now. Savings of the heating demand is first achieved by common energy saving techniques like extra insulation, improved windows, heat recovery of ventilation air, and attached sunspaces, which as something new has integrated pebble bed storage in the floor. Besides, each of eight building blocks utilizes 45 m<sup>2</sup> of roof integrated solar collectors as part of local solar heating system design, primarily for DHW. And for the first time in Denmark a solar heated seasonal storage is used, here with 1050 m<sup>2</sup> of high temperature solar collectors, and a 3000 m<sup>3</sup> water filled seasonal storage insulated and buried in the ground.

## KEYWORDS

Total energy design, solar heating, energy conservation, solar collectors, seasonal storage.

## THE TOTAL ENERGY PROJECT IN HERLEV, DENMARK

The total energy design concept combines the use of general energy savings and solar heating or cooling technology for new building projects. In a new building project, Tubberupvænge, with 92 low density houses near Copenhagen in Denmark approx. 80% of the total yearly energy demand for heating will be saved in this way.

50% is saved by use of different low energy design features, and local solar heating systems. This includes improved insulation, heat recovery of ventilation air, improved window constructions, passive solar heating with attached sunspaces and pebble bed storage in the floor, low temperature heating (55/ 40°C), 150 litre local DHW tanks with improved heat exchanger in each house, and approx. 4 m<sup>2</sup> of roof integrated solar collector for DHW and extra heating of ventilation air. Electrical backup energy in the summer in each housing block is making 4-5 month's stop of the district heating network possible.

60% of the remaining heat demand for the 92 houses is covered by a central solar heating plant with seasonal storage (CSHPSS). Here is used a 3000 m<sup>3</sup> seasonal storage in the ground, which is heated by 1050 m<sup>2</sup> of high temperature solar collectors and, backed up by a nighttime operated electrical heat pump and a combined gas engine/gas boiler heating system. Photos from the CSHPSS of the Tubberupvænge building project is shown in Fig. 1.

In Fig. 2 is shown photos of the building project and the seasonal storage. A diagram of the complete central solar heating plant with seasonal storage is shown in Fig. 3.

The seasonal storage is heated to 85°C by the end of August, and from September heat is delivered from the seasonal storage to the district heating network, depending on the available temperatures. Calculations with the MINSUN program show that it should be possible to cover all the necessary heating demand until December directly from the seasonal storage. When the top temperature in the storage is less than 50°C, the operation strategy is changed so heat will be delivered through a small size nighttime and weekend operated electrical heat pump, (30 kW). This will cool the seasonal storage to a minimum of 10°C in the spring. Supplemental heat after December is supplied from a small gas engine generator system and a gas furnace system. An intelligent control system from the firm Danfoss ensures an efficient operation of the solar heating plant.

The total extra costs to save 80% of the yearly heat demand amounts to approx. 20% of the total building project investment, and about half of the extra costs are paid by the European Communities together with the Danish Energy Council. Calculations indicate that if you limit yourself only to the first step to save 50% of the yearly heat demand, you will only have to invest approx. 5-7% of the total normal building investment, excluding grants from the State and the CEC.

It is the KAB building society together with a local building society in Herlev who are responsible for the Total Energy Project in Herlev. Engineers are Dominia A/S, and Cenergia Aps. are energy consultants and responsible for the Total Energy Design. Main Contractor for the building project is Hosby A/S. Contractor for the seasonal storage is Rasmussen & Schøitz, and Scancon Solar Heating delivers the central solar collector system.

## LOCAL SOLAR HEATING SYSTEMS OF TUBBERUPVÆNGE II.

A 45 m<sup>2</sup> solar collector is integrated in the roof of each of eight housing blocks with 11-12 apartments. The housing blocks have varying orientations (south, south east, east and west).

The solar collector is heating a 2500 litre storage tank placed in a cellar of each housing block. In Fig. 4 is shown a diagram of the local block solar heating systems.

Heat from the storage tank is transferred to local 150 litre DHW tanks with heat exchanger in each apartment, and to the low temperature heating system. A built-in electrical heating element in the storage tank makes it possible to stop operation of the district heating network for the eight housing blocks during 4-5 summer months, leading to large amounts of saved heat losses.

Calculations show that during the summer the difference between solar collectors with east/west orientation compared to south orientation is small (5-10%).

Room heating is as mentioned also covered from the storage tank in the cellar, but only from

the upper half of the storage tank, which during the heating season is partly heated by heat from the heating central through the district heating network. In this way it becomes possible to stop the network operation also during night in periods with limited heating demand.

### FUTURE SYSTEM DEVELOPMENTS

A new total energy project is now being projected for the KAB Building Society, this will be built in 1991 in the city of Ballerup with 100 houses. The firms Dominia, Cenergia and Hosbyg will here optimize and use the most economic solutions from the project in Herlev. It is the aim here to reduce the gas consumption for heating to 40% of normal. At the same time it is intended to use a cogeneration plant with combined production of electricity and heat. A buffer storage will be used for the cogeneration plant. In winter as a 2-3 days storage and in the summer as storage for surplus heat from local solar heating systems.

It is believed that introduction of new solar technology for demonstration in building projects, is important for the development of high quality and economic solar energy systems. It is then possible to involve architects and professional consultants with building and solar system experience, enabling them to make the necessary demands for materials, quality and function. It is, furthermore, possible to achieve better aesthetical solutions and to save alternative building materials and components and thereby obtain a better economy. A continuous use of solar systems in new building projects can be a very useful basis for improvements and more cost effective solutions. This development should in the long run lead to a substantial market, also within the existing housing area where solar systems often are too expensive today.



Fig. 1. Photo of the building project Tubberupvænge in Herlev where a low energy design and 400 m<sup>2</sup> of local solar collectors are used together with a central solar heating plant with 1050 m<sup>2</sup> of high temperature solar collectors and a 3000 m<sup>3</sup> seasonal storage under the wide part of the solar collector field. This total energy system is expected to save 80% of the "normal" gas consumption for heating.

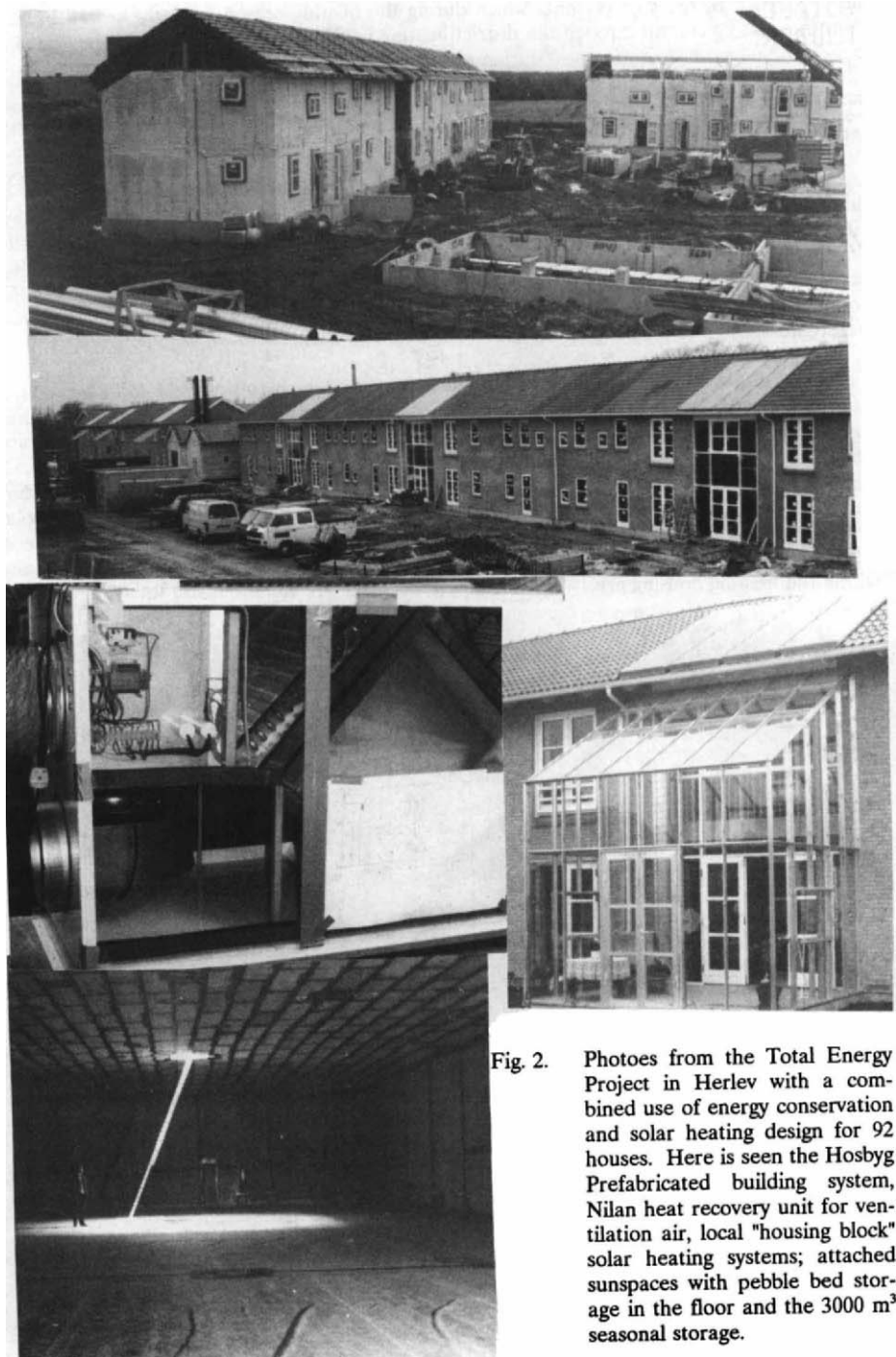


Fig. 2. Photos from the Total Energy Project in Herlev with a combined use of energy conservation and solar heating design for 92 houses. Here is seen the Hosbyg Prefabricated building system, Nilan heat recovery unit for ventilation air, local "housing block" solar heating systems; attached sunspaces with pebble bed storage in the floor and the 3000 m<sup>3</sup> seasonal storage.

## TOTALENERGY SYSTEM TUBBERUPVÆNGE, HERLEV

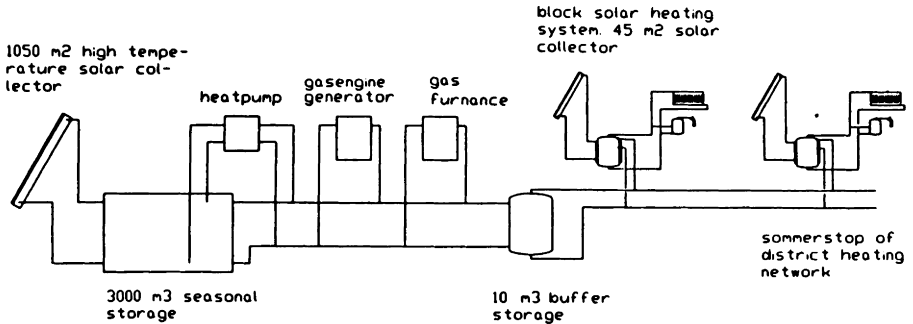


Fig. 3. Diagram of the central solar heating plant with seasonal storage in Herlev, Denmark. Solar heat is supplied from the solar collectors to the seasonal storage, depending on the delivered temperature. The solar collectors are manufactured by the Danish firm Scancon. Heat from the seasonal storage can be used directly, but when the storage temperature is less than 45°C it is used in combination with a small heat pump system.

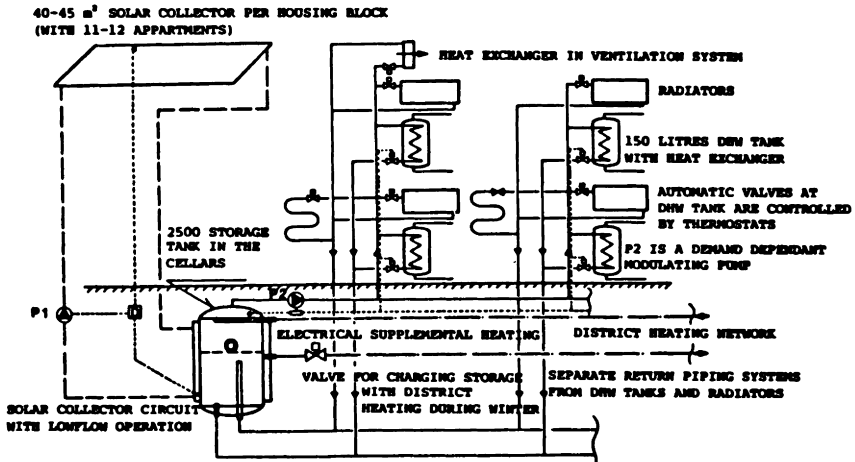


Fig. 4. System diagram of local solar heating systems with 45 m<sup>2</sup> of roof integrated solar collectors for the eight housing blocks in Tubberupvænge. The storage tank in the cellar is designed for "low flow" operation. Electrical supplemental heating is used in the summer to be able to stop the district heating network.

## ENERGY, ENVIRONMENT AND HUMAN DEVELOPMENT IN THE ARAB WORLD

PROFESSOR D J CROOME

Department of Construction Management, University of Reading,  
Whiteknights, PO Box 219, Reading RG6 2BU, UK.

### ABSTRACT

There needs to be an analysis of all climatic issues before deciding any technical solutions. Arabic countries have a wide spectrum of poverty and wealth. World concern about energy and environmental issues challenge the universal tendency of employing advanced technology irrespective of long term social cost.

### KEYWORDS

Building form; materials; dust; precipitation; wind; solar radiation; climate.

### ENERGY, ENVIRONMENT AND HUMAN DEVELOPMENT IN THE ARAB WORLD

Patterns of energy consumption vary greatly as shown in fig. 1 which indicates an annual energy consumption of under 10 barrels of oil per capita in South Yemen to nearly 350 barrels of oil per capita in Kuwait, Iraq, Saudi Arabia, Libya and the Gulf States. Most of the big oil producing countries except Iraq and Algeria are largely desert regions with sparse populations. The remaining Arab countries have larger populations. The remaining Arab countries have larger populations but only small oil resources and these represent about 90% of the people throughout the Arab world.

Egypt has a large population but very modest oil reserves and for these reasons remains comparatively poor. Sudan is also poor but has a lower population and therefore has a better opportunity for balancing needs and resources than Egypt. There are many aspects to consider in viewing future energy horizons. Oil producing states are developing quickly but this poses problems of producing water and electric power at a pace sufficient to keep abreast with these developments. In these countries people have subsidised fuel whereas for neighbouring countries with little oil such as Lebanon, Syria, Egypt, Jordan and Djibouti taxes are high. There is a wide disparity of wealth and resources throughout the Arab world; development rates too are very different.

What are the relevant factors in considering an energy plan for the future? Based on consumption in 1978, Table 1 shows that worldwide coal is by far the most significant fossil fuel with proven and potential lifetimes that are much greater than those for oil, gas or uranium; it accounted for 69.4% of the world reserves in 1979. In terms of world consumption crude oil represented 46.1% and coal 28.4% although crude oil only accounted for 13.9% of proven reserves in 1978.

Table 1: Proven & Potential Reserves of Conventional Non-Renewable Energy Sources: Reserves Stated in Billions of Oil Equivalent (Debs 1982 & Al-Saadi 1981)

Energy Source	Reserves		% Relative to Total		Reserve Lifetime (Years)	
	Proven	Additional	Proven	Potential	Proven	Potential
Coal	3,239	47,197	69.4%	93.7%	226	3,278
Oil	651	1,547	13.8%	3.1%	39	68
Gas	470	1,218	10.1%	2.4%	50	129
Uranium	307	415	6.7%	0.8%	51	73
Total	4,667	50,377	100.0%	100.0%		

Table 2 shows that most fossil fuel reserves are shared between the OECD and the Socialist Blocks. The Arab States have only about 10% of the world proven reserves or 1% of the potential reserves. Tar sand, heavy crude and shale oil developments have limited significance in OPEC and Arab States whereas the OECD Block has more than a 50% share in the distribution.

Table 2: Distribution of Reserves of Non-Renewable Resources Among Producing Blocks.  
(Debs 1982 & Al-Saadi 1981)

Reserves (10 <sup>9</sup> Barrels of Oil)						
Regions		Coal	Oil	Gas	Uranium	Total
OECD Block	Proven	1,483	57	75	151	1,766
	Potential	18,179	256	324	196	18,955
Socialist Block	Proven	1,475	93	171	47	1,786
	Potential	23,856	467	406	158	24,887
OPEC	Proven	4	452	189	7	652
	Potential	29	569	184	5	787
Arab States	Proven		340	74	3	417
	Potential		340	111	8	459
World	Proven	3,239	651	470	307	4,667
	Potential	47,197	1,547	1,218	415	50,377

Table 3 summarises the world situation and it can be seen that Arab countries have less than a 10% share of the world fossil fuel resources and of this Saudi Arabia contributes nearly a third.



Table 3: Distribution of Proven Conventional & New Non-Renewable Resources Among Major Countries (Debs 1982 & Al-Saadi 1981)

Countries	Proven Reserves (10 <sup>9</sup> Barrels of Oil)						Total
	Coal	Oil	Gas	Tar Sand & Heavy Crude	Shale Oil	Uranium	
U.S.A.	888	26	34		204	71	1,223
U.S.S.R.	790	63	164		50	16	1,083
China	463	21	5			12	501
Canada	20	6	16	141		23	206
West Germany	161	0.5	1			0.5	163
U.K.	210	15	5				230
Australia	170	2.1	6			30	208
Poland	143						143
South Africa	118					39	157
India	61	3	2			3	69
Venezuela		18	8	146			172
Arab Countries		340	74	5	60	3	482
Saudi Arabia		168	20				188
Others	215	-	135	-	23	110	471
World	3,239	662.6	470	292	337	307	5,296

This is a broad-brush picture of the energy resource scene but clearly the twentieth century has heralded a massive increase in world population; the fossil fuel reserves are very unevenly distributed and coal is the only fossil fuel with a long-term future.

Populations are increasing and fossil fuel reserves are decreasing so whilst there is a need to develop hospitals, health centre, schools and above all, housing, this has to be carried out within an integrated economic plan, the basis of which must be human development. Already there are examples of rapid development such as in Kuwait but there are positive and negative aspects of these from which lessons can be learnt. Successful development is too often measured in terms of money and comparison with Western growth whereas the most valuable resource is people. All things are serving the development of an Arab civilisation in which all people have a good sense of well-being mentally and physically. The environment, the nature of work and leisure and food are all important if personal satisfaction and aspirations are to be achieved. Within any civilisation there is a culture and this needs to evolve. There are many examples of architecture in which Islamic traditions have been used to good effect. The houses in the Bastikia quarter of Dubai use the wind tower principle to give simple effective cooling and this also contributes to the character of the architecture in a wholesome way; the wind tower used in the Souk at Sharjah is again a functional element but the tile decoration and the metal grille windows grace it in a way which clearly

reflects Arabic thinking and culture.

In his book "Small is Beautiful", Schumacher expresses concern about mankind being distorted by the worship of economic growth and the danger of western man being clever but lacking wisdom. Too often he says we develop things without questioning why we need to pursue these ends with such relentless vigour for such shallow results. If the real mental and physical needs of man are to be catered for then specialised knowledge, especially that of economists, scientists and technologists has to be used carefully and in a systematic manner.

Looking back in history there are certain patterns which are fundamental- simplicity, naturalness and Nature are three key issues which recur in these patterns time and time again. In terms of buildings a consideration of mass, shape, form, orientation and shade can result in less machines to control the climate within them. But these are not new ideas; they are very much part of the language of Islamic architecture. Similarly, it is best to use local materials wherever possible for the fabric of a building because these are readily available, blend with the countryside and are attuned to the climate of the region. Nature, by its climate and landscape, has to be part of the built form expression.

There are human and social needs for new buildings throughout the Arab world. In order to minimise the effects of disparity between countries with respect to fuel reserves, there needs to be a balanced view concerning the energy demand these will make for the people and the economy in general. Energy conscious design has not been predominant so far because money reserves have been very high in the major oil producing countries where most of the building has taken place. In the long-term these countries will have to diversify their interests and some will become fuel importers. Currently the standards of living and community needs vary greatly across the Arab world so there has to be an integrated view towards development. Energy levels need to be as low as possible and alternative renewable resources such as solar energy which is abundantly available need to be developed.

#### Climate in the Arab World

The Arab world occupies a band between the Equator in the south of Somalia and the 37th Parallel North in Algeria. It stretches from Mauritania at 15°W to the tip of Oman at 60°E and comprises some twenty countries in two continents. The predominant religion is Islam.

The countries contain large areas of continental hot desert land but are also strongly influenced by maritime effects from the five different seas onto which they front: the Atlantic and Indian Oceans, the Red Sea and Persian Gulf and, to the north, the eastern Mediterranean. The climatic types are therefore many and various, encompassing the temperate-humid and the hot-arid; the latter is more commonly associated with the Arab world and it is this climatic pattern with which this study is particularly concerned. Within this semi-arid and hot-desert regions predominate; the latter has higher peak temperatures and lower humidities.

Figure 2 is a detailed map showing the climatic classifications of the

Arabian and African countries in terms of both summer and winter conditions. It serves to illustrate the variations in regional climate and emphasises the need for the designer to understand the local climate when undertaking a building design for, while 'typical' climate is a useful indicator of a generic type of building that might be considered, it is only by examining the local weather patterns that an understanding of the possible contribution of the climate to the performance of the building can be approached. Local winds for example are site-specific but highly variable and are frequently exploited with considerable success in indigenous architectural styles.

### Solar Radiation

The intensity of solar radiation and sky clarity are the main reasons for the extreme levels of heat that are encountered in the desert regions. The annual average radiation on horizontal surfaces is in excess of 8 GJ/m<sup>2</sup> in the Sahara and Saudi Arabian peninsulas.

### Wind

The global wind patterns as they affect the countries of the Arab world are illustrated in January and July in figure 3. The countries of continental Africa are subjected to Northerlies and North easterlies for the greater part of the year and the most interesting region is in Southern Saudi Arabia and the Gulf where two systems, the Monsoon from the Arabian sea and the North Westerlies from the Persian Gulf, converge to give what is called the Inter-Tropical Convergence Zone (ITCZ), a zone which moves in the course of the year causing extreme variations in wind patterns in Oman and the other Gulf states. The strong tropical cyclones occur in the summer period and winds as strong as Gale Force 9 have been recorded.

A knowledge of the local winds and their seasonal variations is most important in the passive design of buildings. In most coastal regions the wind speed and direction is considerably modified by the land and sea breezes, particularly at the times when prevailing winds are light (Beaufort force 3 or less). The wide diurnal temperature variations and the consequent differences between air, ground and water temperatures give rise to a large variety of local wind effects. In general the wind blows off-shore in the night and in the early morning; the on-shore breeze sets in towards mid-day and blows until dusk. At times the onset of the sea-breeze may be quite violent and squally; in areas where the mountains slope steeply to the coast the off-shore breeze may also be squally.

Other local winds in the Gulf area include the 'Shamal', a prevailing North-westerly wind particularly strong in June and July; the 'Balat' an off-shore North North-Westerly wind from the coast of Oman which blows from about midnight to midday between December and March; the 'Kaus' (or 'Sharki'), which are South Easterlies in the Persian Gulf occurring ahead of the Westerly depressions between December and March, is an infrequent but strong wind. These are just a few typical examples, but many such local winds occur across the Arab world.

### Precipitation

The high temperatures and extreme levels of insolation which characterise the countries of the Arab world are accompanied by a level of rainfall that is among the lowest in the world. In few places does it exceed 250mm in a year and it is highly intermittent and unreliable so that annual average figures vary widely and can be misleading. Storms normally occur between November and May in downpours where 50mm may fall in twenty minutes and are usually associated with thunderstorms, particularly in the interior. Hail sometimes occurs in association with the thunderstorms and the hailstones may be large. Snow is almost unknown except on the higher mountains and even then it is rare.

Rainfall run-off is normally, in both modern and traditional buildings, discharged from buildings into the street giving rise to the 'traditional' architectural feature of the water spout. Roofs tend to be flat or slightly sloped, evaporation being relied upon to dispose of residual ponded rainfall before it can become a nuisance (not always with the best results for the internal decoration). The more modern cities such as Riyadh are installing surface water drainage systems to alleviate the almost annual flooding problem as, apart from bridging the city to a halt it also poses a considerable health hazard.

### Dust and Sand

Dust and sand carried in the atmosphere are one of the biggest problems for designers of contemporary Arab buildings particularly when natural and passive effects are considered. The atmosphere is rarely free of dust and the problem is exacerbated as cities become larger and the number of motor vehicles increases. The exceedingly small size and low terminal velocity of dust particles tends to make them very difficult to remove by 'natural methods'. Filtration can remove the finest particles but the high resistance to air movement that such high efficiency filters offer necessitates the addition of mechanical means thus negating the 'passive' intention.

It is considered 'normal' in Arab countries to see a slight dust haze for most of the year. Less frequently there are sand and dust storms. A popular misconception exists regarding sand storms due to a failure to distinguish sand from dust. In any arid country when a strong wind begins to blow from a new direction the air becomes charged with a mist of fine particles. Where the surface is alluvial, with little or no sand on it, such as in Iraq or the country around Khartoum, the dust rises in dense clouds to a height of several thousand feet and the sun may be obscured for a long period. This is a dust storm though it often wrongly designated as 'sand storm'. Sand storms tend to be purely local desert phenomena as their particle size (>100 $\mu$ m) requires high wind speed for them to remain suspended.

The international classification of dusty atmospheres is:

Dusty Atmosphere	Visibility (m)	Wind Force	Diameter of Particles
Dust haze	>1000	Light-Calm	Not given
Dust	>1000	>Light	Not given
Dust Storm	<1000	>Strong	<100 $\mu\text{m}$
Sandstorm	<1000	>Strong	>100 $\mu\text{m}$

Dust that has been lifted by strong winds will settle at a velocity determined by the particle size and local air currents. A particle of 0.2  $\mu\text{m}$  diameter has a terminal velocity of 0.6m/day and so, once at a height of 1000-2000m will tend to remain airborne for a considerable period unless brought to earth by air currents.

#### Building Form and Materials

Building form, structure, materials and systems are selected to suit the climatic conditions and achieve a cool and stimulating environment for the people using the buildings besides giving operational economy. Traditional Islamic architecture often displays buildings with heavy facades, limited openings on the external elevations but those that do exist are well shaded. These simple ideas used with modern and traditional materials can produce an energy effective building which is traditionally Arabian.

Figure 4 illustrates the basic form of traditional building from which the environmental impact of the planning can be seen. A combination of mass, shade and ventilation let the buildings breathe in harmony with nature and permit the best range of comfort conditions for occupants inside. Trees, plants and water in the enclosed space cool the air by evaporation, help to keep dust down, provide shade, visual and psychological relief. In addition a cloister type inner courtyard can be featured.

In any location near the equator the roof of the building receives the highest proportion of solar radiation and is also the surface most exposed to the clear cold night sky. To limit the heat gain, the most effective method is to shade or construct a second roof over the first. The outer roof or shading device will reach a high temperature and it is therefore imperative to separate it from the inner roof, to provide for the dispersion of heat from the space between the two and to use a reflective surface on them both. The surface of the lower roof should reflect the low temperature heat and for the outer shading device a white surface is best. A bright metal surface such as aluminium or a white painted surface will have solar absorptivities of 0.1 to 0.5 respectively (see Table 4).

Table 4: Solar Absorptivity Values for Different Materials

Material or Component	Colour or Condition			
	White	Light	Dark	Dirty
Brick	0.2-0.5	0.4-0.5	0.6-0.9	0.5-0.9
Stone	0.3-0.5	0.3-0.5	0.5-0.6	0.5-0.9
Tiles	0.3-0.5	0.4	0.8	0.5-0.9
Asphalt			0.9	
Grey Slate			0.8-0.9	
Asbestos		0.6		
Aluminium	0.1-0.5	0.2		0.4
Copper (tarnished)			0.6	
Water	1m.thick	2m.thick	3m.thick	
	0.56	0.61	0.64	

The amount of incident solar radiation (i) absorbed by a surface depends on its solar absorptivity (α) and its reflectivity (r)

$$\alpha = i - r$$

The radiation absorbed by the material is dissipated through it as heat and some is emitted back into the space by an amount determined by the emissivity of the surface E thus

$$\begin{aligned} \text{Nett gain of energy through material} &= (\alpha - E_a) \\ &= \alpha (1 - E) \end{aligned}$$

For the two examples shown in Figure 5 below the white stone surface and the bright aluminium surface have net gain of 0.03 and 0.192 respectively. If the white surface becomes very dirty the net gain becomes 0.09 and 0.24 for the stone and aluminium surfaces respectively. Values of emissivity are shown in Table 5.

Table 5: Emissivities of Selected Surfaces at Room Temperature

Material	Emissivity	Material	Emissivity
Polished aluminium	0.04	White enamel	0.90
Weathered aluminium	0.40	White paper	0.95
Aluminium roofing	0.22	Plaster	0.91
Polished brass	0.10	Paints	0.95
Oxidised brass	0.61	Ice	0.97
Rough steel plate	0.94	Water	0.96
Weathered stainless steel	0.85	Wood	0.93
Asphalt	0.93	Glass	0.93
Red brick	0.93		

Clearly glass and black surfaces allow a larger solar transmission and hence a high gain to occur.

The roof in Figure 6 shows how to limit direct radiation during the day and maximise the emission of heat outwards at night. The outer element must have a low thermal capacity to ensure quick cooling after sunset. The structure's shading device has a primary objective to cut out the direct radiation from the overhead sun. The second objective is to provide diffused light (absence of glare) to the inner space, yet be architecturally pleasing. The design of a suitable shading device depends on finding a shading mask which overlaps the overheat period as closely as possible. The concrete should be thick enough to achieve a 10-12 hour time lag.

An alternative roof (figure 6b) could be of a more traditional construction with the primary objectives being to limit heat gain and noise intrusion. A well insulated high thermal mass is then necessary with a time lag of 12-14 hours. The outer surface will be light coloured to reflect the incident solar with insulation on the outer face of the structure. The combination of both reduces the heat output to the building.

By placing the thermal mass correctly in the structure the build up of thermal gains will be delayed and will not coincide with highest external temperatures. This results in a reduction of the peak load and in better performance of the airconditioning system.

Figure 7 illustrates the effect of colour and density on the roof cooling load, light colours reduce the cooling load considerably. The effect of mass is more important below about 250kg/m<sup>2</sup>.

Walls also have to give protection against solar heat, external noise, dust and enhance security. The structure must delay and alternate the heat gain so that peak system loads do not coincide with peak external conditions. A well insulated heavy construction is needed. The external face should be light coloured and have a low solar absorptivity. Very few

building blocks have low values and the best that can be expected is something similar to local Riyadh stone, which is a light yellow and has an absorptivity of 0.55 or marble with an even lower value (0.45). A heavy concrete internal skin ensures that the time length is high. For aesthetic reasons the insulation would be placed behind the stone. For hot, dry climates, colour and density are of prime importance for wall construction. Another important element in reducing solar gain through walls is orientation but the effect becomes less significant as the thermal density of the walls increases. With the massive structural density of the wall and limited openings the situation is also favourable for sound insulation.

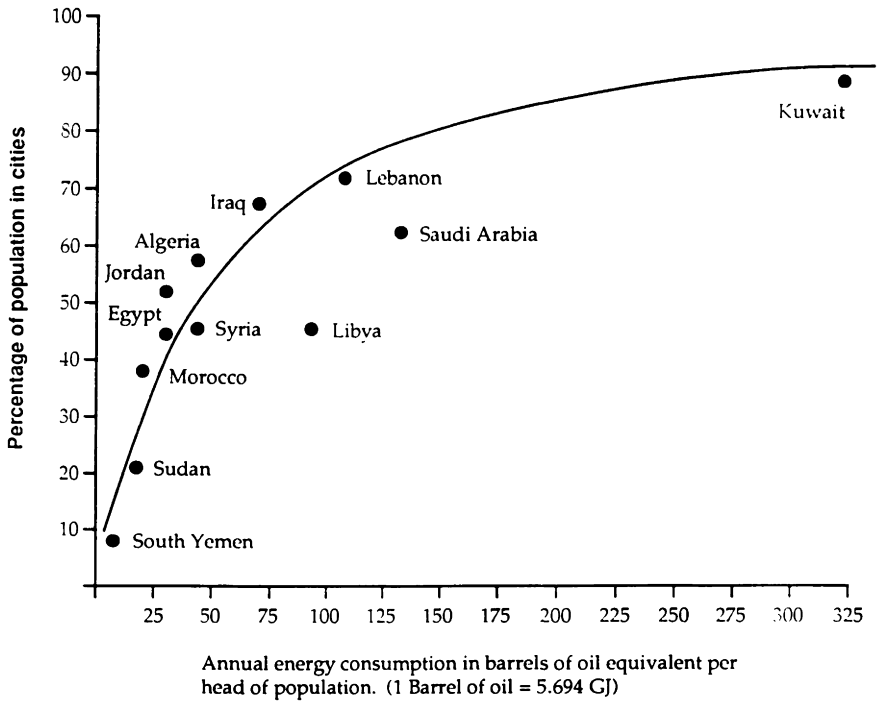
#### Coda

Buildings modify climate; they influence behaviour and culture; they affect the distribution of resources and the ecological pattern of our planet. Human aspirations can only be met when climate, buildings and people are in balance; the dynamic systems and processes which help to achieve this need to work in an interdisciplinary manner so that the hard edges of engineering and architecture are dissolved. Good building design can move freely throughout the climates on Earth as well as through time.

For too long the words building, construction, engineering and architecture have moved uncomfortably with one another and yet distinctions between aesthetics, form and function are arbitrary to say the least. Human thought and life need the stimulus of proactive and reactive forces to give them creative movement. Passive and active approaches to environmental control provide this, so technology can be used not only to achieve technical and economic performance, but also to contribute towards the sensitivity and the emotional effects of the built environment.

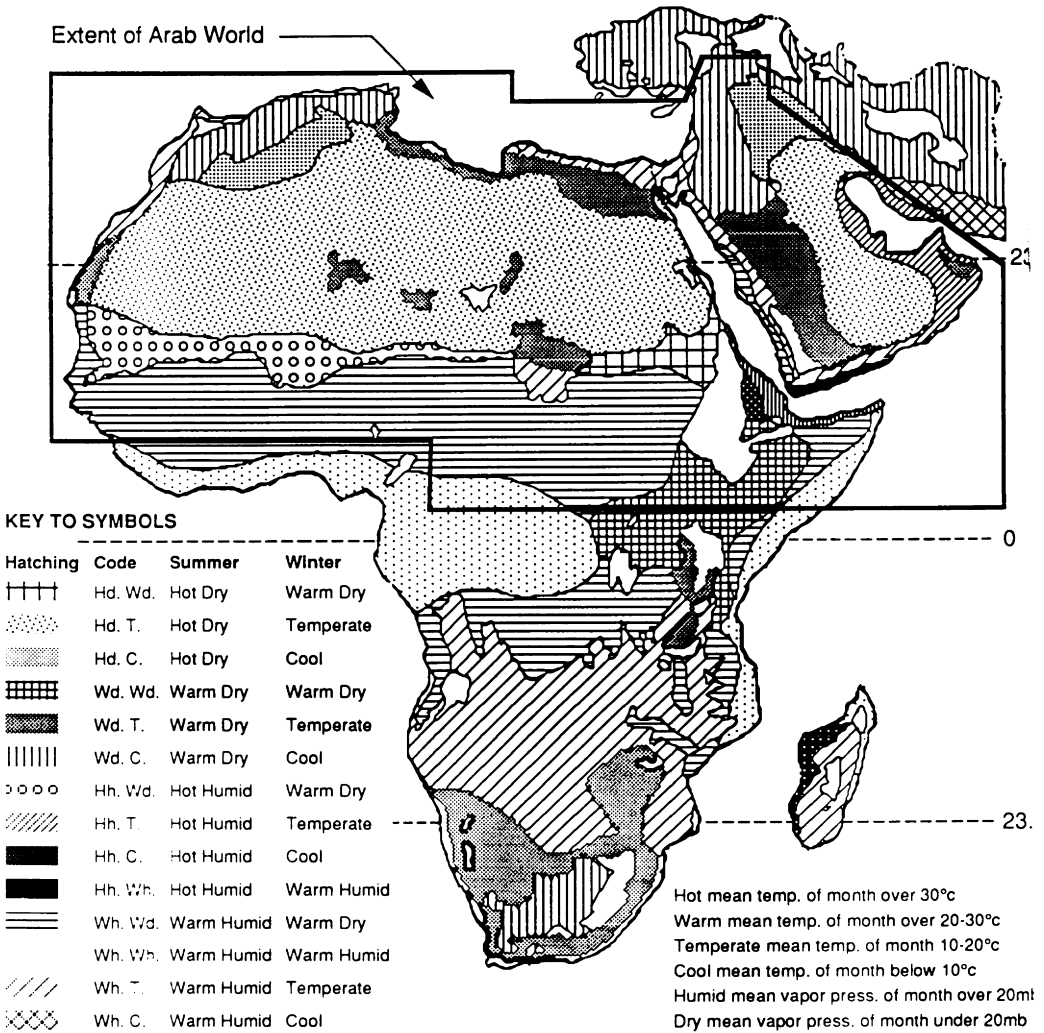
We are learning the languages and this includes understanding how to blend lessons from history with modern technology.





RELATIONSHIP BETWEEN ENERGY CONSUMPTION AND PROPORTION OF POPULATION LIVING IN CITIES FOR SOME ARAB COUNTRIES (DEBS 1982)

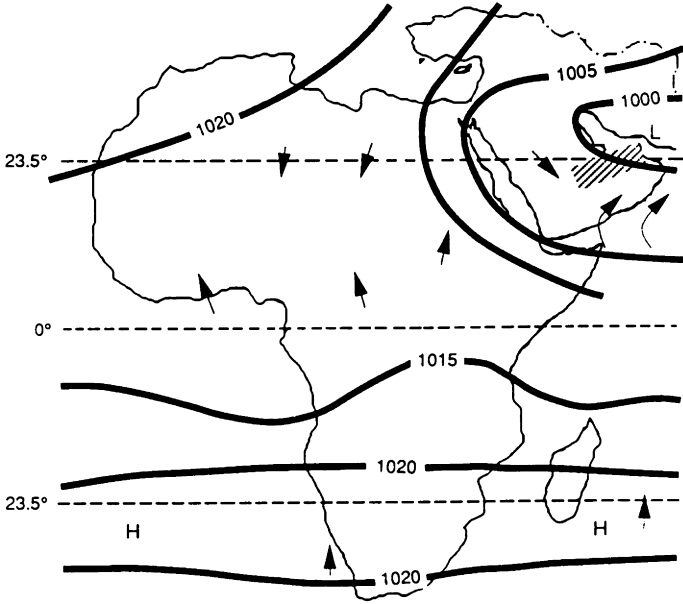
Fig. 1



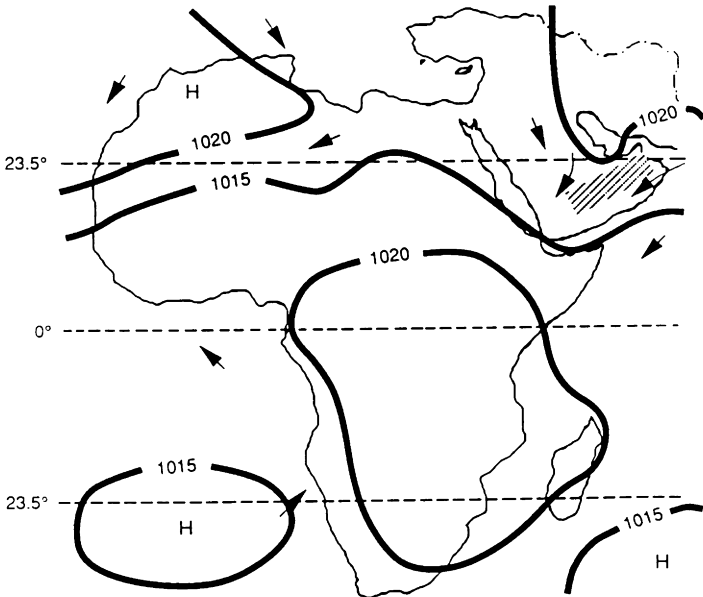
**Major climatic types in Africa and Arabia**

Fig. 2

Fig. 3



**Average Surface Pressure & Windflow Patterns - July (mbars)**



**Average Surface Pressure & Windflow Patterns - January (mbars)**

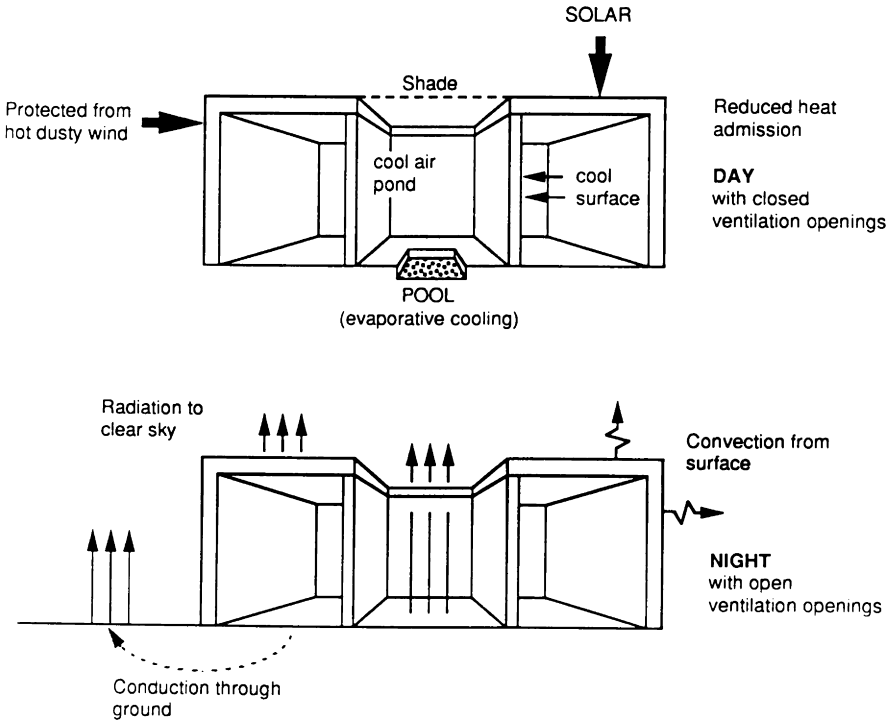


Fig. 4

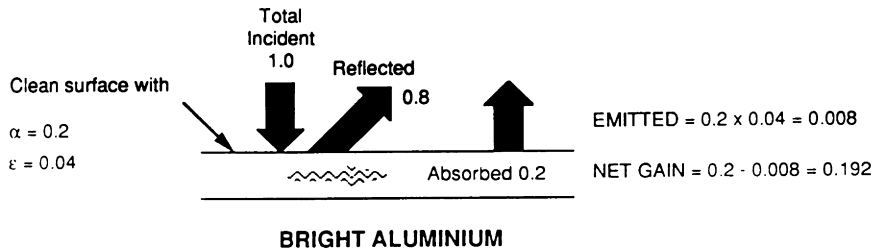
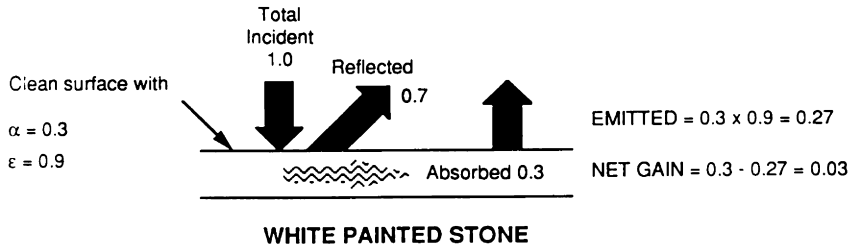


Fig. 5

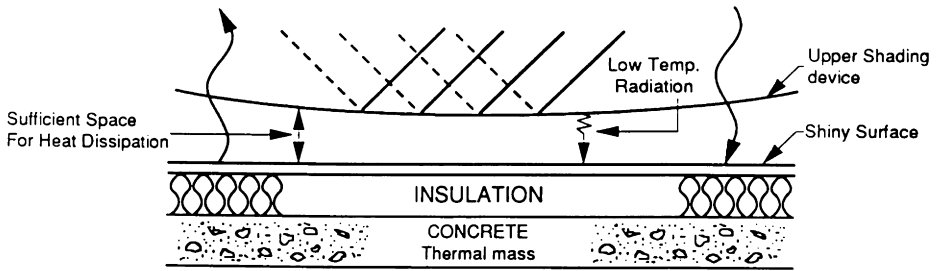


Fig. 6a Shaded and Insulated Roof

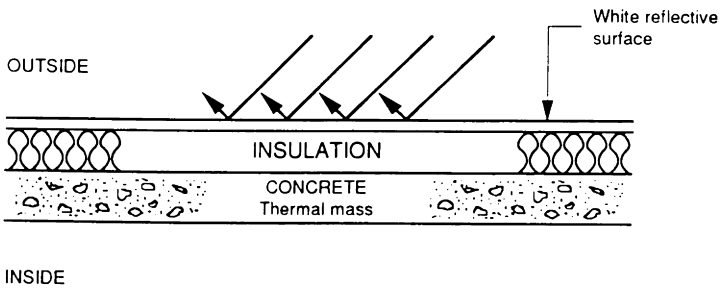


Fig. 6b Traditional Insulated Roof

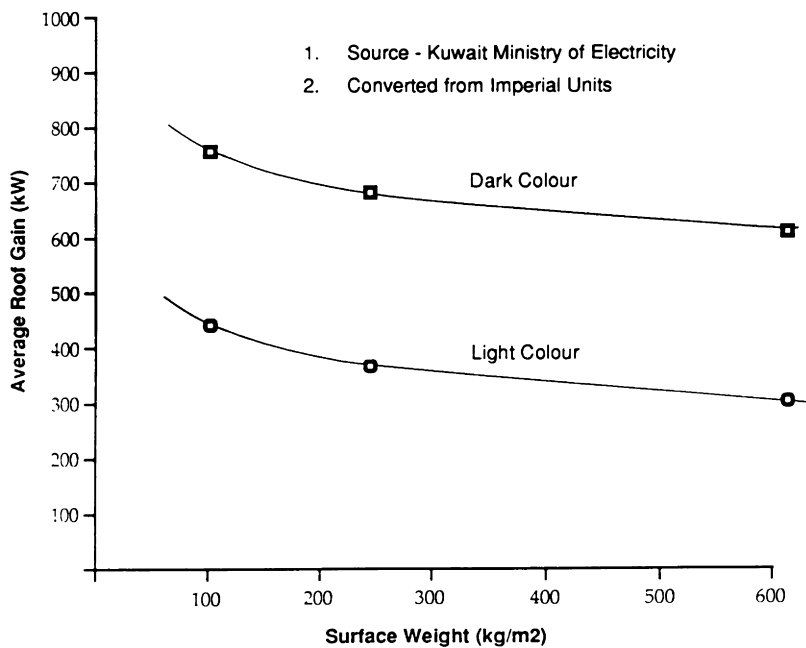


Fig. 7 Effect of surface weight and colour on roof heat gain

## SOME EXPERIMENTS ON IMPROVING THERMAL COMFORT AND INCREASING USEFUL THERMAL GAINS IN SUNSPACES

Kerr MacGregor

Department of Mechanical Engineering, Napier Polytechnic of Edinburgh,  
Colinton Road, Edinburgh, EH10 5DT, Scotland

### ABSTRACT

This paper identifies some strategies for improving both the environmental and thermal performance of attached sunspaces, and describes experimental work to evaluate the performance of one of these strategies. It is concluded that substantial improvements are possible by applying elements of active solar heating to passive solar systems such as sunspaces.

### KEYWORDS

Sunspaces; passive solar; thermal comfort, solar gain, hybrid solar.

### INTRODUCTION

A sunspace or attached conservatory should provide benefits both of amenity and energy savings. However there is often a conflict between achieving reasonable comfort for the occupants and maximising the useful solar gain. If the sunspace is designed and operated as an efficient solar collector it is usually uncomfortable. If it is comfortable the useful energy savings are usually disappointing (James et.al. 1985).

### ANALYSIS OF PROBLEM

An attached sunspace can be considered thermally both as an insulator and a solar collector. It insulates by providing an additional thermal resistance between the building surfaces it covers and the external environment. In addition, when the sun shines it acts as a solar collector. The collected solar heat can be used in the sunspace itself, for example to provide space heating, or it may be transmitted to the adjacent building for space or water heating.

A major constraint on the usefulness of the collected solar heat in a sunspace is the need to provide reasonable thermal comfort for people and possibly also plants. Allowable upper comfort limits on both air and radiant temperatures in the sunspace create engineering



problems in storage and transmission of the solar heat. The intermittent solar gain through glazed roofs is specially problematic.

#### EXISTING SOLUTIONS

Conventional strategies for dealing with or utilising intermittent inputs of solar heat while maintaining reasonable thermal comfort include :

- ( i ) Venting
- ( ii ) Shading
- ( iii ) Passive thermal storage
- ( iv ) Heat transfer to adjacent building.

Venting to atmosphere is quite simple and effective in controlling air temperature in the sunspace. However it is ineffective in controlling radiant temperature and it is also wasteful in terms of utilising solar energy. Shading is quite effective in controlling the radiant temperature experienced by the occupants of the sunspace. However if the shades are reflective they cause wasteful rejection of potentially useful solar energy while if they are absorbant they will heat up and release unwanted heat both by convection and radiation . Passive thermal storage, for example the use of high thermal mass floors and walls is theoretically quite attractive as a means of damping temperature swings in a sunspace but there are practical, economic and aesthetic difficulties in providing large, bare areas of masonry in a living space. Heat transfer, for example by closed-loop circulation of air to the adjacent building is constrained by the need to limit the upper air temperature in the sunspace for comfort purposes and the consequent limitation on the necessary temperature differential between sunspace and building in order to transfer heat without excessive air flow rates. A variation is to use the sunspace simply for open-loop solar pre-heating of ventilation air for the building. This is quite attractive but its energy yield is limited by lack of thermal storage capacity in the sunspace. Neither of the open or closed loop heat transfer strategies addresses the problem of controlling radiant temperatures in the sunspace.

#### ALTERNATIVE SOLUTIONS

In order to overcome the apparent incompatibility between comfort and energy yield in sunspaces I propose a strategy which combines both *shading* and *solar heat collection*. Shading, preferably variable, addresses the problems of thermal and visual discomfort caused by high levels of uncontrolled solar irradiance. Heat collection provides for the controlled and efficient gathering of solar energy which would otherwise be wasted or an embarrassment. If the heat can comfortably be collected at a temperature level significantly higher than the comfortable environmental temperature in the occupied part of the sunspace then the engineering of heat transfer and heat storage is simplified.

Three possibilities for combined or integrated shading and solar heat collection in attached sunspaces are outlined below.

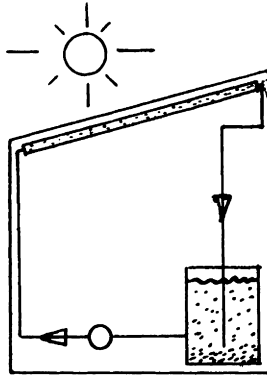


Fig. 1 "FLUID SHADES"

A fluid with dark coloured particles in suspension is pumped through a translucent double-skin panel which is located under the roof of the sunspace. The particles absorb solar radiation and the heat is transferred by the circulating fluid to a store for space or water heating. The concentration of suspended particles, and thus the absorptivity and transmissivity of the panel, may be varied to provide variable shading. This is the subject of a patent application (MacGregor, 1987).

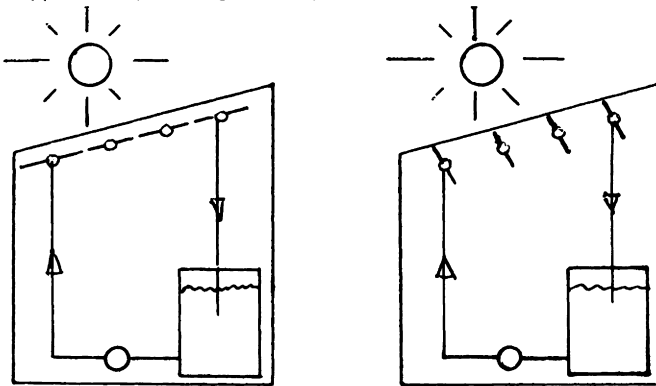


Fig. 2 "FIN SHADES"

Several rows of pipe and fin absorber strips based on solar water heating technology are located under the sunspace roof. The fins may be rotated to provide shading and solar heat collection or to allow solar heat and light to enter the sunspace. Water is circulated by pump through the pipes and transfers the collected heat to a store. The low emissivity rear surface of the fins reduces downward radiant heat transfer by day and upward radiant heat loss at night.

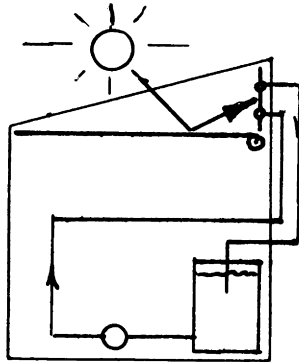


Fig. 3 "REFLECTOR/COLLECTOR"

A reflective blind can be drawn horizontally forward from the back of the sunspace. Much of the solar energy passing through the glazed roof of the sunspace is thus reflected onto a water cooled absorber plate located on the rear wall, either directly or by multiple reflection. The absorber, made of conventional solar water heating materials, experiences quite intensive irradiation and is located in a zone of relatively high air temperature. Collected heat is transferred by pump (or thermosyphon) to a store. By drawing the blind the sunspace is effectively converted into two zones. The upper triangle becomes a moderately efficient solar collector while the lower shaded zone should be reasonably cool and comfortable.

#### EXPERIMENTAL WORK

An experimental test rig to evaluate some of these ideas was constructed on the roof of Napier Polytechnic (Fig. 4)

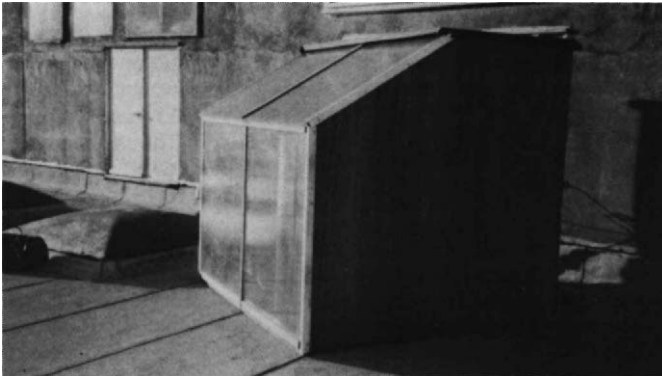


Fig. 4 Sunspace rig for comparative testing.

It consists of two small side-by-side attached sunspace test cells with glazed sloping roofs and vertical south walls (triple skin polycarbonate). The floor and the remaining walls are insulated with polystyrene foam. The structure is made using timber and plywood or

chipboard. This low thermal capacity, high insulation design was deliberately chosen to exacerbate overheating due to solar gain. Thermal comfort in each test cell is assessed by the resultant (or globe) temperature which is the temperature recorded at the centre of a black 100 mm globe which is located centrally at approximately seated head height. The resultant temperature is affected by air temperature, mean radiant temperature and air velocity. For an air velocity of 0.1 m/s, the resultant temperature is the mean of the air and mean radiant temperatures. In one test cell, the *reference* cell, there are no control devices. In the other, the *modified* cell, various control devices and systems can be installed. The performance of the two cells can then be compared under side-by-side weather conditions and the effectiveness of the control devices can be assessed.

A fairly crude but simple measure of the comparative effectiveness of the control devices in improving thermal comfort is defined by the concept Temperature Swing Ratio (TSR)

$$\text{Where TSR} = \frac{\Delta T_{\text{mod}}}{\Delta T_{\text{ref}}} \quad \text{where } \Delta T_{\text{mod}} \text{ and } \Delta T_{\text{ref}} \text{ are the 24 hour}$$

swings in resultant (or globe) temperatures in the modified and reference test cells respectively. The 24 hour swing is taken as the difference between the highest globe temperature in the cell recorded during the day and the lowest recorded during the following 24 hours, usually occurring in the early hours of the morning. The lower the value of TSR, the more effective the control strategy or device.

## RESULTS

The Reflector/Collector concept (Fig. 3) was evaluated using the test cells. An absorber was made from a serpentine grid of 15 mm O.D copper water pipes to which 0.9 mm thick aluminium fins were mechanically and thermally attached using the Clip-Fin method (MacGregor, 1983). The absorber, with a non-selective front surface and bare, shiny rear surface, was mounted on the upper part of the back wall of the modified sunspace. No back insulation was used. An aluminised reflective blind (Reflex-Roll) was stretched horizontally to form the base of a triangular section space with the sunspace roof as hypotenuse and the absorber as the vertical side. Water was circulated by pump through the absorber to a cylindrical storage tank with a capacity of 50 l. The tank was located inside the test cell and, for this test was left uninsulated.

Three operational strategies were evaluated :

- (i) No reflective blind, continuous pump operation.
- (ii) Reflective blind in place, continuous pump operation.
- (iii) Reflective blind, daytime pump operation only (Thermostatic control)

The results are summarised below (Table 1) and a typical 24 hour record is shown in Fig. 5.

STRATEGY	TEST PERIOD	AVERAGE DAILY TEMPERATURE SWING RATIO (TSR)
(i)	10 - 26th October 1989 (17 days)	0.79
(ii)	9th January - 3rd Feb 1990 (19 days)	0.69
(iii)	22nd Feb - 16th March 1990 (20 days)	0.60

TABLE 1. Summary of comparative environmental performance.

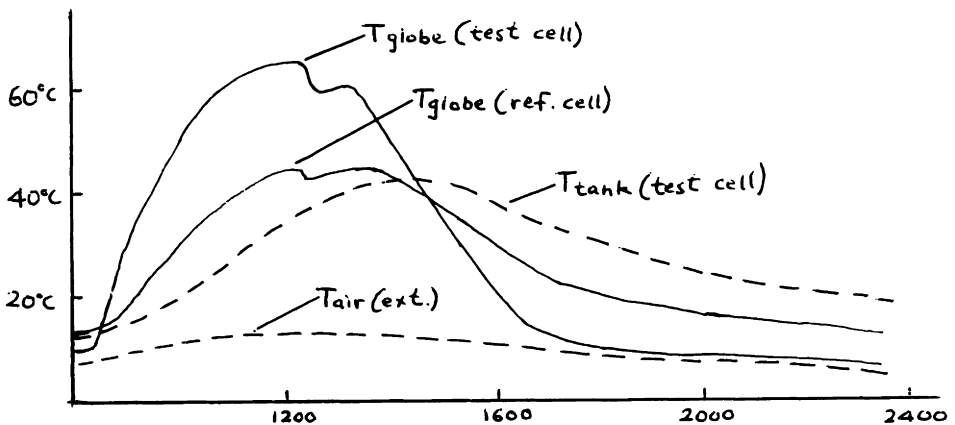


Fig. 5 Typical temperature records in comparative tests.  
DISCUSSION OF RESULTS

Even though most of the testing was done at a time of year when the sun was lower and therefore roof-transmitted solar radiation was less of a problem as regards overheating and discomfort, the results are encouraging. The unshaded (no reflective blind) system reduces temperature swings by about 20%. The addition of fixed reflective shades improves this figure to about 30% while slightly more sophisticated pump control raises it to about 40%.

The benefits of combined roof shading plus collection systems are likely to be more marked when the sun is higher in summer and it should be reasonable to expect temperature swing reductions of the order of 50% or more during this period. Further improvements may also occur if an insulated storage tank is used, with thermostatically controlled release of heat to the sunspace at night.

In these tests the collected solar heat was used entirely for warming the sunspace at night. An alternative is to use it to pre-heat domestic hot water for the adjacent building. The collector performance characteristics of the bare uninsulated absorber plate used in the modified sunspace were measured over a short winter period of several days. With the reflective blind in place the following values were obtained.

$$F_r \sin \alpha = 0.48 \text{ (Intercept of characteristic line)}$$

$$F_{ru} = 10.3 \text{ W/m}^2\text{K (slope of characteristic line)}$$

These figures were based on the irradiance incident on the sloping roof of the sunspace. While it is not strictly valid to compare these figures with those from conventional solar collector testing, nevertheless this appears to be a reasonably performance from a very simple collector which is performing another function (environmental control) in addition to heat collection.

#### FURTHER WORK

It is intended to extend testing of the "Reflector/Collector" system described to include summer operation and pre-heating of domestic hot water. In addition, prototypes of the "Fluid Shades" and "Fin Shades" devices have been constructed and will be tested in a similar manner.

#### CONCLUSION

The use of elements from active solar heating technology to improve both environmental control and also to increase useful energy yield in passive solar systems such as attached sunspaces appears both practical and effective.

#### REFERENCES

- James R and Dalrymple E. J. (1985) Modelling of conservatory performance. Greenhouse and Conservatories (B. Norton, Ed.) UK - 1SES pp 14-21
- MacGregor A.W.K. (1983) The solar clip-fin Proc. ISES Solar World Congress (S.V. Szokolay, Ed)
- MacGregor A.W.K. (1987) Variable Screen. UK Patent Application 8827086.3

## HADEN COURT ENERGY EFFICIENT ESTATE IMPROVEMENT

DAVID CLARKE and ANDREW MYER

David Clarke Associates, 4 Tottenham Mews,  
London W1P 9PJ, UK.

### ABSTRACT

Haden Court is a demonstration project within the Energy Efficiency Office's Energy Efficiency Demonstration Scheme looking at rehabilitation of traditional construction, low/medium-rise flats. It shows that a comprehensive package of energy measures, including both insulation and passive solar features can provide energy-efficient homes cost effectively when applied as part of a general rehab programme - as well as providing additional, non-energy benefits. An energy target of 25-30% below 1985 Building Regulations standards was achieved using available technology - which is still 10-20% below the revised 1990 Regulations. Stage I was completed in May 1990: the cost of the energy measures was £2430 per flat - out of a total of £34800 per flat. With a predicted saving of £110-220/flat per year this achieves a simple payback of 11-22 years.

### KEYWORDS

Energy-efficiency; passive solar; payback; rehabilitation

### EXISTING SITUATION

Haden Court is an estate in North London of 102 flats and maisonettes, in 4 and 5 storey walk-up blocks, built between 1953 and 1958 with solid brick walls and concrete roofs and floors. In 1985 the buildings were hard to heat and suffered condensation problems - similar to tens of thousands of Council-owned properties in London. A feasibility study (funded by the Building Research Energy Conservation Support Unit (BRECSU)) concluded that a combined insulation and passive solar package could be cost effective in conjunction with a normal rehabilitation programme and provide additional amenity benefits. Average savings per dwelling of 6000-10000 kWh/year were identified with a potential replicability in London of 295-660 million kWh/year.

In 1986 Islington Council decided to carry out the recommendations of the feasibility study, as a pilot study for their future estate improvement

programmes. BRECSU agreed to support the project as part of their Energy Efficiency Demonstration Scheme and appointed David Clarke Associates as energy design consultants to advise the Islington Architects Department.

#### TARGETS

The uninsulated buildings penalise occupants compared with residents of new dwellings and reinforce positional disadvantages of top floor or end of block situations. It would seem unacceptable that major rehabilitation programmes should be allowed to provide a new 30 year life for the property without also improving the performance of the building fabric to meet contemporary expectations, as this would create sub-standard dwellings.

The energy target for the project was a 25-30% improvement on requirements for new buildings in the 1985 Regulations, as these levels could be achieved easily with existing technology. This target will still be an improvement on new-build requirements of the revised 1990 Regulations - at Block F, for example, 10-20% better - but this should be seen more as comment on the timidity of the revised regulations than any excess in the target.

#### STRATEGY

The layout of energy measures for the estate was worked out as follows:

##### Conservatories

Conservatories provide energy benefits as well as increased floor area. They are, however, comparatively expensive and so have been applied where the maximum benefit is gained (i.e. to undersized dwellings) and where they can be simply constructed. Careful study of the dwelling sizes and the feasibility of construction resulted in conservatories being proposed to 37 dwellings, in 5 of the 6 blocks.

##### Trombe Walls

Retrofit Trombe Wall applications to South-facing blank walls could have better energy performance than simple insulation, but detailed analysis showed that these were not a viable option for this estate.

##### Roof Space Collectors

The Borough Architect decided at an early stage to add pitched roofs to all blocks, mostly as an aesthetic choice and to provide a roof covering with a longer life. Following this decision, glazing the South slope of the new roof and using existing flues to blow warm air into the dwellings seemed a promising option - particularly as a prototype for urban areas where overshadowing is common to lower floors.

As flats - with greater thermal storage - and maisonettes - which benefit from natural 'stack effect' air circulation - would perform differently with a roof-space collector, it was decided to look at both. The long roof of Block A has a better orientation than Block F and could provide a remote collector supplying eight 2-bedroom flats at the North end, which suffer severe



overshading by the long block itself. The most overshadowed maisonette block is Block B, and a roof-space collector was proposed to the eight mid-terrace 2-bedroom maisonettes to simplify comparison. The site layout also allowed steeper pitched roofs on these two blocks, to optimise the collectors without significantly increasing shading to other dwellings.

#### Enclosure of access galleries

There may be little difference in energy performance between enclosing access galleries to form a buffer space or insulating the walls and windows. In some blocks, the access gallery is recessed with an inadequate wall to the dwelling and uninsulated concrete slabs to the bedrooms above and below; in this case simple enclosure of the access gallery was shown to be as effective in energy terms as more expensive insulation measures, as well as providing amenity to the residents.

Block A not applicable as access was from glazed stairwells.  
 Block B (2nd floor), Blocks C & D (1st and 3rd floors)  
     recessed galleries could be simply enclosed by single glazing between the parapet wall and the downstand beam over.  
 Block E (2nd floor) and Block F (1st, 2nd and 3rd floors)  
     fully exposed galleries would require a structurally independent enclosure.

#### Insulation

Walls. Internal insulation reduces the size of already under-sized rooms. External insulation is more effective, though more expensive, but at Haden Court would conceal good quality facing brickwork. The package optimised a balance of external and internal insulation, and buffering. External insulation was proposed to reduce the locational inequalities of top floors and flank walls. Internal insulation was to be applied on all other walls not buffered by a conservatory or enclosed access gallery.

Roofs. A pitched, insulated roof would be added to all blocks. A low pitch would minimise overshadowing and allow wind-assisted ventilation pre-heat to the maisonette blocks with conservatories, by the use of ridge-vents.

Floors. Uninsulated concrete ground slabs are a major source of heat loss and discomfort, particularly in intermittently heated dwellings, and an insulated floating floor was proposed.

Windows. The windows at Haden Court were galvanised steel in sound condition. They were however, often a poor fit and draughty and were a major source of tenant discomfort and condensation. Secondary glazing was proposed to all North-facing windows (where not buffered) with improvements to all other windows, as necessary.

Plant. Extract fans were to be installed to all kitchens and bathrooms with controlled ventilation to all habitable rooms.

Full central heating is generally inappropriate to low energy buildings. Demonstration projects have shown that reduced heating installations can provide adequate and affordable comfort levels at a considerable capital saving, which can help to offset the cost of the energy measures.

## STAGE I (Block F)

Computer Modelling

Two adjacent flats (1 and 3-bedroom) were modelled in each of 3 positions (ground, middle or top floor): a) as existing; b) as if built to 1985 Building Regulations standards and c) as b) but draught-stripped - to provide the base for the target improvements. All models were run for 'low' and 'typical' internal gains and 'typical' and 'high' heating schedules as most suitable for public sector housing with high levels of occupancy. A wide range of different energy packages were then run identifying the dominant elements of heat loss, minimising the inequalities of position and testing the strategic application of energy measures, to achieve the target savings.

The selected package included: 3 storey conservatory to L/R of 3-bed flats (with balcony to top floor flat); access gallery enclosed to top three floors; external insulation to flank walls and top floor of South-West and North-East elevations (where not buffered by access gallery enclosure); insulated dry-lining to all other external walls; insulated floating floor to ground slab; insulation to roof; secondary glazing to all windows except where buffered by conservatory or access gallery enclosure; controlled ventilation and reduced heating system to all flats.

These measures eradicated inequalities between top and middle floor flats, but restrictions on the thickness of insulation to the ground slab (such as door heights) meant that ground floor flats will perform less well than the others - though this was still a 35-40% improvement over the 'base case' which did not require any insulation to the floor slab. The overall package showed an improvement of 25-33%, in line with the target figure: the intention was that the package of improvements to the whole block should be cost-effective, rather than looking at individual elements or flat types.

Detailed design

Conservatories. Detailed design of the conservatories had to optimise several requirements: size and shape to allow a wide range of activities; the buffer space to cover as much as possible of the living room wall; adequate ventilation paths to pre-heat ventilation air; glazing must be cleanable from inside, or obscured; glass at low level must comply with safety regulations; enough glazing for view from and light to the room behind, to optimise solar gains in winter, but not cause overheating (the S.W. aspect of the conservatories could allow over 6kW solar gains on summer afternoons if fully glazed); need for compliance with Building Regulations is not clearly defined - the District Surveyor for Haden Court accepted that with a door between the conservatory and the living-room, it was an 'enclosed balcony' and need not comply with, for example, fire separation or insulation regulations; geometry and construction to be simple and economic: blockwork construction was chosen, more accurately a 'sun room' than a conservatory.

Enclosure of access galleries. Block F access was more exposed than for the other blocks, with railings rather than a parapet wall and a worse orientation: the decision to enclose was made to provide equality with the other blocks, even though the cost was considerably higher. Because of the greater exposure, additional work would have been required to bring the access to an acceptable standard - for example providing a roof over the top floor gallery and weather-screens to the front doors - and it is the extra-over cost above this and the

provision of insulation, double-glazing and draught lobbies which should be seen as the additional amenity cost of the full enclosure.

Enclosure of access galleries affects the Means of Escape provision: windows from the flats to the galleries were sealed shut and made fire-resistant, and the front doors fire-resistant; smoke doors were required from the enclosed galleries to the main stair and openable ventilation was needed at each level; kitchen extract vents had to be in fire-resistant ducts across the galleries.

Insulation. The original strategy was modified in the light of the greater cost of external insulation, omitting it to the top floor North-East and South-West walls in exchange for internal dry-lining and a greater thickness of roof insulation, while retaining it to the flank walls: this achieved the same energy performance, but at a considerable cost saving. The solid wall and concrete floor construction provided numerous cold bridges, which were cured where practicable by returning the internal dry-lining by 600mm to walls, and to the underside of floor slabs. The ground-slab was insulated throughout but restrictions on thickness to maintain door-heights reduced the effectiveness of this measure.

Windows. As the existing windows were sound and fit for a further 30 years life, the most economic improvement was by modification rather than replacement. Alternatives included: retaining single-glazed windows on the South-West side with draught-stripping and improved night-time insulation; double-glazing existing windows; or secondary glazing. Cost comparison showed that the best buy was secondary glazing to all existing windows not buffered by the conservatories or access gallery enclosure. Garden and balcony access was to be by high performance french windows.

Heating/hot-water installations. Various heating strategies were costed and compared (capital and running costs) for the 1 and 3-bedroom flats. In the 3-bedroom flats it was not appropriate to omit bedroom heaters as it might in maisonettes where convection can adequately heat the upper floors, but it was possible to omit heaters to kitchens and circulation spaces. This number of emitters made a conventional system the most effective gas fired option, although an all electric alternative would have made considerable capital savings with little change to the running costs: the all electric solution was however unacceptable to Islington. Addition of a 'Boilermate' heat store to the conventional system reduced the cost and is claimed to make the system more efficient, by reducing boiler cycling and running the boiler continuously at maximum efficiency.

In the 1-bedroom flats, the most economic solution was provided by gas convector heaters to the living-room and bedroom, an electric heated towel rail to the bathroom and off-peak electric water-heating.

Ventilation. Much of the improvement package is designed to reduce infiltration losses, as these account for around 30% of the losses from the existing building, but it is important that enough controlled, draught-free fresh air is available to ensure a healthy atmosphere - to expel or dilute odours and pollutants, and to prevent condensation. In Block F fresh air is introduced through trickle vents into living and bed-rooms, with some ventilation pre-heat from the conservatories. The North side of the block is tightly sealed by secondary glazing and/or enclosure of the access gallery and negative pressure is induced by fans in the kitchen, bathroom and w.c.s which minimise the risk of condensation (by extracting moist air at source) and draw fresh air into and through the dwelling.

Cost

Tender costs for the energy measures in Stage I were:

	Cost of energy measures (£)	Cost of amenity measures (£)
1. Internal dry-lining (642m <sup>2</sup> )	14740	-
2. External insulation (150m <sup>2</sup> )	9320	-
3. Floor insulation (258m <sup>2</sup> )	3880	-
4. Roof insulation -extra thickness (357m <sup>2</sup> )	340	-
5. Cavity insulation - 2-storey extension only (99m <sup>2</sup> )	460	-
6. Secondary glazing	6880	-
7. Walkway enclosure	14000	14400
8. Conservatories	8000	12210
9. Reduced heating installation	-16310	-
10. Controlled ventilation	<u>2390</u>	-
Total cost of energy measures	f43700 (f2430 ave. per flat)	

Estimates have been made of energy and amenity costs (when benefits apply). For the access gallery enclosure, the cost of the energy part was equated to the insulation package with the same performance: the amenity value was the extra-over cost above bringing the access up to modern standards. The amenity value of the conservatories was estimated on the basis of additional floor area, leaving an energy cost of f1330, which is in line with the acceptable capital expenditure for the predicted energy savings.

These total energy costs represent less than 7% of the contract sum (f626,537 or f34,800 per flat). The predicted savings of f110-220/flat per year (4900-10000 kWh at f0.022/kWh) suggest a simple payback period of 11-22 years, which is worthwhile within the 30 year expected life of the work. It should be remembered, however, that much of the energy work is required simply to bring the flats up to modern standards for their renewed life: if this is not carried out, substandard dwellings would be created. It is not common practice to examine the pay-back period of new plumbing, wiring or roofing and the fact that the energy measures provide a pay-back well within their lifetime should be considered a bonus.

Monitoring is being carried out on Stage I for BRECSU by Wimpey Environmental Ltd, and the results should be published in late 1991.

## LATER STAGES

In May 1989 Islington Council decided that as they could not guarantee funding to the later phases, all energy measures would be dropped. This was particularly regrettable in the light of Haden Court's status as a pilot project and suggests that Islington will continue to rehabilitate properties to an inadequate thermal standard, where tenants can still not afford to heat their homes and condensation will still prevail.

## PASSIVE SOLAR TESTING AND PERFORMANCE PREDICTION

H.A.L. van Dijk and A.C. de Geus

TNO Institute of Applied Physics (TPD)  
P.O. Box 155, 2600 AD DELFT  
The Netherlands

### ABSTRACT

The characterization of passive solar components is due to a number of effects a difficult task. For this reason the CEC-PASSYS project was started. Testcells have been built, testing and evaluation procedures are under development. For the Dutch situation the perspectives by translucent insulated walls have been investigated. The possible energy savings of current wall designs are estimated on 700 to 1200 MJ per m<sup>2</sup> facade. During the summertime the overheating may be a serious problem. Natural ventilation of the airgap is one of the possibilities to reduce the overheating. The conclusions are that the results are sufficiently promising to initiate further and more detailed research and development.

### KEYWORDS

PASSYS testcell, parameter identification, translucent insulation materials, passive solar components.

### INTRODUCTION

A passive solar component (PSC) is mainly characterized by the thermal transmission coefficient (heat loss) and the solar energy transmittance (heat gain). Other important characteristics of a PSC are the heat storage capacity and the airtightness.

In general, it is a complicated task to determine the characteristics of passive solar components. To measure directly the heat transfer and the transmittance for solar radiation in an accurate way is due to the mechanisms involved (free convection, thermal radiation) often not possible. Moreover, the performance of a PSC depends on a number of other factors such as the orientation, competing heat sources, the thermal mass of the building, the size, etcetera. The main task in an experiment is to distinguish these factors and to reveal both the performance of the PSC itself and its interaction with the building and the occupants.

Statistical techniques are of great importance in order to get a maximum of information from a relatively short test sequence. Otherwise the test duration would be excessively long, in particular due to the large time constants of the thermal system.

**RESEARCH OBJECTIVES**

In the research carried out at TNO with respect to passive solar energy systems the following goals can be recognized.

- quantitative determination of the system characteristics for product information;
- full scale testing of new system concepts before applying them into practice, to decrease the risk of costly flaws;
- system optimization;
- system modelling;
- development of simplified design tools for energy savings calculations.

**THE PASSYS PROJECT**

In 1986 the Commission of the European Communities started the international research project on passive solar energy PASSYS. TNO is the Dutch participant in this project. At the moment phase 2 is started. This phase will last until the end of 1991. The aims of the PASSYS project are the following:

- to set up uniform facilities for the testing of passive solar components;
- to develop simplified design tools on the influence of PSC on energy consumption and thermal comfort;
- to develop and validate a selected building energy analysis model (ESP).

The dutch participation in PASSYS is financially supported by NOVEM, the Dutch agency for Energy and the Environment and by TNO.

At a number of locations, spread over the CEC countries a PASSYS testfacility has been set up. This facility consists of four identical outdoor testcells. The open fronts of these full scale cells are faced southward; here the passive solar component can be mounted for testing. In fig. 1 the testcell is schematically presented.

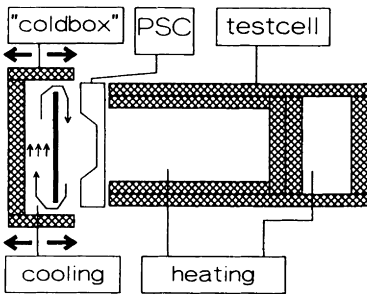


Fig.1. The standard PASSYS testcell, including the TNO addition: the movable coldbox.

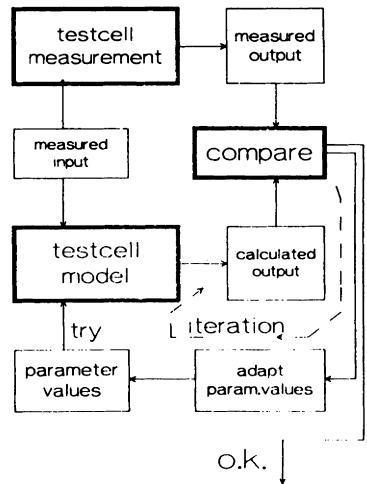


Fig.2. The principle of parameter identification to derive the properties of the PSC from testcell measurements.

The testcell is highly insulated and can be provided with high or low internal lining, to simulate practical situations. Within the testcell a realistic indoorclimate is created, thus simulating as good as possible a real room. During 1988-1989 the facilities in the different countries became operational. The last 2 years of the project will be mainly used to finalize the building up of the facilities, for testing and comparison of testresults from the different countries, but especially for the final choice of a suitable measuring and evaluation procedure and the elaboration of standardized procedures.

A special development at TNO is the movable coldbox. This apparatus (see fig. 1) may be placed in front of a facade which is tested in one of the testcells, and provides an artificial outdoor climate, for example a constant windspeed and a low temperature. By measuring the heatflow through the facade the overall heat transfer coefficient can be calculated. This additional provision transforms the testcell into a full scale "hot-box".

#### DEVELOPMENT OF TESTMETHOD

One of the major goals within the PASSYS project is the development of a good teststrategy in combination with an evaluation technique which enables to get sufficient information from a relatively short test under real, dynamic outdoor conditions. The so-called parameter identification techniques are developed and investigated as a promising evaluation technique. A Parameter identification technique uses mathematical fitting procedures in order to get good agreement between the output of a transient model for the PSC and the measurements carried out on the PSC. In figure 2. the principle of the parameter identification process is given.

The testroom temperature is usually appointed as output variable; input variables are outdoor temperature, solar radiation, heating power etc. The set of parameter values which gives the best agreement between the measured and calculated output variable yields the characteristics. Evidently, one of the basic requirements is that the main PSC and testcell characteristics can be derived from the identified parameter values.

Within the PASSYS project different methods are being compared, in particular with respect to the choice of the type of mathematical model for testcell and PSC.

TNO has developed the parameter identification method MRQT, which can be linked easily to almost any type of model.

#### TEST CONTROL STRATEGY

As a consequence of the application of a technique in which different characteristics are derived from the same testsequence special attention should be paid to the correlation between the input variables: if different input variables, like outdoor temperature and solar radiation are correlated, it is not possible to get a clear separation between the parameters which are supposed to describe the thermal conduct of the system with respect to these respective solicitations (like heat loss and solar gain).

During the period 1988/1989 first test series were carried out; the results were used to reveal childhood diseases in the testfacility and to develop and compare different testmethods.





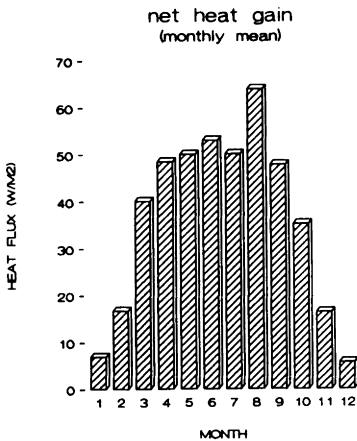


Fig.3. The monthly net heat gain; "reference" TI-wall, South

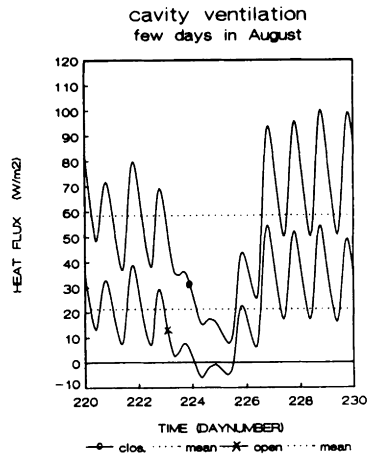


Fig.4. Net heat gain during the summer situation with closed and open cavity for ventilation.

In fig. 3 one can see high heat gains during the summer period. Possible solutions to prevent this are shading devices, overhangs, blinds etc. Unfortunately a number of these solutions have to be mechanically controlled.

A cheap solution is the opening of ventilation slots during the summer season. Calculations have shown that natural convection in the airgap between the wall and the TI material can reduce the unwanted heat penetration in the house with two-third. This option may be promising since it is much cheaper than controlled blinds or shading devices. In figure 4 results for a ventilated and closed reference TI-wall are given, orientation South. Detailed dynamical building simulations must give information whether this option is acceptable in practice with respect to the remaining heat gain.

Calculations indicate that for the Netherlands the possible energy savings by current TI-wall design will be about 700 - 1200. MJ per m<sup>2</sup> TI-wall, orientation South, dependent on the heat demand of the house and compared to opaque insulation.

In practice, the heat gain depends of course on the properties of the TI-wall, the dynamics of the house and the occupants behaviour.

The preliminary conclusions are that TI-walls are quite promising; for large scale applications, however, a cost reduction is necessary. Present high costs are mainly due to the complexity of the overall design which is related to the vulnerability of the material.

### Testcell Experiment

During the period August to October 1989 measurements were carried out in the TNO PASSYS testfacility on an experimental facade. This facade (see fig. 5) had the following elements:

- \* limestone wall of 21 cm;
- \* airgap of 6 cm;
- \* clear glass thickness 8 mm;
- \* PC honeycomb, thickness 10 cm;
- \* clear glass thickness 8 mm;

The frame material is wood.

The measured performance of the TI-wall was lower than expected, mainly due to shortcomings in the construction.

The overall outcome of the experiment, however, is positive: despite an average temperature difference between testcell and ambient of 15 K, the net heat gain was positive. Figure 6 gives the measured heatflux through the facade. A well insulated facade without translucent insulation would have given under the same circumstances an average heat loss of 6 W/m<sup>2</sup>.

Figure 6 also shows the model output after identification of the TI-wall parameters.

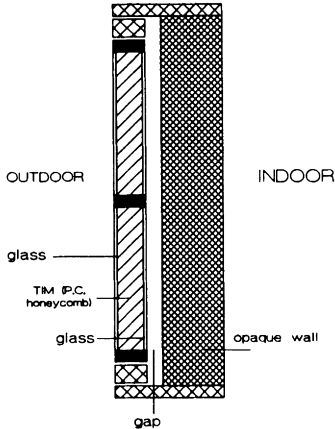


Fig. 5. Construction of the experimental TI-wall.

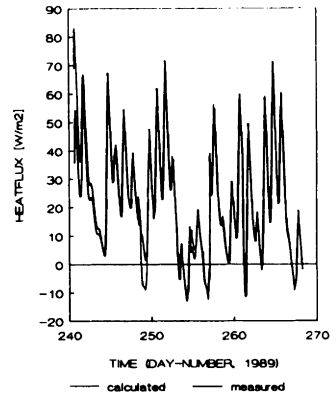


Fig. 6. Measured and identified TI-wall net heat gain during PASSYS test.

## CONCLUSIONS

The CEC PASSYS testcells in combination with advanced test evaluation techniques are a powerful tool for the characterization of passive solar components and their interaction with the indoor environment. Moreover, the full scale tests under real outdoor conditions are very useful to detect shortcomings in the design, before application in occupied buildings.

The first theoretical and experimental results on the application of translucent insulation for passive solar walls are promising. The research on the TI-wall concept will be continued; with the emphasis both on the long and short term goals. To mention are material development, material modelling and testing, guidelines for TI-wall application; testcell experiments and demonstration projects.

In autumn 1990, already, a new PASSYS testcell experiment will start on a "commercial" TI-wall, from a type which is used in recent demonstration projects in Germany. Identical walls will also be tested in some of the other PASSYS facilities.

## ACKNOWLEDGEMENT

Much of the activities reported here have been carried out with the financial support of NOVEM (the Netherlands Management Office for Energy and Environment); also the CEC-DGXII supports financially the PASSYS research project.

NORTHSUN '90,  
UNIVERSITY OF READING, U.K.

**THE JUSTIFICATION OF ENERGY EFFICIENT MULTI-STOREY  
COMMERCIAL BUILDING DESIGN IN MORE TEMPERATE  
CLIMATES.**

**Graeme Robertson**

Department of Architecture  
University of Auckland  
Auckland  
NEW ZEALAND

**Keywords:** Energy, Commercial Buildings, Economic Efficiency, Worker Efficiency,  
Temperate Climate

**Abstract:**

Emissions resulting from human activities are substantially increasing the atmospheric concentrations of the greenhouse gases. These increases will enhance the Greenhouse Effect, resulting on average in an additional warming of the earth's surface. Present high altitude cold climate energy design solutions are likely to require constant revision. This paper addresses the possible solutions in terms of commercial building design, when cooling loads may become more dominant than heating loads.

This paper briefly explores possible energy efficient techniques appropriate for commercial buildings in a temperate climate country such as New Zealand. The likely cost effectiveness is discussed both in terms of energy efficiency and worker efficiency.

This paper suggests that a better method of justifying these possible design solutions lies in the increased output of the workers and not in the possible energy savings.

True environmentally connected high comfort office buildings are possible both economically and architecturally.

**Background**

The earth is warming up. Recent statements (1) suggest that without major change to our rate of emission of greenhouse gases, there will be a rate of increase of global mean temperatures during the next century of about 0.3°C per decade (with an uncertainty range of 0.2°C to 0.5°C per decade). This will result in a likely increase in Global mean temperature of about 1°C above the present value by 2025 and 3°C before the end of the next century. These figures can be reduced only by a substantial change to our approach to living on this planet. Many of the 'problems' of more temperate climates may become those of the higher latitudes.

In the years since the first energy crisis of 1973 a range of design solutions for energy efficient commercial buildings have been developed - normally based on scenarios involving high energy costs and /or severe climatic conditions.

In New Zealand, a temperate climate country in the South Pacific, the lessons to be learnt from the first energy crisis were slow to be assimilated. Energy efficient commercial buildings have been slow to evolve, with relatively cheap energy prices plus a climate that lacks extremes have had an impact on this situation. The need for major design changes for commercial buildings has not arisen. Increasing temperatures in the higher latitudes may well produce somewhat similar results. In New Zealand we find the variations in climate between the north and south (Auckland latitude 37°S, D.D. 1150 and Christchurch, latitude 43°S, D.D. 2420 18.0°C base) produce quite significant variations in energy usages for office buildings (2):

Auckland	850	MJ/m <sup>2</sup> /annum
Christchurch	370	MJ/m <sup>2</sup> /annum

This suggests that warmer temperatures produce higher energy usage for office buildings where the cooling load dominates and yet less in buildings where the heating was dominant e.g. hotels (3):

Auckland	550	MJ/m <sup>2</sup> /annum
Christchurch	930	MJ/m <sup>2</sup> /annum

Global warming will see these temperate climate characteristics repeated in climates that are significantly colder at present and employ a range of energy saving techniques (double glazing, atria etc) which will no longer be applicable.

The need to design buildings to conserve energy is certainly not seen as a necessary factor in New Zealand at present.

To continue to argue to design professionals and the developers of commercial buildings that an 'Energy Efficient' option is desirable is less than justifiable. The economic basis is just not sustainable at the present time as possible savings from energy efficiency contribute such a minor part to the total running costs of a typical tenant company and is a relatively small factor in the costs of the building owner.

This need for a better argument for justification developed into a study of 22 Auckland office buildings during 1988 and 1989. The preliminary results suggest that savings in labour costs attributable to a more efficient environment (environmentally connected natural environment) are of critical importance and do in fact suggest a building form quite different from the norm.

#### Tenant Comparative Costs

In terms of the dollar outlay over the 40 year life cycle of an office building it is generally recognised (4,5) that 2-3% is spent on the initial costs of the building and equipment, 6-8% on maintenance and replacement and 90-92% is generally spent on personnel salaries and direct benefits. These figures are quoted universally, they have been tested in the current Auckland study (6) with some results at variance to a slight degree (Table 1).

- a) The 40 year life cycle used in the quoted studies is irrelevant in the current scene with a 10-15 year economic life being often used - with the result being an even greater emphasis on the reduction of capital costs and annual costs (energy costs) being even less critical.

- b) The figure for personnel salaries seems to fit better in the 80-87% range than the higher percentages quoted in American studies particularly.
- c) Because of the vast range of leasing agreements the maintenance and replacement component along with running costs (including energy costs) is difficult to define precisely but fits within the 5-8% range.
- d) Energy costs typically make up between 0.3% and 2.2% of annual costs of running an Auckland CBD office.

Component	%	Notes
Personnel Costs (Salaries and direct benefits)	80-87	Depending on the nature of the business, size and status/efficiency.
Leasing costs (or Capital replacement in case	1.5-8	The variability of procedures is immense of owner occupied space) which with factors such as quality, position, age, size etc produces an imprecise pattern.
Air conditioning/heating maintenance	0.5-5	This figure varies widely because of the non-existence, nature and age of plant.
Lifts	3-4	
Cleaning	2-5	
Building maintenance	0.5-2.5	The variability of leasing agreements is a factor with the inclusion of external maintenance costs as a tenant responsibility being a growing trend.
Energy	0.3-2.2	Generally this is an electricity cost although 2 cases involved an LPG input.
Other	1.5-8.5	This figure includes aspects of fire, office equipment, communication, rates and insurances. It was difficult to compare like with like.

Table 1 Auckland CBD Office Annual Costs (Tenants)

#### Owner Comparative Costs

To obtain a full picture of a commercial building's energy use one must also investigate the position of the building owner as often, depending upon the lease arrangements, there may be costs associated with common areas etc.

A recent study in Auckland of 20 buildings (7) totalling 206,364 m<sup>2</sup>, for the 1987-88 year, suggests that the total expenditure for energy usage in common areas, including electricity for air-conditioning, lifts, escalators and common area lighting, amounts to on average just NZ\$10.09/m<sup>2</sup>. The total income for the building averaged NZ\$199.05 i.e., 5.07%.

Therefore, from these figures, it is difficult to expect the owners of the commercial buildings to be particularly interested in energy saving, if, to achieve those savings, significant capital expenditure is involved.

Quite clearly the assumption that energy efficiency is in itself a desirable aim in the design and production of temperate climate commercial buildings is faulty. To go to extreme lengths by introducing changes to the typical building in terms of form, external design treatments, daylighting, natural ventilation etc for energy efficient/cost saving reasons cannot be justified even at no extra capital cost, particularly in a climate as moderate as that of Auckland, New Zealand.

**Productivity and Satisfaction**

Productivity is a broad concept which includes not only employees' work performance but also associated organisational costs such as employee turnover, absenteeism, tardiness, required overtime, vandalism, grievances and mental and physical health. Historically, much of the research (8) (9) on productivity has relied on using measures of employee satisfaction as indicators of productivity.

Herzberg (10) concluded from a study of 1685 workers from a range of job types and levels in particular organisations that there was however a distinct difference between aspects of the work environment that were contributing to satisfaction and those relating to dissatisfaction. Herzberg concluded that the "opposite of job satisfaction is not job dissatisfaction but, rather, no job satisfaction and, similarly, the opposite of job dissatisfaction is not satisfaction, but no job dissatisfaction". Aspects of the work environment contributes similarly to job dissatisfaction. Archea (11) concluded that environmental characteristics that influence this level of work process include both architectural properties and architectural attributes. Architectural properties are aspects such as size of office, number of walls, heating, ventilation, air conditioning, lighting, ergonomics and relationships to support services. Architectural attributes are peoples' attitudes and perceptions related to those properties, for example, assessments of openness, noise, enclosure, lighting and temperature. Hedge (12) points out that from a survey of 896 office staff that even though the ambient environment was supposedly being maintained around an 'optimum' level in physical terms, adverse reactions to this were still quite pronounced (Table 2).

Ambient Conditions	%	Agreement
Temperature	- too hot	48
	- too cold	21
Ventilation	- desire to open window	77
	- too stuffy	61
Lighting	- prefer more daylight	76
	- lighting too bright	33

Table 4 Employee reactions to the ambient environment in offices - Hedge (12).

The preliminary results from the Auckland study (6) involving in excess of 560 office workers suggest a similarly very high level of dissatisfaction with the quality of the office environment with clear contradictions arising on aspects of temperature (too cold, too hot), ventilation (too stuffy, too draughty, don't know) and lighting (too bright, wrong angle, too glarey, too dark). The clear conclusion, because of the high level of dissatisfaction and contradiction, is that office staff desire to be able to control their own environments more than the present air conditioned offices allow. A call for greater connection with the external environment? A call for more environmentally connected or energy efficient building forms?

If a more environmentally connected commercial building can produce a slight improvement in office worker efficiency (say 5%) then in terms of the total economic structure of the firm this 5% saving will have a greater impact than saving 100% of energy costs. Here is the justification for buildings that exhibit all the common features connected with not just comfort but also energy efficiency - form, external design treatments, daylighting, natural ventilation etc.

### Conclusions

In more temperate conditions the future for the energy efficient commercial building is indeed good and quite justifiable in economic terms if the approach incorporates other aspects of efficiency i.e., that related to the inhabitants of the office space. Efficiency arising from the increase in worker output because of a more satisfied feeling concerning the work environment brought about by more control of that environment and less artificial inputs, will far outweigh any possible energy savings in the foreseeable future. Buildings will become more energy efficient as part of the process to achieve this end. These temperate climate lessons may well have an application in higher latitude climates as global warming takes hold.

### References

1. Intergovernment Panel on Climate Change Working Group 1, Scientific Assessment of Climate Change report to IPCC 25 May 1990
2. NZERDC Report 115 Commercial Sector Energy Use, 1985
3. Ibid
4. Wineman J.D., The Importance of Office Design to Organisational Effectiveness and Productivity, Behavioural issues in Office Design, Van Nostrand, Reinhold 1986
5. Brill M, Mansell D. and Quinlan M., The Office Environment as a Tool to Increase Productivity and Quality of Life, Buffalo, New York: Bosti
6. Robertson G., Energy Design, Commercial Buildings, Proceedings Australia N.Z. Solar Energy Society, Buildings Group Conference, Hobart 1989
7. Verwer P., Operating Performance Handbook - Office Buildings Auckland CBD 1987-88, Building Owners and Managers Association of New Zealand, Auckland Branch
8. Lawler E.E. and Porter L.W., The Effect of Performance on Job Satisfaction, Industrial Relations 7,1967
9. Locke, Job Satisfaction and Performance, Organisational Behaviour and Human Performance 5, 1970
10. Herzberg F., One More Time: How do you motivate employees?, Concepts and Controversy in Organisational Behaviour, Good Year Publishing, 1976
11. Archea S., The Place of Architectural Factors in Behavioural Theories of Privacy, Journal of Social Issues 33, 1977
12. Hedge A., The Impact of Design on Employee Reactions to their Offices, Behavioural Issues in Office Design, van Nostrand Reinhold, 1986

ENERGY AUTONOMY FOR RURAL SCHOOLS AND  
HEALTH CLINICS IN THE VENEZUELAN LLANOS

DAVID HOLMES

Department of Engineering, University of Reading  
Whiteknights, P.O. Box 225, Reading RG6 2AY, UK

ABSTRACT

When designing power systems for rural villages, more attention should be paid to the ways in which power is used than to the way it is generated. By reducing power requirements, photovoltaic systems, which have numerous external benefits, can be made more competitive with diesel generators thereby saving money and encouraging greater rural self-sufficiency.

KEY WORDS

Solar power, basic rural services, Venezuela

INTRODUCTION

In identifying the factors which contribute to the ongoing exodus of the population from the rural areas of the developing countries, energy must play a prominent role. On the demand side, high energy consumption in urban areas is undoubtedly a major attraction. On the supply side, because of economies of scale and lower unit distribution costs, investments in urban energy projects are far more cost effective, on a per capita basis, than rural projects.

Consequently, the lifeline from the city providing fuel, basic materials, parts and skilled labor has become increasingly tenuous. Ironically, those villages which were most fortunate, in terms of receiving an initial endowment of modern amenities have found the backward turn of the ratchet the most painful.

Rural Venezuela represents an interesting case in point. Following the oil boom of the early 1970's, nearly every small community of a few hundred inhabitants, even in the



more remote parts of the country, received diesel generators and water pumps. The rural dispersed population also benefited in the form of new schools, dispensaries, and a government sponsored program of free, truck delivery of potable water.

Today, large numbers of the diesel engines are broken-down or operate only sporadically. The rural water delivery system is in constant crisis and rural schools and health clinics suffer chronically from lack of maintenance and essential facilities. Professional absenteeism is widespread and notorious.

#### THE POLITICAL IMPACT OF DIESEL POWER

One of the little recognized aspects of the introduction of diesel power to the rural areas was to undermine the monopoly of power of the traditional rural strongmen, who have dominated rural life in Venezuela throughout much of its history. As the newly created oil wealth began to trickle down to the rural areas it facilitated the formation of a pervasive patronage system, which was used to consolidate the power of the dominate political parties. It helped create a whole generation of new leaders whose local support rested fundamentally on the ability to attract patronage funds. And the maximum symbol of the power of these new leaders was to obtain a pair of diesel motors to generate electricity and pump water for the village or town. However, because of reduced oil earnings and the debt crisis, the government has been unwilling or unable to maintain the rural network of diesel motors, much less to expand it. In all likelihood this is a permanent feature of the new economic and social order.

This financial crisis at the center has accordingly provoked a corresponding crisis in rural leadership. It is no exaggeration to say that the major preoccupation of most rural councils today is to keep the diesels operating. And their increasing failure to deliver is a major factor in the current drive to overthrow or change the old order. This could be a very healthy sign for developing a more representative democracy in rural areas, but the gains are likely to be short-lived unless alternatives are found for maintaining basic public services. Either local governments must receive greater subsidies, both in terms of money and skilled people, or they must somehow generate more resources locally. But it is very doubtful that consumers, who currently pay only a small fraction of the actual operating costs, would be now willing to pay the whole cost. Greater subsidies are unlikely and would only tend to perpetuate the current debilitating state of dependency on the central authority.

## ALTERNATIVE ENERGY FOR RURAL SCHOOLS AND CLINICS

To mitigate the ill effects of this progressive decline in living standards, the logical strategy is to encourage a more efficient use of available power as well as to promote the application of technologies which encourage greater local autonomy.

An example, drawn from the experience of a Venezuelan oil company in trying to improve rural services in its zone of influence is illustrative. In 1979, the Maraven Oil Company, (former Shell de Venezuela), one of the affiliates of Petroleos de Venezuela, was assigned an area of approximately 15,000 square kilometers in the Orinoco Tar Belt for exploration and development. As part of the new government policy, dating from nationalization of oil in 1975, the company assumed an obligation to improve the quality of life of the population in its area of influence.

Most of the rural dispersed population had access to a school or health clinic. But these facilities lacked basic amenities such as light and water, although, in theory, water was available via the rural delivery system. Water was usually stored on site in old oil drums fitted with a makeshift lid and water quality was, accordingly, a serious problem. Also, for lack of water, it was impossible to use the flush toilets that had been initially installed. In some cases, conventional latrines, with all of their incumbent problems of flies and odors, were substituted. Not surprisingly, intestinal infections were widespread. A study of 2000 campesino and indian children, in the area, (Sampson, 1990), revealed that 85% were infected.

Under these conditions, it was difficult to persuade teachers and nurses to live in the area, although the lack of amenities was by no means the whole problem. Consequently, professional absenteeism was rampant.

## DESIGN OF THE BASIC SERVICES PACKAGE

While the natural resources endowment of the area is generally poor, solar energy abounds. As a rough measure, average irradiance over a horizontal surface, measured over a period of 15 years was equal to 218 W/m<sup>2</sup> (Venezuelan Air Force Data, 1955-1970). Furthermore, while ground water is scarce, rainfall is relatively generous, averaging about 1200-1500 mm per annum. However, the great bulk of the rain falls during a six month rainy season, followed by six months of almost complete drought. Unfortunately for the schools, the summer vacation break coincides with the rainy season so that during most of the school year, from October to May, drought prevails.

The storage problem was solved using a twenty thousand liter, galvanized metal tank which was designed to supply drinking and washing water to a school of 40 children during the whole school year. Prolonged storage potentially creates a problem of maintaining potability. This problem was solved by inventing a simple, first-flush system (see Fig. 2) which keeps organic matter and sunlight out of the tank, and by limiting user access. In the absence of light and organic matter the tank tends to be auto-purifying. If a pathogen enters, it soon dies for lack of nutrients. Settling provides an additional salutary effect. As an added assurance of quality, teachers and nurses were taught to chlorinate the daily water supply and to monitor the level of residual chlorine with a simple tester.

Photovoltaic panels were then installed to power a small, submersible pump. To save electrical energy, an overhead tank was also installed which avoided switching the pump on and off frequently. Instead, the pump could be operated for a period of around 15 minutes, at hours of peak insolation, to provide a two days supply, which then was available to the user by gravity feed.

To complete the package, (see Fig. 1), a simple roof ventilation system was added to promote air circulation in the classroom and, outside, ventilated, pit latrines (VIP), were constructed. These devices offer sanitary disposal of excrement without the need for water and they eliminate flies and odors associated with the conventional latrines.

## EVALUATION

Since 1985, over 25 units have been installed throughout the area with a high degree of user satisfaction. Maintenance problems have been minor, mostly involving peripheral electrical equipment such as voltage regulators and switches. For this effort, Maraven was awarded the National Prize for Technology Development, 1987, by the Venezuelan National Science Council (CONICIT).

Clearly the solar energy system offers many advantages over a diesel installation. It is quiet, non-polluting, requires no operator, and needs very little maintenance. It also does not depend on external supplies of fuel. On the issue of relative costs, the scale of operation is often decisive. Yet, power requirements, and therefore the selection of technology, are very much dependent on the way in which power is used. In the rush to improve efficiency, and thereby lower cost, manufacturers of photovoltaic panels and project designers often overlook the rather more substantial savings available from optimizing other components of the overall system. In the present example, the selection of a rainwater system, rather than a bore hole to

provide water reduced annual energy requirements from around 78 kWh to 45 kWh, a savings of 42% (Holmes, 1988). This reduction in the power requirement not only saved money but it greatly favored the photovoltaic system since, as is well known, the diesel typically exhibits high unit costs at small power outputs. In fact, a comparison of lifetime, unit costs for this particular system (Holmes, 1988) showed solar to be more than 80% cheaper than diesel. A more telling comparison is found in confronting the unit costs of two complete, service packages, one using rainwater, solar panels, VIP latrines, and convective cooling, and the other, conventional package, using a bore hole, diesel generator, flush toilets, and electric fans. In this case, the unit costs of power generation for the conventional system were more than 60 times higher than those for the alternative system. It could be argued that this is a comparison of 'apples and oranges', yet these are two, competing technology packages which perform essentially the same function.

The economic comparison with the tank truck delivery service, is not quite as clear-cut. Assuming an average lifetime of the rainwater system of 25 years, the unit cost of rainwater is slightly less than that of tank delivery, using existing private rates as the measure of the market cost of providing the service. However, once the rainwater system is installed unit costs depend only on the lifetime of the system unlike truck-delivery costs which are subject to rapid, and unpredictable rises to reflect adjustments in fuel costs (currently highly subsidized) and imported machinery. Furthermore, the reliability of the rainwater system tends to be much greater.

#### CONCLUSIONS

In analyzing rural power problems, it is extremely important to seek ways to improve the efficiency of power consumption as well as to increase power supplies. Experience has shown that adequate water, sanitation and lighting facilities for rural schools and health clinics can be provided more cheaply using alternative technology rather than conventional approaches and that this can indirectly further the goal of greater rural self-sufficiency. This is an especially attractive solution in the context of the current financial and political crisis in Venezuela. But, independently of this crisis, it represents lesson for those who wish to preserve rural life as a viable alternative for the future.

## REFERENCES

- Holmes, D.N. and Vollmann, J.U. (1986). Independencia energetica para escuelas y medicaturas rurales. Memoria Tecnica, Tomo II, 5° Congreso Latinoamericano de Energia Solar, Valparaiso.
- Holmes, D.N. (1988). Energia para escuelas y medicaturas rurales, solar vis. diesel. Memoria, IV Congreso Panamericano de Energia para las Areas Rurales y Aisladas, Habana.
- Holmes, D.N. (1988). Rainwater harvesting for potable water in the eastern llanos of Venezuela. VI International Water Resources Association World Congress, Ottawa.
- Mayer, E.R., Grillet, N., (1983). A solar village in the Amazonas Territory, International Journal of Ambient Energy, 4, 1.
- Morgan, P.R., Mara, D.D., (1982). Ventilated improved pit latrines: recent developments in Zimbabwe. World Bank, Working Paper No. 2.
- Sampson, L.W., (1989). Estudio de las parasitosis intestinales en la zona Zuata de Maraven, Sur del Estado Anzoategui, Venezuela, Caracas,
- Sandia Report. (1987). Water pumping: the solar alternative. Photovoltaic Design Center, Albuquerque.

- 1 GALVANIZED METAL TANK
- 2 PLASTIC BI-GE PUMP
- 3 ELEVATED TANK
- 4 RAIN GUTTER
- 5 FIRST FLUSH SYSTEM
- 6 SOLAR PANEL
- 7 VIP LATRINE
- 8 LATRINE CHIMNEY
- 9 CLEAN-OUT TANK

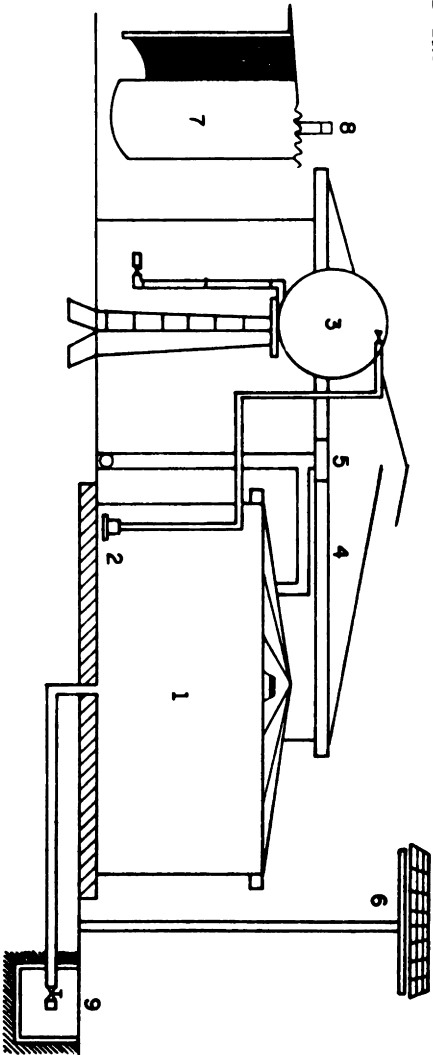


Fig. 1. Basic services package including water, sanitary facilities, electricity, and roof ventilation.



Fig. 2 Details of the first-flush system for keeping debris from the roof out of the tank.

THE SIGNIFICANCE OF THERMAL THRESHOLDS IN THE PERFORMANCE  
OF SOME TRADITIONAL TECHNOLOGIES: THE ICE-HOUSES OF  
BRITAIN AND THE WINDCATCHERS OF THE MIDDLE EAST

DR. S.C. ROAF

Department of Architecture, Oxford Polytechnic,  
Oxford, OX3 0BP

ABSTRACT

Increases in global temperatures this century have caused at least one temperature dependent traditional technology, the ice-house, to cross the thermal threshold dictating its viability in Britain. Study of the windcatchers of the Middle East shows that further increases in regional temperature may render not only types of windcatcher non-viable in some areas, but also traditional dwellings as shelter in some areas. This in turn suggests that limits of settlement in the Middle East would be affected. Such problems and changes should be anticipated and passive solutions sought now.

KEYWORDS

Ice-house; windcatcher; thermal; threshold; climate; desert; technology; global warming; temperature-dependent.

Temperature-dependent Technologies

With a wind or water driven technology one can gauge how efficient it is by easily visible or tangible means: one can count how often a wind-sail, a water-wheel or a grind stone turns, or how much grain is ground or water pumped. However, there are a range of technologies in which their effectiveness rests on the establishment and maintenance of temperature ranges within a building. No one has attempted to quantify the operational temperature limits of such buildings and I believe this is because temperature is invisible and intangible, and is therefore ignored, particularly where the temperature ranges involved are subtle. The need to understand the significance of temperature in buildings is becoming daily more important as is our need to move towards a reliance on passive design solutions to solve problems of heating and cooling buildings. The buildings described below also point to this need for Global as well as regional reasons.



### The Ice-Houses of Britain - a Technology Made Non-Viable by Global Warming

Between 1975 and 1978 I studied the remarkable buildings of the Central Iranian Desert. Among them I recorded the ice-houses of the area. On returning to England I began with a colleague, S.P. Beamon, "The Ice-House Hunt of Britain" in which we tracked down and recorded over three and a half thousand extant ice-houses in Britain. The results of the Hunt along with a history of British and World ice-houses has recently been published (Beamon and Roaf, 1990). Ice-houses were built in every continent of the world to house the natural ice, harvested in winter and then stored until it was required in the hot salad days of summer.

Ice-houses have been built and used since at least the time of the first written records, as cuneiform tablets from Mesopotamia show, even during the hot centuries of the Roman period. However, the ice-house has now ceased to be a viable technology in Britain this century due to a 1°C increase in temperature which has meant that there have been insufficient cold winters to provide a reliable stock of ice for the ice-houses. Thus the ice-house, regardless of the fact that it has also become obsolete for social and technical reasons, is no longer a viable technology in Britain where winter temperatures, although having become only slightly warmer, have crossed the temperature thresholds that divides the building from being a reliable, to a non-viable, technology.

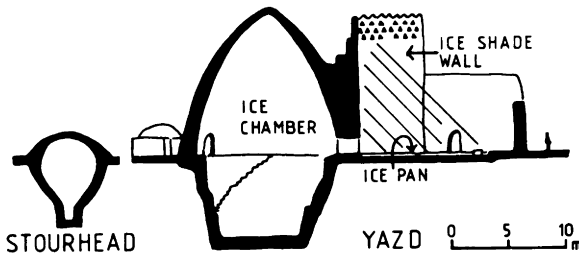


Fig. 2 Comparison between the dimensions of Stourhead ice-house Wiltshire, with a diameter of 5 m (c. 16 ft) and those of the ice-house of Yazd in central Persia (Iran), which has a diameter of 12 m (c. 30 ft).

### The Windcatchers of the Middle East - a Technology Threatened

Windcatchers are also an ancient technology (Roaf, 1991) which are extremely subtle in the way that they can be adapted to local conditions and climates.

Windcatchers operate by drawing moving air from above the building down through its summer rooms in order to cool and/or ventilate them, or their occupants.

In the very hot dry regions of the Middle East, such as Baghdad, the small windcatcher vents on the roof only channel air to the cool deep basements to ventilate them during their afternoon occupation by the extended family in summer. The windcatcher typically only reduces the air temperature from

the roof to the ground floor by 2°-3°C. In Baghdad air introduced into the ground floor summer rooms during the day would be at temperatures of 43°-48°C which is too warm for comfort, even in Baghdad (Roaf, 1991).

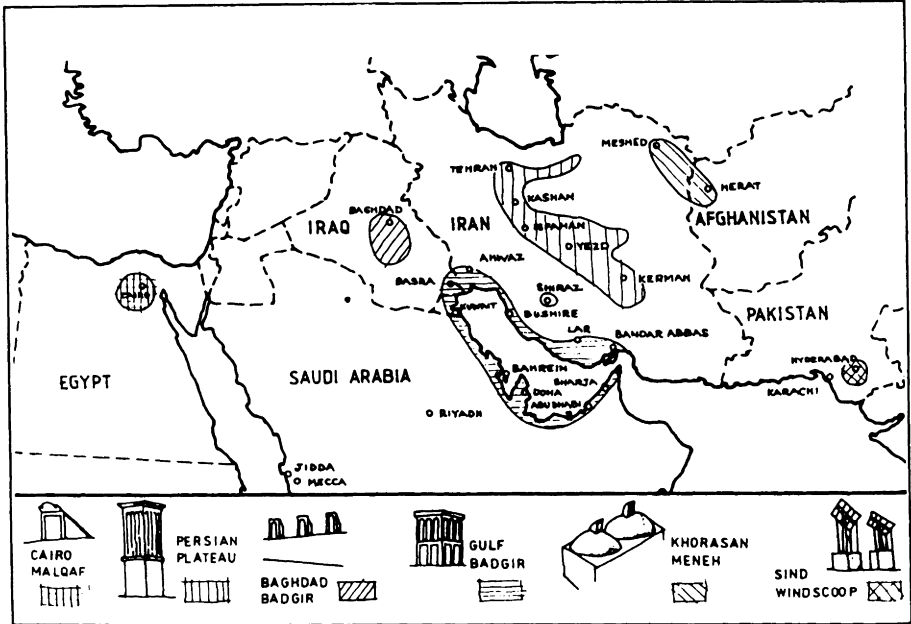


Fig. 2. Map of the windcatcher types of the Middle East.

In the very hot humid Gulf region the windcatchers supply air to the ground floor rooms despite the high temperatures of the area because in this humid climate, when the air temperature exceeds body temperature (37°C) for long periods, the only way the body can lose heat is by evaporative cooling from the skin. In saturated air the only way to increase the rate of heat loss is by increasing the speed of air passing over the skin which a large windcatcher can do effectively.

The most numerous and diverse examples of windcatchers are found in the Central Iranian Desert region, particularly around Yazd, where many settlements, large and small, are topped by seas of windcatchers. The windcatchers recorded in Yazd show how perfectly the climate of the area suits the use of the windcatcher in relation to the local building types and the physiological responses of the body to high temperatures in summer.

In the city of Yazd the windcatchers warm and ventilate the deep basements where people spend the afternoon. The windcatchers also cool the walls of the ground floor rooms during the night and the occupants of the ground floor rooms are cooled by increased convection and evaporation during the mornings and evenings when they sit beneath the windcatchers. But the windcatcher also heats the walls of the ground floor rooms, usually during the late afternoon when the external temperature exceeds the internal

temperature by 2°-3°C - an average figure by which the air temperature is reduced in its path down the tower. As afternoon temperatures in Yazd typically reach around 42°-43°C this usually results in internal temperatures rising to around 39°C in the ground floor rooms below the windcatcher. These figures are perfectly acceptable, and particularly to the Yazdi who retreats to his basement in the afternoon which will be 10°C cooler at around 29°C.

However, in the villages that are on the exposed fringes of the Central Desert, and neither protected by oases or gardens, the indoor afternoon summer temperatures probably rise up to 2°C higher than this resulting in indoor temperatures of up to 41°C in mid-afternoon. These temperatures are on the upper limits of what is physiologically or psychologically acceptable even to this desert population, and are experienced in exposed villages with crude houses, windcatchers and no basements.

I believe that here is another thermal threshold that is being approached and that in the event of a slight increase in global temperatures of 1°-2°C the windcatchers in the exposed desert settlements of Central Iran would cease to be viable to use, but also in turn, would the traditional village houses cease to provide adequate shelter from summer heat.

In terms of the traditional passive solutions to shelter in the Middle East the area would change from requiring the design defenses not of a hot dry climate, to those of a very hot dry climate, notably deep basements and windcatchers serving only the deep basements. In terms of innovative passive solutions solar technology obviously has much to offer. However, the invisibility of the inherent temperature thresholds involved has masked the extent of the possible impact of global temperature increases on the dwelling types and extent of settlement in the Middle East. Or perhaps we are still suffering under the illusion that there are mechanical solutions to these problems.

I suggest that over the next two decades we will see the internal climate of the traditional houses in the Middle East begin to cross such temperature thresholds and we will see whole areas become uninhabited. I would point to what I consider to be immediately vulnerable dwelling types such as the reed houses of the Marsh Arabs of Southern Iraq, the summer houses of the transhumant populations of the Gulf and the single storey dwellings of the exposed villages of the Central Iranian Desert. A rule of thumb may be that areas may be vulnerable if their average July maximum temperatures exceed 43°-45°C.

It would be possible at this stage to introduce a sensible policy for the phased introduction of passive technologies to alleviate increasing problems of summer cooling in the hottest areas of the Middle East; Government sponsored passive technologies such as solar cooling and the incorporation of full and half basements into houses for afternoon use. These technologies could perpetuate the habitability of such regions without the crippling input of energy required for mechanical cooling alternatives.

If nothing else we should at least anticipate the obsolescence of building types in very hot regions and record the fascinating range of dwellings, some of which, such as the reed houses of Southern Iraq, have been occupied for over 5,000 years, before they cease to exist all together.

#### REFERENCES

- Beamon, S.P. and S. Roaf (1990). The Ice-Houses of Britain, Routledge, London.
- Roaf, S. (1991). The Windcatchers of Yazd, MENAS Press, Wisbech, Cambs - in press.

# THE OPTIMUM SELECTION OF THE WINDOW SHADING LEVELS AND OF THE INDOOR VENTILATION RATES AS A DESIGN STRATEGY FOR BIOCLIMATIC COMMERCIAL BUILDINGS.

S. Bertolino<sup>+</sup>, G. Cannistraro<sup>#</sup>, G. Franzitta<sup>#</sup>, G. Rizzo<sup>\*</sup>

<sup>#</sup> Department DEAF  
University of Palermo  
90128 Palermo, Italy

<sup>+</sup> Presently with: IEREN/CNR  
Via Cardinale M. Rampolla  
90142 Palermo, Italy

<sup>\*</sup> University of Reggio Calabria  
c/o DEAF  
Viale delle Scienze  
90128 Palermo, Italy

## ABSTRACT

Ventilation rates, shading level of windows and indoor air temperature are analyzed together in order to single out the optimum mix referred to the thermal comfort situations of thermally moderate commercial buildings. Thermal comfort is here taken into account by means of the Predicted Mean Vote (Fanger, 1970).

A short selection of graphs is proposed, able to provide the simultaneous view of the effects produced, on the PMV, by modifications of the above cited parameters. Graphs can be usefully adopted for the proper design of the glazed surfaces, especially for passive solar buildings.

## KEYWORDS

Predicted Mean Vote, thermal comfort, ventilation rates, shading devices.

## INTRODUCTION

Through the past years, even in commercial buildings, the concepts and the design strategies of the bioclimatic architecture have been largely employed, in order to achieve both relevant energy savings and better levels of the indoor quality.

As it is well known, many parameters meet together to the definition of the thermal quality of the confined environments.

Among them, the amount of solar radiation entering the room through the transparent elements of the envelope and reaching people, is a relevant aspect to take into account. This is particularly important for commercial buildings, where people is assumed to maintain for a long lapse of time the same position and posture.

Another noticeable component of the human thermal sensation is the level of the air flow experienced by people inside the buildings, due both to mechanical or natural

ventilation. Of course, for safety and practical reasons, in service buildings the ventilation is essentially obtained by means of mechanical systems.

For the ventilation rates inside buildings, many rules and technical suggestions are available to designers.

Otherwise, new findings about innovative transparent materials, like glasses with high thermal resistance and materials having changing optical properties, show interesting perspectives on the possibility of suitably operating the thermal performances of the envelope.

## AN OPTIMUM COMFORT MIX

Starting from the above considerations, some graphs are here proposed able to reach the optimization of the shading level of the window and the required ventilation rates for a commercial building, located in a given climate.

The basis parameter for the definition of the optimum mix of shading coefficient and ventilation rate, is here assumed to be the thermal comfort conditions inside the examined room. That is, assuming the target of having a Predicted Mean Vote equal to zero ( $PMV=0$ ), we compute the effects of the presence of the high intensity source of the sun on the thermal balance of the human body (that, notoriously modifies the value of the mean radiant temperature of the room).

Moreover, internal ventilation rates are chosen in order to assure thermal comfort conditions to the occupants, following ASHRAE suggestions and ISO standards.

Effects of different combinations of subjective (clothing and activity levels) and climatic situations (air and mean radiant temperature, relative humidity and relative air velocity) are investigated through the paper.

A comprehensive set of graphs will be presented, where the optimum shading level of the window apertures,  $O_{opt}$ , for each situation is given as a function of the (solar) radiant load (RL) on the human body, for various indoor air temperatures and relative air velocity.

## THE RADIANT LOAD

Following the theory and the symbology adopted by P.O. Fanger (Fanger, 1970), the effect of an high intensity source on the human body radiant load can be expressed in terms of a modification of the mean radiant temperature of the given environment:

$$T_{mrt}^4 = T_{umrt}^4 + T_{imrt}^4 \quad (1)$$

where  $T_{mrt}$  is the modified mean radiant temperature,  $T_{umrt}$  is the mean radiant temperature of the so called "unirradiated" environment, and  $T_{imrt}$  is the mean radiant temperature induced by the presence of the high intensity sources, and the sun among them.

In fact, the irradiated mean radiant temperature assumes the well known expression:

$$T_{imrt}^4 = (A_p \cdot \alpha_{ir} \cdot q_{ir}) / (A_{eff} \cdot \sigma \cdot \epsilon_p) \quad (2)$$

where  $A_p$  represents the projected area factor ( $m^2$ ),  $\alpha_{ir}$  is the mean absorptance of the

clothed human body,  $q_{ir}$  is the mean density of the radiant flux ( $W/m^2$ ),  $A_{eff}$  is the effective radiation area of the clothed body ( $m^2$ ),  $\sigma$  is the Stefan-Boltzmann constant ( $W/m^2K^4$ ), and  $\epsilon_p$  is the emittance of the outer surfaces of the clothed body.

By introducing the term "radiant load", RL (W), as:

$$RL = A_p \cdot \alpha_{ir} \cdot q_{ir} \quad (3)$$

we can write:

$$T_{imrt}^4 = RL / (A_{eff} \cdot \sigma \cdot \epsilon_p) \quad (4)$$

Suitable values of the terms above introduced can be usefully found in the scientific literature. We will not report some of them in a next section of the paper.

We would only remember here that the dependence of the radiant load, RL, by the direction of the spot generating the radiant beam is here given by the term  $A_p$ . In the case of presence of the solar radiation on the human body it takes into account the geometric relative position between sun and human body: as a matter of fact, the projected area depends on azimuth angle and altitude of the sun with respect to the human body.

## WINDOW OPENING LEVEL

By means of the application of the Fanger methodology in the case of presence of high intensity sources, we have generated some graphs that, as a function of the radiant load, RL, provide the optimal opening level of the window rolling shutters for a room characterized by assigned values of air velocity and operative temperature.

The optimal opening rate is here simply intended as the ratio between the optimal glazed surface of the window,  $S_{opt}$ , and the starting value of the glazed surface,  $S_{in}$  (Cannistraro et al., 1990):

$$O_{opt} = S_{opt} / S_{in} \quad (5)$$

Figure 1 shows an example of the proposed graphs. For a metabolic rate of  $58 W/m^2$ , for a clothing ensemble corresponding to a thermal resistance of 1 clo and for a relative humidity of 50%, the optimum value of the opening rate is depicted, for different values of air velocity,  $v$  (m/s), and operative temperature,  $t_{op}$ . Each point of the curves is representative of a "PMV=0" condition and, generally, relates to different combinations of architectural and HVAC solutions.

Points 1, 2 and 3 in the figure are characterized by the parameters described in table 1. As it's easy to note, point 1 indicates that only with the 38% of the glazed initial surface it is possible to reach the thermal comfort situations, when the room is characterized by an operative temperature of  $20^\circ C$  (with relative humidity of 50%) and air velocity of  $0.0 m/s$ . In other words, the combination "RL=60 W,  $t_{op}=20^\circ C$ ,  $v=0.0 m/s$ " is not able to provide the thermal neutral sensation to occupants: in order to reach this goal, one of the solution is the suitable shading of the glazed surface, if air velocity and operative temperature are kept at the initial values.

Starting from this point, by mean of a modification of the air velocity (at a value of  $0.15 m/s$ ), and maintaining at the same value the operative temperature, the thermal comfort

situation can be now obtained with an opening rate of 47%, that means an increase of the 23.6% from the previous value.

Figures 2 and 3 give an example of the graphs that can be produced following the above mentioned methodology. Figures refer to subjective and climatic conditions that are typical respectively of summer and winter situations (ISO, 1984 and ASHRAE, 1981). In figure 2, in fact, air velocity ranges from 0.0 to 0.8 m/s, while operative temperature ranges from 22.8 to 24.5 °C; the metabolic rate refers to sedentary light activity for people dressed with cloths having a thermal resistance of 0.5 clo.

In figure 3 wind velocity spreads from 0.0 to 0.15 m/s, with operative temperature going from 20 to 21.5 °C; the metabolic rate is kept at 1.2 Met and the clothing ensemble refers to a thermal resistance of 1 clo.

**Table I - Values of the parameters referring to points 1, 2 and 3 in figure 1.**

Point no.	RL (W)	$t_{op}$ (°C)	v (m/s)	$O_{opt}$
1	60	20	0.00	0.38
2	60	20	0.15	0.47
3	60	22	0.00	0.13

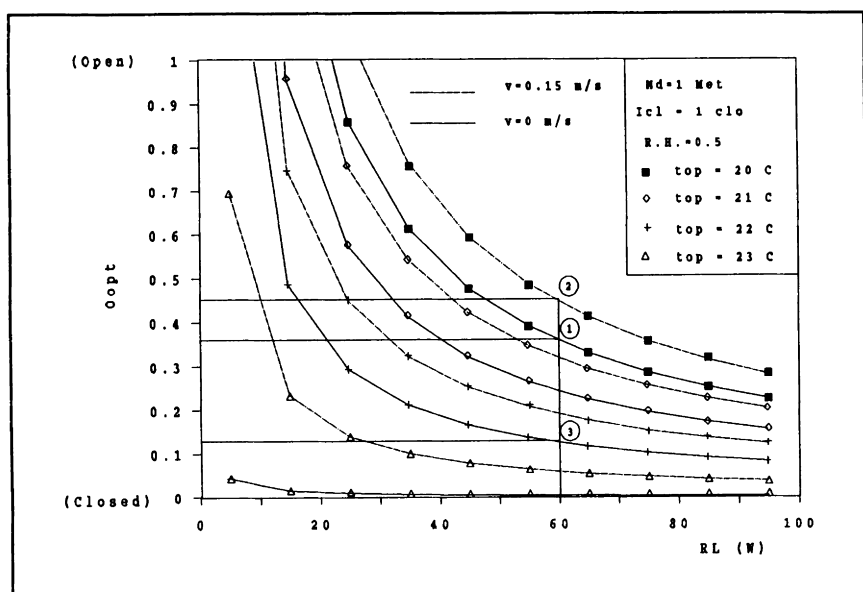


**Figure 1- Opening rate of the window glazed surface as a function of the radiant load, for various values of operative temperature and air velocity (see also table 1).**

The way to enter graphs is the computation of the radiant load, RL. This can be easily made when the value of the density of the flux,  $q_{ir}$ , is known. Moreover, it's important to recognize the azimuth angle and the altitude of the direction from where radiation comes: this allows to properly calculate the projected area  $A_p$  (Fanger, 1970).

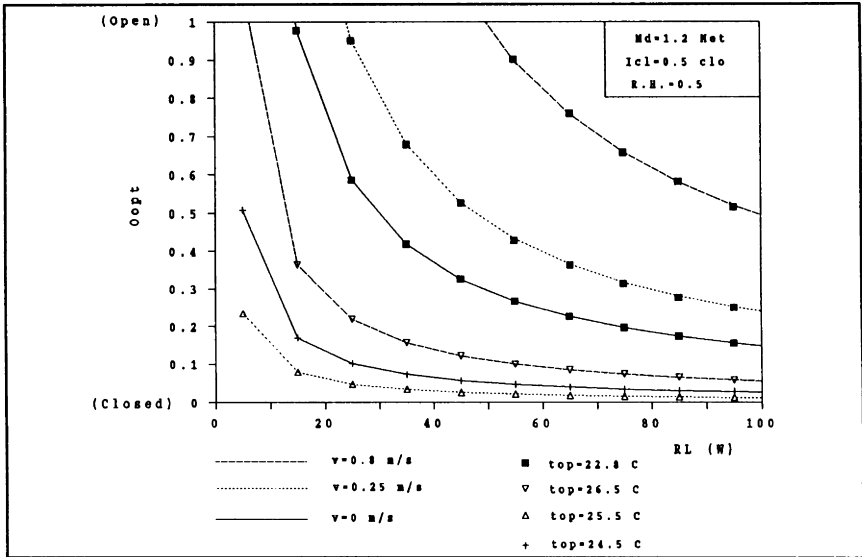


Figure 2- Opening rate of the window glazed surface as a function of the radiant load, for typical summer conditions.

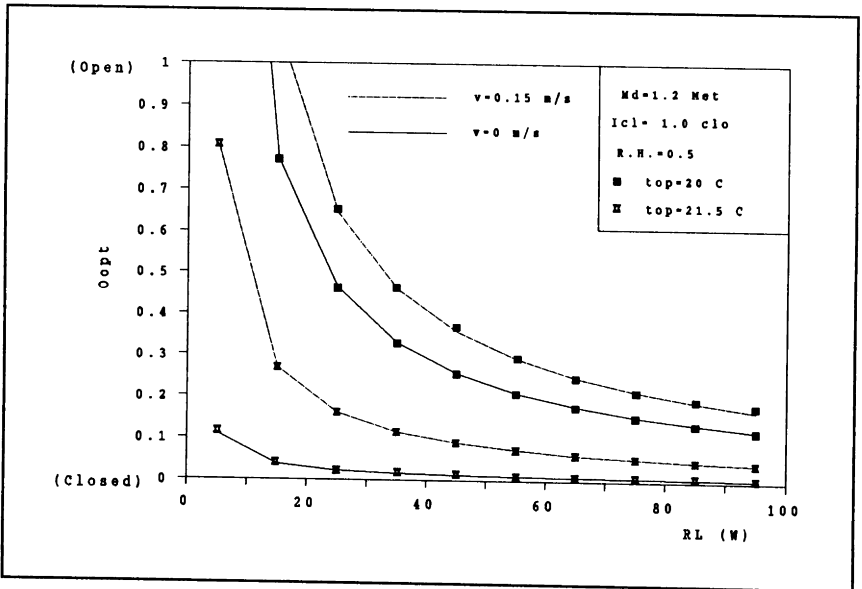


Figure 3- Opening rate of the window glazed surface as a function of the radiant load, for typical winter conditions.



In fact the area factors,  $A_p$ , can be computed by means of the projected area factors,  $f_p$ , with the following relation:

$$A_p = f_p \cdot A_{eff} \quad (6)$$

The parameters to be employed in equations (3), (4) and (6) are reported in tables 2 and 3.

$\alpha_{ir}^*$ (nude body) = 0.95 $\alpha_{ir}$ (clothed body) = 0.95 $\epsilon_p$ (clothed body) = 0.95 $\epsilon_p$ (nude body) = 1.00 $\epsilon_p$ (mean value) = 0.97 $A_{eff}$ (seated persons) = 0.696 $A_{eff}$ (standing persons) = 0.725  <small>* Referred to radiation from IR-sources having colour temperatures of 2500 °K.</small>	Altitude			
	Azimuth	30	45	60
	0	0.303	0.302	0.262
	30	0.297	0.288	0.262
	60	0.280	0.275	0.241
	90	0.243	0.248	0.220

Table 2 - Selected values to be employed in equations (3) and (4)

Table 3 - Projected area factors of seated persons.

## CONCLUSIONS

The aim of the paper is to present a simple method able to provide the optimum combination of shading levels of the window, air ventilation rates and operative temperature, in order to obtain the thermal comfort conditions inside a given commercial building. Since in commercial buildings people is supposed to maintain for a long lapse of time the same position and posture, through the paper we have calculated the PMV only for seated persons.

The effect of the high intensity sources are also taken into account, with special regard to the direct solar radiation entering the room.

## REFERENCES

- Fanger, P.O. (1970). Thermal Comfort Analysis and Applications in Environmental Engineering. Danish Technical Press, Copenhagen.
- Cannistraro, G., Franzitta, G. and G. Rizzo (1990). Correctly Operating the Glazed Surfaces of Buildings for Achieving a Proper Energy Management. Presente at: International Symposium on Property Maintenance Management and Modernisation. CIB W70. Singapore.
- ISO (1984). ISO Standard 7730. Moderate Thermal Environments: Determination of the PMV and PPD Indices and Specification of the Conditions of Thermal Comfort. International Standard Organization. Geneva.
- ASHRAE (1981). ANSI/ASHRAE Standard 55-81. Thermal Environmental Conditions for Human Occupancy. American Society of Heating, Refrigerating and Air Conditioning Engineers Inc. Atlanta.

THE ZERO-ENERGY-HOUSE:  
THE RANKING OF THE SUN IN THE HEAT-REQUIREMENT MARKET

Sabine Knöll and Uwe Welteke  
Ökologische Bautechnik Hirschhagen GmbH,  
D-3436 Hess. Lichtenau, FRGermany

ABSTRACT

The heat requirements of the "Zero-Energy-House" (Dörpe, near Hanover, W.Germany) are covered by solar. First and essential was the consequent cut of energy losses, even superior to the efficient building standards of Sweden. To cover the remaining heat requirement, a solar heating storage system was installed. Compared with the average annual standard heat consumption, it is possible to reach an energy savings rate of 90% with additional construction costs of only an 15%.

The concept

The aim of the "Zero-Energy-House" project near Hanover (Germany 52° 20' north, 155 m high) is to demonstrate that it is possible to completely dispense with the use of fossile energy for heat requirement yet meeting with high standards of comfort.

In the late 1970ies, a group of young people got together who were idealistic enough to develop ecological future technologies before "ecology" had been focused at by the public. The whole project set off as a private initiative. One aim was to build the house inexpensively and to keep the construction simple enough for many volunteers to help and work on the site. What was wanted, was to show how simple, practical ideas as to saving resources could be realized and handled in a daily life situation.

The house, its construction, the choice of the building materials, the way one interacts with the house and the waste handling was planned considering holistic ecological criteria.

The house also serves as a demonstration object. Visitors have access and guided information tours are given. A public relation campaign was started as soon as the building had been completed.

A monitoring programme about the properties of the house and records for scientific investigations presently is being conveyed at the house.

### Energy

The main essential is the idea of completely shifting the energy supply towards the use of renewable energy sources: sun and wind.

Electricity. The electricity supply derives from the use of a wind generator, stored by battery and distributed by a low voltage electricity system. Excess energy is to be fed into the public supply network. (Basically due to administrative impediments, the wind generator hasn't been installed yet.) With all these electrical systems, it is meant to apply energy at its best efficiency, e.g. when using low-consumption light-bulbs that combine durability and economic advantages.

Hot water. Hot water is supplied simply by a solarthermic system and a well insulated water tank.

Heating. Most of the energy wasted can be traced back to heating buildings. Even if modern burners produce significantly less toxic gases than traffic, carbondioxides are considered to be one of the most dangerous pollutants. CO<sub>2</sub> is known to contribute the biggest portion to this dramatic, man-made climate change thus any application of fossile, carbondioxide-releasing energy sources should be avoided!

During the planning stages during the early eighties, it was recognized that only through consistently reducing the energy losses a successful utilisation of an active solar system would be enabled.

During the cold periods of a North German wintertime , with only few hours of sunshine, the passive use of solar energy gains only cover a minor share of the total heat requirement.

Due to the cognition that it is not the energy level (temperature) which has to be provided by heating, but to replace the energy escaped, a heating system always actually balances the losses of the thermal system "house".

All additional surface for more solar gain, e.g. windows facing South, would produce more energy losses than they would be able

to bring into the house. All solar systems which have separate systems for gain and supply of solar energy need cost-intensive energy transport, transformation or storage.

As a consequence the whole house was designed to prevent energy from escaping. In order to this, several energy saving systems were integrated into the concept and carried out thoroughly:

Heat transmittance through walls, windows, floors and roofing had to be minimized. The surface/volume ratio has to be small, which is much easier when bigger units are being built (viz. terrace houses).

Design. The architectural design was based on a half-bowl. There is no cellar except for some crawling space and a well insulated beam construction floor. (1)

The south wall of the two-storey house is vertical. Most of the windows allow the low sloped winter sun to far reach into the rooms. The total surface of all southern windows adds up to 9 m<sup>2</sup>. (2)

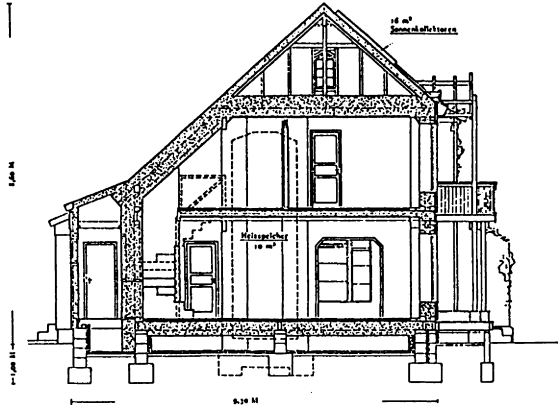
The northern roof was extended downwards and bears a non-heated multifunctional storage space that serves as a thermal buffer. (3)

The attic and the slope roof are both well insulated with another buffer between them. (4)

Building material. Any heat transfer through the surface of the house is by far the most important heat loss factor.

The walls were constructed by the use of two stud systems of 12 cm thickness. The outer surface was stabilized by a wood particle sheathing and protected by wooden weatherstripping and a ventilated air space. The wall cavity was of 12 to 20 cm thick and covered with drywall. Additional airtightening was achieved by using a polyethylene vapour barrier inside and a windtightening paper layer outside. The space between this construction was filled with loose fill cellulose insulation, which again cuts the effects of air leakage. The total insulation thickness ranges from 36 cm (South, floor, ceiling) to 45 cm (East, West) plus buffer and 12 cm insulation (North). The roof is also built with light weight wood construction, but with 55 cm insulation thickness. The k-values vary from 0,083 ... 0,128 W/m<sup>2</sup>K (R = 40 ... 60) (5, 6)  
The exact filling achieved with cellulose insulation sprayed and blown allows a construction with hardly any thermal bridges.

The windows are glazed with  $k = 0,13$  ( $R = 4$ ). During the coldest months, the eastern and western windows may be shut completely and may be temporarily insulated 20 cm thick. The southern windows are to be shielded by an extra well insulated sliding window.



#### Ventilation system

Basically wood frame constructions are insufficient in terms of airtightness because of the numerous joints and cracks. Here emphasis was laid on the multiple tightening of the whole construction. The choice for cellulose fibre improves the airtightness significantly better than mineral fibre. There should not be a single gap or any free air flow in between two wind barriers and it is possible to avoid this with cellulose insulation. Anything that pushes through the envelope was joined together thoroughly to avoid any involuntary air exchange. (7)

This was fundamental in managing the air exchanges needed: In the wintertime, ventilation is done by a heat recovery system. An air to air heat exchanger, equipped with a ventilator provides the rooms with preheated fresh air. The indoor air quality is remarkably good and no noise problems have been reported. With this method 60 ... 70 % of the ventilation losses can be saved.

#### Energy gains

The main energy source for the "Zero-Energy-House" is the sun: remarkable amounts of heating provided through the south windows up to November and from the beginning of February.

As an optimal heat-storage, all inner walls and floors are being made out of solid soil brick layers as thermal mass.

As a matter of fact for the "Zero-Energy-House" in Dörpe this has a considerably smaller effect on the energy balance than previously estimated. ( But this can be expected to be different in sunnier climate zones ,e.g. like in the south of the alps).

A solar greenhouse is also very often claimed to be a vital element of solar architecture. In our case it is more of an additional living space and not actually necessary to the houses energy balance. (8)

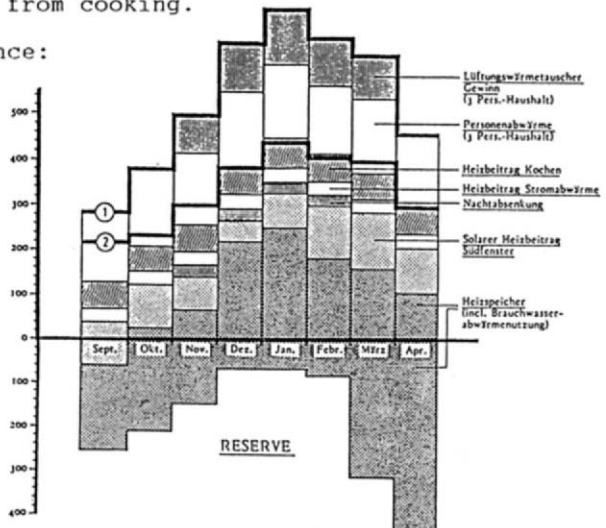
The active heating system is based on 16 m<sup>2</sup> vacuum collectors (9), which heat a tank of 10 m<sup>3</sup> of water (10). This water-storage tank is placed in the middle of the house. It is very well insulated, but there are still losses which in return are gains for the house. The water in the tank again heats up during the autumn and during sunny winter days. Its energy is distributed by a conventional hot water central heating system. The house has a living space of 107 m<sup>2</sup>, of which 97 m<sup>2</sup> are heated.

In January the total losses of the heat transmission with its average temperature of 0° C are as low as 440 kWh, or the equivalent of 37 litres of oil.

The ventilation losses are more or less covered by the energy emission of the users (body heat) of the building.

Solar radiation through the windows and various internal sources like electricity, cooking and savings by reduced night temperature, cover most of the energy losses. It has to be realized, that solar energy gains in January are not adding up to more than the heat from cooking.

The total energy balance:



### Costs:

The total energy supply by the water-storage tank is 2.500 kWh. To make these 2.500 kWh available by the sun, the highest investment cost per unit savings have to be paid compared with all other elements of the house. Nevertheless, during unusually cold winters, a separate heat source (gas heater) may be needed. The storage and heating system is designed for average temperatures of its surrounding.

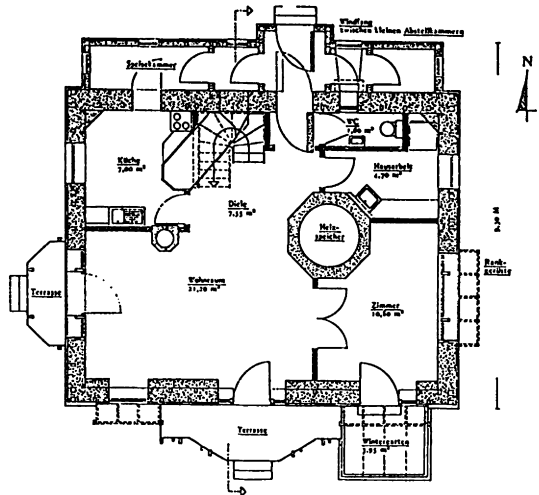
The analysis of cost shows, that in comparison with the average heat requirements of presently conventional housing, about 90 % of energy savings are reached passively, viz. by cuts of requirements: wood frame construction with optimized insulation, heat recovery ventilation system, compact solar oriented house design and temporarily insulated windows.

The construction costs for those 90 % of energy conservation potential are less than the amount required for the remaining 10 %, covered by the solar powered water-storage system.

### Conclusion:

Even in severe climates like in Central Europe, it is possible to cover heat requirements by solar. First and essential is the realization of at least the Swedish building standards. Only consistently reducing the energy losses with the existing technologies would enable a successful utilization of an active solar system.

In more tempered, maritime climates, like in the UK or northern France, the Swedish insulation standards should be sufficient to build "Zero-Energy<sup>4</sup>-Houses.



**TRANSPARENT INSULATION - STUDENT  
RESIDENCES IN GLASGOW**

**Robert Forrest**

**Energy Studies Unit  
University of Strathclyde  
Glasgow  
G1 1XQ  
UK**

**ABSTRACT**

Student residences at the University of Strathclyde have recently been built incorporating the latest development in passive technology - transparent insulation. Solar energy incident upon this face is retained due to a transparent element that has high transmissivity as well as exceptional convection, radiation and conduction suppressing qualities. This transparent insulation material (TIM), composed of a polycarbonate honeycomb, allows maximum utilisation of incident energy for space heating. The development is the largest application of TIM to space heating in buildings.

The overall design of the buildings maximises the use of available free energy and is also vital in ensuring occupant comfort and a pleasant living environment, which ultimately determines the success of the project.

**KEYWORDS**

Passive Solar Energy; Transparent Insulation; TIM; Solar Space Heating; Heat Recovery; Solar Control Shading.

**INTRODUCTION**

The climate of concern over global warming is forcing consideration to reducing greenhouse gas emissions through reduced energy consumption, particularly fossil based. As 40% of total energy demand in high latitude countries is for low temperature heating (space, water and process), energy conservation in buildings has an important role to play.

The use of transparent insulation cladding enables buildings to harness the suns energy at the same time as reducing heat loss. Coupled with proven passive design technology the possibility of substantially reducing or even eliminating the demand for conventional space heating is realised.

Transparent insulation has already been applied to buildings in this role, but to date the developments have been both small in scale and mainly of a research nature (Bollin, 89; Johnson, 89).



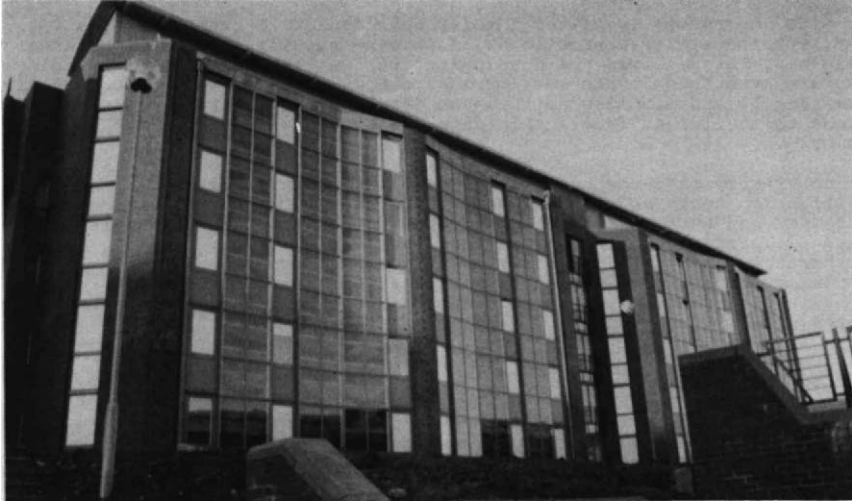


Figure 1: Front View, TIM and high glazing area



Figure 2: Rear view, low glazing area and open aspects

### STUDENT RESIDENCES

The new halls of residence at the University of Strathclyde are an attempt to bring the technology of transparent insulation to commercial fruition. Designed by the Kennedy Partnership and developed by Kaiser Bautechnik, they are the largest example of the application of transparent insulation material (TIM) to space heating in buildings.

The south face of the buildings (Fig 1) consists of a mixture of conventional windows with a TIM facade. The overall impression from the exterior is of a highly glazed building, whilst from the interior the construction appears conventionally solid. The north face, starkly contrasts this, with a greatly reduced glazing area (Fig 2).

The site chosen was ideal for a solar development. A south facing slope that, despite a city centre location, had no shading from trees or other buildings. This allowed the development of two parallel rows of buildings. They are stretched in the east-west direction to maximise the south facing area (Fig 3) and minimise north-south depth to facilitate thermal exchange across the building. They accommodate 376 students in flats of 4 and 8, in 9 blocks.

Two costs come into the question of viability with a new development - construction costs and running costs. The latter takes greater importance with time and here the component devoted to energy conservation is critical, particularly, given current levels of academic funding, for a northern university (Edwards:90). The increased capital cost, of approximately 20%, was offset by an EEC grant under its energy demonstration scheme along with support from the Scottish Development Agency.

### OBJECTIVES

The overall aim of solar architecture must be to design to maintain comfort throughout all seasons, maximising the use of solar energy and minimising the use of conventional energy.

The objectives of this demonstration scheme are to "utilise high technology solar skins... to capture solar radiation and reduce heat loss". Furthermore, the buildings should "demonstrate the importance of solar friendly design at high latitudes".

### TRANSPARENTLY INSULATED FACADE

The 100m<sup>2</sup> of south facing transparently insulated facade is based on technical developments by the Fraunhofer Institut. The TIM in use is 100mm thick polycarbonate honeycomb, in the absorber perpendicular geometry (Fraunhofer, 89). Incident light passes through the high transmissivity honeycomb to heat a darkly painted solid absorber wall (Fig 4). The honeycomb virtually eliminates convective and radiative losses so the retained heat passes through to the interior. The thickness and density of the mass wall dictates the time taken for the heat to reach the interior. In this case a 6 hour delay shifts the peak internal temperatures to match the maximum demand period in the early evening.

Reflective shading devices within the facade, controlled automatically, close at night to further reduce heat losses (Fig 4a). The wall has a U-value of approximately 0.6 reduced to 0.4 when low emissivity shading is closed. Over an entire season, however, the wall appears to have a net negative U-value as the solar gains out-weigh the losses.

The shading serves a further purpose of preventing overheating during periods of high intensity coupled with high ambient temperatures (Fig 4b). Such conditions are most likely to occur during spring and autumn when the sun is low in the sky, vertical insolation reaches a maximum and reflection losses from the cover glass are minimised (see Fig 5). With a high year-round heating load, closely matching the academic year (Fig 5a) the solar fraction of such a wall in Glasgow should be high.

### CONSERVATION AND PASSIVE DESIGN

The use of transparent insulation for space heating is most applicable where a high standard of energy conservation and passive design has already been adopted. The Strathclyde residences utilise a wide number of conservation measures and passive solar features.

Insulation. The buildings are insulated to a level much higher than currently specified in UK building regulations. Outer walls have 150mm of rockwool insulation sandwiched between a dense blockwork inner leaf and a

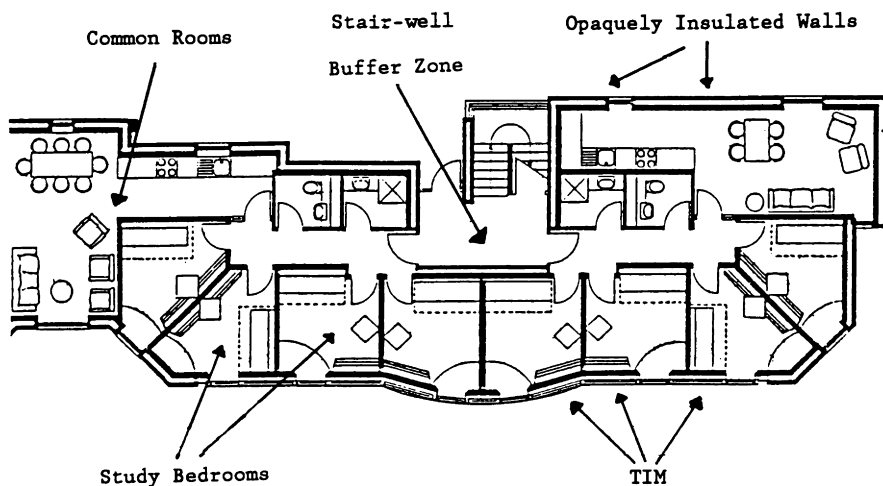


Fig 3: Plan of building, showing location of TIM wall elements

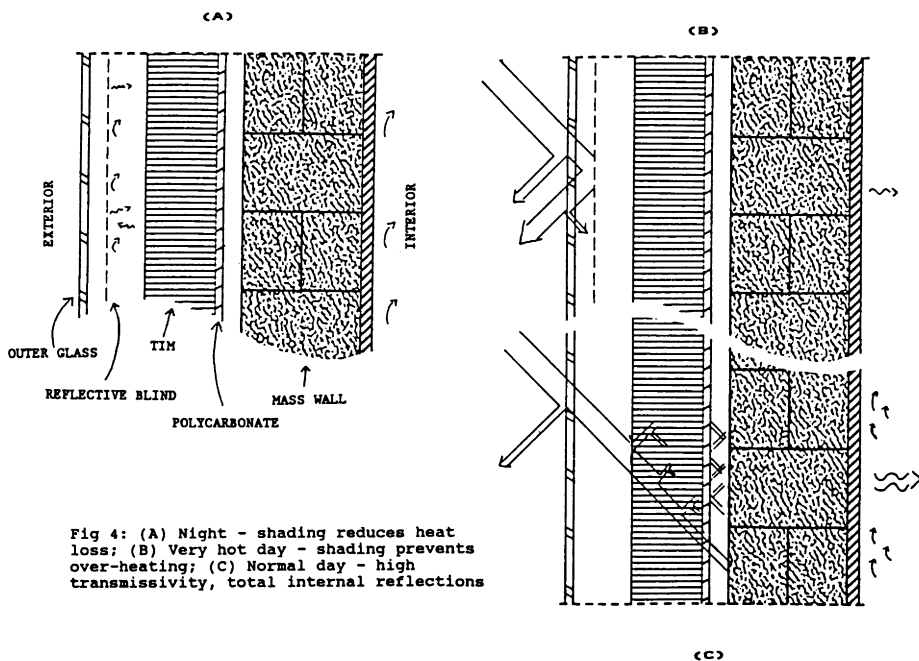


Fig 4: (A) Night - shading reduces heat loss; (B) Very hot day - shading prevents over-heating; (C) Normal day - high transmissivity, total internal reflections

brick outer, giving a U-value of approximately 0.22. The roof and ground floor are also insulated with 100mm glass fibre matting and styrofoam.

**Windows and Blinds.** All north facing windows are small and triple glazed. Some sections accommodate integral venetian blinds between a sealed double unit and a third pane, others are sealed triple units.

Most south facing windows are double glazed with a low emissivity coating on the inner pane, whilst the outer corner bedrooms (see Fig 3) with no TIM benefit from triple glazing. Mounted between the panes are automatic aluminised roller blinds, controlled by a central computer. The blinds are low emissivity coated to reduce radiative losses and when closed they also reduce convective losses by restricting movement within the air gap. The occupants can over-ride the settings for privacy and to control direct solar gains.

**Ventilation and Heat Recovery.** Extensive draught stripping and vapour barriers reduce heat loss through leakage, but result in stuffy rooms and build up of pollutants and condensation. Controlled ventilation is provided in the bedrooms through trickle vents and opening windows.

In the common areas a mechanical ventilation system draws stale air from the shower, toilet and kitchen. Fresh air from the north face is supplied to the common room and hallway and is pre-heated by the exhaust air using a cross-flow heat exchanger. The exchanger has an efficiency approaching 70% and provides a nominal 0.5 air changes per hour, which is boosted by 50% during intensive use, triggered by the shower/toilet and cooker.

**Construction.** In order to retain the heat from casual and free gains, the building has been constructed primarily from high density concrete. This "massive" construction serves to level out temperature swings and so helps maintain a comfortable living environment.

**Lighting.** Compact fluorescent lighting, using 20-25% of the power of incandescent sources are used extensively. In addition to being economical to install, they have the advantage of reducing casual heating not correlated with demand.

**Auxiliary Heating.** Modelling of the buildings' performance (Abacus,88) showed that if severe cold cloudy conditions were to prevail, comfort could be maintained with 200 W auxiliary heating. This is provided by electrical wall mounted radiant heaters. Connected to the central controller, they are automatically switched off to prevent over-heating.

## MONITORING

The buildings are being monitored, over a period of two years, by the Energy Studies Unit at Strathclyde. In addition to determining the overall performance, selected areas are being studied intensively in order to further the understanding of the TIM wall and its interaction with the other design features and to determine occupant reactions.

## CONCLUSION

Transparent insulation offers new possibilities in passive solar design for utilising available energy from the sun, whilst at the same time maintaining high levels of comfort. The residences at Strathclyde see this technology taking a major step towards commercial reality. The lessons learnt from this project will have a major influence upon the future path of TIM.

## REFERENCES

Abacus Simulations Ltd, Report to Kaiser Bautechnik, "Halls of Residence, Phase II", 1988.

Bollin, E., "Newly Built Two Family House with Transparent Insulation in Freiburg", Proc. of the 3rd Workshop on Transparent Insulation Technology for Solar Energy Conversion, 1989.

Edwards, B., "Daylight + Sun = Benign Energy", Interface, Issue 4, University of Strathclyde.

Johnson, K., "A Transparently Insulated Terraced House in the UK", Proc of 3rd Workshop on Transparent Insulation Technology for Solar Energy Conversion, 1989.

"Transparent Insulation Technology for Solar Energy Conversion", Fraunhofer Institut fur Solare Energiesysteme, Freiburg, FRG, 1989.

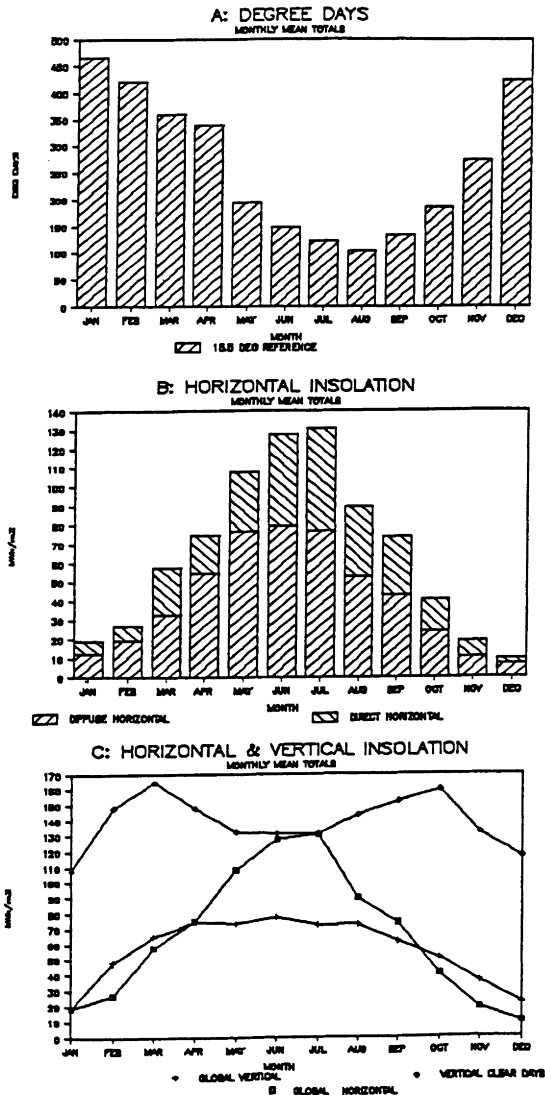


Fig 5: Typical climatic data for the Glasgow area (55.9N, 4.5W) (Source: Met Office, European Solar Atlas)

## PASSIVE SOLAR DESIGN OF A MONTESSORI PRIMARY SCHOOL

R.R. COHEN, P.A. RUYSEVELT AND M. ABU-EBID

Halcrow Gilbert Associates, Burderop Park, Swindon SN4 0QD.

### ABSTRACT

Halcrow Gilbert Associates were requested to provide energy design advice at the post outline planning stage for a new Montessori School in Berkshire, England. The paper describes the design changes which were adopted in order to achieve both important energy savings and a dramatic improvement in the school's internal environment.

The main passive solar features incorporated into the design for the school were a double storey atrium communal area, rooflights to enhance the daylighting of the classrooms and a ridge ventilator driven natural ventilation scheme. The objective was to realise well daylighted classrooms whilst keeping heating costs low and minimising the risks of summertime overheating. Measures to prevent overheating included eave overhangs, blinds under the south-facing roof glazing and nighttime ventilation.

The paper shows how a range of design tools were used to identify the impact of each design change on energy consumptions and environmental conditions. The paper demonstrates the benefits of sophisticated, yet flexible and fast-response, design tools which enable their users to meet the very short deadlines of a real building project.

### KEYWORDS

Passive solar, natural ventilation, daylight, atrium, design tools

### INTRODUCTION

#### Background

Montessori is an educational method founded by an Italian nun about 100 years ago which encourages children to learn by exploration and discovery. The schools have a plethora of equipment and teaching aids, and in this case a farm environment, all so that the children can learn by direct experience. The instigators of this school project felt that the means of providing the children's thermal comfort should also be an integral part of their education. Furthermore, they felt that a climate-responsive energy conscious design would be the most appropriate approach, with the children taking an active role in controlling their environment.

## Integrated Design

The key to climate-responsive energy-conscious design is an integrated approach. The objectives are comfort (thermal, visual, acoustic, air quality etc.) and amenity (function and value); the means are a combination of climate-modifying fabric and energy-driven building services. An integrated design approach should result in a highly satisfactory building environment achieved with the lowest possible energy consumption consistent with a competitive capital cost.

In an ideal situation, the members of a design team would work together from the inception stage to produce a fully integrated design. In this example, HGA did not become involved until after the outline scheme had been developed. However, an initial appraisal of the scheme design showed that the architect's approach to the building form, orientation and siting was basically sound. During a three week period of close co-operation, the design was developed using building simulation software and a range of other design tools to assess daylight availability and natural ventilation air flows.

This example of integrated design in practice demonstrates how a responsive energy advice service can assist the development of a low energy design within the typically tight time constraints of a live project.

### BUILDING FUNCTION, FORM AND ORIENTATION

The school is sited near the bottom of a shallow valley and is to some extent protected from the south westerly prevailing winds by an existing hedge. Shelter-belt tree planting is planned to the north of the school building, and, further away to the east and west.

The school provides two classrooms, each of 100m<sup>2</sup>, plus a communal play area of 55m<sup>2</sup>, for up to 60 primary age children with about 5 teachers. Ancillary spaces include toilets, a kitchen, offices, extensive storage areas (for all the equipment) and a staff room. The school is designed to enable a 100% extension to be added in the near future.

The design has an essentially rectangular plan form, orientated along the north-south axis (see Fig. 1). The extension is planned to be built onto the east-facing elevation, which is therefore minimally glazed. The reception area, headteacher's office and staff room are on the west side. The two classrooms have north and south facing aspects respectively and are linked by a large communal area under a fully-glazed atrium roof. The building form and orientation deliberately minimise the area of east or west facing classrooms, in which direct solar gain and glare is less easily controllable.

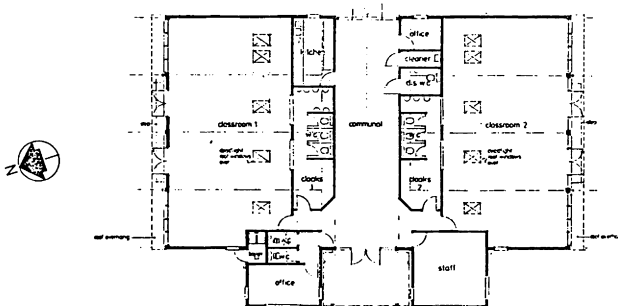


Fig 1. The Montessori School plan

The building is predominantly single storey, with only storage space being provided at first floor level under the pitched roof. The atrium is a full two storey height and should provide a delightfully light and airy space.

Although the overall building depth is approximately 24m, each classroom is effectively only 7.5m deep as each is lit and ventilated via the central atrium as well as directly through the external fabric.

**BUILDING FABRIC**

Glazed Apertures

The design aims to enable all school activities to be carried out in a naturally ventilated, daylight environment, for the majority of the year (see Fig. 2).

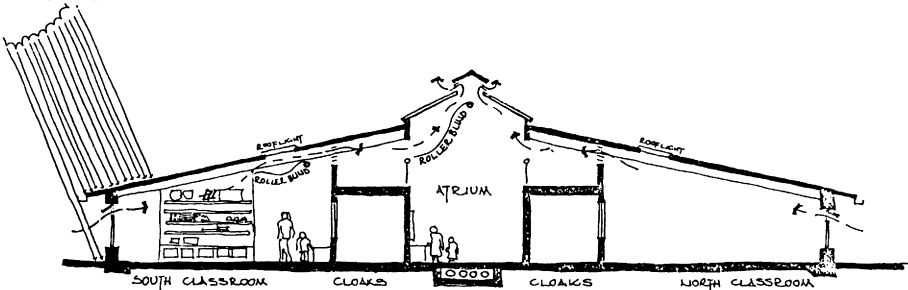


Fig. 2. Section showing some of the passive solar elements

It is certainly more pleasant for children to perform their tasks under daylight rather than artificial light, providing that glare, overheating and thermal discomfort can be avoided. The design endeavours to achieve a high utilisation of daylight through the specification of large window areas and the use of rooflights adjacent to the internal walls. The potential for glare or overheating problems is combated by minimising east and west facing orientations and by the use of appropriate internal and external shading devices. The windows are double glazed to reduce heat loss; a low emissivity coating is specified for the north facing windows to improve the thermal comfort for nearby occupants; the rooflights are single glazed to maximise daylight transmission.

Optimisation of the location and area of the classroom glazing for daylighting purposes was undertaken using a point-to-point daylight factor calculation program called DAYLIGHT. Daylight factor contours in a classroom for the final design configuration are shown in Fig. 3. The average and minimum daylight factors at a working plane height of 0.5m are 5% and 2% respectively.

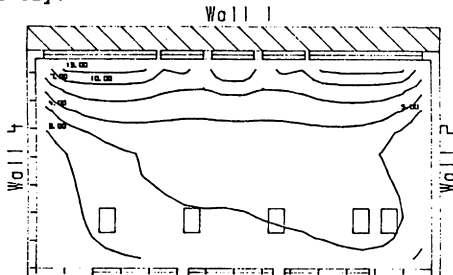


Fig. 3. Daylight factor contours in the south facing classroom



The shading of south facing windows takes the form of a 0.85m overhang above the window which should limit the direct high angle solar radiation incident on occupants sitting near to the windows, a major potential cause of overheating and glare discomfort. The south facing rooflights are shaded by manually operated sail-like internal blinds made of a translucent material.

The communal area, situated on the shorter axis of the plan, has a fully glazed roof of triple skin polycarbonate, which produces an average daylight factor in this space of 22%. This means that electric lighting is necessary for only 34 of the school working hours throughout the year. The south facing roof glazing is also shaded by manually operated blinds. The partitions at high level between the classrooms and the atrium comprise fixed glazing and permanent ventilation louvres. The glazing will serve to introduce some shafts of sunlight into the north classroom.

#### Opaque Fabric

Insulation. The building is insulated to better than the requirements of the 1990 amendment to the Building Regulations. The outer edges of the floor raft are insulated, but the floor is left uninsulated to increase the exposed thermal mass. The 'U' values of the various building components and their contribution to the building heat loss are given in Table 1.

Thermal Mass. The timber-frame structure is relatively lightweight, but the ground floor slab makes the building behave as a medium-weight structure. Internal, block partitions consolidate this process.

Sealing. The compact form produces a reasonably low external to floor area ratio, which, with careful detailing and the use of high performance air/vapour barriers, should constrain air leakage to a low level. Manually operated dampers are provided to seal the ridge ventilators when they are not needed. Similarly, it is intended that the trickle ventilators in the classroom windows are closed outside the occupancy period in winter.

Table 1. Paths of building heat loss

Building Element	'U' Value W/m <sup>2</sup> K	Area m <sup>2</sup>	Heat loss W/K	% of total heat loss
Walls	.33	307	101	10%
Opaque roof	.33	334	110	11%
Ground	.38	346	131	13%
DG Windows	2.80	65	182	19%
Low e DG windows	1.90	17	32	3%
SG Rooflights	5.70	6	34	4%
3 wall polycarbonate	2.40	42	101	10%
Infiltration		Vol=1300m <sup>3</sup>	283	29%
<b>Totals</b>		<b>1117</b>	<b>975</b>	<b>100%</b>
<b>Total per m<sup>2</sup> GFA</b>			<b>.87</b>	

#### Openings For Ventilation

The ventilation strategy is designed to cope with the various potential ambient conditions. In winter, during the occupancy period, the required supply of fresh air is obtained through the large trickle ventilators on the classroom windows. Stale, warm air flows out of the classroom at high level through permanently open glazed louvre partitions into the atrium space, and

leaves the building via louvres in the atrium ridge (see Fig. 2). Outside occupancy in winter, the trickle ventilators are closed and the ridge ventilator is sealed by manually operated dampers. In warm outside conditions, the occupants can open windows to enhance the wind pressure or the stack-driven natural ventilation air flow rate. During hot weather, the building can be cooled down by ventilation at night without jeopardising security, by opening the window trickle ventilators and ridge louvres.

The intentional emphasis on manual control is an integral part of the philosophy whereby the school children take responsibility for correct usage of controls so that they learn by experience how and why the systems work.

## BUILDING SERVICES

### Heating

Space heating is by lphw perimeter radiators fed from a 37kW oil-fired boiler. These provide a means of heating the incoming ventilation air and of combating discomfort due to draughts from the glazing in winter. The heating system controls include thermostatic radiator valves, optimum start/off and external compensation of flow temperature.

### Electric Lighting

A conventional fluorescent lighting installation using T8 tubes is provided to give a working plane illuminance of 300 lux. The luminaires in the classroom are arranged in banks parallel to the main windows. One clearly designated switch is provided for each bank to enable easy manual control of the lights in response to daylight availability. The switches at the classroom entrance are located beneath a rooflight which should encourage people entering the classroom not to switch on the lights unnecessarily.

It is envisaged that the school children will be given responsibility for the monitoring and control of lighting usage. This might include reading the electricity meter and analysing the data.

### Mechanical Ventilation

Extract ventilation is provided to the WCs and internal rooms. The operation of the fans is controlled by occupancy detectors.

## PREDICTED PERFORMANCE

The energy consumption of the building was predicted using an hour by hour annual simulation computer program called SERI-RES. The key outputs in this study were heating demand, electric lighting usage and hourly zone temperatures which indicate the degree of summertime overheating. The predictions for energy consumption data are summarised in Table 2.

Table 2. Predicted annual energy consumptions and costs

End use	Price p/kWh	Consumption kWh/yr	Cost £/yr	Consumption kWh/m <sup>2</sup> yr	Cost £/m <sup>2</sup> yr
Heating (oil)	1.14	33640	384	97	1.11
Lighting (electricity)	6.59	2160	142	6	.41
Totals		35800	527	103	1.52

Lighting: Electric lighting consumption is predicted to be 6 kWh/m<sup>2</sup>; daylighting provides 52% of the total lighting demand which would result if there were permanent electric lighting during the occupied hours.

Heating: Heating demand is predicted to be 68kWh/m<sup>2</sup>, requiring 97kWh/m<sup>2</sup> of oil consumption, assuming a heating season mean boiler efficiency of 70%. The Energy Efficiency Office (EEO) performance yardstick for schools of this type sets the upper limit for the 'good' category at 100kWh/m<sup>2</sup>yr for space heating fuel consumption, whilst 'poor' performance is above 135kWh/m<sup>2</sup>yr for space heating. Whilst comparing modelled data with measured data is fraught with problems, these guidelines indicate that good daylighting performance has not been bought at the expense of a large heating bill.

Energy Costs: The price of oil is taken as 12p/litre and of electricity 6.59p/kWh. Heating and lighting contribute 73% and 27% respectively to their total costs of fl.52/m<sup>2</sup>yr.

Overheating: The two zones of the school which might have a tendency to overheat in hot weather are the south facing classroom and the atrium communal area. The degree of overheating was assessed by counting the number of occupied hours per year that the temperature of each zone was above 27°C.

For the final design, with blinds and nighttime ventilation in operation, the atrium is predicted to have just 16 hours/year over 27°C and the south facing classroom only 3 hours/year.

Sensitivity Studies: A wide range of sensitivity studies were performed both to refine the design and test the robustness of the design to various uncertain parameters. The results are summarised in Table 3.

#### CONCLUSIONS

1. Integrated design of a building aims to achieve an optimum balance between capital cost, energy running costs and environmental conditions. Design tools such as dynamic simulation and daylight factor calculation software have enabled alternative design options for a Montessori School to be evaluated on a timescale compatible with the short deadlines of a real building project.
2. With the aid of appropriate design tools, the judicious sizing and location of the glazing apertures was achieved. Through the use of daylighting, the predicted lighting bill for the school has been halved, whilst maintaining a low heating demand and avoiding excessive summertime temperatures.
3. Overheating has been avoided by a combination of shading devices, stack or wind driven through-ventilation and the use of nighttime ventilation.
4. Control of the building environment and services relies to some extent on the occupants. This has been done partly out of a belief in a preference for manual control and partly to allow the school children to learn about energy and buildings through participation. Minimum fuel bills will only be achieved if a careful monitoring and control programme for the building operation is instigated and maintained.

#### ACKNOWLEDGEMENTS

Financial support for the design advice work reported in this paper from the UK Department of Energy through the Energy Technology Support Unit was much appreciated. However, it should be noted that the contents of this paper do not necessarily represent the views or opinions of the Department.

The authors would also like to express their thanks to Mr Peter Knott, the project architect, and Mr Paul Watkins, co-founder of the school, for their support and receptiveness during the design development.

Table 3. Summary of sensitivity studies of energy and environmental performance predictions

SENSITIVITY STUDY	EFFECT ON AVE. DAYLIGHT FACTOR	EFFECT ON ANNUAL LIGHTING	EFFECT ON OVERHEATING	EFFECT ON ANNUAL HEATING CONSUMPTION
Reduce the atrium rooflight from 3.2m to <u>1.6m</u>	Down by 38%	Up by 6 kWh/yr	In atrium down from 830 to 474 hrs/yr	Down by 1630 kWh/yr (about 5%)
Reduce the atrium rooflight from 3.2m to 1m	Down by 57%	*****	In atrium down from 830 to 173 hrs/yr	Down by 2270 kWh/yr (about 7%)
<u>Reduce north classroom windows</u>	Down by 16% in north classroom	*****	None	*****
<u>Use kappafloat double glazing in north classroom windows</u>	*****	*****	None	Down by 470 kWh/yr (about 1.4%)
Add one rooflight to each classroom (0.5mx14m)	Up by 50% in each classroom	Down 206 kWh/yr (about 10%)	In South classroom up from 42 to 60 hrs/yr	No change
Replace the single rooflight with 8 two skin GRP rooflights each 800x800 mm daylight area	Down by 8%	*****	*****	*****
Replace the single rooflight with 4 D.G. glass rooflights each 560x865 mm daylight area	Down by 25%	*****	*****	*****
Replace the 4 D.G. by 4 S.G. glass rooflights	Up by 3%	*****	*****	*****
<u>Use 5 S.G. glass rooflights instead of 4 S.G. rooflights</u>	Up by 8%	Down 13 kWh/yr (about 0.6%)	In South classroom up from 60 to 63 hrs/yr	Up by 140 kWh/yr (about 0.4%)
Increase the overhang from 0.3m to <u>0.85m</u>	Down by 10% in each classroom	*****	In South classrm down from 52 to 26 hrs/yr	Up by 80 kWh/yr (about 0.2%)
Apply blinds to rooflights	N/A	No change	In South classrm down from 26 to 9 hrs/yr In atrium down from 474 to 179 hrs/yr	N/A
Employ night ventilation	N/A	No change	In South classrm down from 26 to 3 hrs/yr In atrium down from 474 to 89 hrs/yr	N/A
<u>Apply blinds to rooflights and employ night ventilation</u>	N/A	No change	In South classrm down from 26 to 3 hrs/yr In atrium down from 474 to 16 hrs/yr	N/A
DHW from <u>oil boiler</u> or on-peak electricity	N/A	N/A	N/A	With oil: £180/yr With elec.: £450/yr

\*\*\*\*\* = Effect not predicted

N/A = Not Applicable

Underlined text denotes parameter is as fixed in the final design

# **Accurate Field Characterisation of Building Envelope Systems**

Prasad, D.K. & Ballinger, J.A.

SOLARCH: Solar Architecture Research Unit  
School of Architecture, University of NSW  
P.O. Box 1, Kensington, Sydney 2033

## **ABSTRACT**

Growth in the use of glass in buildings has had significant implications on its energy consumption and on plant and equipment used to control conditions. This has led to the development of advanced glazing systems with a range of tailored properties. There has been a corresponding need for accurate characterisation of these glazing systems.

There have been numerous studies internationally in this area, the earliest of these going back to the 1940's. SOLARCH: the Solar Architecture Research Unit of the University of New South Wales has been involved in thermal performance evaluation studies since the early 1970's. Having built and operated Passive Solar Test Cells and other laboratory based equipment it has now built a field model solar calorimeter. The calorimeter is particularly suited for heat gain environments for general Australian conditions. Heat loss studies are undertaken using indoor controlled condition chambers.

This paper discusses the facility and the methods in use for thermal performance characterisation of building envelope systems. It also reports on some early validation studies against other theoretical and experimental methods in use.

## **KEYWORDS**

Glass, Solar Heat Gain, Characterisation, Solar Calorimeter, Field Testing

## **INTRODUCTION**

The need to design energy efficient buildings has been highlighted by a number of studies. In trying to achieve this aim the designer places a great reliance on the thermal and optical input data available on component performance in order to assess the suitability of various alternatives.

Comprehensively developed models for calculating building heating and cooling loads can only be as good as the input data available on the components. It is well established that the error associated with the characterisation of building components can be significant. The absence of uniform standard methods for characterising some of the building components can cause further confusion.

A lot has been documented about the conductive heat transfer calculations and test procedures. Studies internationally (Erhorn et al, 1987 IEA Study; Klems, JH, 1985, LBL Study) have revealed the shortfalls in test procedures, especially the order of differences in values obtained by using the different procedures. Differences due to the choice of standard test conditions and temperature and wind probe locations itself can cause significant error in U-value measurements.

Berman et al (1975) pointed out that seasonal energy costs or benefits associated with windows are substantially

affected by direct solar gains. Johnson et al (1982) emphasised that there is an optimal combination of U-value and shading coefficient from the standpoint of annual energy use. This is certainly true for heat gain dominated climates such as most of Australia. Furthermore, the importance of daylighting contribution to energy efficiency has led to detail consideration being given to visual transmittance and reflectance.

A lot of these studies have been based on theoretical simulations which make a number of assumptions about real time heat flow in buildings. Some of the basic procedures such as the ASHRAE heat transfer analysis have been shown (McCabe, 1984; McCluney, 1984; Rubin, 1985) to have shortfalls. The growing use of advanced glazing systems and the inclusion of novel shading systems are a further cause of concern due to the number of assumptions made regarding the heat flow regime around these systems in use. Their selective dynamic response (spectral, angular and other sensitivity to voltage, light or heat) is of particular concern

This points towards the need for a procedure for accurate and reliable measurement under realistic conditions. This paper reports on the field studies at the SOLARCH: Solar Architecture Research Unit, Sydney, Australia. A field model calorimeter is used to verify larger sample properties against laboratory tested and theoretical results.

### FIELD TESTING

Two key methods of field assessment of thermal and optical performance of glazing systems have been:

- \* comparative assessments using passive test cells.
- \* quantitative (absolute) measurements using calorimeters.

The former have been full size insulated direct gain rooms in parallel, with a control room and one or more test rooms. The inside have largely been unconditioned and a comparative strategy has been devised for component characterisation. Moore (1982) summarised in detail the American use of this procedure. PASSYS program is currently finetuning an advanced adaptation of this procedure for its test program.

At SOLARCH we started using this technique in 1979. In a heat gain dominated climate the inside temperatures in free running cells rise to around 45°C above ambient. Due to the facility dependent nature of such cells it is difficult to quantify all the effects. The use of internal shading devices tends to affect the convective behavior near the glass surface (Smart, 1987).

The use of field solar calorimeters date back to 1945 when ASHRAE built their version in Florida (Parmalee et al, 1945). This resulted in a lot of useful design information for simple systems. Since the 1970's and with the marked growth in the use of glass in buildings, others have been built to varying levels of complexity (NBS, McCabe, 1984; U.A., Yellot, 1965; MOWITT, Klems, 1985; FSEC, 1986; NRCC, Barakat, 1982; U.W., Harrison, 1989; and others in Europe). These have added to the knowledge on field testing but unfortunately most are not in operation. A lot still remains to be researched.

The basic principle in all these has been the detail accounting of heat balances between that gained through test interface and that collected by the absorbent resulting in an increase in its temperature. The inside/outside temperatures are kept closely the same to eliminate conductive transfers. Building on its past experience SOLARCH has built a calorimeter for field characterisation of building components in Australia.

### PERFORMANCE EVALUATION OF GLAZING SYSTEMS

Figure 1 in the appendix illustrates the calorimeter and control systems employed in the SOLARCH facility. The heat extraction consists of a primary chiller unit with an intermediate buffer tank between the calorimeter and the chiller. A high flow rate is maintained in the calorimeter to ensure a uniform absorber plate temperature.

The flow rates in the absorber cooling loop and the air coil are automatically controlled to maintain the average absorber temperature and average air temperature to within a specified tolerance of ambient temperature (usually 1K). The heat extracted from the absorber is removed by the heat exchanger in the return line to the buffer tank or by direct temperature control of the buffer tank from the chiller tank.

All control operations are determined by a real time monitoring and control program in an on-line computer. The primary control function is to maintain the average absorber temperature and air temperature within 1K of ambient temperature. A secondary control function is to maintain a minimum temperature difference of 5K between the absorber and air coil input and output flow lines in order to minimise errors in thermal energy evaluation.

The primary control functions are achieved by automatic adjustment of the flow rates in the absorber and air coil lines and by operator specification of the temperatures of the buffer tank and chiller tanks. The design points for the buffer tank and chiller tank are 5K and 10K below ambient respectively. The chiller tank temperature is specified by the user in the setup data file and then maintained automatically by software control of the chiller system compressor. A dead band of 2K (user specified) on the chiller tank should be used to minimise compressor cycling.

The energy flows into the absorber plate and the air space of the calorimeter are monitored by measuring the flow rate and temperature change of the two water cooling circuits. The energy lost through the walls of the calorimeter and the energy input by the absorber circulating pump, air circulating fan and air reheater are subtracted from the total thermal energy output to give the net energy transmitted by the window system. The on-line program averages all measurements over 10 sec and displays the most recent readings on a mimic diagram of the system. One minute averages of all parameters are stored on a running results file. The running results may be viewed at any time by the operator or displayed graphically.

### USER INTERFACE FOR CONTROL AND DATA ANALYSIS

The control program has been structured so that the user can specify all parameters relevant to the calibration of transducers, control functions and data recording. The main operation specification file contains all control function set points and data stability tolerances. The user should edit this file to control the setup for each test. The control state and graphical data display functions available to the user are:

1. Solar calorimeter - a mimic diagram of the system and control data.
2. Absorber plate temperatures
3. Absorber water temperature
4. Absorber air temperature
5. Buffer and Chiller tank temperature
6. Solar radiation
7. Solar angles
8. Shade coefficient
9. Air flow rates
10. Heat collected by absorber
11. Heat collected by cooling coil

The run time user interface to the data display and control functions is via pull down menus on the screen. The pull down menu structure depends on the display page the user has selected.

### RESULT FILES

Measurements collected during a test are analysed and stored at 3 levels. The minute by minute records of all temperatures, flow rates, energy flows and computed transmission are stored in a file DD-MMM.TMP where DD= day of month; MMM = month eg 04-MAY.TMP. The stability of the calorimeter operation is over intervals defined by the user. Each minute all stability tolerances are evaluated. When a valid test period is observed the measured and computed results are written to file. A typical graphical result file is shown in Figure 2.

### CALORIMETER CHAMBER

Figure 3 shows a photograph of the test facility in use. The test sample size is within the range 1.80m X 1.20m, inclusive of frame. The chamber can be manually aligned to all usable altitude and azimuth combinations. It is on a mobile chassis for transportability.

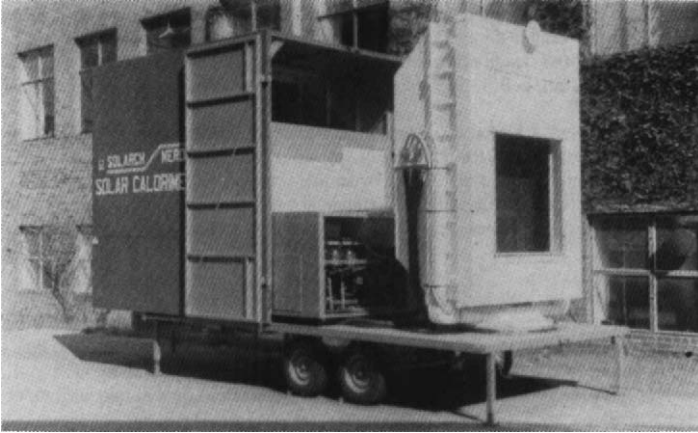


FIGURE 3 A PHOTOGRAPH OF THE TEST FACILITY

### RESEARCH PROGRAM

The first phase of the study currently under way is looking at two sample, a 3mm DSA reference and a commonly applied 6mm tinted glass (TS21). The results have been validated using manual calculation procedures and manufacturers specification. The correlation has been accurate to 94%. Detail sensitivity tests are now under way to establish facility characteristics and variability to ambient conditions. This paper is therefore a progress report on the overall testing program. The facility will be used to provide a service to the industry and be an integral part of a proposed standards development project. An inside scanning system with radiation and photosensors is being mounted for further data extraction.

### CONCLUSION

The need for accurate field measurement of component performance is evident. The study of solar gains and visual transmission through glazing systems is underway to provide further information on product performance.

**Acknowledgement:** This project was supported by the National Energy Research Development & Demonstration Council, DoPIE, Canberra.

### REFERENCES

- Ballinger, J.A., Prasad, D.K., Morrison, G.L. (1990); *The Establishment of a Solar Calorimeter*, NERDDC Project Report 1273, DoPIE, Aust.
- Barakat, S.A. (1984); *NRCC Passive Solar Test Facility: Performance of Direct Gain Units*, NRCC DBR Report No. 215.
- Berman, S.M., Silverstein, S.D. (1975); *Energy Conservation and Window Systems*, APS Conf. Proc. No. 25, American Inst. of Physics.
- Dijk, H.A.L. (1989); *PASSYS Solar Testing and Performance Prediction*, Proc. 2nd Euro. Conf. Arch., Paris.
- Erhom, H., Stricker, R., Szerman, M. (1987); *Test Methods for Steady State Thermal Transmission*, IEA Annexe XII Report on 'Windows and Fenestration'.
- Johnson, R., Selkowitz, S., Winkelmann, F., Zentener, M. (1982); *Glazing Optimisation Study for Energy Efficiency in Commercial Office Buildings*, Lawrence Berkeley Report 12764.
- Klems, J.H. (1985); *Toward Accurate Prediction of Comparative Fenestration Performance*, Lawrence Berkeley Laboratory Report 19550.
- Klems, J.H., Keller, H. (1986); *Measured Net Energy Performance of Single Glazing Under Realistic Conditions*, Lawrence Berkeley Laboratory Report 20346.
- McCabe, M.E., Hancock, C.E., Migom, M.V. (1984); *Thermal Performance Testing of Passive Solar Components in the NBS Calorimeter*, USDOE, NBSIR 84-2920.
- McCluney, R. (1987); *Determining Solar Radiant Heat Gain of Fenestration Systems*, Passive Solar J. 4(4).
- Moore, F. (1982); *Passive Solar Test Modules*, Passive Solar J., vol. 1 No. 2 pp91-103.
- Parmalee, G.V., Aubele, W., Huebscher, R.G. (1945); *Measurement of Solar Heat Transmission Through Flat Glass*, ASHVE Trans. No. 1333.
- Rubin, M. (1982); *Calculating Heat Transfer Through Windows*, 'Energy Research - Vol. 6 pp341-349.
- Smart, M., Ballinger, J.A. (1987); *A Simple Empirical Procedure to Estimate Shading Factors*, ANZSES Conf. Proc. ANU Aust.



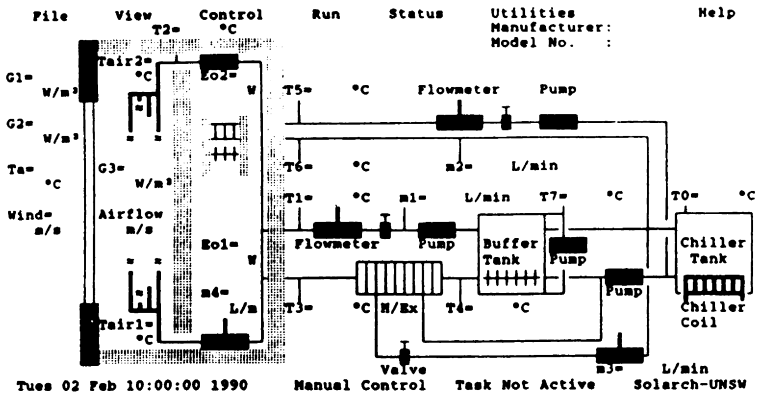


Figure 1 Calorimeter and Control System

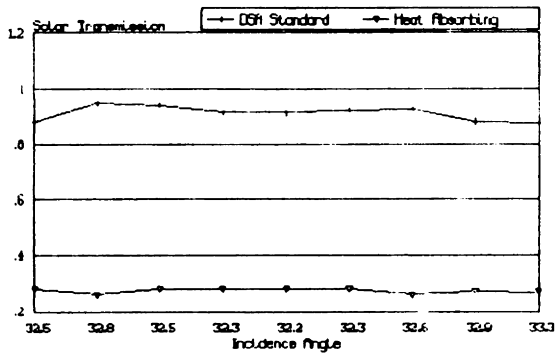
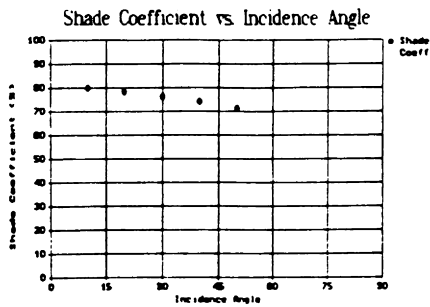


Figure 2 Typical Graphical Output

EVAPORATIVE AIR COOLING IN  
ISLAMIC ARCHITECTURE

AKRAM A. ZUHAIRY and A.A.M.SAYIGH

Department of Engineering, University of Reading,  
Whiteknights, PO Box 225, Reading, RG6 2AY, U.K.

ABSTRACT

The utilisation of evaporative air cooling in Islamic architecture is discussed in this paper. Several systems are presented for which description, operational method and climatic conditions are discussed. The systems which are discussed in this paper; they are completely passive. Some of them are going to be compared with active cooling systems. It shows that some of the passive systems are more efficient than the active ones. They always blend with the needs and the environment.

KEYWORDS

Fountain; Salsa'beel; A'cool; Wind tower; Courtyard house concept.

Introduction

Islamic architecture implemented evaporative air cooling as one of the passive cooling techniques utilised in different types of climates. It was mainly used in the hot-arid regions of that part of the world. Several evaporative air cooling techniques have been used according to the climatic conditions and the available resources.

Some of these techniques are presented in the following discussion. It is important to notice that almost all of the presented evaporative cooling systems are passive ones. These systems do not only work effectively as cooling systems but also take into consideration the aesthetic appeal of the living environment.

The Fountain as an Evaporative Air Cooler

Fountain (Nafora or Fasquia, in Arabic) is a very essential architectural concept in the Islamic architecture. When water is scarce, talking about hot-arid regions, the fountain is recognised as a valuable architectural work of great aesthetic appeal. Moreover it works as an evaporative air cooling system, specially when located in a way of an air stream or a wind passage. The latent heat of water evaporation is absorbed from the passing hot-dry air stream. The process is an adiabatic humidification process in which part of the sensible heat of the air stream is transferred to latent heat. Therefore the sensible heat of the air stream decreases and its DBT decreases, while on the contrary its latent

heat increases. Due to this fact the fountain is used in both the traditional and the contemporary Islamic architecture as a passive cooling system or part of a complex passive cooling system such as in the middle of a courtyard house, in the exit air from a wind tower or located in an air stream passage inside a living room as shown in Fig.1.

#### The Salsa'beel as an Evaporative Air Cooler

It is a kind of fountain composed of an inclined marble plate carved in a wavy pattern on which water stream is trickling. It is an option provided when there was not enough water pressure for operating a fountain, and can be considered as a transposition of the fountainhead placed outside the fountain [7]. The carved wavy pattern, as it reflects and enhances the formation of water waves as an aesthetic view in the living area, also creates more surface area to enhance the water evaporation on that surface. Air cooling by salsa'beel works in a similar manner as that of the fountain. The idea of salsa'beel operation is very simple in which water trickles over the inclined surface of the marble tile. As water accumulates between the carved wavy pattern of the tile; it tends to flow on it in a wavy form, as shown in Fig.2. As water reaches the bottom edge of the marble tile it moves into a marble channel which as creating more aesthetic appeal it provides more water surface area for the evaporative cooling process.

#### The "A'cool" as an Evaporative Air Cooler

Ancient Bedwins of Arabia used to sell evaporative air coolers to people settled in cities. These coolers were named "A'cool", which is an Arabian word. An A'cool is made of desert thorn and namely a special type of thorn called camel thorn or A'cool thorn. The thorn is used as a packing media that acts as an evaporative air cooling surface. It is packed between two layers of palms' sticks formed in a grid shape frame as shown in Fig.3. The sticks tied together with palm leaves to form the above mentioned grid shape frame. The camel thorn has a major advantage which is moisture retention for a long period of time compared with other types of plants. This advantage reduces the amount of water consumed in the process of evaporation and therefore helps in the conservation of water, the most precious element in the hot arid desert climates. Moreover the capability of moisture retention keeps the camel thorn green for a long period of time and this gives an additional advantage of aesthetic appeal to the A'cool. In fact its green appearance indicates the freshness of the camel thorn as a packing media which usually lasts for more than two months before it dries and therefore needs to be changed. The A'cool is usually fixed on a window or sometimes on a door opening facing the prevailing wind or a local wind. Since air is hot and dry in these areas, A'cool is wetted with water and therefore when air passes through the wet media of camel thorn it operates as a direct evaporative air cooler. This cooling process is an adiabatic humidification process in which the latent heat of water evaporation on the wet media is absorbed from the outdoor hot dry air stream while passing through the A'cool. The entering air stream sensible heat decreases, whilst its latent heat content increases. The DBT decreases, simply because some of the sensible heat originally present in the entering ambient air is converted into latent heat.

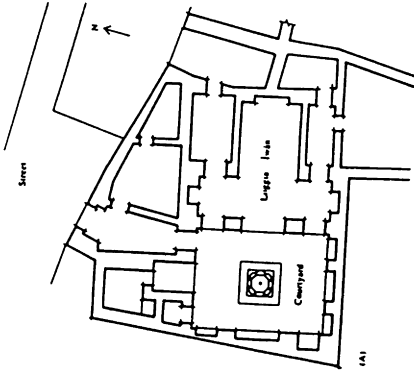
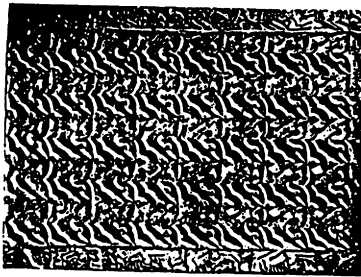
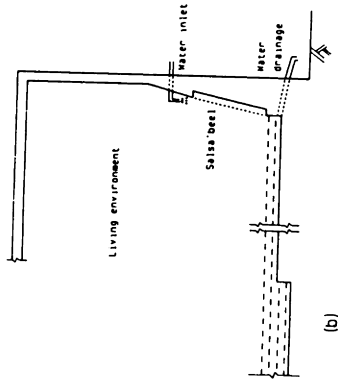


Fig 1. A fountain in the middle of a courtyard house as a passive cooling element (7)

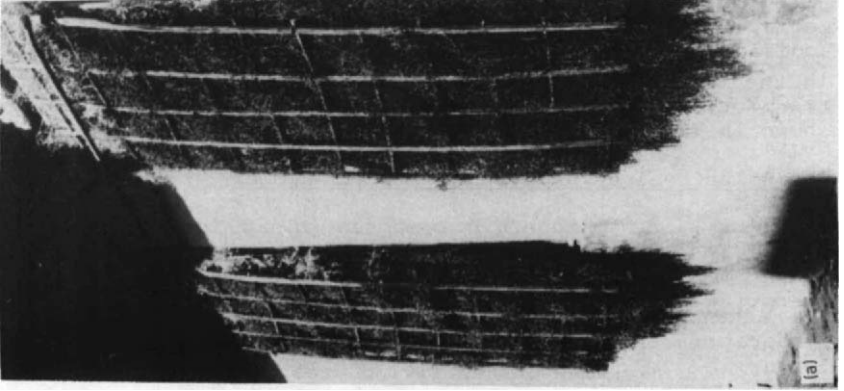


(a)

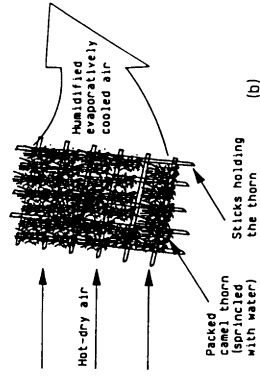


(b)

Fig 2. A salsa'beel: (a) A salsa'beel carved in a wavy pattern - (b) A salsa'beel in a living environment (7)



(a)



(b)

Fig 3. The "A'cool": (a) The A' cool fixed on windows of a traditional house in Baghdad - (b) A schematic diagram showing the idea of A'cool as an evaporative air cooler.

Air humidity increases after it passes through the A'cool wet media, and in hot dry climates this humidification action gives an additional pleasant comfort feeling.

#### Psychrometric Charts and Climatic Conditions

Fig.4. shows a hypothetical psychrometric chart showing a comparison between the cooling effects of the presence of a direct evaporative cooler, an A'cool, a Salsa'beel or a fountain in a living environment. Further investigation and experimental work is needed to prove the ranking of the cooling efficiencies of these systems.

The above mentioned systems works as follows : the air cools evaporatively along a line of constant wet bulb temperature (WBT) moving it from conditions at point A to these represented by the points B<sub>1</sub>, B<sub>2</sub>, B<sub>3</sub> or B<sub>4</sub>, while the ambient air DBT is reduced its humidity increases. The cooled air then gets mixed with room air improving its conditions to those shown at points C<sub>1</sub>, C<sub>2</sub>, C<sub>3</sub> or C<sub>4</sub>.

The WBT of the entering air conditions (point A in the chart) is the most limiting factor for the efficiency of these systems. The above mentioned systems are more efficient in hot dry climates. They are not going to provide the desirable comfort in hot-humid climate this is due to the fact that the humidity will increase to unpleasant level with less achievements in reducing the DBT. If the indoor conditions have a relative humidity exceeding 70-75% RH, the above mentioned systems will cease to function.

#### Wind Tower as an Evaporative Air Cooler

Wind is a very important factor in the design of buildings specially when air movement and ventilation are necessary in achieving human thermal comfort. In hot-arid climates a window cannot function as one unit capable of providing the required natural lighting, ventilation and view. This is because of the nature of that climate which can be characterised by high temperature accompanied by large diurnal range (18-22°C) and dusty winds of fixed diurnal and seasonal patterns. It is also characterised by high solar radiation and hot days with hot draughts and high radiation rate to the sky during the night with cool nights. Therefore, people living in these areas found it impossible to design windows that function as a lighting, ventilation and view source, as well as being able to resist the above mentioned characteristics of that climate. Due to high solar radiation and to prevent excessive illuminance and glare in the living environment, windows must be small. The suitable size of window for day-lighting is usually insufficient size for the required ventilation. Large windows also allows more dust to enter specially when knowing that dust is more concentrated in the lower layers of the wind zone. Air gusts are normally dry and hot. Therefore for people living in these areas in order to overcome the problem of excessive illumination, dust and hot dry winds they have to find another sort of windows different from the common ones.

A normal but small window can be provided in such climate to function as a daylighting and viewing source. Shading devices are good solutions to overcome the problem of excessive direct solar

radiation. Special types of shading devices can be designed to provide both shading and privacy. The third function of a window which is ventilation. It can be interpreted as part of the window area transpositioned to a more convenient location of the building structure where it is mostly needed in order to achieve comfort. This transpositioned part must function to overcome the problem of hot air draughts, dust and sand storms as well as utilising the characteristic of cold nights to cool the hot days. Moreover it works as an evaporative air cooler by utilising the characteristic of hot-dry air during the day.

Wind towers were found to be a good solution to overcome the above mentioned problems of the hot-dry climate. It can be considered as the part of the overall area of the windows in the building required for ventilation removed from their places and placed on top of the building for more convenience.

It is not the aim of this discussion to present the history, theory, design and operation of wind towers, which have been presented by several contributors [2, 3, 4, 5, 7, 8 & 9], rather than presenting its partial operation as an evaporative air cooling system.

When a fountain, a pool or a salsa'beel is placed in the way of the outflowing air from a wind tower, as shown in Fig.5, further air cooling can be achieved. An additional pleasant thermal comfort will be achieved from the action of humidification of the hot-dry air.

This system works as a complete passive cooling since no active parts are added (such as pumps or fans). The wind tower as a cooling system was found to be a more efficient one when compared with several modern evaporative air coolers [2].

Several modifications have been presented in the literature, some of which are shown in this paper. The modifications presented are the ones related to evaporative cooling. Other possible modifications covering the cooling aspects of the wind tower are well documented in the literature. Fig.6 presents an old modification in the wind tower that enhances the evaporative cooling effect of the tower. The modification is simply by providing a row of porous pottery jars just after the inlet of the tower and charcoal on grating before the exit of the tower. A pool of water is usually provided in the bottom of the tower. Jars are filled with water which wet the surface of the jars, moreover droplets of water from the bottom of the jars will also wet the charcoal; excessive water ends into the pool provided at the bottom of the towers' exit.

When hot-dry air passes through the tower it gets humidified and evaporatively cooled when contacting with the wet surfaces of the jars, the water droplets, the charcoal and the pool water surface. Additional to the humidification and cooling effects it also cleans air from the suspended solids of dust which is a common feature of the wind in hot arid climates.

The wind tower of Fig.7 implements another modification that utilises evaporative cooling concept [7]. The evaporative cooling

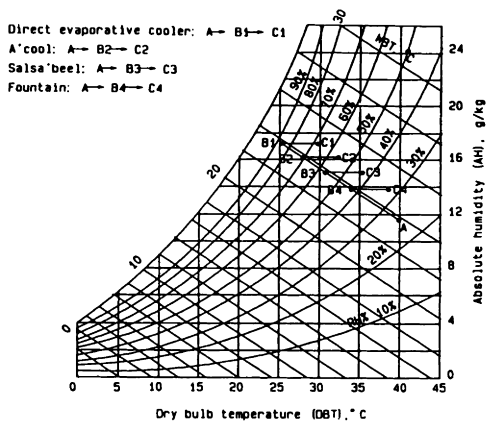


Fig 4. A hypothetical chart shows the ranking of cooling efficiencies for different systems

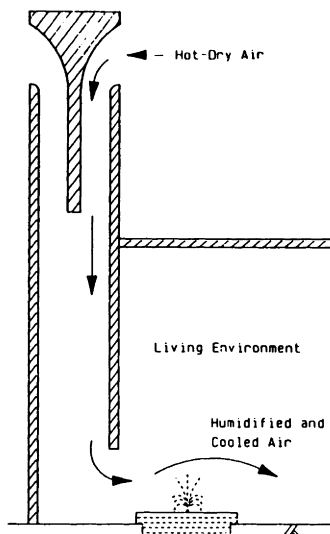


Fig 5. A wind tower functioning during the day as an evaporative air cooler.

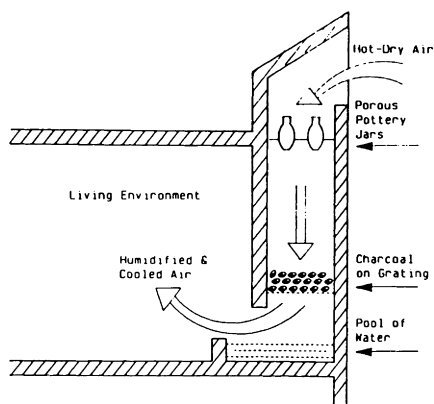


Fig 6. A row of porous pottery jars just after the inlet of a wind tower to enhance the evaporate cooling action.

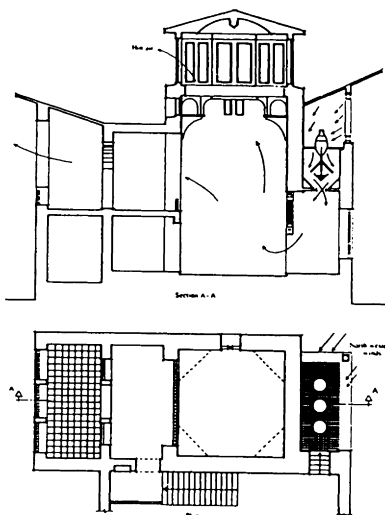


Fig 7. A specific type of wind towers called malqaf (wind catch) provided with witted baffles to enhance evaporative air cooling. Designed by H Fathy.

system is simply an inverted Y-shape metal plate on which charcoal is placed and held in place by grating on top of it. Another V-shaped plate is suspended with the Y-shaped plate and also filled with charcoal. Water is pumped to the upper part of the tower and sprinkled on the charcoal. When hot dry air passes over the wet charcoal surface it gets humidified and evaporatively cooled before entering the living environment. The same tower can be further modified [7] by providing a salsa'beel and / or a fountain in the passage of the air while leaving the tower, as shown in Fig.8. Salsa'beel or a fountain in the living environment not only enhances the evaporative air cooling of the tower but also provides an aesthetic appeal to that environment.

When an underground water stream is available or the water table is high in the site of the building, the wind tower of Fig.9 can be a good evaporative air cooler [2]. As the underground water temperature is normally low, this provides the system with an additional cooling factor. Therefore this system is employing a more cooling efficiency when compared with several other towers. The house is connected with the underground water with shafts such as D. Air enters from point d of the tower with high velocity. While entering it carries the cold air at point c to the other parts of the room. At point a the transported air enters again and gets circulated through the underground water passage therefore further cooling is achieved. The underground water can be utilised by several neighbours by implementing the same system in each house.

Another wind tower incorporated several modifications [3] is shown in Fig.10 in which only the evaporative cooling modifications are intended here for discussion. The system is capable of directing more air to the living space and capable of storing and retrieving coolness with a higher efficiency. Moreover the tower is provided with unglazed clay conduits sprayed with water from the upper part of the tower. When hot-dry air passes over the wet surface of the clay conduits evaporative air cooling takes place. Therefore air enters the living space with a much lower temperature. This tower is also successfully functioning in removing dust particles from the entering air and therefore passing clean air to the living space.

A wind tower incorporating an evaporative air cooling media [5] of thick celdek evaporation pads made of special paper honeycomb have been designed and constructed in a test house. The cooling efficiency of the tower was investigated.

A wind tower for passive cooling and heating in hot-arid regions was successfully designed [4]. The cooling mode of the tower utilised evaporative cooling pads across which hot-dry air passes and leaves the pads as a humidified and cold air.

#### Psychrometric Charts and Climatic Conditions for Wind Towers

Different designs of wind towers tend to have different psychrometric charts, when considering the final cooling effects. A typical psychrometric chart can be considered as that shown in Fig.11 which is related to the cooling effects of the wind tower



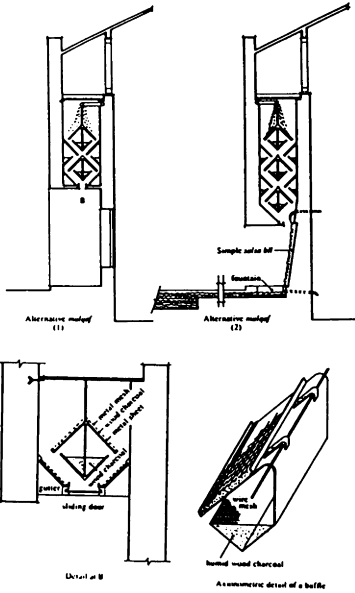


Fig 8. Two other alternative malqafs to that of fig 7. (7)

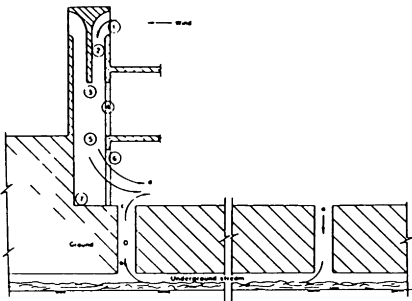


Fig 9. A cross section of a wind tower in conjunction with an underground water stream. (2)

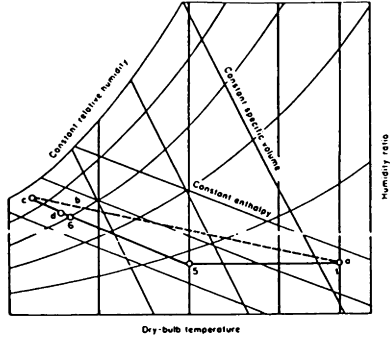


Fig 11. The psychrometric presentation of air conditioning process of the wind tower and underground water stream shown in Fig 9 (2)

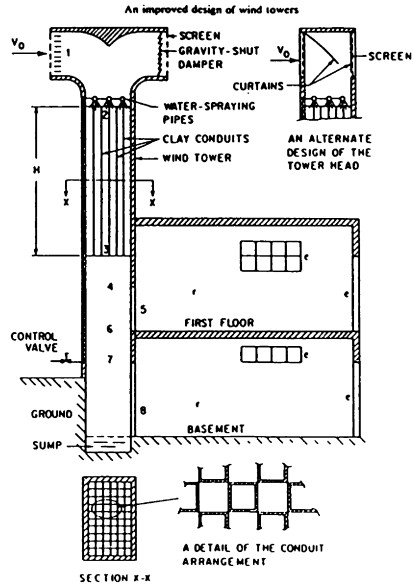


Fig 10. A cross section of a wind tower incorporated several modifications. Designed by M. Bahadori. (3)

presented in Fig. 9 [2].

Wind towers can be used as cooling systems in hot dry climates and the cooling effect of the tower can be enhanced when provided with evaporative cooling parts. The systems can also be used in warm humid climates where air circulation is important in achieving thermal comfort. A wind tower for both passive cooling and heating was reported [5] and proved to be efficiently operating.

#### Evaporative Air Cooling in the Courtyard Concept

It is not the aim here to discuss the courtyard concept, which has been well studied by several other workers [6, 7 & 9], rather than discussing the utilisation of evaporative air cooling as one of the passive cooling techniques utilised by the courtyard concept.

A simple description of the courtyard concept is provided in Fig.12. It is usual to provide a pool or a fountain at the centre of the courtyard for the purpose of evaporative air cooling. The presence of the fountain (or the pool) surrounded by the rooms provide a shelter for the fountain from the direct flow of the hot-dry winds and therefore limits the amount of evaporated water. This is good decision making knowing that water is precious in the hot-dry climates, and therefore it is good to use it for cooling purposes providing that excessive evaporation is prevented. A salsa'beel might be provided in another part of the house such as a living room. An A'cool is provided to serve a room or a number of rooms or spaces inside the house. Several A'cools are possibly provided each to serve a certain space of the house. These are usually fixed on window openings.

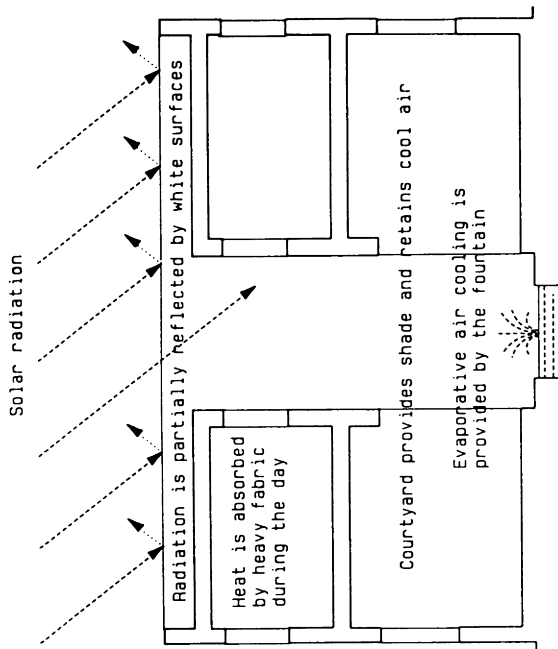
During summer some of the houses are provided with two A'cools standing in an L-shape opposite to the main entrance. A third A'cool is used to cover the previous two A'cools. The main entrance door is kept open and the three A'cools structure serves as an evaporative air cooler and as a curtain that keeps the house private. The green looking of a number of A'cools in front of the entrances of several courtyard houses adds an additional aesthetic dimension to the alleyway.

The courtyard flat roof usually used for sleeping during summer times and water sprinkling on the roof, before sleeping is a common practice. The idea of sprinkling water on the roof is to create evaporative cooling as an additional cooling method to the cooling by radiation to the sky which is a natural phenomena in hot-arid regions. The rooms of the courtyard house which are away from the courtyard breeze are usually provided with wind towers similar to that shown in Fig.5.

Therefore the courtyard concept can be considered as an extreme case of the utilisation of evaporative air cooling.

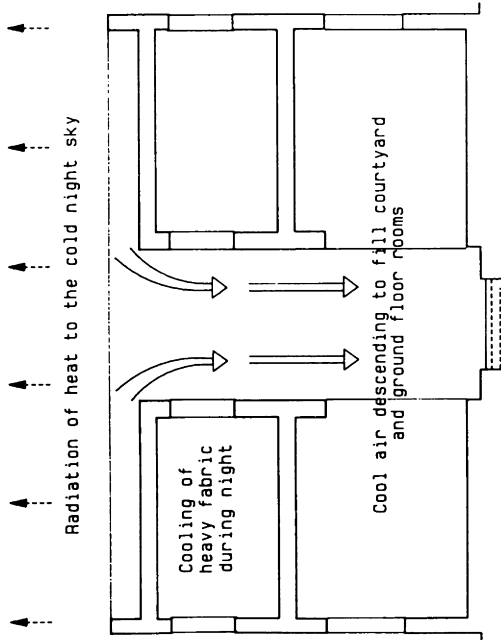
#### Conclusion

The discussed evaporative air cooling systems are not the only implemented ones by the Islamic architecture. They are only presented as examples from some Islamic regions. Other evaporative air cooling systems can be found in other regions of the Islamic world. The presented passive evaporative air cooling systems can



CONDITION DURING DAY

Solar radiation heats the heavy fabric during the day and partially reflected by the white surfaces. The courtyard provides shade and retains the cool air of the previous night. The presence of the fountain provides evaporative air cooling.



CONDITIONS AT NIGHT

Building fabric loses heat during the cold night by radiation to the sky. A pool of cold air builds up in the courtyard and the ground floor rooms.

Fig.12. The courtyard concept which utilises evaporative air cooling as part of the complex passive cooling system.

be characterised by their design simplicity, aesthetic appeal, quietness and good efficiency which are very important parameters in any architectural design. Some of the presented systems were found to be more efficient when compared with several modern evaporative coolers. Further modifications and studies are still required before implementing these techniques as part of the modern architecture, although some have been successfully used in some modern buildings.

#### Aknowledgement

The authors like to aknowledge the help of Dr. S.M. Al-Azzawi in supplying the photograph and some of the discussion about "A'cool" concept.

#### REFERENCES

1. Al-Azzawi, S. (1989). The courtyard of indigenous and oriental houses in Baghdad. In the Courtyard as Dwelling. pp. 59-84, Traditional Dwellings and Settlements Working Paper Series (Series ed. Al-Sayyad N. & Bourdier J.P.) IASTE, Univ. of California, Berkeley.
2. Bahadori, M.N. (1979). Natural cooling in hot arid regions. In: Solar Energy Applications in Buildings. pp. 195-225 (Edited by A.A.M.Sayigh) Academic Press, New York.
3. Bahadori, M.N. (1985). An improved design of wind towers for natural ventilation and passive cooling. Solar Energy J., 35, 119-129.
4. Bahadori, M.N. (1988). A passive cooling/heating system for hot, arid regions. Proceedings of the 13th National Passive Solar Conference (M.J.Coleman, ed.), pp. 364-367. American Solar Energy Society, Inc., U.S.A.
5. Bajwa, M.M. et al. (1987). Architectural manifestation of the passive solar cooling strategies for the Gulf Region of the Kingdom of Saudi Arabia. Proceedings of the 1987 European Conference on Architecture, Munich, F.R.Germany.
6. Burberry, P. (1977). Ambient energy and building design, building design criteria. Ambient Energy and Building Design Conference Proceedings. pp. 153-171. Construction Industry Conference Centre.
7. Fathy, H. (1988). Natural Energy and Vernacular Architecture. The United Nations University (Arabic Edition). Beirut, Lebanon.
8. Karakatsanis, C., Bahadori, M.N. and Vickery, B.J. (1986). Evaluation of pressure coefficients and estimation of air flow rates in buildings employing wind towers. In: INTERSOL 85 (E.Bilgen, ed.), 2 pp. 769-774. Pergamon Press.
9. Szokolay, S.V. (1980). Environmental Science Handbook for Architects and Builders. The Construction Press Ltd., Lancaster, England.

POTENTIAL OF ATTACHED SUNSPACES IN THE SOUTH OF ARGENTINA  
AND DESIGN GUIDELINES

John Martin Evans, Silvia de Schiller, Maria Veronica Snoj  
and Jose Reyes.

Programa de Investigacion "Habitat y Energia"  
Facultad de Arquitectura, Universidad de Buenos Aires,  
Pabellon 3, Piso 4, Ciudad Universitaria,  
(1428) Capital Federal, Republica Argentina.

ABSTRACT

Attached sun spaces and glazed extensions to buildings act as passive solar systems with a relatively low efficiency. This paper analyses the useful solar heat obtained using sun spaces attached to dwellings in different regions of Argentina. The results show that they perform well in Patagonia, southern Argentina, where attached sun spaces offer other climatic and functional benefits in a region with high wind speeds and low rainfall. Design guidelines are provided, based on a study of alternatives which increase useful solar heat gain.

KEYWORDS

Sun spaces; solar systems; patagonia; Argentina; solar radiation; glazing; climate.

INTRODUCTION

Attached sun spaces and glazed extensions act as passive solar systems of relatively low efficiency, providing less useful solar heat gain than direct gain systems and Trombe walls of the same effective exposed area. However, they provide additional benefits such as extra living space for intermittent use, protection from strong winds, space for plants protected from frosts, and a transition between indoor and outdoor spaces, which may be used to provide an entrance with low heat losses or a thermal buffer. At the same time these spaces may suffer from summer overheating and reduced ventilation to habitable rooms.

It is therefore important to identify the region where attached sun spaces perform well and to clarify the design variables which influence the useful heat gain (Evans et al, 1989). These two aspects are studied in this paper. Simple design recommendations are presented, allowing the designer to evaluate alternative solutions in relation to the solar-thermal properties as well as functional, aesthetic and other factors involved.

## CRITERIA FOR THE USE OF ATTACHED SUN SPACES

Four criteria are proposed to identify climatic variables that favour the use of attached sun spaces. The criteria adopted are useful solar heat, avoidance of summer overheating, wind protection and low rainfall. They define the geographical region where benefits of sun spaces are optimized.

1. Useful Solar Heat: The useful solar heat is the energy received by the sun space and transmitted through the shared wall to the building, when this is required, replacing conventional fuels and improving comfort conditions. The useful solar heat gain was estimated for 60 towns, 20 sun space designs and three insulation levels. The Passive Solar Handbook Method (Balcomb and Jones, 1983) was adopted, using data prepared for Argentina (Fabris and Yarke, 1986). Figure 1 shows the typical variation of useful solar heat gain in Argentina for a sun space with double glazing, vertical walls and 30' roof slope, opaque insulated lateral walls, without night insulation. The rate of dwelling heat loss per unit temperature difference per unit area of dwelling/sun space wall is 8.45 Watts/m<sup>2</sup>'C. Other configurations show similar distributions with minor variations and a clear general tendency:

- i). The low latitude, low altitude region in the north has low useful solar heat gain, due to the mild winters with low heating demand.
- ii). The western limit of the country, with high altitudes, has high demand due to low temperatures, coupled with high solar radiation intensities.
- iii). The useful solar energy increases at higher latitudes in the centre and south due to colder and longer winters, which increase heat demand.
- iv). In the far south and west, useful solar energy diminishes slightly due to low angle winter sun and increased cloud cover.

2. Summer Overheating: Attached sun spaces are prone to summer overheating, as they are difficult to shade from high angle sun. Overheating can be controlled in regions where the maximum average monthly temperatures do not exceed the upper comfort limit. With good ventilation, sun spaces will rarely exceed comfort levels and heat transfer to the dwelling will be low and unlikely to cause unwanted temperature increases. A maximum monthly temperature of 25'C was chosen as the proposed upper limit to control overheating of the sun space. In areas of high temperature swings, partial heating may be required at night, even though daytime temperatures are comfortable or hot. In this case, a heavy, high heat capacity wall between sun-space and dwelling can provide a useful fly-wheel effect, delaying heat transfer for several hours. The sun space itself may suffer from high midday temperatures, but the dwelling still benefits. A maximum average monthly temperature of 20'C is proposed to avoid overheating of the dwelling when the summer range exceeds 15'C. Figure 2 shows the areas defined using recent met. data (S.M.N. 1986). The high altitude region in the north and west of the country is excluded using these criteria.

3. Wind protection: The patagonian region is characterized by very strong and persistent winds. The attached sun space provides an intermediate indoor/outdoor space protected from these winds. Figure 3 indicates the distribution of average annual wind speeds which have maximum values on the southern atlantic coast.

4. Low rainfall: Attached sun spaces may also be used for cultivating plants, protected from low temperatures. Plants may require partial winter heating to avoid frosts as attached sun spaces are inherently badly insulated. Plants may also require protection from excessive temperatures in summer using the previously proposed criteria.

The possibility of cultivating plants in attached sun spaces provides additional benefits in Patagonia, as the combination of climatic factors limits cultivation in conventional gardens: very low rainfall, low temperatures and high winds. Figure 3 also shows rainfall distribution in Argentina. The hatched area has an annual average rainfall of less than 500 mm, the minimum required for tree growth without artificial irrigation. Humidity from sun spaces can also improve indoor comfort in this dry region.

The four criteria related to climatic variables allow the definition of the region where attached sun spaces can be used with greatest benefit. This region is shown in Fig. 4 and extends over the greater part of Southern Patagonia. Although the useful heat gain is slightly less in the far south, (Tierra del Fuego), attached sun spaces still provide an attractive and energetically useful addition to dwellings. This evaluation defines a region which coincides with the zone where glazed galleries are found in the traditional "estancias" (sheep farms) in the south of Patagonia.

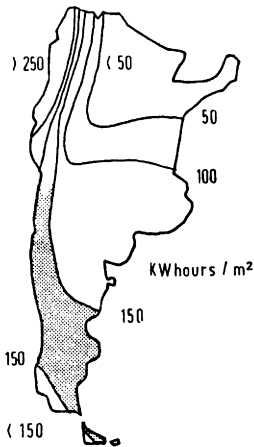


Fig.1. Useful solar heat gain.

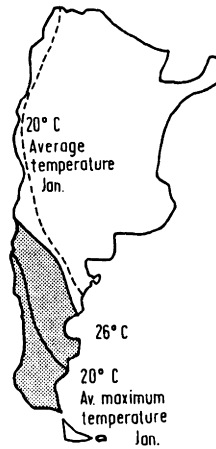


Fig.2. Avoidance of overheating.

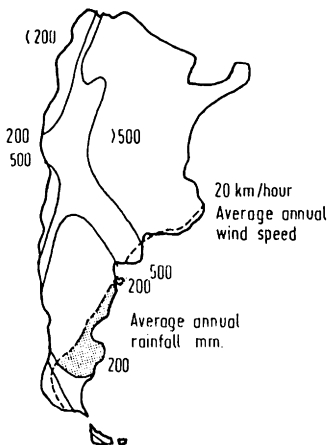


Fig.3. Wind and rain criteria.

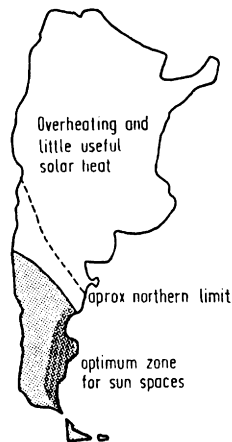


Fig.4. Zone for attached sun spaces.

## OPTIMIZING USEFUL SOLAR GAIN

The comparison between different sun space designs in the same locality indicates the design variables that influence useful solar gain, such as use of nocturnal insulation, combinations of vertical and/or inclined glazing, thermal properties of the wall between sun space and dwelling and treatment of the lateral walls of the sun space: glazed, insulated or shared with the dwelling. The following recommendations will improve solar gains though variations in useful solar gain with different designs are often small and the relative importance of alternatives also varies slightly with latitude:

1. Nocturnal Insulation: The variable that provides the greatest increase in useful heat gain is effective night insulation. This must be provided in the form of insulated shutters, which reduce night heat losses without interrupting daytime gains with open shutters. This element is especially beneficial in the far south where night temperatures are lowest. Despite the benefits, effective insulated shutters are difficult to design and costly to install, especially in the high wind speed area in southern Argentina. In practice, insulated shutters are rarely used with attached sun spaces.

2. Geometry: The geometric configuration of the attached sun space is the second most important design variable. 50' inclined glazing was found to provide more solar energy; vertical and 30' glazing give average levels and vertical glazing, (glazed galleries) provide lower levels. Although glazed galleries with vertical glazing are the least efficient as solar systems, they are the easiest to protect from sun and hail. An east facing gallery of this type has been incorporated in the solar house at Abra Pampa, with positive results (Lesino, et al, 1990). It provides useful morning heat and humidity, while avoiding midday overheating.

3. Wall between dwelling and sun space: There are three alternatives for walls between attached sun spaces and dwellings, allowing energy transfer by radiation, convection or transmission. A glazed wall transmits direct solar radiation, especially with low angle winter sun which can penetrate directly into the dwelling, after passing through the sun space. However, glazed walls transform sun spaces into rather more elaborate direct gain systems, where the main solar gain is received directly in the dwelling space. A heavy, high heat capacity wall of dense brick or concrete receives solar energy on the inner sun space wall and transmits this to the dwelling by conduction, with a time lag. An insulated lightweight wall with controllable high and low level vents allows heat transfer by convection. The evaluation shows that the convective transfer is not as effective as the conduction transfer, even when the improved insulation to reduce heat losses is taken into account.

High heat capacity walls are therefore preferred; they also avoid moving parts or controls. In practice, the three alternatives can be combined in the same wall; windows or glazed doors allow direct gain and convection, while a heavy wall provides accumulation and transmission. Glazed openings should not exceed one third of the dwelling/sun space wall and incorporate double glazing or internal insulated shutters to reduce night heat loss.

4. Lateral walls: The treatment of lateral walls also affects the efficiency of sun spaces. It was found that opaque insulated walls performed slightly better than glazed lateral walls (attached sun spaces) or lateral walls shared with the dwelling (intergrated sun spaces), though differences are not significant.



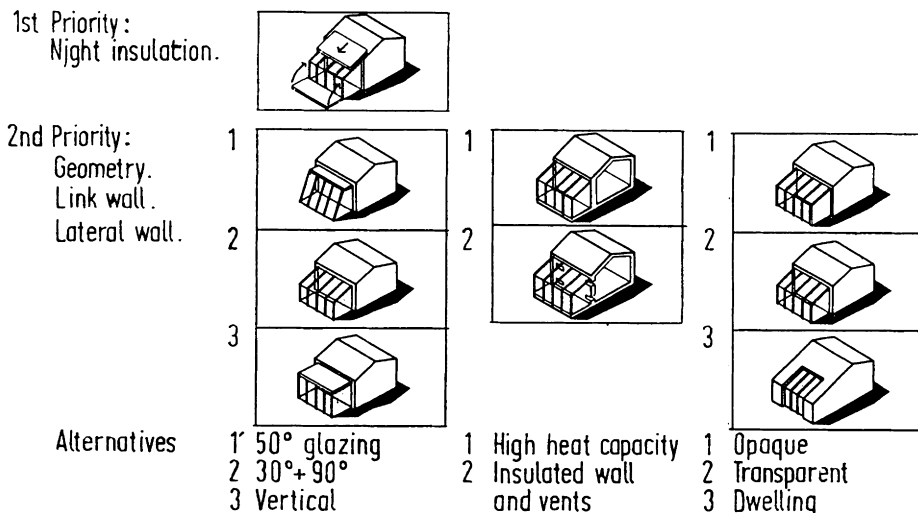


Fig. 5. Order of priority for design alternatives

#### CONCLUSIONS

Sun spaces may be difficult to justify as passive solar systems to provide partial energy to dwellings. However, they offer other advantages to improve the quality of life, especially in the inhospitable patagonian region, where they provide more useful solar energy than in other regions of Argentina. In this region summer overheating can be controlled, wind protected spaces are required and indoor plants can compensate for scarce natural vegetation.

However, the use of the sun space in different seasons depends on the duration of comfortable temperatures. High temperature swings, convection currents, partial shading and stratification make confort analysis even more complicated. A test cell has been constructed in the Faculty of Architecture to study these problems. Measurements are in progress and a computer model for the prediction of sun space performance is being calibrated. Design guidelines will be further developed when the results of measurements in the test cell and output from the model become available.

#### REFERENCES

- Balcomb D. and R. Jones (1983). *Passive Solar Design Handbook*, Vol. 3. American Solar Energy Society. Washington, D.C..
- Evans, J. M., S. de Schiller and A. Perez Anaclerio, (1989). Use of passive solar systems in high latitudes in Argentina. In *Proceedings North Sun '88* (L. Broman and M. Ronnelid, eds.) pp 245-250. Swedish Council for Building Research. Stockholm.
- Fabris, A. and E. Yarke (1986). *Tablas de Cociente Carga Colector para 60 Localidades de la Argentina*. Instituto Solar Arquitectura. Buenos Aires.
- Lesino, G., (1990 - in press). *Comportamiento de la casa solar de Abra Pampa*. In *Actas de la XIII Reunion de Trabajo, ASADES*, Salta.
- S.M.N. (1986). *Estadísticas Meteorológicas 1971-1980*. Servicio Meteorológico Nacional. Buenos Aires.

## PASSIVE SOLAR BUILDING DESIGN IN THE HUNGARIAN BUILDING INDUSTRY

DR. JUDIT PINTÉR

Technical University of Budapest  
H - 1111 Budapest, Műegyetem rkp. 3. Hungary

### ABSTRACT

The application and the result of the passive solar architecture depends primarily on the knowledge of the architect-designers and on the quality of the construction process itself too. There are new developments in the Hungarian building industry too. There has finished a new regulation which is now concentrated onto the solar technology. There has prepared a data bank of the buildings tested, which experiences are available for all the designers. there have established new educational programs for different educational levels on passive solar. There are collected the possible failures indicating the ways how to repair those. Because of the great volume of the reconstruction design, there are many instructions for these works. All these works are directed and connected by a complex marketing work which one provides the success of the program.

### KEYWORDS

Standards, informations, education, reconstruction, marketing, comfort-design.

### STANDARDS

For the modernization of the regulations there were carried on a very comprehensive research in the last few years in Hungary and as the result of it, was prepared the new prescription in 1989. The new regulation is concentrated to the solar energy. Its' requirements are given

for the specific volume of the building. With the calculation methods and data the regulation helps to determine the applicable amount of solar energy. It gives several possibilities to fulfil the energetical demands, so it urges to use the solar radiation energy on different ways / e.g.: thermal insulation /. Therefore it initiates to use the solar energy in the buildings.

#### RECONSTRUCTION

Beside the construction of the new buildings, - because of the slow increase in their volume - it is very important the problem of the existing buildings. In the same time when the solar energy systems are integrated to old buildings there is necessary to apply a control-system to control the traditional heating system. Here is one of the point, where the architectural and the building physics knowledge have to be connected. There are several methods to apply passive elements in old buildings, like insulating-shading constructions. In the case of reconstruction for example sometimes there is a need to change the flooring-system and in this case it is possible to improve the active thermal storage capacity of the buildings. By a general reconstruction can prepare a subsequent thermal insulating work, and can add a new green-house to the old building. The possibilities of the changes in the orientation of an existing building needs more modification in it's functional arrangement, but in some case this work also helps to the energy economy of the building. Such a modification is useful just in that case, if the ageing of the very building itself needs also a general reconstruction. The reconstruction work costs much more than a construction of a new building, so the results are also restricted. Therefore it needs very careful design work, because they have to count with many existing factors.

#### DATA OF THE EXISTING PASSIVE BUILDINGS

There is a need to know the proper information from the methods and possibilities tested earlier. It means, that it is an important data how the passive elements work in the real built construction, because that depends on the construction process as well. This elaboration of the data-collection was carried on in the same time of the elaboration of the new standards. These evaluations give information about the possible failures also, and orientation for the further developments and research.

## EDUCATION

For the effective work on the field of passive solar design it is needed to educate the workers in the industry, the researchers, the developers, the architects, the mechanical engineers, the contributors, the contractors at each level. This education has to be present not only at the technical field. Because of its complexity it is important to involve into this activity the problems of the economy, environment, comfort-studies, etc. The aim of the education is to give to the proper people the proper knowledge from the research and from the industry as well, as soon as possible. For this point of view it is important for the educators to have a very close connection with the industry and research institutes too.

## THE MARKETING ACTIVITY OF THE DESIGNER

The main role of the architect-designer is to facilitate the communication between the demands of the users and the products of the industry by the particular methods of the design. To fulfil this role the designer needs also information on the new products appeared in the market and about the new standards, etc. On the base of these knowledge can carry on the special solar marketing work the architect designer too.

## SUMMARY

The above complex coordinated activity is necessary for the effective passive solar building. Therefore in the building industry it needs the cooperation of different institutes, factories, companies, universities, professions.

TOWN PLANNING FOR SOLAR ENERGY  
URBAN DEVELOPMENT FOR SOLAR RIGHTS IN HIGH LATITUDES

Silvia de Schiller, John Martin Evans and Gabriela Casabianca.

Programa de Investigación "Habitat y Energía"  
Facultad de Arquitectura, Universidad de Buenos Aires,  
Pabellon 3, Piso 4, Ciudad Universitaria,  
(1428) Capital Federal, Republica Argentina.

ABSTRACT

In southern Argentina, the useful solar energy received in conventional housing and passive solar systems increases up to latitudes 47' - 50'S due to the higher heating demand and the longer heating season. This paper analyses the problems of protecting solar rights and avoiding over-shadowing at these high latitudes. Recommendations for planning criteria are given for high latitudes, based on a study of solar energy resources and heating demand in over 100 towns in Argentina from latitude 22'S to 55'S. Densities are indicated for different subdivision characteristics and design guidelines are given for solar access in high latitudes.

KEYWORDS

Building densities; high latitudes; planning codes; solar radiation; subdivisions; sunlight; Argentina.

INTRODUCTION

Continental Argentina stretches from latitude 22'S to 55'S and has a wide range of climates and varying solar energy resources according to latitude, altitude, cloud cover, etc.. This study aims to identify criteria for housing sunlight standards in these different regions, as the widespread benefit of solar energy can only be assured when there is effective building control to avoid excessive overshadowing and protect solar rights. Planning codes can ensure adequate winter sun without unduly limiting building heights and densities at latitudes up to 40'S (Evans and de Schiller, 1988a). Sunlight is more difficult to ensure at higher latitudes where winter sun is lower and shadows are longer.

This paper analyses heating requirements, solar energy resources and solar geometry in high latitudes of Argentina, where useful solar heat is available (Evans and de Schiller, 1988b). Recommended densities and design guidelines are proposed, based on the maximum dimensional building limits to control overshadowing of adjacent plots.

### EXISTING SOLAR RIGHTS AND STANDARDS

Solar rights were promoted in the United States during the 1970's, to ensure that collectors were not overshadowed by adjacent buildings. Since these were often placed on roofs, some proposals emphasised solar rights for this surface (Arumi and Dodge, 1977). Later studies proposed similar safeguards for fachades, with reduced solar exposure (Knowles, 1981).

Sunlight standards for housing, which are used in most of northern european countries since the 1950's, usually require 1 or 2 hours of direct sun in a proportion of habitable rooms on a specified date with additional conditions such as maximum angles of incidence and minimum solar altitude. Low sun has weak radiation intensities and may be blocked by distant obstacles, while high angles of incidence reduce radiation transmitted through glazing and wall thickness may shade direct sun.

An analysis of these existing standards and proposals indicates that they often depend on latitude and availability of direct sunlight. In high latitudes with increased winter cloud cover, dates further from the winter solstice are chosen and fewer hours of sun are required. Minimum sunlight hours also depend on solar energy use: flat plate collectors and passive solar systems require more sun than domestic windows.

### ZONES FOR THE APPLICATION OF SOLAR RIGHTS IN ARGENTINA

Information on the heating demand and solar energy availability (S.M.N., 1986; Pracchia et al., 1986) was prepared for 113 localities in Argentina, using monthly data of solar radiation, heat demand, latitude, altitude, etc.. This data was used to determine regions where similar conditions indicate the need for common responses to "solar access". Heat demand and solar radiation during the four winter months were studied. Two climatic criteria, radiation and degree days, coincided with locational criteria, latitude and altitude, to define 6 zones, shown in Table 1 and Fig. 1.

Table 1. Zones for the application of solar rights in Argentina.

Zone	Solar radiation	Degree days	Latitude	Altitude
Zone 1	> 6 KJ/m <sup>2</sup>	> 150 / month	22'S to 30'S	> 1000 m
Zone 2	> 4 & < 6 KJ/m <sup>2</sup>	< 150 / month	22'S to 30'S	< 1000 m
Zone 3	> 6 KJ/m <sup>2</sup>	> 220 / month	30'S to 38'S	> 600 m
Zone 4	> 4 & < 6 KJ/m <sup>2</sup>	150-220 / month	30'S to 38'S	< 1000 m
Zone 5	> 3 & < 6 KJ/m <sup>2</sup>	> 220 / month	38'S to 47'S	-
Zone 6	< 4 KJ/m <sup>2</sup>	> 400 / month	47'S to 55'S	-

### DEVELOPING CRITERIA FOR SOLAR RIGHTS

Studies were made of typical subdivisions and existing private sector and government financed projects to determine the range of typical plot sizes, set-backs from plot boundaries and critical relationships for receiving sunlight in corner plots. A spread sheet was used to calculate maximum plot ratios, building densities and population densities according to plot sizes, sunlight standards, floor heights, building depths, set-backs, height plot boundary walls and space standards. These variables apply the limiting planes from Table 2, which indicate the maximum dimensional limits of buildings to avoid overshadowing of adjacent buildings and plots.

Table 2. Angles of inclined planes that form the solar envelope to provide 2 hours of direct sunlight.

Date	Latitude	Orientation of the plot boundary; east or west of north.										
		0	10	20	30	40	50	60	70	80	90	100
22/6	54.8	-	-	-	11	12	14	10	-	-	-	-
	53.8	12	12	13	13	15	15	13	-	-	-	-
	51.6	14	14	15	17	19	18	16	13	-	-	-
	49.3	16	16	18	20	22	21	19	15	-	-	-
	47.7	18	18	20	23	24	23	20	17	-	-	-
	45.0	20	21	23	26	27	25	24	20	15	-	-
42.0	23	24	26	30	30	29	26	23	17	12	-	
15/7	54.8	12	13	14	15	17	16	15	-	-	-	-
	53.8	13	14	15	17	18	18	16	10	-	-	-
	51.6	16	16	18	20	21	20	18	15	-	-	-
	49.3	18	19	20	23	24	22	21	17	-	-	-
	47.7	20	20	22	25	25	24	23	19	14	-	-
30/7	54.8	16	16	18	20	21	20	18	15	-	-	-
	53.8	17	17	19	22	22	21	19	16	-	-	-
	51.6	19	20	22	24	24	23	21	18	14	-	-
	49.3	21	22	24	27	27	26	23	21	16	-	-
	47.7	23	24	26	29	29	28	25	22	17	10	-

Notes: Minimum solar altitude = 10'. Maximum angle of incidence = 67.5

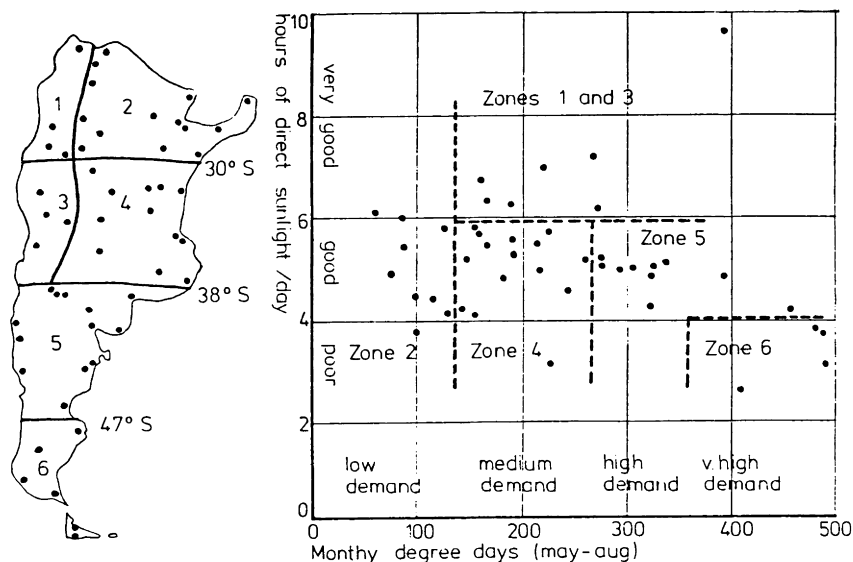


Fig 1. Regions for the application of solar access standards  
a). Solar regions (Table 1), b). Radiation and degree days.

Walls at the plot boundary will shade part of the plot. With partial shading, higher densities can be achieved, so two cases were considered:

- i). Without walls at the plot boundaries, planes start at 0,0 m.
- ii). Walls at plot boundaries, planes start at a height of 2,5 m.

In Zones 1 to 4 (latitudes up to 38'S), reasonable densities for housing layouts can be achieved with 2 hours of sun, as high angle sun does not require wide spaces between buildings on the winter solstice. 4 hours of direct sunlight may be received at medium residential densities, but 6 hours of sun requires limitations of orientation: North +/- 30'.

In Zone 5, solar access is more difficult as planning limitations are more restrictive. It is still possible to receive mid-winter sun though this will result in reduced densities, especially in the south. Densities and building heights have to be progressively decreased as latitudes increase.

In zone 6, it is very difficult to achieve a standard of 2 hours of sun on principal building fachades during the winter solstice with reasonable residential densities: possible orientations are also restricted. The date for establishing sunlight standards and maximum densities must be adjusted to achieve a balance between economy, sunlight and other design factors.

Table 3 shows the plot densities that can be achieved using inclined planes from Table 2 to form an envelope for a typical plot. Two cases are presented: free-standing buildings with set-backs from all site boundaries and buildings with party-walls on both lateral boundaries as shown in Fig.2. Free standing buildings in small plots must have low densities to allow direct sunlight in adjacent plots; plot sizes should exceed 20 m x 40 m to achieve useful densities. Solar envelopes for buildings with party walls allow plot ratios between 1 and 2, even in high latitudes.

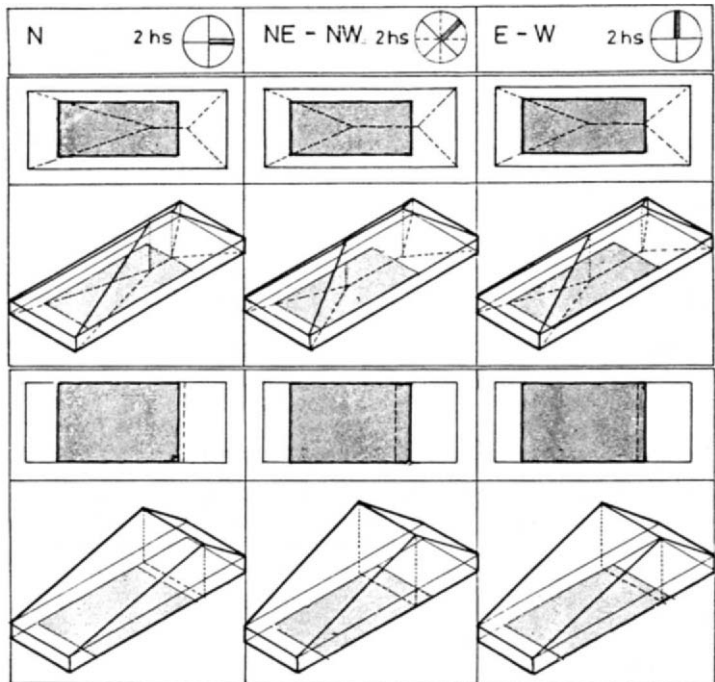


Fig 2. Examples of solar envelopes in Rio Gallegos, latitude 50'S to allow 2 hours of sun in adjacent plots at 2.5 m.



### RECOMMENDATIONS FOR SOLAR STANDARDS IN HIGH LATITUDES

The following recommendations are based on our studies of building form and density in relation to sunlight on fachades with different orientations:

All housing should receive at least 2 hours of direct winter sunlight through windows in main fachades. At least half of the habitable rooms of each dwelling, including the living room, should have windows on this fachade. Dates (and solar declination) for verifying winter sun are as follows: between lat. 52'S and 55'S (Tierra del Fuego), July 30 (18.42); between lat. 48'S and 52'S (south of Santa Cruz Province), July 15th (21.52); north of lat. 48'S (centre and north of Santa Cruz Province), winter solstice: June 22 (23.45).

These windows should be placed in north facing fachades, with a maximum deviation of 70' to the E or W of N to receive 2 hours of sun. Direct sun is not considered useful and is discounted when the angle of incidence exceeds 67.5' or when the solar altitude is below 10'.

When buildings are grouped in parallel rows, the relation between building height and distance between buildings should allow an angle of 15' between a horizontal plane and an inclined plane projected from the sill of the window to the highest point of the roof of opposite buildings. Windows orientated between 20' to 60' E or 20' to 60' W, allow reduced distances between buildings, with a plane inclined at 18'. Alternatively, houses may be designed to receive 1 hour of sun on E and W fachades with limiting inclined planes of 15' on both sides of the building. Streets with continuous rows of buildings orientated E-W will have permanent shade in winter, and may suffer from ice and snow accumulation. Spaces between parallel buildings with a NE-SW or NW-SE orientation will have more direct sunlight.

In collective housing projects, as opposed to single family dwellings in individual plots, up to 10% of the dwellings may receive less than 2 hours of direct sunlight, if this allows other benefits such as closer grouping for energy savings or wind protection. These dwellings must have a view onto a space with a minimum of 2 hours of direct winter sunlight.

With complex building forms or special cases, graphical methods or model studies may be used to test and improve direct sunlight standards. Using these methods, it may be possible to achieve slightly closer grouping of buildings than that indicated in these general recommendations.

Table 3. Range of building density (building area as a proportion of net site area) for typical residential plots.

Building type: Boundary wall height:	With free perimeter		With lateral party walls	
	0 m	2.5 m	0 m	2.5 m
Zone 1 and 2	0.1 - 0.5	0.7 - 1.0	1.0 - 2.0	1.0 - > 2.0
Zone 3 and 4	0.1 - 0.5	0.7 - 1.0	0.5 - 2.0	1.0 - > 2.0
Zone 5	0.1 - 0.5	0.7 - 1.0	0.5 - 2.0	1.0 - > 2.0
Zone 6	0.1 - 0.5	0.7 - 0.9	0.3 - 0.9	1.0 - 2.0
Plot characteristics:	Plot	15 x 40m	Plot	10 x 40m
	Side building line	1.2m	Side building line	0.0m
	Front building line	3.0m	Front building line	3.0m
	Back building line	8.0m	Back building line	8.0m

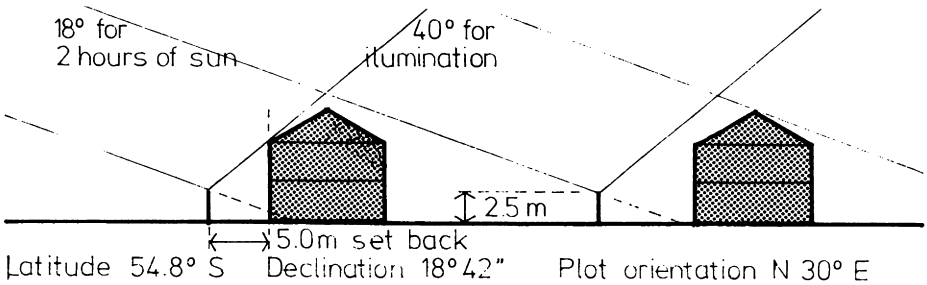


Fig. 3. Use of inclined planes to form solar envelopes.

### CONCLUSIONS

Planning controls to ensure reasonable standards of sunlight in urban areas must be based on simple evaluation criteria and allow acceptable densities and forms of urban development. This study shows that simple building controls can be incorporated in planning codes to obtain established levels of sunlight in latitudes from 38°S to 55°S. These standards can be applied in low and medium density residential areas without restricting existing forms of building development. The next stage of the study is the drafting of standard clauses for planning codes in different zones and discussions with municipal authorities with a view to incorporating these criteria in current planning legislation.

### ACKNOWLEDGEMENTS

The authors of this paper acknowledge the support of ENTECAP (the National Authority responsible for the proposed New Capital project) for the initial studies on solar rights and the research fellowship granted by Buenos Aires University to develop further solar access studies.

### REFERENCES

- Arumi, F. N. and L. R. Dodge (1977). The formal implication of solar rights. *Energy and Buildings*, 1, 183-191.
- de Schiller, S. and J. M. Evans (1988). Healthy buildings in a new city: Bioclimatic studies for Argentina's new capital. In *Healthy Buildings '88* (B. Berlund and T. Linvall eds.) Vol I, pp 121-131, Swedish Council for Building Research, Stockholm.
- Evans, J. M. and S. de Schiller. (1989). Use of passive solar systems in the high latitudes of Argentina. In *Proceedings North Sun '88* (L. Broman and M. Ronnelid, Eds), pp 245-250, Swedish Council for Building Research, Stockholm.
- IRAM 11,603 (1980). Acondicionamiento termico de edificios: clasificacion bioambiental de la Rep. Argentina. Instituto Argentino de Racionalizacion de Materiales, Buenos Aires.
- Knowles, R. L. (1981). *Sun Rhythm Form*. M.I.T.Press, Cambridge, Mass.
- Pracchia, J., A. Fabris y A. Rapallini. (1987). Tablas de datos meteorologicos para 118 localidades. Actas de la XII Reunion de Trabajo de ASADES. ASADES, Buenos Aires.
- S.M.I. (1986). *Estadisticas Meteorologicas 1971-1980*. Servicio Meteorologico Nacional. Buenos Aires.

## THE APPLICATION OF THE DOUBLE ENVELOPE STRUCTURE WITH CONVECTIVE LOOP IN A PASSIVE SOLAR BUILDING

Liu Antian  
Wu Xiangsheng  
Liu Yi

Department of Management Engineering, Logistics Engineering  
College, Chongqing, Sichuan, China

### ABSTRACT

This paper discusses the application of the double envelope structure with convective loop in a passive solar building. That is, the stable air in the double envelope loop is changed to circulating air moving through the passage. Natural convection from a south facing Trombe wall carries the heated air up through the space in a double-skinned roof. The moved air then passes down through the north wall to an underground thermal rock storage bed. At night, single direction dampers prevent the air from reversing. Thus, the air gap acts as an additional sealed thermal insulation. Practical survey indicates that the passive solar building adopting double envelope structure has good heating effect. This method is an advanced and rational one that incorporates direct gain and convective loop methods.

\* \* \* \* \*

Passive solar heating system is the solar heat using system which incorporates the building and the heating facility as one. In winter, this system can collect, storage and distribute solar heat effectively. In summer, it can obstruct solar radiation and dissipate the heat excess. In designing of the passive solar building, the following should be dealt with correctly:

- a. To reduce heat loss, carry out the insulation design properly.
- b. Install sufficient solar heat collectors on the south wall.
- c. Install sufficient heat storage devices in the building.
- d. Arrange the heating room against the collectors and storage devices.

In accordance with these principles, the authors developed a double envelope structure heating model first in China. Test data indicated that this new type of passive solar building had good heating effect.

### 1. DOUBLE ENVELOPE STRUCTURE

The double envelope structure with convective loop is shown in Fig.1. It contained the improved Trombe wall, the double envelope convective loop and the underground thermal rock storage bed. The double envelope convective loop was built within the roof and north wall. Therefore, the improved Trombe wall, the roof, the north wall and the space above the rock bed formed a circulating air passage. In sunny day, natural convection from the south facing Trombe wall carried the heated air up through the convective loop in the roof. The moving air then passed down through the convective loop in the north wall to the underground rock storage bed. In its circulating process, the heated air heated the walls.

Thus, the wall temperature was raised. The heat excess was stored in the rock bed for the use in cloudy days. The circulation of air could be natural convection. It also could be forced convection created by small-sized fans. Therefore, in designing of the double envelope structure with convective loop, the resistance of the air circulation should be reduced as low as possible. In constructing of the double envelope structure, clog or block of the convective loop must be avoided. In the night, single direction dampers installed in the convective loop prevented the air from reversing. The air in the circulating passage acted as an additional thermal insulation layer, thus reduced the heat loss.

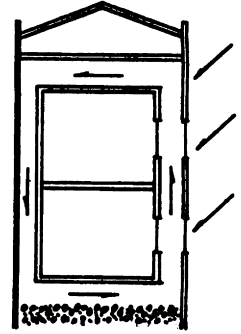


Fig.1 double envelope structure with convective loop

Compared with the direct solar heating system, double envelope structure heating system not only made more use of the heat gain of windows but also strengthened the insulation of walls. Therefore, good indoor temperature stability was achieved. Compared with the traditional Trombe wall, this new heating system had the heat collecting function of convective loop but need not build special heat storage wall. Because of the circulation of the heated air, temperatures of the four sections of the surrounding structure were raised and the comfort condition of the building was improved.

2. THERMALTECHNICAL TEST

In order to examine the heating effect of the double envelope structure with convective loop, two winter thermal condition tests and one summer thermal condition test were conducted. These tests were carried out before the passive solar building went into use, on the condition that there was no supplementary heat sources. Fig.2 shows the daily maximum and minimum temperatures of the standard room (referred to the room heated by the double envelope

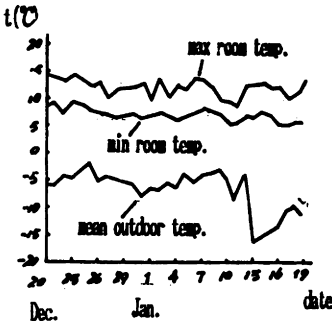


Fig.2 Daily max and min room temperatures and daily mean outdoor temperatures of the standard room

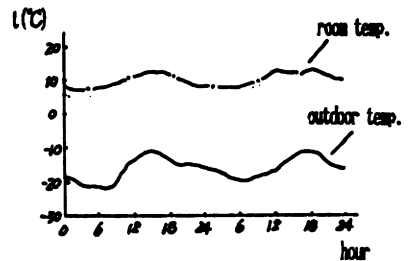


Fig.3 The hourly temperature of the standard room in two days (Jan.13-14, 1989)

structure with convective loop) and the daily mean outdoor temperature. The figure indicates that the highest fluctuation of room temperature was  $6^{\circ}\text{C}$ . Therefore, the standard room had good temperature stability and fine heating effect. The hourly temperatures of the standard room in two days are given in Fig.3. The maximum difference of room temperature and outdoor temperature was more than  $25^{\circ}\text{C}$ . In view of this, the standard room had good heating effect ---- the improved Trombe wall absorbed solar heat effectively, and the double envelope structure with convective loop had good insulating function. Fig.4 illustrates the hourly temperatures of the north wall's interior surface of the standard room and the compared room (referred to the solar heating room which did not possess the double envelope structure). As Fig.4 shown, at night, the temperature of the north wall's interior surface of the compared room was higher than that of the standard room. It was because that the higher heat loss of east breast wall made the air temperature of the standard room decreased, thus resulted in lower surface temperature. In the daytime, temperature of the north wall's interior surface of the standard room was higher than that of the compared room. It was because that the moving air in the double envelope convective loop heated the north wall of the standard room. The heated wall then heated room or reduced the heat loss. Therefore, higher room temperature was acquired. Fig.5 shows the maximum temperatures of the standard room and the compared room in ten days. Test results made known that in summer, overheating could be avoided completely if windows were timely opened for ventilating.

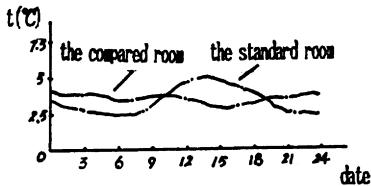


Fig.4 Hourly temperatures of the north wall's interior surface of the standard room and the compared room (Jan.13, 1989)

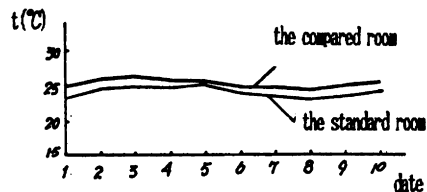


Fig.5 Max indoor temperatures of the standard room and the compared room in ten days (August, 1988)

### 3. CONCLUSION

Test results proved that the double envelope structure with convective loop heating system was an advanced and rational heating system. It had such characteristics like,

1. Ordinary solar building uses solid material as insulating layer, but the double envelope convective loop structure changed the fixed layer to air layer. In the daytime, the moving air heated the room and the heat excess was stored in the rock bed. In the night, single direction dampers installed in the convective loop prevented the air from reversing. The air layer acted as an

night, single direction dampers installed in the convective loop prevented the air from reversing. The air layer acted as an additional thermal insulating layer, thus reduced the heat loss. Compared with the direct solar heating system, the double envelope convective loop heating system either satisfied the need of heating, or raised the temperature stability of the building.

2. The double envelope convective loop structure depended on natural convection to carry the heat gain. The surrounding structure of room was heated by the moving air and the surface temperature of the wall was increased. This led to even temperature field and comfortable condition.

3. The advantage of sunspaces is that it can be used as the buffer area to reduce heat loss. But it takes some of the architectural area. The double envelope convective loop structure also had the advantage of reducing heat loss and by constructing this structure, architectural area was put to a better use.

4. In summer, overheating could be completely avoided if the windows were timely opened for ventilating.

#### REFERENCES

- (1) Liu Antian and Wu Xiangsheng, A Passive Solar Heating Building Adopting Attached Sunspaces or Double Envelope Convective Loop, Meeting Trans. of Solar Energy Applications in Developing Countries, 1989.
- (2) Qu Zhenliang, Designing of Passive Solar Building, 1987.
- (3) Guo Xiaoguang, Design and Usage of the No.1 Solar Building in Weifang, China, Acta Energiæ Solaris Sinica, Vol.6, No.2, 1985.
- (4) Wu Xiangsheng and Liu Antian, Discussion of the Heat Gain Ways of Passive Solar Building, Annual Meeting Trans. of H.V.A.C. of the Southwest District of China, 1989.

# SUPER-INSULATED WINDOWS WITH SILICA AEROGEL

NICK BJØRN ANDERSEN and LARS OLSEN

Dept. of Energy Technology and Dept. of Building Technology,  
DTI, Danish Technological Institute  
P.O Box 141, DK-2630 Taastrup, Denmark

## ABSTRACT

Development of a prototype double-glazed window with evacuated silica aerogel filling, which can give major impact on low energy building construction, retrofitting and architecture, is described. The influence of silica aerogel windows on the energy consumption in houses has been investigated.

The contribution is an evacuation technique and edge sealing, which can sustain the vacuum within the window pane and thus partly ensure its insulating properties and partly protect the aerogel from absorption of atmospheric moisture. The edge sealing is carried out by a technique, giving reduced heat loss through the edges.

The center U-value obtained was below  $0.7 \text{ W}/(\text{m}^2 \cdot \text{K})$ , which is twice as good as the best industrial products.

## KEYWORDS

Silica Aerogel; Evacuation; Window pane; Passive Solar Energy; Insulation

## INTRODUCTION

The fragile, ultra-porous and highly insulating glass material *silica aerogel*, first produced at the American Stanford University in 1931, seems to be on the way to practical usage in windows, solar collector panels and solar walls. In the latter half of the 1980's, interest began to arise in utilizing aerogel as a transparent heat-insulation material. This has, inter alia, occurred as a result of development projects at the Technical University, Lund, Sweden, and has then resulted in a commercial production by the Swedish company, Airglass AB (Sten Henning, 1990).

Airglass AB has within recent years made great progress in the process of producing a more handy, highly transparent aerogel, which is suitable as a practical, insulating layer, between two ordinary glass panes.

Several R&D Institutes are interested in the implementation of transparent insulation material, also The Danish Thermal Insulation Laboratory at the Technical University of Denmark, where an aerogel-based solar collector has been constructed (Svendsen and Jensen,1987). It was the Danish Ministry of Energy's EFP research programme which finally gave significant impetus to Danish research of aerogel's potential in buildings. Finance from such research programmes has enabled the Danish Technological Institute's departments for Energy Technology and Building Techniques to cooperate in development of a 55 x 55 cm prototype window pane on the basis of a 15 mm thick aerogel tile produced by Airglass AB in a construction protected by a 4 mm thick glass pane on both sides.

If the current well-founded hopes for a continued development of silica aerogel are fulfilled, the material can thus become one of the key elements in fulfillment of the anticipated energy-political aim towards reducing consumption of fossil fuels (Andersen,1988).

## SILICA AEROGEL

The principal component of silica aerogel is the same as that of ordinary glass - silicon dioxide, which is the main constituent of beach sand. Silica aerogel is monolithic and amorphous with a certain inhomogeneity. The solid material, which only forms a small fraction of the volume, consists of fine particles of almost pure silicon dioxide. The main part of the volume is air.

The basis for production is a jelly of silicon dioxide particles and liquid alcohol. During the normal production process, the alcohol is withdrawn in an autoclave at a temperature of 270°C and at a pressure of approx. 90 bar (Henning,1990). The material is produced with densities ranging from approx. 70 to 250 kg/m<sup>3</sup>. Changes in density will change the properties significantly.

The density of the aerogel used in this context was around 110 kg/m<sup>3</sup>.

The material is quite brittle and fragile, but developments are in progress making the material more elastic. The compressive strength is 3-4 bars, which is enough to withstand vacuum. The modulus of elasticity is about 10 MPa at a density of 100 kg/m<sup>3</sup>.

### Solar transmission

The material is characterized by a very low index of refraction, approx. 1.02 to 1.04. As a result, aerogel behaves nearly like air concerning reflections at surfaces. The absorption of the spectra of solar radiation is also very small but some scattering in the aerogel occurs (Hunt and Berdahl,1984), which gives a slight colouring of the material. Viewed against a dark background the material seems slightly blue and against daylight it seems yellow.

### Thermal transmission

Apart from the density, the transmission of heat in silica aerogel is dependant on the internal air pressure. The main part of the possible reduction in thermal conductance is obtained at a pressure below 100 mbar. Thermal radiation is transmitted through aerogel thus contributing to the overall thermal transmission. This can be expressed by means of an apparent thermal conductivity, which is shown in fig. 1.



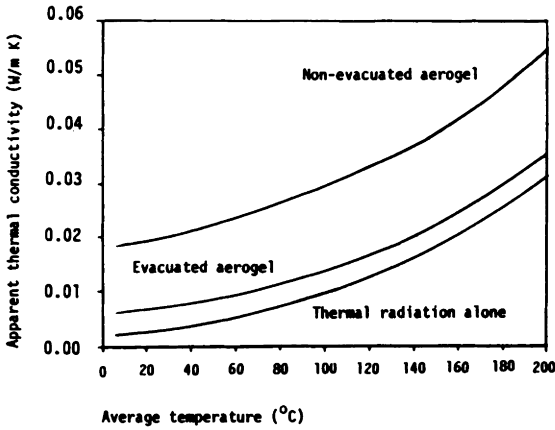


Fig.1 Apparent thermal conductivity versus mean radiative temperature for silica aerogel. Assumption: emissivity of glass on both sides.

The radiation term will take into account the emissivity factor of the glass facing the aerogel. The size of this term depends strongly on a mean radiative temperature in the construction (Caps and Fricke,1986). As an insulating material, even non-evacuated aerogel is better than other known materials.

The solar transmittance as a function of the angle of incidence is shown in fig. 2 .

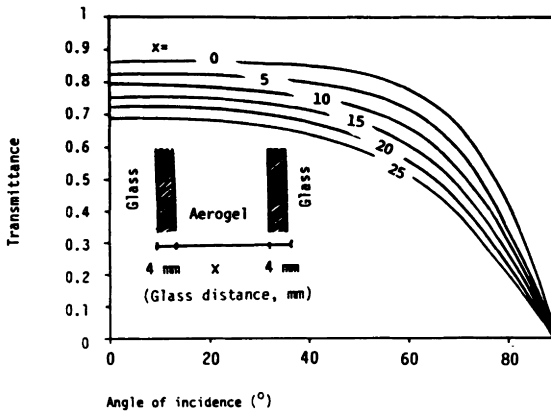


Fig.2 Solar transmittance versus angle of incidence. Parameter: X = glass distance in [mm].

## OPTIMIZING AEROGEL WINDOW PANES

The advantages of aerogel materials for window applications are: good solar transmission, very low heat transmission and a fair, perhaps also acceptable visual transparency. Using thicker aerogel tiles, it is possible to obtain U-values as low as required. However, thicker tiles at the same time reduce the amount of transmitted light and energy. Construction of aerogel based window panes is thereby affected by both effects in order to optimize the performance. The sealing of the two panes and the window frame must be paid great attendance, as cold bridges easily can spoil the good center U-value of the window.

For comparison it can be suitable to describe the performance of window panes by a resultant U-value, which incorporate the solar gains. This U-value is specific for the actual window construction, orientation and surroundings. Thus, the value are only valid for a certain window in a certain building. In fig. 3 are shown the resultant U-values for southfaced windows with the heat capacity factor of the house as a parameter. The heat capacity factor, which is between 0.0 and 1.0 expresses the ability to use the solar gains. Conventional new danish houses are meeting a value of about 0.5, an extremely heavy house will meet a value of 1.0 . It is seen in fig. 4 that a minimum of resultant U-value is reached with an aerogel thickness of 16-20 mm for southfacing windows.

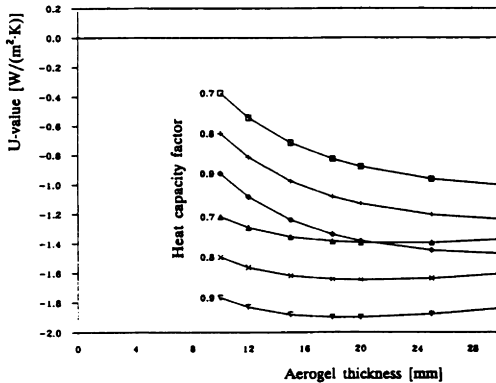


Fig.3 Resultant U-values for aerogel panes versus aerogel thickness. Heat capacity factor of the house 0.7-0.9; Non-evacuated (3 upper curves), Evacuated (3 lower curves).

A study has also been made in order to evaluate the effect of aerogel windows on the annual net energy consumption in traditional detached houses and in low energy houses with heavy constructions and with a lot of southfacing windows. Assuming that the internal heat production from people etc. is used before taking advantage of the passive solar gains, several simulations have been made. The computed consumptions shown in fig. 4 do not include domestic hot water, neither electricity.

It is seen from this figure, that an adequate thickness of aerogel is 10-15 mm. From an economic point of view the lower thickness, perhaps 10 mm, can be appropriate, whereas from a technical point of view about 15 mm of aerogel was chosen for prototype production.

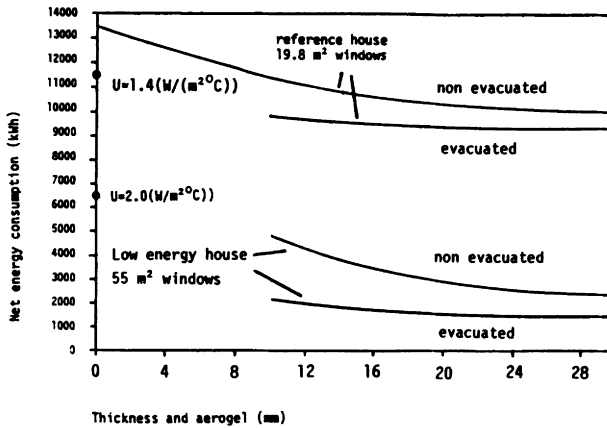


Fig.4 Reduction in energy consumption in houses with evacuated and non-evacuated aerogel windows.

#### PROTOTYPE PERFORMANCE

With the aim of producing an evacuated window pane with silica aerogel filling, research has been carried out on adequate sealing methods and evacuation processes. The seal chosen is in principal based on existing standard isobutanol rolls combined with a metal film; the latter to prevent diffusion through the seal. Some preliminary results (Andersen,1988) pointed out that aerogel between two glass panes was difficult to evacuate through holes in the edges due to insufficient air permeability. The prototype, therefore, was produced in a vacuum chamber. When a sufficient low vacuum was obtained within the chamber, assembling of the second glass pane took place with a remote controlled instrument. One advantage of the technique utilized is, that it does not leave holes in the sealing edge. An evacuated window pane, produced in this way with an aerogel thickness of 14.5 mm is shown in fig. 5 .

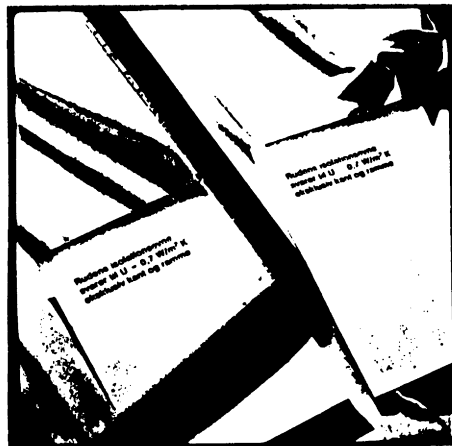


Fig.5 Two identical papers, one behind an evacuated aerogel window pane.

It has not been possible to measure the obtained absolute vacuum in the construction after leaving the vacuum chamber, but a measure of the level of vacuum is indirectly given by the measured center U-value. By use of two evacuated window panes with silica aerogel sized 55 x 55 x 1.5 cm. the U-value was measured in a guarded hot box construction giving as a result a U-value of 0.7 W/(m<sup>2</sup> K).

In order to check the durability of the vacuum seal, the weight of the construction is measured regularly. Until present, no longterm increase in the weight have been introduced.

## DISCUSSION

The center U-value of a prototype has been found to be lower than 0.7 W/(m<sup>2</sup>·K), excluding heat loss through the frame edge. This is twice as good as the very best thermal windows on the market, and four times better than traditional double-glazed windows. Utilization of such aerogel window panes comprises significant energy savings, since calculations show that heat loss through windows at present amounts to a quarter of the total heat loss from buildings.

Aerogel is still a very brittle building material and difficult to produce in a usable form. Even though the aerogel prototype window pane approaches the demands which should be met for clarity, the visual transparency of silica aerogel still cannot tolerate comparison with ordinary window glass. Variations in pore size and particle size cause a certain light scattering. In addition, non-uniform thickness of the aerogel tile causes disturbances in visual transparency. Improvement of the aerogel material is necessary. Airglass AB are working on development of an even clearer aerogel.

The edge solution is under development, because the need for avoiding thermal bridges increases at the same rate as the insulation properties of the window pane.

On a long term basis, DTI is seeking extended industrial cooperation concerning development of commercial aerogel products.

## REFERENCES

- Henning, S. (1990). *Airglass - Silica Aerogel*, Swedish Council for Building Research, Stockholm.
- Svensden, S. and K.I.Jensen.(1987). Flat Plate Solar Collector with Monolithic Silica Aerogel. From: ISES Solar World Congress 1987, Hamburg
- Andersen, N.B. (1988). Aerogel Window Panes - Energy Savings in Houses. In: *Transparent Insulation in Solar Energy Conversion for Buildings and Other Applications*. Proceedings of the 2nd International Workshop in Freiburg, F.R.G. (L.F.Jesch, Ed.), pp. 17-19.
- Hunt, A.J. and P.Berdahl (1984). Structure Data for Light Scattering Studies of Aerogel. Materials Research Society. *Better Ceramics Through Chemistry*, Vol. 32. Brinker, Clark and Ulrich, North holland, New York
- Caps, R and J. Fricke (1986). Radiative Heat Transfer in Silica Aerogel. In: *Aerogels*. Proceedings of the First International Symposium, Würzburg, Fed. Rep. of Germany September 23-25, 1985. Proceedings in Physics 6. J.Fricke, Ed. ,Springer-Verlag, Berlin, Heidelberg, New York, Tokyo.

APPLICATION OF ENVIRONMENTAL ENGINEERING TO THE  
DESIGN OF MOSQUES IN SAUDI ARABIA

PROFESSOR D J CROOME

Department of Construction Management, University of Reading  
Whiteknights, PO Box 219, Reading RG7 2BU, UK.

ABSTRACT

Throughout history mosques have been built which reflect the sanctity of their use. Modern technological solutions can sacrifice simplicity and produce noise, dirty conditions and an increased need for maintenance. Solutions which respect the environmental needs of a mosque are discussed.

KEYWORDS

Comfort; thermal adaptation; acoustical environment; lighting.

APPLICATION OF ENVIRONMENTAL ENGINEERING IN THE DESIGN OF  
MOSQUES IN SAUDI ARABIA

The aim is to produce an environment offering simplicity, dignity and spiritual quality that is conducive to meditation and concentration. The spaces should be quiet, shaded, airy and without distraction while being efficient in operation and easy to maintain and clean.

These ideas can be achieved by an environmental design that considers the natural response of the Mosque to the environment, a response that can be modelled and controlled by the use of mass, form, height and materials to moderate the extremities of climate. Daylight and fresh air must be brought into the building for it to function and this involves the punctuation of the building fabric by discrete openings and channels which must not allow the ingress of noise and dust.

The area climate of Riyadh is characterised by being part of the Central Arabian anti-cyclone. The air mass is polar continental, generally in a SE direction over the dry land mass to the North, thus there is very little cloud cover and rainfall; the sun shines intensely and continuously; the air flowing over the arid land to the North is intensely hot. The combination of clear sky and dry land produces high mid-day air temperatures with frequent peaks of 50°C and average peaks of 46°C. During the night, high radiation to the clear sky from the dry land produces 'low' night temperatures. In summer the day-night temperature

range is about 10°C but in winter this may be as high as 25°C. During the day the ground is heated by solar radiation and the air nearest the ground acquires the highest temperature. In calm conditions the air within 2m of the ground remains stratified in layers of differing temperatures. Mixing of the hotter and cooler layers take place as the heat build up of the lower layer becomes great enough to cause an upward eddy of warmer lighter air, causing local dust storms. At night the ground loses heat by radiation and after sunset its temperature falls below that of the air and the direction of heat flow is reversed from the air to the ground. This phenomenon is known as temperature inversion.

The direction of the wind, the hot land mass which it travels over and the absence of rainfall result in very dry conditions during the summer months and evaporation rates are rapid.

The above statements are general and a study of local conditions are required to determine 'site' parameters. However some general statement can be concluded for the designers to include in their analysis of building form and construction.

- PEAK TEMPERATURES 50°C  
AVERAGE PEAKS 46°C
- INTENSE RADIATION  
900-1000 W/m<sup>2</sup>
- VERY LOW HUMIDITY LEVELS  
DURING SUMMER
- LOCAL DUST STORMS
- COOL CALM NIGHTS
- CLEAR SKIES, PRODUCING  
UNCOMFORTABLE GROUND  
GLARE
- LARGE DIURNAL TEMPERATURE RANGE
- VERY LITTLE RAINFALL AND ONLY  
DURING OCTOBER TO MARCH  
(100 mm PER YEAR AVERAGE)

#### Mass, Materials and Building Construction

A Mosque in Saudi Arabia is used for prayer five times each day at Sunrise (Fajr), Noon (Dhuhr), Mid-afternoon (Assr), Sunset (Maghreb) and Night (Isha), each prayer time lasting approximately twenty minutes. The Friday sermon during Noon prayer lasts approximately one hour. This intermittent occupancy suggests the use of the traditional thick construction with a dense inner structural leaf to absorb the short-term variations in solar gain. A moderately high level of insulation behind the inner leaf will reduce the temperature to which the inner surface is subjected. The outer leaf will be of medium weight material which provides a balance between

insulation properties and thermal storage effects. The fabric should provide a barrier to the flow of heat such that a thermal time lag of 10-12 hours is achieved. If the Mosque was airconditioned this would greatly reduce the cooling load by limiting it to internal gains and the requirements of fresh air for the occupants.

### Thermal Comfort

The internal environment of the Mosque needs to feel cool. Comfort conditions will vary from person to person but field studies carried out throughout the world have shown a close relationship between the preferred indoor temperatures and the mean outdoor temperature. This data provides a background of experience against which to consider indoor temperatures for the Middle East.

Higher temperatures are acceptable in spaces with transitory occupancy. Such spaces are often useful in many types of buildings in order to provide a buffer zone between warm outside conditions and the cooler ones inside thus allowing a gradual acclimatisation thereby avoiding thermal shock. Where a buffer zone is provided the temperature differential between outside and inside should be limited to about 15°C.

Normally internal temperature swings are limited to about 2 to 4 deg C to take into account economic considerations for the building structure and plant provisions but higher temperature swings are permissible in spaces with intermittent occupancy.

In hot-arid climates the band of comfortable internal temperature  $\theta$  is wider than that experienced in Europe. The light clothing worn in the Middle East means that higher temperatures are acceptable physiologically and these can be estimated using the equation:

$$\theta = 37 - M [0.05 + 0.7 (R_{cl} + 0.113)]$$

Where  $R_{cl}$  is the clothing resistance and  $M$  is the metabolic rate. People praying will have a metabolic rate of about  $M=60 \text{ W/m}^2$  and their clothing will have a thermal resistance of about  $R_{cl} = 0.047 \text{ m}^2\text{C/W}$  thus an acceptable temperature would be:

$$\theta = 27.3 \text{ deg. C}$$

In practice airconditioning systems in the Middle East are usually designed to temperatures of between 22 and 26°C in accordance with Western practice for continuously occupied spaces assuming the metabolic rates and hence the degree of activity is the same. There has been a fashion recently to imitate this practice for a building like a Mosque using airconditioning. Mechanisation needs maintenance, space and is often dirty and noisy - the opposite characteristics of purity, tranquility and serenity are needed in Mosques.

Internal relative humidity is also related to external conditions. When the outside relative humidity is low as in Riyadh, then the inside relative humidity should also assume lower values in the order of 45 to 50% but for coastal locations with high humidities the inside values will

be relatively higher.

Relative humidity affects the body sweat rate and this is an important mechanism for body heat loss especially when the internal temperature rises above about 26 deg.C. But again a broader tolerance is permissible for transitory occupancy.

Air movement is also important to disperse heat and moisture but care should be taken to avoid draughts. Ventilation should be sufficient to dilute odours and distribute cool air as well as keeping a fresh atmosphere. A fresh air supply quantity of 5 to 10 litres per second per person should be allowed using passive means wherever possible.

### Acoustical Environment

Sound plays an important role in creating atmosphere. In mosques there is a conflicting requirement because speech intelligibility is important for sermons but due to the size of some mosques and the variability of voice projection a loudspeaker system may be necessary.

Materials have an important effect on the sound environment. Hard materials are cold and give a reverberant space whereas soft materials are warm and produce a dry sound environment.

Religious spaces invite an open acoustic because reverberation is associated with the uplifting of the spirit. Besides, any internal sounds which intrude on prayer will be amplified, and this instills a discipline of quiet thus heightening concentration. On the other hand speech intelligibility is impaired by reverberation and as a consequence the reverberation time is usually restricted to 0.8 to 1.2 seconds for speech auditoria, whereas in a mosque corresponding values would be 1.5-2 seconds. The Imam has to project his voice over 30 metres in larger mosques and should be raised above the audience to minimise the effect of audience absorption. The human voice must be 22 decibels above the background sound level for 80% intelligibility. For this to be achieved with a background sound level criterion of 25 dBA then a 47 dBA voice sound level is needed at the back of the space for clarity. Over a distance of 30 metres assuming an attenuation of 0.7 dB per metre the voice level at the front would need to be 68 dBA. A normal raised male voice level is about 73 dBA.

In order to avoid echoes the direct and the reflected pathways should not be more than 15 metres apart.

High sound levels in a large space can produce reverberant masking and thus certain consonants in the speech will not be clear. A recommended volume per person in speech auditoria is usually  $3.5\text{m}^3$ , whereas in a mosque this factor is often nearer  $10\text{m}^3$ . A reverberation time criterion of about 1.5 seconds can be achieved by the use of a carpet having a sound absorption coefficient greater than 0.15 and the use of sound absorption materials applied to back walls.

Many mosques contain an open cloister-like wall so it is now customary to use voice amplification systems so that the Imam will be heard outside where people can congregate.



Clearly, there has to be great restraint in distributing air to the space so that it is quiet; any equipment should be located as far away as possible. In addition the structure should have a mass of at least 400 kg/m<sup>3</sup> to give adequate sound insulation; this will also increase the thermal inertia of the Mosque.

### Lighting

Natural and artificial lighting need to be soft in character and evenly distributed throughout the space. Indirect lighting is preferable so that visual distraction is minimised. One solution for introducing indirect perimeter day-lighting is to use a system of screened skylights between columns to light the interior areas to a uniform level. Lighting should give a minimum daylight factor of 2% which equates to a floor luminance of 500 lux on a bright day. If the skylights are located near the top of columns then filtered daylight washes down them and they appear luminous so helping to diffuse the light.

Artificial lighting within the prayer hall of a mosque can be installed so as to re-create the effect of natural daylighting. The illuminance of artificial lighting will be lower than natural daylighting but it can be designed to come from a similar direction and to be of similar colour. The level of natural lighting on the floor of the spaces in the mosque will vary throughout the day and around the year due to the angle of incidence of the sun on the building surface. The resultant illumination will not be uniform throughout the area.

The apparent colour of daylight is not constant, as the special distribution at any particular time depends upon the scattering and absorption of the sun's light in the prevailing atmosphere. The correlated colour temperature (K) of daylight is in the range of 5000K to about 10,000K. The colour of daylight is important if artificial lighting is to in any way resemble natural lighting; this is an important factor in selecting the type of electric lamps. For example, mercury vapour lamps could be mounted and concealed in the rooflight arrangement to achieve a certain resemblance to natural lighting (correlated colour temperature would be approx 3700K whereas Sodium lamps are 2000K). A similar system would be adopted around the perimeter using linear fluorescent fittings to emulate the direction of the natural light.

External lighting of Minarets for example may be achieved by floodlighting from a distance or by locating downlighting fittings or even fluorescent luminaries at high level. The first solution is preferable as it is more discreet and allows complete control of glare as well as being more accessible for maintenance. Courtyards can be lit artificially by either linear or downlighting luminaries mounted around the perimeter at high or, alternatively, by a lighting system incorporated into the courtyard sunscreen.

### Coda

There is a danger of the developed nations providing a glamorous image of modern technology to Third World countries. Any attraction may be false and may simply provide a way of spending money. Mosques are sacred places and have an aesthetic rooted in Arabic culture. Environmental engineering solutions need to reflect the peace, serenity and spiritual values demanded by the brief for a mosque.

IEA Task XI  
Integrated Knowledge Based Solar Design Tool (ISOLDE)

O.C. Mørck  
CENERGIA ENERGY CONSULTANTS  
Stationsvej 3, DK 2760 Måløv  
Denmark

co-workers:  
Ida Bryn, SINTEF, Norway  
Nicolas Morel, EFPL, Switzerland  
Rolf Stricker, Fraunhofer Inst., Germany  
Gianni Silvestrini, CNR-IEREN, Italy

ABSTRACT

One specific activity of Task XI of the IEA Solar R&D Programme, carried out by a small working group designated the Expert System Working Group, deals with the development of an Integrated Knowledge Based Solar Design Tool, ISOLDE. ISOLDE basically provides computerised access to the Task XI information through expert system advise, and video-disc illustrations. Besides, the system will provide access to design calculation and simulation tools.

KEYWORDS

IEA; passive; hybrid; solar; integrated; knowledge based; design tool.

INTRODUCTION

Within Task XI "Passive and Hybrid Solar Commercial Buildings" of the IEA Solar R&D Programme a number of activities has been undertaken. These activities cover the areas: case study analyses, advanced case study analyses, parametric sensitivity studies, and compilation of design guidance for the strategies, principles and systems, which have been investigated. The results of this work are presented in several documents, a slide set of the case studies, and in one main design guidance book, designated the source book. To provide alternative (computerised) access to the results of the TASK XI activities a working group has been put together within the task to develop a solar design tool for passive and hybrid solar commercial buildings.

The information arisen from the task activities are to a large extent in a form which can be characterised as knowledge opposed to calculation formulas. On the other hand, some of the results stemming from the parametric sensitivity analyses obviously

exist in the form of numbers, and finally, to verify a proposed building design, calculation and/or simulation methods are necessary. Taking the consequences of the very nature of this mixture of information and methods the working group decided to work towards the development of an Integrated Knowledge Based Solar Design Tool, which has been given the acronym ISOLDE. For those not familiar with the terminology of Artificial Intelligence (A.I.) and Expert Systems, it is in place to explain that the term knowledge based refer to the use of certain programming tools stemming from R&D on A.I. allowing the programmer to embed knowledge in the computer program in a straightforward way using almost plain english.

### OBJECTIVES

The objectives of the development of ISOLDE has been defined in a working document specifying the functional requirements to the design tool. The presumption for these requirements is that the user shall be able to use the tool from the very beginning of a design process, through the selection of techniques to implement in the building, to the final design optimisation based on a simulation method. It was further agreed that the tool also should be useful outside an actual design situation, as an educational system. As mentioned above it is a primary objective to provide computerised access to the experience and information derived from the TASK XI activities.

### IMPLEMENTATION

To meet the functional requirements as specified above it was decided to develop the system in three separate parts: General advise, case oriented advise, and calculations/simulations. Figure 1 presents the overall architecture of the system.

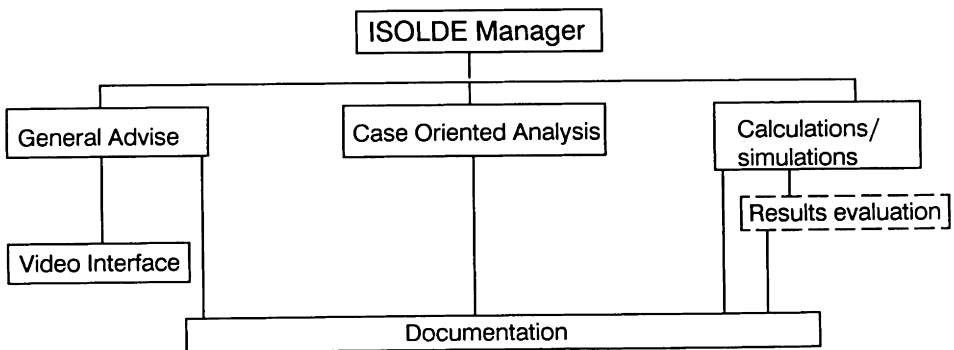


Fig. 1 Overall system architecture

Definitions

The working group found it useful to agree on the following terminology definitions:

- Strategies: Cooling, Heating, Daylighting
- Principles: Ventilation, Shading, Evaporative cooling, etc.
- Systems: Atria, Trombe walls, air solar collectors, etc.
- Concepts: Combinations of strategies, principles and systems

General Advise Part

The general advise part has been designed to serve two purposes: To present advise on different solar strategies, principles and systems either for the programming phase of an actual building project, or as an educational introduction for building designers.

This part of the design tool has been designed to present advise to the user in a logical hierarchical way, starting with solar strategies, continuing with the principles and finally the specific information about the individual systems. The information represented about each principle/system have been ordered under the following headlines:

- Principle/ system definition
- Advantages/ disadvantages
- Side-effects to other strategies/principles/systems
- Design advise
- Rules of thumb for design

Atria takes a special role, as it does in the Task itself, as atria as a system can take many different forms and can be chosen for a combination of strategies.

To supplement the textual advise the system will provide access to illustrations of the different solar systems in the form of slides presenting actual buildings featuring these techniques. The slides, presenting the case study buildings of Task XI, have been transferred to video-pictures, which can be shown on an ordinary PC VGA-colour screen using a special graphics card.

Case oriented analysis

Before entering into this part of the system it is anticipated that a solar system, and energy/comfort strategy has been chosen for a specific project, and that the architect/engineer wants to know what performance to be expected. This part will also be introduced by a menu of choices and explanations.

First, the user have to specify the characteristics of the actual building project by providing additional input on:

- climatical specification
- building description and use (proportions, orientation, thermal properties of building components), advise on appropriate ranges of variables should be available.
- energy/ comfort strategy
- solar system (e.g. atria typology)

The results is to be presented as graphs, showing the sensitivity of chosen building performance parameters, characterising energy, comfort, and daylight conditions, to selected independent variables. A rating structure making comparison between various strategy combinations/ solar systems is to be developed. The implementation of this part of the ISOLDE requires the development of a means to place the actual system within the regions of system parameters of known performance.

### Calculations/simulations

This will be implemented as an interface to established calculation/simulation programs. This interface is intended to include:

- advise on how to simulate (zoning of buildings for respectively temperature, energy and daylight calculations; how to simplify the building specification)
- interface to chosen calculation/simulation programs
- transfer of already given data to calculation/simulation programs
- use of ready to use input data sets stemming from previous simulations (one example only). This could be input data files from the Task parametric sensitivity runs.

Results evaluation. A module which allows some evaluation/interpretation of results from the calculation/simulation programs. It would include:

- a set of performance benchmarks for each climate to allow for comparisons between predicted performance of the actual system to make it possible to "rate" the performance.
- a specified range of acceptable values for for example:
  - max/min temperatures
  - utilisation factor
  - energy use pr sqm.
  - max pover pr sqm.
- duration of temperatures above a certain limit.

### Documentation

Documentation in the form of printed material should in principle be available from all parts of the system. The way this is going to be implemented is not established yet.

## IMPLEMENTATION PLAN

The development of the ISOLDE system is planned to happen along the following main milestones:

1. November 1990: Complete draft system of the general advise part.
2. August 1991: Complete draft system including all three parts.
3. December 1991: Final version of complete system.

## FLUIDIZED TROMBE WALL SYSTEM

Murat Tunç

Thermodynamics Department, Technical University of Istanbul,  
Mechanical Engineering Faculty,  
ITU, Istanbul, TURKEY

### NOMENCLATURE

- $a$  : Width of the channel [ m ]  
 $c_p$  : Specific heat of the fluid [ kJ/kg K ]  
 $c_{pt}$  : Specific heat of the particles [ kJ/kg K ]  
 $c_{pg}$  : Specific heat of the gas [ kJ/kg K ]  
 $\bar{d}_p$  : Average diameter of particles [ m ]  
 $g$  : Gravitational acceleration 9.801 [ m s<sup>-2</sup> ]  
 $H_L$  : Total heat gain of the fluid at the outlet of the channel [ kWs ]  
 $k$  : Thermal conductivity [ w/ m °C ]  
 $L$  : Height of the channel [ m ]  
 $m$  : Mass flow rate [ kg/sec. ]  
 $M$  : Fan power [ HP ]  
 $P$  : Pressure at the outlet of the fan [ Pa ]  
 $Pr$  : Prandtl number  
 $Q$  : Volumetric flow rate [ m<sup>3</sup> /sec. ]  
 $T$  : Temperature [ °C ]  
 $T_0$  : Inlet temperature of the fluid [ °C ]  
 $T_{aveL}$  : Mean temperature of the fluid at the outlet of the channel [ °C ]  
 $T_g$  : Glass temperature [ °C ]  
 $T_w$  : Wall temperature [ °C ]  
 $u$  : Velocity in the X direction [ m/sec. ]  
 $u_0$  : Inlet velocity of the fluid [ m/sec. ]  
 $u_{mf}$  : Minimum fluidizing velocity [ m/sec. ]  
 $v$  : Velocity in the Y direction [ m/sec. ]  
 $\alpha$  : Thermal diffusion coefficient [ m<sup>2</sup>/sec. ]  
 $\beta$  : Coefficient of volumetric thermal expansion [ K<sup>-1</sup> ]  
 $\rho_p$  : Particle density [ kg/m<sup>3</sup> ]  
 $\rho$  : Air density [ kg/m<sup>3</sup> ]  
 $\mu$  : Dynamic viscosity [ kg/m.sec ]  
 $\nu$  : Kinematic viscosity [ m<sup>2</sup>/sec. ]  
 $\epsilon$  : Voidage of fluidized bed  
 $T_g$  : Glass temperature [ °C ] ;  $T_w$  : Wall temperature [ °C ]

## ABSTRACT

The purpose of this study is to perform a mathematical modelling of an air-fluidized bed solar collector and thermal analysis of the system via computer simulation. A new model for an air-fluidized solar collector is developed which is based on "Trombe Wall" structure and theoretic and experimental studies on fluidized beds. Computer solutions are obtained for temperature, and velocity fields and for the power extracted from the system.

### KEY WORDS

Trombe wall; Fluidized beds; solar heating;

## INTRODUCTION

The Fluidized Trombe wall system is a new concept. In this system the gap between the wall and the glass is fluidized by using high absorbance and low density particles.

The present work consist of two main parts. In the first part, the classical trombe wall system is analyzed. Governing equations are solved and the heating capacity of the system is obtained.

In the second part of this study, the medium between the glass and the wall of trombe system is fluidized by using low density particles. The system under consideration is depicted in the figure-1.

Air enters the channel from the bottom and leaves at the top. A filter is placed at the top of the channel to keep the fluidized particles inside the channel.

In this system air as a heating fluid, is in a direct contact with particles which increases the overall efficiency of the system.

The temperature and velocity profiles between the glass and the wall are determined for the Classical and Fluidized trombe wall systems.

The flow is assumed to be laminar. The total rate of heat absorption is calculated for both systems.

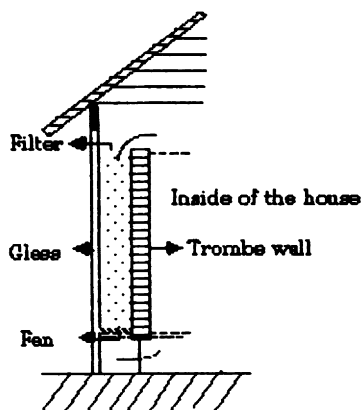


Figure 1. Description of the fluidized trombe wall system

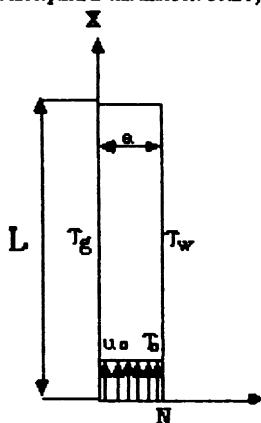


Figure 2. The geometry of the flow problem in trombe wall channel.

## THEORY

### a) Formulation of the conventional type trombe-wall model.

The flow geometry of interest in trombe wall channel is depicted in Figure-2.

The flow is assumed to be steady, laminar, compressible. The pressure defect as a function of height is assumed to be linear for low flow rates [2]. Governing equations of continuity, momentum and energy are:

$$\frac{\partial u}{\partial x} + \frac{\partial v}{\partial y} = 0 \quad (1)$$

$$u \frac{\partial u}{\partial x} + v \frac{\partial v}{\partial y} = -\frac{1}{\rho} \frac{dp}{dx} + \nu \left( \frac{\partial^2 u}{\partial x^2} + \frac{\partial^2 u}{\partial y^2} \right) + 9\beta (T - T_0) \quad (2)$$

$$\rho c_p \left( u \frac{\partial T}{\partial x} + v \frac{\partial T}{\partial y} \right) = k \left( \frac{\partial^2 T}{\partial x^2} + \frac{\partial^2 T}{\partial y^2} \right) \quad (3)$$

The boundary conditions are :

- 1)  $x=0$  and  $0 \leq y \leq a$   
 $u = u_o$   $v=0$   $T=T_o$   $P=P_o$
- 2)  $0 \leq x \leq L$  and  $y=L$   
 $u=0$   $v=0$   $T=T_w$

Heat gain from the channel is calculated as follows :

$$H = \int_0^L \rho u a c_p (T_{ave} - T_o) dy \quad (4)$$

b) Formulation of the fluidized bed from the wall model.

It is assumed that minimum fluidization condition is prevailing inside the channel. Where the total pressure drop inside the channel is equal to the weight of the particles. The fluidization velocity may be calculated as follows [3].

$$u_{mf} = \frac{\mu_g}{\rho d_p} \left\{ \left( (25.25 + 0.0651 Ar)^{0.6} - 25.25 \right) \right\} \quad (5)$$

where

$$\mu_g = \frac{b \cdot T^{a/2}}{s + T}$$

$$b = 1.458 \cdot 10^{-6} \text{ [ kg/m.s.K}^{1/2} \text{ ]} \quad (6)$$

$$s = 110.4 \text{ [ K ]}$$

and  $Ar$  is Archimedes number :

$$Ar = g d_p^3 (\rho_p - \rho) / \mu_g^2$$

Because of the low operating temperatures thermophysical properties of the particles and air are assumed to be independent of temperature.

Energy equation for the air can be written as follows :

$$\rho c_p u \left( \frac{\partial T}{\partial x} \right) = k \left( \frac{\partial^2 T}{\partial x^2} + \frac{\partial^2 T}{\partial y^2} \right) + q \quad (7)$$

in the equation-7  $q$  term represents heat transfer from particles to air.

Boundary conditions are :

- 1)  $0 \leq x \leq L$   
 $u = u_{mf}$   
 $0 \leq y \leq a$
- 2)  $0 \leq y \leq a$  and  $x=0$   
 $T=T_o$

#### THE METHOD OF SOLUTION :

The equations were solved using a forward marching, line-by-line implicit finite-difference technique permitting iterations on each new line.



A rectangular grid [Figure 3], across the channel width is used to establish the increments of the finite-difference approximations to the equations (1), (2), (3) and (7).

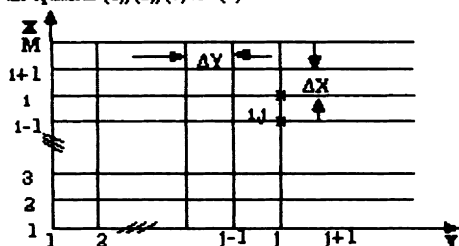


Figure 3. Grid for finite-difference representations for solution.

## DISCUSSION OF RESULTS

### a) The conventional trombe wall system .

In the Figure-4 variation of  $u$  velocity across the channel is depicted for three different wall lengths and for a constant volume flow rate. At the lower flow rates, surface friction is largely responsible for the initial acceleration of the fluid. That's why a clear indication of the heating effect is noted in  $u$  velocity by the more rapidly moving layers of fluid a small distance from the surfaces and progressive decrease in the velocity within the central region.

Similar results are presented in the Figure-5 for a different volume flow rate. At higher flow rates, the  $u$  velocity profile shows a parabolic development soon after entry when the plates are of equal temperature.

As the glass temperature is lowered progressively more a symmetric  $u$  velocity profiles are obtained.

In the Figure-6 and Figure-7 the variation of  $v$  velocity across the channel width is shown for different flow rates and lengths.  $v$  velocity component represents the movement of the fluid across the channel gap caused by a combination of friction and heating.

During the asymmetric heating the fluid flow away from the cooler surface is considerably greater than from the warmer side.

Figure-8 and Figure-9 illustrate air temperature variation across the channel gap for two different flow rates. The coolest portion of the fluid is the fastest moving central layer for higher flows and symmetric heating. During the asymmetric heating fluid temperature near the warmer wall increases.

The total heat extracted from the system as a function of height is depicted in the Figure-10.

### b) Fluidized trombe wall system $u$ velocity profiles is almost horizontal across the channel width as expected.

This  $u$  velocity variation is shown in the Figure-11 and Figure-12 for two different volume rates and for several channel lengths.

The fluid temperature variation across the gap is depicted in the Figure-13. The temperature of the fluid increases near the warmer wall. But, due to the heat transfer from the particles to the air, the temperature profile is almost linear.

In the Figure-14 the heat extracted from the system as a function of channel length is illustrated for two different flow rates. If we compare the results of this figure with the Figure-10, it is apparently can be seen, the superiority of the fluidized system over the conventional one. The numerical results obtained in this work indicate the fluidization of the trombe wall channel appears to be a visible concept. Fan power requirements for  $Q=0.018\text{m}^3/\text{sec}$  and  $Q=0.035\text{m}^3/\text{sec}$  are calculated to be 0.81 HP and 1.61 HP respectively.

## REFERENCES

1. H. Akbari and T.R. Borgers, " Free convective laminar flow within the Trombe wall channel", *Solar Energy*, vol. 22, pp. 165-174, 1979.
2. D. Kunii, O. Levenspiel, *Fluidization Engineering*, Krieger Publishing Co. Huntington, NY., 1977.
3. S. Ergun, *Chem. Eng. Progr.*, vol. 48, pp. 89-95, 1952.
4. F. Trombe, J. F. Robert, M. Cabanot and B. Sesolis, Some performance characteristics of the CNRS solar house collectors, *Passive Solar Heating and Cooling, Conf. and Workshop Proc.*, pp. 201-222. Albuquerque, NM, Los Alamos Scientific Laboratory of University of California, Los Alamos, NM 87545, (18-19 May 1976).
5. J. D. Balcomb, J. C. Hedstrom and R. D. McFarland, Simulation as design tool. *Passive Solar Heating and Cooling, Conf. and Workshop Proc.*, pp. 201-222. Albuquerque, NM, Los Alamos Scientific Laboratory of University of California, Los Alamos, NM 87545, (18-19 May 1976).

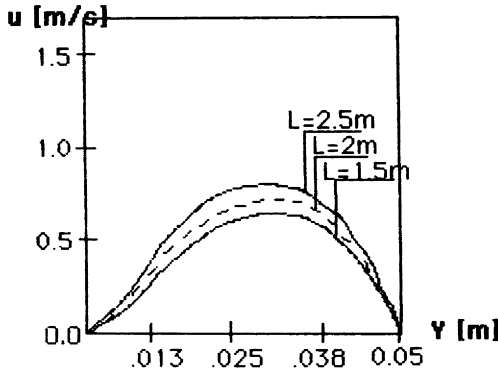


Figure 4.  $u$  velocity profile for three different heights and for  $Q=0.007 \text{ m}^3/\text{sec}$ .

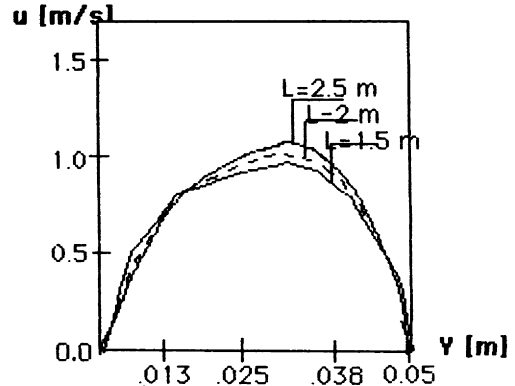


Figure 5.  $u$  velocity profile for  $Q=0.014 \text{ m}^3/\text{sec}$

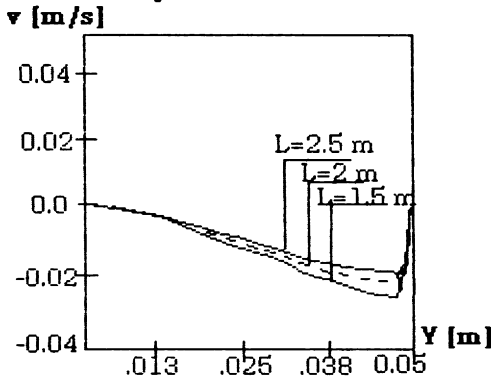


Figure 6.  $v$  velocity profile for  $Q=0.007 \text{ m}^3/\text{sec}$

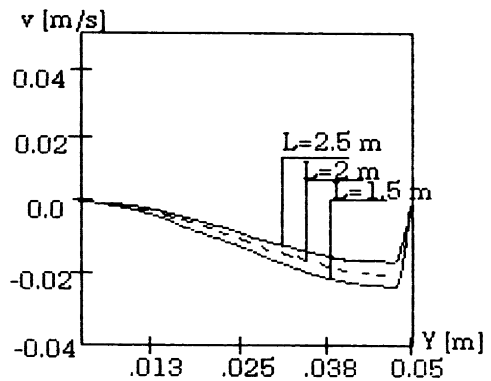


Figure 7.  $v$  velocity profile for  $Q=0.014 \text{ m}^3/\text{sec}$

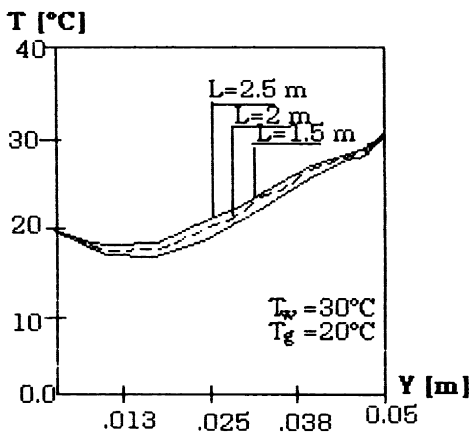


Figure 8. The temperature variation of the air across the channel width for  $Q=0.007 \text{ m}^3/\text{sec}$

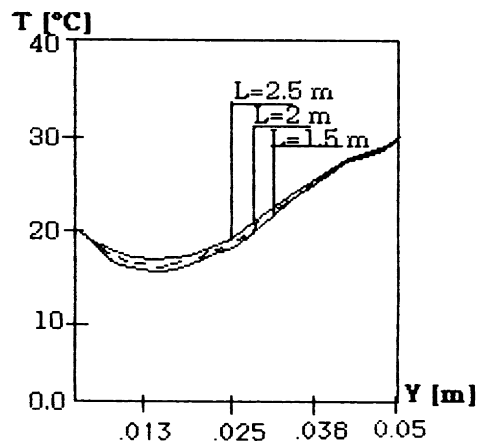


Figure 9. The temperature variation for  $Q=0.014 \text{ m}^3/\text{sec}$

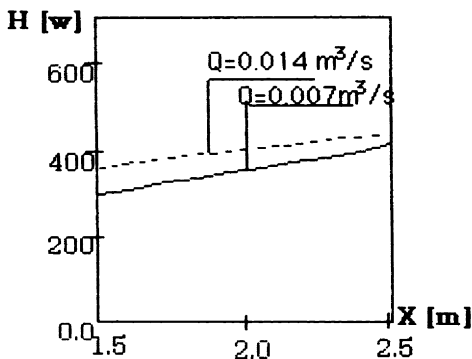


Figure 10. The extracted total heat as a function of height.

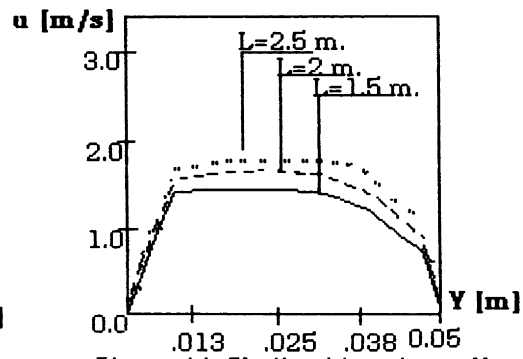


Figure 11. Fluidized trombe wall, u velocity profile for  $Q=0.035 \text{ m}^3/\text{sec}$ .

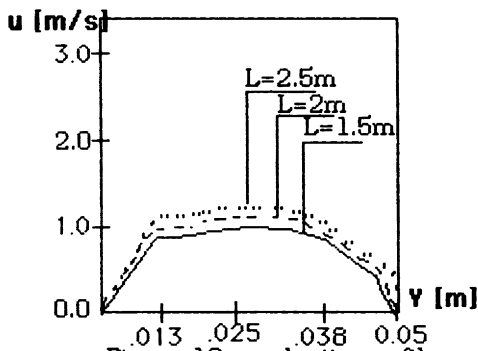


Figure 12. u velocity profile for  $Q=0.010 \text{ m}^3/\text{sec}$

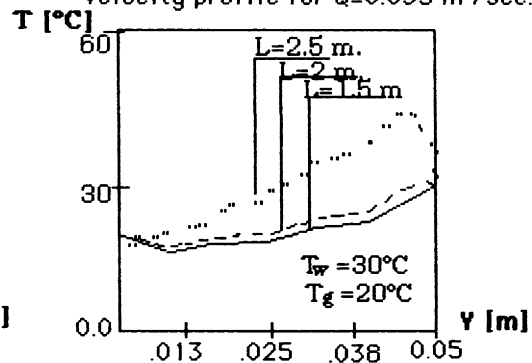


Figure 13. The temperature variation of the fluid for  $Q=0.035 \text{ m}^3/\text{sec}$

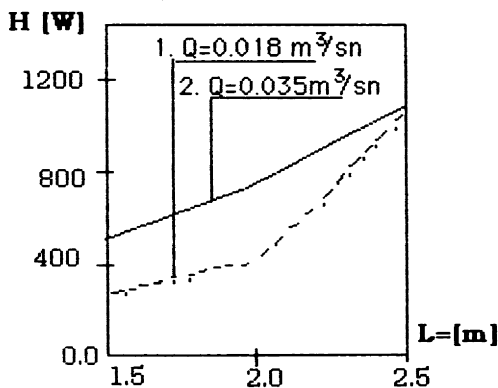


Figure 14. The extracted total heat from the fluidized system.

**NON-DOMESTIC BUILDING DESIGNS INCORPORATING  
PASSIVE ENERGY SYSTEMS**

P.A. Ruyssevelt\*, R.R. Cohen\*, W.B. Gillett\*, and I. McCubbin\*\*

\* Halcrow Gilbert Associates Ltd  
Burderop Park, Swindon SN1 0QD, UK

\*\* Energy Technology Support Unit for the Department of Energy  
Harwell Laboratory, Oxfordshire OX11 0RA, UK

**ABSTRACT**

A series of design studies is being sponsored by the Department of Energy to investigate the practical application of passive solar technology in non-domestic buildings. The first set of eight studies is complete (Campbell et al., 1987), and two further sets managed by Halcrow Gilbert Associates (HGA) and Building Design Partnership are under way. This paper presents the results of HGA's first group of three studies in the light industrial building sector. These studies illustrate the opportunities to produce marketable low energy designs in which the architectural form plays the major role in generating a comfortable internal environment. The studies also show that such designs need cost no more than their conventional counterparts. A second group of studies in out-of-town office developments has started and the initial results are equally encouraging.

**KEYWORDS**

Industrial, Buildings, Energy, Design, Studies, Passive, Solar, Daylight, Rooflights, Cost.

**DESIGN STUDIES**

The objectives of the current set of HGA design studies are to:

- ◆ produce a series of case studies demonstrating best practice in the application of passive energy systems to a range of building types.
- ◆ act as a mechanism for transferring technology from R&D projects to the architects and clients involved in the studies, and ultimately to the design community and construction industry at large.
- ◆ generate data on the cost, performance and amenity benefits of non-domestic passive buildings.
- ◆ develop practical building designs that can act as a seed bed for live building projects.

In each design study, the suitability of various passive energy techniques is explored for a particular building type by asking a firm of architects to propose a design that uses them effectively. The brief for each study is prepared in consultation with a client who has offered to cooperate in the study. These "quasi-clients" are also involved in the evaluation process.

The key factors used to evaluate the proposal are energy performance, environmental performance, amenity, and capital cost. In order to judge these factors in context, a 'typical' reference building of a more conventional design is also assessed. To be successful the proposal must not only use less energy than the reference, but the value of the energy saving must be seen to justify the capital cost of providing it. The design proposal is developed through an interim scheme to a final sketch design with formal assessment at both stages.

The twelve non-domestic design studies managed by Halcrow Gilbert Associates have been divided into four groups of three. Each group of design studies concentrates on a particular building sector which has been selected with reference to a previous market study (Duncan *et al.*, 1983). The first group of studies involve light industrial buildings.

### INDUSTRIAL BUILDINGS

A recent study has shown that fairly simple energy conservation measures such as; reducing fabric U values to  $\sim 0.4\text{W/m}^2\text{K}$  and incorporating high performance loading bay doors, can reduce the space heating requirement of industrial buildings by up to 40% (Hughes, 1989). After applying these energy conservation measures there is only limited potential for further displacing space heating with passive solar gains. This is particularly true of buildings which have a high level of internal heat gains. There is however, considerable scope for saving energy by displacing artificial lighting with daylight, and since the energy saved is electricity the financial value and environmental benefits have greater significance.

The three types of accommodation typically provided by industrial buildings, offices, workshops and warehouses have distinct requirements for temperature, lighting levels and other environmental criteria. In the schemes presented below, the architects were asked to consider carefully the environmental requirements of each space at the outset of the design.

#### Jestico + Whiles Design

The furniture maker SunarHauserman required a high quality building with a strong visual image for its European HQ. In their proposal, Jestico + Whiles designed each of the three main areas, offices, assembly shop and warehouse, with an environmental responsiveness appropriate to its function.

A 2120m<sup>2</sup> warehouse is located at the north end of the building in the form of a well insulated box with small windows. The storage of light sensitive materials and the low comfort temperature requirement of this space meant that daylight and solar heat gains would not have been welcome.

The central section of the building is occupied by a 1030m<sup>2</sup> assembly shop which is daylight through two south facing rooflights running the length of the building. Facing the brighter southern horizon, a smaller glazed area is required to achieve a given level of daylight and hence heat loss can be reduced. Each rooflight is shaded by a series of louvres suspended in an extension of the curved roof frame. These shading devices allow diffuse light and low altitude solar radiation to enter, but reject high altitude summertime solar radiation. Ductwork and service zones have been designated in order to limit the obscuration of the rooflights.

The 1530m<sup>2</sup> offices are located to the south of the assembly space, separated by a courtyard which enables an otherwise deep plan office to be daylit and natural ventilated, as well as providing a pleasant recreation space. On the southern elevation horizontal shading extends through the fenestration to form an internal light shelf with the intention of improving the distribution of daylight by reducing daylight levels close to the window and increasing them further away. The luminaires and their control system have been carefully designed to respond to the availability of daylight.

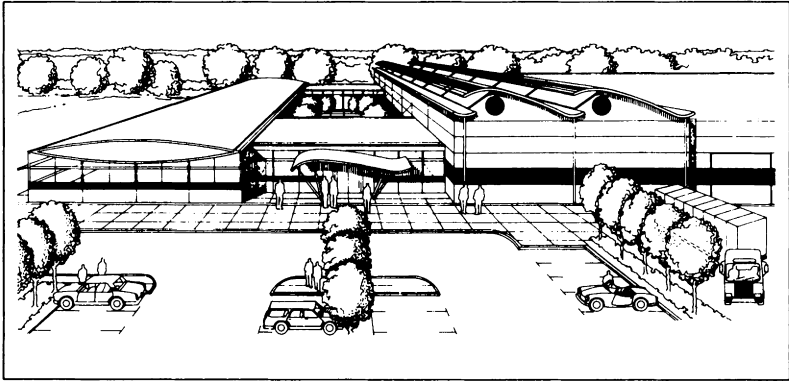


Fig. 1. Jestico + Whiles design for SunarHauserman

**Scheme Assessment.** Nearly 60% of the lighting energy demand should be saved by comparison with the reference buildings, but the heating demand likely to be 50% higher. In energy cost terms the design achieves an overall saving of 22% compared to the reference building. It is important to realise that savings in lighting energy demand do not translate directly into energy cost savings since the maximum demand element of the tariff is unlikely to be reduced in the winter period when lights will be on at least part of the time. Generally, the value of daylighting and solar heat gains outweigh the cost of the heat lost through the windows and rooflights. The exception is the north office facade onto the courtyard which is excessively glazed.

By comparison with the reference buildings, which suffer badly from overheating (a common complaint in many factories), the final design shows no overheating in any area of the building. Visual comfort should be considerably enhanced in all areas as a result of the careful design of external and internal shading devices.

The estimated cost of the final design at £450/m<sup>2</sup> is within the original client budget of £485/m<sup>2</sup> and shows a cost reduction of £42/m<sup>2</sup> from the interim scheme design. SunarHauserman's managing director concluded that "the design represented an excellent investment .... and could be funded by normal financial institutions."

#### The Ryder Nicklin Partnership Design

Graphex Industrial Art are a design conscious company who required a new facility for manufacturing signs and exhibition materials. In their compact square shaped design, the Ryder Nicklin Partnership provided 1762m<sup>2</sup> of double-height workshop and 894m<sup>2</sup> of office space on two floors. The main feature of the design is the so-called "responsive roof" which comprises five 'Toblerone' shaped rooflights with sloping faces orientated

north/south. Reflective roller blinds operate under the south face of the rooflights responding to temperature and solar radiation in order to combat

overheating and glare. At the interim design stage the building had six rooflights and a substantial amount of side glazing in the workshop, the combined effect of which were very high levels of daylight. Removing one rooflight and much of the side glazing reduced both the building heat loss and the capital cost without affecting the lighting energy savings.

In this design the offices are located at the north end of the building since the extent of internal heat gains suggested that solar gains during the heating season would not be useful. Facing north, it was possible to size the double glazed windows to provide adequate daylight without the need for shading. Daylighting in the first floor office is supplemented by one of the rooflights which has a horizontal leylight underneath it to prevent cold down draughts and to diffuse incoming solar radiation.

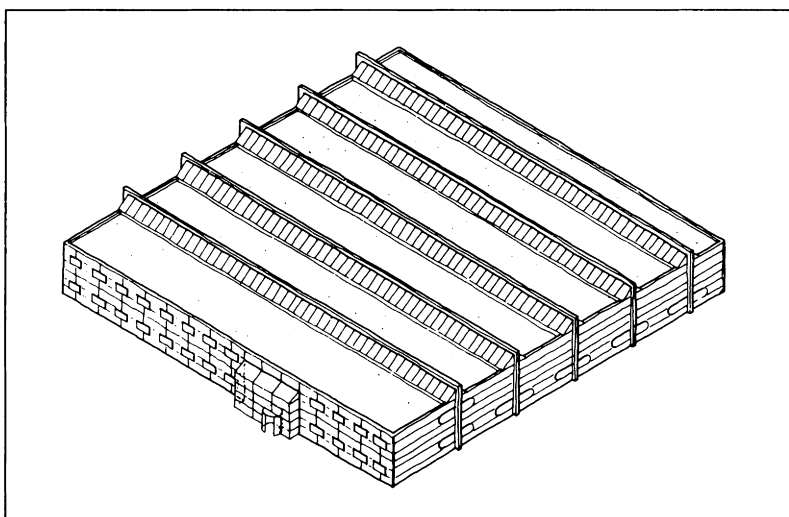


Fig. 2. Ryder Nicklin design for Graphex

**Scheme Assessment.** Nearly 60% of the lighting energy demand and 20% of the heating energy demand should be saved by comparison with the reference building. In energy cost terms the design achieves an overall saving of 36% compared to the reference building. On balance, the value of daylighting and solar heat gains are substantially larger than the cost of heat lost through the windows and rooflights.

The rooflights provide evenly distributed, adequate levels of daylight in nearly all areas. The roller blinds under the south face of the rooflights, and openings for natural ventilation in the north face combine to limit overheating to less than 2% of the working year in the workshop.

The estimated cost of the final design at £412/m<sup>2</sup> is £4/m<sup>2</sup> less than the estimated cost of the reference building and shows a cost reduction of £55/m<sup>2</sup> from the interim proposal. In the client's opinion "...the advantages of daylight and a view to the outside can not be overestimated. The design appears to offer ample opportunities to create an excellent working environment." Graphex were "very impressed" with the predicted annual energy cost saving of £2,150.

### The ECD Partnership Design

English Estates presented The ECD Partnership with a very tight budget (£332/m<sup>2</sup>) within which to design a speculative industrial building containing 1600m<sup>2</sup> of workshop space and 600m<sup>2</sup> of office space. English Estates normally require the provision of rooflight areas at least equivalent to 10% of the floor area in their speculative industrial buildings. In response to this brief ECD applied considerable effort to optimising the size and location of rooflights in order to obtain good daylighting with minimal overheating.

As with the Ryder Nicklin design, offices, workshops and stores are all enclosed in a simple rectangular building. GRP rooflights are incorporated in continuous strips as far as possible on the north facing slopes of the roof. Physical scale models were used to establish daylight levels and distribution patterns. The resultant uniform distribution of daylight in the workshop allows the artificial lighting system to be controlled by a single switching circuit. The offices in this design are located on two floors at the north of the building and are daylit by north facing windows, thereby avoiding the need for expensive solar shading.

Natural ventilation of the workshop is achieved in the summer months by opening the loading bay doors, and if necessary operating fans at high level in the east and west facades. In the offices, natural ventilation is enabled through controllable low level vents and opening skylights.

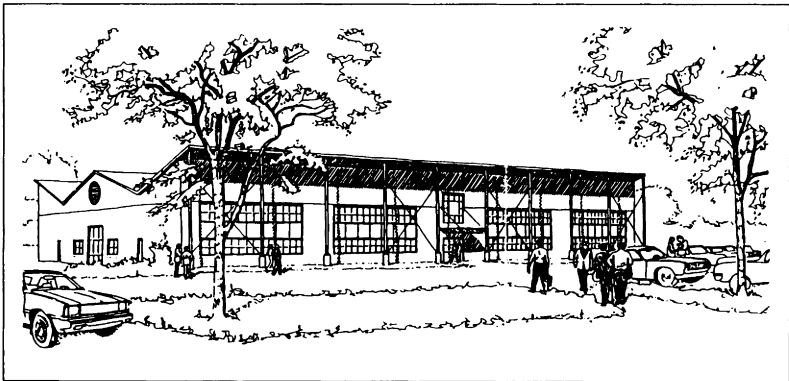


Fig. 3. ECD Partnership design for English Estates

**Scheme Assessment.** The ECD design gives rise to 50% savings in lighting energy demand and only a small increase in heating energy demand compared to the reference building. Overall, the annual energy cost savings amount to 30%, or £1,570. The design is estimated to cost £6/m<sup>2</sup> (2%) more than the reference building due to larger rooflight areas and lighting controls.

Diffusing GRP rooflights located on the north facing roof slopes will reduce glare, but are unlikely to eliminate it. The predicted incidence of overheating at 4% of the working year is substantially less than that predicted for the reference building.

Overall, the design is a credible and attractive solution to the provision of this type of low cost industrial building. Recognising the wide range of potential tenants and owners for their buildings, English Estates felt that this design approach could be best employed where the type of building occupant was identified at the outset.



Table 1. Energy and cost data for designs and reference buildings

Client Architect		SunarHauserman Jestico + Whiles		Graphex Ryder Nicklin		English Estates ECD Partnership	
		Design	Ref.Bldg	Design	Ref.Bldg	Design	Ref.Bldg
Capital Cost	£/m <sup>2</sup>	£450	£485	£412	£416	£338	£332
Heating	kWh/m <sup>2</sup> /yr	53.7	35.7	29.1	35.7	42.3	36.3
Lighting	kWh/m <sup>2</sup> /yr	14.5	33.0	14.3	33.0	15.7	33.8
Heating Cost	£/m <sup>2</sup> /yr	£.94	£.62	£.51	£.62	£.74	£.64
Lighting Cost	£/m <sup>2</sup> /yr	£.80	£1.61	£.91	£1.61	£.93	£1.74
Fuel Cost	£/m <sup>2</sup> /yr	£1.74	£2.23	£1.42	£2.23	£1.67	£2.38
% of Year Overheated		0%	25%	2%	25%	4%	22%

### Important Lessons

This group of design studies has so far revealed that:

- ♦ there is considerable potential for saving energy through the exploitation of daylight in industrial buildings.
- ♦ both north and south facing rooflights can be employed to daylight workshops, but south facing rooflights must be shaded.
- ♦ integration of artificial lighting systems and their controls with daylighting is vitally important if energy savings are to be realised.
- ♦ performance and cost assessment undertaken at the early stages of design can lead to improved energy performance at a lower capital cost.
- ♦ the final design costs are very close to the targets - demonstrating that low energy design need not involve higher capital expenditure.
- ♦ predicted energy savings have both significant financial value and important environmental benefits.

### ACKNOWLEDGEMENTS

The work reported here is fully funded by the Energy Technology Support Unit for the Department of Energy. The performance assessments were undertaken by YARD and cost assessments were performed by Davis Langdon & Everest. Specialist advice was provided by D Hawkes of Cambridge University, P Owens of Pilkingtons, N Vaughan of UWIST and A Richens of Ferguson & Partners.

### REFERENCES

- Campbell, J. and White, K. (1987). *Passive Solar Design Studies in Non-domestic Buildings (Phase 1)*. Report No. S-1157 to the Energy Technology Support Unit for the UK Department of Energy.
- Duncan, I P and Hawkes, D. (1983) *Passive Solar Design in Non-domestic Buildings*. Report No. S-1110 to the Energy Technology Support Unit for the UK Department of Energy.
- Hughes, D. (1989). Low Energy Factory Buildings. In: *Building Services, The CIBSE Journal*. February 1989.

# A NEW INTERPRETATION OF OLGYAYS' METHOD FOR THE ORIENTATION AND DESIGN OF A BUILDING OF MINIMAL ENERGY CONSUMPTION

A. ELAĞOZ\* and M. KÜÇÜKDOĞU+

\* Ass. Prof. Dr., Mimar Sinan University  
College of Arch., Fındıklı, İstanbul. TR

+ Prof. Dr., İstanbul Technical University  
College of Arch., Taşkısıla, İstanbul. TR

## ABSTRACT

The procedure is an optimization of the total percent of the sunlit area and the thermal effect due to the beam component of total solar energy on the vertical exterior surfaces of a building of minimal energy consumption, in Olgays' bioclimatic chart which considers temperature, solar energy, wind, precipitation, relative humidity and vapor pressure. The procedure is a new and comprehensive interpretation of Olgays' well known Overheated Period charts, by replacing the second position of the observer in hourly simulation by the original gnomonic diagrams based on the first position of the observer. The procedure is presented for the use of architectural, urban planning, and energy engineering purposes.

## KEYWORDS

Passive Solar Architecture, Olgays' Method, Energy Conservative Design, Orientation, Shadow Analyses

## ENERGY CONCIIOUS DESIGN AND PASSIVE SOLAR ARCHITECTURE

Substitution of passive solar systems for use of fossil fuels in buildings to keep the environment biologically clean, can make important contributions to the health of individuals and the global ecosystem, as well as contributing to the energy economy. Passive solar architecture integrates energy conservation with passive solar heating, natural cooling and daylighting for a comfortable building of % 50-90 less operating energy.

Hour-by-hour simulation provides the backbone for design analysis. For smaller or simpler buildings simplified methods are usually based on monthly analysis. For larger or more complex buildings, the use of the current generation of powerful microcomputers are advised in simulation directly for design (Balcomb and Jones, 1988; Little, 1979; Kusuda, 1980).

## Solar Radiation Data for Passive Architecture

Much of the past solar radiation data will be rehabilitated and additional data will be collected in the future; however, it is unlikely that the hourly data to be taken will be extended to cover surfaces other than the horizontal for the majority of the stations. Using Liu and Jordan's (1960, 1961, 1963) empirical correlations, it is possible to estimate monthly average daily total radiation on a horizontal surface, divide the daily total into direct and diffuse components, convert each component into hourly values, and then compute the hourly value of either component on a surface of any orientation desired (Duffie-Beckman, 1980; Kusuda-Ishii, 1977).

## Shadow Analysis Techniques

Shadow analysis techniques for building energy studies are examined in two parallel groups of classification (Elagöz, 1989):

- A. The methods deal either with the building as a whole or only with the windows.
- B. Shading and solar influences on a building can be understood from two different observer positions (Wright, 1982):

1. **The observer stands at the ground or the building element and looks toward the Sun.** The entire yearly movements of the Sun and relationship to the modifying intermediate conditions are seen at one time; thus, from the single station point, the observer has a yearly picture of solar movement. The disadvantage of this technique is that every position of the subject surface must be separately analyzed with a new drawing and accompanying calculations. For a total analysis, a continuous three-dimensional site volume must necessarily be broken into discrete representative points each of which is separately analyzed. Without intermediate obstructions any point on a site is equivalent in a solar analysis, since solar rays are parallel. However when the obstruction is large or close, its influence on different station points may be quite varied. Since the proximity of the obstruction determines the degree of variation in complex situations, differences may be considerable. Therefore, the movement or location of shadows is impossible to analyze, for only by accident can one determine whether the discrete object point is at a shadow edge; total overshadowing effects and shadow patterns cannot be seen, nor can the entire building be examined at one time.

2. **The observer is located at a spot between the Sun and the building.** By considering both the Sun and the entire building at once, all surfaces in any orientation can be observed under solar illumination. The relationship of one portion of the site can be understood acting on another portion of the site.

Numerous examples (Elagöz, 1989) show that the observer, generally, is in the first position in the methods dealing only with the windows, and he is in the second position in the methods which consider the building as a whole.

Gnomonic Projections (or Sun Path Diagrams) as having significant emphasis in Olgyays' method, have been widely used

for shading study techniques. The sun-path diagrams are the most efficient tools to draw shadows on horizontal surfaces but share the common failings mentioned below:

1. They require several kinds of constructed drawings such as plans, elevations, sections which are time consuming to make
2. are illustrative of only one view slice, and are true for only one observation point in the project.
3. usually assign the 21st of each month as a representative monthly day. This simplification ignores the characteristics of day-to-day solar movement, which is less rapid at the solstices than near the equinoxes.
4. The charts themselves, require special scaling and are unmanageable in their sizes.

### NEW PROCEDURE

The procedure is a new and comprehensive interpretation of Olgays' well known Overheated period charts. By replacing the second position of the observer in hourly simulation by the original gnomonic diagrams based on the first position of the observer, the procedure gets closer to the aims of Olgays' (1963) method in the interpretation of architectural principles, site selection, sol-air orientation, solar control, environment and building forms, wind effects and air-flow patterns, and finally the thermal effects of materials. It is compiled in two parts and eleven steps as follows :

The first part of the procedure deals with the changes in the sums of the total annual percents of sunlit areas (sunny portion of total exterior walls/total area of exterior walls) of a building relative to the changes in location, form and the orientation. In the second part, the thermal energy of the direct component is added to the variables mentioned above. Thus, each wall is taken into consideration separately, with the changes of intensity of direct solar energy and the percentages of sunlit area on it.

1. Olgays' bioclimatic chart is adapted to the geographical place. The Overheated and the Underheated periods for selected hours of daytime are marked for selected days. For the selected hours of the selected days
2. percentages of sunlight on the walls of the building of a given orientation are computed, with any shading algorithm of parallel projection.
3. areas of sunlight ( $m^2$ ) on the walls of the building of a given orientation are computed,
4. total percentages of sunlight on the building are computed and grouped under two intensities, e.i. the Overheated and the Underheated.
5. The annual sums of the total percentages of sunlight for the Overheated and Underheated periods are divided by the number of the Overheated and Underheated daytime hours respectively. This step gives the intermediate result.
6. Solar thermal energy due to the beam component of hourly radiation is computed for each orientation ( $KJ/m^2.h$ ).
7. Solar thermal energy due to the beam component of hourly radiation is computed for each wall ( $KJ/h$ ).
8. Total solar thermal energy gain of the building due to the beam component of hourly radiation is computed ( $KJ/h$ ).
9. Annual hourly solar thermal energy gains of the building

- due to the beam component of solar energy are grouped under two intensities, the Overheated and the Underheated.
10. The annual sums of solar thermal energy gains of the building due to the beam component of solar energy for the Overheated and Underheated groups are divided by the number of Overheated and Underheated daytime hours respectively.
  11. The results of the fifth and tenth steps are evaluated comparatively.

The first part of the procedure is applied to three blocks (Fig.1) of the same area and height, but of different design, for Istanbul and Antalya and for 1., 11., and 21. days (Fig.2) of the months with Zeren's (1962, 1967) adoption of Olgyay charts. For the second part, however, only the second block is examined for Istanbul, and only for 21. days (Fig. 3, 4) of the months. Hence comparisons of two sets of meteorological data and all the parameters mentioned above may be seen clearly from the graphics relative to the changes in eight orientations. e.i., N, NE, E, SE, S, SW, W, and NW.

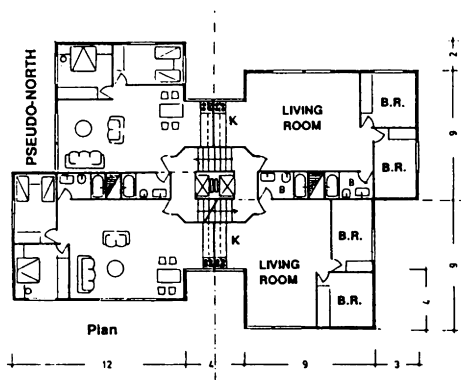


Fig. 1. Plan

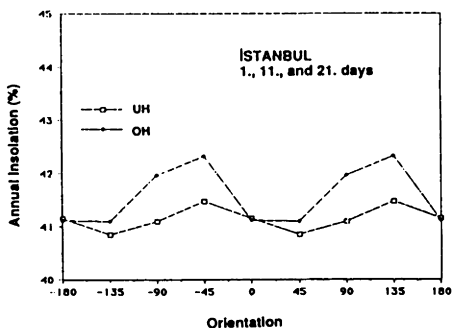


Fig.2. Intermediate Result

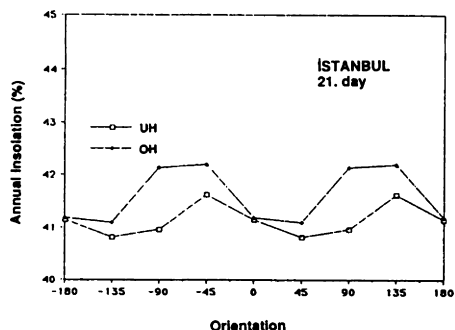


Fig.3. Intermediate Result

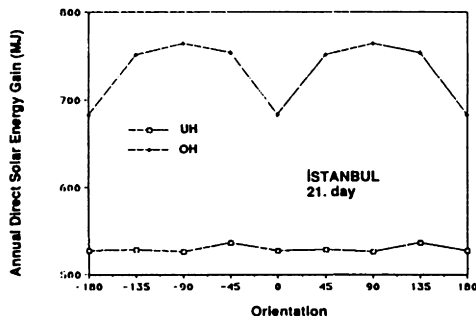


Fig.4. Final Result

Although percentages of sunlight on the vertical exterior walls are computed with program Sunlight, a shading technique based on a parallel projection algorithm and the inclusion of the thermal effect mentioned above is done by Liu-Jordan's well known equations, the procedure is applicable to other scientists' formulae and shadow analysis models as well.

## RESULT

The procedure may be used to generate a wide variety of building blocks and to define alternative proportion of block's sides. The irradiance load and the climatological effects on external surfaces of building blocks may be evaluated for any orientation, time of day and for different localities to define physical characteristics of building surfaces. The procedure generates useful information for the control of solar and climatological environment and to develop building regulations for planning control. Thus the procedure may be employed in conjunction with other performance criteria for a synthesis of an integrated architectural solution.

## REFERENCES

- BALCOMB, J.D. and JONES, W.A. (1988). Workbook for Workshop on Advanced Passive Design, Bled, Yugoslavia, March 21-25.
- DUFFIE, J.A. and BECKMAN, W.A. (1980). Solar Engineering of Thermal Processes. Wiley-Interscience, New-York.
- ELAGÖZ, A. (1989). Enerji Korunumlu Yapıların Yönlendirilmesi ve Bicimlendirilmesi için Yeni Bir Metod. Ph.D.Diss., İTÜ.
- KUSUDA, T. (1980). Review of Current Calculation Procedures For Building Energy Analysis. NBSIR 80-2068.
- KUSUDA, T. and ISHII, K. (1977). Hourly Solar Radiation Data for Vertical and Horizontal Surfaces on Average Days in the USA and Canada. NBS BS Series, 96, US Dept. of Commerce.
- LIU, B. and JORDAN, R.C. (1960). The Interrelationship and Characteristic Distribution of Direct, Diffuse and Total Solar Radiation. Solar Energy, 4, 1-19.
- LIU, B. and Jordan, R.C. (1961). Daily Insolation on Tilted Surfaces Toward the Equator. ASHRAE Journal, 3, 53-59.
- LIU, B. and JORDAN, R.C. (1963). A Rational Procedure for Predicting the Long Term Average Performance of Flat Plate Solar Energy Collectors. Solar Energy, 7, 53-74.
- LITTLE, A.D. (1979). Building Energy Analysis Computer Programs With Solar Heating and Cooling System Capabilities. EPRI Report ER-1146, Mass.
- OLGYAY, V. and OLGAY, A. (1963). Design With Climate. Princeton University Press, New Jersey.
- WRIGHT, (1982). Pseudoshadows for Site Planning. ASHRAE Transactions, 368-386.
- ZEREN, L. (1962). Türkiyenin Tipik İklim Bölgelerinde En Sıcak Devre ve En Az Sıcak Devre Tavini-I, İTÜ, İstanbul.
- ZEREN, L. (1967). Türkiyenin Tipik İklim Bölgelerinde En Sıcak Devre ve En Az Sıcak Devre Tavini-II. İTÜ, İstanbul.

\*\*\*

The authors express their gratitudes to Dr. James P. CONLON for his precious contribution with creating program Sunlight.

PASSIVE SOLAR ENERGY AS A FUEL  
1990 - 2010

S H BURTON AND J DOGGART

The ECD Partnership  
11-15 Emerald Street London WC1N 3QL

**ABSTRACT**

This paper is based on a study carried out for DGXII of the Commission of the European Communities in 1989/90 on the current and potential future use of passive solar energy in buildings throughout Europe. Presented here are the results for eight northern countries, Belgium, Denmark, France, West Germany, Ireland, Luxembourg, the Netherlands and the UK.

**KEYWORDS**

Buildings; cooling; energy; heating; lighting; solar.

**PURPOSE OF THE STUDY**

The study set out to answer three main questions:-

How much solar energy is currently used in buildings in the European Community?

How much solar energy could be used in the future, in the years 2000 and 2010?

What could be the consequent reduction in pollution, particularly the reduction in carbon dioxide (CO<sub>2</sub>)?

**USING SOLAR ENERGY**

Making use of the sun's energy has always been an essential part of living. All buildings can be designed to make use of the sun for heating and to exclude the sun to stop overheating. The sun also provides natural daylighting inside buildings.

Passive solar definitions:

This study looks at the use of passive solar energy in all buildings for heating, cooling and lighting. Heating by passive solar energy was defined as the sun entering a building directly through the windows or indirectly through sunspaces, wall panels etc, and being used or stored inside the building with little or no use of fans or pumps. Cooling by passive solar design was defined as shading, natural ventilation and the use of naturally cooled air (from the ground or evaporative cooling) to stop a building overheating. Daylighting by passive design was defined as allowing natural light to enter deep into a building and ensuring that artificial lighting is only in use when natural lighting is insufficient.

Passive design in new buildings, refurbishments and for retrofitting.

All buildings make use of some solar gain for heating and lighting and this use can be increased at any stage in the building's life. The simplest and most effective way is at the design stage, when solar heating, cooling and daylighting measures can be incorporated with minimal extra cost or inconvenience. During major refurbishment, some solar measures can be introduced with significant effects. Lastly, some solar measures can be added on to a building at any time, sunspaces, shading devices, transparent insulation cladding, etc.

**ESTIMATING SOLAR ENERGY USE**The "spreadsheet" and information sources.

The method used was to build up the total solar usage from all the constituent parts, in all the constituent countries. A computer "spreadsheet" was developed, one for each country, and available information, estimates and projections inserted. Information was collected from published sources such as the CEC Eurostats data, unpublished papers and documents and experts in each country. Much of the information required was simply not available, so estimates were made on the basis of what was available, comparison with other countries and expert opinion. The spreadsheet approach makes future updating, when new information becomes available, fairly straightforward.

Base and "technical potential" solar contributions.

The "base case" solar usage was defined as the contribution of passive solar design to heating and cooling loads if no action is taken to increase the usage in the future. The base case does not include any solar contribution for daylighting in either houses or non-domestic buildings.

The "technical potential" solar contributions to heating, cooling and lighting were defined as the maximum achievable overall in



the years 2000 and 2010, taking into account technical difficulties such as overshadowing but assuming that otherwise all houses would be built or refurbished according to solar principles. Clearly this potential will not be achieved without drastic measures. This is discussed later.

#### Solar heating in houses.

Using solar energy to heat houses is the best researched and documented area in the field of passive solar research. The current, or base, solar usage was built up for each country from the number of houses, their gross heating demand and the percentage solar contributions as determined from monitoring projects. New build, refurbishment and demolition rates were used together with solar contributions monitored in new and refurbished solar houses to estimate technical potential solar contributions for 2000 and 2010.

#### Solar cooling in houses.

The need for cooling in houses was only considered for countries in southern latitudes but this includes France to a small extent. Passive or natural cooling design is estimated in this study to currently provide half of the demand in houses where cooling is necessary but where air-conditioning is not used. In the small proportion of houses already using air-conditioning, no passive cooling contribution was considered. The possible contribution of passive design for the years 2000 and 2010 was built up from new build and refurbishment rates assuming increased natural design contribution rates to the cooling demand.

#### Daylighting in houses.

Daylighting in houses was not considered as an area of solar gain since auxiliary lighting is not normally required in houses in the daytime so no savings can be made by improved design.

#### Offices, factories, schools etc.

The non-domestic sector has far more diverse building types and less information is available. Broader estimates were made mainly on the basis of current energy usage and estimates of increases in energy consumption available from CEC research. New build and refurbishment rates were forecast and estimates made of possible solar contributions from case studies and other research. Solar contributions to heating, cooling and lighting for year 2000 and 2010 were built up in this way.

#### Pollution savings from solar design.

Pollution savings in terms of CO<sub>2</sub>, SO<sub>2</sub>, NO<sub>x</sub> and nuclear waste for each country were calculated based on the fuel split within that

country and the total equivalent savings resulting from the solar design.

#### Development of new technologies.

The estimates are made on the basis of the use of tried and tested methods and components for maximising solar gain. Whilst on the one hand it is unlikely that all these will be implemented, on the other hand it is possible that new technologies will be developed which could significantly increase solar usage. Over the next 20 years the development of transparent insulation seems likely to have the most significant effect.

### **RESULTS - SOLAR ENERGY USE AND POLLUTION REDUCTION**

#### Solar energy use in 1990 compared with other fuels.

Passive solar energy at present supplies the eight northern countries of the European Communities with the equivalent of 61 million tonnes of oil equivalent (mtoe) of primary energy per annum. In the building sector alone (ie excluding industrial process heat and transportation energy use) solar energy supplies 11% of the total (figure 1). Thus it is clear that solar energy is already a very important fuel in northern Europe.

#### Solar energy use in the future.

Over the next 20 years, if no specific action is taken to promote the use of passive solar energy, a small rise of 4.5% above the 1990 levels is predicted by the year 2000, falling back to the 1990 level by the year 2010. The reduction is due to reduced heating demand resulting from higher insulation standards. However if action is taken, the potential exists to greatly increase the use of solar energy. By the year 2000 the overall amount could be increased by 22% of the 1990 usage, an increase of more than 13 mtoe, and by 2010 the amount by 43%, or more than 26 mtoe per annum.

These potentials are the maximum technically possible and include allowances for buildings which cannot be oriented optimally etc. In practice the potential will be reduced by such factors as low take up rates and poor design and operation.

#### Where most solar energy is used.

Figure 2 shows the increase in individual solar contribution in the 5 categories (domestic heating, non-domestic heating, domestic cooling, non-domestic cooling and non-domestic lighting) for the eight countries.

FIGURE 1

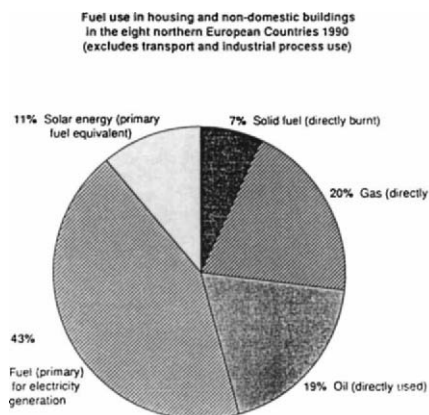
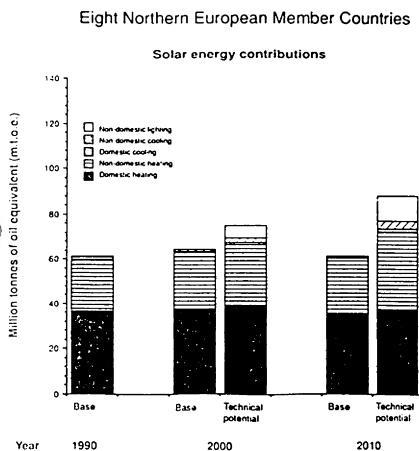


FIGURE 2



Solar contributions to heating (nearly 60 mtoe per annum) are the largest, in absolute terms, and the largest increase is forecast in solar heating in non-domestic buildings at over 11 mtoe per annum by 2010 and reflects the relatively high rates of new construction and refurbishment in this sector compared to housing. Nearly as large is the increase in the use of daylighting in non-domestic buildings, an increase of 11 mtoe per annum by 2010.

The contribution of passive solar design to the reduction of cooling loads gives much smaller savings than that to the reduction of heating loads, due to the small need for cooling in northern Europe.

#### Atmospheric pollution savings from the use of solar energy.

At present passive solar design saves 162 million tonnes of CO<sub>2</sub> per annum, 0.7 million tonnes of SO<sub>2</sub> and 0.2 million tonnes of NO<sub>x</sub> (Oxides of Nitrogen).

Figure 5 shows the pollution savings arising from the use of passive solar energy for all eight countries.

If the technical potential solar contributions determined in this study were achieved, the amount of CO<sub>2</sub> saved per annum by the year 2010 would rise to 223 million tonnes, an increase of 38%. The annual saving in CO<sub>2</sub> production below 1990 levels, due to solar design, could be 30 million tonnes by the year 2000 and 61 million tonnes by the year 2010.

Potential savings in SO<sub>2</sub> and NO<sub>x</sub> are shown to reduce in the future due to implementation of legislation to reduce emissions of these gases from power stations. If targets for reduction in emissions are met, the problems associated with emissions of SO<sub>2</sub> and NO<sub>x</sub> (principally "acid rain") will thus be greatly reduced.

FIGURE 3

Solar energy usage in the eight northern countries 1990

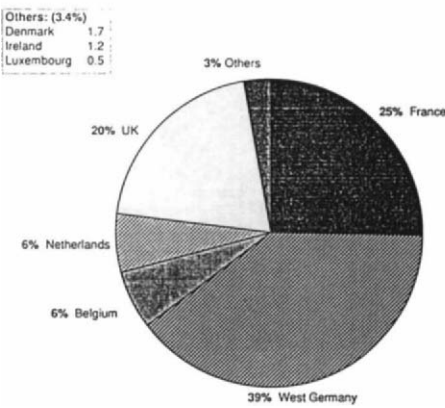


FIGURE 4

Population in the eight northern countries 1990

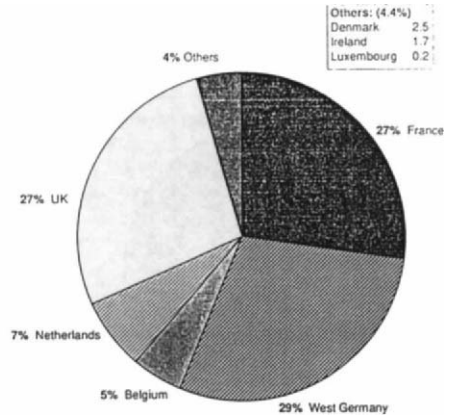
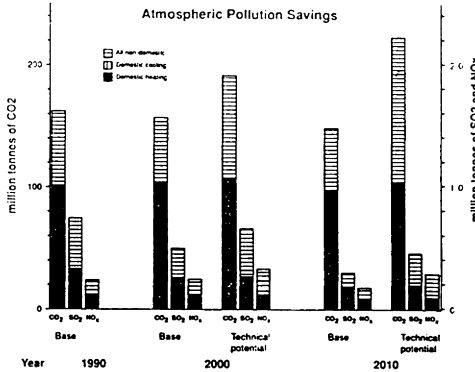


FIGURE 5

Eight Northern European Countries



Two countries, Germany and the UK, currently contribute two thirds of the savings in CO<sub>2</sub>, due to solar design. France contributes only 13% to the savings due to its large nuclear energy sector. The picture is broadly unchanged by 2010, if the technical potential is achieved.

Nuclear waste savings from the use of solar energy.

At present solar energy reduces nuclear waste by more than 18% from that which would be produced without the solar contribution. Five countries use nuclear power but France dominates and contributes around 77% of the 1990 savings and 67% of the 2010 potential savings. Overall, solar design could increase savings of nuclear waste by around 67% by 2010.

## SUN, WIND AND ENERGY AT HIGH LATITUDES

G.S. SALUJA

Department of Building and Environmental Engineering,  
University of Ulster at Jordanstown, Newtownabbey,  
Co Antrim, BT37 0QB, Northern Ireland, U.K.

### ABSTRACT

A comparison is made between northern and southern latitude locations of the U.K. with regard to energy requirements and the availability of solar and wind energy. Two case studies are presented, one of passive solar heating of local authority council housing at a latitude location of  $58^{\circ}\text{N}$ , and another of wind energy for holiday chalets at a latitude location of  $60^{\circ}\text{N}$ . Finally a case is presented to combine solar and wind energy to reduce the mismatch between the availability of energy and its requirements.

### KEYWORDS

Sun; wind; energy; solar and wind energy; energy at high latitudes.

### INTRODUCTION

In the north of Scotland the question is still frequently asked, "Is there enough sunshine for harnessing solar energy?". The case for higher solar energy utilisation, specially for passive solar heating, could not be more straightforward. Firstly, the irradiation on south facing inclined and vertical surfaces at higher latitudes is not significantly less than that at lower latitudes. Secondly, almost year round requirement for space heating at higher latitudes makes the match between energy needs and the availability of solar energy more attractive. Finally summer overheating at higher latitudes is less problematic.

In the case of wind energy the match between energy needs and its availability is much more in tune. In the U.K. higher latitude locations are generally windier than lower latitude locations. Also, the seasonal variations in solar and wind energy densities complement each other.

### AVAILABILITY OF SOLAR RADIATION AND ENERGY REQUIREMENTS

Although the incidence of solar radiation on a horizontal surface decreases

with increasing latitude, the north/south divide is not clear cut. For example, over a 30 year period, Aberdeen recorded 3.71 average daily bright sunshine hours, compared with 3.65 hours at Durham, 3.55 hours at Birmingham, and 3.74 hours at Greenwich (Meteorological Office, 1963). These locations lie at latitudes of 57.1, 54.3, 52.5 and 51.5°N.

Table 1 shows yearly irradiation on horizontal and south facing (vertical and 45° inclined) surfaces and Degree Day data (base 18°C) grouped at two monthly intervals for Lerwick, Aberdeen and Kew (Page and Lebens, 1986).

Table 1. Yearly global irradiation and Degree Days for three locations (Values in brackets show % of Kew values)

	Location		
	Kew (51.5°N)	Aberdeen (57°N)	Lerwick (60°N)
Yearly irradiation (kWh/m <sup>2</sup> )			
Horizontal	941 (100%)	864 (91.8%)	786 (83.5%)
South (Vertical)	743 (100%)	747 (100.5%)	641 (86.3%)
South (45°)	1051 (100%)	1003 (95.4%)	882 (83.9%)
Degree Days (base 18°C)			
January, December	817	936	917
February, March	718	1009	865
April, November	589	743	778
May, October	381	562	630
June, September	194	371	472
July, August	158	289	404
Yearly total	2820	3756	4056

For a south facing inclined surface (optimum for active systems) gap in availability of solar radiation between Aberdeen and Kew is narrowed considerably, compared with irradiation at a horizontal surface. For passive solar applications, a south facing vertical surface in Aberdeen receives somewhat more irradiation than in Kew, reversing the trend of 8.2% lower incidence on a horizontal surface. The Degree Day figures in Table 1 illustrate that much higher space heating load at higher latitude locations is present between May and October. The lower latitude locations are more likely to be unable to utilise the available radiation and in many situations a problem of overheating may occur. Utilisation of active and passive solar thermal systems rarely exceeds 30-40% and 15-25% respectively.

#### AVAILABILITY AND POTENTIAL UTILISATION OF WIND ENERGY

The wind data recorded at the Meteorological Office (MO) sites is not a good indicator for the availability of wind power, as the logging equipment is usually located on a flat ground and at a low anemometer height of around 10 m. There are several sites which have potentially higher wind regime than those at the MO sites. The MO site data on mean annual wind speeds for the period 1971-80 is given in Table 2 (Page and Lebens, 1986).

Table 2. Mean annual wind speeds (m/s) at U.K. locations

Plymouth	5.5	Cambridge	4.8	Belfast	4.9
London	3.7	Birmingham	4.4	Newcastle	4.7
Cardiff	5.0	Manchester	4.5	Glasgow	4.5
Aberporth	6.5	Sheffield	4.0	Aberdeen	5.0
		(1973-80)		Lerwick	7.1

The wind energy density ( $W/m^2$ ) is proportional to (wind speed)<sup>3</sup>. Doubling the height of wind utilisation point would increase wind energy density by 30% to 60% or more depending upon the topography of the site. European Wind Atlas (Troen and Peterson, 1988) classifies whole of Scotland and western coast of Ireland as having best wind resource in Europe. Theoretical maximum power extracted by a wind turbine generator (WTG) has been estimated by A. Betz as 59.3% of the wind energy density. In practice it is more likely to be 40% for the best machine. Further limitations reduce the wind speed/power coefficient to 2-2.5 instead of 3. In Shetland and Orkney a wind turbine generator could harness at least twice as much energy as possible from many mainland locations.

#### CASE STUDIES

##### Passive Solar Flats at Stile Park, Stornoway, Western Isles (58°N Latitude)

The project consists of 22 energy conscious single person flats which were designed in 1983/84 and built in 1985. The flats were planned in typical Scottish tenement fashion, in pairs on each side of a common access stair, in two and three storey terraces. Service areas were located to the north and living area and bedroom in a 5.8 m frontage south facing aspect. The entry space was designed as a sunporch which also acted as a buffer zone. The living room had an additional window. Thus advantage was taken of direct gain and thermo-circulation from the sunporch. An independent solar collection feature was the glazed south surfaces of the common stairs. Surplus gains from sunporch and living area could be vented to the stairwell. The third feature was a glazed roof collector area which charged the rock-bed store by the help of a differential sensor and a fan. Any surplus heat from the stairwell was vented to the roof space. Manually controlled flaps provided natural thermo-circulation of rock-bed store heat, thus completing the thermal loop. Figure 1 shows the general arrangement of the flats highlighting passive solar features. Low level monitoring data and occupants' reaction were recorded during first two years of occupation from August 1985 to June 1987. With the help of Environmental Systems Performance (ESP) model, it has been estimated that the solar contribution amounted to between 25% and 33% of the total energy requirements. Details of this study are published elsewhere (e.g. Saluja *et al*, 1988). Occupants' reaction has been favourable and the demand for the flat is high despite a slight rent levy. Although the flats were built on the basis of council cost guidelines, the passive solar features were estimated at ?400/flat (1983 ?) and a payback period of 10 years was calculated at the design stage.

Further Developments. Western Isles Islands Council also built a similar number of family houses at the Stile Park Development during 1985-86 incorporating the sunspace concept, with the provision of a short duct to the

north side and a differential sensor to transfer the surplus heat. These houses are currently being monitored under a DoE contract. The Council is embarking on another set of passive solar flats at the nearby Spring Field Road Development. These flats will have sunporch, glazed stairwell and roof collector, but no rock-bed store.

The Gordon District Council Howford Housing Scheme, currently under construction in Inverurie, near Aberdeen, includes six units in shelter housing with a passive glazed facade of S-SW, as well as a roof collector. One of the features of these units is to admit maximum daylight by providing strategic spacing between different houses. The houses are scheduled to be completed in summer 1991 and will also be monitored under a DoE contract.

#### Wind energy for Easterhoull chalets at Scalloway (60°N Latitude) in Shetland

This project was sponsored by the Commission of the European Communities (CEC) as a demonstration scheme to provide wind generated electricity to tourist isolated and island communities. It provided electricity for 11 all-electric holiday chalets and the owners' house. The project was sanctioned in 1984 and a 55 kW wind turbine generator (WTG), with two induction generators rated at 11 kW and 55 kW and a tower height of 22.3 m, was installed in August 1985. Figure 2 shows the layout of the scheme. The WTG was connected to the island's diesel grid. Detailed description of the project can be found elsewhere (e.g. Saluja, 1989a and 1989b). Daily records were kept of energy production, its import from and export to the grid during the monitoring period of 33 months. The location of WTG was not ideal as it was shadowed by a surrounding hill when the wind was blowing from east or south east. Some important results are summarised below.

Machine availability and production of wind generated electricity: Over the 33-month monitoring period the WTG produced 368,103 kWh of energy and the availability of the machine was 97%. In 1986 the machine produced 152,308 kWh of energy (a capacity ratio, actual output/output at rated power, of 0.31) at an average annual wind speed of 7.41 m/s at Lerwick. The WTG produced energy for 67% of the period in 1986. When normalised at long term mean annual wind speed of 7.21 m/s at Lerwick and predicted for the WTG site, the production should have been 198,700 kWh of energy, based on performance curve of the WTG, resulting in the energy loss of 30%.

WTG cost, electricity tariffs and economics of installation: The total cost of installation was £41,102 (1985 £). Insurance cost for the first five years was £1,108 and regular servicing cost was around £300 per year. Electricity tariffs include availability, reactive energy and unit charges. In 1989 the unit charge was £0.0518/kWh and excess of energy exported to the grid earned £0.0258/kWh (this compared very favourably with the mainland North of Scotland rate of £0.0186/kWh). Since 1985, the cost of importing energy from the grid has increased and the income from export of the surplus energy has decreased. Consumption during 1986 was 118,411 kWh and only 43% of wind generated energy was directly used. The payback period was estimated at 10.7 years. However if the utilisation factor increased to 60%, 80% and 100%, then payback periods would reduce to 9.5, 8.6 and 7.8 years respectively. These calculations ignore local authority rates payable.

Operational and maintenance problems: Remoteness of the location put some strains on the O & M schedules and costs. No planned service contract was taken out, resulting in some delays. The WTG performed well until a fatal day of 28 December 1988. As a result of high wind speeds and severe



gusting, power cuts and machine malfunction the nacelle fell off the tower onto the ground and the system had to be scrapped. The owner, manufacturer and the insurance company accepted part liabilities and an amicable settlement was reached. Provision of improved controls in the later models of WTGs has considerably reduced the chances of such fatalities.

#### PROSPECTS OF COMBINING SOLAR AND WIND ENERGY

Table 3 shows the estimated solar energy density at a 45° south facing surface (Page and Lebens, 1986) and wind energy density at a 20 m (Troen and Peterson, 1988) for long term monthly averages for Aberdeen and Lerwick. Solar and wind energy complement each other and reduce seasonal variation in total energy which is also more in tune with energy needs of buildings. The cost aspects could easily provide an economic case for large solar areas and small wind turbines. Combination of wind energy for electricity and solar energy for thermal needs would prove immensely beneficial to the mankind.

Table 3. Wind and solar energy densities ( $W/m^2$ ) at Aberdeen and Lerwick Meteorological Office Station locations

Month	Lerwick			Aberdeen		
	Wind (20 m)	Solar (S)	Total	Wind (20 m)	Solar (S)	Total
January	975	15	990	295	45	340
February	650	58	708	165	75	240
March	715	100	815	325	90	415
April	435	156	591	210	115	325
May	325	163	488	180	110	290
June	295	189	484	150	120	270
July	250	166	416	110	105	215
August	250	148	398	90	105	195
September	495	106	601	150	95	245
October	585	66	651	170	80	250
November	845	30	875	305	50	355
December	1105	10	1115	295	40	335
Annual	577	101	678	204	115	319

#### REFERENCES

- Meteorological Office (1963). Averages of bright sunshine for Great Britain and Northern Ireland 1931-60. H.M.S.O., London.
- Page, J. and Lebens, R. (Eds.) (1986). Climate in the U.K. - a handbook of solar radiation, temperature and other data. H.M.S.O., London, 391 pp.
- Saluja, G.S. (1989a). The success and failure of the 55 kW Scalloway wind turbine generator. In: Proc. BWEA St Andrews Workshop (Twidell, J. Ed.).
- Saluja, G.S. (1989b). Wind energy for Easterhoull chalets (EUR 12117). European Communities Commission, Luxembourg. 79 pp.
- Saluja, G.S., Porteous, C.D.A. and Holling, A. (1988). Operating experience of passive solar heating at 58°N latitude. Solar World Congress, Hamburg, Pergamon Press. 6 pp.
- Troen, I. and Peterson, E.L. (1988). European Wind Atlas. Riso National Laboratory, Riso, Denmark, 600 pp.

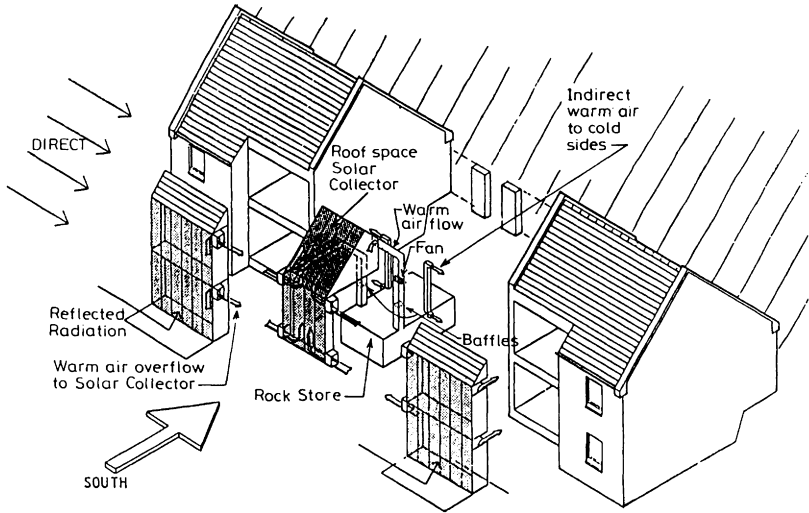


Fig. 1. Passive solar features of Stile Park Flats at Stornoway, Isle of Lewis, Scotland (58°N Latitude)

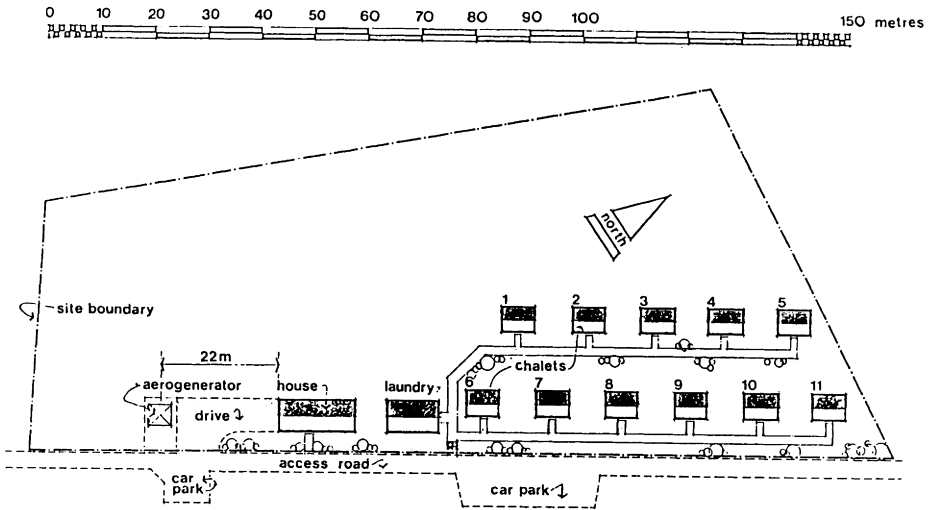


Fig. 2. Site layout of wind turbine generator installation for Easterhoull chalets at Scalloway, Shetland Islands, Scotland (Latitude 60°N)

**STORAGE BATTERIES FOR PHOTOVOLTAIC APPLICATIONS  
- A COMPARATIVE STUDY**

Kazim Raza and A.A.M.Sayigh  
Department of Engineering  
University of Reading  
Whiteknights  
Reading (Berks) RG6 2AY

**ABSTRACT**

Proper choice of storage batteries in photovoltaic systems (those which require storage) is very essential for the system reliability and to meet the load demand throughout the operational life. Battery voltage and capacity are the most important parameters to know. This paper discusses the battery requirements for PV applications (the exact requirements of the battery system for PV use is a complex one, considering the electrochemistry involved, different battery designs, and control systems) and the battery storage systems at present available for selection. The final decision however should base on optimization of parameters such as energy and power density, current demand, cycle life, required maintenance, service temperature range, safety aspects and the costs of both the battery and the control system which must control both the rate and level of charge and discharge.

**INTRODUCTION**

Electric power produced by solar cells is highly dependent upon the amount of sunlight the solar cells receive. Since the insolation level ( $W/m^2$ ) changes as a result of variations in atmospheric conditions, the PV output would fluctuate. Unlike solar thermal plants that have thermal inertia, the response of PV output to any change in solar intensity is immediate. Because of its intermittent nature, PV power generation systems are usually oversized and need some form of energy storage back up. In most cases the back up provided is in the form of "batteries" (i.e an energy storage device or reservoir that when charging directly converts electrical energy into chemical energy). By connecting it to a consumer device/apparatus, the stored energy is received during discharge. The DC output from the solar cell array can either be used to charge the battery or be transmitted directly to the load. For an AC output it is essential to incorporate an inverter with the system. The battery size (capacity) chosen should be able to meet the load demand reliably throughout the duty cycle and life. Sizing requires the typical input characteristics of the solar array, the kW profile over an average day, month and year, max. and min. kW, insolation data, environmental conditions, and system voltage.

## REQUIREMENTS FOR PV APPLICATIONS

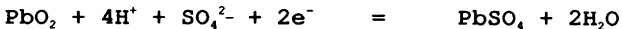
All installation and applications of batteries have their particular characteristic needs as common car batteries have to deliver a high current for a small period of time, a traction battery supplies current for a longer duration and so. Similarly, PV systems operate to supply load for extended periods and batteries are discharged to a higher depth of discharge (DOD). The exact requirements of the battery system for PV use is a complex one, however, in brief to satisfy most of the requirements of PV application, battery should have following characteristics<sup>1</sup>

1. Low cost ( ~ \$ 100 /kwh)
2. Withstands deep depth of discharge ( ~ 80 %)
3. Cycle life >4000 cycles
4. Withstands overcharge and overdischarge
5. No maintenance requirements
6. Capability to indicate the state of charge

The battery having all the above mentioned characteristics is not available as yet. Nickel hydrogen mainly used in space applications meet most of the requirements except cost<sup>2</sup>. At present lead-acid and nickel cadmium batteries are mostly used in photovoltaic systems compromising some of the disadvantage. A table at the end is presented giving the comparison among the battery systems.

### LEAD ACID BATTERY

Lead acid cell, more consistently named the "lead acid oxide cell" commenced in 1859 with the construction by the French physicist, Gaston Plante, of the first practical rechargeable cell, consisting of two coiled lead strips, separated by a linen cloth, which forms the basis of the most widely used secondary battery. The detail and theory of electrochemical reactions can be found in the literature<sup>3,4,5</sup>. The basic reactions are, at positive electrode (PbO<sub>2</sub>),



at negative electrode (Pb)



The overall electrochemical reaction is



The electrolyte density vary from 40% by weight of H<sub>2</sub>SO<sub>4</sub> (1.30 Kg dm<sup>-3</sup>) at full charge, with an associated open circuit voltage (OCV) of 2.15V at 25°C to about 16% by weight of H<sub>2</sub>SO<sub>4</sub> (1.1 Kg dm<sup>-3</sup>) when fully discharged, with an OCV of 1.98V<sup>6</sup>. Major advantages and disadvantages are listed as under

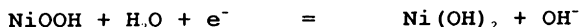
- ADVANTAGES: 1. Long life ( ~ 300-400 cycles depending on DOD)  
 2. Ability to be discharged to a very low value  
 3. Relatively good cell voltage; 2.1V/cell approx.  
 4. Fairly acceptable energy density; 12 Wh/lb  
 5. Satisfactory safe working temperature range -18°C to 43°C  
 6. The completely reversible reactions produce little physical

change in plates

7. Uses comparatively cheap and plentiful material
  8. Low operating and initial cost over other systems<sup>7</sup>
  9. Delivers both low and high currents
  10. Use of gel electrolyte enables full discharge to be employed without sulphating even if left in this condition for 28 days
- DISADVANTAGES: 1. Utilizes one of the heaviest metals, lead.  
2. Develops stratification over the period of time which reduces the performance  
3. Low service life; 3-5 years

### NICKEL CADMIUM BATTERY

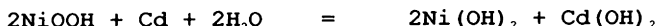
In a nickel cadmium battery system, the positive plate is nickel hydroxide and negative plate is a mixture of cadmium and iron. The reaction occurring on these plates (electrodes) can be found in literature<sup>7</sup>. Most simply the reactions are at positive plate



at negative plate



The overall cell reaction commonly acceptable is



The electrolyte in Ni/Cd is a solution of potassium hydroxide with a density of 1.18 to 1.23 g/ml<sup>6</sup> which may also contain 15-50 g/l lithium hydroxide to improve the cycle life of the positive plate, especially at elevated temperatures. Nickel cadmium cell behaviour is strongly temperature dependent, and gives longest life at about 5°C to 15°C<sup>8</sup>. Charge control method, voltage limit (temperature compensated)/current taper, optimizes the life of Ni/Cd battery<sup>9</sup>. The cost of nickel cadmium system is generally higher than that of lead acid so that overall cost of energy storage is 5-7 times higher. However, long cycle life, low maintenance and high reliability have made it an obvious choice for a number of applications. The basic features of the system

- ADVANTAGES: 1. Outstanding long life both in shelf and operation  
2. Low maintenance cost  
3. Holds a constant voltage over the normal discharge time  
4. Good performance at low temperatures  
5. Able to accept high charge/discharge rates, high overcharge and can remain, discharged for long periods without damage  
6. Higher service life >10 years<sup>10</sup>  
7. Standard cell potential; 1.299V at 25°C
- DISADVANTAGES: 1. Expensive storage system  
2. Very high self discharge  
3. Very low charge efficiency at low charging currents  
4. Check of charge condition is not possible

### NICKEL HYDROGEN BATTERY

This system is the hybrid of hydrogen electrode technology of the fuel cell and nickel electrode from alkali secondary cells. The battery generally consists of nickel oxide and hydrogen electrodes separated by zirconium oxide cloth or asbestos felt separators used to immobilize the 30% KOH aqueous electrolyte. The principle cell reaction is



It has an OCV of 1.5-1.6V, in its fully charged state. The system have the following advantages

1. High cycle life  $\sim$  6000 cycles at 80% DOD<sup>2</sup>
  2. Higher energy density >25 Wh/lb
  3. Deep depth of discharge capability
  4. Insensitive to overcharge and overdischarge
  5. Offer substantial weight savings
- But with these good features it also posses some undesirable
1. Degradation of nickel electrode<sup>2</sup>
  2. High cost as compared to other systems

#### SOLID STATE BATTERY

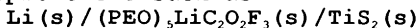
Considerable effort has been focused in recent years on the development of secondary(rechargeable) ambient temperature lithium batteries, due to the desirable characteristics generally associated with primary batteries including high gravimetric energy density, volumetric energy density, long charge retention times(10 years or more<sup>11</sup>), absence of any possible leakage or gassing. These could be constructed with excellent packing efficiency for the active components, without separators and using simple light weight containers.

##### 1. LITHIUM MOLYBDENUM

This system is approx.50% higher in energy density than that of state of the art NiCd and proportionately higher than that of sealed lead acid. The charge retention capability of the system is excellent, with a charge retention time in excess of 8 years. The system utilizes a lithium metal as anode and a granular molybdenum disulphide as the cathode, having open circuit voltage approx. 2.30 V for a cell in fully charged state.

##### 2. LITHIUM POLYMER

The mechanical flexibility of the polymer enables solid state cells to be designed with optimized electrode/electrolyte interface configuration(e.g. composite electrodes). A number of polymers are in use which attracted the great attention for further improvement such as



which has an emf 2.60 V at 25°C<sup>5</sup>. The main advantages are

1. High energy density; 60-70 Wh/Kg depending on the rate of discharge
2. Inherent safety below 110°C for electrical, mechanical and

thermal abuse

3. Wide ambient temperature operating range;  $-20^{\circ}\text{C}$  to  $70^{\circ}\text{C}$
4. Charge retention capability of greater than 8 years
5. Leak proof construction
6. Low cost as compared to other rechargeable systems
7. Extremely long shelf life
8. Excellent packing efficiency

DISADVANTAGES. 1. Anode is not 100% reversible

2. Cell cannot accommodate gross changes in electrode volume.

### CONCLUSION

The study was done as a part of the research work to look into the battery systems suitable for photovoltaic applications functionally as well as economically, making the PV systems reliable and cost effective to other conventional energy supplying systems. At present no battery system meets all the requirements of the PV applications, however, it is concluded that lead acid battery seems to be more promising due to its availability, cost and fair operation during the operational life. In colder regions Nickel cadmium can perform the job at best.

### REFERENCES

1. Kapur, V.K., and Chu, K.P.A., Battery requirements for PV energy storage, Proceedings of 16th intersociety energy conversion engineering conference, Atlanta, Georgia, Aug.1981, pp.685-688.
2. Miller, E.L., Nickel Hydrogen as an alternative to lead acid and nickel cadmium systems in non space application, IECEC, 75 Record (1975)
3. Mantell, C.L., Batteries and energy systems, McGraw Hill book company, 1970
4. Handbook of secondary storage batteries and charge regulators in photovoltaic systems (Exide Management and technology co.), Yardley, PA (USA), Aug.1981
5. Vincent, C.A., Modern Batteries, Edward Arnold, 1984
6. Barak, M., Electrochemical power sources, A.Wheaton & Co.ltd. (1980)
7. Smith, G., Storage batteries, Pitman publishing, 1971
8. Gross, S., Unsolved problems of nickel cadmium batteries, Proceedings of 16th intersociety energy conversion engineering conference, Atlanta, Georgia, Aug.1981
9. Halpert, G., The design and application of nickel cadmium batteries in space, Journal of power sources, 15(1985)
10. Williams, H.H., Field experiences with batteries in PV systems, Proceedings of INTLEC, 87, Stockholm (1987)
11. Stiles, J.A.R., Performance characteristics of lithium molybdenum disulphide rechargeable battery, Proceedings of INTLEC, 84, New Orleans, USA (1984)
12. Clark, R.P., et.al., Prospects for advanced storage battery technologies, IEEE Transactions, 1984.

10,12

## COMPARISON OF BATTERIES FOR PV APPLICATIONS

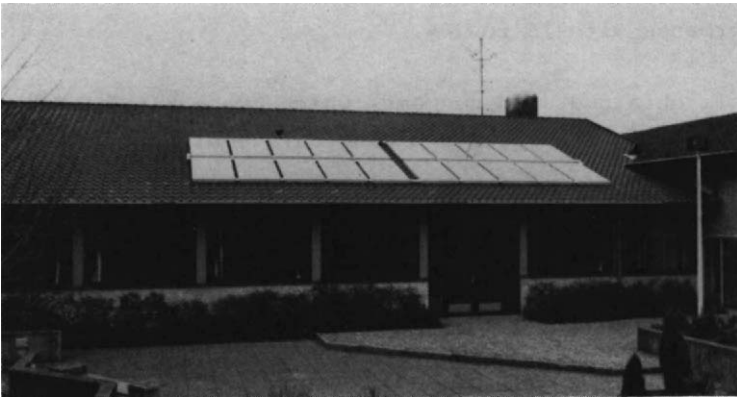
	<i>Ni/Cd</i>	<i>Lead acid</i> <i>(consumer type)</i>	<i>Lead acid</i> <i>(Industrial type)</i>	<i>Ni/H<sub>2</sub></i>
<b>self discharge</b>	<b>very high</b>	<b>low</b>	<b>low</b>	
<b>Cycle life</b>	<b>high</b>	<b>low</b>	<b>high</b>	<b>very high</b>
<b>Charge efficiency</b>	<b>very low (at low A)</b>	<b>very good</b>	<b>very good</b>	<b>good</b>
<b>Cycling ability</b>	<b>good (80% DOD)</b>	<b>low (50% DOD)</b>	<b>good (80% DOD)</b>	<b>very good (80% DOD)</b>
<b>Charge monitoring</b>	<b>not possible</b>	<b>possible</b>	<b>possible</b>	<b>possible</b>
<b>Service life</b>	<b>&gt;10 years</b>	<b>3-5 years</b>	<b>&gt;10 years</b>	<b>&gt;10 years</b>
<b>Cost</b>	<b>very high</b>	<b>low</b>	<b>high</b>	<b>very high</b>



A 44 m<sup>2</sup> Low Flow Solar System for Domestic Hot Water

by

**Torben Esbensen**  
**Consulting Engineers FIDIC**  
**Möllegade 54-56, Dk- Sønderborg**  
**Denmark**



A solar system for heating of domestic hot water has been constructed at Søfartsskolen situated in Sønderborg in Jutland.

Søfartsskolen is a boarding school with 96 seamentrainees.

The system has functioned without problems since January 1988 and is now being monitored.

The system is the first in Denmark designed for larger applications than single-family houses and making use of the attractive low flow principle based on lower flow, smaller piping and stratification in the storage tank.

It is probably also among the first larger systems internationally operating after this principle.

As in most larger solar applications the system is supplying heat for both the domestic hot water use and the considerable heat losses in the circulating piping of the hot water.

It is expected that the monitoring period will clarify the advantages and disadvantages using the low flow principle for larger systems.

For small system experiments at the Thermal Insulation Laboratory at the Technical University of Denmark have shown, that the low flow principle can increase the thermal performance with 15 to 20%.

This is obtained with systems, which are a little cheaper than normal systems since piping have smaller dimensions.

The system is of significant importance for the future design of larger solar systems in northern countries. If expectations are met it will function as prototype for these systems. Furthermore the monitoring project will add knowledge about the low flow principle to be used for future design tools.

The monitoring project is financed by the Danish Agency of Energy. The system has been designed by consulting engineers Esbensen.

The monitoring is performed by the Danish Solar Energy Testing Laboratory, while the evaluation is performed by the Thermal Insulation Laboratory.

Investment

44 m <sup>2</sup> solar collectors installed	Dcrs	60.000
Piping in the collector circuit	Dcrs	15.000
2000 litre storage tank including heat exchanger	Dcrs	30.000
Piping in the storage circuit	Dcrs	16.000
Insulation of pipes and storage tank	Dcrs	18.000
Solar collector liquid	Dcrs	3.000
Electrical supply	<u>Dcrs</u>	<u>4.000</u>
	Dcrs	146.000
Project fee	<u>Dcrs</u>	<u>24.000</u>
	Dcrs	160.000
VAT	<u>Dcrs</u>	<u>35.000</u>
	Dcrs	195.000
30% governmental grant	<u>Dcrs</u>	<u>58.000</u>
Total price for the system-owner	Dcrs	137.000 =====

Output for a normal system :

22.000 kWh (500 kWh/m<sup>2</sup>) x 0,45 Dcrs = 9.900 Dcrs/year.

Simple pay-back period : 14 years

Estimated output for a low-flow  
system-----

26.000 kWh (600 kWh/m<sup>2</sup>) x 0,45 Dcrs = 11.700 Dcrs/year

Simple pay-back period : 12 years

Heating demand :

Total domestic hot water : 73.000 kWh/year

Heat loss in the circulating pipes: 54.000 kWh/year

127.000 kWh/year

## GHANA'S RENEWABLE ENERGY DEVELOPMENT PROGRAMME

C.Y. WEREKO-BROBBY AND I.K. MINTAH

National Energy Board  
Private Mail Bag  
Ministries Post Office  
Accra, Ghana

### ABSTRACT

Renewable energy resources in the form of fuelwood, charcoal and direct sunshine provide most of Ghana's energy requirements. Fuelwood and charcoal together contribute over 80% of the country's energy consumption and enormous amounts of natural sunshine are used for both domestic, agricultural and industrial activities. However, the continued supply of woodfuels is threatened by deforestation and desertification which are being accelerated by the rapidly expanding population, timber operations and shifting agricultural cultivation. The excessive and inefficient burning of woodfuels, especially during charcoal production and use is also putting pressure on the country's forests and causing considerable environmental degradation.

Ghana's Renewable Energy Development Programme aims to assess the availability of renewable energy resources; to examine the technical feasibility and cost-effectiveness of promising renewable energy technologies; to ensure the efficient production and use of the country's renewable energy resources; and develop the relevant information base that will facilitate the establishment of a planning framework for the rational development and use of the country's renewable energy resources.

### KEYWORDS

Cassamance Kiln; Half-Orange Brick Kiln; "Ahibenso"; Improved Coalpot; KVIP toilet.

### INTRODUCTION

Renewable energy resources in the form of fuelwood, charcoal and direct sunshine provide most of Ghana's energy requirements. Fuelwood and charcoal together contribute over 80% of the country's energy consumption and enormous amounts of natural sunshine are used for both domestic, agricultural and industrial activities, especially to dry agricultural export commodities and forest industry products. However, the continued supply of woodfuels is threatened by deforestation and desertification which are being accelerated by the rapidly expanding population, timber operations and shifting agricultural cultivation. The excessive and inefficient burning of woodfuels, especially during charcoal production and use is also putting pressure on the country's forests and causing considerable environmental degradation.

## THE NEB RENEWABLE ENERGY WORK PROGRAMME

The NEB's Renewable Energy Programme, which has been designed to tackle the woodfuels supply and attendant environmental problems, aims: to assess the availability of renewable energy resources in Ghana; to examine the technical feasibility and cost-effectiveness of promising renewable energy technologies; to ensure the efficient production and use of the country's renewable energy resources; and develop the relevant base that will facilitate the establishment of a planning framework for the rational development and use of the country's renewable energy resources. The specific projects designed for the achievement of the overall objectives are grouped under two broad headings of BOIMASS and SOLAR ENERGY.

### BIOMASS

The Biomass activities of the NEB are aimed at conserving forest resources through improved production methods decreasing demand through the use of more efficient cooking devices; expanding the use of other biomass energy sources such as biogas and logging and wood processing residues; planning for the future security of biomass supply through the implementation of a sustained programme of forest regeneration and afforestation; and substituting other fuels for woodfuels. The specific projects include the following

#### Conserving Forest Resources through Improved Production Methods

An improved method using the Cassamance kiln developed in Senegal, was demonstrated to 42 people in separate activities in Kumasi ( a major sawmilling centre) and Jema/Ampoma in the transition zone. Trial firings of both the traditional earthmound and Cassamance kilns showed that the Cassamance yields more charcoal (about 16%) than the traditional kiln, and that the Cassamance kiln carbonises wood four times faster than the traditional earthmound method. A post-training monitoring exercise was conducted to determine the extent of adoption of the improved method showed that although the Cassamance kiln technique had advantages over the traditional method in terms of the yield and shorter carbonisation period, there were certain factors which limited its immediate adoption by the traditional charcoalers. Whilst the Cassamance technique required twenty-four hour surveillance, charcoalers using the traditional earthmound method were able to leave it unattended to engage in other income-generating activities such as farming and hunting. Also, whilst the traditional method required virtually no investment, the Cassamance technique required the procurement of a mettalic chimney which is an essential part of the kiln. Demonstration of the Cassamance technique is continuing in the Kumasi area alongside efforts to introduce improvements to the traditional method.

In addition to the above activities, the NEB is also demonstrating and evaluating the economic viability of the use of sawmill residues for charcoal production in Half-Orange Brick Kiln. This activity is aimed at encouraging sawmillers to incorporate charcoal making activities into their operations if this should prove to be economically viable.

#### Decreasing Demand For Woodfuels through Efficient Cookstoves

Most urban households depend on charcoal as fuel for meeting their cooking needs. However, due to the increasing scarcity of our forests, this fuel is becoming more and more expensive. This problem is aggravated by the fact that the traditional coalpot is very inefficient and wastes fuel. The Improved Charcoal Stoves activity is aimed at disseminating improved stoves in urban households, including the development of local capability in the fabrication of such improved stoves.

A locally designed stove "the Ahibenso" improved stove, has achieved average charcoal savings of 30-45% in field tests carried out in 800 household in

Accra over a nine-month period. An expenditure survey also showed that larger families consume less charcoal per person than smaller families. An average figure of about ₵9 per person/day was found for a sample of 340 households. Savings in household charcoal expenditure amounted to about 15-20%.

An assessment of the acceptability or otherwise of the new stoves was conducted using the retention rate of the stove models that participating households preferred most. At the end of the field tests about 90% of the trial households preferred the "Ahibenso" model and wanted to buy it even though they felt it was too expensive, especially in areas inhabited predominantly by the low-income group. Even when the participants were offered the stoves at a 50% discount, they could still not afford. However, 55% of the trial households have so far purchased the "Ahibenso" model. Also 20% of the households opted for the "Improved Coalpot" which is an improvement on the traditional coalpot and costs only slightly more than the latter.

The next phase of this activity, which is on-going, involves the dissemination of the "Improved Coalpot" and "Ahibenso" models in the Regional Capitals and other selected urban centres to monitor the stoves and to assess their long-term performance.

#### Expanding the Use of other Biomass Sources

In order to counter the ecological damage that has resulted from the excessive dependence on woodfuels, the NEB is assessing the use of other biomass resources such as biogas generated from both animal and human waste through pilot testing of the technology. The first pilot project was undertaken on a cattle ranch at Shai Hills with Chinese Government technical assistance and was used to teach local artisans to construct and operate biogas digesters. Two other pilot projects are underway at Appolonia, near Afienyaa and also at Okponglo, near Accra.

The objectives of the Appolonia village project are to study the various factors that may influence the transfer of biogas technology in Ghana; and demonstrate the full socio-economic benefits of biogas technology and thereby accelerate the process of biogas transfer in Ghana. The Appolonia project converts both animal and human waste to biogas which provides cooking energy to selected households. In addition, ten digesters of 50 cubic meter capacity are being constructed to produce biogas to generate electricity for lighting up the village. The Okponglo Integrated Biogas Project involves the provision of a KVIP (Kumasi Ventilated Improved Public) toilet, whose human waste is converted to biogas for cooking and to generate electricity to light up the area and use its substrate as fertiliser for landscaping and vegetable farming.

Preparatory work for phase 2 has also started. This phase will consist of the extension of the integrated approach to biogas development to areas with a high concentration of feedstock, especially in the Northern Regions. A preliminary assessment has been carried out in the Bimbila district where a biogas programme started a few years ago is at a standstill due to a number of problems such as: (a) insufficient skill in the construction of digesters; (b) lack of basic tools for the construction work; and (c) lack of transportation to convey construction materials to the selected sites. Since the local populations have shown great enthusiasm for the project, it is important to offer assistance to them, as well as to other communities facing the same problems, in order to maintain their interest.

Another activity being pursued in this area is the promotion of the use of logging and wood processing wastes as a source of energy. This includes the commercial production and use of sawdust briquettes as an energy source for commercial and industrial activities such as baking and brick and tile

manufacture. As a further measure, the use of sawdust and logging residue for charcoal production in brick kilns is being investigated. This activity has the advantage of promoting currently unused residues.

#### Planning for the Future Security of Biomass Supply

This objective is to be achieved through a sustained programme of forest regeneration and afforestation, especially in areas where intense charcoal production activities have destroyed the land and created environmental and ecological problems. In this regard under the Improved Charcoal Production activity the NEB is investigating the relocation of charcoalers from the transition zone to the areas where timber operations are carried out and where logging residues abound. A demonstration activity is in progress in a Kumasi-based sawmill to evaluate the economic and technical feasibility of using timber offcuts for charcoal production in brick kilns. This activity will also investigate the possibility of introducing this method of charcoal production to the timber producing areas. The NEB is also developing an afforestation programme in collaboration with the relevant public agencies.

#### Substitution of other Fuels for Fuelwood

In order to reduce the country's dependence on fuelwood and charcoal, the NEB is promoting the use of other fuels as a substitute. Thus, activities have been initiated to increase the use of liquefied petroleum gas in urban households. The Government has abolished the sale of LPG cylinders and introduced new marketing arrangements by which the cost of the cylinder is amortised over its life. Smaller size LPG cylinders have also been introduced to make gas accessible to the low income groups and also measures are being strengthened to ensure the safe use of LPG. Since one of the constraints to the wider use of LPG has been the high cost of stoves, the NEB is investigating the technical feasibility of local production of multi-fuel stoves which can use both LPG and charcoal and which will be affordable to low income groups.

### SOLAR ENERGY PROJECTS

The successful exploitation of Ghana's solar energy resources to pump irrigation water, dry crops, improve communication and health facilities and provide opportunities for access to modern recreational and educational facilities will foster rapid improvements in the living standards of the country's predominant rural population. To turn the enormous solar energy potential into real benefits, the NEB has embarked on a programme to assess and quantify the resource base, monitor the performance of existing solar installations and demonstrate promising solar energy technologies for selected applications. The specific activities being implemented are:

#### Solar and Wind Energy Resources Assessment

This activity involves a comprehensive assessment of the country's solar and wind energy resources to establish the necessary information base for accurate design and siting of solar installations. The NEB has already completed an assessment of existing climatic data on solar and also the state of equipment at meteorological stations all over the country. Further work to be implemented will involve upgrading of the equipment to ensure that all the necessary information will be collected. The existing data and subsequent ones to be collected will be analysed and compiled into the appropriate form (e.g. solar maps) for the design and sizing of solar installations.

This project started in January, 1988 with the installation of solar radiation measuring equipment at the Meteorological Services Department (MSD) Radiation Centre at Legon and three synoptic stations at Kumasi, Tamale and Navrongo. All the twenty-two (22) synoptic stations belonging to the MSD

have been visited to evaluate their status and data acquisition systems, particularly their accuracy and reliability.

The NEB is currently analysing the following meteorological data acquired from MSD: Solar Radiation-Daily Monthly Mean and Hourly Mean of 17 synoptic stations for 10 years; Sunshine Duration-Daily Monthly Mean of 10 synoptic stations for 10 years; Relative Humidity-Daily Mean at synoptic hours for 10 years; and Wind Speed-Daily Mean at synoptic hours for 10 years.

#### Monitoring the Performance of Solar Systems in Ghana

About 220 solar-powered systems have been installed all over the country including 163 communication equipment, 29 vaccine storage refrigerators and 27 other installations consisting of lighting, solar-powered pumps and ventilation equipment. Most of these installations have not performed as expected due to incorrect design and siting. In spite of these observations there is no systematic programme for monitoring and evaluating the performance of these installations, even though adequate information on the performance of these systems under local climatic conditions will be extremely useful for selecting appropriate systems for future applications and increase confidence in the promotion of solar photovoltaic devices in the country.

The objective of this activity is to monitor and evaluate selected solar photovoltaic installations in three different climatic zones in the country and compare their actual performance with design objectives. A nationwide census of solar installations established that most of the installations were not functioning properly due to incorrect orientation of the equipment as a result of which they are covered by shadows at certain periods of the day; poor quality storage batteries which malfunctioned after less than one year of installation; and inavailability of spare parts to carry out effective maintenance of certain components of the installations. Thus, over 80% of the communications equipment have operational problems (poor audio output) due to incorrect selection of the components. Also, out of the four solar water pumps identified, only two were found to be working; one of them had never worked. However, it was observed that the solar refrigerators had a better track record than the other installations since only two of the eleven inspected had malfunctioned.

On the basis of the above observations, some installations have been selected further study, involving the use of solar PV measuring equipment to monitor the performance of these installations.

#### Demonstration of Integrated Solar Power for Villages

The solar energy activities also cover demonstration and evaluation of solar energy technologies such as water heating, portable lighting and battery charging. To assess the potential contribution of solar energy to the Government's National Electrification Programme, the NEB intends to demonstrate and evaluate the concept of an integrated solar-powered village, relying entirely on solar energy to meet its electricity needs.

Twelve villages have been shortlisted for detailed screening, which should lead to the selection of one or two for the implementation of the pilot project. Each of the villages is at least 50km away from the national grid and the solar power option is perceived to be cheaper than connection to the grid. Some of the other criteria used for the screening of the villages are accessibility and road net work; economic and agricultural potential, solar insolation and annual sunshine hours.



# IMPROVED SOLAR OPTICAL PROPERTIES OF A NICKEL PIGMENTED ANODIZED ALUMINIUM SELECTIVE SURFACE

E. WÄCKELGÅRD, T. CHIBUYE and B. KARLSSON

Solid State Physics, Department of Technology, Uppsala University, Box 534, S-751 21 Uppsala, Sweden.

## ABSTRACT

Since commercially produced nickel pigmented aluminium absorbers show large scattering in their solar optical parameters a program for preparation, characterization and optimization of this surface has been initiated. In this laboratory program surfaces with optimum properties of  $\alpha=0.95$  and  $\epsilon=0.13$  have been prepared, while the best factory produced commercial absorber have values of  $\alpha=0.95$  and  $\epsilon=0.19$ . The emittance is critically dependent on the thickness of the surface oxide, while the absorbance depends both on thickness and nickel content. The importance of measuring the hemispherical emittance is pointed out.

## KEYWORDS

Anodic; aluminium oxide; nickel pigmented; solar absorption; thermal emittance; reflectance.

## INTRODUCTION

An ideal solar selective surface should have 100% absorbance for wavelengths shorter than  $2 \mu\text{m}$  and zero emittance for wavelengths longer than that, if the solar absorber surface have a temperature around  $100^\circ\text{C}$ . The solar and blackbody spectra both have low intensity at this wavelength as seen from Fig. 1. A variety of different surfaces have been tested and fulfill to some extent these conditions. One of the most frequently used commercial material, in solar absorbers is nickel pigmented aluminium oxide on aluminium. The production cost of this surface is low and it has fairly good selective properties and is quite resistant to degradation. The physical principle for the optical properties of such a surface is that the nonabsorbing plain oxide is changed to highly absorbing in the visible part of the wavelength region due to small nickel particles which are incorporated in the aluminium oxide. The presence of these particles introduces an absorbing component in the dielectric host matrix which changes the optical properties according to the mean field theory (Sievers, 1979).

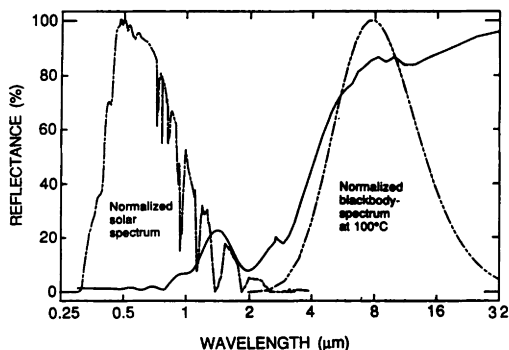


Fig. 1. The solar spectrum and blackbody spectrum at 100°C are plotted together with the reflectance of a SUNSTRIP™, nickel-pigmented aluminium oxide on aluminium solar selective surface.

One example is illustrated in Fig. 1 by the reflectance of a SUNSTRIP™ surface. Three main features deviate from the ideal case. First, the transition between high and low absorbance of the cermet layer is broad and overlaps with both the solar and blackbody spectrum. Secondly, optical interference effect within the double layer is inevitable and the interference maximum in the range 1-2  $\mu\text{m}$ , where the film has insufficient absorbance, reduces the solar absorbance. In the case of the SUNSTRIP™ surface in Fig. 1 this fortunately coincides with a low intensity interval of the solar spectrum. The third drawback with this type of cermet layer is the rather strong absorption bands of the oxide in the wavelength region 8 - 25  $\mu\text{m}$  (Tartre, 1967). There are also some absorption bands in this wavelength region originating from phosphor anions of the electrolyte, which has been incorporated in the aluminium oxide during formation (Tran Tach Lan *et al.*, 1964). These bands affect the 100°C emittance severely.

The aim of our project is to improve the solar selectivity of this type of solar absorber material. Sunstrip absorbers installed in different solar systems show large scattering in their optical properties.  $\alpha$ -values of 0.90 - 0.95 and  $\epsilon$ -values of 0.14 - 0.25 are obtained when different samples are characterized (Dolley and Hutchins, 1987; Roos *et al.*, 1988). A project for the preparation of this surface on a laboratory scale has therefore been initiated, where the physical effects which determine and limit the solar optical properties are analyzed

### SAMPLE PREPARATION

The aluminium substrate used was rolled aluminium covered with an electroplated aluminium layer, 10  $\mu\text{m}$  thick and of 99.98% purity. The samples were cut in pieces of 35x50 mm and cleaned before anodization. They were immersed for about 10 s in a concentrated alkaline detergent solution and immersed for five minutes in 1 M nitride acid. Finally they were rinsed in distilled water and dried quickly in a nitrogen gasflow.

The electrolyte used for anodization was a 2.5 M phosphoric acid at  $(19.5 \pm 0.5)$  °C. A constant dc-voltage of 10 V was used for producing oxide layers of up to 0.5  $\mu\text{m}$  which appeared to be

the limiting thickness before growth and dissolution of the oxide reached a state of equilibrium. For thicker coatings the voltage was set to 15 V. The samples were anodized in pairs, clamped together back to back. Since they both got the same oxide thickness, one of them could be kept as an anodized reference to the pigmented twin sample.

The following nickel-pigmentation was also carried out electrochemically, in a solution of pH 4.7 containing: 30 g NiSO<sub>4</sub>, 20g (NH<sub>4</sub>)<sub>2</sub>SO<sub>4</sub>, 20 g MgSO<sub>4</sub> and 20 g H<sub>2</sub>BO<sub>3</sub> per litre distilled water. The pigmentation process took between 4 and 6 minutes in order to get a visually dark surface of the sample. The initial ac-voltage of 17 V was kept constant during the first two minutes. The current had then dropped to about 350 mA. After this the voltage was continuously adjusted to maintain this current.

## MEASUREMENTS

The optical reflectance measurements were performed with a Beckman 5240 double beam spectrophotometer in the 0.35 - 2.5 μm wavelength range. The Beckman instrument was equipped with a 198851 integrating sphere for measuring the hemispherical reflectance with a BaSO<sub>4</sub> reference plate.

The spectral reflectance in the infrared wavelength range between 2 - 50 μm was scanned with a Perkin Elmer 983 infrared double beam spectrophotometer using a reflectance accessory with nearly normal incidence of the incoming light. An evaporated aluminium film on glass was used as a reference. The infrared reflectance data presented here are not corrected for the less than 100% reflectivity of the reference. Since this measurement only accounts for the specular part of the radiation the measured reflectance is too low compared to the reflectance data from the integrating sphere measurements in the overlapping region around 2 μm. This mismatch is however only noticeable for the highly reflecting samples.

The solar absorptance was calculated from the integrating sphere measurements using ASTM solar data. The normal emittance at 100°C was calculated from the infrared reflectance data corrected for the emittance of the aluminium reference used in the measurements. The total hemispherical emittance was measured calorimetrically at 100°C.

The thickness of the anodic layer was estimated from the interference fringes in the visible wavelength region using a refractive index of 1.7 for the aluminium oxide (Pastore, 1985).

## RESULTS

An anodic oxide layer formed in an acid solution has a porous structure with the pores perpendicular to the surface (Keller *et al.*, 1953). During pigmentation the pores are filled with nickel particles starting from the bottom of the pores (Andersson *et al.*, 1980; Uchino *et al.*, 1979). The filling factor - volume fraction of nickel to the total cermet volume - depends on both pigmentation current and pigmentation time in combination with how large the total pore volume of the specific oxide is. The total pore volume is largest for oxides anodized in phosphoric acid and at lowest possible voltage (Keller *et al.*, 1953). A pore volume as large as 30% of the total oxide volume can then be obtained (Pavlovic and Ignatiev, 1986). Our oxides are not quantitatively analyzed yet but they were anodized under the condition for maximized pore volume.

In order to investigate how the optical properties of the sample changes progressively during the anodization-pigmentation process, a sample were measured before cleaning, after anodization and after one, two and four minutes of pigmentation. The corresponding reflectance curves are presented in Fig. 2.

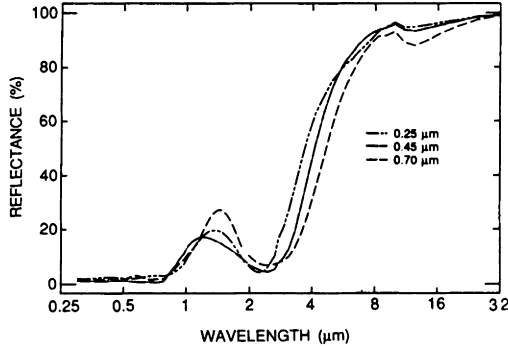


Fig. 2. The reflectance of a  $0.35 \mu\text{m}$  thick sample has been measured between subsequent steps of the pigmentation process.

The anodized sample has an oxide thickness of  $0.35 \mu\text{m}$ . The overall reflectance is reduced owing to some etching of the aluminium surface during the cleaning.

It is seen how the nickel changes the optical properties of the film from being highly transparent to highly absorptive in the short wavelength region. This absorbing region is shifted towards longer wavelengths with increasing nickel content in the oxide. However, in the infrared wavelength region, the transparency of the oxide is not altered severely by the pigmentation. It is therefore possible to select a suitable part of the wavelength region where the cermet film transforms from highly absorbing to nonabsorbing by adjusting the pigmentation time and current obtaining a specific nickel content in the oxide. When the film gets optically thicker with increased nickel content, the interference pattern is also changed in a similar manner, shifting the annoying first maximum out of the wavelength region of the solar spectrum. The sample has after four minutes of pigmentation a solar absorption of 0.95 and a hemispherical emittance at  $100^\circ\text{C}$  of 0.13.

The selective properties of the cermet can also be changed by varying the oxide film thickness. Figure 3 shows the reflectance curves of samples of thicknesses  $0.25 \mu\text{m}$ ,  $0.45 \mu\text{m}$  and  $0.7 \mu\text{m}$  pigmented under identical conditions. The transition wavelength region between high and low absorbance is shifted towards longer wavelengths with increasing film thickness. The thickest cermet layer has pronounced absorption bands in the  $8\text{-}25 \mu\text{m}$  wavelength region. This gives a large contribution to the emittance which is 0.22 for this sample. The thinnest film also has some extra absorption at about  $6 \mu\text{m}$  which is a feature of heavily pigmented samples. This is interpreted as the pores in this thin oxide being filled up to the surface. This sample has a hemispherical emittance at  $100^\circ\text{C}$  of 0.13 and the  $0.45 \mu\text{m}$  thick sample has 0.15. The samples have the same solar absorbance of 0.95.

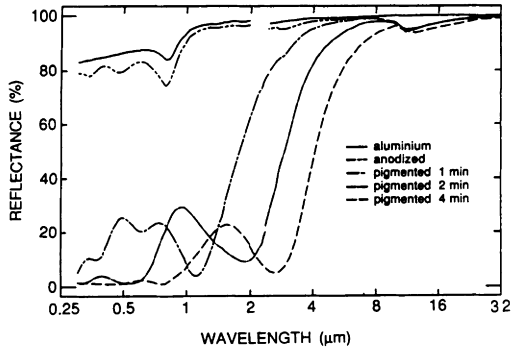


Fig. 3. Aluminium oxide of different thickness but pigmented under identical conditions.

The samples which have the best solar selectivity are presented in Table 1. For comparison we present both the normal emittance calculated from the reflectance data and the hemispherical emittance measured calorimetrically. The later one determines the radiation losses from the absorber. It is important to note that the hemispherical emittance is higher than the normal emittance.

Table 1. The samples with the best solar absorption and emittance at 100°C are presented in the table.

Oxide thickness ( $\mu\text{m}$ )	Solar absorbance	Normal emittance at 100°C	Hemispherical emittance at 100°C
0.25	0.94	0.11	0.13
	0.95	0.11	0.14
0.35	0.95	0.12	0.13
	0.96	0.12	0.16
	0.95	0.12	0.15
0.45	0.95	0.10	0.14
	0.95	0.12	0.15
	0.96	0.12	0.15
0.70	0.96	0.12	0.16
	0.94	0.15	0.21
	0.95	0.17	0.22

## DISCUSSION

The data of Table 1 shows that high absorbance can be obtained for all the chosen oxide thickness. The emittance is however increased with film thickness mainly because of the deeper absorption bands in the 8-25  $\mu\text{m}$  range. The thickest oxide of 0.7  $\mu\text{m}$  is therefore not suitable regarding the solar optical properties. All samples of thickness between 0.25 and 0.45  $\mu\text{m}$  have fairly low emittance values, and compared to the hemispherical emittance of the plain anodized samples the emittance is nearly unchanged after pigmentation. Most of the nickel pigmented solar absorbers found in the literature have an oxide thickness of 0.6 - 0.8  $\mu\text{m}$  and therefore higher emittance values than thin oxides. A thicker oxide layer is not completely pigmented, it has a top oxide layer which is almost free from nickel (Andersson *et al.*, 1980) which could be preferable regarding degradation. Samples of thickness 0.45  $\mu\text{m}$  or thinner are more fully pigmented. We have not yet investigated how the degradation affects nickel pigmented aluminium oxide in the thickness range between 0.25 - 0.7  $\mu\text{m}$ .

An improvement of the emittance from  $\epsilon=0.22$  to 0.13 corresponds to a suppression of the  $U_L$ -value for a teflon equipped glazing of around 0.5  $\text{W}/\text{m}^2\text{C}$ . According to Karlssons relation (Perers and Karlsson, 1990) this increases the annual heat production of a flat plate collector operating at  $T=70^\circ\text{C}$  with  $35\text{kWh}/\text{m}^2$ . An increase of the absorbance from  $\alpha=0.90$  to 0.95 corresponds under identical conditions to a similar annual increase of  $35\text{kWh}/\text{m}^2$ . This means that optimization of the absorber surface has the potential of increasing the annual heat production of flat plate collectors installed in the large swedish collector field by around 10%.

## REFERENCES

- Andersson, Å., O. Hunderi and C.G. Granqvist (1980). Nickel pigmented anodic aluminum oxide for selective absorption of solar energy. *J. Appl. Phys.*, **51**, 754-764.
- Dolley, P. R. and M. G. Hutchins (1987). Accelerated ageing and durability testing of spectrally selective solar absorber surfaces. In: *Advances in Solar Energy Technology* (W. H. Bloss and F. Pfisterer, Ed.), **1**, 682-685, Pergamon Press.
- Keller, F., M. S. Hunter and D. L. Robinson (1953). Structural features of oxide coatings on aluminum. *J. Electrochem. Soc.*, **100**, 411-419.
- Tran Thach Lan, F. Naudin and P. Robbe-Bourget (1964). Étude de la constitution des films d'oxyde anodique par absorption infrarouge. *J. de Phys.*, **25**, 11-14.
- Pastore, G. F. (1985). Transmission interference spectrometric determination of the thickness and refractive index of barrier films formed anodically on aluminium. *Thin Solid Films*, **123**, 9-17.
- Pavlovic, T. and A. Ignatiev (1986). Optical and thickness properties of anodically oxidized aluminum. *Thin Solid Films*, **138**, 97-109.
- Perers, B. and B. Karlsson (1990). This conference.
- Roos, A., B. Karlsson and L. H. Andersson (1988). Optical properties and durability of solar absorber surfaces based on anodized aluminium. In: *Proceedings from North Sun'88* (L. Broman and M. Rönnelid, Ed.). 539-544. Swedish Council for Building Research, Gävle.
- Sievers, A. J. (1979). Spectral Selectivity of Composite Materials. In: *Topics in Applied Physics: Solar Energy Conversion* (B. O. Seraphin, Ed.), **31**, 57-114. Springer Verlag.
- Tartre, P. (1967). Infra-red spectra of inorganic aluminates and characteristic vibrational frequencies of  $\text{AlO}_4$  tetrahedra and  $\text{AlO}_6$  octahedra. *Spectrochimica Acta*, **23**, 2127-2143.
- Uchino, H., S. Aso, S. Hozumi, H. Tokumasu, Y. Yoshioka (1979). Selective surfaces of color-anodized aluminum for solar collectors. *Nat. Techn. Report*, **25** 994-1004.

# FOURIER ANALYSIS OF DAILY SOLAR RADIATION DATA IN EGYPT

**M.T.Y. TADROS**

Faculty of Science, Physics Department  
Mansoura University, Mansoura - Egypt.

*and*

**M.A. MOSALAM SHALTOUT**

National Research Institute of Astronomy  
and Geophysics, Helwan, Cairo - Egypt.

## ABSTRACT

*The aim of this work has been to obtain a Typical Annual Time function by the application of a calculating procedure based on a Fourier analysis to a daily solar radiation data of 8 stations of different climatic conditions in Egypt.*

*This function allows to estimate the most probable value of the Global Solar Radiation for every day of the year. The deviation for the annual average, of any year in the period (1981 - 1986), from the annual average obtained by the Typical Annual Time Function is less than 5 %.*

## KEY WORDS

Solar radiation over Egypt, Fourier analysis

## INTRODUCTION

The determination of the Global Solar Radiation (GSR) is very important in different scientific applications. Recently, it has been recognized that the type of statistical information on solar radiation has generally been published in the professional literature is insufficient for sizing and optimizing solar energy systems of very high solar fractions. For example, the kinds of empirical and even analytic design methods that are appropriate for solar energy systems of intermediate solar fractions do not offer adequate accuracy in the optimal sizing of stand-alone photovoltaic systems [1]. Therefore, Solar Radiation Data (SRD) should be "time series" analyzed. A statistical meaningful projections of these data into the future will be given by the analysis for a past period of these "time series" [1, 2].

Shaltout [3] calculated the input solar energy for 77 sites in Egypt using the relative humidity and the cloudness observations with deviation about 5% from the observed values.

Mehanna [4] gave a system of simple linear equations to estimate monthly mean value of GSR over Egypt with deviation about 10 % from the observed values.

A method of calculation has been developed by Alberto and Recio [5] to obtain a Typical Annual Time Function using Fourier analysis for Barcelona.

Also, Baldasano Recio et al [6] had been obtained the Typical Annual Time Function by the application of a calculation procedure based on a Fourier analysis to SRD of 21 stations in Spain.

Helwa and the authors [7] determined the GSR for different latitudes in Egypt by using The Fourier analysis of daily SRD for the year 1982.

**DATABASE**

It is possible to subdivide the climatological regime of Egypt into different regions as Upper Egypt, Western Desert, Middle Egypt, Cairo area, Delta and Suze Canal, Red Sea and Mediterranean Sea [3]. Therefore, we had choiced our available data to cover the most climatological regions. Actually we could not obtain any data for Sinai and the Red Sea regions. The daily SRD, in our study, were obtained from Solar Radiation and Radiation Balance Data [8]. The names and the climatological regions as well as the available years for each station are indicated in table 1.

**Table 1 : Names, Climatological region, and years of data for 8 stations**

Station	Climatological region	Years	
Aswan	Upper Egypt	1981, 1983 - 1986	5
Kharga	Western Desert	1981 - 1986	6
Asiut	Middle Egypt	1982 - 1986	5
Cairo	Cairo area	1981 - 1986	6
Bahtim	Cairo area	1981 - 1986	6
Tahrir	Delta and Suze Canal	1981 - 1984, 1986	5
Mersa Matrouh	Mediterranean Sea	1982 - 1986	5
Sidi - Barrani	Mediterranean Sea	1985, 1986	2

**METHOD OF ANALYSIS**

The procedure of Fourier analysis depends on the fitting of a trigonometric function (sine and cosine components). The analysis by this procedure allows to estimate the amplitude and the phase angle for different harmonics, as well as the percentage of representation of each harmonic in the data (annual variance). To obtain a Typical Annual Time Function, as detailed in [5, 7, 9], we had used the following expression :

$$S(D, r) = SM_T + AM_T(r) \cos(2\pi Dr/N - \theta_T(r)) \dots \dots \dots (1)$$

where S(D,r) is the estimated daily GSR for any harmonic r, (r = 1, 2, ....., N/2 for 1st, 2nd harmonic, ..... etc), and for any day D, (D = 1, 2, ..., N); N is the total number of days. SM<sub>T</sub> is the annual average of the daily GSR, AM<sub>T</sub>(r) and θ<sub>T</sub>(r) are the annual amplitude and the phase angle, respectively, corresponding to the specified harmonic r.

Our method of analysis for obtaining the Typical Annual Time Function consists of two stages:

1. The first stage is to obtain the representative equation of each year, for different stations, by applying Fourier analysis to the set of annual series year after year.
2. The second stage is to obtain the representative equation for the average of all the available years, day by day, for each station. The representative equation in this case will be called Typical representative equation or Typical Annual Time Function.



## RESULTS AND DISCUSSIONS

The annual variance, has been estimated by the application of Fourier analysis to obtain either the annual representative equation or the Typical representative equation (corresponding to the first harmonic, varies between 73 % and 97 %. The harmonic is the best harmonic describes the Annual Solar Radiation [5, 7, 9]. Accordingly, the first harmonic will be used in this work.

The annual average ( $SM_T$  in  $MJ/m^2$ ), the amplitude ( $AM_T$  in  $MJ/m^2$ ), Phase angle ( $\theta_T$  in degree) and the percentage of presentation of the Typical representative equation in the measured data variance; % VAR) are given in table 2. The same variables with the percentage deviation of the annual average for the yearly representative equations, of each station, from the corresponding Typical representative equation are given in tables 3-10.

**Table 2 : Parameters of the Typical Annual Time Function for analyzed stations.**

Station	Year	$SM_T$	$AM_T$	$\theta_T$	% VAR
Aswan	5	23.50	6.60	- 0.1984	94.7
Kharga	6	22.88	6.91	- 0.1758	96.1
Asiut	5	21.75	7.90	- 0.1314	95.9
Cairo	6	19.02	8.46	- 0.1043	97.1
Bahim	6	19.96	8.68	- 0.1043	97.1
Tahrir	5	19.93	8.62	- 0.1261	97.0
M.Matrouh	5	20.58	9.71	- 0.0952	96.4
Sidi-Barrani	2	19.74	9.40	- 0.1221	91.7

**Table 3 : Parameters of the yearly representative equation with deviation of annual average from Typical average for Aswan.**

Years	$SM_T$	$AM_T$	$\theta_T$	% VAR	% Deviation
1981	24.57	6.71	- 0.2254	88.7	4.55
1983	23.53	6.53	- 0.1476	73.0	0.13
1984	23.33	6.83	- 0.1916	86.1	- 0.72
1985	23.13	6.49	- 0.1631	86.2	- 1.57
1986	23.03	6.52	- 0.2715	92.2	- 2.00

**Table 4 : Parameters of the yearly representative equations with deviation of annual average from Typical average for Kharga.**

Years	SM <sub>T</sub>	AM <sub>T</sub>	$\theta_T$	% VAR	% Deviation
1981	23.84	7.16	- 0.1810	89.0	4.20
1982	22.84	6.84	- 0.1471	84.2	- 0.17
1983	23.13	6.91	- 0.2070	90.5	1.09
1984	22.58	6.58	- 0.2200	87.0	- 1.31
1985	22.70	7.21	- 0.0958	83.7	- 0.79
1986	22.10	6.81	- 0.2171	92.1	- 3.41

**Table 5 : Parameters of the yearly representative equations with deviation of annual average from Typical average for Aslut.**

Years	SM <sub>T</sub>	AM <sub>T</sub>	$\theta_T$	% VAR	% Deviation
1982	21.65	7.85	- 0.0906	84.3	- 0.46
1983	22.07	7.93	- 0.1366	88.1	1.47
1984	22.20	7.90	- 0.1744	90.4	2.07
1985	21.50	7.96	- 0.0875	83.0	- 1.15
1986	21.31	7.90	- 0.1761	91.2	- 2.02

**Table 6 : Parameters of the yearly representative equations with deviation of annual average from Typical average for Cairo.**

Years	SM <sub>T</sub>	AM <sub>T</sub>	$\theta_T$	% VAR	% Deviation
1981	19.82	8.50	- 0.0903	87.5	- 4.21
1982	19.10	8.74	- 0.0875	86.4	0.42
1983	18.87	8.59	- 0.0970	85.3	- 0.79
1984	19.16	8.37	- 0.1588	86.5	0.74
1985	18.51	8.35	- 0.0809	82.5	- 2.68
1986	18.62	8.46	- 0.1552	87.0	- 2.10

**Table 7 : Parameters of the yearly representative equations with deviation of annual average from Typical average for Bahim.**

Years	SM <sub>T</sub>	AM <sub>T</sub>	$\theta_T$	% VAR	% Deviation
1981	20.93	8.89	- 0.1057	88.3	4.86
1982	19.75	8.77	- 0.0777	86.8	- 1.05
1983	19.79	8.75	- 0.0871	85.8	- 0.85
1984	20.02	8.46	- 0.1579	88.1	0.30
1985	19.25	8.68	- 0.0688	82.5	- 3.56
1986	19.99	8.54	- 0.1389	85.7	0.15

**Table 8 : Parameters of the yearly representative equations with deviation of annual average from Typical average for Tahrir.**

Years	SM <sub>T</sub>	AM <sub>T</sub>	$\theta_T$	% VAR	% Deviation
1981	20.71	8.59	- 0.1168	87.2	3.91
1982	19.81	8.65	- 0.1120	87.0	- 0.60
1983	19.88	8.82	- 0.0749	85.9	- 0.25
1984	20.06	8.75	- 0.1584	88.9	0.65
1986	19.16	8.31	- 0.1797	87.5	- 3.86

**Table 9 : Parameters of the yearly representative equations with deviation of annual average from Typical average for Mersa Matrouh.**

Years	SM <sub>T</sub>	AM <sub>T</sub>	$\theta_T$	% VAR	% Deviation
1982	20.59	9.96	- 0.0556	84.2	0.05
1983	20.73	9.88	- 0.0733	85.9	0.73
1984	21.23	9.63	- 0.1039	86.9	3.16
1985	20.51	9.82	- 0.0945	83.9	- 0.34
1986	19.81	9.31	- 0.1613	87.0	- 3.74

**Table 10 : Parameters of the yearly representative equations with deviation of annual average from Typical average for Sidi Barrani.**

Years	SM <sub>T</sub>	AM <sub>T</sub>	$\theta_T$	% VAR	% Deviation
1985	20.51	9.82	- 0.0945	83.9	- 0.34
1986	19.81	9.31	- 0.1613	87.0	- 3.74

From tables 3-10, it is clear that the percentage deviation of the annual average for the yearly representative equation, from the average of the Typical one, is less than 5 %. Also, the yearly variance for all the stations is less than that of the Typical Annual Time Function (table 2). This indicates that the Typical Annual Time Function obtained by this method of analysis gives a best fitting for the data of a long period. The longer of the period of the data is the better for determining the Typical Annual Time Function with more accuracy.

Figures 1-8 show the daily values of GSR measured during 1986 and the corresponding representative equation for all the analyzed stations. Figures 9-16 show the representative equations for the period from 1981 to 1986 (dashed lines) and the corresponding Typical Annual Time Function (dotted lines) of the different climatological regions.

Figures 13 and 14 show that there is a similarity for the Typical Annual Time Function of Bahtim and Tahrir. Their maximum values are 28.63 MJ/m<sup>2</sup> in 25th of June for Bahtim, 28.54 MJ/m<sup>2</sup> in 24th of June for Tahrir and minimum values are 11.28 MJ/m<sup>2</sup> in 25 th of December for Bahtim, 11.31 MJ/m<sup>2</sup> in 24th of December for Tahrir. Therefore, Tahrir region can be related to the climatological GSR regime of Cairo area.

The remarkable decrease of the amounts of GSR for Cairo (maximum 27.47 MJ/m<sup>2</sup> in 25<sup>th</sup> of June and minimum 10.61 MJ/m<sup>2</sup> in 25<sup>th</sup> of December, Lat. 30° 05' N and Long. 31° 17' E, see Figure 12) with respect to Bahtim, Lat. 30° 08' N and 31° 15' E (see Figure 13) could be attributed to the air pollution in Cairo.

It is clear, also, from Figures 9, 10 and 11 that, the Upper Egypt region have the maximum values of GSR (maximum 30.13 MJ/m<sup>2</sup> in 20<sup>th</sup> of June and minimum 16.9 MJ/m<sup>2</sup> in 19<sup>th</sup> of December for Aswan). The Western Desert GSR regime is lower than that of the Upper Egypt but higher than that of the Middle Egypt (maximum 29.79 MJ/m<sup>2</sup> in 21<sup>th</sup> of June, minimum 15.96 MJ/m<sup>2</sup> in 21<sup>th</sup> of December for Kharga and maximum 29.65 MJ/m<sup>2</sup> in 24<sup>th</sup> of June, minimum 13.85 MJ/m<sup>2</sup> in 23<sup>th</sup> December for Asiut).

Figures 15, 16 show that the Mediterranean Sea region is similar to that of Cairo area in winter (minimum 10.33 MJ/m<sup>2</sup> in 24<sup>th</sup> of December for Sidi-Barrani and 10.86 MJ/m<sup>2</sup> in 26<sup>th</sup> of December for Mersa Matrouh). In summer, it is similar to that of Middle Egypt (maximum 29.13 MJ/m<sup>2</sup> in 24<sup>th</sup> of June for Sidi-Barrani) or the Upper Egypt as in Mersa Matrouh (maximum 30.29 MJ/m<sup>2</sup> in 26<sup>th</sup> of June).

### CONCLUSIONS

A Typical Annual Time Function is obtained for 8 measurement stations, in Egypt, of daily GSR over a horizontal surface by the application of a computational method based on Fourier analysis.

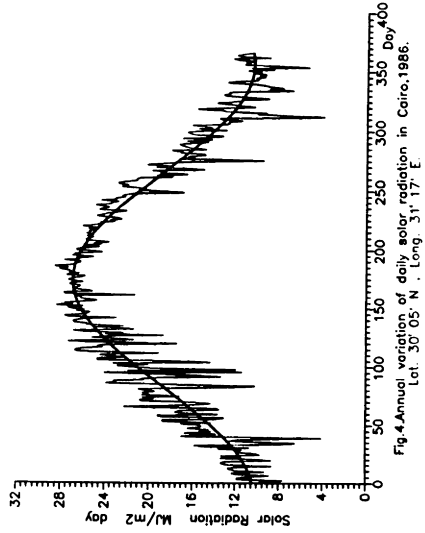
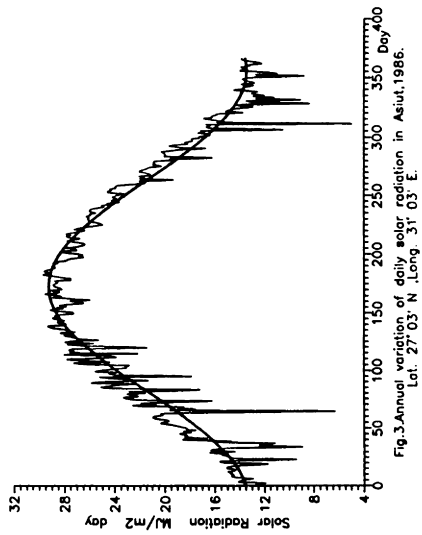
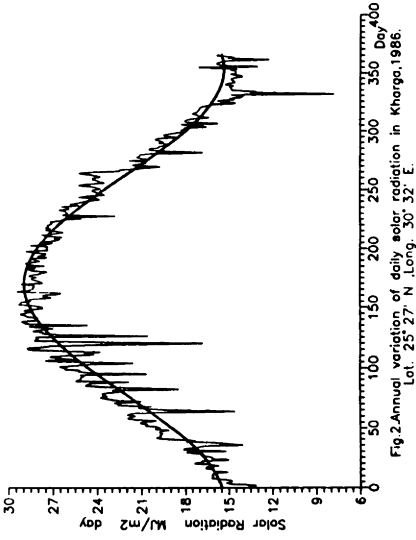
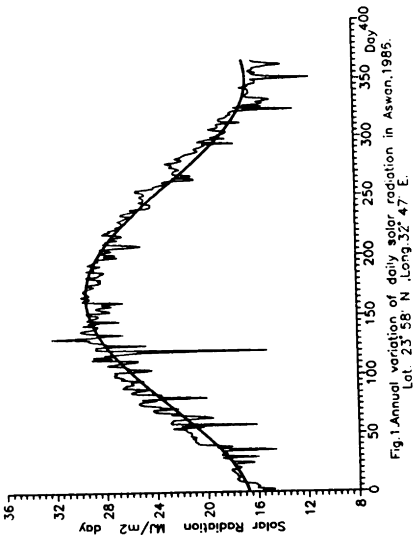
The percentage of representation, for the data, obtained by yearly representative equation, corresponding to the first harmonic, varies between 73 % and 92 %. The Typical representative equation gives the mentioned percentage between 91 % and 97 %. The percentage of other harmonics is less than 2.5 %.

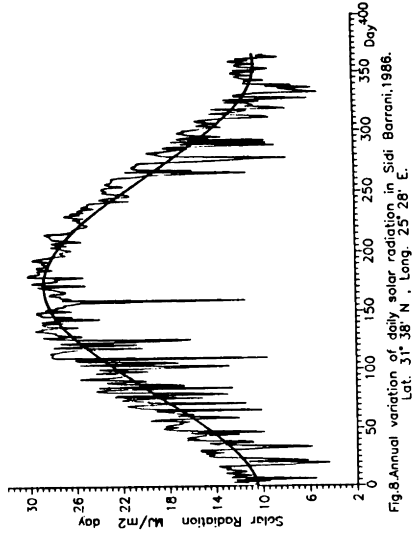
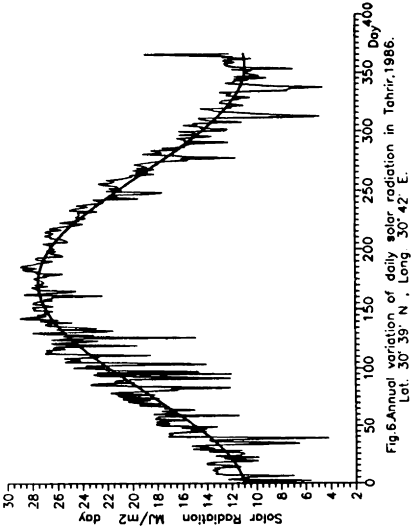
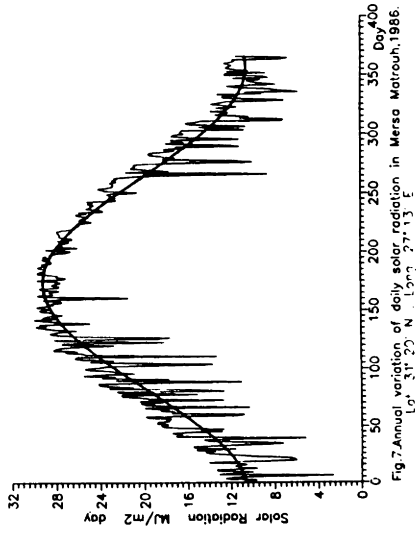
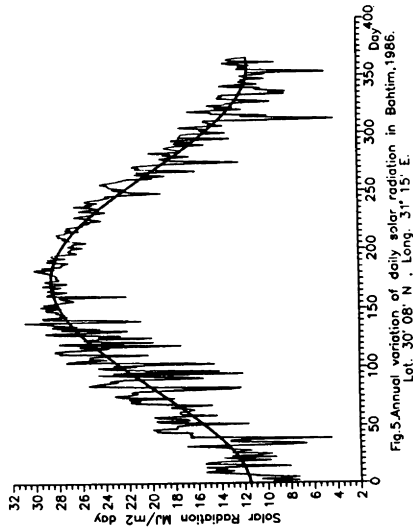
The climatological GSR regime of the Mediterranean Sea is similar to that of Upper Egypt region, in summer, and is similar to that of Cairo area, in winter.

The obtained Typical Annual Time Function, for each station, allows to estimate the most probable value of the GSR for every day of the year. The deviation of the annual average, of any year, from that obtained by the Typical Annual Time Function, in the period from 1981 to 1986, is less than 5 %.

### REFERENCES

1. J.M. Gordon and T.A. Reddy, Time series analysis of daily horizontal Solar Radiation. *Solar Energy* 41 (3), 215 - 226 (1988).
2. C.E.P. Brooks and N. Carruther, *Handbook of Statistical Methods in Meteorology*, 2nd ed., 412 PP. Her Majesty's Stationary Office, London (1978).
3. M.A.M. Shaltout, Solar Energy Input to Egypt, Helwan Institute of Astronomy and Geophysics Bulletin, No. 271, 113 pp Egypt, (1981).
4. A.M. Mehanna, *Meteorological Research Bulletin*, Egypt, 8, p69 (1971).
5. C.S. Alberto and J.M. Recio, Fourier Analysis of Meteorological Data to obtain a Typical Annual Time Function. *Solar Energy* 32(4), 479 - 488 (1984).
6. J.M. Baldasano, J. Clar and A. Berna, Fourier analysis of daily Solar Radiation data in Spain. *Solar Energy* 41(4), 327 - 333 (1988).
7. N.H. Helwa, M.T.Y. Tadros and M.A.H. Shaltout, Simple Method for Computation of Solar Radiation for different Latitudes in Egypt. *Indian Engineer (I) Journal - IDP*, 68, 53 - 60 (1988).
8. **Solar Radiation and Radiation Balance Data.** The World Net Work, Voeikov Main Geophysical observatory, Leningrad, USSR (1981 - 1987).
9. R.C. Balling, Jr., Harmonic analysis of monthly insolation levels in United States. *Solar Energy* 31(3), 293 - 298 (1983).





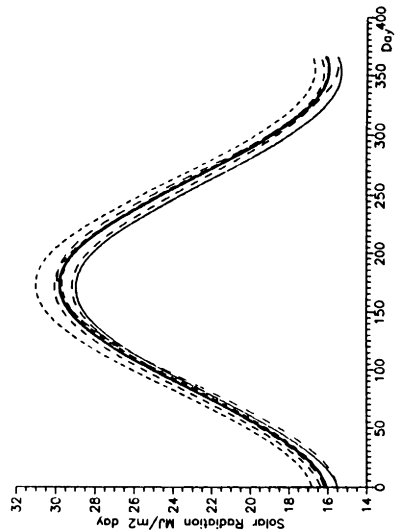


Fig.10.Representative equation of each year for Kharga.

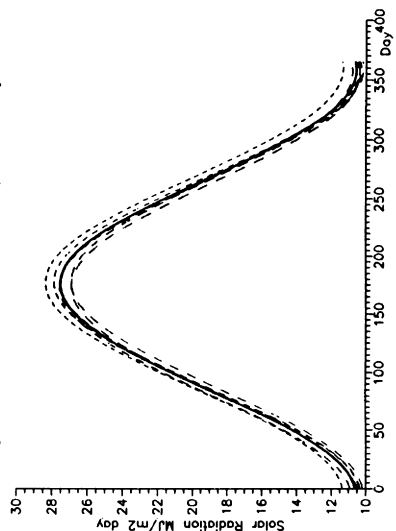


Fig.12.Representative equation of each year for Cairo.

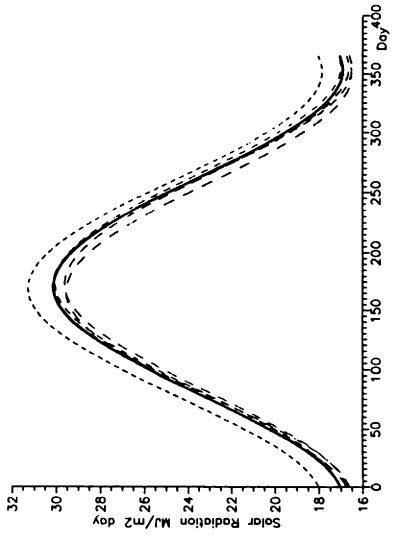


Fig.9 Representative equation of each year for Aswan.

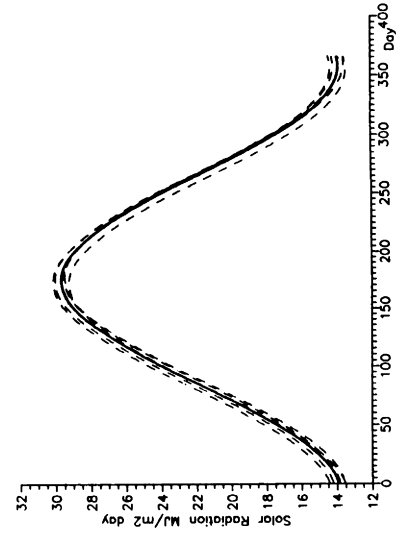


Fig.11.Representative equation of each year for Aslut .

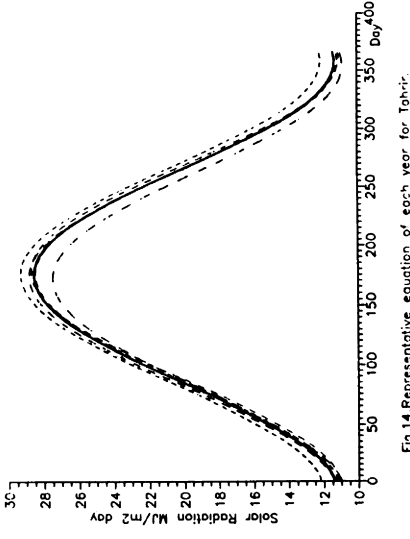


Fig.14.Representative equation of each year for Tahrir.

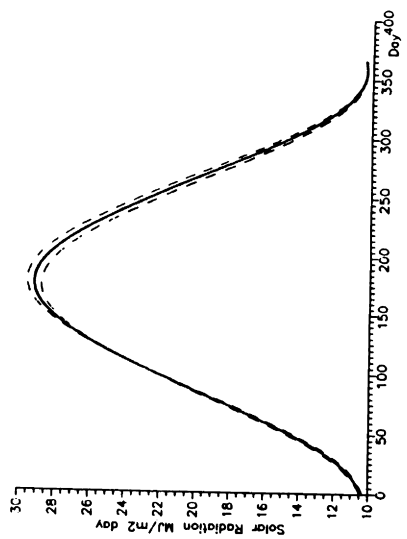


Fig.16.Representative equation of each year for Sidi-Barroni.

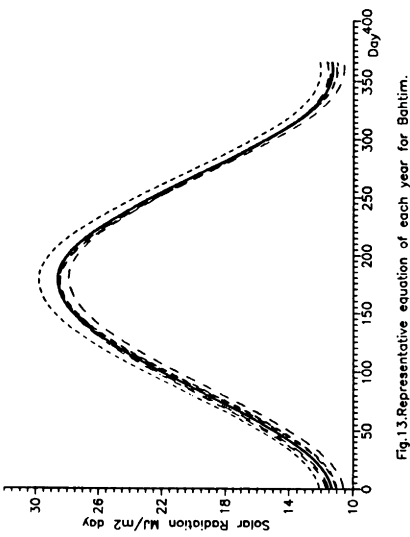


Fig.13.Representative equation of each year for Bahim.

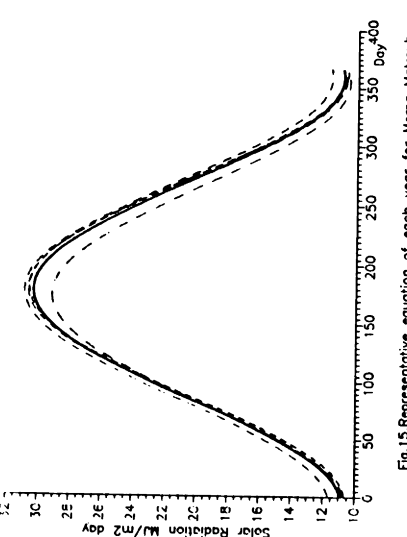


Fig.15.Representative equation of each year for Mersa Matrouh.



## MODELS FOR ESTIMATING SOLAR IRRADIATION AND ILLUMINATION

J.A. OLSETH\* and A. SKARTVEIT

Geophysical Institute, Division of Meteorology  
University of Bergen, Allégt. 70, N-5007 Bergen, NORWAY.

\* also at The Norwegian Meteorological Institute, Oslo.

### ABSTRACT

There is an increasing demand for detailed data on irradiance and illuminance on hourly basis both for horizontal and for sloping surfaces. This paper describes models for estimating these detailed data from long-term global irradiation and also presents examples of how these models are used to produce the required detailed data for the Norwegian solar energy community.

### KEYWORDS

Hourly solar irradiance and illuminance, models.

### INTRODUCTION

Mean global radiation yields monochromatic radiance integrated with respect to wavelength, solid angle and time. But a large number of radiation-driven processes are both non-linear and spectrally selective, and they also depend on the orientation of the irradiated plane. Therefore, the requested data relate to e.g. specific locations and time resolutions, to specified sloping planes (e.g. solar collectors, windows) or to specified parts of the solar spectrum (the entire solar spectrum or e.g. ultraviolet radiation, photosynthetic active radiation, daylight illumination). Such detailed data often have to be modelled from less detailed, existing data (most often mean global radiation, which are the most abundant solar radiation data).

In earlier papers (Olseth and Skartveit, 1985 and 1986) solar radiation data on annual, monthly, and daily basis have been presented for Norway. In this paper a brief survey of the work done to provide the Norwegian solar energy community with detailed solar radiation data on hourly basis is presented.

## MODELS

The frequency distribution of hourly global irradiance has been modelled in terms of solar elevation, season and monthly mean values of global radiation (Olseth and Skartveit, 1987a). This frequency distribution, given in Fig. 1, shows a characteristic bimodal pattern with the highest frequencies (modes) at high and low solar radiation. The bimodality, which is a result of the typical "U-shaped" frequency distribution of cloud cover, may be highly significant for non-linear radiation-driven processes.

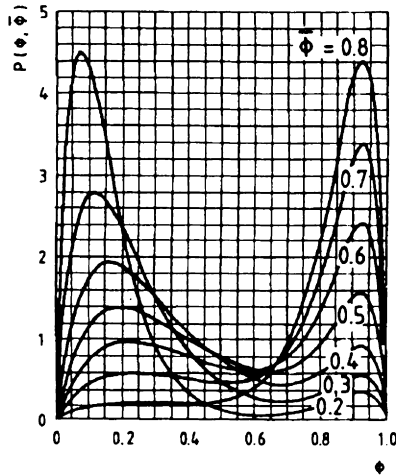


Fig. 1. The probability density function  $P$  of hourly clearness index  $\phi$  (observed global/estimated clear sky global) for various monthly mean indices  $\bar{\phi}$ .

A model for the partition of hourly global irradiance into its diffuse and direct components, as a function of clearness index and solar elevation, has been developed and verified (Skartveit and Olseth, 1987). This model, given in Fig. 2, together with a model for the angular distribution of diffuse radiance (Skartveit and Olseth, 1986) yields a complete description of the angular distribution of hourly global irradiance as a function of solar elevation and global irradiance. The model for the angular distribution of diffuse radiance accounts for the facts that the diffuse radiance increases with decreasing angle from the sun in cloudless weather, and that it increases with decreasing angle from zenith at overcast. Given global irradiance and surface albedo, these models can be used for estimating irradiances on arbitrarily orientated planes.

By a physically based interpolation between published models for cloudless (Bird and Riordan, 1986) and overcast (Stephens *et al.*, 1984) conditions, a model (Olseth and Skartveit, 1989),

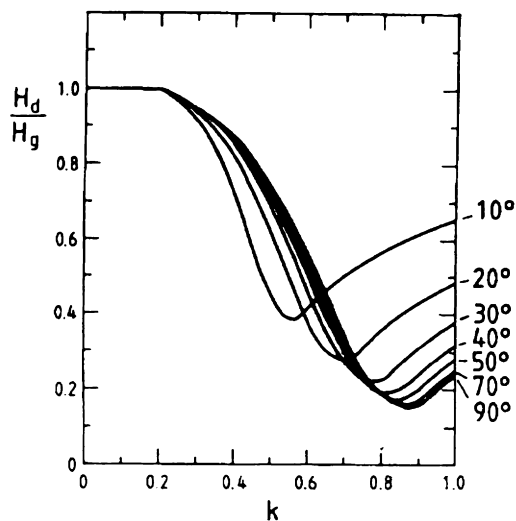


Fig. 2. Modelled hourly diffuse fraction  $H_d/H_g$  (diffuse/global) as a function of clearness index  $k$  (observed global/extraterrestrial global) for various solar elevations.

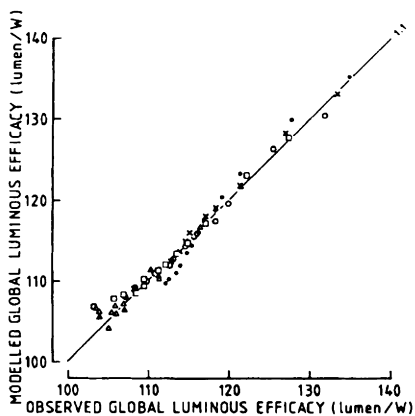


Fig. 3. Modelled vs. observed group mean values (groups according to solar elevation and sunshine duration) of hourly global luminous efficacies (illuminance/irradiance) for Bergen (60.4°N, 5.3°E), 1965-72 (22988 hours).

giving the spectral composition of direct and diffuse radiation, under arbitrary cloudiness and solar elevation, has been developed and verified. In the model the diffuse radiation is decomposed into radiation from cloudless sky, radiation transmitted through thick clouds, and radiation transmitted through thin clouds or/and reflected from thick clouds. The spectral composition of each of these three components and of the direct radiation is subsequently estimated. This model is used for estimation of daylight illumination from global radiation data, and it is tested against daylight data from Bergen (Fig. 3).

## RESULTS

With monthly mean values of global radiation as the only input, the models described above have been used to produce tables giving duration (for each month and for the whole year) of hourly solar irradiance (entire spectrum) upon 11 differently orientated surfaces for 16 Norwegian stations between  $58^\circ$  and  $70^\circ$  N (Olseth and Skartveit, 1987b). From these tables the expected response of non-linear radiation-driven processes can be estimated, and Fig. 4 shows examples of what can be read from the tables for one of the stations, namely Lillehammer.

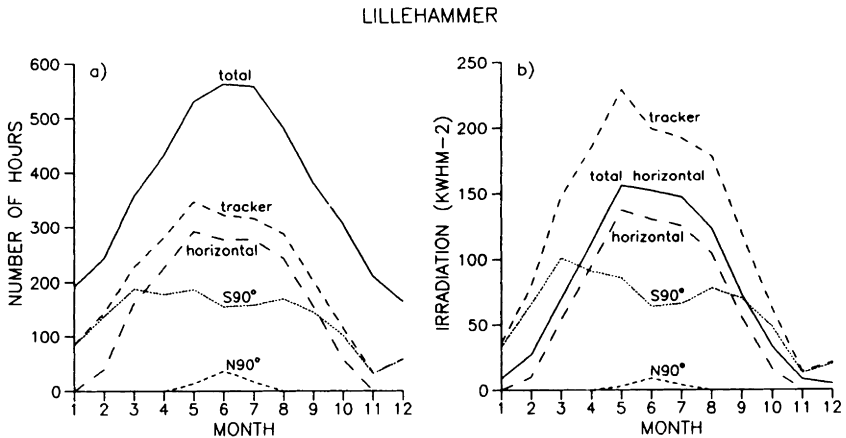


Fig. 4. a) Monthly number of hours with sun above free horizon (total), and with hourly irradiance above  $200 \text{ Wm}^{-2}$  for a horizontal surface (horizontal), a sun-tracking surface (tracker), and vertical surfaces heading towards south ( $S90^\circ$ ), and north ( $N90^\circ$ ) for Lillehammer ( $61.1^\circ\text{N}$ ,  $10.5^\circ\text{E}$ ). b) Monthly global irradiation (total horizontal), and monthly irradiation during hours with irradiance above  $200 \text{ Wm}^{-2}$  for the same surfaces as in a).

Similar tables, giving duration of daily illumination (total and diffuse) upon the horizontal and 4 vertical surfaces for different parts of the day, have also been produced (Skartveit and Olseth, 1988). From such tables summations can give the illumination statistics for a given room/window-geometry and a given length of working-day, and Fig. 5 gives examples of what can be read from the tables for Lillehammer in June.

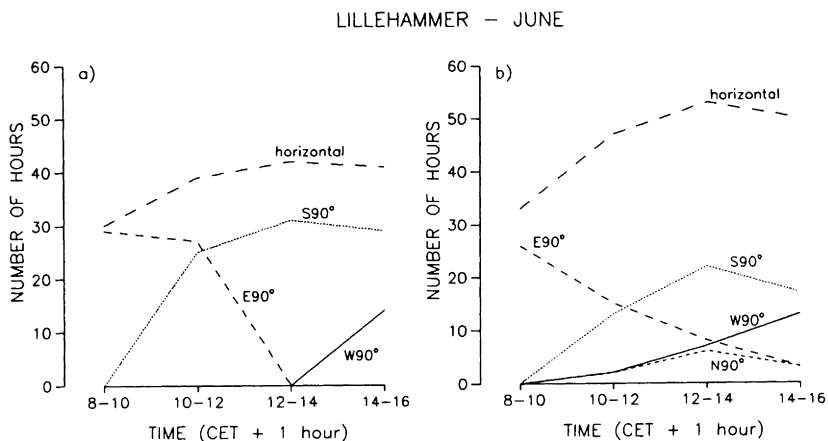


Fig. 5. Monthly number of hours with a) total illumination above 40 klux, and b) diffuse illuminance above 20 klux for an horizontal surface (horizontal), and for vertical surfaces facing south ( $S90^\circ$ ), west ( $W90^\circ$ ), east ( $E90^\circ$ ), and north ( $N90^\circ$ ) for 4 different two-hours intervals during the working-day for Lillehammer in June (CET + 1 hour is daylight saving time in Norway).

### Acknowledgments

This work was supported by a grant BA 8002.16422 from the Norwegian Council of Scientific and Industrial Research.

### REFERENCES

- Bird, R.E. and C. Riordan (1986). Simple solar spectral model for direct and diffuse irradiance on horizontal and tilted planes at the earth's surface for cloudless atmospheres. *J. Climate Appl. Meteor.*, **25**, 87-97.
- Olseth, J.A. and A. Skartveit (1985). Radiation Handbook (in Norwegian). *Klima*, No. 7, Norwegian Meteorological Institute, Oslo.

- Olseth, J.A. and A. Skartveit (1986). A solar radiation data handbook for Norway. Proceedings from NORTH SUN '86 - Solar Energy at High Latitudes, June 10-12, 1986, Copenhagen pp. 276-281.
- Olseth, J.A. and A. Skartveit (1987a). A probability density model for hourly total and beam irradiance on arbitrarily oriented planes. Solar Energy, 39, 343-351.
- Olseth, J.A. and A. Skartveit (1987b). Duration tables of hourly solar irradiance on 11 surfaces for 16 Norwegian sites (in Norwegian). Meteorological Report Series, University of Bergen, 1 - 1987.
- Olseth, J.A. and A. Skartveit (1989). Observed and modelled hourly luminous efficacies under arbitrary cloudiness. Solar Energy, 42, 221-233.
- Skartveit, A. and J.A. Olseth (1986). Modelling slope irradiance at high latitudes. Solar Energy, 36, 333-344.
- Skartveit, A. and J.A. Olseth (1987). A model for the diffuse fraction of hourly global radiation. Solar Energy, 38, 271-274.
- Skartveit, A. and J.A. Olseth (1988). Duration tables of hourly total and diffuse illumination on 5 surfaces for 16 Norwegian sites (in Norwegian). Meteorological Report Series, University of Bergen, 7 - 1988.
- Stephens, G.L., S. Ackerman and E.A. Smith (1984). A shortwave parameterization revised to improve cloud absorption. J. Atmos. Sci., 41, 687-690.

DYNAMIC COLLECTOR MODELS FOR 1 HR TIME STEP DERIVED FROM  
MEASURED OUTDOOR DATA.

Bengt Perers and Håkan Wallekun  
Studsvik Energy  
S-61182 Nyköping  
Sweden

ABSTRACT

The aim of this work is to determine effective models, for solar collectors, that can be used in conventional simulation programmes with 1 hour time steps. The same model is used both for parameter identification and simulation. This will lead to excellent accuracy when extrapolating results to long term performance. The method can also be used for in situ testing. Test periods of less than one week can be sufficient.

KEYWORDS

Collector testing; Collector modelling; Simulation; Multiple regression.

INTRODUCTION

This contribution is an extract from a new Studsvik Report (Perers et al., 1990) describing improved methods for simulation, measurement and evaluation of solar energy systems. Most of this work has been financed by the Swedish Council for Building Research. The participation within IEA SH&C Task VI and III has been very important for this work.

The basic experimental results for this modelling work was presented in a report (Perers 1977) about outdoor collector testing in the Swedish climate. A test rig was built according to the NBS 899 test standard. To achieve reliable results in our climate in reasonable time a rotating teststand and a model with correction for thermal capacitance was introduced.

The same model including incidence angle correction was used for on line simulation of the collector array for the Studsvik Solar Heating Central built in 1978 with good results (Perers 1980). Also the storage heat losses and heating load was simulated directly in the measurement computer. This turned out to be a very useful tool for checking of the system operation and component performance. The agreement with measured data was very good during regular operation. Since then the same type of model has been used with small improvements in all of our measurement projects when there are solar collector arrays in the system.

This was the starting point to search for the inverse method, to identify model parameters from measured data. The parameter identification presently used is multiple regression and can be done with standard statistical programmes as MINITAB. For extrapolation to long term performance any detailed simulation programme like MINSUN, WATSUN or TRNSYS can be used that contain the same collector model that is used here.

#### THE BASIC MODEL FOR GLAZED COLLECTORS

The collector array model for glazed collectors is an improved Hottel Whillier Bliss equation. Four terms are added for Incidence angle modifiers for beam and diffuse irradiation, second order heat loss term and a one node dynamic term.

The basic model used for simulation and parameter identification of the collector array output Q112 for collectors with glazing is of the form:

$$Q_{112} = G_{100_b} F'(\tau\alpha) K_{\tau_{ab}}(\theta) + G_{100_d} F'(\tau\alpha) K_{\tau_{ad}} - F'UL_1(DT) - F'UL_2(DT)^2 - F'U_w(DT)w - mc_e \frac{dT_f}{dt} - U_p(DT) \quad (1)$$

Where:

Q112	= collector array thermal output.	[W/m <sup>2</sup> ]
G100 <sub>b</sub>	= direct solar radiation coll. plane.	[W/m <sup>2</sup> ]
G100 <sub>d</sub>	= diffuse solar radiation coll. plane.	[W/m <sup>2</sup> ]
F'( $\tau\alpha$ )	= zero loss efficiency for the collector.	[-]
K $_{\tau_{ab}}$ ( $\theta$ )	= incidence angle modifier for direct rad.	[-]
K $_{\tau_{ad}}$	= incidence angle modifier for diffuse rad.	[-]
$\theta_{\tau_{ad}}$	= incidence angle for direct rad.	[°C]
F'UL <sub>1</sub>	= first order heat loss factor.	[W/(m <sup>2</sup> *K)]
F'UL <sub>2</sub>	= second order heat loss factor.	[W/(m <sup>2</sup> *K <sup>2</sup> )]
F'U <sub>w</sub>	= wind dependence in the heat loss factor	[Ws/(m <sup>3</sup> *K)]
w	= windspeed near the collector	[m/s]
DT	= temperature difference between fluid mean temperature and ambient.	[K]
mc <sub>e</sub>	= Effective one node thermal capacitance for the coll. array incl.piping.	[J/(m <sup>2</sup> *K)]
$\frac{dT_f}{dt}$	= average fluid temperature change between two measurement scans.	[K/s]
U <sub>p</sub>	= Heat loss factor for piping in the array per m <sup>2</sup> of collector aperture.	[W/(m <sup>2</sup> *K)]

Presently the incidence angle modifier K $_{\tau_{ab}}$ ( $\theta$ ) is modeled with the standard b<sub>0</sub> expression:

$$K_{\tau_{ab}}(\theta) = 1 - b_0 * (1/\cos(\theta) - 1) \quad (2)$$

This equation is acceptable for glazed collectors for incidence angles up to 70°. For higher angles and other collector designs improved models are required to achieve the best accuracy. The accuracy of this model also influences the values of the other parameters in the equation especially when using all day values.



## PARAMETER IDENTIFICATION WITH MULTIPLE REGRESSION

This kind of parameter identification for solar energy applications has been described, for example, by (Proctor 1984). He focused on efficiency testing under stationary conditions and did not involve modelling of the incidence angle, or thermal capacitance effects.

Parameter identification with multiple regression was tested for the first time in 1985 with in situ data from the Södertörn Solar District Heating Test Plant with a high performance flat plate collector giving very promising results (Perers et al., 1987). The optical parameters were especially very well determined, as was the  $b_0$  value.

The method was also tested for an unglazed rubber collector. The wind-dependence in the optical efficiency and the increase in the optical efficiency when putting a single glazing on such a collector could be explained. (Both effects come from the low heat transfer rate in the rubber absorber mat) (Walletun et al., 1986) and (Perers 1987).

When testing the same unglazed collector indoors in a solar simulator at the National Testing Institute in Borås we could identify unmeasured longwave radiation in the range of 50-100 W/m<sup>2</sup> from the solar simulator by this method (Perers 1987). The  $F'(\tau\alpha)$  was too high. But when allowing a zero offset in the equation the parameters were comparable to the outdoor results. When checking the wavelength range for the pyranometer and pyrgeometer used there was a gap between 2.5 and 4  $\mu\text{m}$  where the hot lamps of the simulator could radiate enough energy to explain the offset.

Since then this method has been used with good results for the modelling of other prototype collectors tested at the Studsvik Solar Test Field, leading to a better understanding of the energy flows in the collectors. This is important for further collector development.

We are still in the process of improving the use of this tool as a means for precise collector modelling with a high degree of absolute accuracy in each parameter.

## TEST REQUIREMENTS

The method does not require any extra sensors compared to standard outdoor collector testing but the orientation of the solar sensors parallel to the collector plane and placing and radiation shielding of the ambient temperature sensor becomes extra important with this method.

The test installation needs no special control equipment and also in situ data can be used. The only extra test requirement is that the collector flow has to be continuous for all hours that are used, so that the inlet and outlet temperatures reflect the internal state of the collector.

In case of the Studsvik Solar Test Field the pumps in the collector loops are running 24 hours so that all day values can be used. This increases the variation range for the input parameters and gives a better basis for the regression analysis in a shorter time.

It should also be pointed out that the hours used for parameter identification does not have to be in sequence. Therefore days with data gaps can be used without problem.

## RESULTS

Table 1 shows the model parameters for each month from April to September during 1989. The input data are 65 hr periods from longterm measurements at the Studsvik Solar Testfield. The periods are chosen randomly, except for August where the shadow band was not adjusted for the first period chosen. All hours are used from sunrise to sunset and for some periods also some dark hours.

The collector is an 11 m<sup>2</sup> Long Ground Based Flat Plate Collector (LGB), double glazed with Solatex glass and one teflon layer, Sunstrip absorber and 50 mm polyurethane backinsulation. The expected parameters are 0.75/0.15/0.68/3.5/10000 approximately for this design.

Table 1. Model Parameters from Multiple Regression.

MONTH	$F'(\tau\alpha)$	$b_0$	$F'(\tau\alpha)K_{rad}$	$F'UL$	$mc_e$	STDEV	$R^2$
[No]	[-]	[-]	[-]	[W/m <sup>2</sup> K]	[J/m <sup>2</sup> K]	[W/m <sup>2</sup> ]	[-]
4	0.739	-0.137	0.652	-3.181	-8654	8.23	0.998
5	0.756	-0.125	0.712	-3.625	-12095	11.60	0.997
6	0.763	-0.196	0.738	-3.572	-9713	12.60	0.996
7	0.777	-0.146	0.742	-3.909	-9304	11.82	0.996
8	0.746	-0.123	0.660	-3.225	-9446	12.29	0.994
9	0.743	-0.130	0.671	-3.168	-8986	8.95	0.998

There is a systematic seasonal variation giving higher optical and thermal loss parameters in the summer. Better modelling of the incidence angle effects will lead to more stable results during the year. By choosing only hours between 6.00 and 18.00 the variation is reduced.

Also the modelling of the heat losses can be improved with terms for second order heat losses and wind speed dependence. In this case the wind coefficient  $F'U_w$  was near expected values ( $\approx 0.25$  Ws/(m<sup>3</sup>\*K)) but the standard deviation was in the same range as the parameter and was left out in the model. Preliminary investigations show that the location of the ambient temperature sensor is very critical for the determination of these second or third order terms. New data with several ambient temperature sensors will show how large the influence can be.

It should also be pointed out that none of the 65 hr periods used have been chosen to have some special kind of weather. A systematic selection of input data will certainly improve the reproducibility in the method. Of course also real variations in outdoor collector performance may have some influence as air infiltration, dust and dew on the glazing and internal moisture effects. No correction or sorting of data has been done to reduce these effects in this case.

In figure 1 and 2 we can see how well the model fits the measured data for two periods in April and September. This kind of fit can probably be achieved with many other five parameter models, but in this case the stationary part of the model corresponds closely to the models used for collector testing and for simulation programmes. This makes the results much more interesting and the dynamic effects have been taken into account in a very simple one node model that could be used also in simulation programmes with one hour time steps.

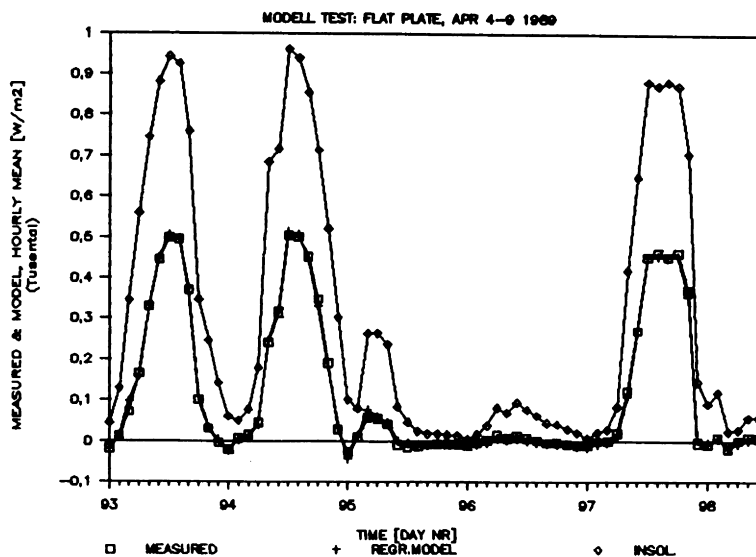


Fig 2 Measured collector output April 4-9 compared to model result with parameters from multiple regression. For comparison the global insolation in the collector plane is also shown.

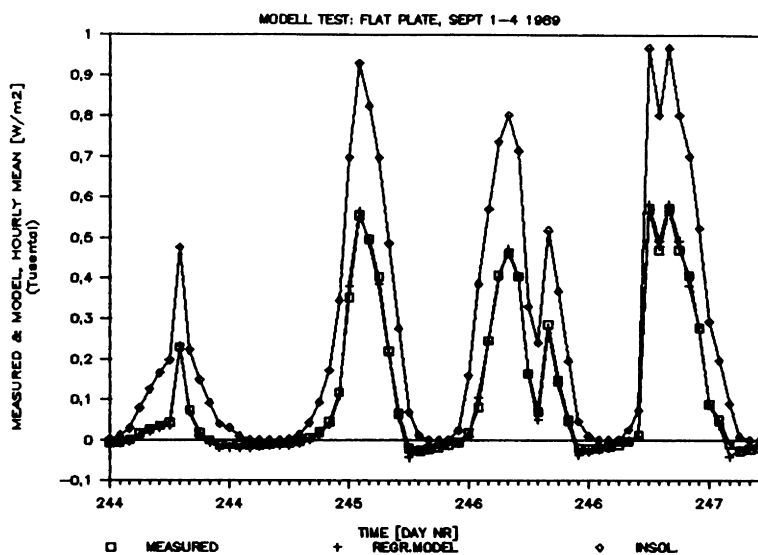


Fig 2 Measured collector output September 1-4 compared to model result with parameters from multiple regression. For comparison the global insolation in the collector plane is also shown.

As an indication of the validity and accuracy of the model the correlation coefficient and standard deviation are given in table 1. The standard deviation corresponds to an average error of less than 5% compared to the measured results. This is in the range of the measurement accuracy in this case. For example the cosine response of the pyranometers will show up here, and the accuracy of the diffuse radiation measurements. These second or third order effects have to be investigated further.

The correlation coefficient is better than 0.99 indicating that the model is statistically acceptable. The standard deviation of the individual parameters also shows that they are significant. For example, the zero loss coefficient for direct radiation has typically a standard deviation of less than 2% (T-ratio greater than 50). Also the dynamic factor has a standard deviation of less than 10% of the actual value (T-ratio greater than 10).

### CONCLUSIONS

At present the model can describe the hourly collector performance very well for the whole day, not only for the operating time.

The model used is physically sound and in most parts identical with existing detailed models for instantaneous collector performance described in standard textbooks as (Duffie et al., 1980).

The model can be used directly in most detailed simulation programmes. The thermal capacitance effects can be taken into account accurately with a simple one node model for 1 hr time steps.

### REFERENCES

- PERERS, B., I. HULTMARK (1977). Bestämning av momentan verkningsgrad för två plana solfångare. (Measurement of instantaneous efficiency for two flat plate collectors). Univ. of Linköping, Sweden, IFM-IKP-IFM-EX-66
- PERERS, B., B. KARLSSON and H. WALLELUN (1989). Simulation and Evaluation Methods for solar energy systems. Application to new collector designs. Studsvik AB, Sweden. (STUDSVIK/ED-90/4)
- PERERS, B., R. ROSEEN (1980) Solvärmecentralen i Studsvik, Resultat 1980. (Solar Heating Central in Studsvik, Progress report 1980. Studsvik AB, Sweden. (STUDSVIK/E1-80/141).
- PROCTOR, D. (1984). A Generalized Method for Testing all Classes of Solar Collectors. Part I, II and III Solar Energy Vol. 32. No. 3. 1984
- PERERS, B., P. HOLST and H. ZINKO. (1987). The Södertörn Solar District Heating Test Plant. Results 1982 - 1985. Studsvik AB, Sweden. (STUDSVIK-87/1)
- WALLELUN, H. and B. PERERS. (1986). Vindens inflytande på oglasade solfångare respektive solfångare med konvektions hinder. (Wind influence for unglazed collectors and collectors with convection suppressing glazing). Studsvik Energy, Sweden. (STUDSVIK/ED-86/15)
- PERERS, B. (1987). Performance testing of unglazed collectors, wind and longwave radiation influence. Internal report presented to IEA Task III. Studsvik Energy, Sweden.
- DUFFIE, J. A., W.A. BECKMAN. (1980). Solar Engineering of Thermal Processes. John Wiley & Sons, New York 1980.

## ECONOMICAL PROSPECTS FOR SWEDISH SOLAR SPACE HEATING SYSTEMS WITH SEASONAL STORAGE

J.-O. Dalenbäck and T. Jilar

Department of Building Services Engineering  
Chalmers University of Technology  
S-412 96 Gothenburg, Sweden

### ABSTRACT

In Sweden there has been comprehensive R & D work concerning large-scale solar heating technology since the middle of the 1970's. Several plants with seasonal storage have been built and evaluated extensively, and at present plants to be built in the 1990's are being considered.

The present development is concentrated on systems in which high performance flat plate collectors produce heat at 50-100°C for space heating and domestic hot water purposes. Today the system design is very simple compared to earlier examples.

For water heat storage, the most promising field seems to be underground technologies. Suitable constructions are thermally insulated pits for volumes above 10,000 m<sup>3</sup> and uninsulated rock caverns above 100,000 m<sup>3</sup>. New pit constructions are under development in prototype plants. Here different sheet metal applications for water sealing are being investigated. Rock cavern construction is an established technology. One example is the Kungälv plant planned for the 1990's. Here, 75% solar heat to cover the demands of a small town requires 125,000 m<sup>3</sup> of collectors and 400,000 m<sup>3</sup> of rock caverns.

The economical prospects are very interesting for the 1990's. Solar heat costs in the order of US\$ 0.04-0.07/kWh are predicted in Sweden and significantly lower costs are possible in other countries.

### KEYWORDS

Residential solar heating; seasonal storage; system design; heat costs.

## INTRODUCTION

This paper briefly describes the Swedish technology and economy for central solar heating plants with seasonal storage in water. The description is concentrated on pure solar heating system concepts. A pure solar heating system with seasonal heat store is one in which solar collectors produce heat at a sufficiently high temperature to allow it to be used directly or after storage for space heating and domestic hot water purposes. In this context no upgrading through use of, for instance, heat pumps should be necessary.

The main feature that must therefore be required of a pure solar heating system with seasonal heat storage is that it must be possible to store and abstract heat at a high, directly usable temperature level, i.e. 50-90°C. In these respects, there is still limited experience from the use of natural ground heat stores while from a general point of view heat storage in water can be regarded almost as established technology. This applies to above-ground technology (e.g. tanks) while in-ground technology (e.g. pits) is still under development.

Since the middle of the 1970's there has been a significant progress in the Swedish development of large-scale solar heating technology. An interesting field of application is the far developed Swedish group and district heating technology.

## SYSTEM DESIGN AND PERFORMANCE

During the last decade several plants with seasonal heat storage have been built in Sweden for experimental purposes. Based on the experiences obtained from these plants, feasible systems should be designed according to the principle shown in Fig. 1.

A very simple system design has been achieved which gives operation security as well as low cost possibilities. The design incorporates separate heat charge and discharge circuits connected to the store. The solar collectors feed the store on two alternative levels. The collector as well as the charge circuit is designed for a low, constant flow rate corresponding to a maximum temperature raise in the order of 30-40°C. The upper inlet is used for temperatures above 80°C else the lower inlet is used. Similarly, heat for the load is drawn from two alternative levels, and use is made of the temperature stratification in the water volume with a minimum of complications. An auxiliary boiler is used when the store temperature is insufficient for the load. The plant should be rated to provide maximum 70-80% solar heat coverage of the annual heat load.

Concerning the choice of a suitable type of solar collector experiences have been gained through Swedish developments in large-scale solar heating technology since the 1970's. Rapid developments in the field of high performance flat plate collectors have taken place. Thermal performance standards have been improved and collector array costs have been lowered to a great extent. The results have been achieved by a combination of several factors. The area of the panels has been increased tenfold. Panel mountings and connections have been simplified and heat losses from piping and panels have been reduced.

It appears possible to design for around  $360 \text{ kWh/m}^2$  of annual thermal yield in Sweden if the mean operating temperature is  $65\text{--}70 \text{ }^\circ\text{C}$ .

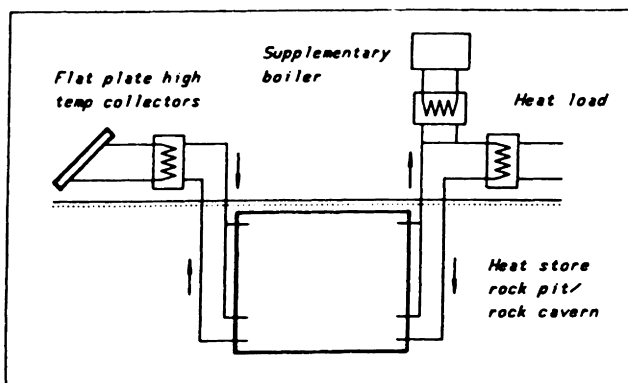


Fig. 1. Feasible system principle for solar heating plants with seasonal heat storage in water.

The array configuration is a large number of groups of collectors connected in parallel. Each group contains, in turn, about 10 collectors connected in series. A large  $12 \text{ m}^2$  modular solar collector is used. It has single-glass cover, a selective absorber coating and a sheet of teflon plastic between the glass and absorber plate in order to minimize convection losses.

For heat storage in water the most promising field today seen from an economical point of view seems to be underground technology. Suitable constructions are thermally insulated pits for volumes above  $10,000 \text{ m}^3$  and uninsulated rock caverns above  $100,000 \text{ m}^3$ . For a solar heat coverage of 75% a store volume of  $10,000 \text{ m}^3$  corresponds to a heat load of about 1300 MWh/year and  $100,000 \text{ m}^3$  to a heat load of about 14,000 MWh/year.

In Table 1 the land area and ground volume requirements for three cases are presented.

In the first example the pit store is supposed to be 10 m deep why the required roof area is about  $1600 \text{ m}^2$ . Here only 13% of the collectors can be placed and land area must be found for the majority of the collectors. In Sweden, new pit constructions are under development in prototype plants. The research work is focused on water sealing problems and different sheet metal applications are studied with respect to sealing properties as well as building technology.

The third example is taken from a prestudy for a very big solar heating plant planned to be in operation in the 1990's in the town of Kungälv in the west of Sweden. The design objective is to meet 75% of the heat load which is 56 GWh/year by solar heat. The total heat storage capacity demand is 23 GWh corresponding to about  $400,000 \text{ m}^3$  of water-filled caverns. The suggested store configuration is a cavern volume horizontally measuring

154x110 m formed by a number of cross-linked cavern units having a width of 20 m and a height of 30 m. The top level of the cavern body is located 40 m below the ground surface level. The building technology for rock caverns is very well known from the field of crude oil storage. Since 5 years a 100,000 m<sup>3</sup> Swedish cavern plant constructed in a similar way is in operation for seasonal storage of heat (the Lyckebo plant).

Table 1. Examples of land area and ground volume requirements for cases with 75% solar heat coverage.

Type of heat store	Heat load (MWh/year)	Store volume (m <sup>3</sup> )	Collector area (m <sup>2</sup> )	Land <sup>1)</sup> area (m <sup>2</sup> )
Insulated pit	2,100	16,300	5,400	11,900
Uninsulated rock cavern	14,100	100,000	32,700	71,900
Uninsulated rock cavern	56,300	400,000	126,000	280,000

<sup>1)</sup>For collector array.

## ECONOMICS

Under this chapter solar heat costs at the present technological stage of development and at one forecasted stage of development for the end of the 1990's are presented. All the costs are expressed in 1988 money value.

In table 2 specific costs today for collectors, heat stores and interconnecting piping plus control equipment are given in three plant cases. The plants are sized in order to provide a solar heat coverage of 75%. The costs include the labor cost for design work while for the store costs even costs for initial water-filling and upheating are included. The cases are the same as the ones in Table 1.

Table 2. Specific costs today for collectors, heat stores and interconnecting piping plus control equipment.

Type of heat store	Heat load (MWh/year)	Specific costs		
		Collectors (US\$/m <sup>2</sup> )	Heat store (US\$/m <sup>3</sup> )	Piping + control (US\$/m <sup>2</sup> ) <sup>1)</sup>
Insulated pit	2,100	240	59	16
Uninsulated rock cavern	14,100	225	25	16
Uninsulated rock cavern	56,300	190	20	16

<sup>1)</sup>Related to collector area.



Solar heat costs have been calculated under the following financial conditions:

- Depreciation time
  - Collectors + piping + control : 20 years
  - Heat store 40 years
- Maintenance cost/year (% of the investment)
  - Collectors + piping + control : 1%
  - Heat store 0,5%

Here the solar heat cost is defined as the cost for solar heat abstracted from the heat store and providing 75% of the annual demand for the connected heat load. In order to obtain the complete heat cost for 100% delivery the cost for the supplementary heat should be added.

The solar heat costs today for the three cases are presented in Table 3. Also presented are the costs related to the forecasted stage of development at the end of the 1990's. Here the collector array cost for the pit-plant is supposed to be US\$ 130/m<sup>2</sup> and for the cavern-plants US\$ 115/m<sup>2</sup>. Furthermore the annual thermal yield is supposed to be 440 kWh/m<sup>2</sup> corresponding to 40% annual efficiency. In a second developed alternative even heat store costs are supposed to be lowered. Here the heat store costs are 30% lower than the ones given in Table 2.

Table 3. Solar heat costs today and at one forecasted stage of development at the end of the 1990's.

Type of heat store	Heat load (MWh/year)	Solar heat costs		
		Today (US\$/kWh)	Developed collectors (US\$/kWh)	Developed collectors + heat stores (US\$/kWh)
Insulated pit	2,100	0,118	0,077	0,066
Uninsulated rock cavern	14,100	0,082	0,046	0,041
Uninsulated rock cavern	56,300	0,069	0,041	0,038

For heat storage in natural ground volumes very promising concepts are systems with vertical ducts. Here the development is focused on construction methods for coils in soft ground and boreholes in rock. Forecasted solar heat costs during the next decade are in the order of US\$ 0,045/kWh for coils in clay and US\$ 0,055/kWh for boreholes in rock for heat loads above 10,000 MWh/year.

## REFERENCES

- Claesson, T., J. Gräslund, G. Hultmark, T. Jilar (1988). Seasonally Stored Solar Heat in Kungälv - A Basis for Heat Supply Planning in the 1990's. The Swedish Council for Building Research, Report R104:1988, (in Swedish).
- Dalenbäck, J-O (1988a). Large-Scale Swedish Solar Heating Technology - System Design and Rating. The Swedish Council for Building Research, Document D6:1988.
- Dalenbäck, J-O (1988b). Swedish Solar Heating with Seasonal Storage - Design Studies. Dept. of Building Services Engineering, Chalmers University of Technology. Paper submitted to Jigastock '88, Paris 1988.
- Jilar, T. (1985). Large-Scale Solar Heating Technology - Ingelstad, a Solar Group Heating Plant without Heat Pumps. The Swedish Council for Building Research, Document D2:1985.
- Jilar, T. (1988). The Sun Town Project - Swedish Plans for the Biggest Seasonal Storage Plant in the World. Dept. of Building Services Engineering, Chalmers University of Technology. Paper submitted to Jigastock '88, Paris 1988.

## FURTHER R & D NEEDS FOR SWEDISH SOLAR HEATING TECHNOLOGY 1990-1993

AN EXPERT GROUP PLAN SPONSORED BY THE  
SWEDISH COUNCIL FOR BUILDING RESEARCH

T. Jilar and B. Nordell

Department of Building Services Engineering  
Chalmers University of Technology  
S-412 96 Gothenburg, Sweden

### ABSTRACT

In the 1970's when the Swedish development seriously started, experimental plants were built with the primary aim of testing various technologies. The economical aspects were of secondary interest which, in many cases, resulted in high costs and even in poor quality. In the second plant generation during the 1980's, R & D was concentrated upon lowering costs and enhancing performances for the most promising system concepts. Systems are included here for DHW, and for combined DHW and space heating designed for solar heat coverages between 30% and 80% of the annual heat requirement.

In the named plan, the state of the art and the R & D needs are described with the focus upon residential heating. Included are systems for multi-family houses, incorporating roof-integrated solar collectors and short-term heat storage. More developed construction and urban planning methods for roof integration is stressed here, as well as systems flexible for size expansion, e.g. through connection to an external seasonal heat storage.

Also included are district heating systems for solar heat supply of up to a couple of hundred flats. Ground or roof based collectors and seasonal heat storage in water-filled pits or ducts in deep ground are considered here. Emphasis is placed on more efficient high temperature flatplate collectors, more simple piping systems and further development of heat insulation and water-sealing methods for pit storage as well as high temperature practical tests for duct storage.

### KEYWORDS

Residential solar heating: state of art; experimental building needs

## INTRODUCTION

It is now approximately 10 years since the solar energy technology started to be seriously developed in Sweden. During the 70's, experimental installations were built mainly for testing purposes and without any significant consideration to cost which, in many cases, was extremely high, at the same time as results were poor. In line with results produced from this first generation installation, continued development efforts during the 80's has concentrated on lowering costs as well as improving performances for the most promising types of systems with regard to possible competitive power for the future Swedish heating market. Among these are partly systems for solar heated domestic hot water in multi-family houses, partly solar heating systems even for a minor part of the space heating load, as well as systems with seasonal heat storage which can cover the bulk of the total annual heating demand.

The area of responsibility of the Swedish Council for Building Research (BFR) - the built-up environment - consists mainly of space and domestic hot water heating but even bathing facilities are included. BFR's expert planning group for solar heating technology consists of some 10 experts who have compiled the basis for the BFR's 3-year R & D plan for 1990-1993. This basic report will be published in the summer of 1989.

Solar heating systems to heat buildings and domestic hot water is usually divided into two groups, "individual systems" and "group systems". "Individual systems" usually mean that the solar collectors are placed on the roof and storage is inside the building and used for diurnal storage of solar heat. By "group systems" this often means that solar collectors are placed on the ground and that storage is placed away from the building and used either for seasonal storage or diurnal storage. A group system can, however, also have solar collectors placed on the roof. A group system via an extended network is the simplest way to meet heating demands which serve several buildings, whereas an individual system for one or two buildings is best carried out via a more local network. Larger group systems are sometimes called "district heating systems" but no distinct or well defined boundary exists.

The three-year plan describes the development situation and the background for the Swedish solar heating technology within the mentioned area. With regard to individual systems, this includes systems for multi-family houses, single-family houses and premises such as hospitals. With regard to group systems, this mainly includes smaller systems, such as those which provide heating for up to a few hundred apartment units.

## EXPERIENCES AND CONTINUED DEVELOPMENT NEEDS

For the different application areas within Swedish active solar heating technology, the main experiences and continued development needs are given below. The named development needs, in the most cases, are strongly connected to increased field experimental building activities.

Group systems:

## Experiences:

Technically seen, well developed principal solutions exist for large solar heating plants with ground-assembled solar collectors and diurnal or seasonal heat storage in water-filled tanks, ground pits or rock caverns. Basic developed design methods exist for systems with solar heating of large groups of buildings which cover the greater part of the annual heating demands, or only the heating demands during the summer months.

Very good technical and economical development possibilities are judged to exist for group systems of various sizes.

## Development needs:

- More effective and rationally manufactured high temperature solar collectors
- Complete systems with a very simplified piping connection
- Direct ground seasonal storage of heat with high temperatures.
- Heat insulation and water-sealing methods with high durability for pits.

Individual systems for multi-family houses:

## Experiences:

Technically, relatively well developed solutions exist for solar heating installations in private multi-family houses with roof-mounted solar collectors and diurnal storage in water-filled tanks. Practically developed design methods exist for systems which supply solar heating for buildings with up to one-third of the annual heating demand

Economically, systems which supply heating below a coverage of 20% are preferred. Systems for only domestic hot water heating in newly built houses are the most interesting.

## Development needs:

- More effective and rational roof-mounted high temperature solar collectors.
- Architecturally suited roof-mounted collectors which fit into newly built areas.
- Effective combinations with supplementary heating systems
- Methods for expansion of individual systems to group systems

### Individual Systems for single-family houses:

#### Experiences:

Technically, relatively simple package solutions for installations in both new and older houses exist. Similar supply options as in multi-family houses exist and the solar heat coverage can, for suitably utilized small housing systems, be equally as good as in multi-family houses.

From an economical point of view, a relatively strong development is needed in order to make these systems competitive. An assessment is that systems installed in a newly built houses has the best development possibilities.

#### Development needs:

- More effective and simple integrated systems for newly built standard houses

### SUGGESTION FOR SUBSTANTIAL CONTRIBUTION WITHIN EXPERIMENTAL BUILDING ACTIVITIES

According to this plan, in the majority of the solar heating installations it most interesting to use high temperature solar collectors which are efficient at a temperature of between 60 to 100°C. Such solar collectors are assumed to be incorporated in all the below mentioned cases. There are applications where lower or higher temperature demands can be met and where other types of solar collectors can be of interest when cost and performance are considered jointly. Firstly, however, more extensive system-related studies are needed before experimental building projects can be considered.

Within the group of experimental building projects suitable for quick application are the following specific examples:

#### Group systems:

- Building of two to three heating plants in new building areas with heating loads of approx. 1,500 - 2,000 MWh/year which corresponds to approximately 200 - 300 apartments in multi-family houses. One of the plants should have ground heat storage in clay and the other, storage in a water-filled ground pit. The pit should be constructed according to the principle which is most suitable in the on-going prototype investigations. The ground heat storage should eventually be tested, partly in connection to heating systems with very low temperature demands, i.e. floor heating systems or via heating in cavity walls, and partly in connection to more normal low temperature systems, i.e. oversized radiator systems. Coverage by solar heating should in all areas be at least 60%.
- Building of a plant in a building area with a heating demand of approx. 10,000 MWh/year - which in a newly built area corresponds to approx. 1,400 apartments in multi-family houses. For heat storage

water-filled rock caverns with temperatures of up to approx. 100°C should be used. Solar heating coverage should be at least 60%. An alternative is the expansion of the already existing Lyckebo plant which includes 100,000 m<sup>3</sup> of rock caverns, where large ground areas are available, with approx. 22,000 m<sup>2</sup> of solar collectors.

#### Individual systems in multi-family houses

- Building of two to three plants in new building areas which consist of at least 100 apartments. The solar heating system should be of a combined type, and supplementary heating should be provided via local group distribution networks where diurnal storage can be utilized advantageous for all heating supply.

One area can be provisionally planned for successive expansion of the number of houses and one for direct expansion but with a later connection to some kind of seasonal heat storage. The third area can be planned as a cross between the other two, but provisionally differentiated from them with respect to some important factor, i.e. number of storeys, degree of exploitation, etc.

The degree of solar heating coverage should be about 30% in all areas.

#### Individual systems in single-family houses

- In some standard house areas, 10-20 houses should be equipped with combined systems or domestic hot water systems. A detailed follow-up of the solar heating results and heating loads should continue for the next few years.

HELIOGASIFICATION OF VEGETAL WASTE  
OF AGRICULTURAL PRODUCTION

N.G.EFENDIEVA, P.F.RZAEV, Sh.D.SHAKHBAZOV,  
S.Ya.AKHUNDOV

Sector of Radiation Researches of Azerbaijan  
Academy of Sciences, Narimanov Avenue, 31 "a"  
Baku, 370143, USSR

ABSTRACT

Our paper deals with the problems of development of combustible hydrogen-containing gas production by solar gasification of agricultural wastes.

Kinetical parameters are determined and gas formation process is optimized.

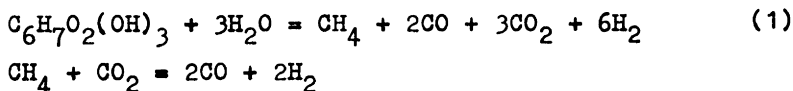
KEYWORDS

Solar pyrolysis; solar gasification; solar gasifier.

The processes of coal gasification by means of solar power give the possibility of saving the organic fuel employed for support of heat of the formation and superheating of vapor reactions (40%).

The given paper is devoted to the prospecting of regional available raw materials in specific conditions of Azerbaijan, and in connection with this to the essential widening of assortment of the carbon-containing materials. The paper concerns, as well, the problem of transfer from the standard fuel by means of utilization of biomass in the process of gas-formation at solar power plant (vegetal waste of agricultural production-stems of cotton, grape and tobacco), the waste make up to 5 million tons per year in our republic.

Experimental studies showed that high-temperature steam conversion of cellulose occurred as:





No lignin separation is required for the hydrogen generation from vegetative wastes by similar reaction, i.e. the biomass can be used here without pretreatment (Paushkin et al., 1986)

Vegetative waste thermal decompositions were studied by derivatographic and chromatographic analyses upon heating in nitrogen atmosphere, and gas product identification to estimate the amount of volatile products released and various stages of thermal decomposition, thermal effects, and variations in vegetative mass weight.

The starting materials were vegetative wastes of the following composition:

Wastes	C <sup>r</sup>	H <sup>r</sup>	N <sup>r</sup>	S <sub>O+H</sub>
Tobacco	46.0	6.3	0.56	-
Vine	46.9	6.6	1.0	0.26
Cotton	44.5	6.7	1.2	0.77

Thermal characteristics of vegetative mass decomposition obtained on the MOM derivatograph (Hungary) are listed in Table 1.

Table 1. Thermal characteristics of vegetative mass decomposition

Object de- nomination	Temperature interval, °C, of weight losses, %, per com- bustible mass						Overall de- composition, %	
	150- 200	200- 300	300- 470	470- 600	600- 800	800- 1000		
I Cotton	4	32	17	14	4	2	81	
II Vine	-	22	20	22	8	6	86	
III Tobacco	-	20	27	10	7	3	77	
	Differential thermal analysis, °C						Differential thermo- gravimetric analysis, °C	
	Endothermal effect			Exothermal effect				
	I	II	III	I	II	III	Decomposit- ion start- ing temper- ature	Maximum temperature of decompo- sition rate
I	570	720	790	220	400	-		
II	620	700	800	-	400	480	240	320
III	570	730	790	-	400	-	240	300

The analysis of Table 1 shows that vine stems undergo the

most marked thermal decomposition, up to 86%, in 20 to 1000 °C temperature range.

Thus vegetative waste utilization for combustible gas production in addition to the considerable economical and ecological effect gives real prerequisites for the wasteless technology.

To produce combustible gas according to the scheme (1) of temperature decrease intensification and price reduction of gas generation from vegetative stock using solar energy we employed in our work salt mixtures of alkali metals in the following combinations:

$KCl + K_2CO_3$ ;  $K_2SO_4 + Na_2CO_3$ ;  $K_2SO_4 + NaCl$ ;  $K_2SO_4 + Na_2SO_4$   
(Lang et al., 1982).

When catalyst mixtures of 6 weight % were used for steam conversion, average combustible gas yield increased 1.2 to 1.5-fold as compared to the initial material - noncatalyzed solid fuel.

The process kinetical characteristics were calculated from

$\mathcal{d} = 1 - 1^{-kt^n}$ . To determine reaction rate constant  $k$  and reaction order ( $n$ ) we employed the least-squares approximation so that  $\mathcal{d} = 1 - 1^{-kt^n}$  was rewritten as  $y = \bar{a}t + b$  where  $y = \ln(1 - \mathcal{d})$ ;  $a = n$ ;  $b = \ln k$ ;  $\bar{t} = \ln t$ .

$a$  and  $b$  regression factors were determined from the measurements taken at  $m$  experimental points ( $m > 2$ ), i.e. by defining  $a$  and  $b$  from  $m$  equations of  $y = \bar{a}t + b$  we can find the conversion degree.

The  $\mathcal{d}_c = f(\tau)$ ;  $v_c = f(\tau)$  and  $v_c = f(\mathcal{d}_c)$  variations were computed on the ES 1033. Calculation results are given in Table 2.

It appears that in this case the catalyst particle penetration into vine stems is of major importance and results in the surface development, decrease of activation energy, and acceleration of thermal destruction.

On the other hand, experimental studies have revealed that efficient solar gasification of vegetative mass into combustible hydrogen-containing gases occurs at lower temperatures (800°C) with subsequent magnification of the solar gasifier reaction volume and productivity buildup for the solar power plant (Effendieva et al., 1989).

The investigation of impurity elements in wastes and the products of their processing is of interest since the part of agricultural wastes as potential energy carriers and available raw material is growing in importance.

We used quantitative spectral analysis for the determination of said microelements. For spectral analysis, ash residue

Table 2. Kinetical characteristic calculations of vegetative mass solar gasification in the presence of  $K_2CO_3$ ,  $K_2SO_4$  catalysts and their mixtures of the following content:  $KCl+K_2CO_3$ ;  $K_2SO_4+Na_2SO_4$ ;  $K_2SO_4+NaCl$ ;  $K_2SO_4+N_2CO_3$

Specimen	n	K	k	Activation energy E, kcal/mole
Vine stem gasification without catalyst	1.3	0.004	0.000074	27
$K_2CO_3$	1.32	0.012	0.000213	19.4
$KCl + K_2CO_3$	1.02	0.009	0.000626	21.5
$K_2SO_4$	1.03	0.007	0.000315	24.3
$K_2SO_4 + Na_2SO_4$	1.6	0.010	0.000230	22.0
$K_2SO_4 + NaCl$	1.13	0.008	0.000362	22.1
$K_2SO_4 + Na_2CO_3$	1.2	0.009	0.001340	21.5

specimens were prepared both in stimulated conditions on the laboratory plant /I/ and in natural conditions /II/ on the solar power plant. The DFS-8-1 spectrograph was used in the analysis. The photos of the spectra of samples and standard specimens were taken on the used in research photographic plates of "spectrographic type I" with 4 GOST unit sensitivity.

The spectrograms obtained were qualitatively identified on the MBS 2 microscope and SP 3 spectral projector with 20-fold magnification.

The results of microelement composition analysis in vine stems are given below for I and II conditions, in %:

I.  $Mg > 1$ ;  $Pb - 0.0095$ ;  $Cr - 0.012$ ;  $Ti - 0.065$ ;  $Si > 1$ ;  $Mn - 0.075$ ;  $Ga - 0.07$ ;  $Fe > 1$ ;  $Ni - 0.0035$ ;  $Al > 1$ ;  $Ca > 1$ ;  $Mo - 0.00035$ ;  $V - 0.0010$ ;  $K > 1$ ;  $J - 0.00095$ ;  $Cu - 0.065$ ;  $Zr - 0.0070$ ;  $Zn - 0.25$ ;  $Ag - 0.000055$ ;  $Nb - 0.0065$ ;  $Na > 1$ ;  $Sr - 0.095$ ;  $Co -$  not detected;  $Sn -$  not detected;  $Ge -$  not detected.

II.  $Mg > 1$ ;  $Pb - 0.0035$ ;  $Cr - 0.0047$ ;  $Ti - 0.40$ ;  $Si > 1$ ;  $Mn - 0.078$ ;  $Ga - 0.0044$ ;  $Fe > 1$ ;  $Ni - 0.0025$ ;  $Al > 1$ ;  $Ca > 1$ ;  $Mo - 0.00024$ ;  $V - 0.0097$ ;  $K > 1$ ;  $J - 0.011$ ;  $Cu - 0.060$ ;  $Zr - 0.0058$ ;  $Zn - 0.030$ ;  $Ag -$  not detected;  $Nb - 0.00016$ ;  $Na > 1$ ;  $Sr - 0.035$ ;  $Sc - 0.0080$ ;  $Cd -$  not detected;  $Sn - 0.0047$ ;  $Ge -$  not detected;  $Ba - 0.040$ .

Analysis of the results obtained in (I) and (II) showed that

high mineral component content in ash residue determines the efficiency of its utilization both as plant growth stimulator and as mineral fertilizer. Moreover, K and Na presence in ash residue of vine stems (the same apparently refers to cotton and tobacco stems) results in the capability to catalytically affect both solar pyrolysis and solar gasification promoting thermal destruction rate and combustible gas yield increases at lowered temperatures.

So, utilization of vegetal waste in conditions of Azerbaijan for production of combustible gases gives not only considerable economical and ecological effects but creates the real prerequisites for wasteless engineering.

#### REFERENCES

- Effendieva, N.G., Sh.D.Shakhbazov, P.F.Rzayev and S.Ya.Akhundov (1989). Calculation of kinetical characteristics of vegetative mass solar gasification (MS deposited in the VINITI No.163-B89 Dep.).
- Lang, R.J. et al. (1982). Catalytic coal gasification: USA Patent No.4318712 GJOJ 3/54.
- Paushkin, Ya.M., Yu.M.Zharov, L.P.Nikanorova and Ye.G.Gorlov (1986). Fiz. Khimiya, No.5, pp.1169-1171.

DECREASE OF HYDROGEN CONTENTS DURING THE PERIOD OF THREE YEARS  
IN a-Si:H FILMS AND CHANGE IN EFFICIENCY OF ITO/ p i n a-Si:H/Al  
SOLAR CELL

A. Kolodziej and S. Nowak, Institute of Electronics, Academy  
of Mining and Metallurgy, Al. Mickiewicza 30, 30-059 Krakow,  
Poland

A-Si:H films and ITO/p i n a-Si:H/Al Solar Cell have been prepared by dc magnetron technique during of the simple vacuum process. The influence of deposition parameters of the process on electrical and optical properties of a-Si:H films was investigated. The infrared vibrational absorption spectra method was used to estimated the total hydrogen concentration and, particularly, to evaluate the Si-H to Si-H<sub>2</sub> bonds relation. The hydrogen content in the film over the period of three years is examined. The decrease is about 25 at %, depends on the Si-H to Si-H<sub>2</sub> bonds relation and on sample environment. Simultaneously, the efficiency of the solar cells decrease from 6 % to 4 % (mean values).

## 1. Introduction

The application of hydrogenated amorphous silicon ( a-Si:H ) started with realization of solar cells in 1976. Since then, other possibilities for this relatively new semiconductor materials have been found <sup>1-3</sup>.

In our work, dc magnetron sputtering was used to obtain the a-Si:H and ITO/p i n a-Si:H/Al structure. The deposition system, the film preparation method, electrical and optical properties were described already in <sup>4-6</sup>.

The scheme of our present system is shown in Fig.1 and Fig.2. DC magnetron technique was several practical advantages:

1) good control of the hydrogen content both in the chamber and in the films, and the Si-H to Si-H<sub>2</sub> bond relation, as well, 2) tight control of the substrate over wide range, 3) the

possibility of sputtering composite targets, 4) practically, the avoidance of toxic gases, 5) the possibility of a high deposition rate, 6) low sputtering voltage of less than 320 V, giving a limited influence of the energetic ions on heterostructure and hydrogen bonds of the film.

A duo-magnetron system ( magnetron plus an additional magnet on shield ) was used for deposition of the film, in order to obtain more homogeneous horizontal magnetic field, and consecutively greater erosion area of the target and smaller target voltage. Furthermore, a +30 V-biasing of the inner screen surrounding the magnetron, and that of the outer shield improve evacuation of thermal electrons from ionization area which do not heat created films.

In the paper, the three year old samples, stored in a simple transparent box placed in a room close to a window, are examined. Only the flawless a-Si:H films of hydrogen content in the range 16 to 21 at % with predetermined optical characteristics and hydrogen bonding modes were considered to evaluated time induced degradation. There were to reasons of the studies.

First, the comparison of the time dependent changes of electrical and optical properties of the films and the p i n structures versus decreasing total hydrogen content.

Second, numerical calculations of the changes of the Si-H to Si-H<sub>2</sub> contents ratio and their individual degradation rates in order to optimize technology of manufacturing process.

### 3. Experimental.

The scheme of experimental apparatus for obtaining the a-Si:H films and the p i n structures by dc magnetron technique, during the single vacuum process is shown in Fig.1 and Fig.2. The base pressure, which is qualifying process parameter determining the final quality of the films amounted to some  $5 \times 10^{-7}$  Torr.

The detailed description of all possible technological functions and procedures will be given in a paper being prepared for publication.

The growth species were generated by a dc planar magnetron sputtering sources from polycrystalline of 100 mm diameter Si target. The additional shield and magnet at +30 V potential between target and substrate were used. During the deposition, biased substrate at -100 V potential is oscillating 8 cm over the target. We can vary the horizontal magnetic field from 500 to 1500 Gs in order to stabilize the ion process.

The effectiveness of the hydrogenation process measured in terms of reduction rate of defect gap states in sputtered layers is largely controlled by various deposition conditions such as the hydrogen partial pressure  $p_{H_2}$ , argon partial pressure  $p_{Ar}$ , substrate temperature  $T_g$ , input power  $P$  and substrate bias  $V_B$ .

Our previous measurements show that the best films were obtained under the conditions listed in Table I.

Table II contains their characteristic parameters and changes after 3 years. The 3- years old samples and p i n structures made with standard technology but on the base of the "f" and "g" a-Si:H films is shown in Fig.3. The sheet resistivity of ITO was  $30 \Omega/\square$ . The conversion efficiency were 6% for "f" and 5.5% for "g".

The infrared vibrational absorption spectra were measured with a Digital FTS-spectrometer in  $400-4000 \text{ cm}^{-1}$  range.

The films were deposited onto the polished Al substrate <sup>5-7</sup>. Other electrical and optical parameters were measured by the field effect transistor and photocurrent methods <sup>2,3,5,6,8</sup>.

### 3. Results and discussion.

As an example three old spectra and three new spectra and corresponding values of hydrogen content are presented in Fig.2,3 and Table III, respectively. They show the evaluation of the absorption spectra with variation of substrate temperature, substrate bias dissipated power and time in the wavenumber range  $500-750 \text{ cm}^{-1}$  and  $1900-2300 \text{ cm}^{-1}$ .

The wagging mode centered on  $645 \text{ cm}^{-1}$ ,  $641 \text{ cm}^{-1}$  and  $638 \text{ cm}^{-1}$  for the curves c,f,g,c<sub>3</sub>,g<sub>3</sub>, respectively, was used to determine

total amount of bonded hydrogen by means of the Paul and Anderson's formula (1981) modified to H/Si % ratio. The determined constant of proportionality and the density of the a-Si:H films were about  $1.5 \times 10^{19} \text{ cm}^{-2}$  and  $5 \times 10^{22} \text{ cm}^{-3}$ , respectively. The time evolution of these spectra indicate that in "g" samples hydrogen content decreases quicker than in "c" and "f" films. The integral absorption of the stretching modes was determined after deconvoluting the absorption into two Gaussians centered around marked points in Fig.3 with the exception of "g" curve which showed practically only Si-H<sub>2</sub> bonds.

Evaluated ratio Si-H<sub>2</sub> to Si-H bonds is about 0.9 for sample "f" and changes to 0.8 for sample "f<sub>3</sub>". It indicates that Si-H bonds are more time stable than Si-H<sub>2</sub> bonds.

The other results of calculations in the form of the ratio of Si-H amount at the beginning of the test to that after 3 years shown in Table III. They indicate also time dependence degradation of hydrogen bonds and additionally prefer the samples which are Si-H rich.

They are important for optimization of a-Si:H technology in order to obtain the films with domination of Si-H bonds. In our case, only a few well-defined samples have been available and thus only approximate determination of time degradation process was possible.

The efficiency of "f" and "g" p i n structures in the time have been decreased to 5 % and 4 %, respectively.

An annealing have been given better properties of the films and structures. It may be associate with creation of new Si-H bonds from involved hydrogen in the degradation process. Samples, which were stored in the outside with high level of SO<sub>x</sub> and NO<sub>x</sub> (environment in Cracow) have been completely degraded.

#### 4. Conclusions.

The results of the investigation show that the time dependence, spontaneous degradation of the a-Si:H films



(without light and thermal shocks) may be connected with stabilization of various bonds for Si-H and Si-H<sub>2</sub>. Our idea is to produce the material with the hydrogen content 18-20 at % and prevailing number of Si-H bonds, compared to the number of Si-H<sub>2</sub> bonds. However, we know that it is only a part of the problem of the degradation of the film. Many authors discuss broken bond stabilization 9-11.

#### References

1. Y.Hamakawa, (ed.), Amorphous Semiconductor Technologies and Devices, JARECT, vol.16 (1984)
2. J.D.Joannopoulos, G.Lucovsky, (ed.), The Physics of Hydrogenated Amorphous Silicon, vol.1, Springer, Berlin 1984
3. A.Kolodziej, S.Nowak, Thin Solid Films, vol. 175 ,37, (1989)
4. A.Kolodziej, T.Pisarkiewicz, Acta Phys.Polonica, vol.A73,(1988)
5. A.Kolodziej, AGH Press, Cracow, Poland, vol.7,3,(1988) 361
6. A.Kolodziej, T.Pisarkiewicz, Acta Phys.Polonica,vol.A75 (1989)
7. W.Paul, D.Anderson, Solar Energy Materials, vol5,(1981)229
8. T.D. Moustakas,Hydrogenated Amorphous Silicon, Semiconductors and Semimetals,ed.J.I.Pankove, NY,1984,vol.21A
9. M.Pinabasi, N.Maley, N.A.Myers, J.R.Abelson, Thin Solid Films vol.171,(1989)
- 10.J.Kakalios, R.A.Street, W.S.Jackson, Phys.Rev.Lett., vol.59(9), (1987)1037
11. D.E.Carlson, Appl.Phys.A. vol.41(1986)305

TABLE I

Deposition parameters of a-Si:H films

Series	P (Wcm <sup>-2</sup> )	T <sub>s</sub> (°C)	P <sub>H<sub>2</sub></sub> (%)	P <sub>Ar</sub> (%)	P <sub>total</sub> (mTorr)	V <sub>B</sub> (V)
c	6	250	50	50	10	-50
f	3	250	50	50	10	-100
g	3	300	50	50	10	-100
h	3	>550	50	50	10	-100

TABLE II

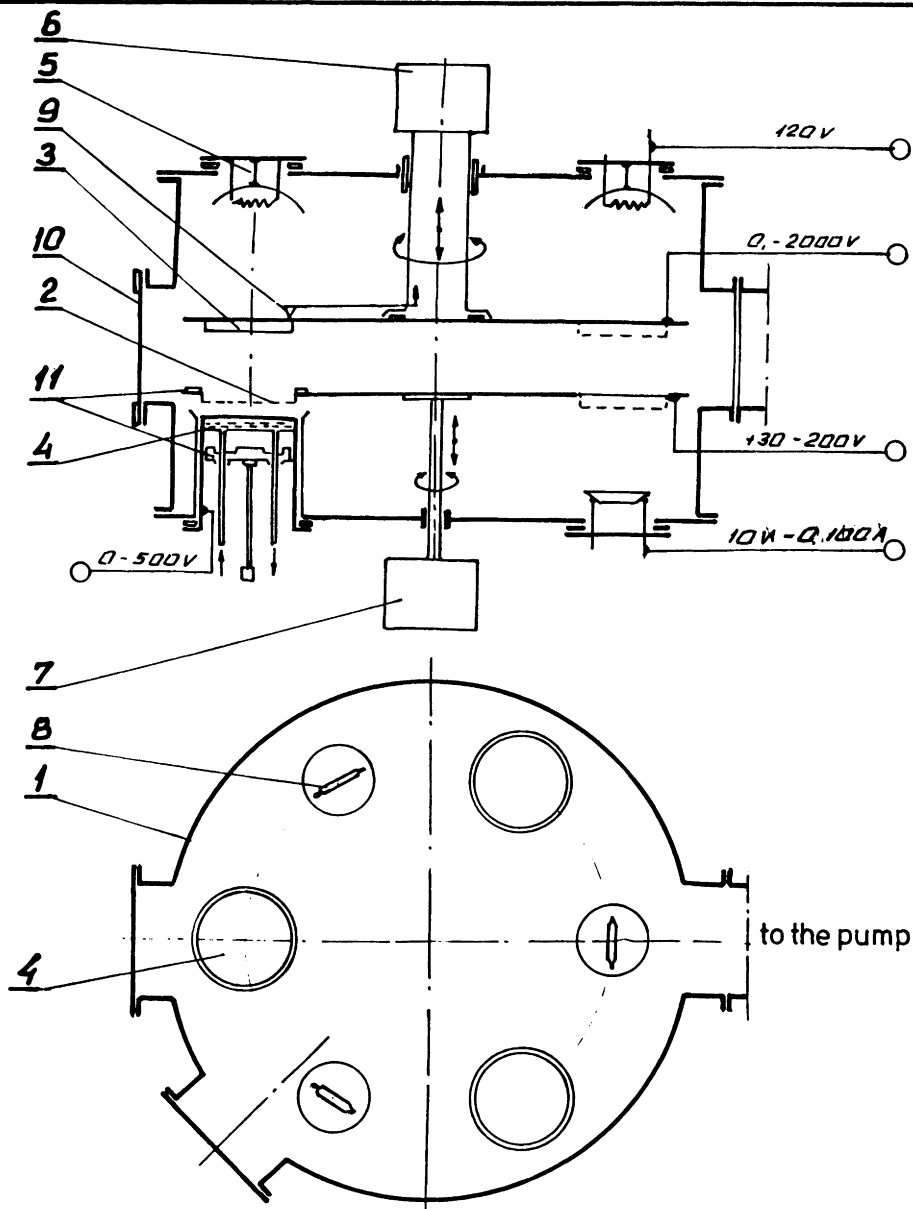
Characteristics of the a-Si:H films and their time changes after 3 years:

Series	Hydrogen content H to Si (%)	Oxygen content O to Si (%)	Optical band gap (eV)	Density of states (cm <sup>-3</sup> eV <sup>-1</sup> )	Dielectric constant	Light-to-dark conductivity ratio $\sigma_{ph}/\sigma_c$
c, c <sub>3</sub>	19, 15	2, -	1.90, -	4x10 <sup>16</sup> , -	8.5, -	10 <sup>4</sup> , 5x10 <sup>4</sup>
f, f <sub>3</sub>	21, 17	2, -	1.92, 1.90	4x10 <sup>16</sup> , 6x10 <sup>16</sup>	8.5, -	10 <sup>5</sup> , 5x10 <sup>4</sup>
g, g <sub>3</sub>	18, 12	3, -	1.80, 1.72	8x10 <sup>16</sup> , -	8.0, -	10 <sup>3</sup> , 10 <sup>2</sup>
h, -	- , -	8, -	1.5, -	- , -	- , -	- , -

TABLE III

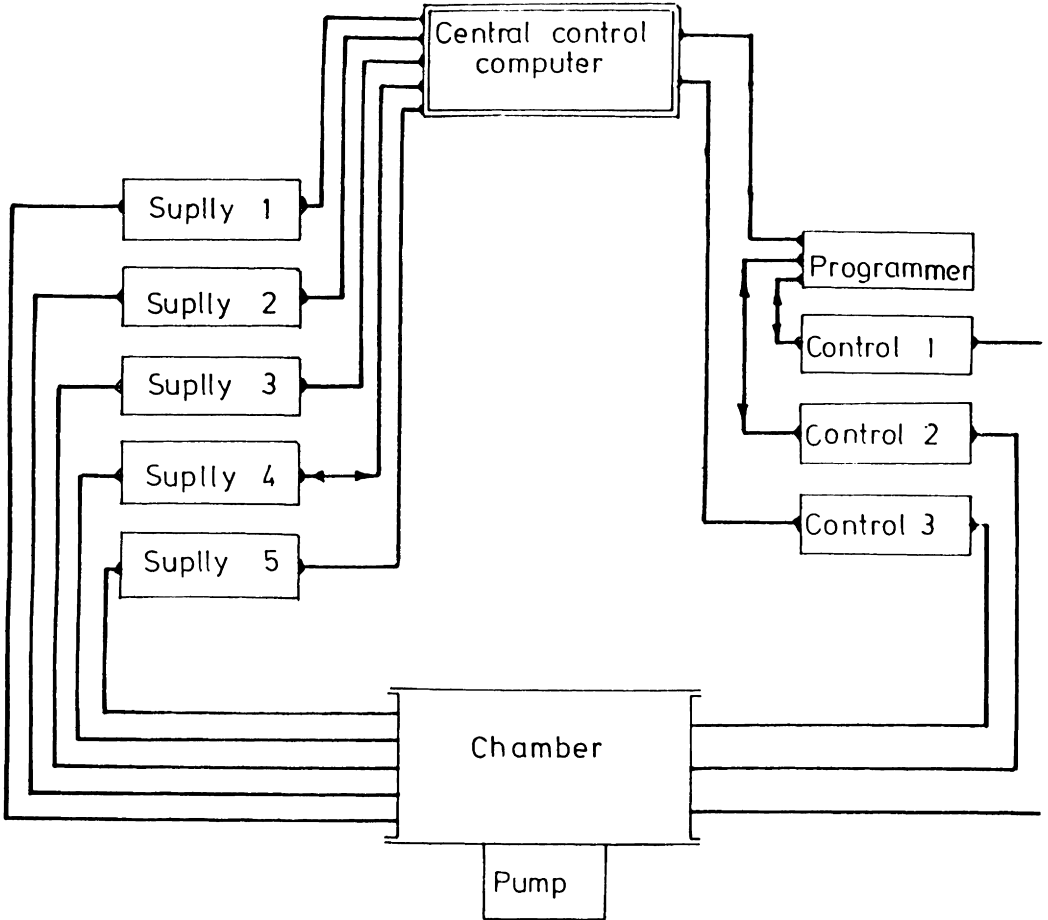
Results of calculation in the form of the ratio of bonds amount at the beginning of the test to that after 3 years

Series	Ratio of amount hydrogen after 3 years to hydro- gen at beginning (%)	Ratio of amount Si-H bonds after 3 years to Si-H bonds at beginning (%)	Ratio of amount Si-H <sub>2</sub> bonds after 3 years to Si-H bonds at beginning (%)
c <sub>3</sub> /c	78	82	75
f <sub>3</sub> /f	81	85	78
g <sub>3</sub> /g	61	-	65



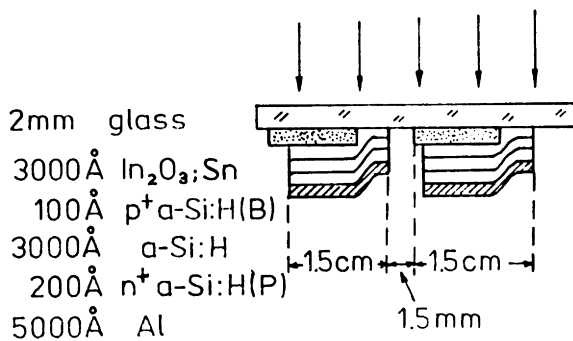
### 1. Schematic diagram of magnetron arrangement

1-view of the chamber and magnetron and vapor sources, 2-shield with mask, 3-oscillating sample and substrate, 4-magnetron, 5-heater of the substrate, 6-driver of substrate, 7-driver of shield, 8-vapor source, 9-temperature control, 10-load window, 11-magnets. Possible moves and supplies are marked as arrows and voltages, respectively.

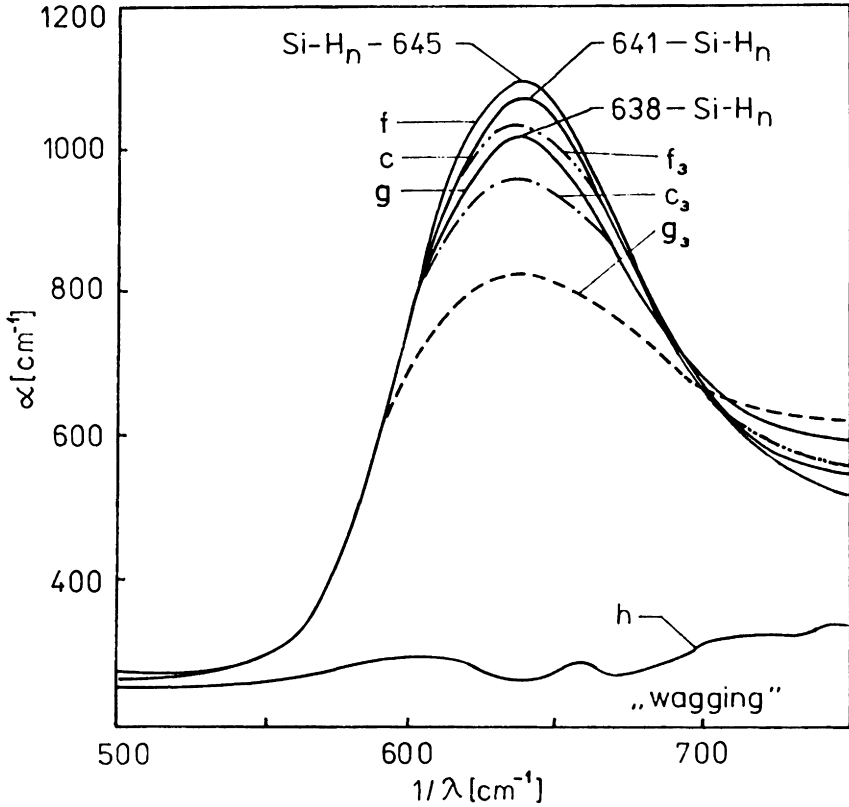


## 2. Block diagram of total magnetron arrangement.

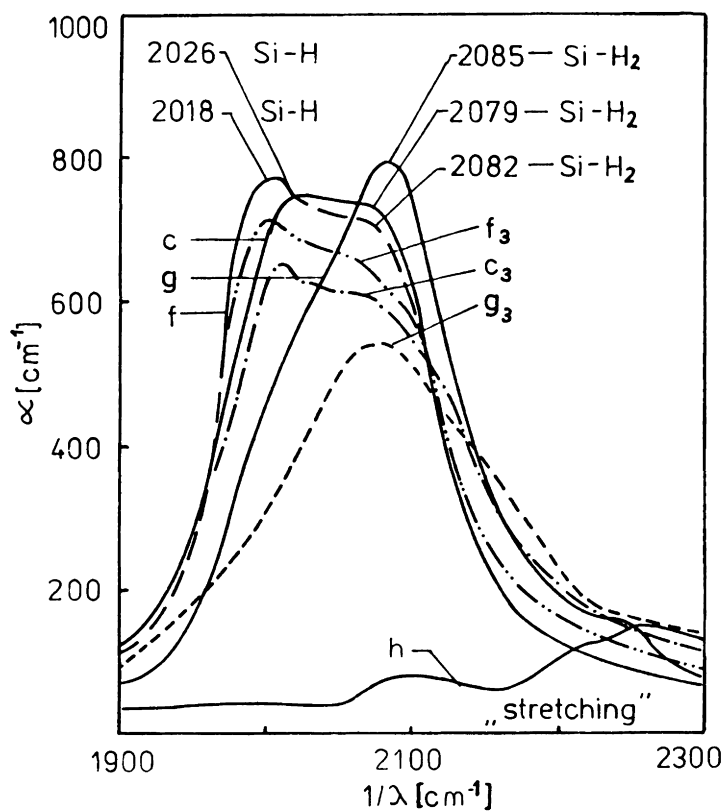
Control 1- programable pressure electronic unit with absolute baratron, Control 2-four channel mass flow system, Control 3- vacuum driver, Programmer -flow/pressure display system, Supply 1- 0-500 V supply of magnetrons, Supply 2- 10V,100 A supply of vapor sources, Supply 3- 0-120V supply heaters, Supply 4- 0-2000V of substrate ( polarization and ion cleaning), Supply 5- 0-100V supply of shields.



3. The scheme of a-Si:H solar cell of p i n structure.  
 Area of the single element is  $4.5 \text{ cm}^2$ .



4. Infrared absorption spectra for films: c, f, g, h measured three years ago and  $c_3, f_3, g_3$  measured at present in the range  $500-750 \text{ cm}^{-1}$ . The film are deposited on Al substrate.



5. Infrared absorption spectra for films: c, f, g, h measured three years ago and  $c_3, f_3, g_3$  measured at present in the range 1900-2300 cm<sup>-1</sup>. The film are deposited on Al substrate.

PARAMETRIC STEADY STATE  
SOLAR POND ANALYSES-A NUMERICAL APPROACH

P.T.TSILINGIRIS

Council of Technological Research, Commercial  
Bank of Greece, Sofocleous 11,  
Athens 122, Greece.

Department of Electrical Engineering, National  
Technical University of Athens, 42 28th October  
str., 106 82, Athens.

ABSTRACT

Preliminary feasibility investigations for the design of solar ponds, which are steadily recognised as potential low-cost solar collectors for a variety of applications, requires first order steady-state performance predictions. The present work refers to the development of a simple and powerful microcomputer model, suitable for the fundamental design of solar ponds.

KEYWORDS

Solar Ponds, Large scale solar-thermal conversion, Heat Storage.

INTRODUCTION

Among several analytical models presented in the literature, steady-state analyses (Kooi 1979, Hawlader 1980, Wang et al 1983), offer the advantage of simplicity to derive first order performance and design optimisation, using limited amount of simple easily accessible, meteorological data. The present work refers to the development of an advanced level, alternative to the already published steady state, microcomputer model, which provides a physical insight into the effects of parameter variation in basic design of ponds.

THE THEORETICAL MODEL

The fundamental computer model (Tsilingiris 1988, b), refers to a large pond which consists of a gradient zone (G.Z.), bounded by the upper and lower convecting zones (U.C.Z. and L.C.Z. respectively) at the levels of  $x_2$ ,  $x_1$  and  $x_3$  measured from the surface.

Heat transfer in G.Z. is described by,



$$-\frac{d}{dx} \left[ k_b \cdot \frac{dT(x)}{dx} \right] - \frac{I(x)}{x} = 0 \quad (1)$$

with,

$$I(x) = \alpha \cdot r \cdot I_0 \cdot h(c \cdot x) + (1-\alpha) \cdot r \cdot I_0 \cdot h(c \cdot x) \cdot h \left[ c(2 \cdot x - x) \right] \quad (2)$$

where  $\alpha$  the bottom absorptivity,  $r$  the reflection loss,  $c$  factor to account the actual path length  $I$  the total average solar radiation and  $h(x)$  its fraction reaching at the depth  $x$ , which though may be even more favorable, (Tsilingiris 1988,c), it is assumed to follow Rabl-Nielsens model.

The heat transfer in the soil is described by the equation,

$$\frac{d}{dx} \left[ k_s \cdot \frac{dT(x)}{dx} \right] = 0 \quad (3)$$

where  $k$  the thermal conductivity and subscripts  $b$  and  $s$  refer to brine and soil respectively. The first boundary condition of the problem is the heat balance in the U.C.Z.,

$$I_0 \cdot (1-r) [1-h(x)] + k_b \cdot \left. \frac{dT}{dx} \right|_{x=x_1} = (h_r + h_e + h_c) \cdot [T(x_1) - T_a] \quad (4)$$

where  $h_r$  the radiative heat transfer coefficient with the sky temperature given by the expression (Idso et al, 1988)

$$T_s = (T_a + 273) \cdot (1 - 0.261 \cdot \exp(-7.79 \cdot 10^{-4} \cdot T_a^{0.25})) - 273. \quad (5)$$

Evaporation and convection heat transfer coefficients are given by, (I.H.V.A.E. Guide 1970, and Lunde 1979)

$$h_e = (9.15 + 7.76 \cdot V_s) \cdot (p_s - RH_s \cdot p_{sa}) / (T_s - T_a) \quad (6)$$

$$\text{and } h_c = 4.5 + 2.9 \cdot V_c \quad (7)$$

where  $V_s$ ,  $p_s$ ,  $p_{sa}$ ,  $RH_s$ ,  $T_s$ ,  $T_a$  wind velocity, saturated water pressures at surface temperature and in the ambient air, relative humidity, surface and ambient temperatures respectively. The second is the heat balance in the L.C.Z.,

$$I \cdot (1-r) \cdot h(x) - \frac{q}{e} - k \cdot \frac{dT}{dx} \Big|_{x=x_2} + k \cdot \frac{dT}{dx} \Big|_{x=x_3} = 0 \quad (8)$$

where the second term corresponds to heat extraction rate and the third boundary condition is the fixed underground water temperature at a fixed depth underneath the bottom of the pond.

The brine and soil are subdivided into a number of uniform temperature slabs the heat balance of each one of which is translated to its finite difference form and the set of equations are solved simultaneously by the triangular factorisation method while top surface temperature is calculated iteratively by a conventional microcomputer. Selection of an optimum space mesh requires numerical experiment.

RESULTS AND DISCUSSION

Assuming that conditions of stability and boundary migration, which have also been extensively considered elsewhere (Hull et

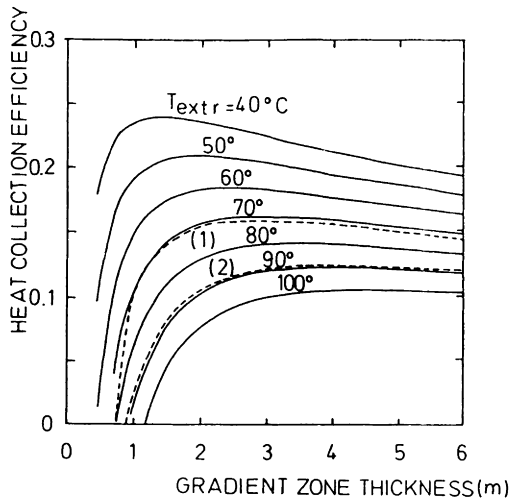


Fig.1. Calculated heat collection efficiency as a function of G.Z. thickness for various extraction temperatures and U.C.Z. thickness of 0.2 m

al 1987, Tsilingiris 1988, a) are fulfilled, and that climatic conditions correspond to a sunny mediterranean country (yearly average total solar insolation and ambient temperature 180 w/sq.m. and 18.1 deg.C. respectively) derived heat collection efficiency as a function of gradient zone thickness is shown in fig.1 for heat extraction temperatures from 40 to 100 deg.C. for an U.C.Z. thickness of 0.2 m. Broken lines (1) and (2) correspond to an U.C.Z. of 0 and 0.5 m respectively at 80 deg.C. Optimum heat collection efficiency (solid) and G.Z. thickness

(broken lines) as a function of heat extraction temperature for an U.C.Z. thickness of 0 to 0.5 m is shown in fig.2.

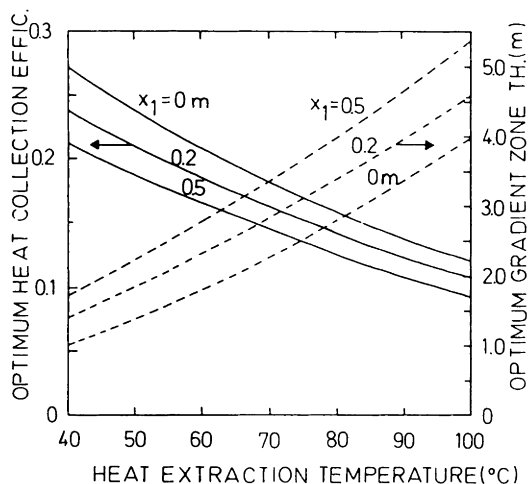


Fig.2 Optimum G.Z. thickness and heat collection efficiency as a function of heat extraction temper. with parameter the U.C.Z. thickness.

Upon a further simplification of the assumptions made, it is possible to compare derived results with those by Kooi's model. In fig.3 a close agreement between the results (typically 3 %

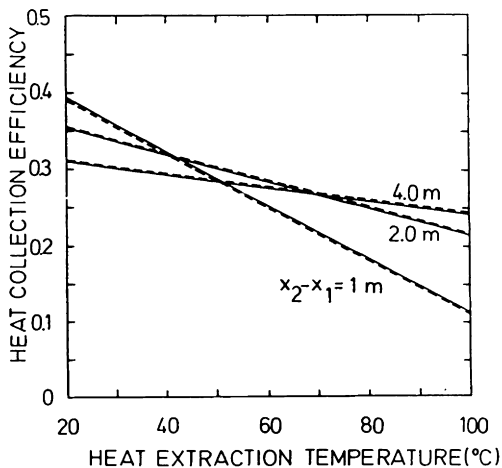


Fig.3 Comparison between the present simplified (solid) and Kooi's model (broken lines).

discrepancies) of the present (solid line) and Kooi's model (broken line) are shown as a function of heat collection efficiency for a G.Z. thickness of 1,2 and 4 m.

#### CONCLUSIONS.

Solar pond steady state analyses provide a good first approximation to thermal performance and offer an efficient method to design and optimising solar ponds under given meteorological and local conditions.

Owing to the difficulty of improving the assumptions already made in the published analytical models, an alternative numerical model was developed for investigating various effects, among which basic pond geometry soil conditions and optimum design are presented here.

Finally, comparisons which were possible after simplifications of the present model have shown very good agreement with Kooi's steady state model.

#### REFERENCES

- Hawlder M.N.A.,1980, The influence of the extinction coefficient on the effectiveness of solar ponds, Solar Energy, Tech.note,25,461-464.
- He X.,Golding P.,Nielsen C.,1988, The determination of internal stability in a salt gradient solar pond",proc. pf the Conf. Int. Progress in Solar Ponds, 107-117,I.I.E.
- Hull J.R.and Katti Y.,1987, Microconvection effects at gradient zone boundaries, Proc.A.S./I.S.E.S.,493-497,Portland.
- Institution Heating, Ventilating, Air Conditioning Engineers (I.H.V.E.) Guide, 1970, Book C, London.
- Idso S.B.,Jackson R.D., 1969, Thermal radiation from the atmosphere, Journal of Geophys.Research, pp 5397-5403.
- Kooi C.F.,1979, The steady state salt gradient solar pond, Solar Energy,23,37-45.
- Lunde P., 1979, Solar Thermal Engineering, John Wiley & Sons.
- Rabl A.R. and C.E.Nielsen,1975, Solar ponds for space heating, Solar Energy, 17,1-12.
- Tsilingiris P.T.,1988, The process of convecting breakdown in the gradient zone of salt gradient solar ponds, Proc. of the Conf.Int.Progress in Solar Ponds,pp.93-99,I.I.E.
- Tsilingiris P.T.,1988, Computer simulation modelling,thermal performance and design optimisation for solar ponds in Greece, Solar & Wind Technology,Vol.5,No.6,645-652.
- Tsilingiris P.T.1988, An accurate upper estimate for the transmission of solar radiation in salt gradient ponds, Solar Energy,40,41-48.
- Wang Y.F.and Akbarzadeh A., 1983, A parametric study on solar ponds,Solar Energy,30,555-582.

CENTRAL SOLAR HEATING PLANTS WITH SEASONAL STORAGE-  
A SITE SPECIFIC FEASIBILITY STUDY FOR 8 LOCATIONS  
IN THE FEDERAL REPUBLIC OF GERMANY

R. Kübler, L. Mazzarella, N. Fisch, E. Hahne

Institut für Thermodynamik und Wärmetechnik (ITW)  
Universität Stuttgart  
Pfaffenwaldring 6, FRG-7000 Stuttgart 80

ABSTRACT

Site specific studies for solar heating plants are carried out in a project "Solar District Heating". Long-term storage and collector arrays for the heating of housing areas in the FRG are considered. During a pre-study phase systems are evaluated for eight locations, two of these will be further investigated in the design phase starting in October 1990. The projected solar fraction lies in the range of 60 to 75 % of the yearly heat demand of typically 200 residential houses or 300 flats (about 3000 MWh/a). The goal for heat cost is below 0.2 DM/kWh including distribution system and supplement heat. In this contribution an overview is given on the results of the pre-studies. Design, dimensioning as well as an economic analysis are presented in detail for two of the locations.

KEYWORDS

Solar heating, seasonal storage, solar collectors

INTRODUCTION

The work carried out under the Task VII "Central Solar Heating Plants with Seasonal Storage (CSHPSS)" of the IEA Solar Heating and Cooling Programme has shown (Dalenbäck 1990) that it is possible to heat housing areas with a solar fraction of 60 - 80 %. Experiences with this technology in Sweden has demonstrated (Dalenbäck 1988) that, with the potential performance improvement and cost reduction for seasonal heat storages and high efficient flat plate collectors, solar heating can become competitive with conventional heating technology within a few years. Own work of the authors (Hahne 1989) in the Task VII has shown that similar systems under German conditions could deliver heat for less than 0.2 DM/kWh to residential homes. This work is now continued and applied to real housing areas in the study "Solar District Heating".

The project is carried out in close cooperation with Chalmers University of Technology (Gothenburg, Sweden) and Studsvik Energy AB (Nyköping, Sweden).

## AIMS OF THE FEASIBILITY STUDY

The aim of this study is to investigate the technical and economic feasibility of central solar heating plants at specific sites in the Federal Republic of Germany. In the pre-study phase (September 1989 - September 1990) eight locations are considered (see table 1), the two most suitable systems will be planned in detail during the design phase (October 1990 - June 1991). During the pre-study phase the geological conditions for the heat storage and the possibilities for the installation of collectors are investigated. The expected thermal performance of the systems is determined by computer simulation with the program MINSUN (Mazzarella 1989). The cost for storage construction, collector array, heat distribution system and for the auxiliary heating are estimated and the expected heat cost will be calculated.

During the second phase a detailed system design is elaborated and a call for tenders is issued for the heat storage, the collector array and the heat distribution system to result in a realistic cost basis for the construction of one of the systems. The aim is to show, that with a 50% subsidy on the investment cost, a first pilot plant can be built and operated economically competitive with conventional heating systems.

## DESCRIPTION OF PRE-STUDY LOCATIONS

Due to the great interest in the study from communes and local utilities the initial number of 4 or 5 pre-study locations has been extended to eight. The locations are all listed in table 1. The radiation data in table 1 are taken from the respective test reference years which might differ slightly from the actual local long term averages. The annual heat demand includes distribution losses.

Six out of the eight housing areas (except Wolfsburg and Rottweil) are under planning, in some cases the available roof area and the expected heating energy demand had to be estimated. For all six planned areas only roof integrated collectors or collectors on flat roofs can be considered due to limited ground available. The solar fraction is in most cases limited to about 60 % due to the available roof area.

For the construction of the heat storage (cylindrical pit, partly buried in ground) good conditions can be found at Stuttgart, Hamburg, Ulm and Wolfsburg while at Düsseldorf (4-5 m), Offenburg (2-4 m) and Leutkirch (1-2 m) the groundwater level limits the depth of the storage.

At Rottweil the heat storage shall be used mainly for surplus heat in summer from a planned heat and power plant fired with wood, the solar fraction thus is only about 11 %.

The pre-studies for Hamburg, Rottweil, Düsseldorf and Offenburg have been completed, the possible collector area lies between 3000 and 6720 m<sup>2</sup> and the required storage volume ranges from 4,000 to 50,000 m<sup>3</sup>. The large storage volume is required for the system at Rottweil, where mainly surplus heat during the summer from the heat and power plant will be stored. As the system at Rottweil is not a "classical" solar heating plant, no further investigations will be carried out for this particular system under this project.

Table 1. Summary of pre-study sites

Site	No. of flats	Heat demand MWh/a	Total horizontal solar radiation kWh/m <sup>2</sup> ·a
Hamburg	193 RH	3,244	977
Rottweil	1,230 RH	18,100	1,119
Düsseldorf	55 RH + 55 MFH	1,460	977
Offenburg	75 RH + 175 MFH	2,409	1,109
Stuttgart	120 RH + 360 MFH	5,000	1,119
Wolfsburg	23 RH	600	928
Leutkirch	67 RH + 110 MFH	2,993	1,072
Ulm	161 RH + 120 MFH	3,345	1,119

MFH = Flats in multi-family houses, RH = Residential Homes

## RESULTS OF THE PRE-STUDIES FOR HAMBURG AND OFFENBURG

### General Description

In this section the results of the pre-studies for Hamburg and Offenburg are presented in more detailed form (see table 2.). In Hamburg 193 residential homes will be built, each with an annual heat demand of about 12 MWh for heating and 4 MWh for domestic hot water. In Offenburg, which is located in the south-western part of Germany, a relatively compact housing area with about 70 % of all flats in multi-family houses is being planned, detailed information and plans will not be available before autumn 1990. The yearly total radiation is about 15 % higher in Offenburg than in Hamburg, the number of degree-days is about 15 % lower than in Hamburg.

### System Design

For both places the same system concept (see fig. 1) has been assumed. The auxiliary heat demand shall be met by natural gas (price 52.- DM/MWh)

The high efficient flat plate collectors are mounted on the roofs, delivering the heat to the central heat store via a heat exchanger. As heat transfer fluid a water/glykol mixture is used, the collector pipes are placed in the same ditch as the heat distribution system. For the economic calculations a price for the whole collector-system of about 450.- DM/m<sup>2</sup> was assumed (depending on the piping length), which is based on offers from manufacturers for collector arrays larger than 1000 m<sup>2</sup>.

The storage medium is water. The heat storage is an earth pit of cylindrical shape (7 - 10 m deep), partly buried in the ground. Due to shortage of available ground, for both cases a concrete top was chosen for the storage, that can be covered with soil. A pre-design by a large construction company has shown, that the cost for this type of storage

would be 130.- DM/m<sup>3</sup> for a volume of 13,000 m<sup>3</sup> (Hamburg) and about 175.- DM/m<sup>3</sup> for a volume of 4,000 m<sup>3</sup> (Offenburg). The projected insulation thickness on top of the heat storage is 0.4 m and 0.2 m on the side walls. Insulation of the bottom is only required, if the ground water level is close to the bottom of the storage.

The domestic hot water (DHW) is heated centrally and distributed by separate pipes. This allows for a better use of the heat storage due to the low fresh water temperature, and leads to up to 5 % higher solar fraction. Moreover it allows for an operation of the heating network independent of the needs for DHW-heating (minimum supply temperature 55 °C) in the individual houses. An economic analysis shows, however, that for the Hamburg system decentralized DHW-heating in each group of houses (3-8 houses per group) is cheaper due to the quite long piping required .

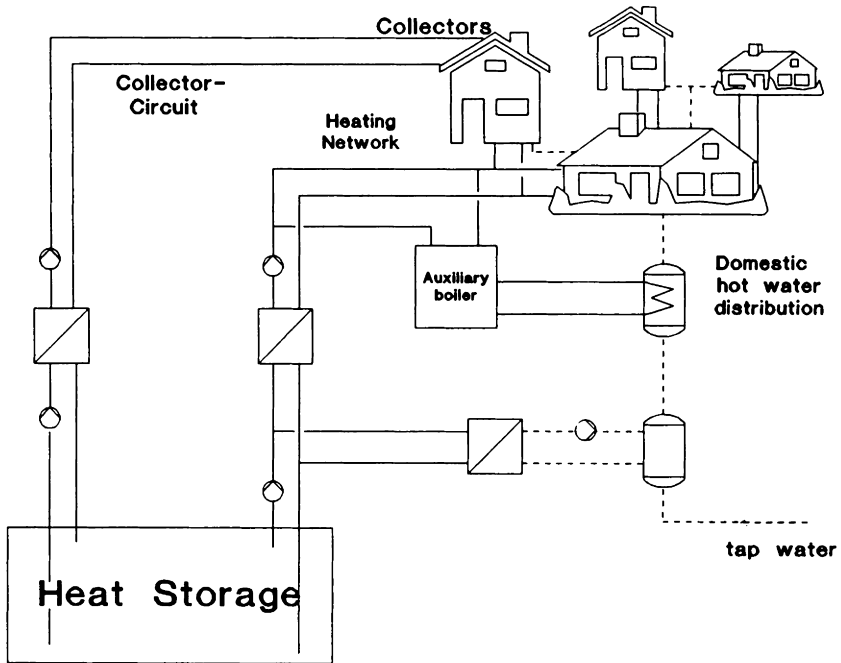


Fig. 1: Scheme of the System

### Thermal Performance

Design and thermal performance data are presented in table 2. With the system in Hamburg a solar fraction of 62 % can be achieved, while in Offenburg due to the limited collector area on the multi-family houses only about 48 % are possible. It has to be stressed, however, that the available roof area has been estimated based on the projected total building area. Due to the lower solar fraction for the Offenburg system, the heat storage



can be kept relatively small. The considerably larger solar gain per  $m^2$  of collector area is mainly due to the more favourable climate (higher insolation) and to lower heat losses in the storage (the portion of solar heat directly supplied to the load is higher, so less heat must be stored).

Table 2. Design data and thermal performance of the systems at Hamburg and Offenburg

Item	Unit	Hamburg	Offenburg
No. of degree days	K·d	3,903	3,319
Heat demand of the houses	MWh/a	3,088	2,330
Total solar radiation (horizontal)	kWh/m <sup>2</sup> ·a	977	1,109
Collector area	m <sup>2</sup>	6,720	3,000
Storage volume	m <sup>3</sup>	13,000	4,000
Solar contribution to load	MWh/a	2,006	1,144
Solar gain/collector area	kWh/m <sup>2</sup> ·a	299	381
Solar fraction	%	62	48

### Energy Cost

For comparison with the cost goal of 0.2 DM/kWh, i.e. 200.- DM/MWh, the cost of heat delivered to the houses has been calculated (see table 3). For the above described basic system design the expected cost amount to 248.- DM/MWh for the system at Hamburg and to 154.- DM/MWh for Offenburg. For the cost calculations the annuity method was applied with a real interest rate of 6 % and an expected lifetime for all system components of 20 years. The fairly large cost for operation, maintenance and administration include also depreciation and exchange of heat meters and accounting of the heat.

Table 3. Heat cost and their distribution for the systems at Hamburg and Offenburg (all prices in DM/MWh delivered, real interest rate 6 %, expected lifetime 20 years)

Item	Hamburg	Offenburg
Heat cost (price of energy delivered)		
base case, separate DHW distribution	248	154
common heat distribution	236	
common distribution, floating storage top	224	
Contribution to heat cost (base case)		
collectors	79.88 (32%)	44.38 (29%)
heat storage	50.47 (20%)	27.86 (18%)
distribution network	46.4 (19%)	24.16 (16%)
fuel (gas)	21.49 (9%)	28.9 (19%)
operation, maintenance, administration	42.35 (17%)	23.38 (15%)
auxiliary boiler, building	7.91 (3%)	5.57 (3%)

The large difference in the total heat cost has several reasons. The difference in the solar fraction, first of all, leads to a smaller solar system and to the burning of more cheap gas for the Offenburg system, which reduces the heat cost. The solar system at Offenburg delivers more useful heat at lower investment cost (smaller storage, shorter piping). The structure of the area (compact in Offenburg, residential in Hamburg), finally, leads to higher cost for the heat distribution system in Hamburg.

With the cost structure used in this investigation with cheap gas as auxiliary, no cost minimum for the combined system exists for a finite collector area, i.e. the heat cost minimum occurs at zero solar contribution.

#### DISCUSSION AND FUTURE WORK

The investigations carried out under this project so far have shown that the cost goal of 0.2 DM/kWh for heat delivered to the houses can be achieved in a pilot project. The project has already after one year created a lot of interest from the part of solar collector manufacturers, who are willing to improve the thermal performance of their collectors and the design to meet the needs of central solar heating plants. Five different high efficient flat plate solar collectors are presently tested at the Institute ITW), one more will be mounted on short notice.

Before the construction of a Pilot-CSHPSS in the FRG a number of pilot installations for a realistic test of the components will be realized. This comprises a large collector array, connected to a district heating network, one or two large roof-integrated collector arrays (100 - 200 m<sup>2</sup>) and a high-temperature earth-pit heat store.

#### REFERENCES

- Dalenbäck, J-O. (1988). *Large Scale Swedish Solar Heating Technology - System Design and Rating*. Document no D6:1988, Swedish Council for Building Research, Stockholm. (National report, Task VII, IEA SH&CP)
- Dalenbäck, J-O. (1990). *Central Solar Heating Plants with Seasonal Storage - Status Report*. Document no D14:1990, Swedish Council for Building Research, Stockholm. (Final report, Task VII, IEA SH&CP)
- Hahne, E. (1989), M. Hornberger and N. Fisch. Solar Assisted District Heating Plants with Long-Term Heat Storage, *Proceedings of the ISES Solar World Congress*, Kobe, Japan, (in print)
- Mazzarella, L. (1989). *Central Solar Heating Plants with Seasonal Storage - the MINSUN simulation Programme, application and user's guide*, Politecnico di Milano, (report, Task VII, IEA SH&CP)

*Acknowledgement: This project has been funded by the Federal Ministry for Research and Technology under the contract number 032 8867 A, the authors gratefully acknowledge this support.*

## DEVELOPMENTS IN WAVE ENERGY

L.J.Duckers

Energy Systems Group  
Coventry Polytechnic

Ocean waves are generated by wind passing over extensive stretches of water. Because the wind is originally derived from solar energy we may consider waves to be a stored, moderately high density, form of solar energy.

The possibility of extracting energy from ocean waves has intrigued man for centuries but it is only in the past two decades that technically suitable devices have been proposed.

In general these devices have few environmental drawbacks. The economic projections for some devices look extremely promising and especially so in areas of the world where the wave climate is energetic. The north east Atlantic is a particularly favourable area.

Figure 1 illustrates the wave energy mates for Western Europe. From Reference 2 it is clear that energy potentially available from the European wave resource is enormous.

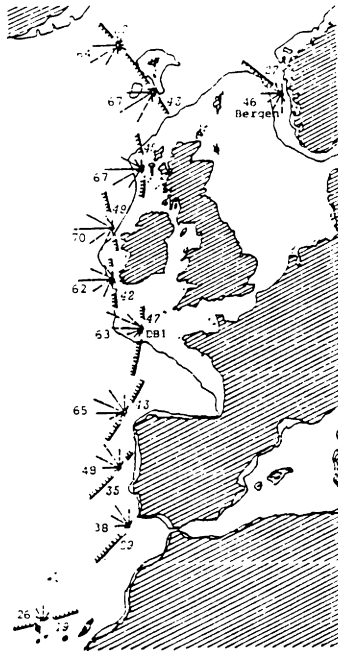
The wave climate is not steady, indeed seas vary on a minute by minute basis as well as seasonally. It is important to note that generally the most energetic Atlantic seas occur during the winter when the demand for electricity is greatest. The variation in wave height, period and power with time means that devices have to be carefully designed for optimal energy capture and have also to be able to withstand the considerable loadings that result from the largest storms.

The oil crisis of 1973 stimulated considerable activity in wave energy development in the United Kingdom and a number of teams were established working on a wide variety of devices. It is fair to say that by the late 1970's Britain led the world in wave energy research but that the 1982 decision by the Department of Energy to curtail the programme caused the loss of many of these teams and their accumulated expertise. The basis for the decision was, and still is, the subject for much debate and the arguments will not be rehearsed here. A review of wave energy is now being conducted by the Department of Energy and it is to be hoped that a new research programme will be formulated by 1992.

Other countries, notably Norway, and Japan now have prototype devices under test and Portugal, Denmark, Sweden and Eire are also undertaking research.

### The Technology

In order to capture energy from sea waves it is necessary to intercept the waves with a structure which can respond in an appropriate manner to the forces applied to it by the waves. If the structure is fixed to the seabed or seashore then it is easy to see that some part of the structure may be allowed to move with respect to the fixed structure and hence convert the wave energy into some mechanical energy (which is probably subsequently converted into electricity). Floating structures can be employed, but then a stable frame of reference must be established so that the 'active' part of the device moves relative to the main structure. This can be achieved by the application of inertia or by making the structure so large that it spans several wave crests and hence is reasonably stable in most sea states. A classification of offshore point absorbers is attempted by Folley reference 3.



Wave power estimates for western Europe based on the UK Met Office wind-wave hindcast model (Norwegian Met Inst model for Bergen). Wave roses show mean power from each  $30^\circ$  sector ( $2.5^\circ$  for DBI), with marks at  $5 \text{ kW/m}$  intervals. Gross power levels are shown (in  $\text{kW/m}$ ); and also net power  $P_\theta$  (numbers in *italics*) crossing lines (|||||) whose direction  $\theta$  maximises  $P_\theta$  for the particular site.

Figure 1

An important subgroup of wave energy devices are the bed and shore mounted ones since, excepting the Japanese vessel, Kaimei, they are the only ones so far tested as prototypes at sea. As a fixed frame of reference and with good access for maintenance they have obvious advantages over the floating devices, but do operate in reduced power levels and may ultimately have limited sites for future deployment.

Probably the majority of devices tested and planned are of the oscillating water column (OWC) type Figure 2 is a schematic representation of an OWC.

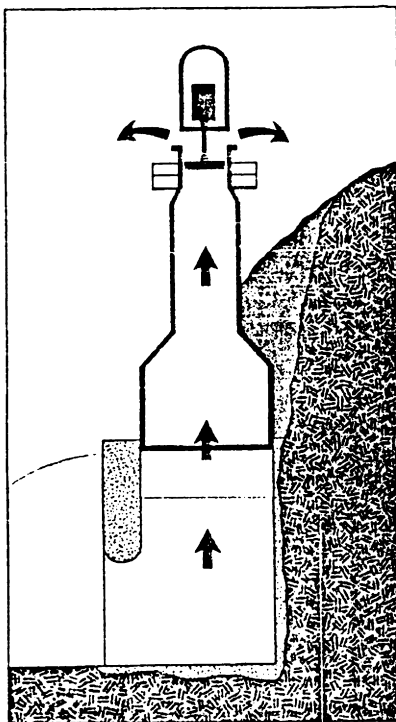


Figure 2 A shore mounted O.W.C

An air chamber pierces the surface of the sea and the contained air is forced out of and then into the chamber by the approaching crests and troughs. On its passage from and to the chamber the air passes through an air turbine generator and so produces electricity.

A novel air turbine, the Wells, which is self rectifying and has aerodynamic characteristics particularly suitable for wave application, is proposed for many OWCs.

Oscillating water columns have been built in Norway, Japan and Scotland (see reference 1) and are proposed for the Azores by the Portuguese (reference 4). Kaimei was a floating collection of OWCs which was first tested in 1977. A further four (fixed) OWC type devices have been tested as prototypes in Japan. Three other prototypes have been tested in Japan, all having mechanical linkage between a moving component, such as a hinged flap, and the fixed part of the device.

In Norway a device for capturing water at an elevated level as a result of waves running up a tapered channel has proved to be very successful. TAPCHAN, as it is called, needs very careful location as it is susceptible to tides and wave direction.

Floating devices, such as the Clam and Duck from the United Kingdom, are rightly thought to be next generation devices, due to the difficulties of working in 50-100 m depth of water.

They would be able to harvest more energy since the wave power is greater offshore than in shallow water and since there is little restriction to the deployment of large arrays of such devices.

The Clam is a floating rigid toroid. Twelve air cells are arranged around the circumference of the toroid and these cells are all coupled together by an air ducting which contains twelve Wells turbines. Thus the air forced from one cell will pass through at least one turbine on route to other cells. Each cell is sealed against the water by a flexible rubber membrane.

The Edinburgh Duck was originally envisaged as many cam-shaped bodies linked together on a long flexible floating spine which was to span several kilometres of the sea. More recently interest has centred on the case of a single Duck which would demonstrate the technology at full scale and because of point absorber effects would produce significant amounts of energy.

### Economics

Wave energy, like many other renewables energy technologies, has high capital costs but low operating costs. The high capital costs arise from the need to build and deploy large structures to capture small amounts of energy as the "energy density" of wave environments is quite low around 50 kW per metre. On the other hand the operating costs are low because one has to consider only operational, repair and maintenance costs, which together might only amount to a few percent per annum of the capital cost, and there is no cost associated with the fuel, the waves - unless governments impose an abstraction tax.

The consequence of high capital cost, but low operating cost, is generally a long pay back period, and this seems to be a major drawback as far as government and commercial investors are concerned. This is particularly true in the United Kingdom where, for commercial investment pay back periods exceeding about three years are often regarded as too long.

Wave energy is a long term technology, it will take some further years of research and development to produce prototypes of some devices and to refine the design of others.

Wave energy is also a long term technology in the deployment of a particular device. Whilst it is impossible in this short paper to present a complete economic model Figure 3, adapted from Reference 5, serves to illustrate the influence of discount rate and value of electricity generated on the the long term value of an investment in a wave energy station. The capital cost is taken as £1000 per installed kW, operating cost is 3% per annum and the value of electricity is £0.03 and £0.04 per kWh, index linked. Discount rates between 3 and 15% are employed. It is clear that the pay back period is always long, the discount rate is very important, favouring the Japanese who currently enjoy very low discount rates, and that the value of the output is also critical. Being an environmentally clean technology it may be that the value of the output should be enhanced with respect of electricity derived from some of the conventional sources.

Finally this simple model shows that, provided that a positive payback is achieved, the returns on investment in wave energy can be considerable in the longer term.

#### Possibilities For The Future

Wave energy is already being utilised in some parts of the world. Where a remote island has expensive conventional energy and a reasonable wave climate it is likely that prototype devices may be economically viable. In the longer term a major contribution from wave energy will probably arise from the deployment of arrays of floating offshore or near shore devices and there is still a research and development programme required in this area. For example a prototype clam device and testing programme would probably cost £25M over five years. Such a programme would be aimed at confirming the claims made for the performance of the device, giving confidence to its structural integrity and allowing refinement and cost optimisation of the design. We should not close our minds to the possibilities for other devices, emerging in the future with enhanced cost effectiveness.

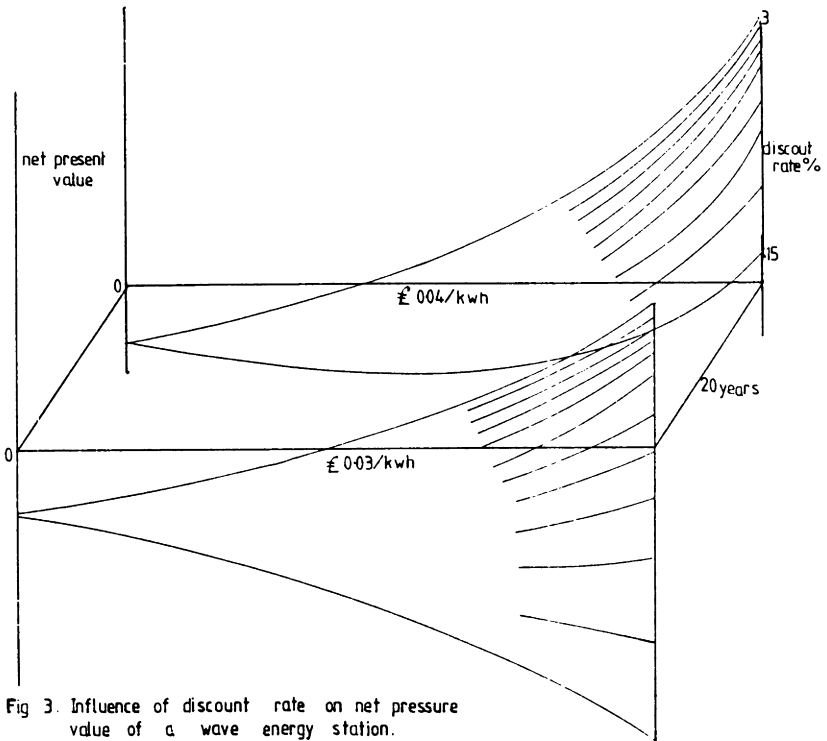


Fig 3. Influence of discount rate on net present value of a wave energy station.

### References

- (1) WAVE ENERGY DEVICES Ed. Duckers L.J. Meeting C57, Coventry, November 1989 The Solar Energy Society Kings College, Campden Hill Road, London
- (2) Mollison D. in (1) pp28-31 The European Wave Power Resource
- (3) Folley M. in (1) pp69-73 Classification of Wave Energy Converters
- (4) Wave Energy Project in Portugal. OWC demonstration plant. Falcao, A.F, Gato, L.M.C, Teresa Pontes, M., Sarimento AJNA ISES Solar World Congress, September 1989, Kobe, Japan.
- (5) Turner D.M. private communication April 1990.



Presentation of PRESIM  
A user-friendly preprocessor for TRNSYS

Svante Nordlander\*, Mats Rönnelid\*, Per Isakson\*\* and Lars Broman\*

\* Solar Energy Research Center (SERC)  
Univ. College of Falun/Borlänge  
Box 10044, S-781 10, Borlänge, SWEDEN

\*\* Monitoring Center for Energy Research (MCE)  
Royal Institute of Technology  
S-10044 Stockholm, SWEDEN

ABSTRACT

PRESIM is an interactive graphical computer program for producing input data for modular HVAC system simulation programs. Version 1.0 runs on IBM compatible DOS computers and produces input data for the TRNSYS simulation program, version 12.2. The user works with a drawing of an HVAC system model on a graphical computer screen, much in the same way as with a CAD-system. PRESIM has been tested for half a year by experienced TRNSYS users and is now officially released and available through SERC and other distributors.

KEYWORDS

Solar energy, computer simulation, front end, TRNSYS

INTRODUCTION

Computer simulation programs are important tools for evaluating the performance of HVAC systems. There are good programs which offer an almost unlimited variety of HVAC systems to be modelled and simulated. However, the methods to describe and change the system model under study are not user-friendly (Broman and Nordlander, 1987).

With a better user interface more people would do better simulation studies. The most used modular simulation program for solar systems is TRNSYS (Klein and co-workers, 1983). A number of efforts to develop a better user interface for preparing TRNSYS input data have been made. So far, none of them has gained a wide acceptance.

SERC at the University College of Falun/Borlänge and MCE at the Royal Institute of Technology, in collaboration with the Solar Lab at University of Wisconsin, now have developed PRESIM, a graphical front end for the TRNSYS simulation program. The structure of PRESIM would also permit interfacing to other simulation programs with a similar input data structure.

DESCRIPTION OF PRESIM

With PRESIM a user can create, store, retrieve and change system drawings and input data for TRNSYS. The user works with a mouse and manipulates a drawing of an HVAC system model on a graphical computer screen, much in the same way as with a CAD-system. The user interface is similar to a Windows or Macintosh program. The program runs under DOS on an IBM AT, PS/2 or compatible machine with 640 kb memory, minimum 2 Mb free disk space, and EGA or VGA graphics screen. Drawings can be plotted on HP-compatible plotters and a number of laser and dot matrix printers.

A PRESIM system model consists of components and connections. Typically, each symbol on the screen represents a component in the simulation program. As far as possible, standard ISO symbols are used. The connections are multi-dimensional, e.g. one line on the drawing may represent both temperature and mass fluid information. Figure 1 shows an example of a screen.

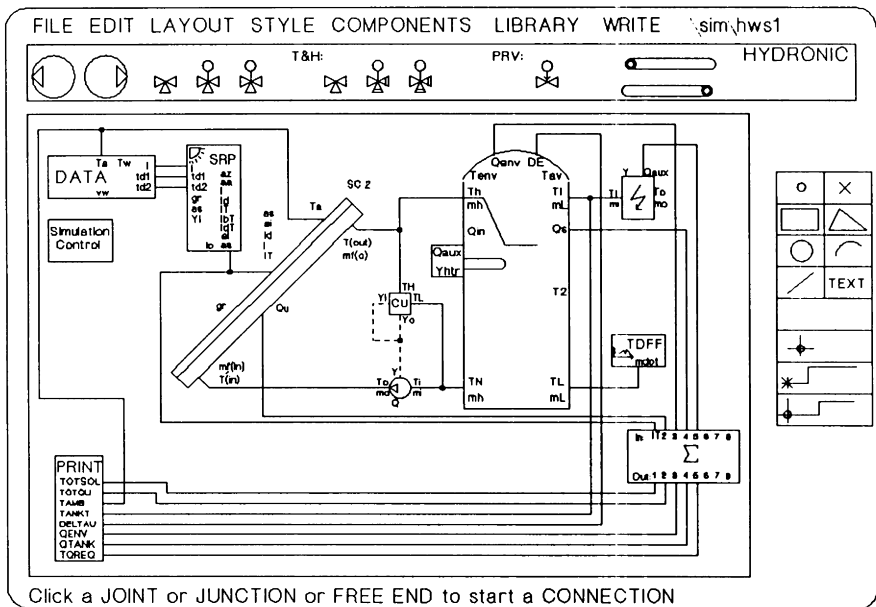


Figure 1. The computer screen during a PRESIM session.

Parameter values such as collector area and efficiency, heat exchanger properties and so on are entered in screen forms with help texts and unit conversion. The user may save copies of individual components, with parameter values, and thus build a library of ready-to-use components. The standard PRESIM library contains all standard TRNSYS types with a few exceptions. It is also possible for the user to create PRESIM components for user developed TRNSYS components. Figure 2 shows a typical parameter form for a storage tank component.

IN1: Stratified storage tank, 3 nodes IN2: Variable inlet. No aux heater. PRESIM type: 1019 TRNSYS type: 4 Short label: S Tank Long label : Solar storage tank CM1: CM2: TRNSYS manual 4.3.1			
PARAMS	15	PG_UP	
		PG_DW	
1	Variable inlet	-	2
2	Tank Volume	m3	600
3	Specific heat of fluid	kJ/kg-C	4.19
4	Density of fluid	kg/m3	1000
5	Tank loss coefficient	W/h-m2-C	0.09
6	Height of node 1	m	4
7	Height of node 2	m	4
8	Height of node 3	m	4
INPUTS	OUTPUTS	PARAMS	DERIVS
			EXPAND SHRINK

Figure 2. The parameter form for a storage tank.

Often a TRNSYS component functions differently depending on modal parameter settings, so it must be represented by two or more PRESIM components. For example, the TRNSYS Type 3, a storage tank, may have a fixed or variable inlet, and each of these two modes is represented by one PRESIM component, with different graphic symbols.

## TESTING AND RESULTS

The program has been tested by a number of experienced TRNSYS users during spring and summer 1990, among those: Sorane SA, Lausanne, Switzerland; Solar Lab, University of Wisconsin, USA; Institute of Thermodynamics, University of Stuttgart, Germany; C.E.T.I.A.T, Villeurbanne Cedex, France; Laboratoire de Thermodynamique, Universite de Liege, Belgium. In general the testing has proved the program to be most useful. A number of valuable comments and suggestions, and a few severe shortcomings and fatal bugs have been reported.

## DISTRIBUTION OF PRESIM

Version 1.0, which is now released, produces input data for the TRNSYS simulation program, version 12.2. Next PRESIM version will support TRNSYS 13.0. The program comes with complete documentation in English and a component library which includes 82 PRESIM components, representing 41 TRNSYS types.

The license fee for PRESIM is \$300 and the program is available from:

PRESIM Coordinator  
 Solar Energy Research Center (SERC)  
 Univ. College of Falun/Borlänge  
 Box 10044  
 S-781 10 Borlänge                      Tel.: +46 243 73757  
 SWEDEN                                      Fax.: +46 243 73750

INET Bart, Fisch, Kubler  
 Böhmisreuteweg 20  
 7000 Stuttgart 1  
 West Germany

TRNSYS coordinator  
 University of Liege  
 Laboratory of Thermodynamics  
 Rue Ernest Solvay, 21  
 B-4000 Liege  
 Belgium

TRNSYS Engineer  
 Solar Energy Laboratory  
 University of Wisconsin-Madison  
 1500 Johnson Drive  
 Madison, WI 53706  
 USA

#### ACKNOWLEDGEMENT

We greatly acknowledge the support by W. A. Beckman. The work presented here was carried out with financial support from the Swedish Council for Building Research (BFR) and the Swedish National Energy Board (STEV).

#### REFERENCES

Broman, L. and S. Nordlander (1987). New Swedish simulation and design tool for solar heating systems, A preliminary study (In Swedish). University College of Falun/Borlänge, Borlänge, Sweden.

Klein, S. A. and coworkers (1983). TRNSYS, a transient system simulation program. University of Wisconsin-Madison, WI, USA.

## A SOLAR HEATING PLANT WITH SEASONAL STORAGE The Särö Project

Jan-Olof Dalenbäck, Lic Tech

Dept. of Building Services Engineering  
Chalmers University of Technology  
S-412 96 Göteborg, Sweden

Phone: +46-31721153 Fax: +46-31721152

### ABSTRACT

A new solar heating plant, with a novel storage design, has been built in a new residential building area south of Göteborg, Sweden. The plant will provide a part of space heating and DHW requirements in 48 flats, using roof-integrated solar collectors and a newly developed insulated and water-filled steel tank. The main scope of this RD&D project is to evaluate system performance and economics with advanced roof-integrated collectors and seasonal storage in new small residential building areas.

### KEY WORDS

Solar heating, seasonal storage, residential heating.

### INTRODUCTION

The evaluations of the solar heating plants Ingelstad and Lambohov (1980-83) showed that both cheaper and more efficient solar collectors and heat stores were required to make solar heating with seasonal storage competitive with conventional smaller heating plants (100-500 residential units). They also revealed substantial scope for cost reductions in the system design, particularly the piping and control (Dalenbäck, 1988a).

A pre-study for a new smaller solar heating plant was initiated in 1984, with the objective of designing a cheap insulated heat store together with a cheap and simple system, as new collector designs were developed in other projects. The Särö project is the most recent result of this study. The solar collectors are financed using the same kind of governmental building loans as for the houses, while the storage is financed by experimental building loans.

### DESCRIPTION OF THE SURROUNDINGS

Särö is located on the Swedish west-coast about 20 km south of Göteborg. The average annual outdoor temperature is 7 °C, the heating design temperature is -16 °C and the annual global solar radiation on a horizontal surface is close to 1 000 kWh/m<sup>2</sup>. The

building area is located in a small valley between rocky hills and consists of a group of nine small multifamily houses with two floors. The houses have ordinary roof slopes (27°) and the collector roofs are facing SSE to SE.

## SYSTEM DESIGN

The collectors cover about 60 % of the SSE to SE facing roof area. The solar collectors, as well as the space heating and domestic hot water (DHW) systems in the houses, are connected to a small central heating plant via insulated iron pipes in the ground. The storage is close by the heating plant and supplementary heating is managed by a conventional oil boiler.

### Solar Collectors

The solar collector used is an advanced version of the roof-integrated collector type previously used in several Swedish projects (Sunstrip absorber, acrylic cover). In Särö this collector type is complemented with a convection barrier (TPFE-foil), thus improving the thermal performance using a large temperature difference in the water heat store. The total collector aperture area is 800 m<sup>2</sup>, and the collectors were built and put into operation during the late summer 1989.

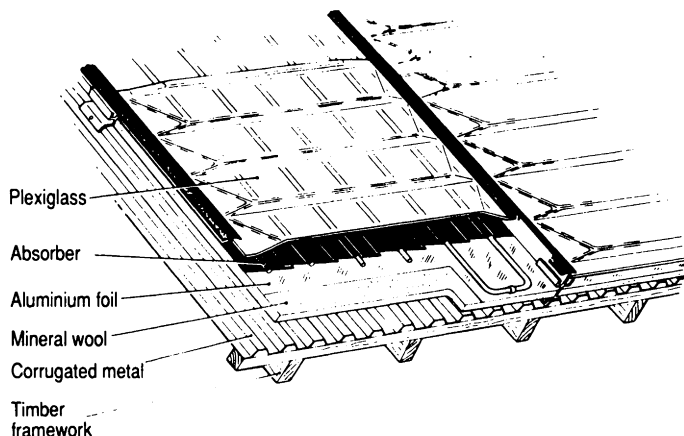


Fig. 1. Roof-integrated collectors. The collector in Särö has a convection barrier (TPFE foil) between the acrylic cover (plexiglass) and the absorber.

### Heat Store

The final choice for the storage design in Särö fell on a cylindrical conventional tank construction, in combination with loose mineral wool insulation (blown into place), placed in a rock pit. A spray polyurethan insulation in combination with plastic sheets (HDPE, TPFE) or reinforced spray concrete as water-proofing liners were two other alternatives that was studied in advance.

The tank was rolled together on site out of 4 mm galvanized steel plates with a special equipment. As this tank can have a self-supporting top the outer roof construction was changed from an original design with concrete slabs to aluminium sheets on iron beams, which is much cheaper. The height of the tank is 7 m and the water volume is close to 700 m<sup>3</sup>.

The heat store was originally supposed to be a rectangular insulated and water-filled rock pit, water volume of about 1 400 m<sup>3</sup>, with a self-supporting top similar to an earlier R&D project in Väjö (Dalenbäck, 1988b).

The pit excavation was done already in 1988 in connection with the planning of the building area and the final construction was supposed to be completed in the beginning of 1990. The change of storage design to a cylindrical tank (inside a rectangular pit) resulted in a reduced storage volume. The main advantages with this construction is that it is an established technology and that the usable temperature range can be large, about 35-95 compared to 35-80 °C for the original design.

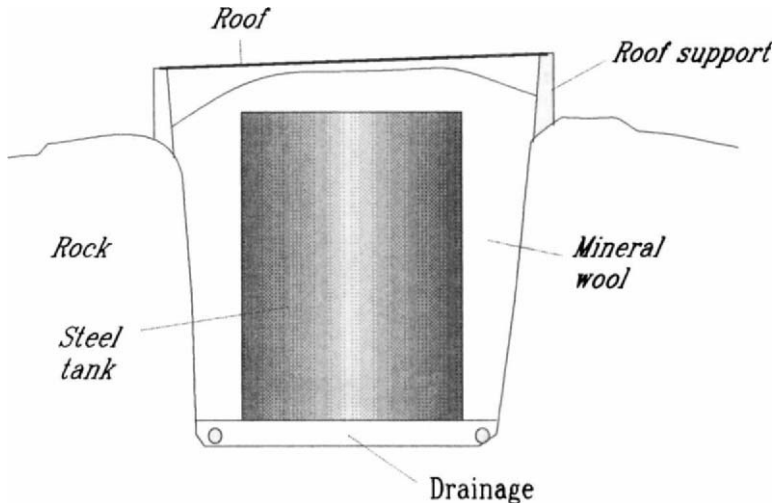


Fig. 2. Särö - Schematic drawing showing the storage design.

### Space heating and DHW

The load is space heating and DHW for a small residential building area with 48 flats in multifamily houses. The houses are calculated to have an annual heat requirement of the order of 400 MWh, including DHW and distribution losses. The space heating system is a low temperature hydronic radiator system with a 55 °C supply temperature required at an outdoor design temperature of -16 °C. The characteristic supply temperature requirement is 50 °C for DHW, and the characteristic return temperature is 35 °C.



## SYSTEM OPERATION

The system operation is similar to the system operation in other late R&D projects (Dalenbäck, 1988a). The main difference is that there is a direct connection between the collector circuit and the load circuit in Särö. This will not improve the performance but it reduces the amount of piping in connection to the storage. The interaction between these two circuits will be evaluated.

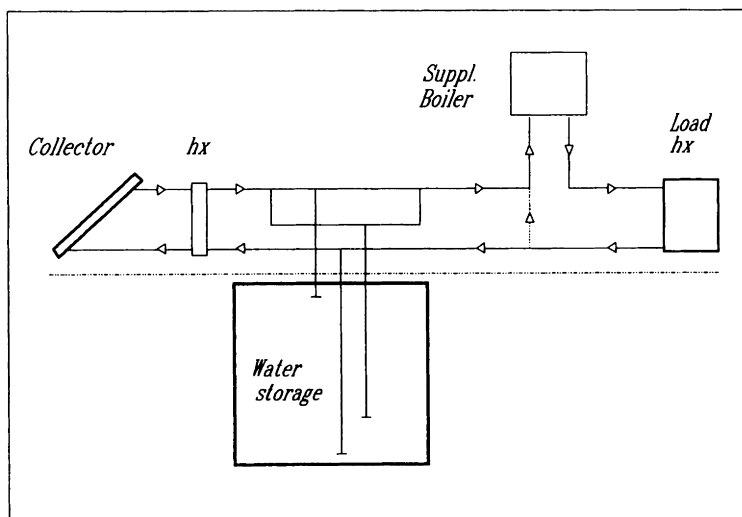


Fig. 3. Särö - System schematic diagram.

The system in Särö has been in operation with a short-term storage tank (boiler buffer storage) since autumn 1989 and the seasonal storage was put into operation in May 1990. The plant is controlled using a few conventional and simple thermostat control units.

## THERMAL PERFORMANCE

### System Rating

Previous evaluations of solar heating systems with seasonal storage have resulted in some general guide-lines concerning the rating of these systems (Dalenbäck, 1988a and 1990). A desirable solar fraction of around 70 % requires about 2.5 m<sup>2</sup> of collectors per MWh annual load and about 2.5 m<sup>3</sup> of water volume per m<sup>2</sup> of collector area.

### The Särö Project

Thermal performance calculations for the Särö plant were carried out at an early stage. The calculations were made with the simulation program SUNSYST (Gräslund, 1986). Simulations were made for an average climatic year and an estimated annual heat load of about 400 MWh. 800 m<sup>2</sup> of roof-integrated collectors (with convection barrier) and a 1 400 m<sup>3</sup> water heat store were expected to give a desirable solar fraction of the order of 65 %.

The actual built plant consists of 800 m<sup>2</sup> of collectors but the volume of the water heat store is only 700 m<sup>3</sup>. This gives about 2.1 m<sup>2</sup> of collector area in relation to MWh of annual load. Furthermore, the storage volume is less than 1 m<sup>3</sup> per m<sup>2</sup> of collector area, due to the R&D characteristics of the project, which followingly will result in a lower solar fraction close to 40 %.

The performance with the actual sizing will be calculated with the simulation model SIMSYS, as well as TRNSYS, in connection to the evaluation of the plant. A preliminar estimation of the performance is shown in Fig. 4.

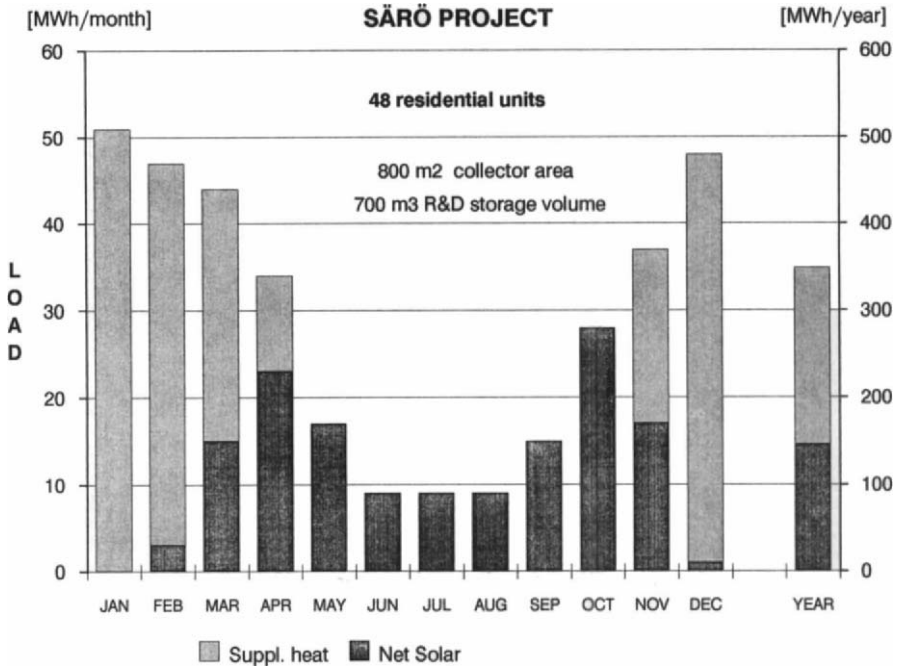


Fig. 4. Särö - Preliminar simulated thermal performance with actual R&D storage volume.

**DISCUSSION**

The main scope of this project is to gain experience from the new seasonal storage design. The final design is based on conventional technologies to a large extent. An estimated investment cost, based on construction experience in Särö, is around 900 SEK/m<sup>3</sup> for a storage volume of the order of 2 000 m<sup>3</sup>. This cost is less than the investment cost for a conventional insulated steel tank, and there are great possibilities to reduce this cost by a careful commission of a new larger storage. This storage design is, furthermore, also possible to use in an ordinary pit design in ground.

## REFERENCES

- Dalenbäck, J-O. (1988a). *Large-scale Swedish Solar Heating Technology - System Design and Rating*. Document no D6:1988, Swedish Council for Building Research, Stockholm. (National report, Task VII, IEA SH&CP).
- Dalenbäck, J-O. (1988b). *The Swedish Pilot Plant Kronhjorten - Description and some Experiences from Design and Construction*. Report no 1988:2, Dept. of Building Services Engineering, Chalmers University of Technology, Göteborg.
- Dalenbäck, J-O. (1990). *Central Solar Heating Plants with Seasonal Storages - Status Report*. Document no D14:1990, Swedish Council for Building Research, Stockholm. (Final report, Task VII, IEA SH&CP).
- Gräslund, J (1988). *Solar Heating with Seasonal Storage in a Residential Building Area in Särö*. Report no R16:1988, Swedish Council for Building Research, Stockholm. (In Swedish)

## SOLAR DHW SYSTEM EVALUATION WITH F-CHART

Barbro Briheim, M Sc and Jan-Olof Dalenbäck, Lic Tech

Chalmers University of Technology  
Dept. of Building Services Engineering  
S-412 96 Göteborg, Sweden  
Phone: +46-31721153 Fax: +46-31721152

### ABSTRACT

Several solar heating systems with roof-integrated collectors have been installed in multifamily houses during the last five years in Sweden. The outstanding features of the systems are the flexibility and the large amount of conventional heating technology in the system design. Measured performance agrees with F-Chart calculations, and F-Chart could thus be used to estimate the performance of these systems in different locations. The performance for DHW systems in Göteborg, Sweden and Madison, U.S. are shown as an example.

### KEYWORDS

Solar heating, domestic hot water, measured performance, F-Chart.

### INTRODUCTION

The type of solar heating system described in this paper is the result of some years research and development on roof-integrated collectors in combination with a careful use of conventional heating technology. This system can be installed in new-built or existing multifamily houses, and it can be combined with many types of conventional heating such as oil, gas, electricity, wood-chips, etc. The reduction of conventional heating, under Swedish conditions, is about 10-40 % depending on design and characteristics of the load.

The evaluation of this type of system covers construction and performance documentation, validation of design methods using measured climate and actual load profiles, as well as, simple and realistic performance estimations for new systems. Design and measured performance for two systems, Åsa and Hammarkullen (Dalenbäck, 1987), and F-Chart calculations for the Åsa system (Dalenbäck, 1989) have been presented earlier. This paper includes mainly a presentation of F-Chart calculations for the Hammarkullen system.

## DESCRIPTION OF THE OVERALL SYSTEM

The system in Hammarkullen is designed to pre-heat domestic hot water (DHW) in two multifamily houses with about 400 flats. The south-facing roofs on the houses are covered with 1 527 m<sup>2</sup> (aperture area) of roof-integrated solar collectors at 24° inclination. The collector area is divided into four systems and each system incorporates a 20 m<sup>3</sup> water storage tank. Storage tanks and necessary equipment are placed in small rooms in connection to district heating sub-units in the cellars.

The installations were made in connection to a retrofit project in 1985. The main intention was to re-build the roofs from flat to inclined.

### Domestic hot water system

The DHW systems are connected to heat-exchangers of copper in the storage tanks. The water in the tanks are heated with the collectors, and the DHW heat-exchangers are connected so that the cold water supply inlet is in the bottom, where the collectors are connected. The hot water outlet is connected to district heating heat-exchangers for supplementary heating.

A very simple control system with conventional thermostats is used and the solar DHW system does not need any special supervision in comparison with a conventional heating system.

### Solar Collectors and Storage Tank.

The collectors consist of selective Sunstrip absorbers under a cover of acrylic. Insulation, absorbers and cover are mounted on the roof on top of a corrugated sheet of aluminium. The connecting pipes are also mounted on the top of the sheet. Propylene glycol is used as anti-freeze protection in the pressurized collector circuit.

A well insulated pressureless (atmospheric pressure) water tank is used as short-term storage. The tank is quadrangular and built of steel-sheets on site. The ratio between the width and the length can vary depending on the space available. Walls are put up on the open sides of the tank, when the construction of the tank is finished. Blocks of polyurethane are placed under the tank and the spaces between the tank, the roof and the walls are filled with about 20 cm spray-polyurethane, all to minimize cold bridges.

### Costs

The investment cost is about 2 000 SEK/m<sup>2</sup> (1 USD = 6.0 SEK, June 1990) including collectors, storage tank, control and overhead, which is promising low. The annual net collector yield is about 900 GJ/m<sup>2</sup> in a system with both space heating and DHW, solar fraction of around 20 %, and about 1 400 GJ/m<sup>2</sup> in a system providing pre-heated DHW, solar fraction of around 40 %, under Swedish conditions.

## THERMAL PERFORMANCE

The annual requirement for DHW in 100 flats was estimated to 1 030 GJ. System analysis and design studies for Hammarkullen were made with a simulation model called "SUNSYST" (Bernestål, et.al, 1985) and the contribution from the solar system was estimated to 480 GJ, which is 47 %.

Measured performance 1986-89

Measurements in Hammarkullen during 1986-89 show that the annual DHW load is twice as large as expected an average year. This is mainly due to the fact that the occupancy is higher than expected. The solar fraction is followingly lower then expected, about 30 % as an average. The solar yeild is as expected for the design load, which actually means that it is over estimated. Measured performance for unit no. 39 is shown as example (Fig. 1).

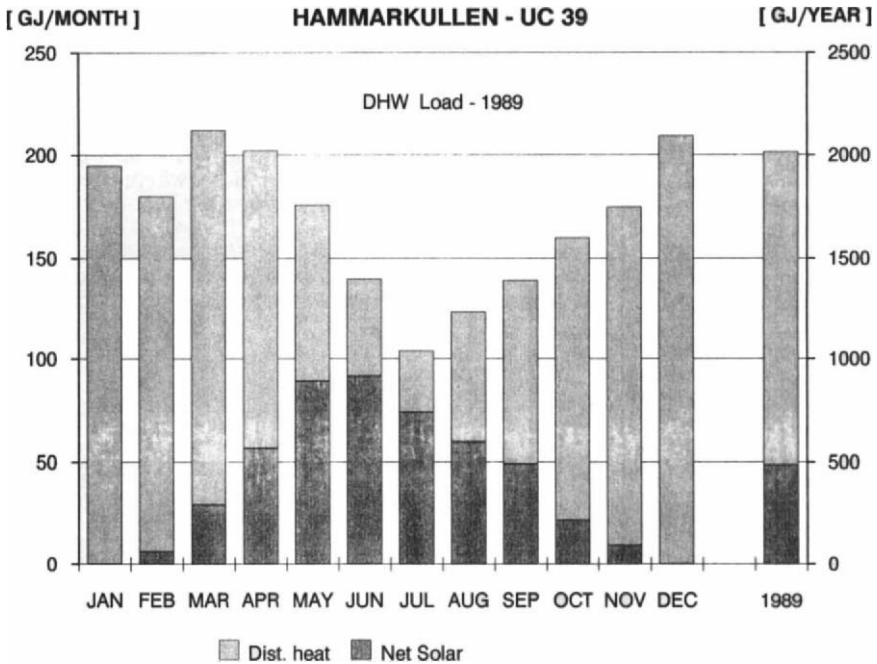


Fig. 1. Measured performance 1989, Hammarkullen no 39.

F-Chart calculations

The F-Chart program has then been used to calculate the performance, using average year load and climate. The parameters used in F-Chart were first calibrated to fit the measured performance during months that were regarded as average months. The result is that, even though the real system configuration differs from the system that F-Chart models, a good agreement was obtained. The calibrated parameters agrees with estimated parameters based on the measurements.

## DISCUSSION

The evaluation shows that F-Chart can be used to estimate the annual performance of this type of solar system with reasonable precision. To know or estimate the size of the load accurately is, however, very essential to make a proper rating of these systems. The performance of a solar system is very sensitive to a correct estimation of the load.

### Other designs, climates and load profiles

The evaluated systems are characterized by system  $F_R(\tau\alpha)$  of 0.7 and  $F_{R,U_L}$  of 5.0 ( $W/m^2,C$ ). Fig. 2. shows the calculated average solar fraction (based on the evaluation in Hammarkullen), as a function of system size, for a 2 000 GJ DHW load in Göteborg.

There is reason to believe that future systems will be improved to have the same  $F_R(\tau\alpha)$  and  $F_{R,U_L}$  of 3.0, by improving the selective properties of the absorber and adding a convection barrier (TPFE foil) in the collector. The result of such an improvement is shown in Fig. 2.

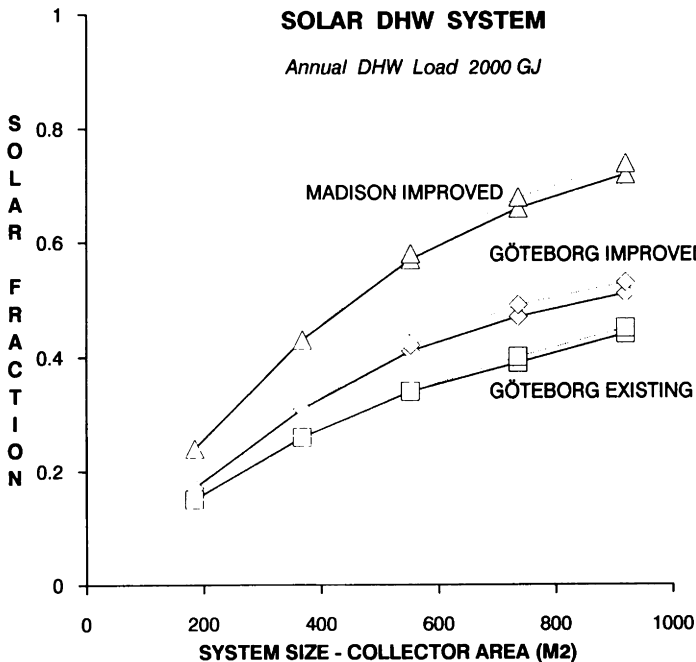


Fig. 2. Solar fraction as a function of system size for a DHW system. Hammarkullen load profile - straight lines, constant load profile - dotted lines.

There is further reason to believe that the annual DHW load profile would effect the performance of the system. Fig. 2. shows that the effect is rather small, assuming that the annual DHW load (in GJ) is the same. The comparison covers an existing load profile from Hammarkullen (similar to Fig. 1.) and a constant load profile.

Also shown in Fig. 2. is the improvement in performance going from a Swedish climate to the more sunny climate in Madison, USA. Taking economics into account gives an optimum solar fraction around 40 % for south Sweden and 65 % for Madison.

### F-Chart

The system parameters used have been validated with F-Chart, using measured monthly solar radiation, ambient temperature and loads, for a number of systems and years. Preliminary results for the Åsa and Hammarkullen systems are shown in Fig. 3. Åsa is designed for both space heating and DHW preparation and Hammarkullen for DHW preparation only.

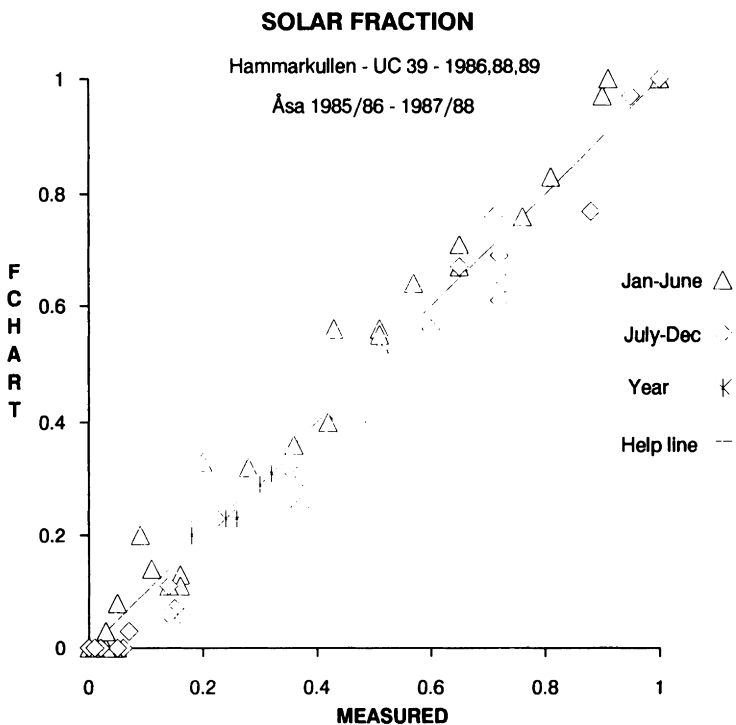


Fig. 3. Measured and calculated solar fractions in Hammarkullen and Åsa.

The comparison between F-Chart calculations and measurements is based on a monthly comparison of the solar fraction. One could imagine that this procedure would not



make sense, as F-Chart is based on average months and symmetrical days. However, the agreement is good except for some months with a large deviation from the average solar radiation.

There is however one cumbersome observation in almost all cases. F-Chart slightly overestimates the performance in the spring and underestimates it in the autumn. There is, so to speak, some hysteresis in the comparison.

One explanation could be that there is a difference between how F-Chart calculates solar radiation on a tilted surface and the real solar radiation on the collector. In that case F-Chart might include statistical parameters not exactly valid for the climate on the Swedish westcoast (Beckman et al, 1984). One thing that might confirm this observation is that there is the same difference between the designs (Bernestål et al, 1984 and Olsson, 1985), which are based on Swedish climate statistics, and F-Chart results.

The f-chart method was presented already in 1977 (Beckman et al, 1977). It is a simple method requiring only monthly average meteorological data which can be used to estimate the long-term thermal performance of solar heating systems as a function of the major system design parameters. This paper is based on calculations with the F-Chart program package (PC version 5.6), with the new  $\dot{U}$ ,f-chart method (Beckman et al, 1980).

## REFERENCES

- Beckman, W.A., S.A. Klein and J.A. Duffie (1977). *Solar Heating Design by the f-chart Method*. Published by Wiley-Interscience, USA.
- Beckman, W.A. and J.A. Duffie (1980). *Solar Engineering of Thermal Processes*. Wiley-Interscience, USA.
- Beckman, W.A., J.A. Duffie and B.L. Evans (1984). F-Chart in European Climates. *Proceedings of the First E.C. Conference on Solar Heating*, Amsterdam, April 30 - May 4, 1984, pp 161-165, D. Reidel Publishing Company, The Netherlands.
- Bernestål, B., G. Hultmark and S. Olsson (1984). *A Solar Heating System for Domestic Hot Water in Multifamily Houses (Hammarkullen)*. Swedish Council for Building Research, Report no. R192:1984, Stockholm. (In Swedish)
- Dalenbäck, J-O. (1987). *Solar Heating Systems for Multifamily Houses*. Dept. of Building Services Engineering, Chalmers University of Technology, Göteborg. (Paper submitted to ISES 87)
- Dalenbäck, J-O. (1989). *Solar Heating Systems for Multifamily Houses*. Dept. of Building Services Engineering, Chalmers University of Technology, Göteborg. (Paper submitted to ISES 89)
- F-CHART User's Manual. Microcomputer version. F-Chart Software, Middleton, Wisconsin 53562, USA.
- Olsson, S. (1985). *A Solar Heating System for Space Heating and Domestic Hot Water in Multifamily Houses (Åsa)*. Swedish Council for Building Research, Report no. R51:1985, Stockholm. (In Swedish)

# INVESTIGATIONS ON SOLAR DHW SYSTEMS COMBINED WITH AUXILIARY HEATERS

G.A.H. van Amerongen, P.W. Bergmeijer

TNO Institute of Applied Physics  
(Technisch Physische Dienst TNO-TU)  
P.O. Box 155, 2600 AD DELFT  
The Netherlands

## ABSTRACT

In the System Test Facility of TNO 7 combinations of SDHW's and auxiliary heaters are tested. The aim of this test was to investigate the interaction between SDHW and auxiliary heater (AH) and to estimate the yearly energy saving potential of each combination. In close co-operation with 2 manufacturer system combinations were installed and prior to the actual test all control systems were checked and in some cases improved. It turned out that most combinations performed less good as expected. The main reasons were found in avoidable heat losses, rather high tapwater outlet temperatures and moderate efficiency of the AH.

## KEYWORDS

Solar domestic hot water systems; auxiliary heaters; dynamic performance testing; control systems.

## INTRODUCTION

During the stage of development most Dutch SDHW systems are indoor tested using solar simulator of TNO. The applied test procedure results in the main parameters of the concerned system. This information for the manufacturers gives necessary feedback to their development activities. However, to estimate the solar contribution of the SDHW or the yearly energy saving an indoor test is not sufficient. In order to determine these values the dynamic outdoor behaviour of the total combination SDHW and AH has to be investigated. Up till now experimental results about several possible combinations were lacking. For that reason a side by side test of 7 SDHW/AH combinations is performed. The combinations were choosen to be typical for the Dutch market. This was realized by inviting both installers and utilities -involved in renting out SDHW systems to users- to propose the combinations to be tested. This involvement of market parties increases the applicability in practice of the results and promotes the tranfer of knowledge about solar systems.

Therefore the test aimed at a more broad set of results than merely the dynamic behaviour of the combinations. The following aims were defined:

- the technical realization of the SDHW/AH systems;
- the detection of failures;
- the evaluation of the control systems;
- the prediction of the energy saving.

## THE INVESTIGATED SYSTEMS

Based on the information from installers and utilities 7 combinations were selected. The combinations can be divided into two groups. In the first type of system combinations the SDHW acts as a separate preheater. Figure 1. shows the schematic outline of this type of combinations. For all systems in this group a gas auxiliary heater is applied. This heater is either a combined central space and tapwater heater or a geyser.

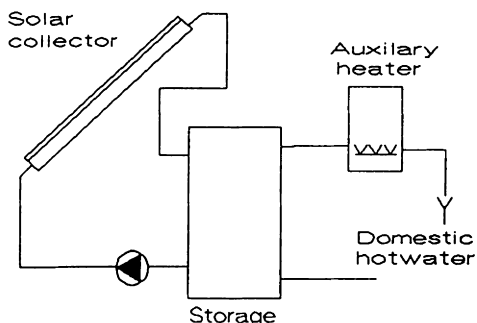


Figure 1. Preheater type

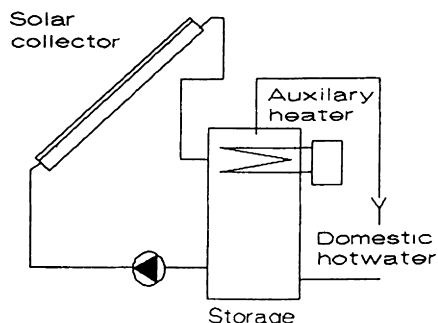


Figure 2. Integrated type

The second group is formed by SDHW systems which included a so-called hot-top. This integrated type of systems is outlined in figure 2. The hot-top is either heated electrical or gas central heated. In table 1 the combinations are summarized.

Table 1 Tested SDHW/AH combinations

comb. no	comb. type	type of SDHW	type of AH
1	preheater	1 <sup>1</sup>	comb. central/tapwater
2	preheater	2 <sup>2</sup>	comb. central/tapwater
3	preheater	2	geyser
4	integrated	1	central heater
5	integrated	2	central heater
6	integrated	1	electrical heater <sup>3</sup>
7	integrated	1	electrical heater <sup>4</sup>

(1) collector area 2.6 m<sup>2</sup>; mantel heatexchanger in primary circuit; solar storage 120 l.

(2) collector area 2.5 m<sup>2</sup>; helix heatexchanger in primary circuit; solar storage 100 l.

(3) switched on during night rate; hot-top setpoint 85°C

(4) hot-top setpoint 65°C; used also day rate electricity if hot-top temperature falls below 40°C

## EXPERIMENTAL SET-UP

The installers of type 1 and 2 SDHW systems were invited to install the 7 combinations in the System Test Facility of TNO. An additional reference system consisting of a central heater combined to a tapwater storage of 80 litres was installed as well. All combinations were equipped with sensors for the measurement of temperatures, flows and control signals.

From all systems hot water was automatically tapped 5 times a day by withdrawing each time 4.6 MJ. So the total daily tapwater draw-off corresponded to 23 MJ being the equivalent of heating 110 litres of water from 15°C to 65°C. The withdrawal of a fixed amount of heat instead of a fixed amount of hot water is in our point of view a more realistic simulation of the use in practice. Moreover in this way the interaction between SDHW and AH will effect the systems energy consumption and gives therefore information about the best combinations. The experiment was carried on during 4 weeks.

## RESULTS

### Technical realization

In general the technical realization of the systems were judged as good. However, it was observed that most systems would suffer from avoidable heat losses. In many cases connections to the hot-top were rather poor insulated as well as the hot-top itself. Moreover it was recommended to the manufacturers to replace the hot water outlets from the top of the storage to those storage regions which have lower mean temperatures.

### Failures

During 4 weeks in wintertime all systems were turned off. After starting up the systems again 3 collectorpumps from SDHW type 1 did not function properly. This may be caused by calcereous deposits due to occasionally filling up the primary circuit from which water can evaporate. This may be a weak point in the design of the drain-down system of this SDHW.

Although only a simple action was needed to bring the pump into operation again, users in practice possibly would not notice this failure immediately. Other failures were not observed during the test period.

### Control systems

Prior to and during the test period the actions of the control systems were monitored and compared to the specified performance. In the first place the tapwater outlet temperatures of the combinations were investigated. It turned out that all systems with a gas central heater produced outlet temperatures in the range of 60°C and 70°C. Although this temperature level is preferable with respect to comfort aspects, a decrease of 10°C would significantly increase the solar contribution.

The combination with the geyser auxiliary produced tapwater with a temperature of 55°C.

For the electrical heated hot-top systems a rather high temperature setpoint is necessary because night rate electricity is used and the heating power of the heaters are limited.

A second point of interest is the number of heating cycles of the gas auxiliaries to heat the hot-top. Theoretically this number has to be lower or equal to the number of tap-water withdrawals. However, for both the mentioned hot-top systems and the reference storage system a daily mean number of 8 cycles was examined. This will have a negative influence on the burner efficiency.

More extensively the temperature difference controllers of the SDHW systems were investigated. It was observed that the controllers of the two SDHW systems showed a completely different behaviour. The controller of type 1 switched on and off the pump too frequently, while in contrary the one of type 2 switched too less. In order to determine the causes of this behaviour the accuracy of both the hardware of the controllers and the measuring method was analysed.

It was concluded that from the two controllers both the device and the sensors showed a satisfying accuracy. However, the measuring method e.g. the place and connection of the sensors, introduced big discrepancies between the actual temperature differences of inlet and outlet of the collector and measured differences by the controller. Prior to test period a number of recommendations to improve the controller actions were implemented in the systems by the manufacturers.

### Energy saving

The measured data from the 7 SDHW/AH combinations was evaluated with help of the STF-method which is developed by TNO (De Geus, 1987). This resulted in typical characteristics for the several components and the total SDHW systems. These characteristics describe efficiencies for dynamic operation conditions as a function of the dimensionless climatological parameter  $Q_{sun}/Q_{load}$ . The efficiencies of the auxiliaries were determined as a function of the daily contribution to the tapwater heating.

Based on these general characteristics yearly energy consumptions were estimated for all 7 combinations. More interesting however would be to know what amount of energy can be saved by the several combinations. To determine those energy savings the definition of reference energy consumptions is required. These references were defined as follows:

- the preheater types have to be compared to the energy consumption of the most efficient combined central and tapwater gas heater.
- the integrated types using a gas auxiliary have to be compared to the above-mentioned reference system (central heater-storage combination)
- the integrated types using electricity for heating the hot-top have to be compared to the well-known electrical storage heaters.

The derived yearly energy saving figures are summarized in table 2.

Table 2 Reference yearly energy consumption and energy saving for the 7 tested combinations.

comb. no	type of SDHW	ref. energy consumption (m <sup>3</sup> natural gas) (kWh-e)	energy saving (%)
1	1	380	43
2	2	380	41
3	2	380	31
4	1	422	39
5	2	422	23
6	1	2565	39
7	1	2565	51

From these results the following conclusions were drawn.

- The reached energy saving by the combinations were lower than an expected value of 50% based on model calculations.
- The preheater types performed better than the integrated types. The main reason was found in avoidable losses from the hot-top. The difference in energy saving of the combinations 6 (hot-top temperature 85°C) and 7 (65°C) proves this effect.
- The combinations proposed and installed by manufacturer 1 showed in general a better performance than the combinations of 2. This is caused by a somewhat bigger collector area, a better collector efficiency and a bigger solar storage.
- The extremely low performance of combination 5 was due to the low-flow in the primary circuit without optimizing the collector and heatexchanger for such a flow.

#### GENERAL CONCLUSIONS AND RECOMMENDATIONS

This investigation showed clearly that the actual energy saving of a SDHW heavily depend on the performance of the total combination of SDHW and auxiliary heater. Experiments under dynamic conditions for both irradiance and tapwater withdrawal are necessary to investigate the interaction between SDHW and auxiliary heater and to check the control systems.

In order to market reliable combinations with an optimized energy saving potential the following recommendations has to be taken into account by the manufactures and installers.

- Improve insulation in particular for the integrated types.
- Install in SDHW system 1 a system to detect pump failure or redesign the primary circuit to avoid calcereous deposit.
- Choose a lower tapwater outlet temperature in order to maximize the solar contribution.
- Improve the auxiliary control for hot-top heating in order to minimize the number of burner cycles.

- Improve the accuracy of the pump control systems or replace existing types by irradiance-level controllers.
- Improve the general performance of SDHW system 2.
- With respect to optimized energy saving install combinations of the preheater type using gas auxiliaries with a high performance, electronic ignition and a tapwater outlet temperature of 55°C.

## REFERENCES

De Geus, A.C. (1987); An evaluation method for Solar Energy Systems monitored in the TPD System Testfacility, ISES Congres 1987, Hamburg, West Germany.

OBTAINING OF METALLIC AMORPHOUS MATERIALS  
USING CONCENTRATED SOLAR ENERGY

LITVINENKO Yury M. and PASICHNY Vladislav V.

Institute of Materials Science of Academy of  
Sciences of the Ukrainian SSR; 3, Krzhizhanovsky  
str., Kiev-252180, USSR

ABSTRACT

The obtaining of metallic amorphous ribbons by method of spinning with using of concentrated solar energy are described.

KEYWORDS

Solar energy, metallic amorphous materials, spinning.

Metal-amorphous materials are used in the field of electric energy conversion, in techniques of magnetic and video recording, electromagnetic protection and as corrosion-proof and radioresistant materials as well.

A gradual transition is observed in the research of metal-amorphous materials from the field of pure science to that of technology. The investigation is aimed at obtaining materials under certain conditions and in needed quantity to produce various classes of devices and articles. Fast quenching of liquid alloy is most commonly used of various methods for obtaining metal-amorphous materials. The technique consists in rapid transformation of a liquid jet to a thin layer on the metal surface and in the quenching of this layer at a speed of about  $10^6$  K/s mainly due to heat conduction.

The method of spinning based on pouring out a jet of melted alloy onto the outer cylindrical surface of a disk revolving around a horizontal axis is among the simplest and most productive ones. The technique is used to produce metal amorphous strips 1-2 to 100 mm wide (Davis, 1983). The output of such devices is determined by the strip production speed reaching a few kilometers per minute (Polk et al., 1984).



The disk rotational speed is 3-20 ths revs/min. The disk (its diameter being 200-400 mm) is usually made of a high heat-conductive material, copper for example. To obtain a better contact between the quenched melt and the disk cylindrical surface the latter is polished. Water cooling is used to increase the disk heat capacity. The liquid alloy cooling speed is  $10^6$  K/s.

The technique may be used to produce soft magnetic, hard magnetic, corrosion-proof and other materials in the form of a strip. Usually an inductor supplied with a high-frequency powerful generator is used as a heating source. But when laboratory research needs a small amount of metal-amorphous material, the use of such sources is doubtful. The authors succeeded in applying a combination of the device for spinning and heating plants utilizing arc xenon lamps and the Sun.

Solar heating had been used before to obtain certain oxide systems in a metastable condition (Asimov et al., 1983, Lopato et al., 1981, Rewcolevschi et al., 1975). The mechanical part of the device was based on the "hammer and anvil" principle where the liquid alloy drop was flattened between two heat-conducting surfaces. The work of this low-productive device resulted in a thin oxide film of heterogeneous structure with amorphous and crystalline phases available simultaneously. Application of the spinning method to obtain metal-amorphous materials under solar heating is one more step on the way of effective utilization of solar energy in the amorphous material production process.

Main production operations were studied under laboratory conditions in the "Uran-1" unit. When working with radiant heating sources under earth conditions principal difficulties consist in spatial arrangement of the system components where it is necessary first of all to take into account the direction of gravity which determines to a considerable extent the direction of the poured out jet, on the one hand, and the mirror heater elements forming a high-density radiant energy region around the focus, on the other. When heated by xenon lamps and the Sun the starting material was in a one-side soldered quartz tube with the outside diameter up to 10 mm and wall thickness about 1 mm. In the soldered bottom there was an orifice 1-2 mm in diameter. The melting point of the used FeCoNiSiB and FeCoSiB alloys is not higher than 1473 K, therefore their melting did not destruct the transparent quartz container. The liquid alloy was blown out by argon under a pressure of 20 kPa onto the disk cylindrical surface.

The mirror parabolic concentrator with a 1500 mm diameter, 650 mm focal distance and a focal spot of 6 mm in diameter was used for heating the alloys by solar radiant energy. Inside the paraboloid there was a fixed motor for rotating the aluminium disk to 100 mm in diameter by means of a direct current source placed on an external turning platform. The disk polished cylindrical surface to 15 mm wide was water-cooled from within. The disk rotation speed was not higher than 3000 revs/min. The quartz tube with the starting alloy was

fixed perpendicularly to the disk cylindrical surface in such a position that the lower part of the tube and its butt end with the orifice fell within the region of the focal spot.

The starting FeCoNiSiB and FeCoSiB alloys were melted for 1-2 min and blown out by argon under a pressure up to 20 kPa. The solar plant operated in an automatic regime of the Sun tracking, that was responsible for stability of heating.

Strips 1 mm wide and to 50  $\mu$ m thick were obtained. They were exposed to a differential thermal analysis. During isochronal heating in vacuum at a rate of 5 K/min the released heat corresponding to the transition to a crystalline state within a 831-868 K range was observed. It is close to the corresponding values for commercial metal-amorphous strips of the same composition. X-ray diffraction analysis of the obtained strips was made in CrK radiation. The starting alloy in a crystalline state was used as a primary standard. The diffraction patterns showed the absence of a crystal phase in the obtained strips.

The suggested techniques for production of metal-amorphous materials by means of concentrated solar energy are more advantageous economically as compared with the routine ones based on a more expensive induction heating. The advantages are especially effective for the Earth regions where there are many sunny days in a year and for outer space.

The one-step process for production of strips from melts has technological advantages. The spinning device with the solar energy concentrator will permit obtaining metal-amorphous materials from melts of systems containing refractory metals and metals with high affinity for oxygen. Servo systems can maintain the continuity of heating for the crucible with the starting alloy. The form of the directed pouring out jet and the melt pouring out itself with the gravity absent will be provided by a small pressure of the inert gas in a closed crucible. In this case there will be no gas loss. The poured out jet does not practically produce a braking effect on the rotating disk, therefore a powerful motor is not needed. The use of solar energy for rotating the disk makes it possible to create a self-contained production process for metallic and metal-amorphous materials in the form of strips. The obtained materials may be used right away for scientific-and-technological research and practical purposes.

#### REFERENCES

- Azimov S.A., G.T.Adylov et al. (1983). Sverkhostraya zakalka vysokotemperaturnykh materialov v usloviyakh luchistogo nagreva. In: Ispolzovanie Solntsa i drugikh istochnikov luchistoy energii v materialovedenii. pp. 183-187. Naukova dumka, Kiev.
- Davis, H.A. (1983). Methods of rapidly quenching. In: Bystrozakalennyye metally (B.Cantor, Ed.). pp. 11-30. Metallurgiya, Moskva.

- Lopato L.M., A.V.Shevchenko et al. (1981). DAN USSR, Ser. A., 7, 80-83.
- Polk, D.E. and B.C.Giessen (1984). Application of metallic glasses. In: Metallicheskie stekla (J.J.Gilman and H.J.Leamy, Ed) pp. 12-39. Metallurgya, Moskva.
- Rewcolevschi N., A.Rousnet., F.Sibieude (1975). Techniques of ultrafast quenching (splat cooling) for refractory oxides. High Temperature - High Pressure, 7, 209-214.

PROSPECTS OF A SOLAR COMMUNITY FOR REDUCING  
ENVIRONMENTAL DAMAGE AND SAVING FOSSIL FUELS

AGHAREED M. TAYEB

Faculty of Engineering, El-Minia University  
El-Minia , Egypt

ABSTRACT

The huge increases in oil prices since 1973 virtually guarantee that the major portion of the world will never drive most of its energy from petroleum . Thus, new energy sources should be widely sought as replacements for conventional ones. Added to this are the fastly growing problems of environmental pollution and lastly the up-to date problem of the ozone layer. Thus, new energy sources will act as a two-blades weapon both for satisfying the increasing human energy demands and for minimizing the environmental pollution. Putting in mind that the human being is the main constituent of any community his vital requirements to survive are studied. These requirements are food, housing and transportation. Next, an attempt is made to satisfy these requirements partially or totally by solar energy. This is illustrated through a flow diagram describing both the energy requirements and the suitable ways to satisfy it .

KEYWORDS

Solar energy, environment, fossil fuels, energy requirements

INTRODUCTION

Fuel and electricity prices, already at record highs, are seen to double again in the next few years (Smith and Fazzolare , 1980). Thus, energy conservation offers a way to significantly reduce facility operating costs.

One way of energy conservation is changing to other energy modes. New technology is available for many industrial processes , for heating and cooling buildings, for lighting and

agriculture . New technology is urgently needed for energy efficient transportation. Unresolved are the issues of how best to educate and inform the public, especially in the Third World, and to install new values appropriate for the future.

The solar community is a new community suggested such that most of its energy requirements can be fulfilled by solar energy. Therefore the main considerations taken into account have been to meet all the energy needs of the community through locally available, renewable and non-polluting sources.

#### HUMAN SURVIVAL REQUIREMENTS AND MODES OF SOLAR ENERGY UTILIZATION IN EACH

specially speaking, the basic requirements of a human being are food, housing and transportation. Modes of utilizing solar energy in each of these requirements are studied in detail and are illustrated in Fig. 1.

##### 1. Food:

The food required for human beings may be of plant origin or of animal origin.

Food of Plant Origin: In a highly populated world, practical ways of sanitarily preserving foods would be welcomed, yet especially in the last 20 years, the charges for fossil fuels and the prospect of depletion and scarcity of these fuels have drawn interests back to solar drying instead of such large scale, energy consuming systems. Besides obtaining clean solar-dried products, there exists large resemblance with natural drying in taste, appearance, and odour which are important factors in marketing and selling the products. Different designs for solar driers were developed by the author ( Tayeb 81, 82, 83a, 86, 83b ). Among these designs are:

1. Solar cabinet dryer
2. Solar collector dryer
3. Mixed mode dryer
4. Rotary solar dryer, and
5. Solar fluidization dryer.

The first three designs were used for drying grape, fig, apricot, apple, carrot, potato, onion, garlic, tomato, parsley and spinach. The last two designs were used for drying different grains, sesame and peanut.

Food Processing: The next competitive technique that follows drying is food processing through canning, sterilization or others. The most important supply for these processes is hot water up to 70° which can easily be obtained from solar water heaters.

Solar Water Heaters: Are known to be the least polluting and less expensive way of heating water. It can supply hot water both for industrial processing steps and for domestic uses.

Green Houses: To guarantee a more or less self sufficient solar community with respect to food requirements, green houses are introduced into agriculture. It has been found that using this

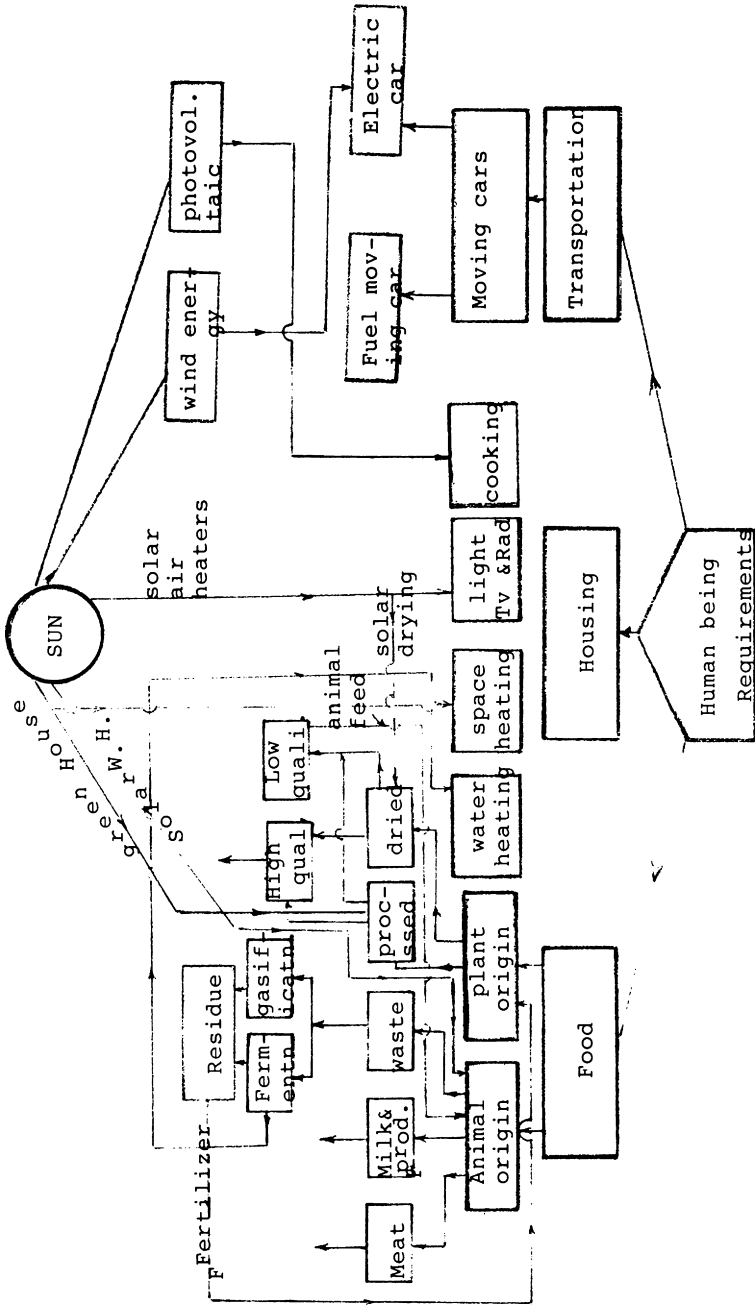


Fig. 1 Human Survival Requirements and Modes of Solar Energy Utilization in Each

technique in agriculture could increase the production of cucumbers and tomatoes five folds( Perera 1980 ).

Food from Animals: A suitable number of animals, cows, buffalows and chips could be grown up in the present solar community. These animals would supply the necessary requirements of meat and milk and its products. The food required for these animals may be fresh or as dried feed. The dried feed can be got from one of these sources after some additions:

1. Scraps from drying fruits and vegetables
2. Wet vegetable wastes from canning and other processes, and
3. Reject material from sorting machines in a drying or canning plant .

Bio-Fuels: When growing up animals, their refuse are not thrown away. It is digested to produce methane and/or ethanol to be used as a source of energy for domestic purposes and transportation. The residual sludge from the fermentation process is used directly as a rich fertilizer for plants.

## 2. Housing:

House equipment such as refrigerators, T.Vs, radios, water heaters, lighting means, cookers and stoves are all necessary. These equipment need a high portion of energy and if it can be operated by another source of energy other than the electric energy, it would be a good achievement.

Warmth: Solar water heaters and solar air heaters can supply a hot fluid which could be circulated in tubes through the house to provide a comfortable environment.

Lighting: photovoltaic cells could be used to provide the electric energy required for lighting houses.

Water Heating: Water heating for domestic uses is easily accomplished through solar water heaters.

Cooking: A wide range of design varieties for solar cookers have been known. Related to cooking is refrigeration to preserve the cooked or even uncooked food for time of use. A solar powered refrigerator( Sun World 1980) has been used for this purpose.

## 3. Transportation :

The most common facility for transportation in any community is cars which can be solar augmented to be suitable for use in the suggested solar community. Three types of fuels, other than the conventional ones, could be used for moving cars and all of which originated from solar energy. These fuels are electricity, wind power and methanol.

The electrically-driven car( Fujinaka 1986) works by secondary batteries which have been previously charged from photovoltaic cells. A less attractive alternate is to mount the photovoltaic cell panel on top of the car. The wind-driven car(El-Bassuoni

and Tayeb 1986) uses the kinetic energy of a moving air stream to rotate a wind turbine fixed over the roof of a moving car. A suitable generator can be coupled with the wind turbine to generate the electricity required for driving the car. The alcohol-driven car ( Acioli 1982) moves by burning ethanol in its engine in the presence of  $O_2$  . The ethanol is obtained as a fermentation product of the animal refuse in the present solar community. Either blended with gasoline or pure, alcohol offers advantages over gasoline as an automotive fuel.

### CONCLUSION

1. The basic concept of the solar community evolved out of the need to promote change from energy dependence to energy autonomy, from external control to self-reliance, from electrification to energisation, from inequitable to equitable distribution and above all from non-renewable to renewable energy sources. Therefore the main considerations taken into account have been to see that all the energy needs of the community are met through locally available, renewable and non-polluting sources.
2. It is not enough that the energy source be available, the technology to put it to use must also be available.
3. Solar energy is the most important renewable energy source and it can supply energy by means of : solar water heaters, air heaters, photovoltaic cells, wind-powered machines and methanol production.
4. Matching energy resources, energy needs and devices to be used has to be planned carefully to ensure techno-economic viability and social acceptability in the long run.
5. A limited community could be almost completely powered by solar energy through simple and non-expensive devices.

### REFERENCES

- Acioli, J.D. The Alcohol Fueled Program of Brazil. Sun World 6, No.2, p.39, 1982.
- El-Bassuoni, A.A. and Tayeb, A.M.(1986). Non-Conventional Energy Sources for Automobile Application. Proceedings Intl. Conf. on the Development of Alternative Energy Sources and the Lessons Learned since the Oil Embargo, North Dakota, USA.
- Fazzolare, R.A. et. al.(1980). Changing Energy Use Future. Energy Conv. & Management, 20, p.219.
- Fujinaka, M.(1986) The Solar Electric Car. Sun World, 10, No.3
- Perera, J.(1980). Arabs Turn Their Eyes to the Sun. New Scientist, Feb.
- The Solar Powered Refrigerator(1980). Sun World, 4, No.5, p.161.



Tayeb, A.M.(1981). Investigation of a New Drying Unit for drying Different Agricultural Products Using Solar Energy. Ph.D.Thesis, El-Minia University, Egypt.

Tayeb, A.M. et.al. (1982). Solar Fruit Drying in Egypt. Progress in Solar Energy, ASES.

Tayeb, A.M. and Veziroglu, T.N.(1983). A Solar Collector Dryer. Alternative Energy Sources V,Part A , Elsevier Science Publishers .

Tayeb, A.M. Modern Solar Grain Dryer . J. Solar & Wind Technology, vol.3, No.3, pp.211-214 (1986).

Tayeb, A.M. (1983), Solar Fluidisation Drying. Proceedings, 6th. Miami Intl. Conf. on Alternative Energy Sources, Miami, Florida , USA.

PC-PROGRAMMES  
FOR  
SOLAR HEATING SYSTEMS

J.E. NIELSEN

Solar Energy Lab., Dept. of Energy Technology, Danish Technological Institute,  
P.O. Box 141, DK-2630 Taastrup, Denmark

ABSTRACT

Several user-friendly PC-programmes for solar heating systems have been developed. Manufacturers and designers are using them for optimizing components and systems. Following programs are available:

- DIMSOL : Design of collectors.
- FLOWSOL : Calculation of pressure conditions and flow distribution in collectors and systems.
- DISTSOL : Design of systems for district heating.
- POOLSOL : Design of systems for pool heating.

KEYWORDS

PC-programmes, design of collectors, design of solar heating systems, district heating, pool heating.

INTRODUCTION

Based on fundings from the Danish Ministry of Energy and the Ministry of Industry a package of user-friendly design tools (PC-programmes) for the solar industry has been developed by the Solar Energy Lab. These programmes are now widely used by manufacturers and system designers in the proces of optimizing components and systems.

## DESIGN OF COLLECTORS - DIMSOL

The DIMSOL programme calculates the efficiency of a solar collector based on a very detailed description of the collector construction. On the top of this calculation different built-in simplified system calculations can be used, so it is possible directly to evaluate the influence of the collector construction on the system performance.

The collector is described with data of the cover (if any), the absorber and the insulation. Also information on the slope, flow, wind, irradiation, outside temperature etc. must be given. While giving data to the program an online help is given with explanation and examples of the actual parameter. When all the data is given it is possible to get a cross section of the collector to check the geometry.

The efficiency is calculated as a function of the difference between the mean collector fluid temperature and the outdoor temperature. This is done by calculating the efficiency at six different values of the just mentioned temperature difference and then approximate the results to a second order equation. Also stagnation temperatures in covers and absorber are printed out.

The programme gives you the opportunity to investigate the influence of a specific collector construction parameter on the collector efficiency. This is done very easily by specifying the interval of the parameter variation - the programme then gives you the corresponding variation of the constants in the second order equation for the efficiency. On this basis it is possible to detect critical values of the parameter.

Perhaps the strongest facility of the programme is the possibility to evaluate directly the influence of a change in the collector construction on the annual output of a system. The programme is supplied with simplified algorithms for calculation of the different solar systems types: Domestic hot water, combined domestic hot water and space heating and constant temperature systems. These systems are very simply described by collector size and system load. So, to evaluate the influence of a certain construction detail of the collector i.e. a collector parameter, an interval of this parameter is given to the programme and the programme will give out the variation of the annual output for the specified system and furthermore the necessary collector area to achieve the output of the reference system. It is then easy to compare the marginal overheads due to a change in construction to the corresponding higher system output or savings in collector area.

The program is very popular among the manufacturers of collectors.

Executing time of the program is very short: normally only a few seconds on an 80286 PC.

Calculations done by DIMSOL are compared with measured collector efficiencies with really good agreement.

## FLOW DISTRIBUTION - FLOWSOL

Determination of the flow distribution in and the pressure loss across a collector and an array of collectors is done by the programme FLOWSOL. Collector channels, tubes and/or pipes are to be described in the input data. On line help and guidelines for pressure loss across bendings, valves and other fittings are given.

In the programme there are three levels of calculation. 1) Collector (distribution in collector channels), 2) Section (distribution in collectors), 3) System (distribution in sections). To calculate a certain level, one has to calculate all the underlying levels first.

The results of the program are visualisation of the flow distribution, pressure drop as a function of the flowrate and the performance reduction due evt. bad flow distribution compared to ideal flow conditions.

General lessons learned by using this programme are:

- only extremely bad flowdistribution influences the collector output significantly
- reversed return-pipe is in many cases not necessary (as a consequence of the above)
- precise results of absolute values of pressure losses are hard to obtain due to uncertainties in inlets, outlets, branches, fittings etc., but the relative flowdistribution is less sensitive to these uncertainties.

The executing time is very dependent on the number of parallel channels to be calculated but is normally in the order of seconds on a 80286 PC.

## SOLAR SUPPLY TO DISTRICT HEATING - DISTSQL

Using the DISTSQL programme one is able to deal with three different combination of solar and district heating:

- central solar heating plant heating the return pipe from the district network
- central solar heating plant for summer heating
- individual solar domestic systems and stopping the network circulation in the summertime

The programme is not able to calculate systems with seasonal storage, only a simple storage model is included for short term storing.

Data on the network are very easily given by simply drawing on the screen a model of the pipes, consumers and producers. On this drawing one can directly write the values of diameters, insulation, annual consumption and so on. Max. 50 branching

points are allowed at the present moment. Solar system data are given in a special menu.

Calculations can be done hour by hour which gives the possibility to check for possible critical high temperatures in situations with high insolation and low load.

DISTSOL is validated with data from the Danish 1000 m<sup>2</sup> system in Saltum and the agreement between measured and calculated results was very good.

Among other things it has been learned from running this program that it could be critical to combine a solar heating plant with a district heating network with thermostat-controlled by-passes.

### POOL HEATING - POOLSOL

Solar systems for outdoor pool heating are rather simple but calculations of these systems are not as simple because of the sensitivity of the uncovered collectors and pools to wind conditions and radiation to the ambient. Estimation of evaporation losses from the pool is also uncertain. Using POOLSOL one can evaluate the influence of these conditions on the performance of the system. The programme simulates the solar system and the pool hour by hour and temperatures during the calculated period are plotted.

Using POOLSOL it is possible to design solar systems for pool heating and also to evaluate the influence of an insulated night cover on the pool. Also the eventually need for auxiliary power an energy can be determined.

POOLSOL is validated with data from a real system and it was shown that it is possible to obtain very reasonable estimates of the performance of such systems.

### LITERATURE

- Nielsen, J.E., Ravn, O. (1986), *Users Manual for DIMSOL*,  
Solar Energy Lab., Danish Technological Institute (in danish).  
Nielsen, J.E., Ravn, O. (1988), *Users Manual for FLOWSOL*,  
Solar Energy Lab., Danish Technological Institute (in danish).  
Nielsen, J.E., (1990), *Users Manual for DISTSOL*,  
Solar Energy Lab., Danish Technological Institute (in danish).  
Nielsen, J.E., Simonsen, J.-M.(1988), *Users Manual for DISTSOL*,  
Solar Energy Lab., Danish Technological Institute (in danish).

ON THE CORRELATIONS BETWEEN DIFFUSE  
AND GLOBAL DAILY SOLAR RADIATION

M. M. KENISARIN, N. P. TKACHENKOVA AND A. I. SHAFEEV

Thermophysical Department  
Uzbek SSR Academy of Sciences  
700135 Tashkent, USSR

ABSTRACT

The relationship between diffuse and global monthly average daily solar radiation on the base of 34 USSR meteorological stations data is investigated. The comparison statistical analysis of the developed and known correlations is given. The observation results of 20 meteorological stations in various parts of world were used as reference data.

KEYWORDS

Global and diffuse radiation, relationship, correlation comparison

INTRODUCTION

The designing of solar installations requires the determination of solar radiation incident on the plane of solar collector. Sloped solar collector receives direct, diffuse and reflect solar radiation. To calculate of total solar radiation it is necessary to know their components. The one of most values needed for determination of total radiation is the relationship between monthly average daily diffuse and global solar radiation incident on horizontal surface,  $H_d/H$ .

This relationship can be find from direct meteorological observation or on empirical relationship (Lui and Jordan, 1960; Klein, 1977; Page, 1961; Tuller, 1976; Iqbal, 1979; Collares - Pereira and Rabl, 1979; Modi and Sukhatme, 1979; Erbs *et al.*, 1982; Ma and Iqbal, 1984). All USSR meteorological stations which observe actinometric data record the global and diffuse radiation. Therefore for many Soviet locations easy to find the relationship  $H_d/H$ . However it is difficult to make it for other regions of world. For instance from 52 Canadian meteorological stations only 4 ones recorde the diffuse radiation (Iqbal, 1979). The similar situation there is in other parts of world also.

Taking into account the unique geographical location of the USSR and the large amount of meteorological stations the authors tried to establish the relationship between the diffuse and global radiation and compare the obtained regression with other known correlations.

### THE PRESENT CORRELATION

In present work the 34 USSR meteorological stations data were used. The location of these stations showed in Table 1. The each of these stations gives 12 monthly daily values

Table 1. Mean bias error and root mean square error of calculated values of the daily diffuse radiation from observed values

Location	Lat. °N	Long. °N	Obs. period	MBE	RMSE	RMSE, %
Petrozavodsk	61.8	34.2	1955-63	-0.007	0.068	-10.8
Sortvala	61.6	30.8	1955-63	0.018	0.070	10.8
Kargopol	61.5	38.2	1954-63	-0.011	0.075	-11.8
Leningrad	60.0	30.7	1953-63	-0.052	0.084	-13.2
Voekovo	60.0	32.0	1953-63	-0.009	0.064	-11.0
Volosovo	59.5	32.5	1954-63	-0.040	0.088	-14.5
Vologda	59.2	40.0	1953-58	0.022	0.081	12.7
Tartu	58.4	26.8	1953-64	0.025	0.068	11.2
Valdai	58.0	33.0	1954-63	0.028	0.073	11.3
Torzhok	57.1	35.0	1956-63	0.057	0.092	14.5
Riga	56.9	24.0	1953-63	-0.032	0.045	7.5
Toropez	56.6	31.8	1954-63	0.070	0.068	10.9
Kaunas	54.9	24.0	1955-63	0.028	0.065	10.4
Smolensk	54.5	32.4	1955-63	0.013	0.075	11.6
Minsk	53.8	27.5	1952-64	0.013	0.040	6.8
Kuibyshev	53.2	50.2	1954-63	-0.007	0.059	11.6
Saratov	51.6	44.2	1954-63	0.026	0.067	12.6
Kiev	50.5	30.5	1952-61	0.007	0.029	5.0
Volgograd	48.7	44.5	1954-63	-0.017	0.052	10.8
Kherson	46.6	32.6	1954-63	0.005	0.036	7.0
Astrakhan	46.3	48.0	1954-63	-0.048	0.064	14.8
Takhiatash	42.3	59.6	1954-63	0.000	0.037	10.2
Tashkent	41.3	69.6	1955-63	-0.078	0.083	24.3
Kara-Bogaz-Gol	41.0	52.9	1954-58	-0.013	0.051	13.5
Fergana	40.4	79.9	1955-63	0.026	0.044	10.4
Leninabad	40.2	69.6	1958-64	0.010	0.037	9.6
Samarkand	39.6	67.0	1957-63	-0.019	0.034	8.7
Yaskhan	39.6	55.8	1953-58	-0.003	0.028	7.6
Ak-Molla	39.4	60.5	1958-64	0.023	0.035	9.7
Chardjou	39.1	63.7	1954-63	0.013	0.034	10.0
Beki-Bent	39.1	50.5	1955-63	0.009	0.017	4.6
Dushanbe	38.6	68.6	1956-63	0.018	0.028	7.1
Ashkhabad	37.9	56.3	1954-63	-0.017	0.028	7.3
Termez	37,2	67.4	1955-63	0.004	0.030	8.4
<b>All stations</b>				<b>0.000</b>	<b>0.056</b>	<b>11.0</b>

of  $H_d/H$  and the relationship between the global and extra-terrestrial daily solar radiation incident on a horizontal surface,  $H/H_0$  or  $K_T$ . At the calculation of the  $K_T$  solar constant  $H_0$  is equal  $1367 \text{ W/m}^2$ .

The polynoms of first, second and third degrees for determination of correlation type were used. The cubic polynom given the minimal errors:

$$\frac{H_d}{H} = 1.191 - 1.783 K_T + 0.862 K_T^2 - 0.324 K_T^3 \quad (1)$$

$$\text{for } 0.15 < K_T < 0.80$$

The mean bias error (MBE) and the root mean square error (RMSE) for evaluation the obtained regression and statistical comparison of present result with other known correlations were used. The estimation of the MBE and RMSE was similar those which has been used by Ma and Iqbal (1984). The calculation results of the MBE and RMSE obtained at using of correlation (1) are presented in Table 1.

#### THE COMPARISON OF VARIOUS CORRELATIONS

For the first time Lui and Jordan (1960) developed a graphical relationship between  $H_d/H$  and  $K_T$ . This graphical relationship Klein (1977) expressed later algebraically as follows

$$H_d/H = 1.390 - 4.027 K_T + 5.531 K_T^2 - 3.108 K_T^3 \quad (2)$$

$$\text{for } 0.3 < K_T < 0.7$$

Page (1981), using data from ten meteorological stations located between  $40^\circ \text{N}$  and  $40^\circ \text{S}$  latitudes, recommended the linear equation:

$$H_d/H = 1.00 - 1.13 K_T \quad (3)$$

Tuller (1976), considered all four actinometric stations of Canada where necessary data are registered, suggested follow equation:

$$H_d/H = 0.84 - 0.62 K_T \quad (4)$$

Taking into account that the diffuse radiation observed on the Resolute station which located above Polar circle Iqbal (1979) excluded these data from consideration. Based on data from other southern Canadian stations he recommended linear equation:



$$H_d/H = 0.958 - 0.982 K_T \quad \text{for } 0.3 < K_T < 0.6 \quad (5)$$

Basing on data of five actinometric stations of the USA Collares- Pereira and Rabl (1976) suggested a equation whouse coefficient vary with season:

$$H_d/H = 0.775 + 0.347 (\pi/180) (\omega_s - 90^\circ) - 0.505 + 0.261 (\pi/180) (\omega_s - 90^\circ) \cos[2(K_T - 0.9)] \quad (6)$$

Modi and Sukhatme (1979) for 12 meteorological stations of India developed regression equation:

$$H_d/H = 1.4112 - 1.6956 K_T \quad \text{for } 0.34 \leq K_T \leq 0.73 \quad (7)$$

Erbs *et al.* (1982) considered data for four US stations which have been used by Collares-Pereira and Rabl recomended new equation:

$$H_d/H = 1.391 - 3.560 K_T + 4.189 K_T^2 + 2.137 K_T^3$$

for  $\omega_s \leq 80^\circ$  and  $0.3 \leq K_T \leq 0.8$

$$H_d/H = 1.311 - 3.022 K_T + 3.427 K_T^2 - 1.821 K_T^3 \quad (8)$$

for  $\omega_s > 80^\circ$  and  $0.3 \leq K_T \leq 0.8$

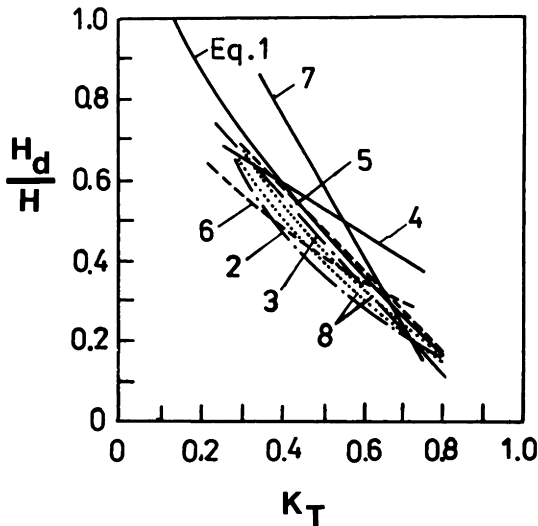


Fig.1. The various type of correlations for  $H_d/H$

So we have several correlations recommended by various investigators. The graphical representation of considered above correlations are given in Fig.1. As shown from this figure the character of this correlations vary different each other. Therefore it is interesting to carry out the statistical comparison of these correlations.

Similar comparison has been made by Erbs *et al.* (1982) and Iqbal (1979). It should be noted that in both works the amount of reference stations was less five. The reference stations included also the stations which have been used for developing of the considered correlations. In addition the amount of considered correlations was limited.

In present work the statistical investigation of known correlations was made on the base of data from 12 foreign and 10 soviet reference stations. Then only one station from ten soviet stations was used for developing the Eq. (1). In Table 2 the geographical location of reference stations is given. The used data are based on long term observations. The initial data have been took from (Erat *et al.*, 1982; Godoy *et al.*, 1982; Turrent *et al.*, 1982; Paltridge and Proctor, 1976; *Handbook*, 1966; Kenisarin *et al.*, 1990.). It should be noted that the

Table 2. Reference stations for statistical comparison of known correlations

Location	Latitude, °N	Longitude, °E
Luonetyarvi, Finland	62.42	25.67
Yakutsk, USSR	61.98	129.42
Kostroma, USSR	57.85	40.98
Moscow, USSR	55.30	39.30
Dublin, Ireland	55.43	6.25
Goose-Bay, Canada	53.30	60.45(*)
Irkutsk, USSR	52.23	104.27
De Bild, The Netherlands	52.20	5.12
Kew, England	51.47	0.30
Czelinograd, USSR	51.20	71.40
Trappes, France	48.77	2.01
Freiburg, FRG	48.00	7.18
Odessa, USSR	46.60	30.88
Montreal, Canada	45.50	73.61(*)
Toronto, Canada	43.80	79.55(*)
Vladivostok, USSR	43.68	132.17
Madison, USA	43.13	89.40(*)
Frunze, USSR	42.90	74.12
Fergana, USSR	40.40	71.77
Melbourne, Australia	37.80(**)	145.00

(\*) - West longitude; (\*\*) - South latitude

all calculation of considered correlation for Italian stations Torino and Crotone give overestimated values of diffuse

radiation in comparison with observed ones. These differences vary from 30 till 70%. We excluded on this reason from consideration these stations. In what follows all conclusions are based only on twenty stations' data.

The calculation show that the Lui-Jordan, Page, Colarres-Pereira and Rable, Erbs *et al.* equations give the underestimating values of diffuse radiation on all reference stations. Modi and Sukhatme equation gives in contrast the overestimating values. In respect to Lui-Jordan, Page, Collares- Pereira and Rabl, Erbs *et al.* equations our results agree with results of statistical analysis obtained by Ma and Iqbal (1984). The generalized results of comparison are presented in Table 3. More detail information about statistical analysis can be find in (Kenisarin *et al.*, 1990)

Table 3. Generalized results of comparison of the eighth correlations for estimating the monthly average daily diffuse radiation incident on a horizontal surface and obtained for twenty reference stations

Equation	MBE	RMSE
Lui and Jordan (2)	-0.107	0.132
Page (3)	-0.043	0.087
Tuller (4)	0.032	0.092
Iqbal (5)	-0.017	0.078
Collares-ereira and Rabl(6)	0.071	0.149
Modi and Sukhatme (7)	0.108	0.143
Erbs et al (8)	-0.056	0.099
Present work (1)	-0.001	0.075

### THE CONCLUSION

The present work shows that the equation (1) obtained on the base of 34 Soviet meteorological stations evenly describes the behaviour of  $H_d/H$  in all investigated latitude intervals. The root mean square error of the determination of diffuse radiation are varied from 11 to 15%. For latitudes less than  $50^\circ$  can be recommend Tuller equation, and for latitudes less than  $50^\circ$  - Iqbal equation. Eqs.(3), (6) and (8) for latitudes less  $50^\circ$  give the noncompensated remainder -0.025, -0.039 and -0.035 respectively. These remainders less than for all reference stations -0.045, -0.074 and -0.059. To use these equations for other regions in separate case it should be revised. Equiations of Lui & Jordan and Modi & Sukhatme it should be used only for those regions wich have beeb obtained for.

## REFERENCES

- Collares-Pereira M. and A. Rabl (1979), The average distribution of solar radiation - correlations between diffuse and hemispherical and between daily and hourly insolation values, *Solar Energy*, 22, 155-164
- Erat B., M. Niemi, O. Jussi (1982). *Energia - ja asunnsystävällinen Kerrostalo. Osa 2*, Valtion painatuskeskus, Helsinki (in Finish)
- Erbs D.G., S.A. Klein and J.A. Duffie (1982). Estimation of diffuse radiation fraction for hourly, daily and monthly - average global radiation, *Solar Energy*, 28, 293-302
- Godoy R., D. Turrent, R. Ferraro (1982), *Solar Space Heating: An Analysis of Design and Performance Data from 33 Systems* Brussels-Luxemburg, EUR 8004
- Handbook on USSR Climate* (1966). 1-34, pt.1, Leningrad
- Iqbal M. (1979). A study of Canadian diffuse and total solar radiation data 1. Monthly average daily horizontal radiation, *Solar Energy*, 22, 81-86
- Kenisarin M.M., N.P. Tkachenkova and A.I. Shafeev (1990). On relationship between diffuse and global solar radiation. *Gellotechnika*, to be published
- Klein S.A. (1977). Calculation of monthly average insolation on tilted surface, *Solar Energy*, 19, 325-329
- Lui B.Y.H. and R.C. Jordan (1960). The interrelationship and characteristic distribution of direct, diffuse and total solar radiation, *Solar Energy*, 4, 1-19
- Ma C.C.Y. and M. Iqbal (1984). Statistical comparison of solar radiation correlations. Monthly average global and diffuse radiation on horizontal surface, *Solar Energy*, 33, 143-148
- Modi V. and S.P. Sukhatme (1979). Estimation of daily total and diffuse insolation in India from weather data, *Solar Energy*, 22, 407-411
- Page J.K. (1961). The estimation of monthly mean values of daily total short wave radiation on vertical and inclined surfaces from sunshine records for latitudes 40°N - 40°S, *Proc. U.N. Conf. on New Sources of Energy*, Paper No. S98, 4, 378-390
- Paltridge G.W. and D. Proctor (1976). Monthly mean solar radiation statistics for Australia, *Solar Energy*, 18, 235-243
- Tuller S.E. (1976). The relationship between diffuse, total and extraterrestrial solar radiation, *Solar Energy*, 18, 259-263
- Turrent D., R. Godoy, R. Ferraro (1982). *Solar Water Heating: An Analysis of Design and Performance Data from 28 Systems*, Luxemburg, EUR 8003,

Design and Application of a Collector Test Facility  
Based on a Solar Simulator

Gunter Rockendorf

Institut für Solarenergieforschung (ISFH)  
Sokelantstr. 5  
3000 Hannover 1; FRG  
tel. 0511/35850-41

ABSTRACT

A solar simulator for the investigation of solar collectors and other solar thermal devices has been developed and is run by the ISFH. Some design details of the light source and the additional units are discussed. Experience with the operation and some results show, that the whole facility may serve as a tool for quick assessment and optimization of solar collectors.

KEYWORDS

Solar simulator; artificial sunlight; solar collector testing; flat plate collector; development and optimization of collectors

INTRODUCTION

The main meteorological values affecting the performance of a collector such as solar irradiation, wind velocity, ambient and sky temperature, show large fluctuations in Central Europe. For that reason collectors can only very seldom be operated in thermal steady-state conditions. Due to this outdoor-tests are very time-intensive and the respective results show a high scattering. However, this problem can be overcome with indoor-tests, using an artificial light source. The main advantage is the free, independent and reproducible setting of the meteorological parameters, which leads to a high reproducibility of the results. A more detailed thermal description of the collector, a quick assessment and an optimization is possible in this way.

An appropriate light source simulates the real conditions with respect to global intensity, spectral and angular distribution, high spatial uniformity and a low level of infrared-irradiance ( $> 3 \mu\text{m}$ ). Ambient temperature and wind velocity at the collector have to be kept constant.

## SIMULATOR DESIGN

The whole test facility consists of a light source, a thermal process unit for the heat transfer fluid, the measurement equipment and some auxiliary devices. The focus is directed towards the development of the low-IR-light-source with solar-similar properties.

### Selection of the lamps

Appropriate lamps should meet the following main criteria: a good approach to solar spectrum, a rather constricted beam and the possibility to design a light source with a high homogeneity in the receiver plane. Further criteria are the energetic efficiency, the durability and degradation, the possibility to adjust the intensity by voltage variations, cooling problems, weight and demand of space, allowed inclination angles and finally the operating costs and the price.

The chosen lamp is Philips type 13117, a halogen lamp with dichroic mirror and a nominal power of 150 watts at 17 volts. The small lamp units allow to design a light source with high uniformity and a narrow angular distribution. A suitable spectral distribution with low price are on the positive side, the problems are the rather low efficiency and the durability.

### Design of the lamp field

The angular radiation distribution of a single lamp was determined and by means of a computer program the irradiance distribution in the receiver-field (i.e. the test-plane), caused by a certain number of lamps in the lamp field, was calculated. After some iterations the number and the positions of the lamps to achieve the needed irradiance level were found. Here a rectangular grid with variable intervals was found to be optimal.

More than 85% of the electric power are waste heat and have to be removed. The installed ventilators (see Fig. 1) force an ambient air stream of approx. 3 m/s through the lamp field.

### The cold sky

Under clear sky conditions the IR-radiation is below the blackbody-radiation of the ambient temperature. Hence the hot lamps have to be thermally decoupled from the test-plane. Fig. 1 indicates, that this is accomplished by a double pane of acrylic glass. The highly transparent channel is cooled with low temperature air. As the acrylic glass shows an emissivity

of about 95 % (wavelength  $> 2.5 \mu\text{m}$ ), it provides a low IR-radiation and serves as a cold sky with selectable temperature. A further advantage is the improvement of the spectral distribution between 1 and  $2.5 \mu\text{m}$ , which is caused by absorption (Table 1).

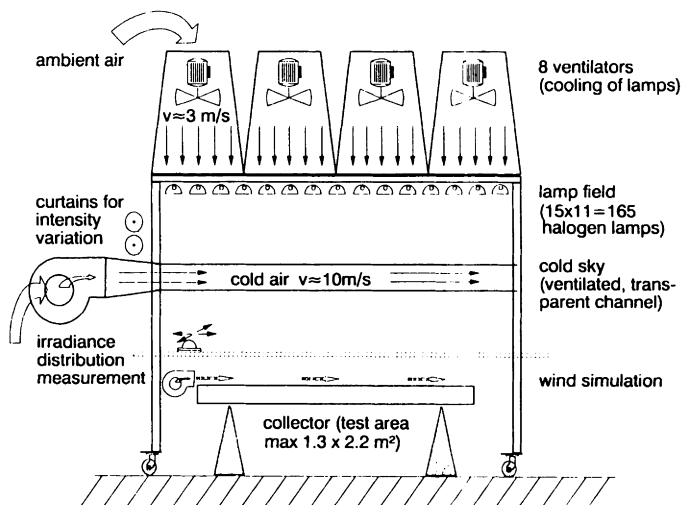


Fig. 1 Schematic side view of the solar simulator

Table 1 Spectral distribution of the light source

Range [nm]	sun at AM 2	bare lamp at 17 V	lamp with cold sky, 17V	lamp with cold sky, 19V
< 400	2.7%	0.5%	0.6%	0.9%
400-700	44.4%	32.0%	39.1%	41.3%
700-1000	28.6%	23.9%	28.8%	30.1%
> 1000	24.3%	43.6%	31.5%	27.7%

#### AUXILIARY DEVICES

Some additional installations are essential for the successful installation of the whole facility.

### Constant Temperature and Flow-Rate

A flow-rate with fluctuations of less than 1 % at a constant temperature of  $\pm 0.02$  K in a range of 15 to 95 °C is delivered by a thermostatic-constant-flow-control-unit. It serves as the fluid-source for collector-inlet.

### Irradiance Distribution Measurement

The accurate determination of the irradiance level in the receiver plane is of primary importance. Even with a rather high uniformity (standard deviation  $\pm 3.3$  %, minimum/maximum  $\pm 8$  %, see Fig. 2) the error e.g. in an efficiency value caused by disadvantageous sensor locations is expected to be in the same order of magnitude. Therefore the mean irradiance over the test object has to be known. This is done by an automatic step by step irradiance distribution measurement (e.g. in a 10 cm x 10 cm - grid). As the behaviour of lamps can change, this procedure will be repeated at the beginning of each experiment, at least once a day.

### Cooling of the Experimental Building

The internal loads (lamps, heaters and machines) of around 30 kW are removed by a cooling system, that allows to keep temperatures constant ( $\pm 0.3$  K) in a range of 18 to 30 °C.

### Electric Power Supply

The irradiance is very sensitive against fluctuations of the voltage in the public grid (intensity  $\sim U^2$ ). The used station gives a constant voltage  $\pm 0.1 \dots 0.2$  %, selectable between 220 and 250 V. That corresponds to a lamp voltage of 16.9 to 19.2 V (13 lamps connected in series). Thus a very constant irradiance during an experiment (better than  $\pm 2$  W/m<sup>2</sup>) is achieved and the intensity level is changeable between 800 and 1000 W/m<sup>2</sup> with only a small effect on spectral distribution.

### Data Acquisition and Sensors

Much care is taken for the choice and calibration of the sensors (temperature: PT100  $\pm 0.05$  K; flow-rate: inductive flowmeters  $< \pm 1$  %; irradiance: pyranometer CM11  $\pm 1$  %). A variable data acquisition system allows flexible collecting of measuring data with high accuracy.



## PERFORMANCE OF THE ISFH-TEST-FACILITY AND EXPERIENCES

The technical data of the simulator are summarized in Fig. 2.

TECHNICAL DATA SUSI I		June 1990
• irradiated area	2.2 x 1.3 m <sup>2</sup>	
• mean irradiance (nominal value)	800 W/m <sup>2</sup>	
• variation of irradiance	300 .. 1000 W/m <sup>2</sup>	
• uniformity (std.dev. / min.max.)	± 3.3 % / ± 8 %	
• angular distribution	77 % within ± 30°	
• IR-radiation (> 3 μm) in testplane	0 .. 10 K below ambient temp.	
• ambient temperature	18 .. 30°C	
• wind velocity above collector	0 .. 20 m/s	
• main beam direction	vertical*)	
• dimension of lamp field	2.45 x 1.50 m <sup>2</sup>	
• distance lamps - receiver	1.30 m	
• number of lamps	165	
• cooling of lamp field	ambient air with 3 m/s	
• nominal power	24 kW	
• efficiency	9.6 %	
*) modification in autumn '90: inclination angle of lamp field: 0 to 90°		

Fig. 2 Technical Data of the Solar Simulator SUSI I

The calculated irradiance was within ± 4.5 % (standard deviation ± 1.3 %). In practice this value could not be reached due to variations in lamp production.

Up to now (June '90) the simulator worked for more than 650 h. Within this time 14 collectors have been investigated. Most measurements were efficiency-curves with different parameters (flow-rate, intensity etc.), besides also stagnation temperatures and instantaneous heating-up curves were made. 11 lamps have failed and were replaced. After 650 h about 10 % of the original intensity is lost. The lamps were ageing differently and so the homogeneity gets worse of up to ± 10 % (minimum/maximum). Also a small change in spectral distribution has been found: the part of the irradiance between 400 and 1000 nm decreases from 68 to 64 % (17 V) respectively 71 to 67 % (19 V) (AM2: 73 %).

Fig. 3 shows the repeated measurement of the efficiency-curve of the same flat-plate-collector. Between both experiments are around 550 h of operation. An additionally performed outdoor-test shows a rather good agreement, the respective efficiency-values are between 0 and 0.02 above the indoor-measurements. A repetition of an efficiency-value gives a relative deviation of less than 1%, the relative accuracy is estimated to be better than 2 %.

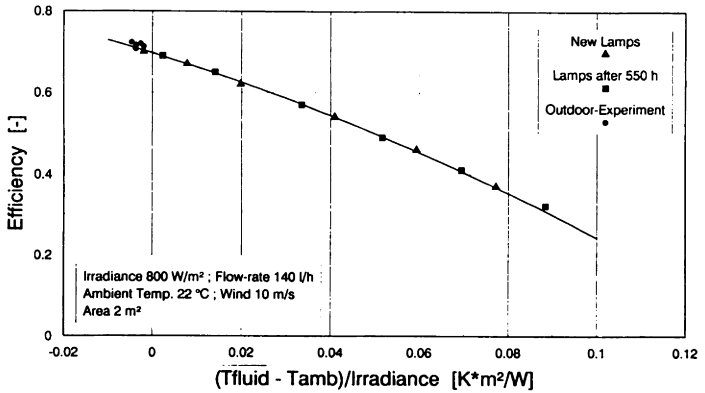


Fig. 3 Efficiency Curve of a Flat Plate Collector with new lamps, after 550 h and under outdoor-conditions

POTENTIAL AND FUTURE WORK

The very stable test conditions allow the accurate investigation and improvement of solar collectors. Fig. 4 shows the efficiency curve of a new collector with parallel connected absorber tubes. This efficiency is a strong function of the flow-rate. A look at the outlet-temperature at 17 l/h gives a large stochastic fluctuation of around  $\pm 4$  °C, all other parameters are kept strictly constant. This could be due to an unequal flow through the tubes. A connection in series indeed brought an improvement of about 4 % absolute.

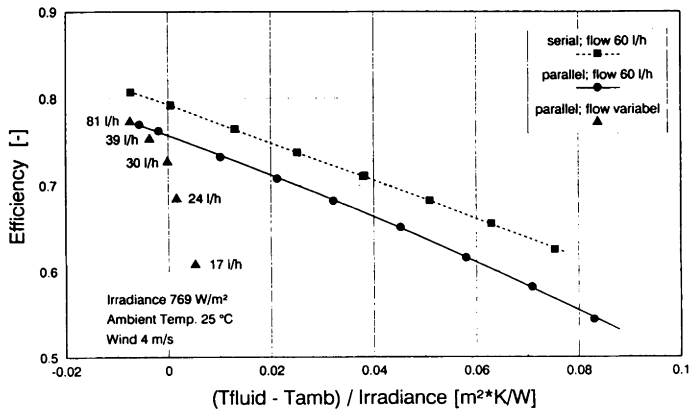


Fig. 4 Efficiency curves for a new collector, at different flow-rates, with parallel and serial absorber tube connection

In Fig. 5 the efficiency of an evacuated flat-plate-collector is presented as a function of inner pressure (all other parameters were kept constant). In this case the optimum pressure seems to be below 100 mbar, just before convection starts.

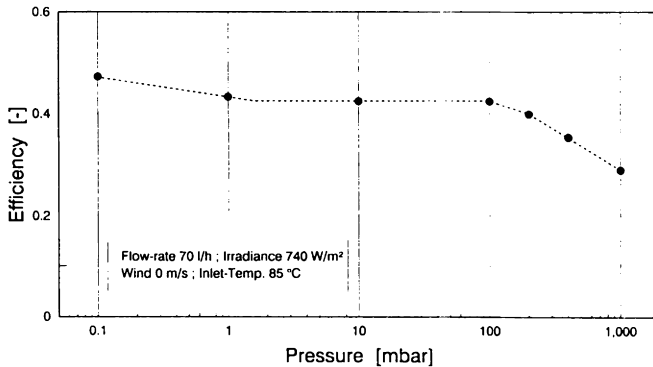


Fig. 5 Efficiency of an evacuated flat plate collector versus collector pressure.

Further experiments have been done with wind velocity or intensity as parameter. In the next months, the simulator will be mounted into a tiltable frame, so that for instance heat-pipe-collectors can be investigated. Furthermore the construction of a high-temperature thermostatic control-unit (up to 180 °C) is planned. This extension of the temperature-range is useful for the assessment of process-heat-collectors, e.g. with transparent insulation materials or low concentrating mirror arrangements ( $C < 2.5$ ).

In discussion is the application as a test device for small passive solar components respectively for photovoltaic systems.

#### CONCLUSION

The solar simulator SUSI I, developed at the ISFH, provides a good and cost-effective artificial light source for the investigation of solar collectors. Assisted by auxiliary devices, measurements can be done with high reproducibility. Thus a more detailed analysis or a thermal optimization of a collector is possible, and a collector-manufacturer can get experimental support to develop new collectors.

# ON THE MECHANISM BEHIND OVERCAST WEATHER

## A Mathematical Discussion

ARNE BROMAN

Solar Energy Research Center  
University College of Falun/Borlänge  
P.O. Box 100 44, S-781 10 Borlänge, Sweden

### ABSTRACT

Since around fifteen years a theory of "chaos" has developed. This theory seems to shed light on many aspects of science, biology, and human endeavors. We shall consider some of its mathematical and empirical facts.

### KEYWORDS

Chaos, weather, overcast, iteration, recursion, nonlinear, Feigenbaum.

### 1. Introduction

Consider Fig. 1. Assume that particles of transparent atmosphere (molecules of oxygen, nitrogen, etc.) repeatedly push alien particles (molecules of water vapour, etc.). Consider a region of space where the speed of the atmosphere particles has a maximum (due to increased temperature, say). The maximum is indicated by the curve in the figure. An alien particle will sometimes be pushed closer to the maximum, sometimes further off.

The axes of Fig. 1 are labelled "space" and "pushes". We think of "space" as three-dimensional, and we think of "pushes" as three-dimensional vectors. (Fig. 1 is very simplified.)

What will be the motion of the alien particles? A person who can answer this question may be able to predict weather accurately. There will probably never be such a person. We restrict our attention to a mathematical model. Infinitely many models can be constructed; our choice is probably the simplest possible. Does this model tell anything about phenomena in nature?

### 2. The model that we consider

Assume that  $k$  and  $x_0$  are given numbers,  $0 < k < 4$  and  $0 < x_0 < 1$ . Consider the sequence  $x_0, x_1, x_2, \dots, x_n, \dots$ , or shorter  $\{x_n\}$ , that is defined by the recursion formula:

$$x_{n+1} = k(x_n - x_n^2) \text{ for } n = 0, 1, 2, \dots \quad (1)$$

The infinite sequence is said to be obtained by iteration.

We define functions  $y = f_k(x)$  by:

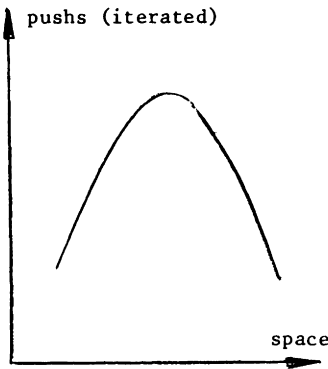


Fig. 1. Particles of clean air push alien particles.

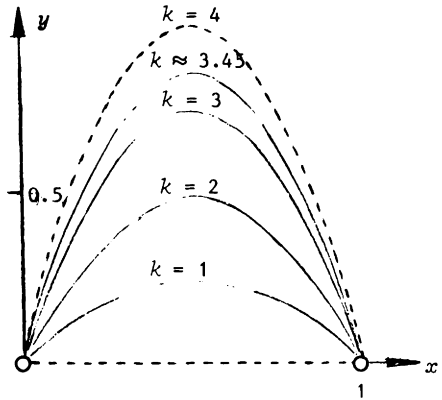


Fig. 2. The curves  $y = f_k(x)$  for certain values of  $k$ .

$$y = f_k(x) = k(x - x^2), \quad 0 < x < 1. \tag{2}$$

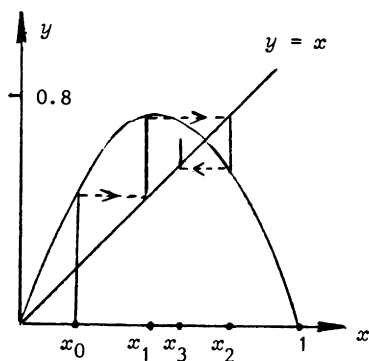
Fig. 2 shows graphs for some of these functions. The curves (parabola arcs) sweep the region between a segment of the  $x$ -axis and the arc  $y = 4(x - x^2)$ ,  $0 < x < 1$ , as  $k$  increases from 0 to 4. The segment, the latter arc (dotted in the figure) and the end points of the segment (denoted by small circles) do not belong to the region. Each curve has a maximum point:  $(1/2, k/4)$ . The  $k$ -values in Fig. 2 are not arbitrarily chosen; we shall see in the following that each of them is of interest. The functions (2) are nonlinear, i.e. they are not polynomials of degree 1.

The dotted segment in Fig. 2 and the iteration formula (1) are our model of "space" and "pushes" in Fig. 1. Our assumptions imply that, for any  $k$  and  $x_0$ , the entire sequence  $\{x_n\}$  is situated in the interval  $0 < x < 1$ .

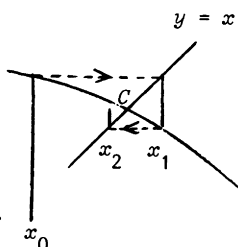
### 3. Visualization

Fig. 3 shows a way to visualize (part of) a sequence (1). The vertical line through  $(x_0, 0)$  intersects the curve (2) at the point  $(x_0, x_1)$ . From there, a horizontal line intersects the bisector  $y = x$  of the first quadrant at  $(x_1, x_1)$ . The vertical line through the latter point intersects (2) at  $(x_1, x_2)$ . Going on in this way, we construct (a finite subsequence of)  $\{x_n\}$ .

Assume  $k > 1$ . Then the bisector  $y = x$  intersects the curve (2) at a point  $C$ , in coordinate form:  $(c, c)$ , with  $c = 1 - 1/k$ . A short computation gives the derivative of the function (2) for  $x = c$ :  $f'_k(x) = 2 - k$ . Hence  $|f'_k(c)| < 1$  for  $1 < k < 3$  and  $|f'_k(c)| > 1$  for  $k > 3$ . These two cases are illustrated in Figs. 4 and 5. Assume that  $k \neq 3$  and that  $x_n \neq c$  is



**Fig. 3.**  $k = 3$ ,  $x_0 = 0.2$ .  
The first few  $x_n$ .



**Fig. 4.**  $k = 2.5$ .  
The point  $x = c$   
attracts  $x_n$ .

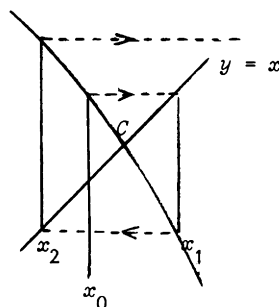


**Fig. 5.**  $k = 3.5$ .  
The point  $x = c$   
repels  $x_n$ .

situated in a small neighborhood,  $N$ , of  $c$  where  $|f_k'(x)| - 1$  does not change sign; such an  $N$  exists, for  $f_k'(x)$  is a continuous function. The figures indicate that, with  $n$  increasing,  $c$  attracts  $x_n$  for  $k < 3$ , while  $c$  repels  $x_n$  for  $k > 3$  (at least for small  $n$ ). To prove this rigorously, use the mean value theorem to show the existence of a number  $\xi$  between  $c$  and  $x_n$  such that  $f_k(x_n) - c = f_k'(\xi)(x_n - c)$ .

Now assume that  $0 < k \leq 1$ . Then, by (1),  $x_{n+1} < x_n$  for all  $n$ . It follows that the sequence (1) is decreasing and, hence, has a limit. Fig. 6 indicates that the limit is zero; a rigorous proof is readily constructed. The case  $0 < k \leq 1$  is of no interest in this article; we turn to larger values of  $k$ .

#### 4. Periods. The cases $1 < k \leq 3$

Consider a sequence (1). There may exist positive integers  $n$  and  $p$  such that  $x_{n+p} = x_n$ . Then the numbers  $x_n, x_{n+1}, x_{n+p-1}$  will come back periodically from  $n$  onwards. We shall say that  $x_0$  gives rise to a periodic sequence or, shorter, that  $x_0$  is *periodic*. If  $p$  is the smallest positive integer with this property, we say that  $p$  is the *period* of  $x_0$ . It is seen that the subset,  $S$ , of periodic starting values  $x_0$  is infinite.

However,  $S$  is a very tiny subset (a denumerable subset) of the interval  $0 < x < 1$ : If  $x_0$  is chosen at random, its probability to be periodic is zero. Fig. 6 and its context show that, for  $0 < k \leq 1$ , no  $x_0$  is periodic. But for  $k > 1$ , there exist infinitely many periodic starting values  $x_0$ , among them the  $c$  in the context of Figs. 4 and 5. This  $x_0$  has the period  $p = 1$ . We take a closer look at  $k$ -values larger than 1:

(a) Assume  $1 < k \leq 2$ . Then the maximum point of the curve (2) is situated to the right of or exactly on the bisector  $y = x$ . Fig. 7 indicates that the sequence  $\{x_n\}$  has the limit  $c = 1 - 1/k$ . This is readily proved, using ideas from figures, such as Fig. 7. Hence, every sequence (1) has the limit  $c$ , and there is only one period:  $p = 1$ .

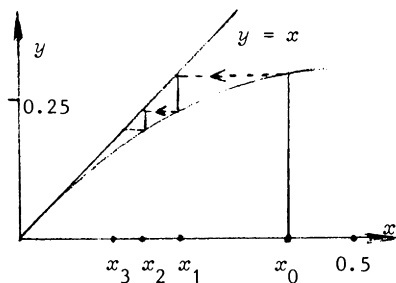


Fig. 6.  $k = 1$ ,  $x_0 = 0.4$ . The diagram suggests  $x_n \rightarrow 0$ .

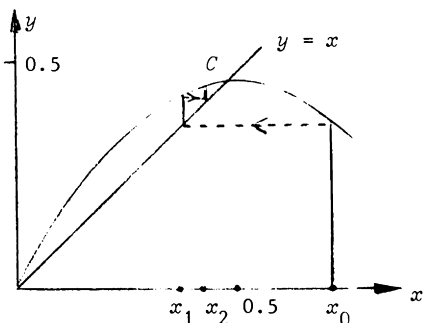


Fig. 7.  $k = 1.8$ ,  $x_0 = 0.7$ . The diagram suggests  $x_n \rightarrow c$ .

(b) Assume  $2 < k \leq 3$ . These cases are harder. Diagrams (as Figs. 3 and 4) indicate that each sequence (1) has the limit  $c = 1 - 1/k$ . Tests on a computer support this observation. (The author made several tests. For  $k = 3$ , a proof is given below in an appendix.) In sum, it is very probable that every sequence (1) has the limit  $c$  and that there is only one period,  $p = 1$ .

### 5. The cases $3 < k < 4$

Fig. 5 and its context indicate that complications occur. These are difficult to master; in what follows we give a résumé of empirical results, almost without mathematical justifications. We pay special attention to periodic starting values, for these have turned out to serve as "skeletons" in our investigations. For  $p = 2$  (similarly for  $p > 2$ ), to find periodic starting values, we define  $f_k(x)$  by (2) and we solve the equation  $f_k(f_k(x)) = x$ .

This is an algebraic equation of degree 4, and it has the roots  $x = 0$  (noninteresting),  $x = 1 - 1/k$  (already known for us) and two more roots. It is verified that these latter roots are real and distinct if and only if  $k > 3$ . An example is given in Fig. 8. This figure shows a part of the curve  $y = f_k(x) = 3.2(x - x^2)$  and a square with three important properties: (1) its sides are parallel to the coordinate axes; (2) it has two vertices,  $A$  and  $B$ , on the curve; (3) it has two vertices on the bisector  $y = x$ . (There is such a square for every  $k > 3$ .) The vertical sides have the  $x$ -coordinates  $x_0 = 0.513$  and  $x_1 = 0.799$ . (Our decimal fractions with more than one decimal are correctly rounded off values of some real numbers.) Hence  $x_0$  (and also  $x_1$ ) is periodic with period  $p = 2$ . Further,  $|f_k'(x_0) \cdot f_k'(x_1)| < 1$ . Repeated application of the mean value theorem then shows that the square in Fig. 8 attracts the polygons of other starting values. It is verified that such an attraction occurs for  $3 < x_0 \leq 1 + \sqrt{6} \approx 3.449$ , while

repulsion occurs for  $x_0 > 1 + \sqrt{6}$ . In the former case, every sequence  $\{x_n\}$  has subsequences  $\{x_{2n}\}$  and  $\{x_{2n+1}\}$  with distinct limits: 0.513 and 0.799 when  $k$  and  $x_0$  are as in Fig. 8.

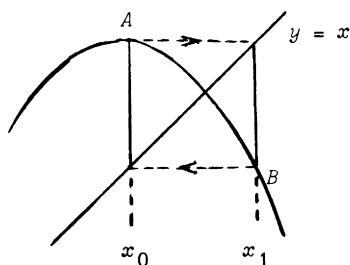


Fig. 8. Period  $p = 2$ ,  $k = 3.2$ ,  
 $x_0 = 0.513$ ,  $x_1 = 0.799$ .

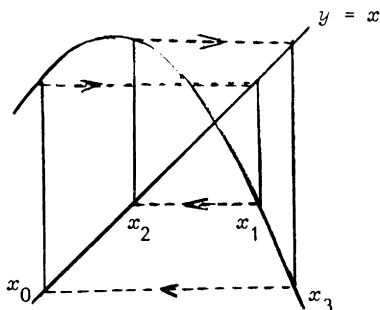


Fig. 9. Period  $p = 4$ ,  $k = 3.6$ ,  
 $x_0 = 0.3552$ ,  $x_1 = 0.5454, \dots$

For  $k > 3.449$ , the square of Fig. 8 is replaced by an octagon; see Fig. 9. It is verified that this octagon attracts for  $k \leq 3.565$ , repels for larger values of  $k$ . Some information (obtained on a computer) on some more values of  $p$  is given in Fig. 10 and accompanying tables. The letters "a" and "r" in Fig. 10 and its tables refer to "attract" and "repel". In Fig. 10, attraction and repulsion are denoted by a whole line and a dotted line respectively. The letter "F" denotes the limit of the sequence  $a_1, a_2, a_4, \dots$  and refers to the American physicist Feigenbaum. The numbers  $a_7$  and  $r_7$  of Fig. 10 have the interest that their difference is quite small:  $r_7 - a_7 \approx 2 \cdot 10^{-7}$ . In Fig. 10 we have abstained from trying to use uniform scales on the axes.

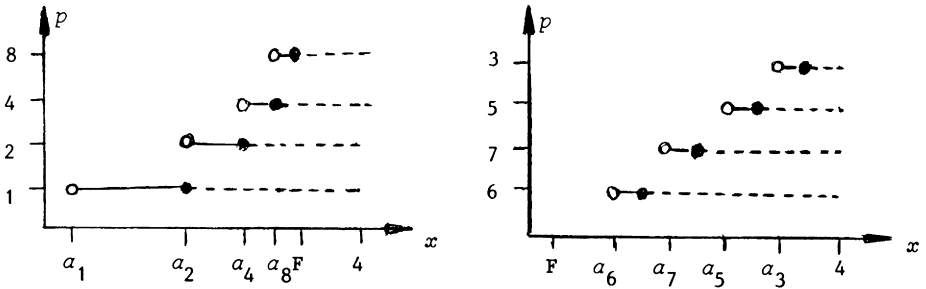
Around 1975, Mitchell Feigenbaum put down a considerable amount of numerical work (partially on computers) on the subject of this article: (1) He discovered the sequence of numbers that we have denoted  $a_2, a_4, a_8, \dots$  (2) He discovered the constant that we have denoted by  $F$ . (3) He discovered that the ratios of successive terms in the sequence  $a_2 - a_1, a_4 - a_2, a_8 - a_4, \dots$  tend to a limit for increasing  $n$ , and that this limit does not depend on the particular function chosen in (2). (The limit is around 4.669. Feigenbaum determined it to 10 decimal places.) This last result is truly remarkable. Gleick (see the reference below) tells a lot about Feigenbaum and his achievements.

## 6. Chaos. The case $k = 4$ . Clouds

Consider Fig. 10. For a nonperiodic starting value  $x_0$ , larger than  $F$ , a sequence  $\{x_n\}$  usually becomes chaotic: The numbers  $x_n$  are tightly packed everywhere in the interval  $0 < x < 1$ . There are some exceptions: tiny intervals for  $x_0$ , as indicated by the right-hand part of the figure. The figure suggests that these intervals are "chaotically distributed".

We illustrate the tight packing by an example. Assume that  $k = 4$ . (We here skip an assumption in Section 2, accepting the dotted curve in Fig. 2.) Assume that  $\{x_n\}$  is a nonperiodic sequence. Let  $x_n$  and  $x_{n+1}$  be successive members of the sequence.





$p$	$a_p$	$p$	$a_p$	$p$	$a_p$	$r_p$
1	1	8	3.544	3	3.8284	3.8285
2	3	16	3.565	5	3.738	3.741
4	3.449	F	3.571	6	3.627	3.631
				7	3.702	3.702

Fig. 10. Starting values for attracting and repelling sequences for some periods  $p$ .

Associate with them angles  $\alpha$  and  $\beta$  as in Fig. 11. Set  $x = x_n = (1 - \cos \alpha)/2$  in the equation  $y = 4(x - x^2)$ . It is readily computed that  $y = x_{n+1} = (1 - \cos 2\alpha)/2$ . Hence  $\beta = 2\alpha$ . Assume (aiming to get a contradiction) that the numbers  $x_n$  are not tightly packed everywhere. Then there is a largest circle arc  $a$  in Fig. 11 (or one among several largest arcs) to which there corresponds no  $x_n$ . Doubling angles gives an arc  $b$  without any corresponding  $x_{n+1}$ , hence a larger arc. (The exceptional case that  $b$  has  $x_0$  as its midpoint is easily disposed of.) The contradiction implies that the  $x_n$  are dense everywhere, i.e. that chaos prevails.

Consider a cloud. Its interior parts remind of our case  $k = 4$ . Its boundary parts have a fine structure, reminding of cases earlier in our text. Many observations in the physical world exhibit similar patterns.

REFERENCES

These two books contain a wealth of ideas from our and related topics. They also contain lots of relevant references:

PAUL DAVIES, *The Cosmic Blueprint*, Heineman, London 1987, viii + 224 pages.  
 JAMES GLEICK, *Chaos/Making a New Science*, Viking Penguin, New York 1987, xi + 352 pages.

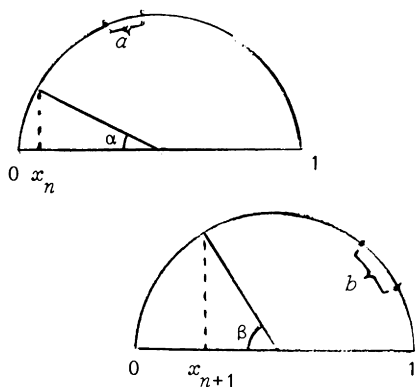


Fig. 11. A certain angle is doubled.

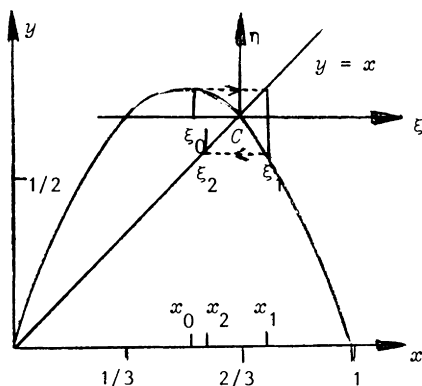


Fig. 12.  $k = 3$ . New coordinates have the origin  $C$ .

#### APPENDIX. THE CASE $k = 3$

Assume  $k = 3$ . This case is a bit tricky, for the expression  $|f'_3(x)| - 1$  changes sign at  $x = c = 2/3$  (see Fig. 12). We assume  $1/3 < x_0 < 2/3$ . (This is no essential restriction: If  $x_0 = 1/3$  or  $x_0 = 2/3$ , then every following  $x_n = 2/3$ ; if  $x_0 < 1/3$ , or  $x_0 > 2/3$ , there is an  $n$  with  $1/3 \leq x_n \leq 2/3$ , and we can use this  $x_n$  as a "new  $x_0$ ".) We introduce new coordinates (see Fig. 12):  $x = 2/3 + \xi$ ,  $y = 2/3 + \eta$ , and we set  $\xi_0 = x_0 - 2/3$ ,  $\xi_1 = x_1 - 2/3$ ,  $\xi_2 = x_2 - 2/3$ . Observing that (2) now is  $y = 3(x - x^2)$ , a computation gives  $\xi_1 = -3\xi_0^2 - \xi_0$ . Then  $\xi_2 = 3\xi_1^2 - \xi_1 = -3(3\xi_0^2 + \xi_0)^2 + (3\xi_0^2 + \xi_0)$ , whence  $\xi_2 - \xi_0 = -27\xi_0^4 - 18\xi_0^3 = -9\xi_0^3(3\xi_0 + 2)$ . This last expression has a positive value, because  $-1/3 < \xi_0 < 0$ . Further,  $\xi_2 < 0$ . Hence the sequence  $\{\xi_{2n}\}$ , with even indices, is increasing, and it has a limit. It is seen that the limit is zero. It follows that the sequence  $\{\xi_{2n+1}\}$ , with odd indices, also has the limit zero. This shows that the original sequence  $\{x_n\}$  has the limit  $2/3$ . Summing up, we have the limit  $2/3$  for  $k = 3$  and every  $x_0$ .

**HEAT TRANSFORMERS FOR SOLAR HEATING:  
PERFORMANCES OF VARIOUS MIXTURES.**

Mauro FELLI and Franco COTANA

Istituto di Energetica, Facoltà di Ingegneria, Università di Perugia, Via Cairoli - Ferro di cavallo - 06100 Perugia, Italy.

**ABSTRACT**

Absorption heat transformers are considered, fed with low temperature water, as coming from flat type solar collectors. The temperature of the water is raised to reach the minimum required value for residential heating. A thermodynamic study is performed and the overall coefficient of performance is discussed as a function of the mixtures properties. Besides a number of mixtures are considered with data collected from Literature, such as: P-T-X equilibrium charts, latent heats, heats of mixing, specific heats, specific volumes. A computer program is developed which allows to get a dynamic response of the performances of a standard residential heating system when the different mixtures are used in the heat transformer. Various operating conditions are examined, which are concerned with the most common climatic situations, and the proper field of application for each mixture is indicated.

**KEY WORDS**

Absorption, Heating, Energy savings.

**1. Introduction.**

The Absorption Machine operating with an inverted cycle is usually referred to as the "heat transformer". Such name is appropriate indeed, because the heat transformer raises a quantity of heat  $Q$  from an intermediate temperature level to a higher level, while another quantity of heat  $Q'$  is lowered from the intermediate level to the environment temperature. The higher level may be the utilization temperature, while the heat source at the intermediate temperature may be waste heat or solar energy. In this way low cost collecting devices, viz. flat-plate solar panels, may be used for applications such as residential heating with higher efficiency. The absorption heat pumps also allow to get the same purpose, but they require a high temperature heat source to feed the generator. On the contrary, the absorption heat transformers need not supplementary heat sources; compared with the absorption heat pumps, however, the heat transformers require a relatively higher temperature of the heating source and that may be a

negative feature when solar plants are utilized. Infact the heat pumps may use solar fluids at any temperature, very close also to the environment temperature  $T_0$ , while the heat transformers have to be seeded by fluids heated to an intermediate temperature  $T_3$  between the environment and the utilization temperature  $T_u$ : as a first approximation,  $T_3$  may be set equal to the arithmetic mean value between  $T_u$  and  $T_0$ .

A research program involving heat transformers is being carried on by the Italian National Council for Research, Energy Finalized Project, in collaboration with the University of Rome "La Sapienza", Department of Technical Physics, and with the University of Perugia, Institute of Energy. The mentioned program consists of a number of steps: first, studying the thermodynamic fundamentals of the heat transformers [1], [2]; second, surveying the applications, especially related to residential heating and solar energy utilization [3]; third, comparing the various fluids performances, in connection with a selected application; the final tool is to design a prototype of the engine.

The present paper is placed within the third step of the research program and illustrates the results of a computer simulation dealing with the utilization of five solute-solvent pairs, which are (first mentioning the refrigerant):

- Ammonia-Aqua ( $\text{NH}_3\text{-H}_2\text{O}$ );
- Aqua-Lithium Bromide ( $\text{H}_2\text{O-LiBr}$ );
- Methanol-Lithium Bromide ( $\text{CH}_3\text{OH-LiBr}$ );
- Methanol-Lithium Bromide-Zinc Bromide ( $\text{CH}_3\text{OH-LiBr-ZnBr}_2$ );
- Difluorochloromethane (R22) - Tetraethylene Glycol Dimethyl Ether ( $\text{CHClF}_2\text{-C}_{10}\text{H}_{22}\text{O}_5$ ).

The comparison is performed with reference to the scheme of a heat transformer feeded at a variable intermediate temperature and which supplies a variable temperature utilizer; this scheme may adequately simulate the situation of a solar assisted residential heating plant.

## **2. Scheme and Hypothesis.**

The simplified internal operating scheme of an absorption heat transformer is sketched in fig. 1 [1], [2]. In addition, a possible layout of the whole system is arranged in fig. 2. The absorber operates at the highest temperature  $T_a$  reached within the engine and it supplies the heating plant at a variable temperature. The evaporator and the generator operate at the same intermediate temperature:

$$T_g = T_e \quad (1)$$

The mean temperature  $T_w$  of the fluid circulating in the solar plant is slightly higher, so that we can write:

$$T_w = T_g + 5^\circ\text{C} (= T_e + 5^\circ\text{C}) \quad (2)$$

We suppose that the collecting devices are flat-plate iron made solar collectors, covered with a 3 mm thin sheet of standard

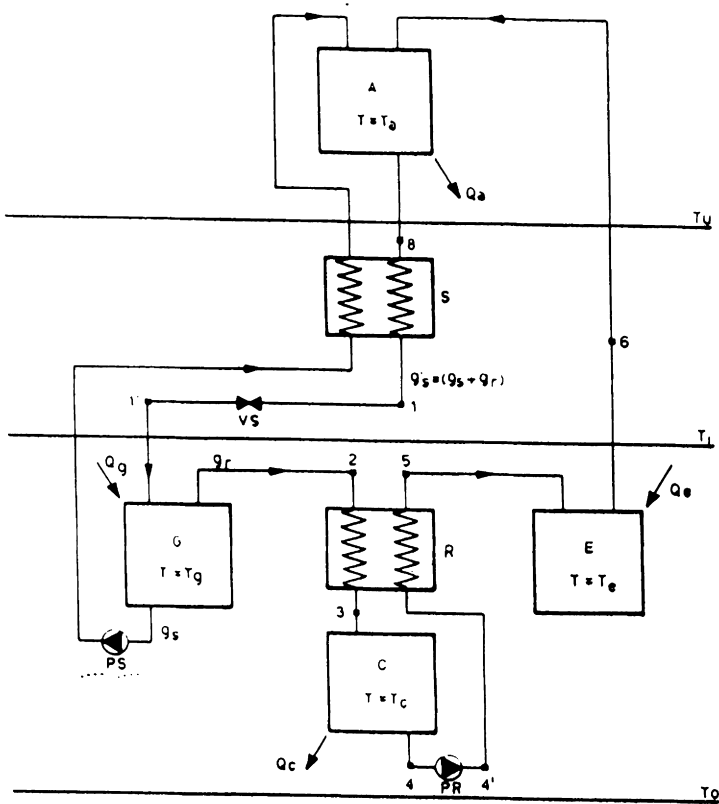


Fig. 1: simplified scheme of an absorption heat transformer.

transparent glass; so we may consider an efficiency of about 0.45, when the difference between  $T_w$  and the environment temperature is set equal to 50°C [4], that is to say:

$$\eta_c = \text{cost} = 0.45 \tag{3}$$

$$T_w = T_o + 50^\circ\text{C} \tag{4}$$

The environment temperature  $T_o$  is supposed variable; infact it is interesting to study the variations of the performances of the system as a function of the variations of the external air temperature. The condenser temperature  $T_c$  has to be slightly higher than  $T_o$  and it may be set:

$$T_c = T_o + 5^\circ\text{C} \tag{5}$$

Finally the ratio  $m$  between the solution and refrigerant flow-rates is assumed constant and equal to 10:

$$m = g_s/g_r = \text{cost} = 10 \tag{6}$$

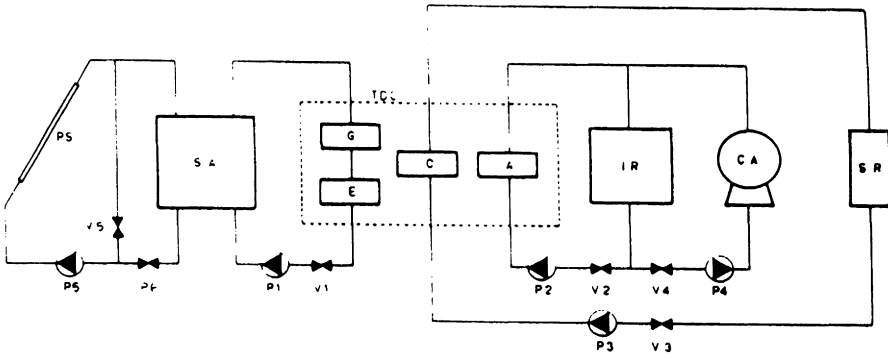


Fig. 2: general layout of a solar heating plant utilizing a heat transformer. PS = solar panel; SA = water tank; TDC = heat transformer; IR = heating plant; CA = furnace; SR = cooling system; P = pump; V = valve.

### 3. Evaluation of the Fluid Parameters.

In order to achieve the calculation of the system performances it is necessary to know the values of some physical properties of the involved fluids, such as:

- specific heat of the liquid refrigerant;
- specific heat of the refrigerant vapour;
- specific heat of the liquid solution at the operating concentration;
- latent heat of evaporation of the refrigerant at variable temperature;
- differential heat of solution at the operating concentrations and temperatures;
- specific volume of liquid refrigerant;
- specific volume of liquid solution.

A relation has been written for each parameter, directly derived from Literature or determined by interpolating of the experimental disposable data from the Literature [5, 6, 7, 8, 9, 10, 11, 12]. These are usually relations containing a number of numerical constants, that have been summarized in table 1, for the different solutions. The form that is assumed for each relation is as follows:

- Specific heat of the liquid refrigerant:

$$\gamma_{p,R} = A_1 + A_2T + A_3T^2 \quad (7)$$

- Specific heat of the refrigerant vapour:

$$\gamma_{p,v} = B_1 + B_2T + B_3T^2 \quad (8)$$

- Specific heat of the solution:

$$\gamma_{p,s} = C_1 + C_2 X \quad (9)$$

Table 1: values of the constants $A_i$ , $B_i$ , $C_i$ , $D_i$ , $E_i$ , $F_i$ , $G_i$ for different refrigerant-absorbent pairs.					
	$\text{NH}_3\text{-H}_2\text{O}$	$\text{H}_2\text{O-LiBr}$	$\text{CH}_3\text{OH-LiBr}$	$\text{CH}_3\text{OH-LiBr-ZnBr}_2$	$\text{CHClF}_2\text{-C}_{10}\text{H}_{22}\text{O}_5$
A1	4.597	4.211	4.172	3.785	4.567
A2	0.0059	$-1.276 \cdot 10^{-3}$	0.0456	$-0.5632$	$-0.6784$
A3	$4.32 \cdot 10^{-5}$	$1.295 \cdot 10^{-5}$	$3.12 \cdot 10^{-5}$	$2.56 \cdot 10^{-5}$	$4.44 \cdot 10^{-5}$
B1	2.059	1.858	12.56	4.38	7.56
B2	0.001343	0.0012	0.00154	0.00212	0.00134
B3	$2.49 \cdot 10^{-6}$	0.0000156	0.0000178	0.0000215	0.0000317
C1	4.18	4.18	4.16	4.19	4.14
C2	0.71	-3.09	-2.12	3.18	-4.17
D1	1262.6	2500.3	1890.8	2408.5	2753.5
D2	-3.5031	-2.227	-4.1973	-3.942	-3.892
D3	-1.359	$-3.11 \cdot 10^{-3}$	$-3.12 \cdot 10^{-3}$	-1.345	-1.762
D4	$2.645 \cdot 10^{-5}$	$4.43 \cdot 10^{-5}$	$3.78 \cdot 10^{-5}$	$2.56 \cdot 10^{-5}$	$4.36 \cdot 10^{-5}$
D5	$-8537 \cdot 10^{-7}$	$-3.78 \cdot 10^{-7}$	$-4.78 \cdot 10^{-7}$	$-2.563 \cdot 10^{-7}$	$-3.45 \cdot 10^{-7}$
E1	2161.7	$5.65 \cdot 10^{-2}$	$3.472 \cdot 10^{-2}$	$3.224 \cdot 10^{-2}$	$4.143 \cdot 10^{-2}$
E2	-2210.8	-41.348	-234.83	-128	-264.92
E3	5742.8	623.31	2198.9	4127.4	3871.8
E4	-10.086	-1531.7	-154.83	-1569.4	-23.78
E5	4380	-1246.2	3421	-3122	-3442
F1	$1.562 \cdot 10^{-3}$	$2.782 \cdot 10^{-3}$	$3.75 \cdot 10^{-3}$	$32.11 \cdot 10^{-3}$	$1.78 \cdot 10^{-3}$
F2	$3.824 \cdot 10^{-6}$	$-2.672 \cdot 10^{-6}$	$123.39 \cdot 10^{-6}$	$1.34 \cdot 10^{-6}$	$11.9 \cdot 10^{-6}$
F3	$-5.944 \cdot 10^{-9}$	$-34.3 \cdot 10^{-9}$	$-3.7 \cdot 10^{-9}$	$-23.8 \cdot 10^{-9}$	$-12.26 \cdot 10^{-9}$
F4	$2.203 \cdot 10^{-9}$	$21.2 \cdot 10^{-9}$	$22.1 \cdot 10^{-9}$	$2.43 \cdot 10^{-9}$	$1.45 \cdot 10^{-9}$
G1	$1.007 \cdot 10^{-3}$	$5.91 \cdot 10^{-3}$	$4.23 \cdot 10^{-3}$	$12.11 \cdot 10^{-3}$	$2.67 \cdot 10^{-3}$
G2	2.15	-3.24	-3.48	-2.32	-12.78
G3	1.332	-123.89	-21.38	-32.78	-43.1
G4	-1.34	3.38	2.11	5.21	7.11

where X is the concentration by mass of the refrigerant.

- Latent heat of evaporation of the refrigerant:

$$r(T) = D_1 + D_2T + D_3T^2 + D_4T^3 + D_5T^4 \quad (10)$$

where T is the absolute temperature.

- Differential heat of solution (variation with temperature):

$$s(X) = E_1 + E_2T + E_3T^2 + E_4T^3 + E_5T^4, \quad (11)$$

where T is the absolute temperature.

- Specific volume of the liquid refrigerant:

$$v_R = F_1 + F_2T + F_3T^2 + F_4T^3 \quad (12)$$

where T is the absolute temperature.

- Specific volume of the solution:

$$v_s = G_1 + G_2X + G_3X^2 + G_4X^3 \quad (13)$$

where X is the concentration by mass of the refrigerant.

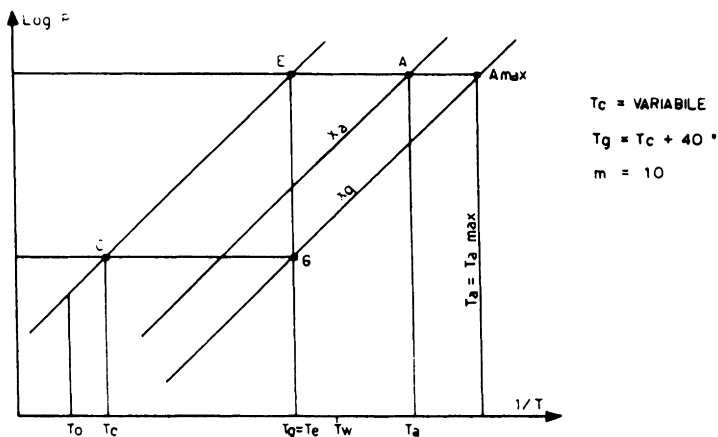


Fig. 3: determination of the thermodynamic conditions of the working fluid on the P-T-X diagram.

#### 4. Engine Operation and Performances

The operation of the engine may be adequately illustrated on the P-T-X chart of the solution, as it is shown in fig. 3. The points C, G, E, A are representative of the thermodynamic conditions of the fluid, respectively, within the condenser, generator, evaporator and absorber. The point  $A_{\max}$  lays on the isotherm  $T = T_{\max}$ , that is the maximum temperature that may be theoretically reached by the engine, when the flow rate of the solution is going to infinite. As the position of the point C varies with the environment temperature  $T_0$ , the positions of the other points are also variable during the operation of the engine; they have been determined for all the fluids, as a step of the calculus, in order to get the values of the engine performances: however, they are not reported in the text, for sake of brevity.

There are two meaningful parameters in order to point out the performances of an absorption machine and, in particular, of a heat transformer: they are the thermal rate and the coefficient of performance. The former takes into account the possibility of an engine of fixed dimension to exploit an assigned thermal request; the latter takes into account the energetic consumptions of the machine. Therefore the former is related to the initial costs of the installation, the latter to the running costs.

We define "useful heat rate" of a heat transformer the quantity of heat rejected from the absorber to the utilizer. It is possible to show that the useful heat rate is given by the



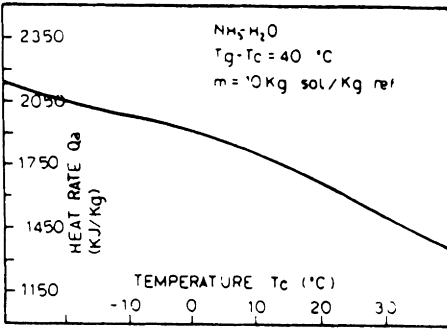


Fig. 4a

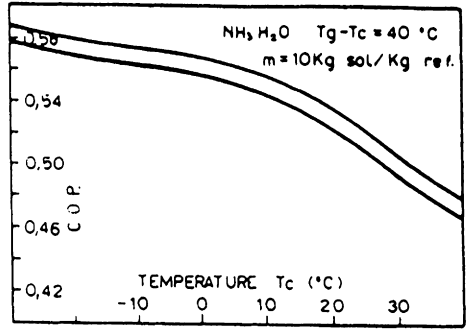


Fig. 4b

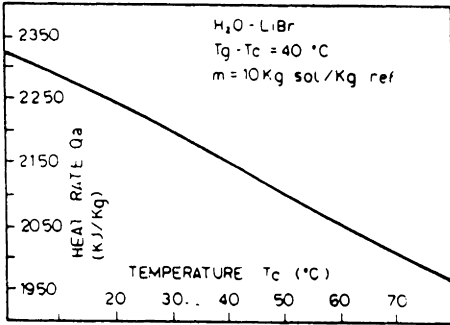


Fig. 5a

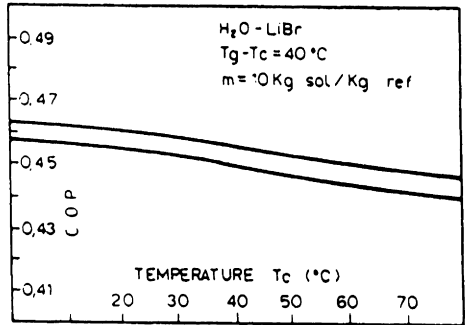


Fig. 5b

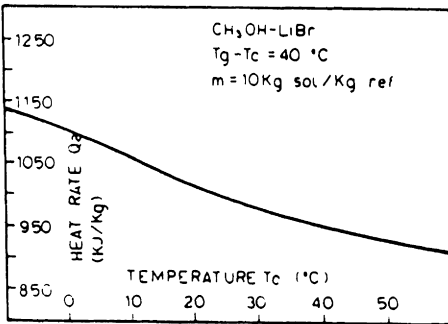


Fig. 6a

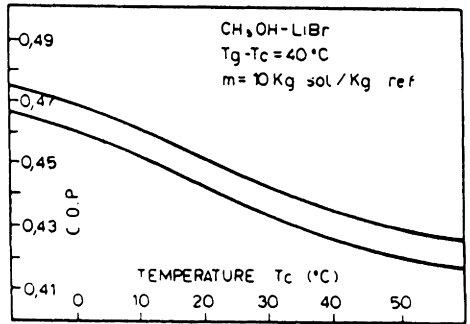


Fig. 6b

following expression [1]:

$$Q_a = r(T_a) + s(X_a, T_a) - \gamma_s(T_a - T_g) [m - \alpha(m+1)] - \gamma_{R,v}(T_a - T_e) \quad (14)$$

We define coefficient of performance (C.O.P.) of a heat transformer the ratio between the thermal rate and the corresponding energy assumed by the engine, that is to say:

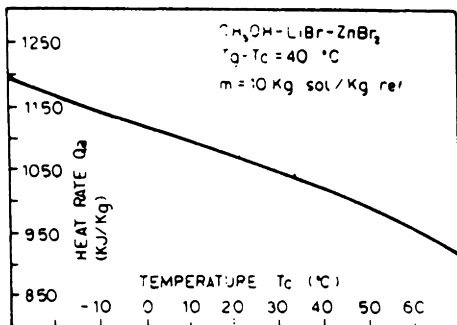


Fig. 7a

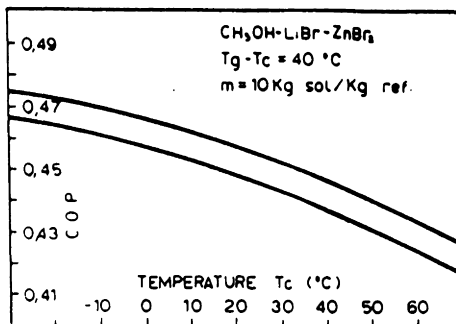


Fig. 7b

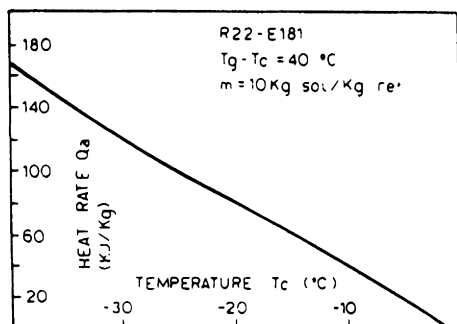


Fig. 8a

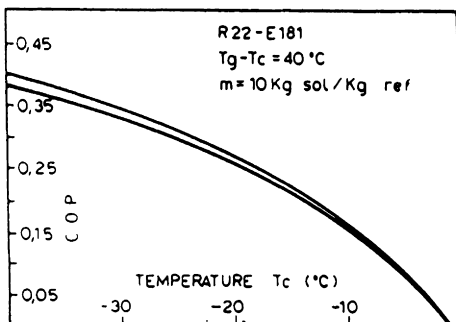


Fig. 8b

$$\text{C.O.P.} = \frac{Q_a}{Q_g + Q_e + L_{PS} + L_{PR}} \quad (15)$$

where  $Q_a$  is given by the (14) and the quantities  $Q_g$ ,  $Q_e$ ,  $L_{PS}$  and  $L_{PR}$  are being calculated by the following expressions [1]:

$$Q_g = r(T_g) + s(X_g, T_g) - (1-a)(m+1) \gamma_s(T_a - T_g) \quad (16)$$

$$Q_e = r(T_e) + \gamma_{R,1}(T_e - T_c) - \alpha_R \gamma_{R,v}(T_g - T_c) \quad (17)$$

$$L_{PS} = \frac{v_s m (P_a - P_g)}{\eta_{PS}} \quad (18)$$

$$L_{PR} = \frac{v_R (P_e - P_c)}{\eta_{PR}} \quad (19)$$

The ratio  $m$  between the flow rates  $g_s$  and  $g_p$  is given, in the particular case of the heat transformer, by the following:

$$m = \frac{1 - X_a}{X_a - X_g} \quad (20)$$

## 5. Results and Discussion.

The relations from (14) to (20) have been introduced in a computer program to explore the variations of the performances with the operating conditions and for the different fluids, whose characteristics are listed in table 1. The results have been set in the form of graphics which correlate the thermal rate and the C.O.P. against the condensing temperature. In the figg. 4, 5, 6, 7, 8 are shown, respectively, the performances of the mixtures  $\text{NH}_3\text{-H}_2\text{O}$ ,  $\text{H}_2\text{O-LiBr}$ ,  $\text{CH}_3\text{OH-LiBr}$ ,  $\text{CH}_3\text{OH-LiBr-ZnBr}_2$ , R22-E181; each figure is divided into two parts, a) and b): the part a) is concerning with the useful heat rate and the part b) with the coefficient of performance.

For all the mixtures the useful heat rate exhibits a meaningful dependance on the condensing temperature, while the coefficient of performance may be considered about constant in a large interval of the condensing temperature: that is in accordance with the usual behaviour of the absorption machines.

The very important result is that the useful heat rate diminishes with the increasing of the condensing temperature, and so, remembering the (5), that diminishes with the increasing of the environment temperature  $T_o$ . Therefore the heat transformer looks very attractive for residential heating applications, because the useful heat rate offered by the heat transformer has the same trend as the heat request of a heating plant.

A comparison between the various mixtures shows that the best performances are offered by the Water-Lithium Bromide mixtures, followed by Water-Ammonia and Alcohol-Salt mixtures. However, the Water-Ammonia mixture is favourable only if the external temperature is very low. The mixture R22-E181 shows very poor performances in all the operating conditions.

## 6. List of Symbols.

A = Absorber;	R = Heat Recuperator;
C = Condenser;	r = Heat of Evaporation (KJ/Kg/);
C.O.P.=Coefficient of Performance;	S = Heat Exchanger between Solutions;
E = Evaporator;	s = Differential Heat of Solution (KJ/Kg);
$E_m$ = Mechanical Energy (KJ/Kg);	T = Temperature (K, °C);
$g$ = Flow Rate (Kg/sec);	v = Specific Volume ( $\text{m}^3/\text{Kg}$ );
G = Generator	VE = Refrigerant Expansion Valve;
L = Mechanical Work (KJ/Kg);	VS = Solution Expansion Valve;
$m = g_s/g_r$ ;	X = Mass Concentration.
P = Pressure (KPa);	
PS = Solution Pump;	
PR = Refrigerant Pump;	
Q = Quantity of Heat (KJ/Kg);	

## Indices

o = Environment;	R = Refrigerant;
------------------	------------------

a = Absorber;	s = Solution;
c = Condenser;	u = Utilizer;
e = Evaporator;	v = Vapour;
g = Generator;	x = Cooling Fluid.
l = Liquid;	

### Greek letters

$\alpha$  = Efficiency of Heat Exchanger S  
 $\gamma$  = Specific Heat (KJ/Kg K).

### 7. References.

- 1) M. Felli: "A Contribution to the Theory of Heat Transformer" (to be published).
- 2) M. Felli: "Lezioni di Fisica Tecnica", Masson, Milano, 1990.
- 3) M. Felli: "Impiego del trasformatore di calore nel riscaldamento residenziale", Atti del Convegno Nazionale AICARR, Roma, 1989, p. 91-105.
- 4) Giacomia, Orioli, Panno: "Prove di efficienza su collettori solari piani", Energie Alternative HTE, 1981, p. 52.
- 5) C.A. Vancini: "La sintesi dell'ammoniaca", Hoepli, 1961.
- 6) R. Plank: "Handbuch der Kältetechnik", Springer-Verlag, 1988, vol VI/B.
- 7) Landolt, Bornstein: "Densities of liquids systems and their heat capacities", 1984, Vol. 1, part. B.
- 8) Landolt, Bornstein: "Heat of mixing and solution", Vol. 2.
- 9) ASHRAE: "Handbook of Fundamentals", 1989.
- 10) N.B. Vargaftik: "Tables of the thermophysical properties of liquids and gases", Hemisphere publ.Co., Washington, 1975.
- 11) E. Schmidt: "Properties of Water and Steam in SI Units", Grigull, 1982.
- 12) M. Coppi, A. de Lieto Vollaro, M. Felli: "Calore specifico di soluzioni in fase liquida: indagine sperimentale su nuovi composti", ESA, Roma, 1984.
- 13) T. Uemura, S. Hasaba: "Investigation of Absorption Refrigerating Machine operating on solution of Methanol-Lithium Bromide", Reito, Jap., vol. 43, 1968.
- 14) T. Uemura, S. Hasaba: "Studies on the Methanol-Lithium Bromide-Zinc Bromide Absorption Refrigerating Machine", Reito, Jap., vol. 44, 1969.
- 15) S.V.R. Mastrangelo: "Solubility of some chlorofluoro-hydrocarbons in Tetraethylene Glyco Dimethyl Ether", ASHRAE Journal, October 1959.
- 16) Kriebel, Loffler: "Thermodynamic properties of the binary system R22-E181", Kältetechnik, vol. 17, n° 9, sett. 1965, p. 266-271.
- 17) M. Jelinek, I.Yaron, I.Borde: "Measurement of vapour-liquid equilibria and determination of enthalpy-concentration diagrams of refrigerant-absorbent combinations", I.I.R. Commission B1, B2, E1, E2 Mons, Belgium, 1981.

## COOLING OF COMMERCIAL BUILDINGS BY MEANS OF LARGE COLD RADIANT CEILINGS

S. Alessandro, F. Butera (\*), G. Rizzo (\*\*), G. Silvestrini (\*\*\*)

(\*) Department of Energetics, University of Palermo, Viale delle Scienze, Palermo, Italy

(\*\*) Institute of Energetics, University of Reggio Calabria, Italy

(\*\*\*) CNR-IEREN, Viale delle Scienze, Palermo, Italy

### ABSTRACT

The possibility of using different cooling tools working with lower radiant temperatures and higher air velocity is explored. Lower energy consumptions may be achieved in specific climates with reasonable levels of thermal comfort.

### KEYWORDS

Cooling, thermal comfort, radiant panels, energy saving

### INTRODUCTION

Attention on energy consumptions for air conditioning of buildings is rapidly rising in many industrialized countries due to the growth of the cooling demand. In 1988 in Italy, for example, for the first time the peak power demand has been recorded not during the winter season, but in the summer time. Moreover, along with the higher importance assumed by the services sector, the number of the commercial buildings is largely spreading. Therefore, new energy saving measures should be introduced in order to minimize the energy consumptions for the climatisation of these buildings. In this work we present a theoretical study concerning the effects of a cold ceiling in connection with a fan.

With the use of such a system, the thermal comfort conditions will be assured in spite of higher air temperature, due to the combination of lower radiant temperatures and the effect of the air movement.

A computer code developed by the authors (Butera et al., 1984), based on the finite differences methodology, will be employed. A check will be performed through two Italian locations and a comparison will be made with a conventional air conditioning system.

Figures 1 and 2 respectively report the mean monthly values of relative humidity measured at the minimum and maximum mean monthly air temperature and the minimum and maximum temperatures for the summer season of two selected locations.

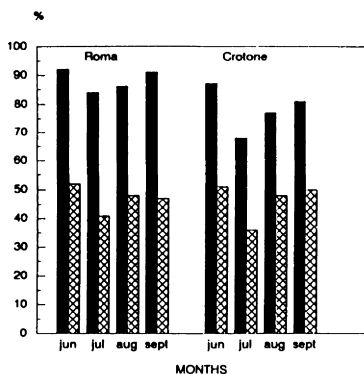


Fig. 1. Mean monthly values of relative humidity

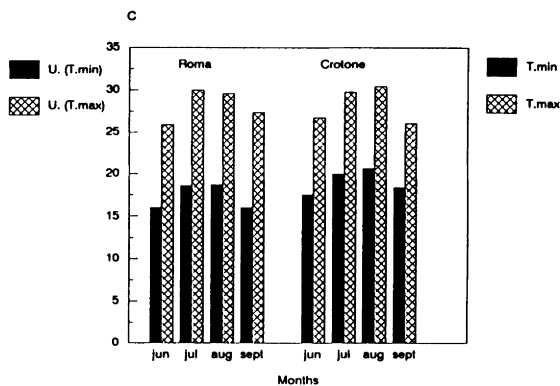


Fig. 2. Mean monthly values of min. and max. temperatures

## THERMAL COMFORT CONSIDERATIONS

It is well known that an appropriate control of the thermal radiant field of confined environments does allow the achievement of the thermal comfort conditions, by means of the modification of the surface temperatures of the surroundings and, as a consequence, of the mean radiant temperature.

The non-uniform distribution of the superficial temperatures of the walls could be sometimes cause of discomfort related to the asymmetric radiant field, even if the air temperature remains confined within the comfort range. But, as demonstrated by P.O. Fanger et al. (1980, 1985), the human body is not particularly sensitive to asymmetric radiation. As a rule for the judgement of the effectiveness of the radiant panel-electric fan system, we adopt here the Predicted Mean Vote (PMV) and the Predicted Percentage of Dissatisfied (PPD), that have been assumed by the ISO standards (1984).

To evaluate the range of thermal comfort of the system analyzed, the Fanger equations have been used in order to define the new comfort limits. In Fig. 3 the upper curve represents the situation with PPD = 10, assuming a modified mean radiant temperature (ceiling temperature is imposed at a temperature of 2.5 °C higher than the dew point temperature) and an air velocity of 0.8 m/sec.

## DESCRIPTION OF THE COOLING PANEL

The equipment here presented mainly consists of a set of tubes, in which water, coming from an underground cool storage or from a conventional chiller, flows. The tubes are equipped with fins in order to facilitate the thermal exchange with the room.

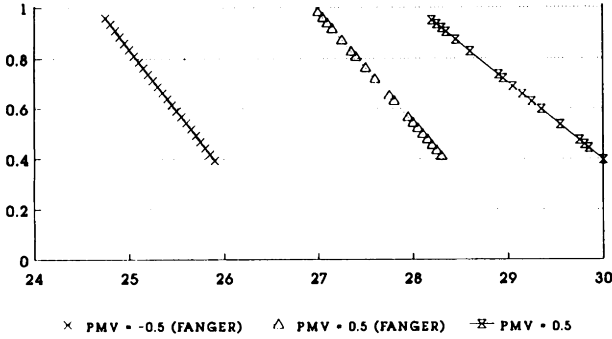


Fig. 3. Comfort ranges in the normal situation ( $T_{rm} = T_a$ ) and in the case study in relation with relative humidity and air temperature

Under the ceiling a row of electric fans provide the appropriate air movement, when the cooling effect of the radiant panel isn't strong enough to generate a comfortable environment (see figure 4).

The control of such a system is quite sophisticated, in the sense that a simulator of human thermal comfort is used (like it is done with the instruments, already in commerce, that analyze all the parameters of the Fanger equations).

There are two steps in the control strategy:

- a) when the PPD is higher than 5% the radiant cold ceiling is activated, in order to lower the surface temperature to a point that is always slightly higher than the dew point, to avoid condensation problems;
- b) when the PPD exceeds 6% the ceiling fans are activated, in order to increase the air velocity near the working persons to 0,8 m/sec.

This value of air velocity comes from the limit established by the ASHRAE (1981) in the case of use of ceiling fans (see figure 5).

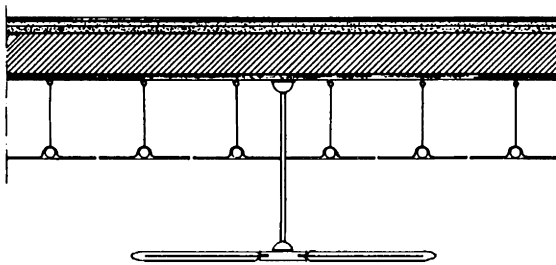


Fig. 4. Section of the false ceiling acting as a cool radiant panel and of the electric fan

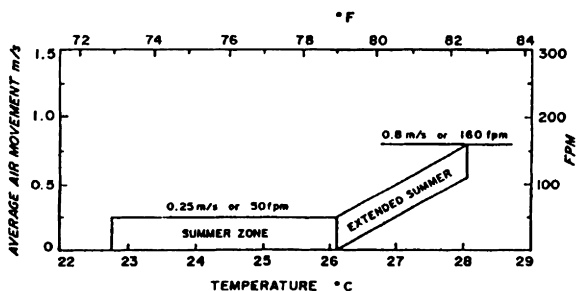


Fig. 5. ASHRAE extended summer comfort zone (ASHRAE, 1981)

It's important to note that such a system, although closely related to the dew point temperature of the room air, does not provide any modification of the latent heat balance of the room. Another relevant characteristic of this radiant equipment is its fitness to be also used during the winter season as a heater radiant panel: for heating purposes this technology is already available.

### THERMAL SIMULATION

In order to evaluate the effectiveness of this system, the energy consumption and the thermal comfort have been compared with those of a conventional cooling system.

An office of  $120 \text{ m}^3$ , with two external surfaces facing north and south and an envelope thermal loss of  $0.60 \text{ W/m}^3$ , has been analyzed for two climatic areas in central and southern Italy.

Table 1 reports the results of the simulation through July and August. As it is possible to note, the values of the energy demand for the conventional system and for the proposed one are quite different: the cooling panel configuration shows a remarkable lower amount of energy consumptions. On the contrary, the sum of the PPD over the considered period is much higher in the case of the cooling radiant panel. As the thermal comfort is a basic element for deciding whether to use or not the radiant panel, we need some more information about it. In Fig. 6 is presented, for example, the distribution of the PPD for the months of July and August in Crotone. From these kind of values it's possible to have an idea about the thermal performance of the system during the examined time and of the periods of better utilizability.

	Cooling system	Energy demand (kWh)	PPD cumulative sum
ROME	Conventional	1677	350
	Radiant panel	789	773
CROTONE	Conventional	1687	379
	Radiant panel	783	809

Tab. 1. Results of the simulations for the months of July and August



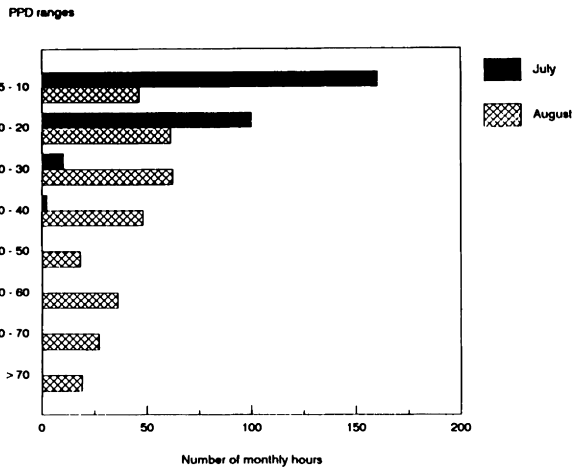


Fig. 6. Distribution of Percentage of Persons Dissatisfied (number of hours during July and August in Crotona)

## CONCLUSIONS

The cooling system here presented demonstrates to be an effective tool in getting a lower energy consumption for the building climatisation. Of course, great attention should be paid to the comfort situations inside the building, that represents an important element in order to decide the use of the system. Since the system is very dependent on the specific building and climate characteristics, careful analysis should be done in order to evaluate the possibility of its application.

## REFERENCES

- Butera, F., Farruggia, S., Rizzo, G., Silvestrini, G. (1984). Il codice di calcolo SMP per la simulazione del comportamento termico di moduli edilizi solari passivi e convenzionali. *Quaderni dello IEREN/CNR*, 1.
- Fanger, P.O., Ipsen, B.M., Langkilde, G., Olesen, B.W., Christensen, N.K., Tanabe, S. (1985). Comfort limits for asymmetric thermal radiation. *Energy and buildings*, 8, 225-236.
- Fanger, P.O., Bahidi, L., Olesen, B.W., Langkilde, G. (1980). Comfort limits for heated ceilings. *ASHRAE Trans.*, 86 (2), 141-156.
- Moderate thermal environments. Determination of the PMV and PPD indices and specification of the conditions for thermal comfort. *ISO 7730*.
- ANSI/ASHRAE Standard 55. (1981) Thermal environmental standards for human occupancy. American Society of Heating, Refrigerating, and Air-Conditioning Engineering.

AN ESTIMATION METHOD OF MONTHLY AVERAGE  
DAILY GLOBAL SOLAR RADIATION ON THE AMBIENT  
AIR TEMPERATURE

M.M.KENISARIN and N.P.TKACHENKOVA

Thermophysical Department  
Uzbek SSR Academy of Sciences  
700135 Tashkent, USSR

ABSTRACT

In present report a simple method of estimation of the monthly daily global solar radiation on monthly daily ambient air temperature is suggested. For determination of regression equation connected noted above values the Fourier series are used. The developed method are used for determination of the solar radiation for 16 location of Uzbekistan and Tadjikistan.

KEYWORDS

Solar radiation, ambient air temperature, simulation

INTRODUCTION

Solar radiation incident on horizontal surface are observed by many meteorological stations. The sunshine hours duration are recorded also on several stations. Suggested in literature correlations (Dibirov and Makhmudov, 1982; Kenisarin *et al.*, 1988; Ma and Iqbal, 1984) permit to estimate of solar radiation on sunshine hours duration. However the distribution of noted stations on the territory of each country is uneven. As known there are many locations where the ambient temperature are registred. To our mind the ambient temperature data can be serve valuable basis for estimating of global solar radiation. The present work deal with the determination of correlation between average daily global solar radiation incident on horizontal surface and average monthly air temperature in same location.

THE METHOD OF ESTIMATION

As known the air temperature is the function of global solar radiation incident on a given geographical location. Therefore

the determination of conversly dependence of the global solar radiation from the ambient temperature has the large practical interest. The global solar radiation and ambient temperature changes have periodical character. However the amplitude this changes in each location can be different from each other significantly. Therefore it is more convenient to consider the dimationless radiation and the ambient temperature change character:

$$\theta_h = (H - H_{\min})/\Delta H \quad (1)$$

and

$$\theta_t = (T - T_{\min})/\Delta T \quad (2)$$

where  $\Delta H = H_{\max} - H_{\min}$  and  $\Delta T = T_{\max} - T_{\min}$

Figure 1 shows typically monthly variation of the dimationless solar radiation,  $\theta_h$  and ambient temperature,  $\theta_t$  for conditions of Tachiotash. As shown the character of these variations is periodical. In this case the variations of  $\theta_h$  and  $\theta_t$  can be written by Fourier series

$$\theta_{h,N} = \frac{A_{h,0}}{2} + \sum_{k=1}^{\infty} [A_{h,k} \cos(\pi k N/6) + B_{t,k} \sin(\pi k N/6)] \quad (3)$$

and

$$\theta_{t,N} = \frac{A_{t,0}}{2} + \sum_{k=1}^{\infty} [A_{t,k} \cos(\pi k N/6) + B_{t,k} \sin(\pi k N/6)] \quad (4)$$

For the difference  $\theta_{h,N}$  and  $\theta_{t,N}$  we have

$$\theta_{h,N} - \theta_{t,N} = \frac{A_0}{2} + \sum_{k=1}^{\infty} [A_k \cos(\pi k N/6) + B_k \sin(\pi k N/6)] \quad (5)$$

where

$$A_0 = (A_{h,0} - A_{t,0})/2 ;$$

$$A_k = (A_{h,k} - A_{t,k}) = \frac{2}{12} \sum_{N=1}^{\infty} (\theta_{h,N} - \theta_{t,N}) \cos(\pi k N/6), \quad k=1, 2, 3, \dots \quad (6)$$

$$B_k = (B_{h,k} - B_{t,k}) = \frac{2}{12} \sum_{N=1}^{\infty} (\theta_{h,N} - \theta_{t,N}) \sin(\pi k N/6), \quad k=1, 2, 3, \dots \quad (7)$$

From Eqs.5 and 1 we have

$$H_N = H_{\min,N} + \Delta H_N \{ \theta_{t,N} + A_0 + \sum_{N=1}^{\infty} [A_k \cos(\pi k N / 6) + B_k \sin(\pi k N / 6)] \} \quad (8)$$

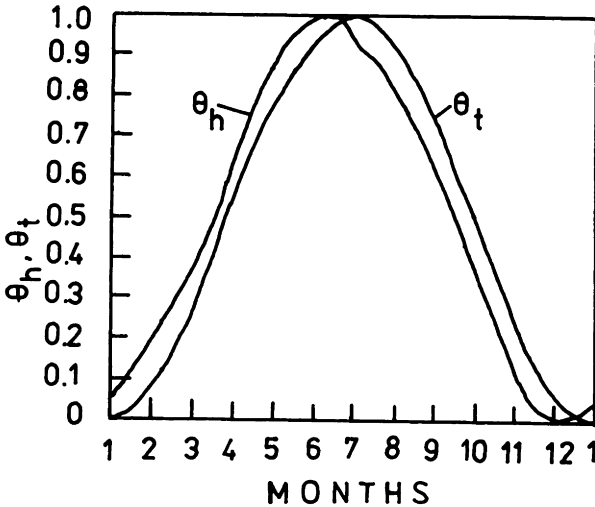


Fig. 1. Dimensionless solar radiation and ambient air temperature changes from months

According Dijakonov (1987) Fourier coefficients found from Eqs.6 and 7 for harmonics number  $m=N/2$  give the minimal standard deviation [4]. We have, as known, only the average monthly daily solar radiation and average monthly daily ambient temperature. In given case  $N=12$  and we can limited in Eq.8 only first six members of Fourier series

$$H_N = H_{\min,N} + \Delta H_N \{ \theta_{t,N} + A_0 + \sum_{N=1}^6 [A_k \cos(\pi k N / 6) + B_k \sin(\pi k N / 6)] \} \quad (9)$$

Using Eqs.6.7 and 9 we can find monthly daily global solar radiation the dependence from monthly daily ambient temperature if we have the data on solar radiation and ambient air temperature in neighbour locations.

## THE RESULTS

Noted above equations were used for determination of Fourier series coefficients for several meteorological stations showed partially in Table 1.

Observed data are grouped in dependence from the nearness of stations each other.  $H_{\min}$ ,  $\Delta H$  and  $\theta_t$  are found by averaging of each group stations data. Typical coefficients of Fourier' series are presented at Table 2. These coefficients were used for determination of the monthly average daily global solar

Table 1. Monthly average daily ambient air temperature and global solar radiation for several reference locations

Mon	Tashkent		Samarkand		Fergana		Chardjou		Termez	
	t	H	t	H	t	H	t	H	t	H
Jan	0.9	6.2	-0.3	7.2	3.2	6.7	0.6	7.7	1.4	8.3
Feb	2.0	8.7	2.3	9.4	0.6	10.0	3.5	12.0	4.9	11.4
Mar	7.6	12.2	7.2	12.0	7.8	13.2	9.3	15.4	11.3	15.1
Apr	14.4	17.6	13.7	17.4	5.2	18.6	16.8	20.5	17.7	20.5
May	20.0	23.2	19.2	22.8	0.8	23.9	23.0	27.8	24.1	25.7
Jun	24.7	26.7	23.5	27.5	4.6	27.3	27.4	30.3	27.5	29.3
Jul	26.9	27.1	25.5	27.5	6.8	26.7	29.2	29.0	29.6	28.0
Aug	24.9	24.4	23.7	25.3	5.0	24.8	27.2	26.9	27.4	25.6
Sep	19.4	19.5	18.8	20.6	9.6	20.1	21.2	21.8	22.3	21.8
Oct	12.6	12.7	12.5	13.6	2.6	13.6	14.2	16.1	15.1	15.5
Nov	6.4	7.7	6.5	8.1	5.6	8.2	7.1	9.9	8.5	10.2
Dec	1.6	5.4	2.1	6.1	0.4	5.4	2.5	6.9	4.6	7.5

t is ambient air temperature, °C; H is global solar radiation, MJ/m<sup>2</sup>

Table 2. Fourier series coefficients

Tashkent-Samarkand-Fergana			Chardjou-Termez	
$A_0 = -0.0275396$			$A_0 = -0.0109873$	
$A_1 = -0.0534929$	$B_1 = 0.0707350$		$A_1 = -0.0340606$	$B_1 = 0.0827031$
$A_2 = 0.0138270$	$B_2 = 0.0441261$		$A_2 = 0.0062042$	$B_2 = 0.0166757$
$A_3 = -0.0225002$	$B_3 = 0.0328554$		$A_3 = -0.0343792$	$B_3 = 0.0251656$
$A_4 = -0.0008973$	$B_4 = -0.0014995$		$A_4 = -0.0000621$	$B_4 = -0.0070008$
$A_5 = -0.0097599$	$B_5 = -0.0022033$		$A_5 = -0.0108903$	$B_5 = -0.0009188$
$A_6 = -0.0012479$	$B_6 = -0.0000004$		$A_6 = 0.0049867$	$B_6 = -0.0000002$

radiation for several locations of Uzbekistan and Tadjikistan showed on Fig.2.

The deviations of predicted solar radiation from observed ones for reference group stations are given in Table 3. From this Table is shown that the maximal deviations are observed for winter months (December and January) when the weather is not stable. Standard deviation for Tashkent-Samarkand-Fergana group stations is less than 5% at maximal value 11.7%. The maximal deviation for the period from April till October less than 4%. Data for Tachiataash showed that instrumental error of suggested method is insignificant. Therefore the accuracy of considered method are determined by stability of weather in separate locations and nearness of reference stations where is registered of solar radiation and ambient air temperature. Noted above method was used for prediction of the monthly average daily global radiation incident on horizontal surface for several locations of Uzbekistan and Tadjikistan. These data are presented in Table 4.

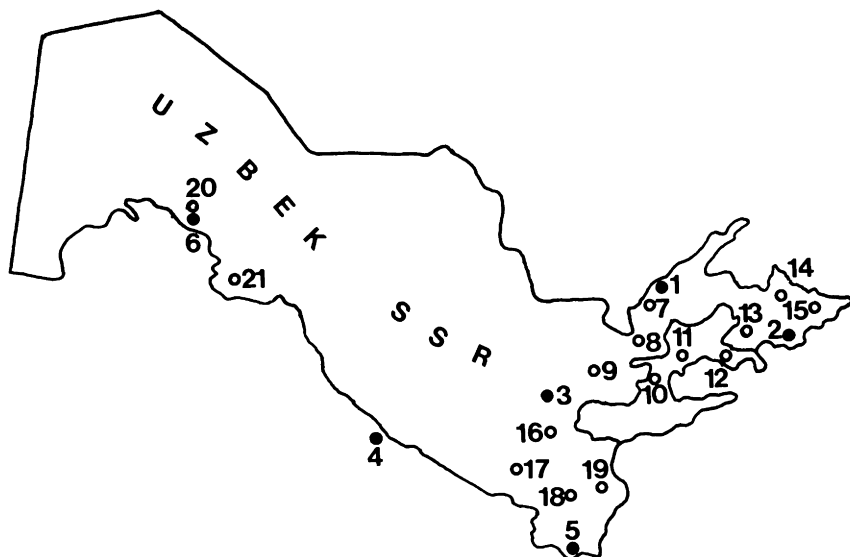


Fig. 2. Location of several meteorological stations of Central Asia: 1-Tashkent, 2-Fergana, 3-Samarkand, 4-Chardjou, 5-Termez, 6-Tachiataash, 7-Chinaz, 8-Gulistan, 9-Djizak, 10-Leninabad, 11- Isfara, 12- Ura-Tube, 13-Kokand, 14- Namangan, 15- Andijan, 16-Kitab, 17- Karshi, 18- Baisun, 19- Denau, 20- Nukus, 21- Urgench

Table 3. Deviation of predicted values of solar radiation from observed values, %

Month	Tash	Sam	Fer	Char	Ter	Tach
January	8.3	-6.8	0.2	3.2	-4.3	-1.7
February	5.9	-2.1	3.0	-4.1	5.1	1.1
March	-0.5	-1.5	2.0	-4.8	4.9	-0.8
April	-0.9	-0.7	1.1	-0.7	1.3	0.6
May	-1.2	1.0	0.3	-4.1	3.7	-0.4
June	1.5	1.3	0.3	-1.0	1.4	0.4
July	0.1	-1.4	1.5	-2.0	1.7	-0.4
August	1.3	-2.1	0.7	-1.9	2.3	0.5
September	1.5	-2.9	1.7	-1.2	0.8	-0.6
October	1.7	-3.4	1.5	-2.2	2.9	0.8
November	1.1	-3.7	3.0	-1.9	0.7	-1.3
December	-0.4	-10.7	1.7	-2.5	3.8	2.0

Table 4. Monthly average daily global solar radiation incident on horizontal surface for several locations of Uzbekistan and Tadjikistan, MJ/m<sup>2</sup>

Loc	Jan	Feb	Mar	Apr	May	Jun	Jul	Aug	Sep	Oct	Nov	Dec
Chi	6.7	9.5	13.2	18.5	24.0	27.7	27.1	24.8	20.1	13.4	7.9	5.4
Gul	6.7	9.6	13.0	18.4	24.0	28.8	27.1	24.5	19.7	13.5	8.0	5.5
Dji	6.7	9.0	11.6	16.9	22.7	27.0	27.1	24.9	20.0	13.0	7.4	5.1
Len	6.7	9.2	12.3	18.1	23.7	27.7	27.1	24.9	19.8	12.8	7.0	4.3
Isf	6.7	10.0	12.4	18.4	23.9	27.5	27.1	25.4	20.2	13.3	7.5	5.0
Ura	6.7	9.0	11.1	16.4	22.2	26.6	27.1	24.5	19.2	12.8	7.0	4.8
Kok	6.7	9.4	13.2	18.8	24.0	27.4	27.1	24.9	20.1	13.2	7.7	5.5
And	6.7	9.5	13.6	18.8	24.0	27.5	27.1	25.1	20.8	14.3	8.5	6.2
Nam	6.7	10.0	13.6	19.0	24.0	27.4	27.1	24.7	20.4	13.8	8.5	6.1
Kit	7.9	11.5	14.0	19.1	24.7	28.8	28.5	26.7	21.6	15.8	10.6	7.8
Kar	7.9	12.6	14.6	19.4	25.3	29.4	28.5	26.3	21.3	15.5	10.1	7.3
Den	7.9	11.8	14.9	20.0	25.6	29.4	28.5	25.9	21.4	15.9	11.1	7.7
Bal	7.9	10.7	13.0	18.0	24.0	28.6	28.5	26.5	22.1	16.5	11.3	7.9
Guz	7.9	11.5	13.9	19.0	25.0	29.3	28.5	26.6	22.2	16.1	10.4	7.4
Nuk	6.5	10.3	13.8	20.3	25.4	28.0	26.4	23.9	19.2	13.8	8.3	5.8
Urg	6,5	10.7	14.0	20.5	25.4	28.2	26.4	24.0	19.1	13.7	8.4	5.9

### CONCLUSION

In this work the new method of the determination of monthly average daily global solar radiation is suggested. Obtained results shows that it may be successfully used for estimation global solar radiation on the ambient air temperature if we have mentioned above data for neighbour locations. The accuracy of method is determined by the accuracy of reference data.

## REFERENCES

- Dibirov M.G., I.S.Makhmudov (1982) To the determination of global solar radiation by calculation method, *Gellotechnika*, No.3, 73-74
- Djakonov V.P.(1987). *Handbook on algorithms and programs on the BASIC for personal computer*, Nauka, Moscow
- Kenisarin M.M., A.I.Shafeev, N.I.Pilatova (1988). The correlation between solar radiation and sunshine hours, *Gellotechnika*, No.6, 62-69
- Ma C.C.Y., M.Iqbal(1984) Statistical comparison of solar radiation correlation. 1. Monthly average global and diffuse radiation on horizontal surface, *Solar Energy*, 33, 143-148
- The Soviet Union* (Geographical Description in 22 volumes): Uzbekistan, Tadjikistan, Moscow, 1967
- USSR Climate Handbook*, v.19,30,31, Pt.1,2, Leningrad, 1966-67



## A METHOD OF DETERMINATION OF THE FLAT PLATE SOLAR ENERGY COLLECTOR OUTPUT

MURAT M. KENISARIN AND NATALIJA P. TKACHENKOVA

Thermophysical Department  
Uzbek SSR Academy of Sciences  
700135 Tashkent, USSR

### ABSTRACT

An equation permitting the estimation of flat plate collector output at fixed inlet and outlet temperatures of working fluid is suggested. The developed method for evaluation of annual and monthly output of several widespread collectors for climatic conditions of Tashkent (41°N), Kiev (50°N) and Leningrad (60°N). Presented method may be used for choosing the necessary type of collector in dependence on the forthcoming operate conditions without preliminary collector tests.

### KEYWORDS

Flat plate collectors, collector output

### INTRODUCTION

Solar energy collectors are widely used recent in space and water heating systems and technological processes. There are the various types of flat plate solar collector produced at present time. Therefore it is complicate on one hand to make the comparison analysis of the collector performance without experimental tests and on other hand to determine the field of their expedient utilization. The possibility of comparison analysis are limited by absence of the simple and universal method of solar collector output estimation. Below such method of determination of the solar flat plate collector output for fixed inlet and outlet temperatures of working fluid is given.

### THE METHOD OF DETERMINATION

Useful energy gain obtained from flat plate solar collector as known can be expressed (Duffie and Beckman, 1980) as

$$Q = A_c F_R [I(\alpha\tau) - U_L(T_i - T_a)] \quad (1)$$

where

$$F_R = \frac{GC_p}{A_c U_L} \left[ 1 - \exp\left(-\frac{A_c U_L}{GC_p} F'\right) \right] \quad (2)$$

- $A_c$  - collector area,  $m^2$ ;  
 $F_R$  - collector heat removal factor;  
 $I$  - solar radiation intensity,  $W/m^2$ ;  
 $\alpha$  - absorptance;  
 $\tau$  - transmittance;  
 $U_L$  - overall heat loss coefficient,  $W/m^2C$ ;  
 $T_i$  - inlet temperature of working fluid,  $C$ ;  
 $T_a$  - ambient air temperature,  $C$ ;  
 $G$  - flow rate,  $kg/s$ ;  
 $C_p$  - specific heat of working fluid,  $J/kgC$ ;  
 $F'$  - collector efficiency factor

Equation (1) is the base of the operated standard tests for flat plate solar collectors (Bankston, 1983; Frid, 1988; Moon, 1982; Moon, 1983). In tests the such standard parameters as  $F_R(\alpha\tau)$  and  $F_R U_L$  are determined. As shown from Eq. (2) the heat removal factor depends significantly on the total flow rate of working fluid and is mainly determined by operating conditions. Parameters  $F_R(\alpha\tau)$  and  $F_R U_L$  are usually determined for several fixed flow rates. Obtained in these conditions parameters are appeared then in the collector certificate. At real operating conditions  $F_R$  may be different from those which were obtained in the tests. This can be lead to the over-estimating predicted output in comparison with real output. Known also that the collector output depends significantly on the outlet temperature of working fluid. The Eq. (1) not gives such dependence in evident form. In that time it is interesting to investigate of collector output for any fixed inlet and outlet temperatures of working fluid.

Duffie and Beckman (1980) showed that the exponential component can be expressed as

$$\exp\left(-\frac{A_c U_L}{GC_p} F'\right) = \frac{I(\alpha\tau) - U_L(T_o - T_i)}{I(\alpha\tau) - U_L(T_o - T_a)} = \frac{A}{B} \quad (3)$$

where  $T_o$  - outlet temperature of working fluid.

Substituting Eq. (3) in Eq. (2) we have for the heat removal factor

$$F_R = - \frac{A-B}{B} \frac{F'}{\ln(A/B)} \quad (4)$$

Taking  $B-A=U_L(T_o-T_i)$  into account and substituting Eq. (4) into Eq. (10) we obtain

$$Q = - A_c U_L (T_o - T_i) \frac{F'}{\ln(A/B)} \quad (5)$$

or

$$Q = \frac{A_c F' U_L (T_o - T_i)}{\ln \frac{I(\alpha\tau) - U_L (T_i - T_a)}{I(\alpha\tau) - U_L (T_o - T_a)}} \quad (6)$$

The last expression establish the relationship between the collector output on one hand and the design parameters  $F', \alpha, \tau, U_L$  and the operating conditions  $I, T_i, T_o, T_a$  on other hand. The Eq. (6) permit to estimate the collector output at any times and any fixed temperatures of working fluid.

The annual collector output of collector with one squire meter of surface can be find by

$$Q = F'_L (T_o - T_i) \sum_{j=1}^{12} \frac{3600 n_j}{\ln \frac{I_j(\alpha\tau)_j - U_L (T_i - T_a)}{I_j(\alpha\tau)_j - U_L (T_o - T_a)}} \quad (7)$$

where subscript  $j$  corresponds the averaging of parameters for  $j$ -month;  $n_j$  is sunshine hours duration.

The output of collectors connected in series is considered by Kenisarin (1990) more detail.

#### THE RESULTS OF COMPARISON

The Eq. (7) was used for comparison analysis of seven most widespread flat plate solar fluid collectors. The calculations were fulfilled for Tashkent, Kiev and Leningrad climatic conditions. The output was carried out for various slope of

solar collectors. Presented below results were obtained for optimal slope angles. Collector efficient factor for all types of collector was 0.95. The typical calculation results of the annual specific output of several collectors are presented in Table 1. The Table presents the collectors output for most widespread working temperatures. More detail information about the output of all seven types collector can be find in (Kenisarın and Tkachenkova, 1990). Fig. 1 illustrates the

Table 1. Annual specific output of several types  
of the flat plate collectors,  $GJ/m^2$

$T_i$	$T_o$	Type of collector								
		Tashkent ( $41^{\circ}N$ )			Kiev ( $50.5^{\circ}N$ )			Leningrad ( $60^{\circ}N$ )		
C	C	1	2	3	1	2	3	1	2	3
10	30	4.23	4.23	4.61	2.22	2.33	2.66	1.51	1.64	1.93
10	40	3.76	3.95	5.51	1.90	2.15	2.59	1.21	1.49	1.88
10	50	3.23	3.67	4.41	1.51	1.96	2.53	0.89	1.32	1.82
10	60	2.53	3.36	4.30	1.02	1.75	2.46	0.34	1.12	1.76
10	70	1.72	3.03	4.19		1.23	2.39		0.91	1.70
10	80	0.75	2.65	4.09		0.83	2.32		0.62	1.64
10	90		2.15	3.98		0.16	2.24		0.08	1.58
10	100		1.57	3.86			2.17			1.51
20	40	3.43	3.74	4.41	1.70	2.01	2.53	1.06	1.38	1.82
20	50	2.94	3.46	4.31	1.35	1.83	2.47	0.77	1.21	1.77
20	60	2.30	3.16	4.21	0.90	1.63	2.40	0.29	1.03	1.71
20	70	1.55	2.85	4.10	0.23	1.41	2.33		0.83	1.66
20	80	0.68	2.48	4.00		1.14	2.26		0.56	1.60
20	90		2.01	3.89		0.76	2.19		0.08	1.53
20	100		1.47	3.78		0.15	2.12			1.49
30	50	2.63	3.25	4.22	1.17	1.69	2.41	0.64	1.11	1.72
30	60	2.05	2.96	4.12	0.77	1.50	2.32	0.24	0.94	1.66
30	70	1.36	2.66	4.01	0.19	1.29	2.27		0.75	1.61
30	80	0.60	2.31	3.91		1.04	2.20		0.50	1.55
30	90		1.87	3.80		0.69	2.13		0.07	1.49
30	100		1.35	3.69		0.13	2.06			1.43
40	60	1.77	2.75	4.02	0.63	1.37	2.28	0.19	0.84	1.61
40	70	1.20	2.46	3.92	0.15	1.17	2.21		0.67	1.56
40	80	0.53	2.14	3.82		0.94	2.15		0.44	1.50
40	90		1.72	3.71		0.62	2.08		0.06	1.44
40	100		1.25	3.60		0.12	2.00			1.38

Collector 1  $\alpha=0.9$ ,  $\tau=0.85$ ,  $U_L=8 W/m^2C$  (ordinary single  
glas collector)  
2  $\alpha=0.9$ ,  $\tau=0.85$ ,  $\tau=5$  (selective coating,  
single glas)  
3  $\alpha=0.92$ ,  $\tau=0.91$ ,  $\tau=2$  (Philips collector,  
1985)

calculation results for two typical mode of operation. Typical monthly output of collector can be find in Table 2. From Tables 1 and 2 obtain the comparison output of different solar collector for various operating temperature modes and climatic conditions.

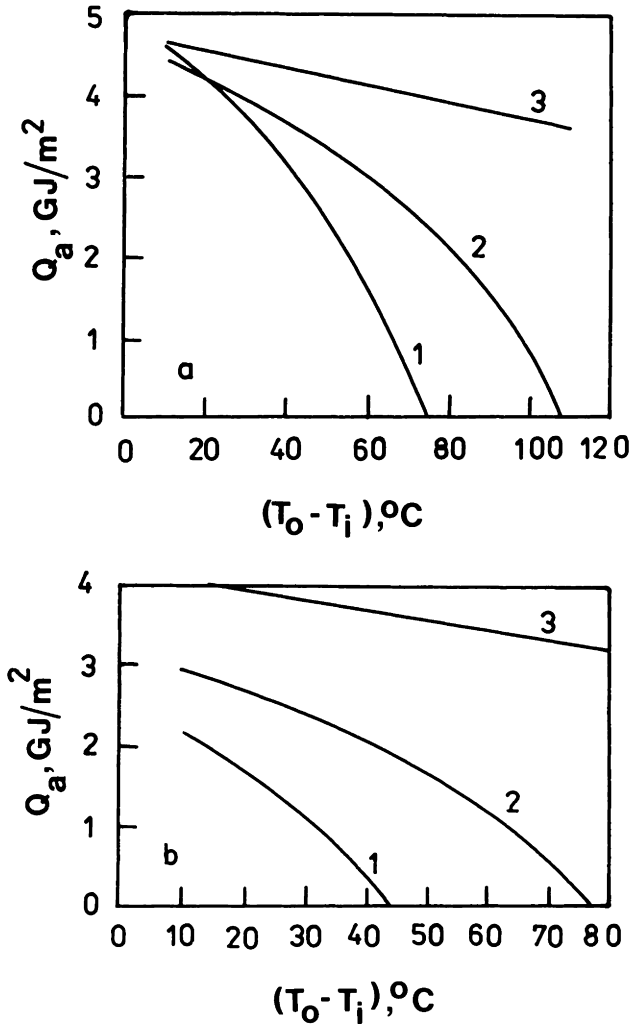


Fig. 1. Annual specific output of several collectors for Tashkent conditions:  
a -  $T_i = 10$ °C; b -  $T_i = 40$ °C

Presented here method permit to the consumers to make preliminary choosing of collector in the dependence on predicted operating conditions and planned place of operation.

For instance, as is seen from Table 2 for summer period at the operating mode  $T_i=10$  C and  $T_o=50$  C is recommended to use the collectors 1 and 2. For winter months and for high temperature modes can be recommend the collector 3.

Table 2. Typical monthly output of several flat plate collectors for Tashkent conditions, MJ/m<sup>2</sup>

Months	Type of collector					
	1			2		
	1	2	3	1	2	3
	$T_i=10$ C; $T_o=50$ C			$T_i=40$ C; $T_o=90$ C		
January	55	107	151	not	0	133
February	66	115	176	avai-	40	156
March	153	198	300	lable	86	219
April	257	289	355		136	300
May	374	408	476		202	400
June	459	477	535		244	447
July	531	540	593		300	503
August	511	527	586		287	497
September	399	429	506		232	433
October	241	292	368		136	311
November	126	170	226		59	190
December	57	101	140		0	129

#### REFERENCES

- Bankston C. A. (1983). *Basic Performance, Cost, and Operation of Solar Collectors for Heating Plants with Seasonal Storage*, Argonne National Laboratory Report ANL/ES-139
- Duffie J. A., W. A. Beckman (1980). *Solar Engineering of Thermal Processes*, John Wiley & Sons, New York
- Frid S. E. (1988). *Thermal Test Methods of Solar Collector*, IVTAN Preprint No. 3-248, Moscow
- Kenisarin M. M. (1990). Flat plate solar collectors output. 1. The method of determination, *Geliotechnika*, to be published
- Kenisarin M. M. and N. P. Tkachenkova (1990). Flat plate solar collectors output. 2. Calculation results, *Geliotechnika*, to be published
- Moon J. E. (1982). Editor, *Results and Analysis of a Round Robin Test Series Using Solar Simulators*, Luxemburg, CEC, EUR 8006
- Moon J. (1983), Editor. *Results and Analysis of a Round Robin Test Series Using a Evacuated Tubular Solar Collectors*, Luxemburg, CEC, 1983, EUR 8757
- Philips Evacuated Tubular Collector VTR 361 (1985). Advertising booklet

SOME RESULTS AND PROSPECTS OF THE USE OF SOLAR  
ENERGY IN MATERIAL STUDY AND PRODUCTION PROCESSES

V.V.PASICHNY

Institute for Materials Science of Academy of  
Sciences of the Ukr.SSR; 3, Krzhizhanovsky st.,  
Kiev-252180, USSR

ABSTRACT

It is reviewed a number of high temperature technological processes using solar energy: thermal treatment of steel, surface melting (vitrification) of building materials such as slag concrete and ceramic glazed plates, thermal cutting by melting of stainless steel and industrial fabrics of glass, silica and asbestos fibres. It takes place the estimation of efficient heat or energy outlay for these processes. The technical characteristics of some solar furnaces are presented.

KEYWORDS

Solar energy, solar furnace, thermal treatment of materials, thermocutting of materials.

A problem of the use of solar heat energy in material study and production processes consists, for the first hand, in finding out the processes which implementation nowadays or in the nearest future will prove to be correct for the given region in accordance with the economical and ecological estimates, for the second hand, in the development of reliable and sufficiently inexpensive solar plants to perform these processes on half-industrial and industrial scales.

The present work purpose is to demonstrate on a number of examples under the laboratory conditions the use of concentrated solar light heat energy in production processes, to show a possibility to, at least partially, replace the traditional energy sources by renewable ones.

The created experimental base promotes the successful performance of different experiments. The base includes 10 solar

furnaces with concentrators 1.0; 1.5; 2.0; 2.8 and 5.0 m in diameter, the last two being metal antennas with pasted facets, the other ones—high-accuracy glass mirrors of search light type. The characteristics of some plants are given in Table 1. All the devices are provided with photoelectrical

Table 1. Characteristics of solar plants

N	Plant index	Power kW	Ømirror (m)	Temperature T max (°C)	Øfocus (mm)	max heat flow (W/cm <sup>2</sup> )
1.	СЦ-2	1,2	1,5	3500	6,0	1500
2.	СЦ-4	1,8	2,0	3400	8,4	1200
3.	СЦ-5	1,8	2,0	3200	8,4	1200
4.	СЦ-6	3,5	2,8	1500	36	80
5.	СЦ-7	8,5	5,0	1500	70	80
6.	СЦ-9	0,7	1,0	2500	2,5	600

systems of automatic tracking the Sun, regulators of heat parameters, the other functional nodes and systems including the chambers with quartz windows to make experiments in vacuum and in the media different in chemical composition. Heat parameters in all the plants are certified using the calorimeters with water-cooled space simulating a blackbody. A special optoelectronic system of temperature measurements has been elaborated (Stegniy et al., 1979). It permits to make measurements in the infrared region in the solar spectrum troughs, which are the result of light absorption by vapours of water and carbon dioxide molecules.

A number of works made earlier at the Institute for Problems of Material Science has show a possibility to use solar furnaces for the study of physicochemical, radiative, thermophysical, mechanical and other physical properties of materials at high temperatures (Kuzovkov et al., 1972; Pasichny et al., 1978; Stegniyy et al., 1979).

A possibility of local thermal treatment of the component elements (teeth, pushers, cutting edges, etc.), which does not result in total heating of the article is of practical interest. The estimate of such a possibility was executed by heating of steel 38ХН3МФА specimens in the focal spot of the plant СЦ-4 (Maiboroda et al., 1986). When the specimen sizes did not exceed the focal spot volume, the steel hardness reached 50-53 HR<sub>C</sub>. But the local heating of the specimens, simulating the half-infinite body, resulted in the increase of hardness to 42-43 HR<sub>C</sub> only, the hardness outside the heating zone being 39 HR<sub>C</sub>. Comparative data of the microstructural analysis evidence for steel recrystallization during heating and, as a consequence, on its hardening. Low hardness in the heating zone is a result of the process of tempering under cooling due to the metal volume heating in the boundary areas. Thus, thermal treatment in the focal spot of the solar furnace



requires the allowance for the factors affecting this process in each separate case (thermophysical properties of the material, the dimensions of focal spot and heated object, etc.).

We think that the processes of the surface vitrification of building materials with the purpose to improve their operation characteristics, to impart new qualities or to change to existing power-intensive processes for the treatment using the renewable power sources can be especially promising as to industrial implementation. The results of the study of two processes are described below: decoration of slag concrete, consisting of the blast furnace slag and cement, and burning of ceramic glazed plates. The both processes were performed by the solar plant *СГУ-6* whose concentrator possessed relatively big focal spot and sufficiently high temperature.

Nowadays, the fire-jet sources of heat are used for the slag concrete decoration which gives the material nice paint and increases its service life owing to the increase of moisture and frost resistance. In our case the article was fastened on the position mechanism in the focal region of *СГУ-6* and automatically passed along the focal plane with the speed ensuring necessary quality of the surface fusion (Pasichny et al., 1986). Optimum conditions of processing have been determined.

The dependence of the slag concrete processing rate on the normal solar radiation is given in Fig. 1. The efficient heat

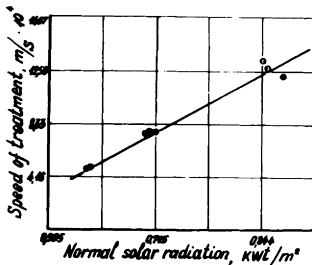


Fig. 1. Dependence of the speed of heat treatment of cement slag concrete on normal solar radiation.

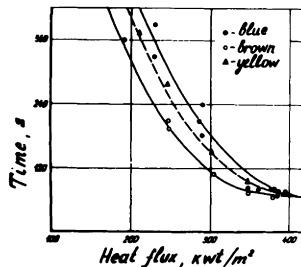


Fig. 2. Dependence of the time of heating of ceramic plates on the heat flow.

of the surface fusion  $H$  was determined as a comparative value characterizing the specific heat expenditures:

$$H = \frac{Q}{B \cdot V}, \tag{1}$$

where  $Q$  is the amount of supplied heat  $\frac{kJ}{sec}$ ;  $B$  - width of the fused zone, m;  $V$  - travel speed of the article in the focal spot, m/s. The efficient heat of the slag concrete article surface fusion obtained from the experimental data is about

13600 kJ/m<sup>2</sup> and this is in good agreement with heat expenditures in case of the use of plasma flow (Zolokitin et al., 1983).

The experiments on thermal treatment of glazed ceramic plates consisted in a single exposure of the specimen 32x30 mm<sup>2</sup> which is completely inscribed into the focal spot of the concentrator *СГУ-6*. Heating was decreased after reaching the uniform fusion of the whole surface. The dependence of heating time on the supplied heat flows for the plates of different colour is given in Fig. 2. The deviations for different compositions are the result of the difference in the emissivity factor. The carried out physicomachanical tests for the specimens burnt in the solar furnace as well as the analysis for water absorption, shrinkage and density have confirmed the complete correspondence of the glaze quality to the requirements of state standart. Calculation of specific expenditures of heat *H* according to the formula analogous to (1) evidences for the fact that, under the heat flows above  $3.5 \cdot 10^5 \text{ W/m}^2$  they are  $3 \cdot 10^7 \text{ J/m}^2$  at an average, which is 4 times as low as under the present production process based on the burning of natural gas. It can be partly explained by the individual character of treatment (absence of heat losses on the conveyer, exhaust gas etc.).

The laser separating cutting of materials is practised on a large scale for the last years. In particular, fusion cutting of industrial fabric permits evoding losses because of swingling of the fabric edges which is usual under mechanical cutting; it also permits reducing the demand of the difficult-to-obtain hard-alloy blade materials. We have estimated the potentialities of cutting by the concentrated solar light of the following industrial fabrics: asbestos fabric AT-1, silica fabric KT-II-TO, glass cloth T. The experiments were made by the plant *СГУ-9* with the concentrator with  $\phi 1.0 \text{ m}$  where the focal spot is less than 4 mm in diameter (Pasichny et al., 1985). Data of the experiments show (Fig. 3) that beginning

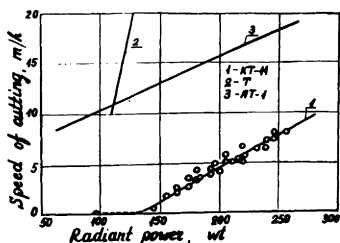


Fig. 3. Dependence of cutting speed of industrial fabric on the power

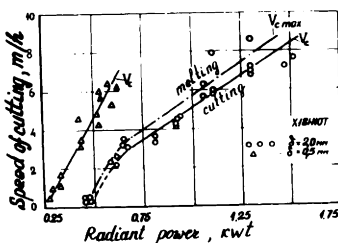


Fig. 4. Dependence of cutting speed of steel X18H10T on the power

from some minimum values the cutting rate is in direct proportion with the supplied energy, the angle of slope to the X-axis being decreased with the rise of the fabric melting point (cur-

ves 1 and 2). Specific energy expenditures are 160; 45 and 28 kJ/m for fabrics KT-11, AT-1 and T, respectively.

The experiments on cutting the alloy X18H10T were carried out by means of the plant *СГУ-5* in the air atmosphere. The sheet material 0.5 and 2.0 mm thick was cutted. The plant power was regulated by the change of the turning angle of the shutters. Dependences of the cutting speed on the energy supplied to the specimen are presented in Fig. 4. The data obtained allowed calculating the specific heat expenditures related to the unit of weight of the cut metal. In the range of the stable process of cutting at  $E_0=1.5$  kW it is about - 5600 kJ/kg (Pasichny et al., 1984).

In conclusion let us note, that there is no essential technical reasons preventing from the practical implementation of the described laboratory processes. The main obstacle is, apparently, the dependence of the use of solar energy on the weather and time conditions and this hampers the planning of industrial production. At the same time the discreteness of processes similar to the described ones, a possibility of their smooth outage and restoration practically at any moment permit retaining the hope to overcome this obstacle.

Thus, the described examples of the experimental use of concentrated solar energy, from our point of view, evidence for great potentialities of the substitution and economy of traditional energy resources in such power-intensive field as material study and production engineering.

#### REFERENCES

- Kuzovkov, E.G., V.S.Dvernyakov, B.A.Lyashenko, V.V.Pasichny, S.A.Kazimirov, N.L.Pozen (1972). Mechanical tests of layered plastic materials using solar plants. *Geliotekhnika*, 4, 47-52.
- Maiboroda, V.P., V.V.Pasichny, N.G.Palaguta, A.I.Stegniy, V.G.Krivenko (1986). Peculiarities of local heat treatment of steel *38XH3MΦA* in the focal spot of solar furnace. *Metalloved. i termobr. materialov*, 1, 59-60.
- Pasichny, V.V., V.S.Dvernyakov, E.S.Podlesnaya, A.D.Kondratenko (1978). Study of characteristics of heat destruction of materials under intensive radiant heating. *Coll. kosmicheskie issledovaniya na Ukraine*, 12, 65-89, Naukova Dumka, Kiev.
- Pasichny, V.V., I.E.Kasich-Pilipenko (1984). Study of the process of cutting by solar energy of the alloy X18H10T. *Geliotekhnika*, 3, 73-76.
- Pasichny, V.V., I.E.Kasich-Pilipenko, V.Ya.Berezhetskaya (1985). On the study of a possibility to cut industrial fabrics by the concentrated solar energy. *Geliotekhnika*, 5, 21-24.
- Pasichny, V.V., V.Ya.Berezhetskaya, G.A.Frolov (1986). On a possibility of decoration of building materials by concentrated solar energy. *Geliotekhnika*, 3, 30-33.
- Stegniy, A.I., A.V.Shevchenko, L.M.Lopato, A.K.Ruban, V.S.Dvernyakov, V.V.Pasichny (1979). Thermal analysis of oxides using solar heating. *Doklady Akademii Nauk. Ukr.SSR*, ser. A, 6, 484-487.
- Zolokitin, G.G., T.F.Romanyuk, N.K.Skripnikova (1983). Surface treatment of silicate articles using plasma technology. In: *The 9th All-Union Conference on High Temperature Plasma Generators*, pp. 284-285, ILIM, Frunze.

# OPTIMAL TEMPERATURE CONTROL OF THE SOLAR HEATING SYSTEMS

Dr. Mithat Uysal

Assoc. Prof. Technical University of Istanbul  
Faculty of Sciences and Letters  
80626 Maslak - ISTANBUL - TURKEY

## ABSTRACT

Temperature control systems based on solar and wind energy differ in two important ways from existing fossil fuel systems. One is that solar systems, at least active solar systems all have some kind of energy storage, the other is that the source of energy in a solar and wind energy system is variable and uncontrollable. Because of these added complications and the high capital investment required for solar and wind energy systems, considerably more sophisticated techniques are required for the design of those systems. In this study, a new technique is applied to the optimal control problem of the solar heating systems.

## SOLAR HEATING SYSTEM

The energy balance equation for the control volume around the storage tank takes into account the rate of energy lost from the tank to the surrounding  $Q_{tl}$ , the rate of solar energy collected  $Q_u$ , the rate of energy supplied to the house by the baseboard heaters  $Q_b$  and the rate of energy change in the storage tank in itself,  $Q_{st}$ :

$$\dot{Q}_{st} = \dot{Q}_u - \dot{Q}_{tl} - \dot{Q}_b \quad (1)$$

where

$$\dot{Q}_{st} = M_s C_p \frac{dT_s}{dt} \quad (2)$$

$M_s$ ,  $C_p$ ,  $T_s$  are the mass, specific heat and the temperature of the storage water respectively. The thermal loss through the tank walls  $Q_{tl}$  is given by:

$$\dot{Q}_{tl} = A_s U_s (T_s - T_r) \quad (3)$$

where  $A_s$  is the tank surface area,  $T_r$  is the room temperature,  $U_s$  is the overall heat transfer coefficient of the tank.

$Q_u$  is given by the following equation [2]:

$$\dot{Q}_u = A_c F_R (\dot{m}_c) [H_T \tau \alpha - U_L (T_s - T_a)] \quad (4)$$

where  $A_c$  is collector area,  $F_R$  is the heat removal factor, is defined as,

$$F_R (\dot{m}_c) = \frac{\dot{m}_c C_p}{A_c U_L} \left[ 1 - \exp \left( -\frac{F' U_L A_c}{\dot{m}_c C_p} \right) \right] \quad (5)$$

$m_c$  denotes the fluid flow rate in the collector,  $H_T$  denotes solar energy rate incident on tilted collector,  $T_i$  denotes temperature of fluid into collector and  $T_a$  denotes ambient temperature. Definition of other parameters may be found in Ref. [2]

The energy supplied to the house can be calculated as follows:

$$Q_b = m_r (C_p)_r (T_s - T_r) \quad (6)$$

where  $T_r$  is room temperature,  $m_r$  is room loop flow rate and  $(C_p)_r$  is coefficient of specific heat for room.

The energy balance equation for control volume around the room can be written as below :

$$(MC_p)_r \frac{dT_r}{dt} = Q_b + Q_{aux} - Q_L \quad (7)$$

where  $Q_b$  is the heat gain from the storage (equation 6),  $Q_{aux}$  is auxiliary heat energy rate,  $Q_L$  is heat losses from the room to the ambient.  $Q_L$  can be expressed as follows :

$$Q_L = U_r \cdot A_r (T_r - T_a) \quad (8)$$

where  $U_r$  is wall thermal conductance and  $A_r$  is the wall area.

OPTIMAL CONTROL OF THE SYSTEM

If  $\bar{T}_r$  denotes a desired set-point temperature for the room a possible "comfort index" is

$$J_C = \int_0^{t_1} (T_r - \bar{T}_r)^2 dt \quad (9)$$

while the measure of the auxiliary energy consumption over the interval  $(0, t_1)$  is

$$J_R = \int_0^{t_1} Q_{aux} dt \quad (10)$$

[3].

If state variables

$$X_1 = T_s - \bar{T}_s$$

$$X_2 = T_r - \bar{T}_r$$

are introduced, the above equations can be written in vector form

$$\dot{X} = (K_0 + F_R K_1 + m_r K_2) X + Q_{aux} B + v(t) \quad (11)$$

$K_0$ ,  $K_1$ ,  $K_2$  and  $B$  are given in the Appendix I. The control variables in this problem are  $m_c$  (or equivalently  $F_R$ ),  $m_r$  and  $Q_{aux}$ . The disturbance signal  $v(t)$  has components,

$$V_1(t) = [A_c F_R H_T \tau \alpha - A_c U_L (T_s - T_a) - U_s A_s (\bar{T}_s - \bar{T}_r) - m_r (C_p)_r (\bar{T}_r - T_a)] / (MC_p)_s \quad (12)$$

$$V_2(t) = [m_r (C_p)_r (\bar{T}_r - T_a) - (UA)_r (\bar{T}_r - T_a)] / (MC_p)_r \quad (13)$$

SOLUTION OF THE OPTIMAL CONTROL PROBLEM

As shown in Eq. (11), the dynamic equation for temperature control systems are nonlinear. However, the equations can be linearized by using the Taylor series approximation as shown in Appendix II. If we use this technique, then Eq. (11) will be transformed to the following equation :

$$\dot{X} = K_0 X + K_1 \bar{F}_R + K_2 F_R \left[ \begin{array}{l} (x - \bar{x}) \\ x - \bar{x}, F_R - \bar{F}_R \end{array} \right] + K_3 x \left[ \begin{array}{l} (F_R - \bar{F}_R) \\ x - \bar{x}, F_R - \bar{F}_R \end{array} \right] + K_4 \bar{x} \bar{m}_r$$

$$+ K_2 \bar{m}_r \left[ \cdot (x-\bar{x}) + K_2 x \left[ \cdot (m_r - \bar{m}_r) Q_{aux} B + v(t) \right] \right] \quad (11)$$

$x-\bar{x}, m_r - \bar{m}_r \quad x-\bar{x}, m_r - \bar{m}_r$

where  $\bar{\quad}$  notation represents the values near the optimal operating conditions. Eq. (11) can be rewritten in terms of  $x$ ,  $m_r$ ,  $F_R$  and  $Q_{aux}$  as below :

$$X = (K_0 + K_1 F_R \left[ \cdot \quad \quad + K_2 m_r \left[ \cdot \quad \quad \right] ) x + K_1 x \left[ \cdot F_R + K_2 x \left[ \cdot m_r + K_1 \bar{F}_R - K_1 F_R \right] \right] \right. \\ \left. \left[ \cdot \bar{x} \quad - K_1 x \left[ \cdot \bar{F}_R + K_2 \bar{x} \bar{m}_r - K_2 m_r \left[ \cdot \bar{x} \quad - K_2 x \left[ \cdot \bar{m}_r + B Q_{aux} + v(t) \right] \right] \right] \right] \right. \quad (12)$$

$x-\bar{x}, F_R - \bar{F}_R \quad x-\bar{x}, F_R - \bar{F}_R \quad x-\bar{x}, F_R - \bar{F}_R \quad x-\bar{x}, m_r - \bar{m}_r \quad x-\bar{x}, m_r - \bar{m}_r \quad x-\bar{x}, m_r - \bar{m}_r$

Eq. (12) is now in the form of the following equation :

$$\dot{x} = H_1 x + H_2 u + H_3 v \quad (13)$$

where  $u$  is an 3-dimensional control input vector representing  $m_r$ ,  $F_R$  and  $Q_{aux}$  and  $v$  is disturbance vector representing ambient temperature, insolation etc.  $x$  is an 2 dimensional state vector, representing temperature deviations from set points.  $H_1$ ,  $H_2$  and  $H_3$  are coefficients of  $x$ ,  $u$  and  $v$  in Eq. (12) respectively.

The control problem under considerations can be stated as follows. Determine the optimal control  $u(t)$  which minimizes the performance index

$$J(u) = \frac{1}{2} \int_0^{t_f} [x^T(t) Q(t) x(t) + u^T(t) R(t) u(t)] dt \quad (14)$$

subject to the dynamic constraints

$$\dot{x} = H_1(t) x(t) + H_2(t) u(t) + H_3(t) v(t) \quad (15)$$

and the initial conditions

$$x(0) = x_0 \quad (16)$$

where  $x(t)$  is an 2x1 state vector,  $u(t)$  is an 3x1 control vector,  $Q(t)$  is an 2x2 positive semi-definite matrix,  $R(t)$  is an 3x3 positive definite matrix, and  $H_1$  and  $H_2$  are respectively, matrices of dimensions 2x2 and 2x3,  $t$  is time parameter,  $t_f$  is the final time, and  $(\cdot)$  represents the time derivative.

It is well known that the optimal control  $u(t)$  for this system is

$$u(t) = R^{-1} H_1^T p(t) \quad (17)$$

where  $p(t)$  is an 2x1 costate (adjoint) variable vector that satisfies the following canonical equations :

$$\dot{x}(t) = H_1 x + H_2 R^{-1} H_1^T p(t) \quad (18)$$

$$\dot{p}(t) = Q x - H_1^T p(t) \quad (19)$$

subject to the terminal conditions :

$$x(t_f) = x_0 \text{ and } p(t_f) = 0 \quad (20)$$

In this study, the new method proposed by O.P Agrawal [4] is applied for solving the optimal control problem of the solar heating system.

If  $dx$  and  $dp$  are arbitrary virtual variations in the state and costate variables, respectively, then using an approach analogous to a variational virtual work approach and the Lagrange multiplier technique, (18) to (20) can be restated as

$$\int_0^{t_f} [\delta x^T W^s(t) (\dot{x}(t) - H_1 x - H_2 R^{-1} H_2^T p(t)) + \delta p^T W^c(t) (\dot{p}(t) - Q x + H_1^T p(t))] dt + \delta [\lambda_1^T (x(0) - x_0) + \delta [\lambda_2^T p(t_f)]] = 0 \quad (21)$$

where  $W^s(t)$  and  $W^c(t)$  are diagonal weighing coefficients matrices associated with virtual variations of state and costate variables, respectively, and  $\lambda_1$  and  $\lambda_2$  are each  $2 \times 1$  vectors of Lagrange multipliers. Matrices  $W^s(t)$  and  $W^c(t)$  may be written explicitly as

$$W^s(t) = \text{diag} [W_1^s(t), W_2^s(t), \dots, W_n^s(t)] \quad (22)$$

$$W^c(t) = \text{diag} [W_1^c(t), W_2^c(t), \dots, W_n^c(t)] \quad (23)$$

where  $W_i^s(t)$  ( $W_i^c(t)$ ) is the weighing coefficient associated with the  $i$ th component of  $\delta x$  ( $\delta p$ ). [4]

Equation (21) is the desired variational formulation for numerical solution of the two point boundary value problems.

### CONCLUSIONS

A new approach incorporating a variational virtual work with weighing coefficients and the Lagrange multiplier technique has been applied to the solar heating systems. In this method, the approximating functions need not satisfy the terminal conditions a priori.

A comprehensive numerical results of the problem will be presented in the next paper.

### REFERENCES

- [1] C.B. Winn, D.E. Hull, *Optimal Controllers of the Second Kind Solar Energy* Vol.23, pp. 529-534 (1979).
- [2] J.A. Duffie and W.A. Beckman, *Solar Energy Thermal Processes*, Wiley, New York (1974).
- [3] P. Dorato, *Optimal Temperature Control of Solar Energy Systems*, *Solar Energy*, Vol.30, No.2, pp. 147-153, (1983).
- [4] O.P. Agrawal, *General Formulation for the Numerical Solution of Optimal Control Problems*, *Int.J. Control*, 1989, Vol.50, No.2, 627-638.
- [5] K. Ogata, *Modern Control Engineering*, Prentice-Hall, Inc. Englewood Cliffs, N. J. (1970).

### APPENDIX I

The matrices  $K_0$ ,  $K_1$ ,  $K_2$  and  $B$  in Eq. (11) in the paper are given by,

$$K_0 = \begin{bmatrix} -U_s A_s / M_s (C_p)_s & U_s A_s / M_s (C_p)_s \\ 0 & -U_r A_r / M_r (C_p)_r \end{bmatrix}$$

$$K_1 = \begin{bmatrix} -A_c U_1 / M_s (C_p)_s & 0 \\ 0 & 0 \end{bmatrix}$$

$$K_2 = \begin{bmatrix} -(C_p)_r / M_s (C_p)_s & (C_p)_r / M_s (C_p)_s \\ (C_p)_r / M_r (C_p)_r & (C_p)_r / M_r (C_p)_r \end{bmatrix}$$

$$B = \begin{bmatrix} 0 \\ 1 / M_r (C_p)_r \end{bmatrix}$$

## APPENDIX II

### LINEARIZING OF THE NONLINEAR MODEL

Consider a nonlinear system whose output  $y$  is a function of the inputs  $x_1$  and  $x_2$ , so that

$$y = f(x_1, x_2) \quad (1)$$

In order to obtain a linear approximation to this nonlinear system, we may expand Eq. (1)

in to a Taylor series about the normal operating point  $\bar{x}_1, \bar{x}_2$ . Then Eq. (1) becomes

$$y = f(\bar{x}_1, \bar{x}_2) + \left[ \frac{\partial f}{\partial x_1} (x_1 - \bar{x}_1) + \frac{\partial f}{\partial x_2} (x_2 - \bar{x}_2) \right]$$

$$+ \frac{1}{2!} \left[ \frac{\partial^2 f}{\partial x_1^2} (x_1 - \bar{x}_1)^2 + \frac{\partial^2 f}{\partial x_1 \partial x_2} (x_1 - \bar{x}_1) (x_2 - \bar{x}_2) + \frac{\partial^2 f}{\partial x_2^2} (x_2 - \bar{x}_2)^2 \right] + \dots \quad (2)$$

where the partial derivatives are evaluated at  $x_1 = \bar{x}_1, x_2 = \bar{x}_2$ . Near the normal operating point, the higher-order terms may be neglected. The linear mathematical model of this nonlinear system in the neighbourhood of the normal operating condition is the given by

$$y - \bar{y} = P_1 (x_1 - \bar{x}_1) + P_2 (x_2 - \bar{x}_2) \quad (3)$$

where

$$\bar{y} = f(\bar{x}_1, \bar{x}_2)$$

$$P_1 = \left. \frac{\partial f}{\partial x_1} \right|_{x_1 = \bar{x}_1, x_2 = \bar{x}_2}$$

$$P_2 = \left. \frac{\partial f}{\partial x_2} \right|_{x_1 = \bar{x}_1, x_2 = \bar{x}_2}$$

[5]



## LOW COST SOLAR COLLECTOR - STORAGE SYSTEMS

Y. TRIPANAGNOSTOPOULOS and P. YIANOULIS

Department of Physics, University of Patras, Patras  
26 110, GREECE

### ABSTRACT

We have designed, constructed and tested two types of low cost solar water heaters. The first is a thermosiphon unit consisting of a flat plate collector in conjunction with a storage tank, using air as a heat exchange working medium, instead of liquid. The second is an integrated collector storage system, using a cylindrical collector-storage tank placed horizontally in a curved mirror envelope. With proper design and operation of these two types of water heaters we can improve their performance, approaching the efficiency obtained by the commonly used and more expensive solar water heaters.

### KEYWORDS

Solar water heater, thermosiphon system, air heater, integrated collector storage system.

### INTRODUCTION

The use of solar water heaters for low temperature applications, as for example for domestic hot water, has shown that there is a need for design and construction of units which combine low cost, good performance and durability. This will help their widespread use in many countries, with favourable meteorological conditions. The units which are commonly used now are of the thermosiphon and the integrated collector storage (ICS) types. Extensive study on these types in our laboratory has led to the design and development of improved models based on air collectors in conjunction with a storage tank for thermosiphon units, and low cost stationary concentrating ICS systems. The collector is based on the principle of the thermal trap for the reduction of thermal losses to the ambient, using air as a working fluid (Caouris et al. 1978).

### AIR THERMOSIPHON UNITS

For the thermosiphon case, particular interest deserves the design employing air as a heat exchange working medium, instead of liquid, used in common thermosiphon collectors. The advantages are: low cost of construction and extended durability, while the thermal efficiency is reduced compared to that with liquid working medium. Recent work on this type of solar heaters (Grupp et al. 1987) has shown that proper design and operation may improve the efficiency, approaching that of liquid medium thermosiphon

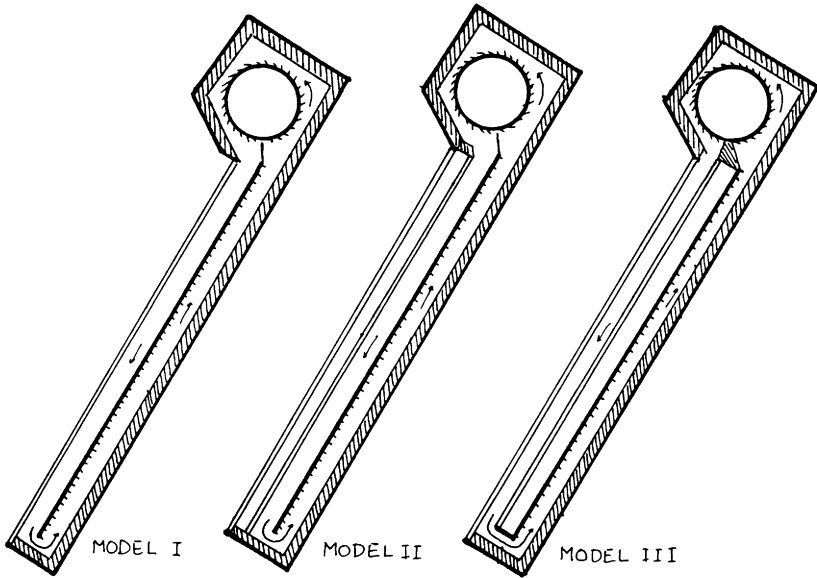


Fig. 1 Cross section of the air thermosiphon units.

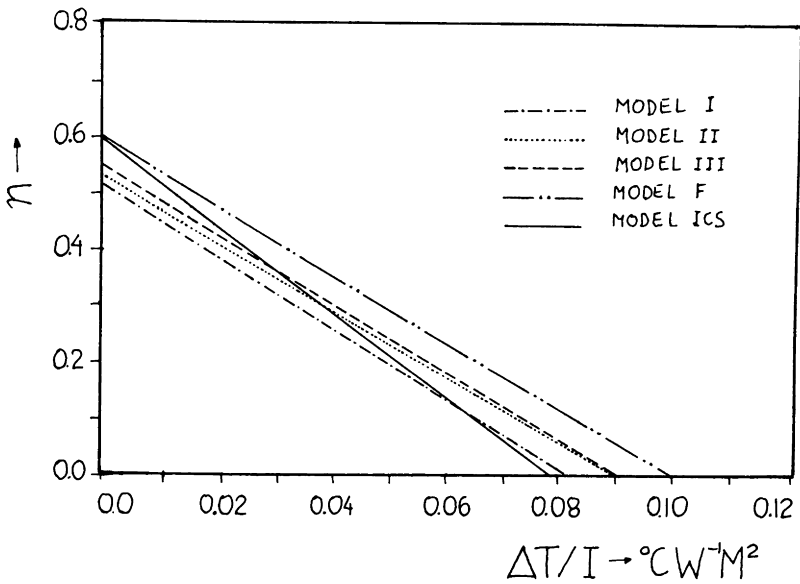


Fig. 2 Efficiency curves for the experimental models.

systems. Our aim is to improve the thermal efficiency of the thermosiphon air circulation between the collector and storage by the increase of the areas of heat exchange and the speed of air circulation.

In figure 1 we show three models operating in a similar way, regarding the thermosiphon air circulation. The lower part of the absorber is shaped in form of fins for increased area of heat exchange. For the same reason we have attached fins on the external surface of the cylindrical tank. This results in improved heat transfer from the hot air to the water in the tank. All three models use two air ducts, the lower used for the lift of hot air to the water tank and the upper for the air return. The ducts are separated from the absorber in models I and II, while for model III there is an interposed layer of hot trapped air acting as an insulator. All models are covered by transparent glass covers.

The experimental study of models I, II and III has taken place in field conditions and included also a common flat plate collector of the thermosiphon type (model F) for comparison. From the results we have calculated the average efficiency  $\eta$  during the day, for each model, as a function of the ratio  $\Delta T/I$ , shown in figure 2. We see that the thermal behaviour of the thermosiphon units with air, is approaching that of the thermosiphon units with water. The difference in efficiencies is mainly due to the smaller efficiency of the air collector, in comparison with the liquid collector, and the fact that the last was used without a heat exchanger (open system). The results show that the use of air collectors is a viable alternative to the thermosiphon units, taking into account cost and durability.

#### STATIONARY CONCENTRATING ICS SYSTEM

For the ICS type he have developed a series of models, which consist of a cylindrical storage-collector tank, in conjunction with a mirror for the increase of the collected solar radiation with the simultaneous reduction of the thermal losses from the tank (Tripanagnostopoulos *et al.*, 1987). In this article we present a simple design of an ICS system with low construction and maintenance cost. In figure 3 we show this inexpensive ICS model, which is constructed from an envelope of polished stainless steel sheet, the internal surface of which acts as a concentrating mirror. The cylindrical tank is placed horizontally and the sides are closed by two flat mirrors. A transparent glass cover is used for all models.

The low cost of the unit is mainly due to the compact and simple design, combined with the absence of additional elements for thermal protection, e.g.: double glazing, selective absorber and thermal insulation of the external mirror surface. This collector is also characterized by the ease of transport, installation and operation. This ICS unit has a satisfactory efficiency during the day for the water heating, but it has a problem in maintaining the hot water during the night (figure 4), because of the relatively high thermal losses to the ambient, from the tank surface. In figure 2 we have drawn, for comparison, the curve of average efficiency  $\eta$  during the day, of an ICS model together with the efficiency of the previous models. We note that the ICS model has a high value for the coefficient of thermal losses due to the minimum thermal protection, compared with the other systems.

On the basis of these guidelines the most efficient operation of the unit is when we use the hot water during the day and few hours after the maximum temperature time.

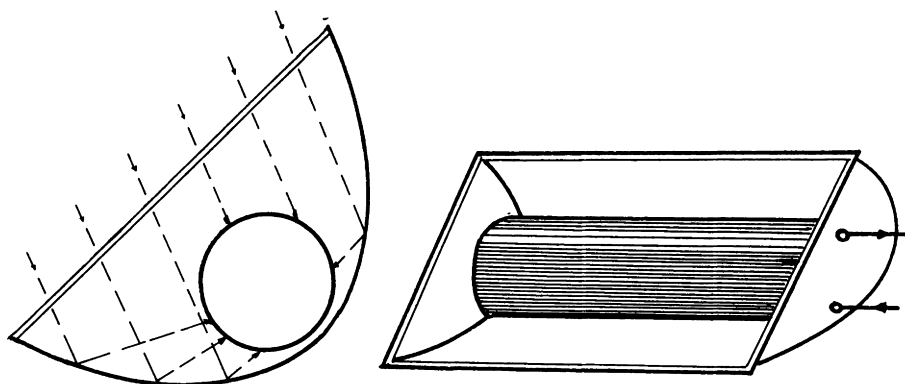


Fig. 3 The stationary concentration ICS model with horizontal cylindrical collector-storage tank.

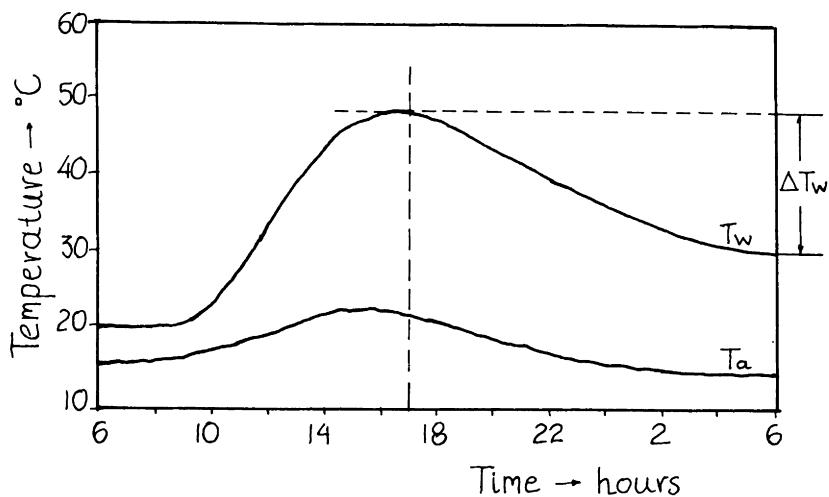


Fig. 4 Variation of mean water temperature of the ICS model without water draining.

However, for the preservation of hot water to cover the needs until late at night we must take some precautions for the thermal insulation of the hot water. For countries, where the water heating for domestic use is done mainly by electric water heaters as it is the case for Greece, there exists the possibility of economically efficient combination of existing water heating installation and ICS type units.

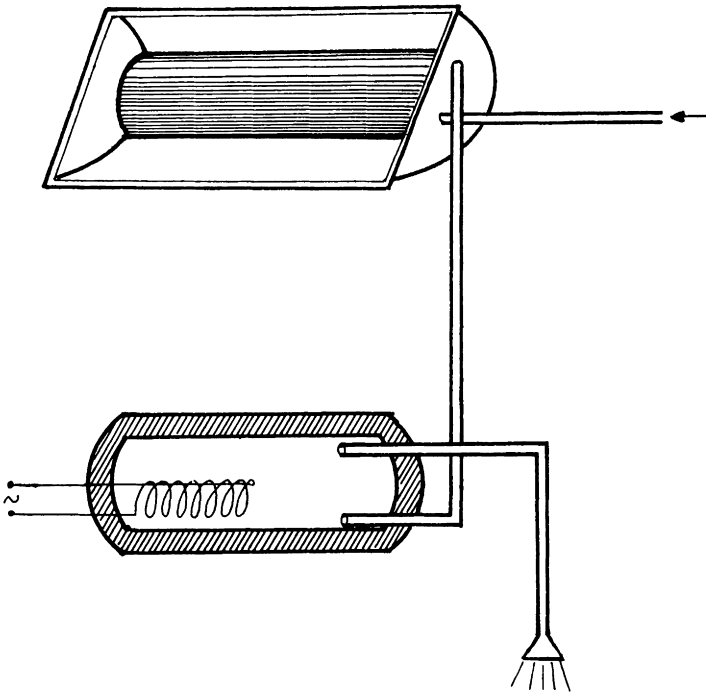


Fig. 5 Connection of an ICS unit in series with an indoor water electric heater.

In figure 5 we present a connection of an ICS unit in series with an indoor electric heater, which serves in the preservation of sufficient quantity of hot water as it passes through the well insulated second unit, if we use hot water during the day and early in the night. For the case of insufficient temperature of water we can operate the second auxiliary source of heat, giving the additional energy .

#### REFERENCES

- Caouris, Y., R. Rigopoulos, J. Tripanagnostopoulos and P. Yianoulis (1978). A novel solar collector. Solar Energy, 21, pp. 157-160.
- Grupp, M., B. Kromer and J. Cieslok (1987). Convective systems: The use of air in thermosiphonic flow in solar thermal systems. A new way forwards cost-efficient appliances. Advances in Solar Energy Technology, Proc. of Int. Conf (Hamburg) Vol.2, pp. 1086-1090.
- Tripanagnostopoulos, J. and P. Yianoulis (1987). Integrated Solar Collector Storage with minimized thermal losses. Applied Optics in Solar Energy II. Proc. of Int. Conf. (Praha) pp.297-299.

# ATTRACTIVE SMALL MARKETED HOT WATER SOLAR HEATING SYSTEMS USING LOW FLOW OPERATION

Simon Furbo  
Thermal Insulation Laboratory  
Building 118, Technical University of Denmark  
DK-2800 Lyngby  
Denmark

## ABSTRACT

Laboratory experiments have shown that solar heating systems using low flow operation perform extremely well.

Preliminary results from a demonstration project indicate, that the promising results for low flow systems in the laboratory can be transferred to systems in practice.

Work is necessary in order to reduce the cost of marketed low flow solar systems. If this work is successful highly attractive marketed solar heating systems making use of low flow operation will be available in the future.

## KEYWORDS

Solar heating systems, domestic hot water supply, low flow operation, laboratory experiments, marketed systems.

## INTRODUCTION

Investigations have shown (van Koppen *et al.*, 1979, Furbo *et al.* 1987, Hollands, 1988), that small solar heating systems using low flow operation and a heat storage, where thermal stratification is built up during sunny periods, are highly attractive.

The thermal performance of such a low flow system is greater than the thermal performance of a "traditional" solar heating system. Furthermore, the cost of a solar heating system can be reduced if the low flow principle is used.

## LABORATORY EXPERIMENTS

Since 1987 the thermal performance of different small solar heating systems for domestic hot water supply have been measured by means of side-by-side experiments at the laboratory, (Furbo *et al.*, 1987, Furbo, 1989). One of the tested systems have as the heat storage a hot water tank with a built-in heat exchanger spiral at the bottom of the tank. The solar collector fluid is pumped through the heat exchanger spiral with a normal flow rate. In this way the heat produced by the solar collectors is transferred to the hot water tank. This system is designed as most of the marketed solar heating systems in Denmark today.

Two identical solar heating systems with a hot water tank with a mantle welded around a part of the surface of the tank, were tested as well. The solar collector fluid is slowly pumped through the mantle from the top to the bottom. In this way it has been possible to determine optimum flow rate and control strategy for a solar heating system with a mantle heat storage.

The volume of each of the hot water tanks is 200 l, and electric heating elements are placed in the top of the tanks. In this way the water is also heated in periods without sunshine.

Identical marketed solar collectors are used in the solar heating systems, which are tested under uniform, realistic conditions.

The investigations showed that the mantle storage system performs best with volume flow rates in the solar collector loop between 0.1 and 0.2 l/min m<sup>2</sup> solar collector, a volume flow rate approximately 7 times smaller than the normal used volume flow rate.

The thermal performance of the mantle storage system is greater than the thermal performance of the heat exchanger spiral storage system.

Figure 1 shows the measured performance ratios between the net utilized solar energy for the mantle heat storage system and the net utilized solar energy for the heat exchanger spiral storage system as a function of the solar fraction for the heat exchanger spiral storage system for different test periods.

Performance ratio=

$$\frac{\text{Net utilized solar energy for the mantle storage system}}{\text{Net utilized solar energy for the heat exchanger spiral storage sys.}}$$

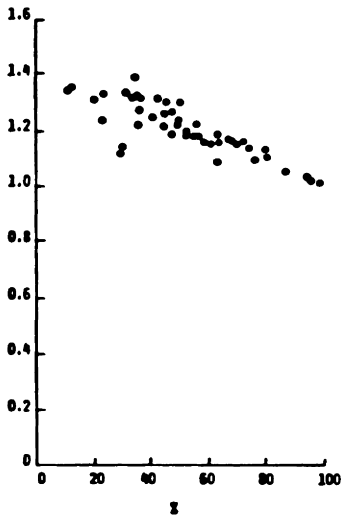


Fig. 1.  
Measured performance ratios for the mantle storage system as a function of the solar fraction for the heat exchanger spiral storage system.

Solar fraction for the heat exchanger spiral storage system.

Each point in the figure represent measurements for a test period of about 1 week. For instance, if a point indicates a performance ratio of 1.20, it means that the thermal performance of the mantle heat storage system was 20 % greater than the thermal performance of the heat exchanger spiral system in the period in question with a duration of about 1 week.

The thermal advantage of the mantle storage system is strongly influenced by the solar fraction. For decreasing solar fraction the thermal advantage of the mantle storage system is increasing. In periods with a solar fraction equal to 100 % for the heat exchanger spiral storage system, the solar fraction of the mantle storage system will also be 100 %, and so the performance ratio is equal to 1.00.

The main reason for the thermal advantage of the mantle heat storage system with a low flow rate is the large advantageous thermal stratification, which is built up in the heat storage of this system during operation of the solar collectors. Only a short period with sunshine is necessary for the water at the top of the tank to reach a temperature level, where the electric heating element will be turned off.

On a yearly basis, how much better perform the mantle heat storage system with low flow rate than the heat exchanger spiral storage system? In order to answer this question continuous measurements of the thermal performance of the two systems have been carried out since June 1989 so, the systems have now been in operation for a year. Each system has a 4.0 m<sup>2</sup> Danish marketed solar collector with a polypropylene absorber. The efficiency of the collector is:

$$\eta = 0.74 - 5.4 \cdot \frac{T_m - T_a}{I} - 0.018 \cdot (T_m - T_a)^2$$

The daily hot water consumption was 200 l, somewhat smaller however in June 1989. The results of the measurements are given in table 1.

The measured net utilized solar energy for the mantle storage system has been 17 % greater than the net utilized solar energy for the heat exchanger spiral storage system during the first year of continuous operation.

The net utilized solar energy for the mantle storage system for the first year of operation was 319 kWh/m<sup>2</sup> solar collector, corresponding to a solar fraction of 48 %. This is a good performance considering the relatively poor efficiency of the solar collectors and the Danish weather conditions.

The difference between the thermal performance of the systems would have been smaller if the daily hot water consumption would have been smaller than 200 l, while the difference between the thermal performance of the systems would have been greater with a greater daily hot water consumption.

#### SMALL MARKETED SOLAR HEATING SYSTEMS

Can the promising results for the low flow solar heating systems be transferred from the laboratory to practice? In order to answer this question a demonstration project was initiated in the spring of 1989. Three Danish producers of solar heating systems: Batec, Aidt Miljø ApS and Aroon Solvarme ApS participate in the project. Each producer build three small solar heating systems using low flow operation in different one family houses.

All the systems are equipped with kWh-meters in such a way, that the hot water consumption and the thermal performance of the systems will be measured during the first year of operation.



Table 1. Measured thermal performances of two 4.0 m<sup>2</sup> laboratory solar heating systems.

System	Month	Tapped Energy kWh	Energy supplied to the electric heating element kWh	Net utilized solar energy kWh	Solar fraction %	
Heat exchanger spiral storage system	June 89	172	35	137	80	
	July	225	63	162	72	
	August	225	85	140	62	
	September	202	91	111	55	
	October	202	151	51	25	
	November	220	189	31	14	
	December	248	232	16	6	
	Jan. 90	247	238	9	4	
	February	222	184	38	17	
	March	240	150	90	38	
	April	227	84	143	63	
	May	228	58	170	75	
	June 89 - May 90.	2658	1560	1098	41	
	Mantle storage system	June 89	172	25	147	85
		July	225	43	182	81
August		225	58	167	74	
September		202	70	132	65	
October		202	136	66	33	
November		220	177	43	20	
December		248	224	24	10	
Jan. 90		247	231	16	6	
February		222	171	51	23	
March		240	132	108	45	
April		227	62	165	73	
May		228	40	188	82	
June 89 - May 90.		2658	1369	1289	48	

Extra performance for mantle storage system.

7 %  
12 %  
19 %  
19 %  
29 %  
39 %  
50 %  
78 %  
34 %  
20 %  
15 %  
11 %  
17 %

## PRELIMINARY RESULTS

By the end of May 1990 six of the planned nine solar heating systems have been installed. Each system has a mantle hot water tank as the heat storage. The hot water tanks are at the top supplied with an electric heating element and/or a heat exchanger spiral in such a way, that the water at the top of the tank can be heated by means of an auxiliary energy source in cloudy periods. This is: The total hot water consumption is tapped from the heat storage of the solar heating system.

Some of the systems have been in operation without problems for months. The measured thermal performances of these systems are given in table 2. The thermal performances of the systems are as great as expected. The preliminary results from the first installed systems with low flow operation therefore indicate, that such systems also in practice can have high thermal performances and that the systems can operate without problems.

The measurements will be continued during the next year and experiences with different designs of low flow systems will be gained.

## CONCLUSION

Measurements have shown, that small marketed solar heating systems making use of low flow operation can have very high thermal performances. The net utilized solar energy for low flow systems can be up to about 20 % greater than the net utilized solar energy for normal solar heating systems.

Therefore there is a need to develop these marketed low flow systems in order to reduce the cost of the systems without decreasing the thermal performance of the systems. If such work is successful it will be possible to market highly attractive small low flow solar heating systems for domestic hot water supply in the future.

## ACKNOWLEDGEMENT

The investigations are financed by the Danish Energy Agency.

## REFERENCES

- Furbo, S. (1989). Solar water heating systems using low flow rates. Experimental investigations. Report no. 89-9, Thermal Insulation Laboratory, Technical University of Denmark.
- Furbo, S., Mikkelsen, S.E. (1987). Is low flow operation an advantage for solar heating systems? Advances in solar Energy Technology, Vol. 1, Proceedings of the Biennial Congress of ISES, Hamburg, 962-699.
- Hollands, K.G.T. (1988) Recent developments in low-flow, stratified tank solar water heating systems. Proceedings North Sun '88, Borlänge.
- van Koppen, C.W.J., Thomas, J.P.S. and Veltkamp, W.B. (1979). The actual benefits of thermally stratified storage in a small and medium size solar system. Sun II, Proceedings ISES Biennial Meeting, Atlanta, Ga, Vol. 2, 576-580.

Table 2. Measured thermal performance of solar heating systems using low flow operation in practice.

\* incl. heat loss for the circulation piping.

System	Month	Hot water consumption 1/day l/m <sup>2</sup> ·day	Average operation time for circulation pump h/day	Energy tapped from the tank kWh/month	Energy supply from: Electric heating element oil burner	Delivered solar energy: exclusive heat loss kWh/month	Delivered solar energy: inclusive estimated heat loss kWh/month	Solar fraction (inclusive heat loss) %	Delivered solar energy: exclusive heat loss per m <sup>2</sup> solar collector kWh/m <sup>2</sup> month	
Birtac: 6.5 m <sup>2</sup> Svenborg 6 occupants	July 89	163	6.7	191	0	191	253	100	39	
	August	178	6.5	228	0	228	290	100	45	
	Sept.	137	5.8	213	0	213	273	100	42	
	October	145	3.8	193	0	117	179	70	28	
	November	140	3.3	203	0	152	111	42	17	
	December	158	2.4	269	0	-88	-26	< 0	-	
	Jan. 90	161	2.5	273	0	357	22	7	3	
	February	161	2.5	234	0	189	45	35	16	
	March	169	2.6	273	0	113	160	66	34	
	April	193	3.0	337	0	28	309	93	57	
	May	275	4.2	576	1	575	637	100	98	
	Birtac: 6.5 m <sup>2</sup> Svenborg 5 occupants	July 89	176	6.9	235	12	223	285	96	44
August		206	7.0	287	30	208	270	87	42	
Sept.		187	6.8	239	17	219	275	93	43	
October		183	4.2	257	0	182	137	75	33	
November		190	2.8	273	0	49	109	35	17	
December		184	1.5	280	0	283	52	17	8	
Jan. 90		218	3.4	325	0	331	86	14	9	
February		216	3.5	304	0	262	42	27	15	
March		255	3.9	384	19	231	135	187	30	
April		245	3.8	385	0	115	237	207	46	
May		215	3.3	332	10	41	261	323	50	
Aldt: Nilsjö Ags 3.8 m <sup>2</sup> Barnhola 4 occupants		Sept. 89	192	5.8	195	90	105	165	65	43
	October	179	2.4	245	214	0	31	30	24	
	November	181	1.1	267	226	0	41	31	26	
	December	146	3.6	236	216	0	10	23	19	
	Jan. 90	196	5.1	335	304	0	31	24	24	
	February	146	3.8	254	200	0	54	29	29	
	March	138	3.6	261	172	0	89	39	39	
	April	160	4.2	278	127	0	151	211	55	
	May	164	4.3	367	97	0	190	252	66	
	Aldt: Nilsjö Ags 3.8 m <sup>2</sup> Madrian 2 occupants	Sept. 90	143	8.9	192	85	107	167	66	43
		May	149	9.6	191	44	147	209	83	54
	Birtac: 8.6 m <sup>2</sup> Garbofors 7 occupants	May 90	464	7.9	775 *	198	544	606	72	70

# CALCULATION OF THE THERMAL PERFORMANCE OF SMALL HOT WATER SOLAR HEATING SYSTEMS USING LOW FLOW OPERATION

Peter Berg and Simon Furbo  
Thermal Insulation Laboratory  
Building 118, Technical University of Denmark  
DK-2800 Lyngby  
Denmark

## ABSTRACT

Experiments have shown that small solar heating systems using low flow operation and a hot water tank with an enclosing mantle perform extremely well.

A detailed mathematical model simulating the thermal behaviour of such solar heating systems has been developed and validated by means of indoor experiments with a mantle heat storage.

The yearly thermal performance of different designs of and operation strategies for small low flow solar heating systems have been calculated. By use of the model it is possible to optimize the design of the system, the operation and control strategy of the system.

The calculated thermal performance of the low flow system is compared to the calculated thermal performance of a traditional solar heating system using a normal flow rate. The calculated increase of thermal performance of the low flow system is somewhat smaller than the measured increase of the thermal performance. Therefore, work is still necessary in order to validate the developed model by means of experiments with a complete solar heating system.

## KEYWORDS

Solar heating system, low flow operation, domestic hot water supply, mathematical model, validation, calculated yearly thermal performance, optimum design and operation strategy, comparison to traditional solar heating systems.

## INTRODUCTION

Investigations have shown (van Koppen *et al.*, 1979, Furbo *et al.*, 1987, Hollands, 1988), that small solar heating systems using low flow operation and a heat storage, where thermal stratification is built up during sunny periods, are highly attractive.

In connection with optimization of low flow systems a validated mathematical model which simulates the thermal behaviour of these attractive systems

will be a useful tool. Therefore work has been initiated in order to develop such a model. The results of this work have been reported (Berg, 1990). A summary is given in the following.

**MATHEMATICAL MODEL**

A schematically illustration of the solar heating system which is taken in calculation is shown in Fig. 1. The heat storage is a hot water tank with a mantle welded around the surface of the tank. This type of tank is commonly used in Denmark as a hot water tank. The solar collector fluid is slowly pumped through the mantle from the top to the bottom.

As shown in Fig. 1 a number of heat storage temperatures, corresponding to a number of control volumes in the water, in the solar collector fluid in the mantle and in the tank material, is taken in consideration. New control volume temperatures are calculated at each time step during the year. In periods with the solar collector in operation the time step is chosen in such a way that the volume of the solar collector fluid in each control volume of the mantle is replaced exact once during each time step. In this way numerical diffusion is avoided.

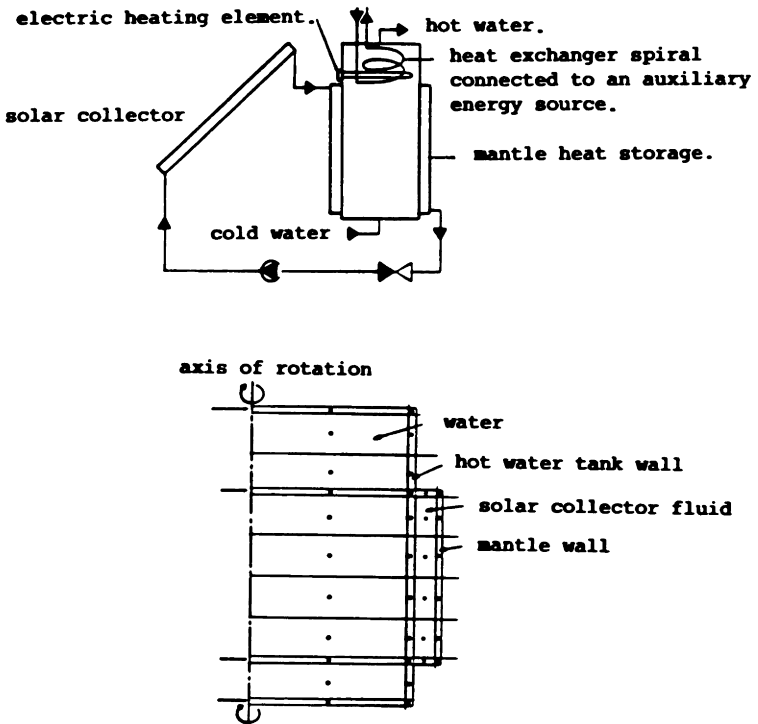


Fig. 1. Schematical illustration of the solar heating system taken in calculation and of the principle of the division of the heat storage in a number of control volumes.

## VALIDATION OF THE MODEL

The mathematical model has been validated by means of different experiments with a 200 l mantle heat storage in an indoor test facility. Tests with different inlet temperatures of the solar collector fluid were carried out.

Measured hot water tank temperatures were compared with calculated temperatures, for different quantities of heat transfer coefficients for the heat transfer between the solar collector fluid and the water in the heat storage. In this way the heat transfer coefficients were determined.

Figure 2 shows for a period with a typical behaviour of the solar collector fluid inlet temperature and two hot water tapings the measured and calculated outlet fluid temperature and heat storage temperatures. The calculated temperatures are in good agreement with the measured temperatures. The good agreement in the experiment shown in Fig. 2 and in a number of other experiments is only achieved by use of different quantities of the heat transfer coefficient between the solar collector fluid and the water for different operation conditions.

## CALCULATED RESULTS

The yearly thermal performance of the solar heating system shown schematically in Fig. 1 was calculated by means of the model. The solar collector area is 4.3 m<sup>2</sup> and the efficiency of the collector is  $\eta = 0.78 - 4.8 \frac{T_m - T_a}{I}$ .

The tilt of the south facing solar collector is 45°. The heat storage is a 200 l hot water tank with a 27 l mantle welded around the lower 5/6 of the vertical surface of the tank. The top of the tank is supplied with an electric heating element for the 5 summer months and a heat exchanger spiral for an oil burner for the 7 winter months.

The daily hot water consumption is 150 l heated from 10°C to 50°C and the Danish Test Reference Year is used as the weather data. Calculations were carried out with different designs and operation strategies. An example of the calculated auxiliary energy supplied to the heat storage as a function of the volume flow rate in the solar collector loop is shown in Fig. 3. The optimum volume flow rate determined in this way is 0.15 l/min m<sup>2</sup> solar collector.

## COMPARISON TO A TRADITIONAL SOLAR HEATING SYSTEM

Additional calculations with an existing model simulating the thermal performance of a traditional solar heating system with a hot water tank with a heat exchanger spiral situated at the bottom of the tank were carried out. The volume flow rate in the solar collector loop was 1 l/min m<sup>2</sup> solar collector.

Based on the results of these calculations and on the calculated thermal performance of the mantle heat storage system with a low flow rate, calculated performance ratios equal to the ratios between the net utilized solar energy for the traditional system were determined.

The corresponding measured performance ratios have been determined (Furbo, 1989, Furbo 1990). Figure 4 shows calculated and measured performance ratios for periods with a duration of one week. It is obvious that the models underestimate the advantage of the low flow systems a little.

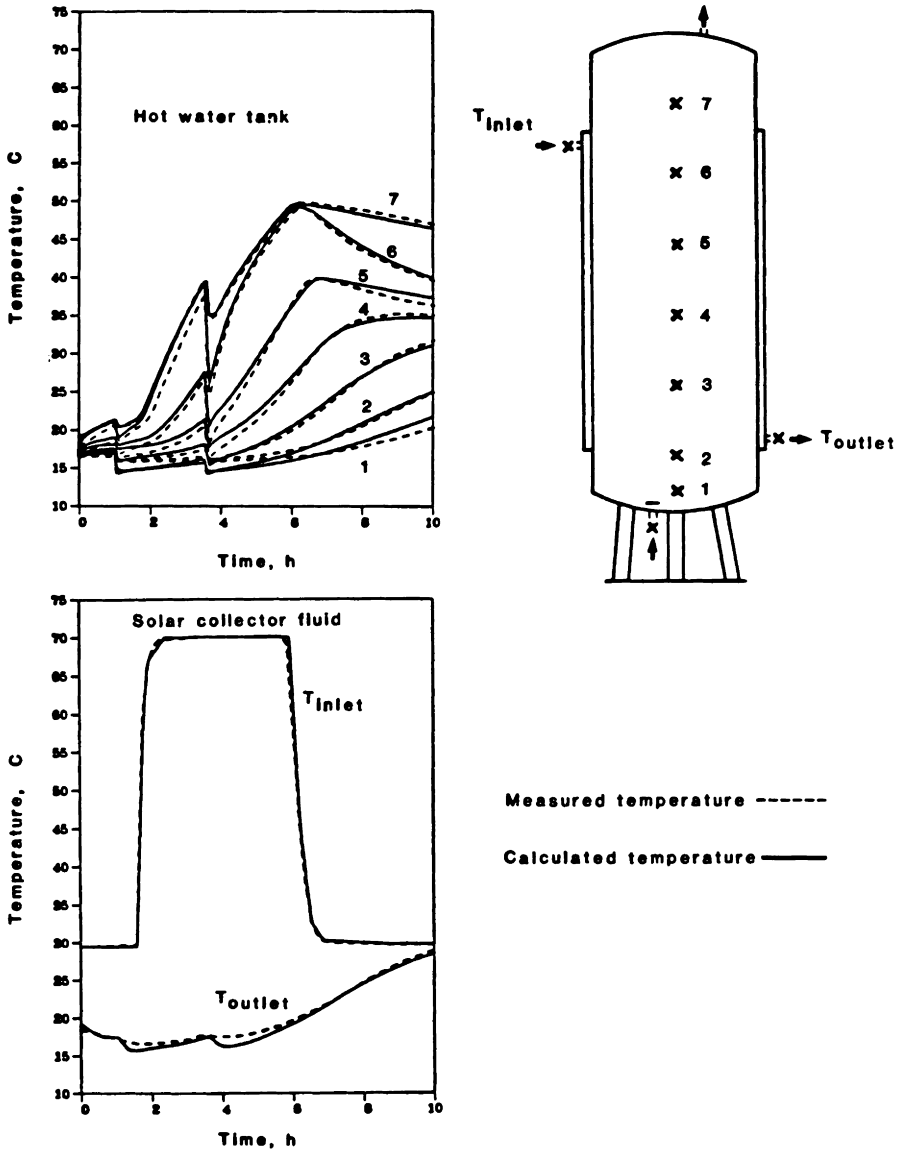


Fig. 2. Measured and calculated heat storage temperatures during a period of operation.

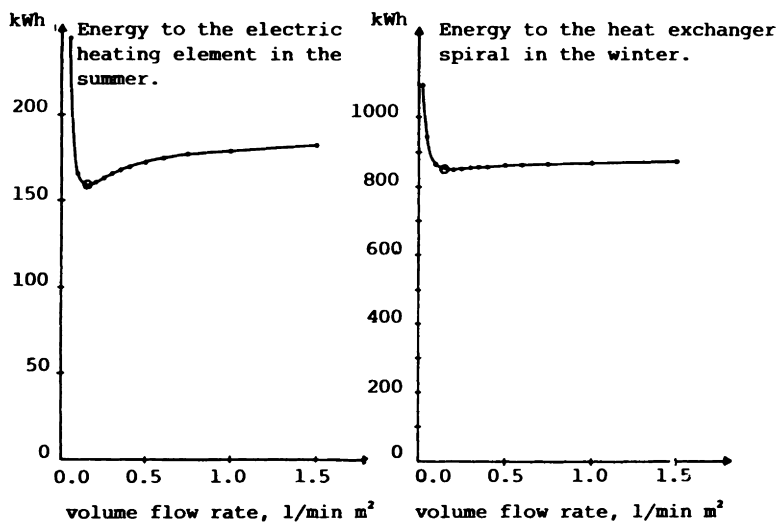
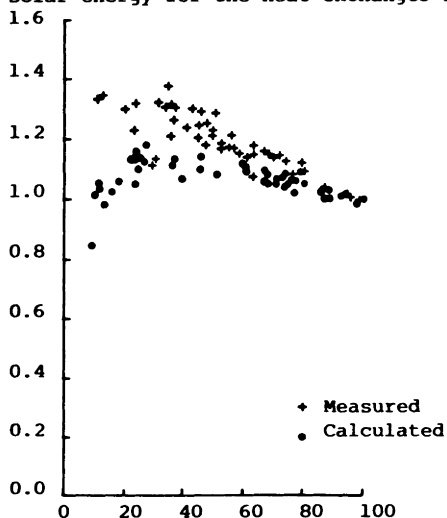


Fig. 3. Auxiliary energy supplied to the heat storage as a function of the volume flow rate in the solar collector loop.

Performance ratio=

$$\frac{\text{Net utilized solar energy for the mantle storage system}}{\text{Net utilized solar energy for the heat exchanger spiral storage sys.}}$$



Solar fraction for the heat exchanger spiral storage system, %.

Fig. 4. Calculated and measured performance ratios as a function of the solar fraction of the heat exchanger spiral storage system.



Work has been initiated in order to elucidate the reasons for the discrepancy between measurements and calculations. It will be elucidated if the average hourly solar irradiance data of the test reference years are sufficient to calculate the thermal performance of the low flow systems, which works in such a way, that the variations in the solar irradiance increases the advantageous thermal stratification in the heat storage.

When this work has been completed the validated model will be a useful tool to optimize the design of small low flow solar heating systems for domestic hot water supply.

#### CONCLUSION

A detailed mathematical model simulating the thermal behaviour of small low flow solar heating systems has been developed. The model has been validated by means of indoor experiments with a mantle heat storage.

By means of the model yearly thermal performances of the attractive low flow systems have been calculated.

Comparisons between calculated and measured performances show that the model underestimate the thermal advantage of low flow systems a little.

Therefore work is necessary in order to validate the model by means of experiments with a complete solar heating system.

#### REFERENCES

- Berg, P., (1990). Højtstående solvarmeanlæg med små volumenstrømme. Teoretiske undersøgelser. Report no. 209, Thermal Insulation Laboratory, Technical University of Denmark.
- Furbo, S. (1989). Solar water heating systems using low flow rates. Experimental investigations. Report no. 89-9, Thermal Insulation Laboratory, Technical University of Denmark.
- Furbo, S., (1990). Attractive small marketed hot water solar heating systems using low flow operation. Proceedings North Sun '90, Reading.
- Furbo, S., Mikkelsen, S.E. (1987). Is low flow operation an advantage for solar heating systems? Advances in solar Energy Technology, Vol. 1, Proceedings of the Biennial Congress of ISES, Hamburg, 962-699.
- Hollands, K.G.T. (1988). Recent developments in low-flow, stratified tank solar water heating systems. Proceedings North Sun '88, Borlänge.
- van Koppen, C.W.J., Thomas, J.P.S. and Veltkamp, W.B. (1979). The actual benefits of thermally stratified storage in a small and medium size solar system. Sun II, Proceedings ISES Biennial Meeting, Atlanta, Ga, Vol. 2, 576-580.

## A VAPOUR-LIFT PUMP FOR SOLAR SYSTEMS

Peter Kjaerboe

Dept. of Heating and Ventilation, Royal Institute of Technology,  
S-100 44 Stockholm, Sweden

### ABSTRACT

A solar heating system with the storage tank situated under the collector can have a natural circulation with a vapour-lift pump. It takes one fifth of the collector's area for generating vapour. The system is simpler and therefore cheaper than a normal system with an electrical driven pump.

### KEYWORDS

Natural circulation; solar heating system; vapour-lift pump.

### INTRODUCTION

A desired feature in a solar collector, is to have a self sustaining circulating system between the collector and the storage tank. Not only do you economize by saving on the pump and regulating equipment, but most importantly the dependence for electricity has been eliminated. One possible arrangement in creating a self sustaining circulation system, is to place the storage tank above the collector. There are a few disadvantages to this arrangement. One of the major drawbacks, is that the storage tank is subject to "wear and tear" from the elements of weather. Heat loss can be considerable, due to the wind factor. Also limited space at the location site can aggravate the shadow producing factor, other arrangements will be assumed here.

### CURRENT AVAILABLE SYSTEMS

Several systems are described in the current literature. Figure 1 shows one example Neaper (1986).

The float switch and the valves have been positioned under the collector, for example, by the condenser and the accumulator. When the condensor tank is filled, the float switch closes vapour pipe (3), the liquid pressure (the condensate) is pressed up into tank (2) and then into the solar collector.

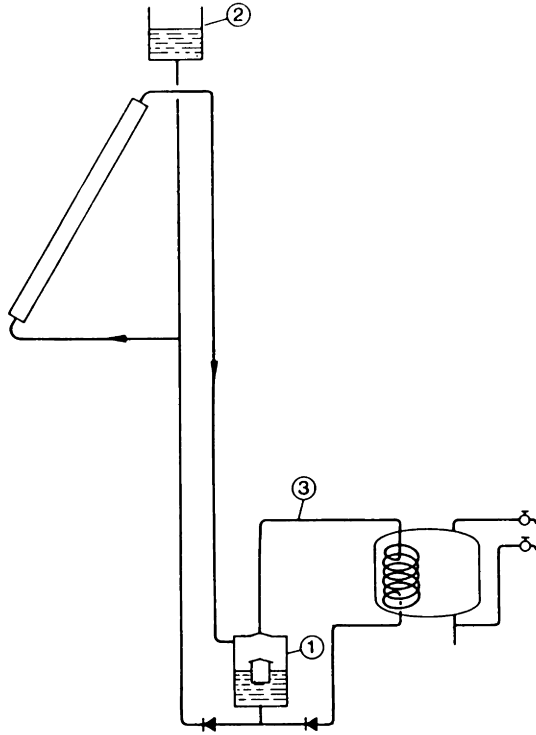


Fig. 1. A float switch in tank (1) shuts vapour pipe (3) and tank (2), which causes the solar collector to be filled with liquid.

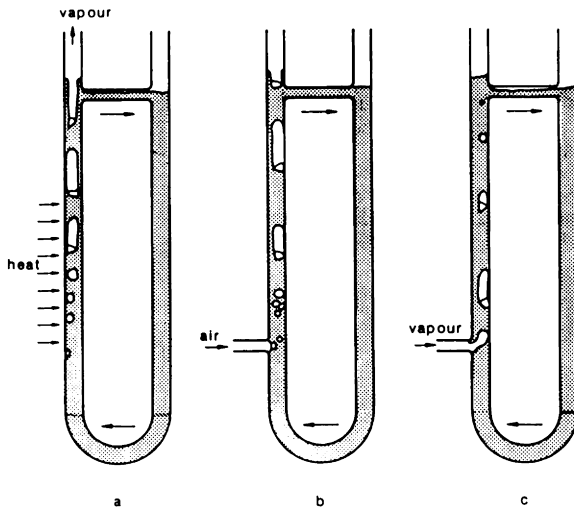


Fig. 2. Procedures for pumping.

Several additional examples for solar collectors, are given by Kjaerboe (1988). Primarily in connection with vapour boilers, where vapour (water in a gaseous state) has a lower density, which results in bringing about circulation in a closed system, Fig. 2a. Note that circulation requires a mixture of fluid and gas, to pump the liquid around the system. Another given example is when several mediums with different boiling points are combined in a mixture. This reaction can be found in cooling systems like the absorption refrigerator, the air-lift pump or Mammut pump, Fig. 2b.

### CHOSEN SYSTEM

Figure 2c illustrates a system where water and water vapour are used. The pumping capacity of the vapour lift pump, Fig. 3, has been measured. The vapour from the solar collector is connected with a pipe to the main flow of the solar collector system. Vapour bubbles will gradually condense in the liquid. The bubbles and liquid will form a mixture with a certain void. The mixture has a lower density, which compensates for the density difference between the two liquid columns, due to the temperature difference when the warmer water stays in the accumulator, and partly for the pressure differences which occurs with the flow.

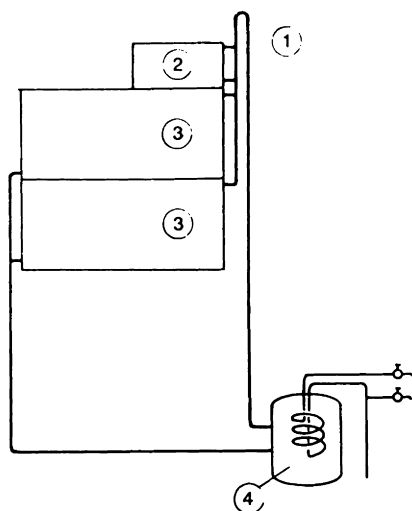


Fig. 3. System with a pump (1), a steam generating solar collector (2), a heating solar collector (3) and a storage tank (4).

### MEASUREMENT PROCEDURES

For the purpose of taking measurements a test rig was installed. An immersion heater generated the vapour, which also preheated the fluid in the vapour-lift pump's inlet. This enabled the measuring of the flow and the pump height depending upon the amount of vapour produced. As well as measuring the inlet temperature respectively at the choke flange, liquid-type pressure gauge and at the thermoelement. Four different pipe diameters, 6, 10, 16 and 22mm were used for the measurements.

## RESULTS

The mass flow and pumheight (= pump work) for different temperatures on incoming liquid see Fig. 4. The pumping work  $P = q\Delta p/n$  can be written as  $P = C\theta^5$ .

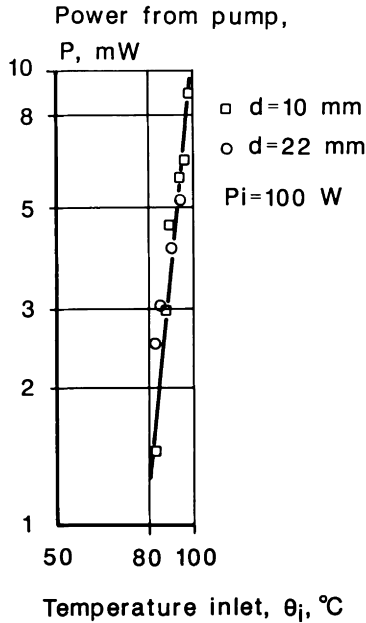


Fig. 4. Performed pumping effect with different temperatures for the incoming fluid.

It is assumed, that there is a connection between the life expectancy of a vapour bubble and the flow, for example Rayleigh (1917). Forcheutz et al (1965) also noted the heat transfer. In this case the heat transfer between the vapour and the liquid is done over a cylindrical boundary cut, instead of a spherical cut. More detailed studies of this should be undertaken. For different flows there will also be different dynamic losses. The results have been simplified according to the measurements taken.

## EFFICIENCY

A pump was installed in the system, to measure the efficiency. This was achieved by estimating the flows for different insulations, see Fig. 5, and by comparing a vapour-lift collector with a conventional solar collector. The latter was assumed to have a slightly lower heat loss e.g. was provided with three a glass cover.

The operating time is less than for a standard solar collector. This was determined when steam generation occurred, i.e. which insolation corresponds to the loss in the collector.

A fundamental property in this case study is that only relatively high water temperatures (85°C-95°C) is achieved at the outlet, see Fig. 6.

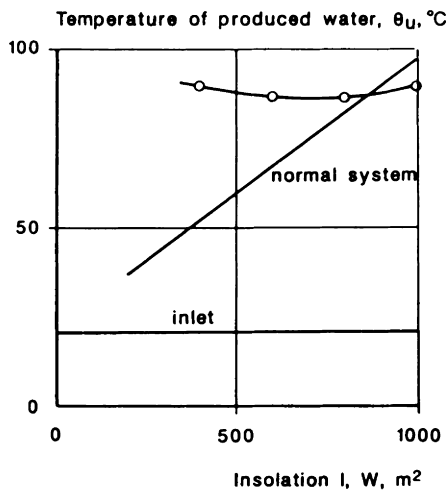


Fig. 5. The systems discharge temperature with different insolation.  $a$  is the area of vapour-lift solar collector to total area of a solar collector.

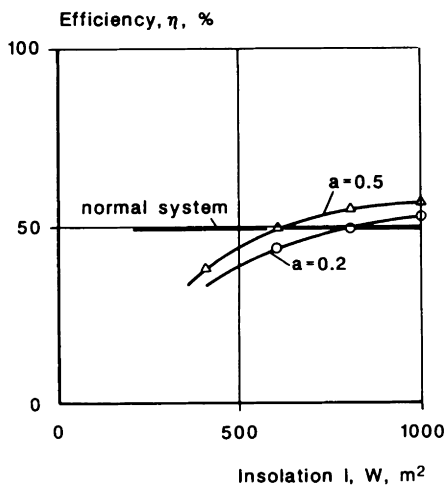


Fig. 6. Efficiency of the two systems depending on the different levels of insolation.  $a$  is the area of vapour-lift solar collector to total area of a solar collector.

## CONCLUSIONS

Comparing a vapour-lift pump with a conventional system:

- o Higher water temperatures (85°C-95°C) results in 40 % reduction in volume for accumulators.
- o Between 10% and 16% reduction of yield during longer periods the area of the collector must be increased.
- o Higher investment costs for components in solar collectors using vapour.
- o Lower investment expenditures for pumps and regulating equipment, no need for electrical installation.

The benefits with self-circulating systems where the storage tank has been located on top of the solar collector (circulating pump not included) are many. The heat losses due to exposure (compare with a storage tank in a closed room) can be ignored. Construction costs are lower. The operating life of the equipment is longer.

A summarized comparison is shown in Table 1. We assume a system with a 5sqm solar collector costing a total of 22,000 SEK, including VAT (value added tax), labour etc. The savings should come to (not including the smaller building volume) about 8%.

Table 1. Consequences and costs when a standard circulation pump is replaced with a vapour-lift pump.

Parameters	Cost Analysis	
	%	SEK
Larger solar collecting area due to lower efficiency	8.0	1,700
Better insulating of the steam generating sections	4.0	800
Piping for the vapour-lift pump	0.5	100
Elimination of the electrical circulation pump	-6.0	-1,400
Reduction for the area of storage tank	-5.0	-1,200
Electricity for operating costs savings over a 15 year time period	-8.0	- 250
Total	-8.0	-1,650

## LITERATURE

- Florschuetz, L., Chao, B.T. (1965). On the mechanics of vapour bubble collaps. *Journal of Heat Transfer*, Trans of the ASME, 5.
- Kjaerboe, P. (1988). Vapour for heat distribution in solar heating systems - Examples (in Swedish). *The Heliograph 1:1988*. Dept. of Heating and Ventilation, Royal Institute of Technology, Stockholm, Sweden.
- Neaper, D.A., Hedström, J.C. (1986). A self-pumping vapour system for hybrid space heating. Conf. Intersol 1985. Pergamon Press.
- Rayleigh, O.M. (1917). On the pressure developed in a liquid during the collaps of a spherical cavity. *Phil Mag N 34*.
- Xin-Shi, Q. (1980). A simple solar collector system using warm water pressure.

## THE EFFECTS OF SUPERCOOLING OF STEAM ON UNIFLOW STEAM ENGINE THERMAL EFFICIENCY IN SOLAR THERMAL POWER STATIONS

DR. B. GHASSEMI\*

Assistant Professor, Science Department  
University of ISFAHAN  
IRAN

### ABSTRACT

The thermal efficiency of uniflow steam engines as employed in solar thermal power stations is reexamined with allowance made for supercooling of the expanding steam by solving the flow equations combined with nucleation theory. The results are in good agreement with experimental measurements. It is shown that all previous unsuccessful attempts in calculating the thermal efficiency (which was always lower than the measured values) can be attributed to the neglected effects of supercooling of the steam during the course of expansion. This study suggests possible improvements to achieve higher performance in steam engines, with consequent increase in cost effectiveness on solar and other applications.

### 1 - INTRODUCTION

This paper describes the effects of the supercooling of the steam on the thermal efficiency of the three cylinders uniflow steam engine developed at the Energy Research centre of the Australian National University and employed at the white cliffs (Australia) solar thermal power station(1). Engine configuration is shown in Figure 1

The thermal efficiency of the engine (the ratio of the heat input to the work output) is mainly depends on the thermodynamics states of steam during the expansion and compression strokes in the cylinders. The previous

---

\*Formerly

Visiting Fellow

Energy Research Centre

The Australian National University

Canberra A.C.T



attempts in calculating the efficiency was based on the assumption, that, the steam remains in equilibrium states(2) and the required data below the saturation line are also obtained from the steam table.

A comparison between the summary of the results obtained by this method and the measured efficiency at different inlet condition is shown in table 1. The interesting point, is that, the measured efficiency is higher than the calculated one.

## 2 SUPER COOLING OF THE STEAM IN STEAM ENGINE

The details of the nucleation theory and its applications to the flow of the expanding steam have already been discussed by numerous investigators (3), (4) and it is beyond the scope of the present paper to review them. Despite the vast amount of information exists in literature for supercooling and thermo-fluid properties of the steam in steam turbines (5), (6), few attempts are made to study the behaviour of steam during its expansion in steam engine (7), (8). In this paper, the thermo-fluid properties of supercooled steam obtained by applying the combination of the nucleation theory to the flow of the expanding steam in steam engine. Figure 2 shows a summary of the variation of the thermo-fluid properties of steam during the expansion in steam engine. It reveals, steam attains a maximum of supercooling  $T_s - T = 28^\circ\text{C}$  and then reverts to near the equilibrium. Figure 3 shows a comparison between the thermodynamics properties of supercooled steam with the data obtained from the steam table. Figure 4 also shows the experimental records of the variation of pressure inside the cylinder obtained by dynamics pressure transducer (2). The humps on the expansion line could be due to the condensation shock. Considering the existance of supercooling in expanding steam in steam engine, the discrepancies between the measured and calculated efficiency can be attributed to this neglected effects.

## 3 RESULTS AND CONCLUSION

Since the location of the maximum degree of supercooling ( $T_s - T$ ) and super-saturation ratio  $P/P_s$  is mainly depends on the time rate of the expansion of the steam ( $P^o = \frac{1}{p} \frac{dp}{dt}$ ) a supercooled steam table with the  $P^o \sim 500 \text{ S}^{-1}$  prepared by solving the flow equations combined with the nucleation theory (9) and used instead of ordinary steam table in obtaining the required steam data

below the saturation line. The calculated efficiency is presented in table 1 which is in good agreement with the measured value. This study reveals, that, the thermodynamics states of the steam during the expansion deviates from the equilibrium states. This fact has to be considered in future design in order to improve the low performance of the engine employed in solar thermal plant.

#### 4 ACKNOWLEDGMENTS

The author wishes to express his gratitude to the authorities of the University of ISFAHAN-IRAN and the Ministry of Science and Higher Education for their financial support.

I am indebted to Professor S-Kanefff, the head of the Energy Research Centre, Australian National University for his permission to use the departmental facilities and his many valuable suggestions during my visiting period. I am grateful to Professor F. Bakhtar, University of Birmingham, U.K. for his permission to follow the calculation procedure developed under his supervision.

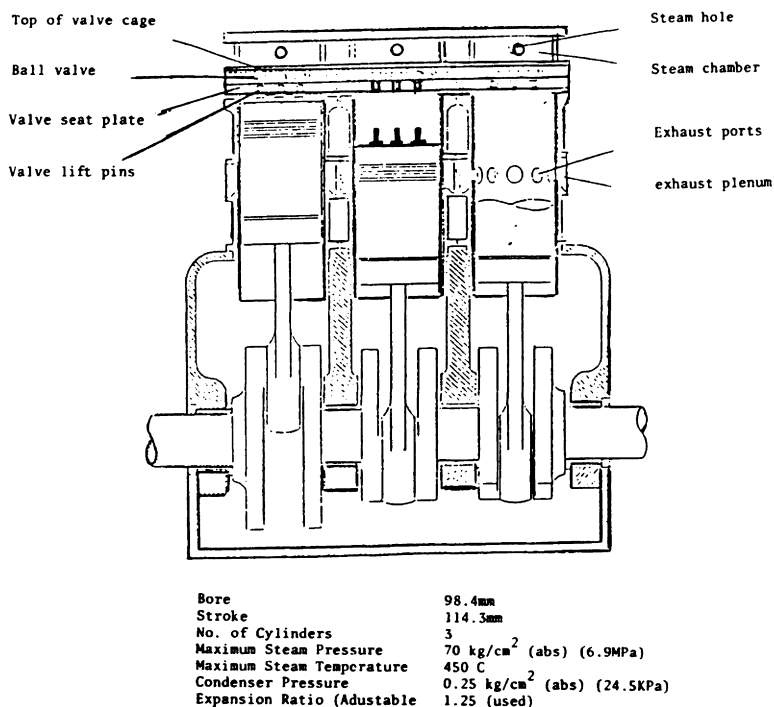


Figure 2: Engine configuration

## REFERENCES

- 1- KANEFF, S., E.K. INALL and R.E. Whelan (1987) "A Range of High Performance uniflow Reciprocating Steam Engines Powered by Solar, Biomass and other Sources of Steam" proc. int solar Energy Society World Congress, Hamburg, 13-18 Sept. Pergamon Press, Oxford.
- 2- Williamson, H.M. and Prasad S.B. (1987) "Performance Evaluation of a three cylinder steam Engine. Research Report EP-RR-45 Energy Research Centre, Australian National University.
- 3- BAKHTAR, F., et al (1975) "Nucleation Studies in Flowing High-Pressure steam", Proc. inst. of Mech Engrs, vol. 189, 41, 75.
- 4- Gyarmathy, G (1976) "Condensation in Flowing Steam" Two-Phase steam flow in turbine and separators edited M.J. Moorc, Hemisphere Publishing Co.
- 5- Bakhtar, F., and Ghassemi, B. (1979), "A study of Nucleating and wet steam flows in high pressure Turbine" Proc. instn Mech Engrs C 191/79 London.
- 6- Ghassemi, B. (1988), "Theoretical study of the Maximum Degree of super-saturation Ratio of low pressure steam during the expansion" proc. Thermodynamics conf. inst. of Engrs, Australia, Brisbane.
- 7- Ghassemi, B. (1989) "Supercooling of steam in steam Engine, Research Report No EP-RR-49 Energy Research Centre, Australian National University Canberra, Australia.
- 8- Ghassemi, B. (1989) "Variation of the thermofluid properties of steam Entering the white cliffs solar power plant. Proc. Australian and New Zealand Solar Energy Conference, University of Queensland.
- 9- Ghassemi, B. (1989) "Tables of supercooled steam, Research Report No EP-RR-50 Energy Research Centre Australian National University, Canberra, Australia.

TABLE 1, Comparison between the measured and calculated efficiency

Inlet P(kPa), T oC	4824,375	4825,362	4686,394	4548,380	4790,416
Measured eff.	14.7	14.6	14.4	14.3	15.1
Calculated efficiency without considering the supercooling					
"	13.8	13.9	13.7	12.6	14.7
Calculated efficiency including the supercooling effects					
"	14.8	14.7	14.6	14.5	15.2

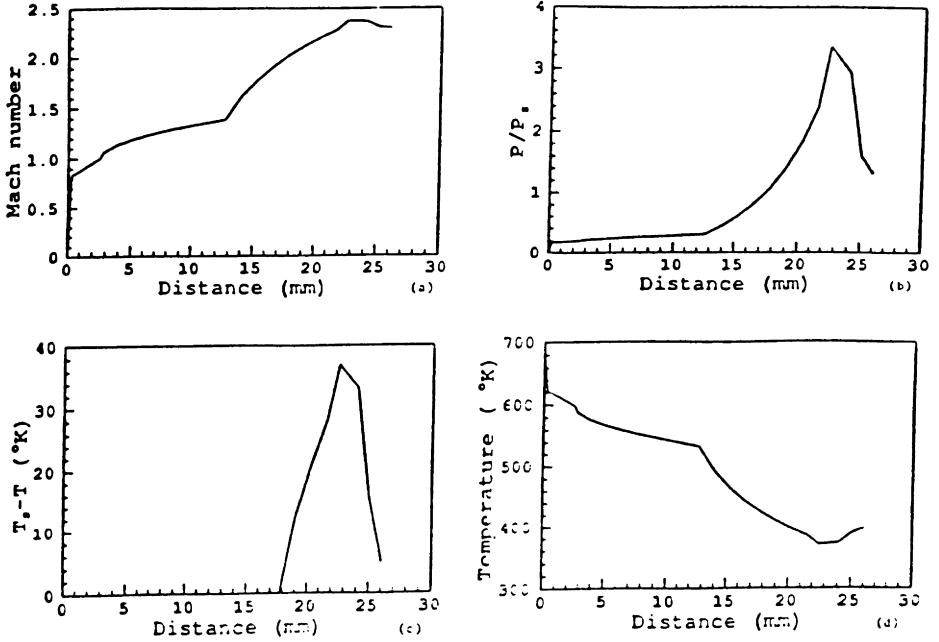


Figure 2: Variation of the thermo-fluid properties of steam

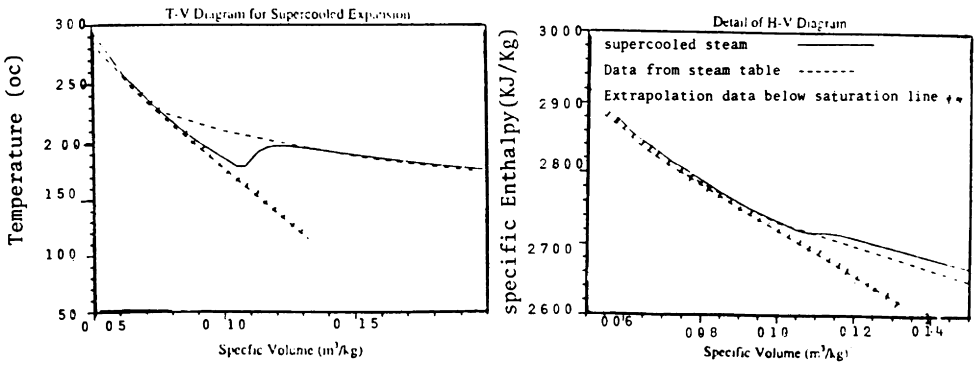


Figure 3: Comparison between the thermodynamics properties of supercooled steam with data of steam table

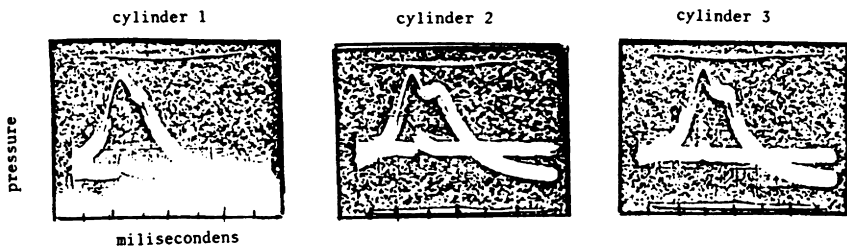


Figure 4: Experimental Records of variation of pressure inside the cylinders.

# OPTIMUM MATCHING OF COLLECTORS IN CPC SOLAR MEDIUM TEMPERATURE WATER HEATING SYSTEM

Yang Xiao-feng

Department of Management Engineering, Logistics Engineering  
Institute of P.L.A. of China, Chongqing, Sichuan, China.

and

Liu Qi-xian

Department of Thermal Power Engineering, University of  
Chongqing, Sichuan, China.

## ABSTRACT

This paper has researched on optimum matching of collectors in the CPC solar energy median temperature water heating system which consists of flat-plate solar collectors and CPC solar collectors, based on the theories and methods of system engineering. The transient performance of optimized system has also been simulated. The Comparison between simulated results of unoptimized system and that of optimized ones shows that the matching of all kinds of collectors in the optimized system is more reasonable, the area of collectors is decreased and the performance of system is improved to some extent too.

### 1. INTRODUCTION

To prove the practical possibility and application value of using the new CPC solar collector system to supply hot water of 150 °C, we developed a CPC solar energy median temperature water heating open-loop system in 1983~1986, which consists of single-glazed and double-glazed flat-plate collectors, CPC evacuated tube-heat pipe collectors, a pump and a number of pipes in series (Fig.1). There are not storage and auxiliary energy heaters in the system. The matching of the three kinds of collectors was not optimized. Besides, to make sure that the CPC collector worked over 70 °C and to reduce cost, the area of flat-plate collector array was increased. Therefore the area of flat-plate collector array was somewhat large, and its temperature increment was overhigh, the area of CPC collector array was small, and its temperature increment was low. Thus,

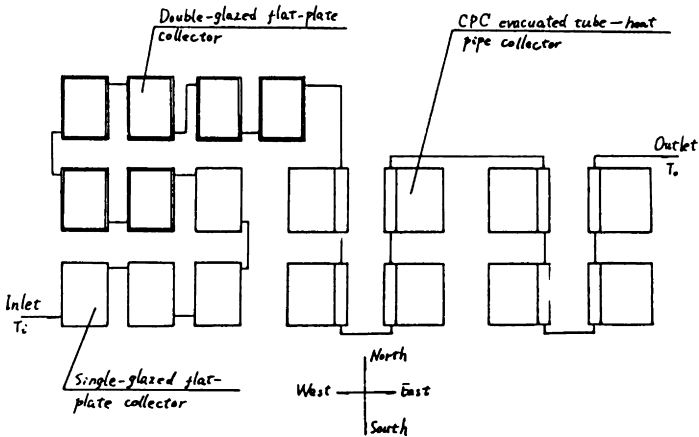


FIG.1 The diagram of CPC solar energy median temperature water heating test system

all collectors did not operated at their optimum temperature range. The outlet temperature of flat-plate collector array was often over  $100\text{ }^{\circ}\text{C}$ , so the heat loss increased greatly, the efficiency decreased rapidly, and then the temperature increment of CPC collector array was reduced, the advantage of CPC median temperature collector was not shown fully.

Here, we introduce the optimum matching method of the three different kinds of collectors mentioned above and the simulation results of the optimized system. The comparison between the simulation results of unoptimized system and that of optimized system shows that after the system has been optimized, the matching of the collectors is more reasonable and cheaper, and the performance of system is improved.

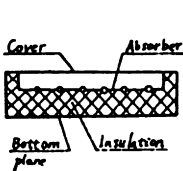


Fig.2 Single-glazed flat-plate collector

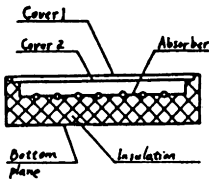


Fig.3 Double-glazed flat-plate collector

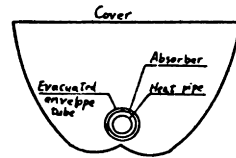


Fig.4 CPC evacuated tube-heat pipe collector

## 2. MATCHING OPTIMIZATION MODEL OF COLLECTORS

### 2(a) Design characteristics of the system

The optimization research of system is a way which makes the design of system more perfectly. In the design of solar energy system, after the types of collectors are determined, the optimization of system is only achieved by choosing reasonably areas of various collectors and their connecting ways. This is a question about the optimum matching of collector parameters ----- it belongs to the question of static optimization question.

The design characteristics of the CPC solar energy median temperature heating . water system is shown as follows:

(1) Heat load: At the average irradiance of  $814.4\text{ W/m}^2$ , the system can supply hot water of approximately  $150\text{ }^{\circ}\text{C}$  and  $50\text{ kg/hr}$ .

(2) This solar energy water heating uses the single-glazed and double-glazed flat-plate collectors, and the CPC evacuated tube-heat pipe collectors. Their construction and types have been fixed.

### 2(b) Hypotheses of optimization

(1) Do not consider the effect of heat capacity of the system, but consider the system to be at static state or warrant static state.

(2) Mass flow rate in the system is kept constant.

(3) Irradiance, ambient temperature and wind speed take their annual average values.

(4) All energy collected by the system may be effectively utilized. There is no question about discharging excess energy.

(5) The collector overall heat loss coefficient and effective transmittance-absorptance product are modified by the heat loss of inlet and outlet ducts of collector.

### 2(c) Mathematical model of matching optimization of collectors

#### (1) Determination of variables

The system has been design to use three types of collectors. The purpose of system optimization is to determine numbers of three types of collectors and their connecting ways. Here, we choose six optimizing variables:  $N_1, N_2, N_3$  are numbers of single-glazed flat-plate collectors, double-glazed flat-plate collectors and CPC evacuated tube-heat

pipe collectors in series respectively, M1,M2,M3 are numbers of single-glazed flat-plate collectors, double-glazed flat-plate collectors and CPC evacuated tube-heat pipe collectors in parallel respectively. The determining of the optimizing parameters of CPC collectors take a CPC trough as one unit.

(2) Restraint conditions

In the system which consists of three collector arrays connected in series, the outlet water temperature of front array is equal to the inlet water temperature of back array. Based on the useful energy gain of collector

$$Q_u = A FR [(\tau\alpha) I - UL (Tf_i - T_b)], \tag{1}$$

the equivalent characteristics of M rows of N collectors connected in series [1] and the requirements of system design, we can derive the following restraint conditions after considering the modifying of heat loss of inlet and outlet ducts of collector to its useful energy gain[2]:

1) The useful overall energy gain of the system must be larger than, or equal to, the energy supplied by the system, i.e.,

$$Q_{ut} > 7397.993 \text{ W, or} \\ G(1) = 7397.993 - Q_{ut} \\ = 7397.993 - \sum \dot{m} C_p [(\tau\alpha)_{j'} I - UL_{j'} (Tf_{ij} - T_b)] \{1 - [1 - M_j A_j FR_j \\ UL_{j'} / (\dot{m} C_p)]^{M_j}\} / UL_{j'} < 0, \quad (j=1,2,3) \tag{2}$$

where  $(\tau\alpha)_{j'}$ ,  $UL_{j'}$ ,  $FR_j$  are the modified performance parameters of first collector in j array.

2) To give full play to good median temperature performance of CPC collectors, the outlet water temperature of second flat-plate collector array (i.e., the inlet water temperature of CPC collector array) should be larger than, or equal to, 70 °C in the series system, i.e.,

$$Tf_i > 343.15 \text{ K, or} \\ G(2) = 343.15 - Tf_{i2} - [(\tau\alpha)_{2'} I - UL_{2'} (Tf_{i2} - T_b)] \{1 - [1 - M_2 A_2 FR_2 \\ UL_{2'} / (\dot{m} C_p)]^{M_2}\} / UL_{2'} < 0. \tag{3}$$

3) The outlet water temperature of the system (i.e., the outlet water temperature of CPC collector array) must be larger than, or equal to, 150 °C, i.e.,

$$T_o > 423.15 \text{ K, or} \\ G(3) = 423.15 - Tf_{i3} - [(\tau\alpha)_{3'} I - UL_{3'} (Tf_{i3} - T_b)] \{1 - [1 - M_3 A_3 FR_3 \\ UL_{3'} / (\dot{m} C_p)]^{M_3}\} / UL_{3'} < 0. \tag{4}$$

4) Three different types of solar energy collectors must be used in the system. In other words, the series number of each type of collectors must be larger than, or equal to, 1, i.e.,

$$M_j > 1 \text{ and } N_j > 1, \text{ or} \\ G(4) = 1 - M_1 < 0, \tag{5} \\ G(5) = 1 - N_1 < 0, \tag{6} \\ G(6) = 1 - M_2 < 0, \tag{7} \\ G(7) = 1 - N_2 < 0, \tag{8} \\ G(8) = 1 - M_3 < 0, \tag{9} \\ G(9) = 1 - N_3 < 0. \tag{10}$$

Since the performance parameters of collectors  $(\tau\alpha)_{j'}$ ,  $UL_{j'}$ ,  $FR_j$ , and  $Tf_{i2}$ ,  $Tf_{i3}$ ,  $T_o$  change with series and parallel numbers of various collectors, the performance parameters of collectors should be repeatedly calculated according to different  $M_j$  and  $N_j$  ( $j=1, 2, 3$ ). Then the obtained results are introduced into restraint equations. So long as optimizing variables  $M_j$  and  $N_j$  ( $j=1, 2, 3$ ) change once, a new set of performance parameters will occur. Because the set of energy balance differential equations of collector is nonlinear, the imitative Newton method is used in finding performance parameters of collectors[3-6].

(3) Model of objective function

The area matching optimization of collectors in the system is to determine reasonably areas and connecting ways of collectors under the condition of meeting the requirements of system design and to make system have the least collector area, therefore

decreasing the cost of system and increasing the efficiency of system.

The minimum sum of areas of various collectors is just the objective function of system optimization, i.e.,

$$f = A_1 M_1 N_1 + A_2 M_2 N_2 + A_3 M_3 N_3$$

$$= \sum A_j M_j N_j, \quad j=1,2,3. \tag{11}$$

After the optimizing variables  $M_j$  and  $N_j$  ( $j=1, 2, 3$ ) are replaced by  $X(k)$  ( $k=1, 2, \dots, 6$ ), the objective function model may become

$$f(X) = A_1 X(1) X(2) + A_2 X(3) X(4) + A_3 X(5) X(6). \tag{12}$$

To sum up, the mathematical model of collector matching optimization is

$$\min f(X) = A_1 X(1) X(2) + A_2 X(3) X(4) + A_3 X(5) X(6)$$

$$\text{Restraint conditions } G(i) = F_i(X) < 0 \quad (i=1,2,\dots,9)$$

$$X \in E^n. \tag{13}$$

### 3. SOLUTION OF OPTIMIZATION MODEL AND CALCULATION PROGRAMME

It is seen from obtained model that objective function and restraint conditions are nonlinear and this is an optimization question under the unequal equation restraint conditions. One can use only the optimizing numerical solution of unequal equation restraint to solve the question. The optimizing solutions of the kind are much more and we choose the penalty function interior point method in indirect solution methods. It is one numerical solution method of nonlinear programming questions which is used most extensively.

Applying the penalty function interior point method on the optimizing calculation of the system, we programed the calculation programme OPTIUM of collector matching optimization in the system. This programme contains an "executive" program and a main program and 25 subroutines.

After running the programme on an IBM-PC microcomputer, the obtained optimal results are shown in Table 1.

Table 1. Results of collector matching optimization in system

Type of collectors	Parameters	Series number	Parallel number	Array area (m <sup>2</sup> )	Outlet water temperature of array (°C)	FR	UL'	(τ α)'
Single-glazed flat-plate collectors		2	2	6.24	54.97	0.5818	10.413	0.7443
Double-glazed flat-plate collectors		2	2	6.24	78.07	0.6653	7.4682	0.7738
CPC evacuated tube-heat pipe collectors		18	2	5.36 (12.36)	150.59	0.982	0.9228	

Notes: The data in the brackets is the sum of aperture areas of CPC collectors. The heat loss of inlet and outlet ducts of collectors is counted into the Performance Parameters of collectors)

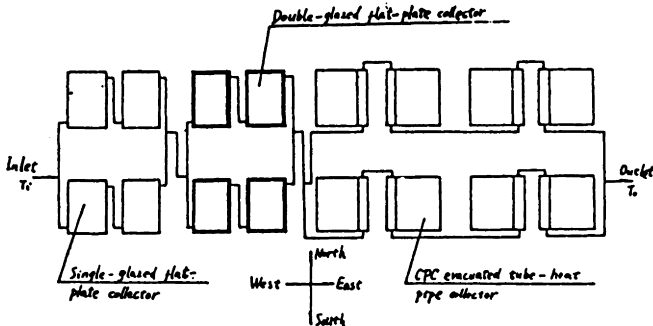
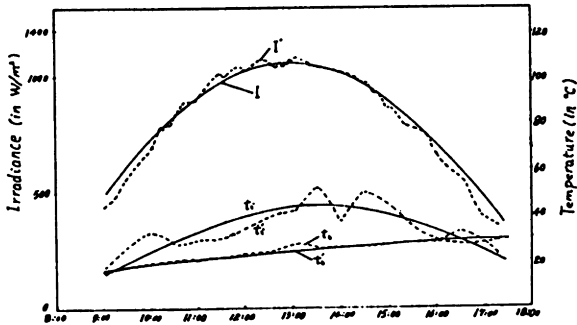
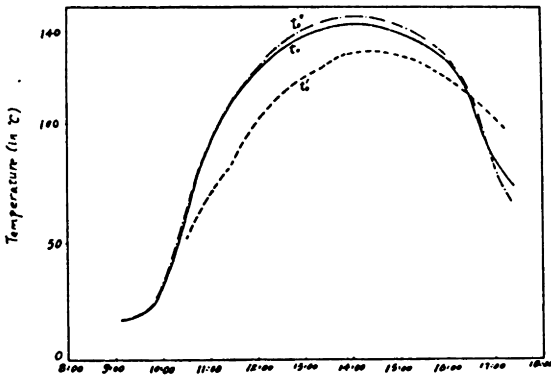


Fig.5 The diagram of optimized system.

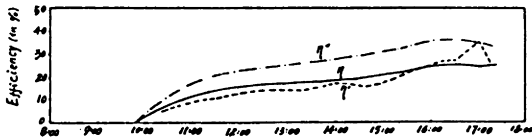




$t$  (Standard time in Beijing, in hr)  
 Fig.6 Disturbing function curves of system. Dotted lines represent the test results and real lines represent the simulation results.



$t$  (standard time in Beijing, in hr)  
 Fig.7 Outlet water temperature of system.  $T^{\circ}$  and  $T^{\prime}$  are respectively simulation result and test result of unoptimized system,  $T^{\circ\circ}$  is the simulation result of optimized system.



$t$  (standard time in Beijing, in hr)  
 Fig.8 Efficiency curves of system.  $\eta^{\circ}$  and  $\eta^{\prime}$  are respectively the simulation result and the test result of unoptimized system, and  $\eta^{\circ\circ}$  is the simulation result of optimized system.

#### 4. SIMULATION OF OPTIMIZED SYSTEM AND COMPARISON BETWEEN PERFORMANCE OF OPTIMIZED SYSTEM AND THAT OF UNOPTIMIZED SYSTEM

For the convenience of making a comparison between unoptimized system and optimized system, the performance of optimized system in Fig.5 has been simulated. Simulation hypotheses are presented as follows:

(1) The mass flow rates are equal in two parallel branch lines.

(2) In the parallel branch lines, the construction characteristics and performance of corresponding same types of collectors are the same, and inlet and outlet water temperatures of their are equal.

The method with which to establish the simulation model of optimized system is the same as unoptimized one. Disturbing functions of simulation, constructions of collectors and connecting pipes are same as that of unoptimized system. Comparing the simulation results of unoptimized system with that of optimized system, it may be found that

(1) The area of flat-plate collectors after optimized is decreased by  $3.12 \text{ m}^2$ . The area decrement is about 10.6 % of original area.

(2) Although the collector area of optimized system is decreased, the outlet water temperature of system is increased by approximately  $3 \text{ }^\circ\text{C}$  on the contrary. This is primarily because the overall temperature increment of flat-plate collectors is decreased and their heat loss is reduced too. Besides, the temperature increment of CPC collectors is increased and their median temperature potentiality is fully brought out. This can be seen in Fig.7.

(3) The efficiency of optimized system is increased by approximately 10 %. See Fig.8. This shows fully the effect of collector matching optimization. As the area of flat-plate collectors is decreased, some of their heat load is transferred to CPC collectors with good median temperature performance. The heat loss of system is reduced and its useful energy gain is increased, and the performance of system is improved to some extent too.

#### 4. CONCLUSIONS

In order to make the area of the collectors in the CPC solar energy median temperature water heating system minimum, we get the matching parameters of three types of collectors, that is, the parameters of the collectors in series and in parallel in the condition of the useful overall energy gain and the required outlet water temperature in the system. Considering that the performance parameters of collectors are the functions of temperature, they are regarded as the functions of the numbers of collectors in series and in parallel in this model.

The comparison between the simulation results of unoptimized system and that of optimized system shows that in the optimized system, the overall area of collectors is decreased, the outlet water temperature of system is slightly increased and the transient transient efficiency of system is increased to some extent too. This fact shows that although the constructions of collectors are not changed, changing the connecting ways of collectors in the system can improved properly the thermal performance of system by the collector matching optimization. It may be seen from this that the optimization research of solar energy system has very important significance for the design of solar energy system. We have made the preliminary discussion on the collector matching optimization, and the obtained method has certain reference value to the optimization research of the system which consists of various types of collectors.

#### 5. NOMENCLATURE

A	collector area ( in $\text{m}^2$ )
$A_i, A_o$	surface areas of inlet and outlet ducts of collector, respectively ( in $\text{m}^2$ )
$C_p$	average specific heat of fluid ( in $\text{J/kg} \cdot \text{ }^\circ\text{C}$ )
FR	heat removal factor
$(\tau\alpha)$	effective transmittance-absorptance product of collector
I	irradiance arrived on tilted surface of collector ( in $\text{W/m}^2$ )

$\dot{m}$	mass flow rate (in kg/s)
$Q_{ut}, Q_u$	useful energy gains of system and collector, respectively (in W)
$M, N$	parallel number and series number of a type of collectors, respectively
$t$	time (in hr)
$T$	temperature (in K)
$\eta$	efficiency of system (in %)
$U_L, U_b$	heat overall loss coefficient and bottom heat loss coefficient of collector, respectively (in $W/m^2 \cdot ^\circ C$ )
$U_t, U_e$	top heat loss coefficient and side heat loss coefficient of collector, respectively (in $W/m^2 \cdot ^\circ C$ )

## Footnotes:

$f$	fluid	$p$	absorber of flat-plate collector
$f_i$	inlet fluid	$f_o$	outlet fluid
$c$	cover of collector		
$c_1, c_2$	first cover and second cover of double-glazed flat-plate collector, respectively		
$j$	when $j = 1, 2, 3$ , it represents respectively the single-glazed flat-plate collector array, the double-glazed flat-plate collector array, and the CPC evacuated tube-heat pipe collector array		
$k$	when $k = 1, 2, \dots, 6$ , it represents respectively some optimizing variable		

## 6. REFERENCES

- [1] Podney L. Onk, Bruce E. Cole --- Appel. Calculation of performance of  $N$  collectors in series from test data on a single collector, *Solar Energy* 23, 535 (1975).
- [2] John A. Duffie, William A. Beckman, *Solar Energy Thermal Process*, Wiley, New York (1980).
- [3] P. I. Cooper, The effect of inclination on the heat loss from flat-plate solar collectors, *Solar Energy* 27 (1980).
- [4] S. Shakerin, Wind-related heat transfer coefficient for flat-plate solar collectors, *Journal of Solar Energy Engineering*, Vol. 109, 108 (1987).
- [5] C. K. Hsiek, Thermal analysis of CPC collector, *Solar Energy* 27, No. 1 (1981).
- [6] M. J. Carvalho, M. Collares-Perceire, J. M. Gordon, Economic optimization of stationary nonevacuation CPC solar collectors, *Journal of Solar Energy Engineering*, Vol. 109, 40 (1987).

A STUDY ON SOIL TEMPERATURE WHEN MULCHED BY  
TRANSPARENT PLASTIC FILM

Sun Xiaoren

Shanxi Science and Technology Information  
Institute, Taiyuan, China

ABSTRACT

This paper mainly deals with the establishment of the relation between mulched soil temperature and solar energy, so that we can use local meteorological data to predict mulched soil temperature at a fixed time. This paper also puts forward an experimental formula for calculating mulched soil temperature, and experiments showed that the agreement between calculated and observed soil temperatures is roughly good.

KEYWORDS

Plastic mulch; soil physics; soil heat transfer; solarization.

INTRODUCTION

In recent years a lot of experiments on plastic mulching have been done all over the world, especially in high latitude area. Experiments showed that plastic mulching can increase the yields of fruits, vegetables and crops, advance harvest. In China experiments showed that the yield of cotton on plastic mulched plots was 15-50% higher than control plots(bare soil).

Studies showed that plastic mulch can raise soil temperature, reduce evaporation from soil, increase dioxide concentration and nutrient, control weeds, protect plants from pests and reduce fruit rotting, Some experiments also showed that plastic mulch can alter the salt content in soil. That is why plastic mulch have good effects on plant growing. And this method is especially useful in arid and cold areas.

Plastic mulch has a close relation with solar energy. But a brief glance at the available literature on plastic film mulch gives the impression that so far not much work on solar heat

transfer analysis has been done. And some work on thermal performance analysis of plastic soil mulch will be useful in this regard.

The aim of this study is to establish the relationship between soil temperature and insolation. Here we should see that there are many other factors affecting soil temperature, such as wind velocity, ambient temperature, soil property and so on. These factors bring difficulty to this study.

#### THERMAL PERFORMANCE ANALYSIS

Plastic mulch is widely used to increase the soil temperature in early Spring, when the solar radiation level may still be relatively low. The soil temperature can be estimated by calculating an energy balance in steady state at day time, or an energy balance for a typical day of a period. This work can be done by equating the heat gains to the heat losses at the equilibrium soil temperature.

#### Bare Soil

Solar radiation received by the soil surface is one of the major components of its energy balance. Part of the radiation received is transformed into heat, which warms soil, plants and atmosphere. And a major part of radiation is absorbed as latent heat in the twin processes of evaporation and transpiration (Koorevaar *et al.*, 1983).

The soil surface also emits radiation, and at the same time the atmosphere absorbs and emits long wave radiation, part of which reaches the soil surface. During day time the heat exchange may be a small fraction of the total radiation balance, but at night the heat exchange dominates the radiation balance.

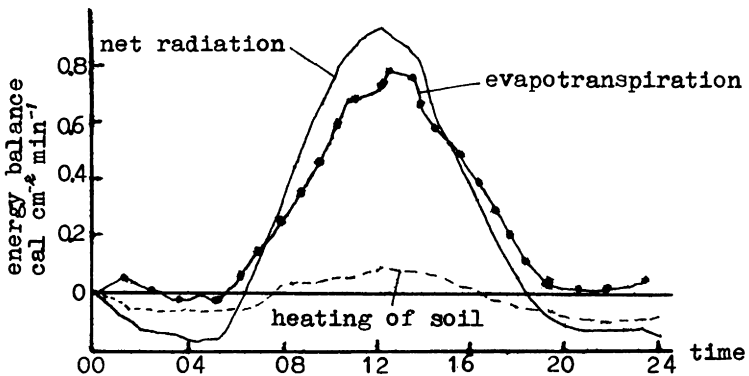


Fig. 1. The diurnal variation of energy in soil

Figure 1 illustrates the diurnal variation of the energy balance in soil (Hillel, 1982). From this figure we can see that during day time energy utilization by evaporation dominates radiation balance. Experiments showed that the patterns of the components of the energy balance differ for different conditions of soil, climate and vegetation.

For bare soil the heat gains are mainly insolation, and the heat losses are due to the evaporation from soil surface, radiation with surroundings, convection and long wave infrared radiation exchange between soil and the sky. So the energy balance equation for bare soil can be written as follows:

$$H\alpha = LE + h_r(T_s - T_a) + h_c(T_s - t_a) + \epsilon R + S \quad (1)$$

where H is the insolation value on horizontal surface;  $\alpha$  is soil absorptivity; LE is the rate of energy utilization in evaporation (a product of the rate of water evaporation E and the latent heat of evaporation L);  $h_r$  is the radiative heat transfer coefficient;  $h_c$  is the convective heat transfer coefficient;  $\epsilon$  is the soil emissivity; R is the long wave infrared radiation; S is the rate at which heat is stored in soil;  $T_s$  is the soil surface temperature;  $T_a$  is the ambient air temperature.

There are some empirical approaches for calculating LE. The method in common use proposed by Penman is based on combination of energy balance and aerodynamic transport considerations:

$$LE = (\Delta/\xi)(H-S) + k d_a / (\Delta/\xi + 1) \quad (2)$$

where  $\Delta$  is slope of saturation vapor pressure curve at mean air temperature;  $\xi$  is psychrometric constant; k is the transfer coefficient for water vapor, empirically  $k=20+V/5$ , where V is the mean wind speed;  $d_a$  is the vapor coefficient deficit, namely  $(e_s - e_a)$ , where  $e_s$  is the saturated vapor pressure and  $e_a$  is the actual vapor pressure (Schwab *et al.*, 1981).

The ratio  $\Delta/\xi$  and the saturated vapor pressure at different temperature is given as follows:

$T_a$ (°C)	10	15	20	25	30	35
$\Delta/\xi$	1.23	1.64	2.14	2.78	3.57	4.35
$e_s$ (mm of Hg)	9.20	12.78	17.53	23.75	31.82	42.18
$e_a$ (mbar)	12.27	17.04	23.37	31.67	42.43	56.24

Radiative heat transfer coefficient  $h_r$  is linearized by the following equation:  $h_r = \epsilon \sigma (T_s^2 + T_a^2)(T_s + T_a)$ . And  $h_c$  is estimated to be  $5.68+3.78V$ , where V is the wind speed (Duffie *et al.*, 1980). R, the long wave infrared radiation exchange, depends on the emissivity of soil and ambient weather condition, such as relative humidity, cloud cover and temperature. In Arizona of USA, calculations estimated that this exchange value ranging from 69 Wm in the Summer to 88 Wm in the Winter (Talwar, 1980).

The thermal flux (i.e. the amount of heat conducted across a

unit cross-sectional area) can be taken as the heat stored in soil.

$$S = k_t \frac{dT}{dx} = D_T C \frac{dT}{dx} \quad (3)$$

where  $k_t$  is the thermal conductivity;  $dT/dx$  is the temperature gradient in the vertical direction;  $D_T$  is the thermal diffusivity,  $D_T = k_t/C$ ,  $C$  is volumetric heat capacity. Experiments indicated that the daily soil storage term is to be of the order of 5-15% of net radiation.

From formula (1), the temperature of bare soil can be expressed as follows:

$$T_s = (H\alpha - LE - \epsilon R - S)/(h_r + h_c) + T_a \quad (4)$$

### Mulched Soil

From the above it can be seen that for bare soil the biggest loss component is the evaporation loss. And plastic mulching film can effectively reduce this loss to nearly zero. Moreover, the infrared radiation loss and convection loss are also reduced to some extent. But at the same time plastic film may reduce the direct absorption of solar energy by 5-20%, depending on the types of plastic film used.

Under steady condition an energy equation for mulched soil is given as follows:

$$H\tau\alpha = h_{r,s-p}(T_s - T_a) + h_{c,s-p}\tau(T_s - T_a) + \epsilon\tau R + S \quad (5)$$

where  $\tau$  is the transparency of plastic film. In this study, we suppose the temperature of the mulched soil surface and the temperature of the plastic film are the same.

From formula (5), we can get an equation for calculating the temperature of mulched soil as follows:

$$T_s = (H\tau\alpha - \epsilon\tau R - S)/(h_r + h_c\tau) + T_a \quad (6)$$

### EXPERIMENT AND DISCUSSION

This experiment was carried out at the University of Melbourne in Australia. Three boxes, each of which measures 0.4 m long, 0.33 m wide and 0.25 m deep, were filled with soil. Two boxes were covered by transparent polyethylene film. Thermocouples were used to measure the temperatures at different depths. The observation was taken during Spring time.

Some of the observed and calculated soil temperature are shown in figure 2. Experiments showed that the agreement between the observed and calculated soil temperatures of both bare and mulched soils is good. So we can use formulae (4) and (6) to predict the soil temperatures of bare and mulched soils based on the local meteorological data.

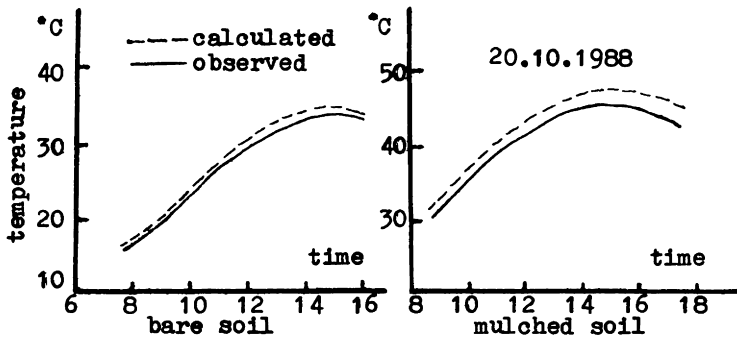


Fig. 2. Observed and calculated temperatures of mulched and bare soils

Experiments also indicated that there were some differences between observed and calculated soil temperatures. In order to predict soil temperature more quantitatively, an error analysis for typical days is needed for correction.

#### CONCLUSIONS

Through this study we can come to the following conclusions:

1. For bare soil the biggest heat loss is for evaporation. And plastic mulching film can effectively reduce this loss.
2. Formulae (4) and (6) can be used for forecasting soil temperature regime under local meteorological conditions. In this way, we can predict the earliest possible date for sowing or predict the highest temperature for solarization.

#### REFERENCES

- Duffie, J.A. and Beckman, W.A. (1980). Solar Engineering of Thermal Processes. John Wiley & Sons, pp123, 137-139.
- Hillel, D. (1982). Introduction to Soil Physics. Academic Press, pp 155-167, 309-320.
- Koorevaar, P. (1983). Elements of Soil Physics. Elsevier Science Publishing Company INC, Netherlands, pp 193-203.
- Schwab, G.O. (1981). Soil and Water Conservation Engineering. John Wiley & Sons, America. pp 53-97.
- Talwar, R. (1980). Swimming Pool Heating. Solar Energy Technology Handbook, Part B. pp15-31.



ABOUT A CONCEPT ON MICROCOMPUTER MEASURING SYSTEM AND  
ITS APPLICATION IN THE FIELD OF SOLAR ENERGY CONVERSION

Dr. A. M. Marinoff

Bulgarian Academy of Sciences, 1618 Sofia, P.O.Box 105,  
Bulgaria

ABSTRACT

The realization of a possible concept on a microcomputer measuring system for electrical, optical and temperature measurements in the field of photoelectrical and photothermal conversion of solar energy is presented in this paper.

KEYWORDS

Solar energy, solar system control, computer control, computer interfaces, software engineering, computer testing, programmed control, thermal variables control, optical variables control, electric variables control

INTRODUCTION

Scientific research in the field of photoelectrical and photothermal conversion of solar energy requires experimental work - for instance measuring of many and different electrical, optical and thermal values which characterize the functioning of the solar energy convertors (solar cells, solar collectors ect.). The experimental research is connected with the usage of different measuring units. This is due to the fact that the studied objects (for instance crystalline and amorphous thin films, insulating films, p-n- and Schottky-junctions, MOS-structures, solar water and air collectors) show a wide variety of physical behaviour. Thus, the variety of measuring tasks make difficult the control of the measuring units and the data acquisition.

In this work a realization of a possible concept on a microcomputer intelligent measuring system for electrical, optical and temperature measurements in the field of solar energy conversion is presented. The microcomputer system can be used also for theoretical modelling of physical processes. The measuring system is based on specialized measuring units and modules of the USA Hewlett-Packard and Perkin-Elmer companies which are connected through the interface IEEE-488-1 with a Hewlett-Packard microcomputer HP9000, series 80 to an integrated open system. The modern microcomputer technique allows for effective usage of the measuring units and the data acquisition. In practice this can be achieved in different ways. There are many possibilities to attain intelligent measuring system (Goetze et al. , 1987).

A microcomputer (MC) is used as a central control and data acquisition unit. The microcomputer carries out the control, the measurement and the acquisition of the measured data. Besides, the different measuring units are equipped with built-in microprocessors. In this case the microcomputer plays a coordinating role in the communication between the measuring units. The actual measuring tasks are performed by the intelligent measuring units. The software support of the measuring system includes the system software for microcomputers HP9000, series 80 and the application software for control, measuring, registering, data acquisition and modelling of a wide range of electrical, optical and temperature measurements developed by us.

#### HARDWARE CONFIGURATION OF THE MEASURING SYSTEM

Fig. 1 represents a principle block scheme of an intelligent measuring system. It contains a MC complete with a standard microcomputer periphery (printer, plotter, floppy disc drive and digiizer) and measuring units (Marinoff, 1987a).

The 8-bit MC has an operating memory of 16k/32k or 128k (which can be expanded to 640k). The operating system (OS) takes 32k and it is realized on ROM's. The range of the OS can be widened with the help of 6 different ROM's. The MC is equipped with the well known measuring interfaces (IEEE-488, RS-232-C, BCD, GPI0 ect. ). This facilitates substantially the control of the measuring units.

The measuring units include a digital voltmeter, programmable power supply (10A, 60V), multiplexer, LCR-meter and spectrophotometers for optical measurements in the range between 200 nm and 50 microns. The spectrophotometers are manufactured by the USA Perkin-Elmer company and the rest of the units- by the USA Hewlett-Packard company. All measuring units except the spectrophotometers have an IEEE-488 interface. The spectrophotometers have a RS-232-C interface and they can be controlled by the same MC.

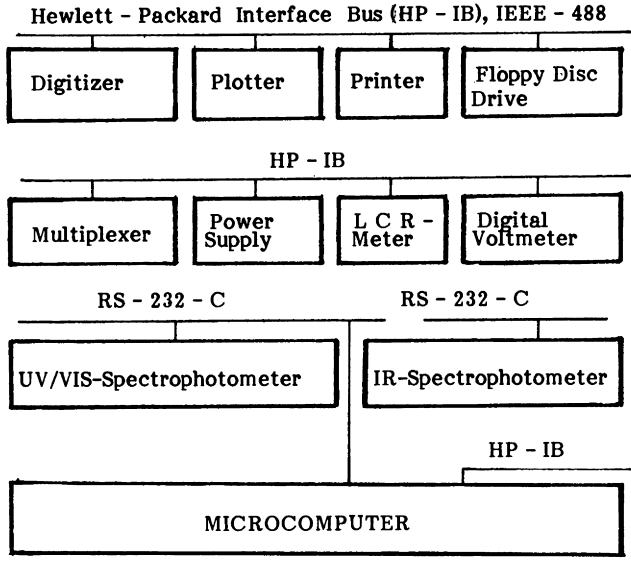


Fig. 1 Principal hardware scheme of the measuring system

#### SOFTWARE CONCEPT

The above described hardware configuration allows for the usage of a measuring system in a wide range of applications. This is provided by both the hardware of every measuring unit and the system and application software. Appropriate hardware and software are selected according to the specific application of the system.

Fig. 2 represents a common block scheme of the application software, developed by us. It is written mainly in HP BASIC and ASSEMBLER for the MC HP9000, series 80 from the USA Hewlett-Packard company (Marinoff, 1987b). Depending on the specific application of the measuring system the data collected from the studied object (for instance solar cell, thin film or solar collector) is received by the computer in three different ways:

- directly through keyboard of the MC if the data is obtained from other units and it is necessary to be stored on magnetic media and registered in appropriate form.

- through the digitizer- for instance by estimation of optical spectra if they are obtained by spectrophotometers without digital output.

- the MC receives the data directly from the measuring units through the interface. This can be attained with the help of specialized program modules, developed for every specific case of application.

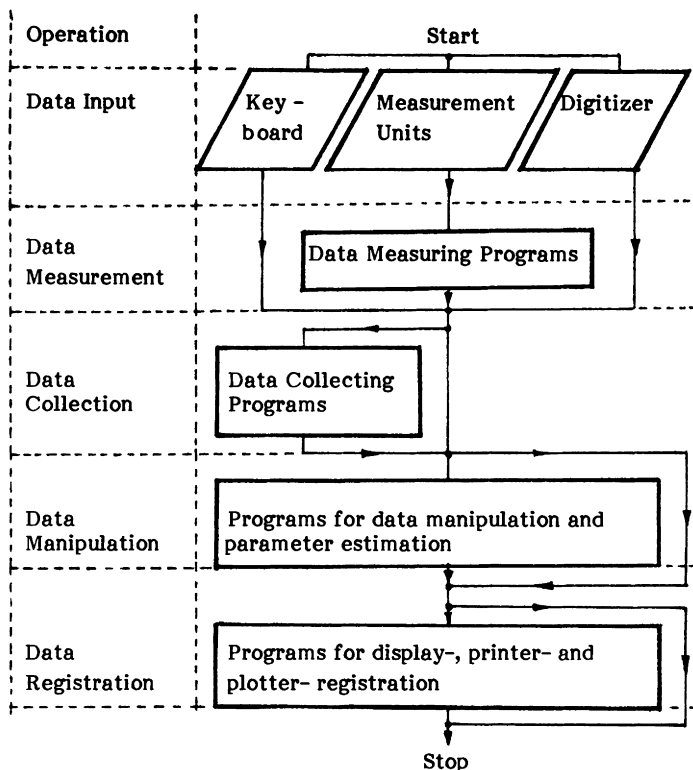


Fig. 2 Principal scheme for the program system design

The software development is governed by several basic principles:

1. A complete application of the characteristics of the OS and the firmware for every data tasks (levels) (data input, measurement, collecting, manipulating and registering).

2. The programming is carried out successively for every level and is based on module principles. Different programming modules are developed for every level. These modules allow for the execution of different electrical, optical and temperature measurements in the field of solar energy conversion.

3. Some attempts were made in order to achieve standard modules for the different tasks.

4. There were other attempts made in order to attain very flexible module organization for a specific data level (for instance for data registration). This could minimize the programming costs for other measuring tasks. For instance, the programming module "data input from digitizer" used in optical measurements can also be used as data input module in electrical measurement tasks. The programming modules for data input from different measuring units have in principle the same structure. There are only insignificant differences, which characterize the hardware of the specific measuring units used in the measurement. The programming modules for data registration are

characterized by high flexibility and they can be used for different purposes with little variations only.

5. A minimum of hardware configuration is to be used for any specific measuring task, characterized by certain criteria. For instance, the measuring of V-A curves for semiconductor diodes and solar cells can be carried out in different ways in accordance with the requirements of the measurement. Hardware variations are possible in case of temperature measurements as well (Marinoff, 1988a). This can result in alteration of the software concept.

The described software concept was applied for the MC HP9000, series 80 but it can be translated to more powerful measuring systems such as VME/VXI or IBM PC/XT/AT based systems, because the latter have turned recently into industry standard. For instance, concerning more powerful systems the MC HP9000, series 300 allows for widening the system to the VME-bus systems (Marinoff, 1988b). In this case it is possible to use IEEE-488- and VME-bus together and to utilize VME driver software for the operating systems BASIC, PASCAL, HP-UX (Hewlett-Packard variant of the operating system UNIX). It is possible to connect a VME-expander with 5 slots to the MC HP9000, series 300. Four slots are reserved for different VME-modules and the fifth slot is reserved for the VME-bus.

With the help of a MS-DOS coprocessor 80286 and appropriate driver programs it is possible to achieve program compatibility between IBM PC/XT/AT and HP9000, series 300 MC's. This leads to integration between the operating systems UNIX and MS-DOS and the usage of hundreds MS-DOS software products is possible.

There is another way to achieve flexibility of the above presented system: with the help of only one program driver and without any hardware modules it is possible to translate the developed application software and to transfer any data files from HP9000, series 80 to IBM PC/XT/AT working in the environment of MICROSOFT QUICK BASIC 4.0. Programs written in series 80 BASIC on MC HP85A, HP85B, HP86A, HP86B, HP87, HP9915 will be automatically translated to MICROSOFT QUICK BASIC 4.0 and run on faster MS-DOS MC's. MICROSOFT QUICK BASIC 4.0 is a fast powerful language which can handle the complex and various programs created on HP9000, series 80. 100 % of the code of general computation programs will be translated. More than 90 % of the graphics programs will be automatically moved to MICROSOFT QUICK BASIC 4.0. Hewlett-Packard Input/Output (HP-IO) commands will be translated as closely as possible to the library supporting the 82900A interface. The RS-232-C HP-IO commands will be translated to work with standard RS-232-C ports. The translator will automatically replace intrinsic functions. The advanced string handling included in HP9000, series 80 advanced programming ROM will be replaced by appropriate functions on the MS-DOS MC's. Matrix ROM functions handling complex manipulations of both matrixes and vectors will be supported. Translating functions of the plotter ROM will allow the user to continue using his graphic equipment in the MS-DOS environment. A MS-DOS file copy utility allows to copy data files and programs SAVED on HP9000, series 80 floppy disc drives.

Another way leading to further development of the existing measuring system is connected with application of the methods of the artificial intelligence, especially the technique of the expert systems and knowledge engineering (Marinoff et al. , 1989).

### CONCLUSION

The measuring system is used for a certain range of measurement tasks (concerning the scientific area of solar energy conversion), but it can be utilized in many other fields of science and technique.

The future application of the above described system will be connected with its widening to more powerful measuring systems such as VXi, IBM PC/XT/AT or IBM PS/2 based systems.

The creation of an expert system on the basis of the currently operating automatic system for control seems to be even more attractive achievement (in terms of the future development).

### REFERENCES

- Goetze, B. and K.-H. Meusel (1987). Personalcomputer in der Messtechnik. Mikroprozessortechnik, Berlin, DDR, Heft 2, 54-56.
- Marinoff, A. (1987a). Universal automatic system for electrical, optical and temperature measurements. Second National Conference with International Participation about Problems of Personal Computers "PERSCOMP'87". 21-24.04.1987, Sofia, Bulgaria.
- Marinoff, A. (1987b). Software for intelligent measuring system for automation of scientific experiments. Scientific Symposium of the High School for Mechanical and Electrical Engineering- Sofia "WMEI Lenin 87". 08-10.10.1987, Sofia Bulgaria.
- Marinoff, A. (1988a). In: Hardware and Software for Real Time Process Control ( J. Zalevski and W. Ehrenberger, ed.), 1988, Elsevier Science Publishers B. V., Amsterdam, New York, Oxford, Tokyo, Chap. 4, pp. 145-150.
- Marinoff, A. (1988b). On a concept for automation system on the basis of IEEE-488-1 bus with possible transfer to VME- bus systems. Fifth International School "Automation and Scientific Instrumentation '88", 11-21.10.1988, Varna, Bulgaria.
- Marinoff, A. and E. Georgieff (1989). About a concept on expert system for control and interpretation of photoelectrical and photothermal solar energy convertors data. Second International Symposium of Socialist Countries "Theory and Application of Artificial Intelligence", 29.05. - 02.06.1989, Sosopol, Bulgaria.

## SOLAR ENERGY ACCUMULATION INTO COMBUSTIBLE GASES

R.M.MUSTAFAYEVA, S.Ya.AKHUNDOV, I.I.MUSTAFAYEV,  
P.F.RZAYEV, I.M.ALIYEV

Radiation Research Department, the Azerbaijan  
SSR Academy of Sciences, 31a Narmanov Prospekt,  
Baku 370143, USSR

### ABSTRACT

The paper deals with the development of solar gasification for oil residues and mazout, in particular, at a high-temperature solar power plant. The compositions of resultant gases, the product heat capacities and the process efficiency have been determined.

### KEYWORDS

Solar power plant; solar gasifier; solar gasification.

At present extensive search for efficient and ecologically pure methods of solar energy conversion into potential energy of combustible hydrogen-containing gases have been carried out both in our country and abroad.

Nowadays certain progress has been achieved in this trend of modern science: solar power plants and solar gasifiers of various configurations have been developed which are destined for solar gasification of solid fuels, non-cultured high-yield plant varieties, and agricultural wastes into combustible gases (Gregg *et al.*, 1980).

Since the Republic lacks its own coal base, a necessity to seek for local "available" material appeared. In Azerbaijan conditions mazout was chosen as such available raw material. The work attempts to develop an efficient way of combustible gas production by thermochemical transformation of oil residues using accumulated heat of solar radiation. Taking the above into consideration, we have developed and tested a pilot solar power plant for solar gasification of oil residue - mazout which is being formed during crude oil treatment at the Baku refineries. The elemental content of Baku sulphur-free mazout in weight per cent is as follows: C = 87.3; H = 11.6; O = 0.6; N = 0.5.

The unit consists of reflecting mirror, solar gasifier, the systems of starting material and oxidizer feeding and dosage, the systems of resultant gas collection, sun-guided systems, control and communication unit.

The thermochemical conversion of mazout at solar power plant is as follows: accumulated solar rays reflected from the reflecting mirror pass to the solar gasifier through the systems of starting material and oxidizer feeding and dosage. Starting material is heated in the reaction volume of solar gasifier to the decomposition temperature ( $\sim 1000^\circ\text{C}$ ) and thus the process of mazout thermochemical decomposition into  $\text{H}_2$ ;  $\text{CH}_4$ ;  $\text{C}_2\text{H}_4$ ;  $\text{C}_2\text{H}_6$ ;  $\text{C}_3\text{H}_6$ ;  $\text{C}_3\text{H}_8$ , etc., takes place.

The composition of reaction products was determined chromatographically. Diversified configurations and modifications of solar gasifiers were used depending on starting material employed and technological conditions of the process (solar pyrolysis or solar gasification).

Experimental studies showed that maximum yields of finite products are obtained upon mazout decomposition at  $800\text{--}900^\circ\text{C}$ ,  $0.1\text{ MPa}$  pressure, and solar radiation intensity of

$3135\text{kJ/m}^2$  hour. In this case combustible gas yield was  $\sim 80$  m/hour. The content of resultant gas in volume % is given below:

$\text{H}_2 \sim 20\text{--}25$ ;  $\text{CH}_4 \sim 30\text{--}35$ ;  $\text{C}_2\text{H}_4 \sim 20\text{--}25$ ;  $\text{C}_2\text{H}_6 \sim 3\text{--}3.5$ ;

$\text{C}_3\text{H}_6 \sim 9\text{--}10$ ;  $(\text{C}_3\text{H}_8 + \text{C}_4\text{H}_{10}) \sim 1\text{--}2$ ;  $\text{CO} \sim 3.5\text{--}4$

Solar gasifier efficiency was determined as the ratio of resultant product potential heats to overall spent energy and was calculated from the following relation:

$$\eta = \frac{\sum G_i Q_i^H}{Q_{\text{starting}} + Q_{\text{accum.}}} \quad (1)$$

Overall calorific power of reaction products was therefore determined from:

$$Q_{\text{prod.}} = \sum G_i Q_i^H \quad (2)$$

The calculation of quantity of heat accumulated during gas formation was performed from the following relation:

$$Q_{\text{accum.}} = Q_{\text{reaction product}} - Q_{\text{mazout}} \quad (3)$$

Having acquired  $Q_{\text{accum.}}$  from (1-3) the solar gasifier efficiency was found as

$$\eta = \frac{Q_{\text{accum.}}}{Q_0} \quad (4)$$

In the conditions under study  $\eta$  was: for (mazout) solar pyrolysis  $\sim 0.28\%$ , for solar gasification  $\sim 30\%$ . Tables 1 and 2



present composition, yield and calorific power of resultant gases for the mazout solar pyrolysis and solar gasification at a solar power plant, respectively.

The analysis of the data obtained showed that efficient solar energy accumulation (or preservation) into combustible gas energy occurs upon thermochemical accumulation of oil residues (mazout) at a solar power plant fed by external heat (due to concentrated solar radiation heat) as opposed to the traditional technology based on internal heat feeding (when actual 35% of mazout are combusted).

Table 1.

Reaction products	Amount			Product calorific power, kJ	
	volume %	weight gr	mass %		
H <sub>2</sub>	22.3	2.321	2.4	26.7	334.8
CH <sub>4</sub>	34.6	28.831	30.2	40.6	1527.4
C <sub>2</sub> H <sub>4</sub>	20.4	29.748	31.1	23.8	1492.3
C <sub>2</sub> H <sub>6</sub>	3.2	5.004	5.2	3.7	249.8
C <sub>3</sub> H <sub>6</sub>	11.2	24.496	25.6	12.8	1198.5
CO	3.5	5.10	5.3	4.08	50.1
Total	95.2	95.6	99.8	111.68	4852.9

Table 2.

Reaction products	Amount			Product calorific power, kJ	
	volume %	weight gr	mass %		
H <sub>2</sub>	23.5	2.1	2.5	27.8	348.6
CO	11.2	14.0	16.7	13.4	168.0
CH <sub>4</sub>	26.2	18.6	22.1	31.1	1118.0
C <sub>2</sub> H <sub>4</sub>	26.5	33.4	39.8	31.6	1875.6
C <sub>3</sub> H <sub>6</sub>	3.5	6.7	8.0	4.2	368.7
C <sub>2</sub> H <sub>6</sub>	1.6	2.2	2.6	1.9	122.5
C <sub>3</sub> H <sub>8</sub>	3.5	7.0	8.3	4.1	380.4
Total	96.0	84.0	100	118.3	4381.

## REFERENCES

- Gregg, D.W., and Grens I.Z., K.W. Taylor, W.R. Aiman (1980). Solar restoring of oil shale. "Proc. 15th Intersoc. Energy convers. Eng. Conf. Energy 21st. Century." Seattle. Wash. 1980. Vol. New York. N.Y., pp.262-267.
- Mustafayeva, R.M., S.Ya. Akhundov, I.I. Mustafayev and P.F. Rzaev (1989). Processes of converting of oil residues and oil bituminous species. 9th Miami International Congress on Energy and Environment, 2, p.269.

TAKING AN INTEGRATED VIEW OF ENERGY ALTERNATIVES  
The hotel industry of Cyprus

J.K. JACQUES and C.Y. KONIS

Department of Business and Management, University of Stirling, Stirling  
FK9 4LA, U.K.

ABSTRACT

Hourly electricity and heat demand data from a large typical seaside Hotel were collected. Various options for satisfying the Hotel's energy demand patterns with mixes of energy supplies of different capacity (cogeneration, wind energy, and solar energy) were investigated with the use of recently developed simulation software. Sensitivity analysis with respect to energy produced and anticipated cost was performed. A 0.5 heat to power ratio for cogeneration was established as optimum. When using energy mixes, cogeneration, must be the largest "supplier". When the participation of wind and solar energy in the energy mix increases, the solution becomes less cost effective. The optimum mix of energy is very sensitive to a reduction of anticipated energy production/collection.

KEYWORDS

Simulation, hotels, cogeneration, solar, wind, energy mix.

INTRODUCTION

Hotel industry is the island's most important industry. The competitiveness of this industry is vital to the economy of the island. With the exception of a 4% contribution of solar energy all energy needs of the island are satisfied by imported oil. Electricity, which is produced by oil fired stations, is the main type of energy used by the hotel industry (45%) Its total sectoral consumption is only second to the sector of cement. Heating needs in most hotels are satisfied by gas oil (42% of total energy consumed in a hotel) and cooking by liquid petroleum gas (13%). Water heating is done, in almost half of the hotels, partly by solar systems and partly by gas oil. Because of various reasons (non availability of data, lack of thorough study and a monopoly covering the production of electricity) no use of electricity production by wind has been done up to this moment. Cogeneration is an option examined only recently (5).

Though theoretically the economics of this option are excellent (a considerable fraction of the rejected heat to the sink is added to the available work), the variation of the demand pattern makes the problem of optimization of the capacity of the systems quite complicated. The solution of the problem of finding cost effective mixes of energy and the adoption of new and better supply pattern that will be making maximum use of various alternative energy sources (i.e wind and solar) will be extremely useful for this and possibly for other industries as well.

The potential of applied microcomputer simulation modelling for cogeneration has been reviewed by a recent paper (5). A microcomputer simulation model designed by Jacques and Muir (3) has been developed and tested. The model aims to simulating random fluctuations of the demand patterns and examining their effect on the overall economic performance of a proposed micro cogeneration project. A complete description of this package and can be found in a recently published paper (3). A distinct advantage of the package exploited fully in the present study is its ability to account for variability in the supply-potential of alter native sources of energy (allows the input in the program of other sources such as solar, wind etc).

## THE PRESENT STUDY

The present study has used the simulation package developed extensively in order to experiment with various mixes of energy supplies (cogeneration, solar, wind) with the aim of drawing useful conclusions as far as the optimum capacities and mixes of these supplies is concerned. Real hourly heat and electricity demand data were collected for three typical "seasons".

The heat input in the model by the solar system configurations each hour was calculated using hourly global radiation data for the specific location provided by the Meteorological Service of Cyprus for tilted surfaces at 50. A panel efficiency of 70 per cent and a system efficiency of 40 per cent was used for locally manufactured installed and priced solar systems.

Wind velocities for the specific site available at a height of 10 meters were transferred to that of the shaft height utilizing data from wind generator manufacturers and the Meteorological Service of Cyprus. Hourly electricity produced for each "season" was then calculated and inputted to model.

Data collection of hourly heat and electricity consumption data is one of the most difficult, vital, time consuming and perhaps costly activities of the investigation. The importance of the existence of "enough" reliable data can not be overemphasized. Figures 1 and 2 present a sample of 3 days of electricity and heat demand patterns.

Seven different cogeneration systems of varied capacity and heat to power ratio of 0.5 were analysed. The choice of the specific heat to power ratio was based on previous study (3) the results of which were reconfirmed in this study. In this simulations no other auxiliary forms of energy were inputted.

Following experimenting of three different energy "mixes" (configurations) that included cogeneration, solar system and a wind generator the effect of varying the capacity of the cogeneration system (between 40 and 140 KW) while maintaining the same wind generator (60 KW) and solar system (250m<sup>2</sup>) was investigated.

The effect of varying the heat power ratio was investigated on a specific configuration and the ratio of 0.5 confirmed.

For the optimum configuration (100KW of cogeneration + 15KW wind generator + 150m<sup>2</sup> of solar heating system) a substitution of the chp power with wind generated electricity and solar produced heat was performed (4 new configurations). For the optimum configuration a sensitivity analysis was performed aiming at investigating (a) the effect of changes in the quantity of heat and electricity input by the specific energy mix and (b) the effect of changes in the cost of the system.

## RESULTS

- (a). Table 1 presents the results of seven cogeneration configuration without any auxiliary energy inputs (i.e solar energy, and wind energy). Yearly benefit and Net Present Worth for each investment are given.
- (b). Table 2 presents the results of five simulation runs. In configuration No 4 cogeneration input varied and solar and wind input was kept constant (thus creating five new configurations). Configuration No 5 presents the results of varying the heat to power ratio of the cogeneration system for a specific configuration.
- (c). Table 3 presents the results of substitution on the configuration with the best financial return of cogeneration capacity with auxiliary sources of energy (solar and wind).
- (d). Table 4 presents the results of a sensitivity analysis performed on the optimum configuration. The test for the cost included only the optimistic case (more close to reality) of reduction in the cost of all equipment involved.
- (e). Figure 1 and 2 present sample heat and electricity demand data for one day of each "season". Three different patterns ( data for three days for each season ) were inputted into the model.

## CONCLUSIONS

The study confirmed previous simulation runs that for the specific demand patterns and needs the optimum range of cogeneration capacity is in the range of 100-120 KW where as the optimum heat to power ratio is 0.5. It was proved that in energy "mixes" the configuration is more cost effective when the largest electricity and heat supplier is the cogeneration system. When the participation of auxiliary energy sources in the energy "mix" increases the configuration becomes less cost effective. The best of the configurations tested was the one that included a cogeneration unit of 100 KW a solar system of 150m<sup>2</sup> and a wind generator of 15 KW. The sensitivity tests proved that the optimum solution is very sensitive to a reduction of energy collected and produced. A future drop of the equipment cost will prove very beneficial to the adoption of this integrated approach of energy "mixes". Financial analysis can be considered to

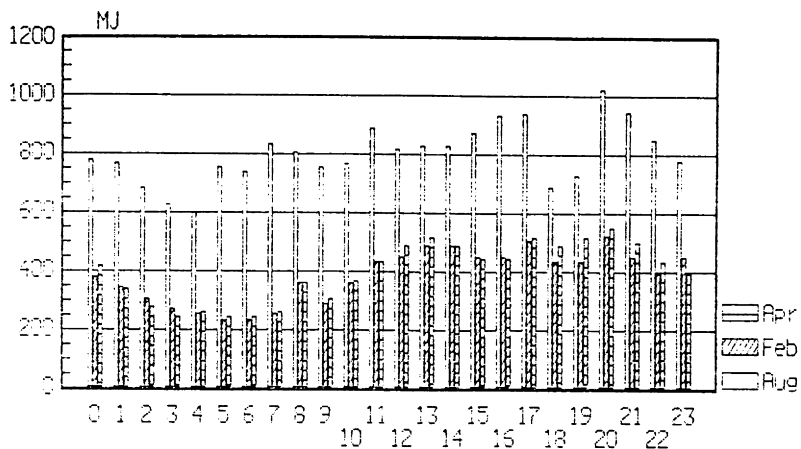
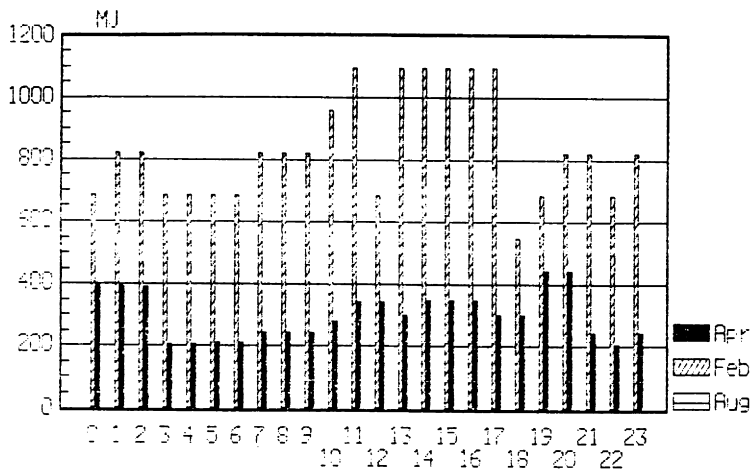


Fig. 1. Sample electricity hourly data



(extremely low demand for August)

Fig. 2. Sample heat hourly data

be on the "tough" side since possible tax allowances for the investments were not included. Further simulation runs with weather and energy data from more hotels is required in order to draw general conclusion for optimum energy "mixes" for the whole of the hotel industry.

Table 1. Results of cogeneration simulations without auxiliary sources of energy.

	40 KW	60 KW	100 KW	120 KW	140 KW	180 KW	200 KW
Capacity	: 40 KW	60 KW	100 KW	120 KW	140 KW	180 KW	200 KW
Cost	: 16000	20000	30000	40000	46000	60000	80000
Heat/Power	: 0.5	0.5	0.5	0.5	0.5	0.5	0.5
Efficiency	: 0.85	0.85	0.85	0.85	0.85	0.85	0.85
Availability	: 0.95	0.95	0.95	0.95	0.95	0.95	0.95
Maintenance	: 1200	1500	2500	2800	3300	4500	5600
Yearly benefit	: 6859	10243	16697	19750	22246	26327	27807
N P V	: -21288	-12088	4796	13881	16756	17511	8480

Table 2. Results for various simulations utilising auxiliary sources of energy.

Configuration 1 : 100 KW Chp + 15 KW Wind + 100 m2 Solar Cost of equipm. : 30,000 Chp + 16500 Wind + 15,000 Solar Total cost : 61,500 Maintenance : 1500 Own Capital : 30,000 Yearly Benefit : 19,051 NPV : 8,030
Configuration 2 : 100 KW Chp + 30 KW Wind + 150 m2 Solar Cost of equipm. : 30,000 Chp + 19,500 Wind + 22,500 Solar Total cost : 70,000 Maintenance : 2,500 Own Capital: 30,000 Yearly Benefit : 19,725 NPV : 81
Configuration 3 : 100 KW Chp + 45 KW Wind + 200 m2 Solar Cost of equipm. : 30,000 Chp + 22,000 Wind + 30,000 Solar Total cost : 82,000 Maintenance : 3,000 Yearly Benefit : 20,883 NPV : -7005 NOTE : Own capital : 30,000, Inter : 9%, Depr. Plan : 10%, Disc. Rate : 20%
Configuration 4 : 60 KW Wind + 250 m2 Solar with 40,60,100,120 and 140 KW Chp each time With 40 KW Chp : Cost 99,100, Maintenance : 1,000 Yearly benefit : 13,752, NPV : -31,493 With 60 KW Chp : Cost 103,100, Maintenance : 1,500, Yearly benefit : 16,866, NPV : -25,940 With 100 KW Chp : Cost 113,100, Maintenance : 2,000, Yearly benefit : 23,272, NPV : -14,982 With 120 KW Chp : Cost 123,100, Maintenance : 2,500, Yearly benefit : 25,965, NPV : -14,073 With 140 KW Chp : Cost 129,100, Maintenance : 2,500, Yearly benefit : 28,382, NPV : -10,546 NOTE : For all mixes in this conf. the "own" capital assumed was 55,000 the depreciation time was 5 years, the repayment of loan 5 years and the discount rate 20%. H/P was 0.5, efficiency 0.85 and availability 0.95.
Configuration 5 : 75 KW Wind + 300 m2 Solar + 100 KW Chp Total Cost : 128,000 Availability : 0.95 Efficiency : 0.85 Maintenance : 1,500 H/P = 0.5 : Yearly benefit : 24,470, NPV : -20,982 H/P = 0.6 : Yearly benefit : 23,668, NPV : -23,152 H/P = 0.75 : Yearly benefit : 22,479, NPV : -26,374 H/P = 1.0 : Yearly benefit : 20,949, NPV : -30,513
NOTE : The depreciation plan used was 5 years, the discount rate was 20% "own" capital was 64,000 and the repayment plan was 5 years.

Table 3. Results of simulations in which chp capacity was substituted with wind and solar input.

Configuration A : 100 KW Chp + 15 KW Wind + 150 m2 Solar Equipment Cost : 30,000 (Chp) + 16,000 (Wind) + 20000 (Solar) Total Cost : 66,000 Maintenance : 2,000 Own Capital : 33,000 Yearly benefit : 20,063 NPV: 10113
Configuration B : 80 KW Chp + 30 KW Wind + 200 m2 Solar Equipment Cost : 25,000 Chp + 19,000 Wind + 27,000 Solar Total Cost : 71,000 Maintenance : 2,000 Own Capital : 35,500 Yearly benefit : 17,409 NPV: -1875
Configuration C : 60 KW Chp + 60 KW Wind + 250 m2 Solar Total Cost : 99,000 Maintenance : 2,000 Own Capital : 49000 Yearly benefit : 17422 NPV : -1759
Configuration D : 40 KW Chp + 75 KW Wind + 300 m2 Solar Equipment Cost : 16,000 Chp + 53,000 Wind + 41,000 Solar Total Cost : 110,000 Maintenance : 2,000 Own Capital : 55,000 Yearly benefit : 14980 NPV:-14990

NOTE : For all simulation above the following financial data were used : Discount rate : 15%,  
Deprec. Plan : 10 years, Loan repayment 5 years.

Table 4. Sensitivity analysis for optimum configuration (100 KW Chp + 15 KW Wind + 150 m2 Solar).

10% more heat and electricity NPV : 10,204 Yearly benefit : 19,775	10% less heat and electricity NPV : 7,583 Yearly benefit : 19,250
20 % more heat and electricity NPV : 10,633 Yearly benefit : 20,096	20% less heat and electricity NPV : 5,928 Yearly benefit : 18,728
10% more cost NPV : 8798 Yearly benefit : 17455	10% less cost NPV : 11,529 Yearly benefit : 22,700
20% more cost NPV : 8090 Yearly benefit : 16950	20% lest cost NPV : 12,135 Yearly benefit : 24276

NOTE : For all financial analysis the following data were used : (a) Electricity price = 4c/KWh,  
(b) Off-peak electricity = 4c/KWh, (c) Boiler Fuel = 1.25 c/KWh,  
(d) Chp Fuel = 0.95c/KWh.

## REFERENCES

1. California Energy Commission. Results from the Wind Project Performance Reporting System. 1988 Annual Report, August 1989.
2. J.H. Horlock. Cogeneration, Combined Heat and Power, Pergamon, (1987)
3. J.K. Jacques and A. Muir. Development of decision algorithms in situations of considerable data uncertainty : stochastic patterns of energy demand and their effect on optimal economic choice for cogeneration. Proceedings, Second International Congress, Industrial Engineering, Innovation in Industrial Engineering, France December 1988, pp301-311.
4. J.K. Jacques, J.B. Lesourd and J.M Ruiz. Modern Applied Energy Conservation. Ellis-Horwood, (1988).
5. J.K. Jacques and C.V. Konis with computer technical assistance from : A. Muir and C. Mitchell. Systems modelling and micro-computing applied to Mediterranean hotel energy conservation planning through cogeneration simulations, Applied Energy Research September (1989).
6. K.S. Bajaj and T. Singh. Cost - effective Energy Management. SIBN 0-912524-22-7, Business News Publishing Co. (1982)
7. Ministry of Agriculture and Natural Resources, Meteorological Service. A study of Surface Winds i n Cyprus. Meteorological Paper Number 8, October (1986).
8. Ministry of Agriculture and Natural Resources, Metereological Service. Solar Radiation and Sunshine Duration in Cyprus. Meteorological Paper Number 10 (Revised) Dec. (1988).
9. W.C. Turner. Energy Management ISBN 0-471-0852-X, 1982, Wiley and Son Inc.

## UTILIZATION OF LOW GRADE ENERGY SOURCES FOR AIR-CONDITIONING USING SOLID-DESICCANT MATERIAL

Y. CARMI, E. KORIN and I. BORDE  
Ben-Gurion University of the Negev, P.O. Box 1025, Beer-Sheva 84110, Israel

### ABSTRACT

A solid-desiccant open-cycle system for cooling and air-conditioning is an attractive means for utilizing low-temperature energy, such as solar, geothermal or waste heat, and for reducing the consumption of conventional energy.

The aim of this work is to study the kinetics of heat and mass transfer in a dehumidifier with parallel sheets coated with a thin layer of sorbent. We have developed a theoretical model which accounts both for Knudsen and for surface diffusion of moisture within the particle. An experimental system for validation testing of the theoretical model was constructed containing sheets 610x250x1 mm in size coated with silica gel (0.22 mm). The outlet air temperature and humidity were recorded and determined as a function of time. In general there is reasonable agreement between the theoretical and experimental data.

### KEYWORDS:

Air-conditioning; dehumidifier; intraparticle diffusion; silica gel; solid desiccant; solar energy; waste heat

### INTRODUCTION

During the past two decades, various open and closed cycles based on a solid desiccant dehumidifier have been extensively investigated for cooling and air conditioning applications. In comparison with the vapor compression system driven by electrical energy, the solid desiccant system offers the possibility of utilizing various energy sources such as waste heat, solar energy, and natural gas. As compared with a liquid-gas adsorption system it has the advantage of simplicity, low maintenance requirements, and reliability.

Many solid-desiccant open-cycle systems (ventilation, recirculation or Dunkle mode) comprise three basic components: an evaporative cooler, a sensible heat exchanger, and a dehumidifier. The air-heat exchangers and evaporative coolers available today can be modified to operate successfully in these applications however, commercially available dehumidifiers, i.e., packed bed type, have the disadvantage of a high pressure drop and high resistance to mass transfer (Clark *et al.*, 1981, Perassan *et al.*, 1987, Biswas *et al.*, 1984).

Since the performance of the dehumidifier has a significant effect on the overall COP in any thermodynamic cycle, a great deal of effort is currently being devoted to developing dehumidifiers which fulfill the special requirements of air-conditioning applications. Generally, there are two ways of improving performance: a) by improving the properties of the solid desiccant; and b) by improving the design parameters and operating conditions. Research has been conducted in both directions at the Energy Laboratory of The Institutes for Applied Research.



Among the various ideas proposed, the concept of air flow through parallel sheets coated with a thin layer of sorbent is considered one of the most promising (UCLA concept). Its main advantages are that it is characterized by a small pressure drop and a low resistance to heat and mass transfer (Biswas *et al.*, 1984, Kravchik *et al.*, 1988). We therefore adopted this concept in our R&D project. Most kinetic studies on mass and heat transfer based on the UCLA concept neglect the solid-side heat and mass transfer resistances (Biswas *et al.*, 1984, Kravchik *et al.*, 1988, Kravchik *et al.*, 1990).

One of the most important design parameters in this concept is the average particle size of the sorbent material. As the particle size increases the mass of solid desiccant in the system and its adsorption capacity increase; on the other hand, the solid-side resistance increases and the mass and heat transfer rate decrease. In order to study this important effect a reliable theoretical model which considers both gas- and solid-side resistances is needed. The aim of this work is to develop reliable theoretical models for heat and mass transfer in the UCLA concept allowing for both Knudsen and surface diffusion of moisture within the solid.

The paper presents the theoretical model, the experimental system for validation testing, and experimental results.

### MATHEMATICAL FORMULATION

The model for the prediction of the transient heat and mass transfer processes in the bed is based on the following assumptions:

- The bed is adiabatic - The heat transfer at the sides of the bed are neglected.
- The air velocity along the bed is constant and uniform.
- The air humidity and temperature depend only on direction of flow.
- Diffusion and conduction in the direction of flow are negligible.
- The processes in the bed are quasi-steady-state.
- The Nusselt and Sherwood numbers are equal ( $Nu_{Dh} = Sh_{Dh} = 7.54$ ) in a laminar regime flow.
- The diffusion of moisture within the particle are characterized by both surface and Knudsen diffusion.
- There are no temperature gradients in the solid particle. ( $B_i < 0.1$ ).
- The temperature of the sheets is the same as temperature of the solid particles.

The energy balance in the air stream is given by:

$$\frac{\partial T}{\partial Z} = \frac{2h_c(T_s - T)}{C_{pg} \rho_g BU} \quad (1)$$

where  $T$ ,  $T_s$  are respectively the temperature of the air and of the solid particle,  $h_c$  is the convective heat transfer coefficient,  $B$  is the distance between the plates,  $U$  is the air velocity,  $C_{pg}$ ,  $\rho_g$  are the specific heat and density of the gas, and  $Z$  is a longitudinal coordinate (in the direction of the flow).

The mass balance of the water vapor in the air stream is given by:

$$\frac{\partial Y}{\partial Z} = \frac{2K_g(Y_{eq} - Y)}{B \rho_g U} \quad (2)$$

where  $Y$  is the air humidity ratio,  $Y_{eq}$  is the humidity of air in equilibrium with the solid desiccant, and  $K_g$  is the gas-side mass transfer coefficient.

The energy conservation within the desiccant felt is expressed as:

$$\frac{\partial T_s}{\partial t} = \frac{2K_g H_{ads}(Y - Y_{eq}) - 2h_c(T_s - T)}{2\Omega d_{sg} \rho_{sg} + \delta_{ss} \rho_{ss} C_{ss}} \quad (3)$$

where  $H_{ads}$  is the heat of adsorption,  $\Omega$  the volume fraction of silica gel in the desiccant film,  $d_{sg}$  the particle diameter,  $\rho_{sg}$  the density of the silica gel on a wet basis, and  $d_{ss}$ ,  $\rho_{ss}$ ,  $C_{ss}$  are the thickness, density and specific heat of the plate, respectively.

Conservation of water in the desiccant particle is described by:

The effective Knudsen diffusion coefficient is:

$$D_{k,eff} = \frac{\epsilon_p}{\tau_g} 22.86 a T^{1/2} \quad (4)$$

where  $\epsilon_p$  is the particle porosity,  $\tau_g$  the tortuosity factor for intraparticle gas diffusion, and  $a$  is the average pore radius.

The effective surface diffusion coefficient is:

$$D_{s,eff} = \frac{D_o}{\tau_s} \text{Exp} [-\mu H_{ads}/RT] \quad (5)$$

where  $\tau_s$  is the tortuosity factor for intraparticle surface diffusion and  $R$  is the  $H_2O$  gas constant,  $D_o$  and  $\mu$  are constant parameters.

The overall effective diffusion is (Pesaran *et al.*, 1986):

$$D_{eff} = D_{s,eff} + \frac{D_{k,eff}}{\rho_{sg}} \frac{\partial Y}{\partial X} \quad (6)$$

$$\frac{\partial X}{\partial t} = \frac{1}{r^2} \frac{\partial}{\partial r} \left( r^2 D_{eff} \frac{\partial X}{\partial r} \right) \quad (7)$$

where  $X$  is the silica gel water content and  $r$  is the particle radius

#### Boundary and initial conditions

$$T(0,t) = T_{in} \quad (1b)$$

$$T_s(z,0) = T_{s,0} \quad (3i)$$

$$Y(0,t) = Y_{in} \quad (2b)$$

$$X(z,0) = X_0 \quad (7i)$$

$$\frac{\partial X}{\partial r} \Big|_{r=0} = 0 \quad (7b_1)$$

$$-\rho_{sg} D_{eff} \frac{\partial X}{\partial r} \Big|_{r=R} = K_g (Y_{eq} - Y) \quad (7b_2)$$

In addition there is an equilibrium vapor pressure relation:

$$Y_{eq} = Y_{eq} [X, T, P] \quad (14)$$

#### Method of Solution

Equations (1), (2), (3), (7), (14) are five equations in the unknowns  $T$ ,  $T_s$ ,  $Y$ ,  $Y_{eq}$ , and  $X$  respectively within the boundary and initial conditions. For numerical solution equations (1), (2), (3) were expressed by a fourth-order Runge-Kutta Scheme and solved simultaneously, while equation (7) was expressed by the Crank-Nicholson Scheme.

### EXPERIMENTAL SYSTEM AND PROCEDURES

A schematic description of the experimental system is given in Fig. 1. The experimental dehumidifier is 250 x 88 mm in cross-section and 610 mm in length. To minimize side effects and approximate adiabatic

operational conditions the system was insulated on all sides with polystyrene. This system can accommodate 19, 25 or 35 sheets 610 x 25 x 1 mm in size, with 1 mm intervals between the sheets. The sheets were made of 1.0 mm thick polycarbonate panels coated on both sides with fine silica gel particles. The silica gel was supplied by BDH Chemical Ltd. (Cat. no. 300614T), and had an average pore radius of 11 Å. The material was sieved and only the 0.20-0.25 mm fraction was used. The particles were glued to the polycarbonate sheets with a silicon rubber adhesive.

The following operational conditions of the bed can be regulated independently: air flow rate, temperature and humidity of inlet. The flow rate was adjusted by an air control valve and measured by an air rotameter (Fisher & Porter Company). A 2 kW electrical air heater equipped with a voltage regulator was used to obtain the desired air temperature. The required relative humidity at the bed inlet was regulated by a wet Raschig-ring column humidifier or by one of the compressed air filter-driers supplied by Thomas Scientific Ltd. Both the relative humidity and the temperatures at the inlet and outlet were measured. Relative humidity was measured ( $\pm 1.5\%$ ) by capacity thin film sensors C80 Hygromer Rotronic). The sensors were periodically calibrated against standard salt solutions. Each probe element was also equipped with a Pt100 resistor sensor which enables simultaneous measurement of the air temperature with an accuracy of  $\pm 0.5^\circ\text{C}$ .

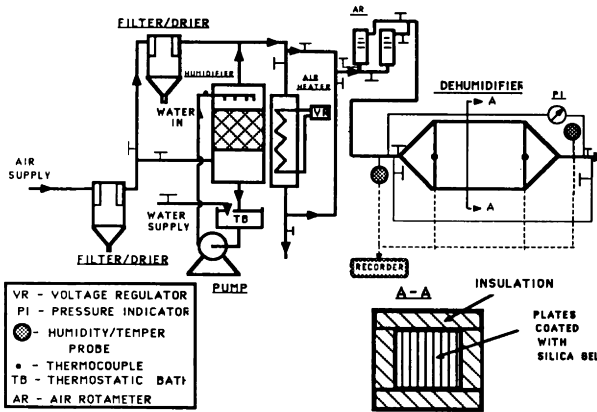


Fig. 1. Schematic description of the experimental system

RESULTS AND DISCUSSION

Figs 2, 3 and 4 compares representative breakthrough curves as predicted by the theoretical model with the experimental results. It can be seen that for low relative humidities (Figs. 2) the match between the theoretical model and the validation test results is generally good; however as the relative humidity increases the degree of agreement decreases (Fig. 3, 4). This effect may be attributed in the main to the equilibrium relation, which we found to be satisfactory up to a level of 45 % relative humidity. This point is currently studied with a view to improving the theoretical model.

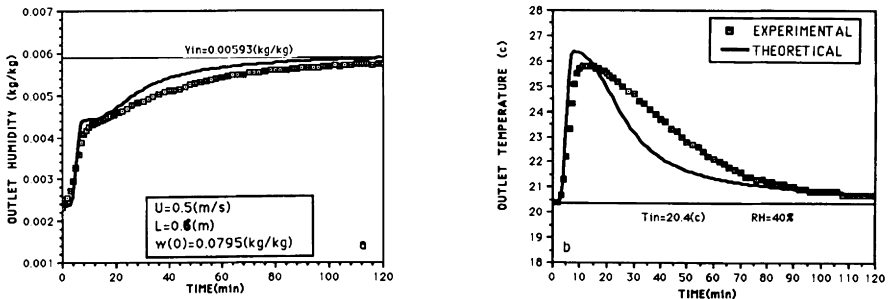


Fig. 2. Comparison between experimental measurements and theoretical results a) outlet air humidity time b) outlet air temperature time (RH = 40%)

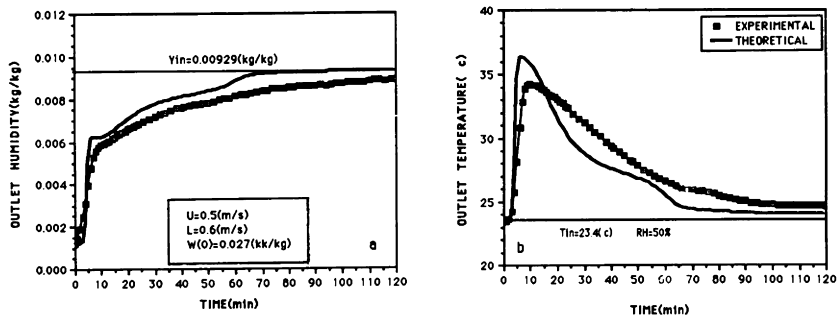


Fig. 3. Comparison between experimental measurements and theoretical results a) outlet air humidity time b) outlet air temperature time (RH = 50%)

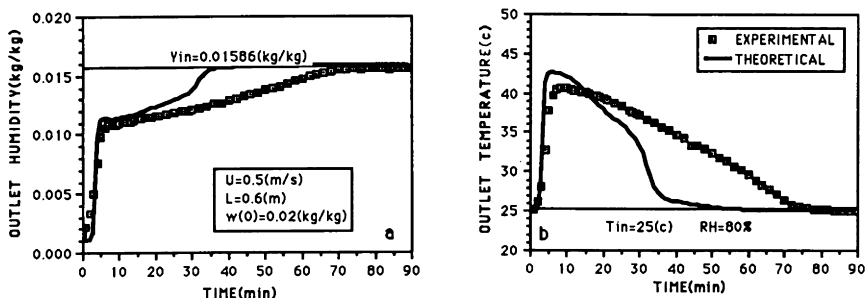


Fig. 4. Comparison between experimental measurements and theoretical results a) outlet air humidity time b) outlet air temperature time (RH = 80%)

## SUMMARY AND CONCLUSIONS

A computerized simulation model for studying the kinetics of heat and mass transfer in dehumidifiers consisting of parallel sheets coated with solid desiccant material was developed. Validation testing of the model was carried out using experimental data corresponding to silica gel as the sorbent material. The model can be improved by using more accurate thermophysical properties of the sorbent material than are currently available in the literature. The model will be used to study the role of the particle size of the solid desiccant material (such as silica gel, zeolites, etc.) and particularly for preliminary evaluation of the performance of new sorbent materials now under development in our laboratory.

## REFERENCES

- Biswas, P., Kim, S. and Mills, A.F. (1985) A compact low-pressure-drop desiccant bed for solar air-conditioning applications, 1: Analysis and design. *J. Sol. Energ. Eng.*, **106**, 153-158.
- Clark, J.E., Mills, A.F., Buchberg, H., (1981) Design and testing of thin adiabatic desiccant beds for air conditioning application. *ASME J. of Solar Energy Engineering*, **103**, 89-9.
- Kravchik, T., Korin, E. and Borde, I. (1988) Investigation of low-pressure-drop solid desiccant dehumidifier for air conditioning applications, Proceedings of 22nd Israel Conference on Mechanical Engineering, p. 183, Ben-Gurion University of the Negev.
- Kravchik, T., Korin, E. and Borde, I. (1988) Studies of the drying kinetics of air flow through thin layers of silica gel. Proceedings of the Sixth International Drying Symposium (IDS '88) OP 625-632.
- Kravchik, T., Korin, E. and Borde, I. (1990) Influence of material properties and heat removal on mass and heat transfer in a solid desiccant dehumidifier. *Journal Chem. Eng. and Process*, **27**, 19-25.
- Pesaran, A. A., and Mills, A.F., (1987) Moisture transport in silica gel packed beds. Theoretical and experimental study. *J. Heat and Mass Transfer*, **30**, 1037-1060.

## Liquid Desiccants for Low Energy Regeneration

M. AL-ZUHAIR AND A.A.M. SAYIGH

Department of Engineering , University of Reading , Whiteknights  
P.o. Box 225 , Reading RG6 2AY U.K.

### Abstract

Liquid absorbents which show promise for solar application include aqueous solutions of Lithium Chloride , Lithium Bromide , and Calcium Chloride , as well as Glycols of the Ethylene glycol group . To achieve good dehumidification regeneration of the weak solution should take place at above 80 deg. C . The purpose of this paper is to experimentally measure the vapour pressure of a mixture of two salts at different molalities at constant total ionic strength . The driving force for dehumidification and regeneration has been calculated and compared with a solution of LiCl only at the same ionic strength . An increase of 16.115% has been observed for a solution having 0.5 moles  $MgCl_2$  and 15.5 moles LiCl upon a solution of 17 moles LiCl only for the regeneration process.

### Introduction

Open-cycle desiccant cooling systems offer a potentially promising alternative to the Absorption and Rankine type methods of solar air-conditioning (1) .

The cooling capacity of an open-cycle absorption cooling system is uniquely determined by the amount of water evaporated from the weak solution . There are different kinds of regeneration equipments , two of which been highly investigated by many scientists , the open collector/regenerator and the packed bed . The open collector/regenerator have been carefully analyzed (2,3) for the use of regenerating the weak solution in an open-cycle . The performance of packed columns have been thoroughly investigated in series of papers by Shulman (4) . The use of a packed column in an open-cycle as a dehumidifier and regenerator have been investigated by Factor (5) .

The regeneration efficiency in a continuous open-cycle , regardless of the heat input to the system by solar energy or other means of energy , is the percentage of the amount of water removed to the amount of water been absorbed in the dehumidifier . Mass transfer is highly dependent upon the difference in the pressure of water in the air and on the surface of the solution . Concentrations of LiBr solutions ranging from 45 wt% to 60 wt% been investigated by Patnaik (6) . The condensation of water vapour from the air was reduced when using weak solution and the evaporation of water from the solution in the regeneration process decreases with increasing solution concentration . The present study concentrate on the vapour pressure of the ternary system Water-Magnesium Chloride-Lithium Chloride and the ternary system Water-Calcium Chloride-Lithium chloride and the effect of those systems on mass transfer driving force .

### Vapour pressure of LiCl solution

Vapour pressure of LiCl solution for different concentrations at temperatures ranging from 25 deg. C to 100 deg. C has been measured and a comparison between our data and Uemura (7) are shown in Figure (1) . An equation of the form :

$$\text{Log}(kPa) = A + \frac{B}{T-C} \quad (1)$$

P : Vapour pressure in k Pa

T : Temperature in Deg. K

$$A = 6.719985 + 0.01368815 X - 0.0003027801 X^2$$

$$B = -1593.132 - 1.736042 X - 0.05884013 X^2$$

X : Concentration of LiCl wt%

after Antoine (8) was chosen to fit the data . The constant C been chosen to be -45.107 (9) . This part of the experiment is to check for the reliability of the system . The mean deviation from Uemura's data was ranging from 1.1 kPa for 10% solution to 0.05 kPa for 40% solution .

### Selection of concentration

LiCl solution with concentrations ranging between 38 and 42 wt% been used in absorption refrigeration machines (7) . 17 moles LiCl solution has the concentration of 41.88% and a total ionic strength of 17 . The ionic strength in defined

$$I = .5 \sum_i m_i z_i^2 \quad (2)$$

I : Ionic strength

$m_i$  : Molality of ion i

$z_i$  : Number of charges on ion i

A total ionic strength of 17 has been chosen in this study . Molality rang for  $MgCl_2$  and  $CaCl_2$  is between 0.5 and 3.5 moles which according to the constant total ionic strength LiCl molality well be ranging between 15.5 and 6.5 moles . Equation (3) is used to control the molalities .

$$17 = 3 \times MgCl_2 \text{ molality} + LiCl \text{ molality} \quad (3)$$

### Vapour pressure of mixed salts

The vapour pressure of a ternary system has been discussed by many scientists. Robinson (10) proposed a method where the vapour pressure lowering of an aqueous solution containing two salts A and B can be compounded additively from the vapour pressure lowering of a solution containing the salt A alone and another solution containing the salt B alone. The additivity rule requires that we use the vapour pressure lowering per mole of salt at the total ionic strength of the mixed solution. He also reports

the vapour pressure of six different combination of salts mixtures at 25 deg. C experimentally and by the additivity rule , the percentage differences were ranging from 0.1 to 2.2% .

Sako (9) reported the vapour pressure of ternary aqueous solution containing 1.057 moles  $MgCl_2$  and 2.905 moles  $CaCl_2$  for temperatures ranging from 49 to 125 deg. C . He used a method proposed by Teruya (11) to calculate the vapour pressure for comparison , the percentage differences were 8.95% at 49 deg. c and 2.24% at 125 deg. C . Out of this we find it necessary to experimentally evaluate the vapour pressure of the ternary aqueous solution in question . Table (1) shows the solubility of  $Mgcl_2$  and  $Cacl_2$  in solutions of  $LiCl$  (12) , it also shows it in molality scale . The experimental vapour pressure data has been fitted to equ. (1) with A and B are functions of molality .

For  $Mgcl_2, LiCl$  solutions .

$$A = 6.889255 + 0.04685054 M - 0.01616207 M^2$$

$$B = -1803.047 + 15.59322 M - 3.874455 M^2$$

M :  $Mgcl_2$  molality ranging from 0.5 to 3.0

For  $Cacl_2, LiCl$  solutions

$$A = 6.983705 - 0.04685054 M - 0.01616207 M^2$$

$$B = -1811.357 + 14.14154 M + 8.48152 M^2$$

M :  $Cacl_2$  molality ranging from 0.5 to 3.5

Table (2) shows the experimental vapour pressure of  $Mgcl_2, LiCl$  solutions compared with the calculated by the additivity rule and table (3) shows it for  $Cacl_2, LiCl$  solutions .

#### Mass transfer approach

The driving force behind the transfer of any substance A from one media to another is the difference in concentration of A between the two medias . In a desiccant system A is water vapour in the air that need to be absorbed in the dehumidification process . In the regeneration of the desiccant water need to be evaporated to concentrate the desiccant for reuse . In both processes the matter is the difference in water vapour pressure . Introducing equ. (4)

$$LMDF = \frac{1-P_{vl}/P_t}{1-P_{vg}/P_t} \quad (4)$$

LMDF : log mean driving force

$P_{vl}$  : solution vapour pressure

$P_{vg}$  : water vapour pressure in the air

$P_t$  : total pressure

If LMDF is +ve then the water well be transferred from the air to the

solution and vice versa . In other word if the solution pressure is lower than the water vapour pressure in the air then the air well be dehumidified , and if the solution vapour pressure is higher than the water vapour pressure in the air the solution well be regenerated .

If we consider a system of 17 moles LiCl solution at 25 deg. C and air at 35 deg. C with 0.015 kg water/kg air specific humidity the LMDF = 0.01788 . If we heat up the same solution to 70 deg. C ,with the same air , the LMDF = -0.04476 . Now if we chose a solution of 0.5 moles  $MgCl_2$ +15.5 moles LiCl for the same conditions above LMDF = 0.017414 for

dehumidification and LMDF = -0.07212 for regeneration . The percentage decrease in the driving force for dehumidification is 2.605% and the percentage increase in the driving force for regeneration is 16.116% .

If we consider a solution of 0.5 moles  $CaCl_2$ +15.5 moles LiCl for the same conditions the decrease in LMDF for dehumidification well be 5.135% and the increase in LMDF for regeneration well be 25.166% , and a solution of 15.5 moles LiCl only for the same conditions , the decrease in LMDF comparing with 17 moles LiCl well be 6.824% , and the increase well be 22.7% .. Therefore adding any amount of  $MgCl_2$  or  $CaCl_2$  to LiCl solution well change

the slop of the pressure curve and results in higher pressure at higher temperature which is shown in Figure (2) .

Any other parameter influence the mass transfer is related to the mass transfer characteristic of the equipment used , the air and solution flow rates , the air temperature , and the solution temperature .

### Conclusion

The open-cycle cooling system is highly influenced by the kind of absorbent used and its dehumidification and regeneration characteristic . One of the most important parameter in selecting a liquid absorbent is it's vapour pressure lowering . Using a mixture of two salts having different vapour pressure characteristic appears to be feasible and offers advantages over one salts solution . A mixture of two salts offers the choice of selecting different molality combination according to the climate condition . whether it is hot and dry or hot and humid , all in relation with the vapour pressure behavior of the mixed salt solution .

### References

- 1- Grossman G. and Johannsen A.. Solar Cooling And Air Conditioning Prog. Energy Combust. Soci. Vol. 7 pp 185-228 , 1981
- 2- Collier R.. The Analysis And Simulation Of An Open-Cycle Absorption Refrigeration System Solar Energy Vol. 23 pp 357-366 , 1979
- 3- Peng C.P. And Howell J.R.. Analysis Of Open Inclined Surface Solar Regenerator For Absorption Cooling Applications Solar Energy Vol. 28 pp 265-268 , 1982
- 4- Shulman H.L.,Ullrich C.F.,And Wells N.. Performance Of Packed Columns A.I.Ch.E. Journal Vol. 1 June , 1955
- 5- Factor H.M. And Grossman G.. A Packed Bed Dehumidifier / Regenerator For Solar Air Conditioning With Liquid Desiccants Solar Energy Vol. 24 pp 541-550 ,1980
- 6- Patnaik S.,Lenz T.,And Lof G.. Performance Studies For An Experimental Solar Open-Cycle Liquid Desiccant Air Dehumidification System



- Solar Energy Vol. 44 pp 123-135 ,1990
- 7- Uemura T.. Studies On The Lithium Chloride Absorption Refrigeration Machine.  
Technology Report Of The Kansai University, No. 9 pp 71-88 ,1967
- 8- Antoine C.. Chem. Rev. Vol. 107 pp 681-836 ,1888
- 9- Sako T.,Hakuta T.,And Yoshitome H.. Vapour Pressure Of Binary ( $H_2O-HCL$ , $-MGCL_2$ ,AND $-CACL_2$ ) And Ternary ( $H_2O-MGCL_2-CACL_2$ ) Aqueous solutions  
J.Chem.Eng.Data.Vol 30 ,pp 229,228 ,1985
- 10- Robinson R.A.,And Bower V.E.. An Additivity Rule For The Vapour Pressure Lowering Of Aqueous Solutions.  
J.Of Research Of The National Bureau Of Standards-A.Physics And Chemistry , Vol.69A ,No 4 ,1965
- 11- Teruya K.,Hosaka S.,Nakano T.,And Nakamori I.. J.Chem.Eng. Jap. 1,9,1976
- 12- Linke W.F.. Solubilities,Inorganic And Metal-Organic Compounds  
4<sup>th</sup> Edi. American Chem. Soci. ,1958

Fig (1)

## Experimental Vapour Pressure Of LiCl Solutions

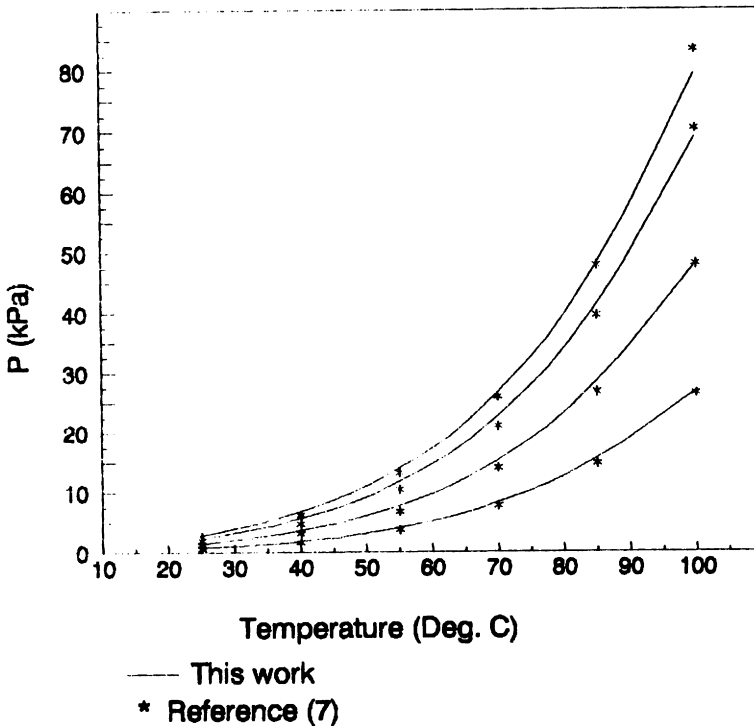


**Table (1)**  
**Solubility Of  $MgCl_2$  And  $CaCl_2$  In Solutions Of  $LiCl$**

$LiCl$ wt%	$MgCl_2$ wt%	$LiCl$ Moles	$MgCl_2$ Moles	$LiCl$ wt%	$CaCl_2$ wt%	$LiCl$ Moles	$CaCl_2$ Moles
45.85	0.00	19.813	0.000	46.15	0.00	20.216	7.869
43.10	2.66	18.751	0.520	42.54	3.78	18.693	7.608
40.00	5.78	17.402	1.120	41.62	5.45	18.548	5.971
38.00	6.99	16.294	1.334	39.23	8.30	17.636	3.973
35.40	8.32	14.837	1.552	34.97	12.13	15.593	3.374
33.90	9.34	14.088	1.728	28.31	17.22	12.280	2.848
29.30	13.70	12.125	2.524	24.72	20.51	10.646	2.089
22.00	18.00	8.950	3.151	19.48	24.64	8.223	1.425
18.90	20.00	7.296	3.438	8.02	36.66	3.419	0.827
8.40	28.30	3.130	4.695	3.08	42.47	1.334	0.634
0.00	35.40	0.000	5.755	0.00	45.98	0.000	0.000

**Table (2)**  
**Vapour Pressure Of  $MgCl_2$ ,  $LiCl$  Solutions At Rounded Temperatures**

Molality	T(K)	P(kPa)*	P(kPa)**	dev.
$MgCl_2$ 0.5 $LiCl$ 15.5	298.15	0.63719	0.64447	0.007
	313.15	1.59042	1.57939	0.011
	328.15	3.60286	3.52014	0.082
	343.15	7.51686	7.23810	0.278
	373.15	14.6156	13.8902	0.725
1.0 14.0	298.15	0.69345	0.69675	0.005
	313.15	1.72653	1.70594	0.020
	328.15	3.90250	3.78951	0.113
	343.15	8.12573	7.78889	0.356
	373.15	15.7708	14.8993	0.901
1.5 12.5	298.15	0.74822	0.75303	0.004
	313.15	1.89008	1.83249	0.027
	328.15	4.19872	4.05889	0.139
	343.15	8.73195	8.29969	0.432
	373.15	16.8269	15.8485	1.080
2.0 11.0	298.15	0.80039	0.80732	0.007
	313.15	1.98676	1.95905	0.029
	328.15	4.48711	4.32626	0.158
	343.15	9.32761	8.83047	0.487
	373.15	18.0773	16.8276	1.249
2.5 9.5	298.15	0.84886	0.86160	0.012
	313.15	2.11022	2.06560	0.024
	328.15	4.76315	4.56763	0.165
	343.15	9.80536	9.36128	0.544
	373.15	19.2033	17.8067	1.396
3.0 8.0	298.15	0.89260	0.91588	0.023
	313.15	2.22214	2.21215	0.009
	328.15	5.02230	4.66700	0.155
	343.15	10.4565	9.69205	0.584
	373.15	20.2832	18.7658	1.507
		37.0663	33.6462	3.420

\* Smoothed values

\*\* Calculated using the additivity rule

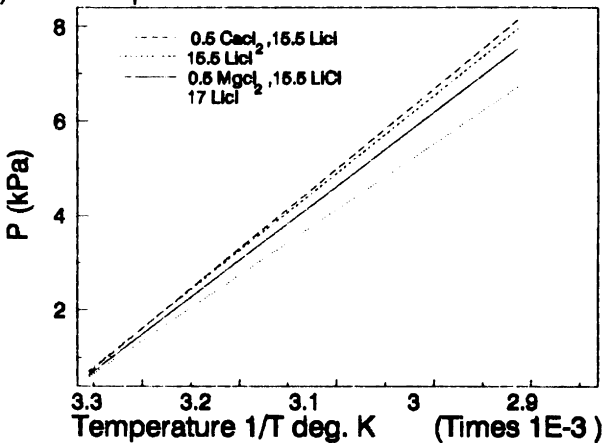
Mean deviation = 0.629 (k Pa)

**Table(3)**  
**Vapour Pressure Of CaCl<sub>2</sub>,LiCl Solutions At Rounded Temperatures**

Molality	T(K)	P(kPa)	P(kPa)*	Dev.
CaCl <sub>2</sub> 0.5 LiCl 15.5	298.15	0.6827	0.6632	0.029
	313.15	1.7082	1.6082	0.101
	328.15	3.8826	3.5691	0.283
	343.15	8.1202	7.4272	0.693
	358.15	15.823	14.298	1.525
	373.15	29.009	25.927	3.073
1.0 14.0	298.15	0.7108	0.7182	0.005
	313.15	1.7875	1.7837	0.003
	328.15	3.9905	3.9475	0.043
	343.15	8.3002	8.1471	0.153
	358.15	16.094	15.698	0.406
	373.15	29.373	28.448	0.927
1.5 12.5	298.15	0.7551	0.7793	0.024
	313.15	1.8607	1.9191	0.058
	328.15	4.1672	4.2958	0.013
	343.15	8.6051	8.8671	0.262
	358.15	16.578	17.074	0.496
	373.15	30.074	30.985	0.911
2.0 11.0	298.15	0.8183	0.8423	0.024
	313.15	1.9940	2.0746	0.081
	328.15	4.4213	4.8443	0.223
	343.15	9.0484	9.5870	0.538
	358.15	17.289	18.482	1.173
	373.15	31.137	33.484	2.347
2.5 9.5	298.15	0.9048	0.9053	.0007
	313.15	2.1752	2.2301	0.055
	328.15	4.7861	4.9827	0.228
	343.15	9.9502	10.307	0.657
	358.15	18.282	19.848	1.567
	373.15	32.900	36.003	3.403
3.0 8.0	298.15	1.0202	0.9683	0.052
	313.15	2.4156	2.3655	0.030
	328.15	5.2201	5.3411	0.121
	343.15	10.439	11.027	0.588
	358.15	19.533	21.237	1.704
	373.15	34.515	39.522	4.997
3.5 6.5	298.15	1.1739	1.0773	0.096
	313.15	2.7308	2.5408	0.189
	328.15	5.8089	5.8484	0.039
	343.15	11.453	11.748	0.293
	358.15	21.157	23.039	1.882
	373.15	36.952	41.041	4.089

\* Calculated using the additivity rule  
 Mean deviation = 0.774 k Pa

**Fig (2)** **Vapour Pressure Of Different Solutions**



AUGER ELECTRON SPECTROSCOPY AS A TOOL OF ELECTRONIC  
AND CHEMICAL INFORMATION

BY

NORREDDIN. S. BISHENA, DEPARTMENT OF PHYSICS  
UNIVERSITY OF THE SEVENTH OF APRIL  
ZAWIA - LIBYA

ABSTRACT :

The present paper reviews the nature and the mechanism involved in the production of Auger electron and its relation to local electronic and chemical environment the shapes and positions of corresponding spectra determine the chemical environment at the site of the initial core-hole of Auger electron . Measurements and analysis of the energy shifts of the Auger peaks together with oxygen adsorption effect on the spectral distribution of the emitted Auger electrons are related to local electronic density of states .

INTRODUCTION :

The wide range of (AES) usage made it a dependable technique for researchers and scientists to obtain quantitative elemental measurements and analysis . Knowledge of chemical environment changes through changes of Auger electron spectra gave better understanding of oxidation mechanisms of the surfaces of solids .

Being a two - electron process, fig. 1, AES is uniquely distinguished from other processes involving one electron only , such as X - ray photoelectron spectroscopy (XPS) . Both XPS and processes may be initiated by either an incoming photon or electron . Since the final state of Auger process leaves the system with two valence-holes compared to one valence-hole in XPS , this tends to complicate the spectrum analysis , on the other hand , a greater surface sensitivity of AES compared to XPS was

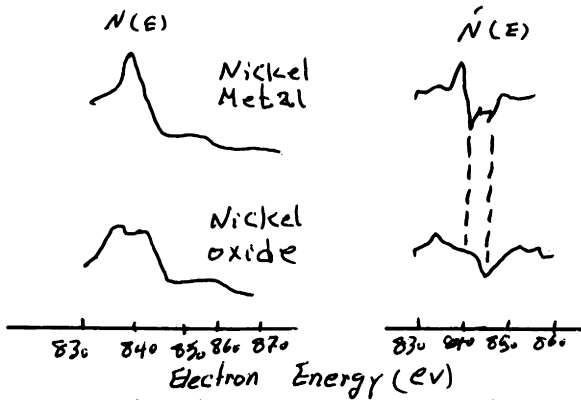


Fig 3. Changes in the LMM Auger From Pure Nickel and Nickel oxide.

binding energy . Secondly , the change in the outer electron configuration upon formation of the solids which in turn makes significant difference in core level binding energy (9).

#### LINE SHAPE CHANGES:

It is shown that Auger electron c.c.v. signal from a metal should have a shape which is directly relatable to the valence band density of state of the metal while the lineshape of the c.v.v. signal should depend on the self-convolution of the valence band density of state (10,11,12 ) .

Silicon is a material to which most theoretical attention has been given (13,14,15,16 ) . Calculations made by several researchers have shown that an independent electron theory together with the proper calculation of the matrix element for Auger transition involved, lead to very good agreement between theoretical and loss corrected experimental Si-L<sub>23</sub>VV signals .

In some cases core-valence-valence (c.v.v) spectrum of metals do not bear simple relationships to ground state valence band density of state distribution , Copper is an example of such material as illustrated in fig , (5). Both loss corrected LVV and MVV lines from copper have been compared with valence band density of state and been found distorted. One type of distortion is due to satellite Auger intensity superimposed on the L<sub>23</sub>VV line as in fig, (5). These distortions resulted

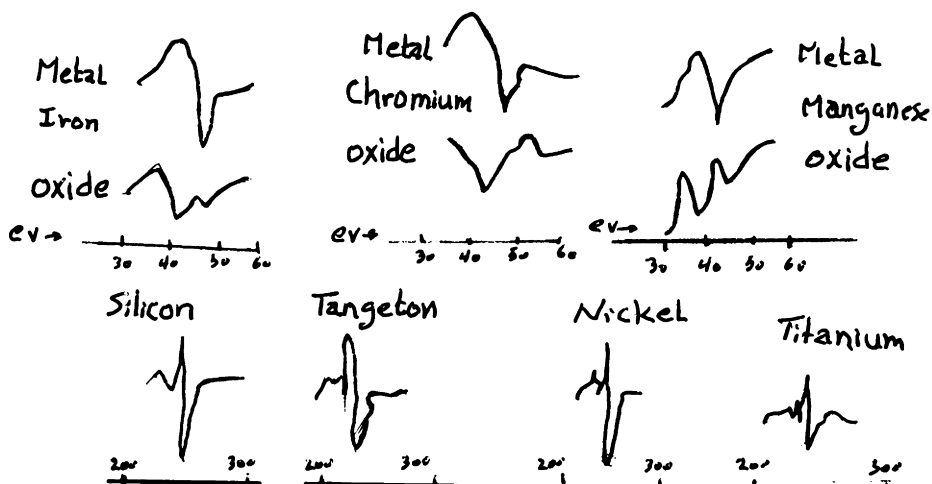


Fig. 2. Chemical effects in Auger peak shape and position

the complication involved may be gained by considering the energy level diagram in fig. (4)? In part (a) levels  $i, j, k$ , are assumed to be core levels with a specified energy values  $E_i, E_j, E_k$ , respectively, which are measured with respect to some reference level. In part (b) one electron was removed from the  $i^{\text{th}}$  core-level, as a result Auger transition (core-core-core) denoted  $asi-j-k$  transition would be occur. This transition would involve one electron in the  $j$ -level dropping down in energy to fill the  $i$ -level with the energy made available by this process being given to a second electron in the  $k$ -level. If this energy is sufficient the  $k$ -electron will escape the ion and be detected as Auger electron.

In the case of multi-atom system in which we assume an atom as in fig. (4), embedded, with energy diagram like that in part (c) where the core levels  $i, j, k$ , of the atom appear relatively narrow but with different energy values  $E_i, E_j, E_k$ , the change in these energy levels are chemically induced changes that one would like to measure and interpret using core-level spectroscopy. Changes in the core levels energy are due to either sharing or transfer of valence band electrons to bring about the bonding of the atom to its neighbours, and to the resulting changes in the electrostatic potential in the core region of the atom. Even in the formation of elemental solids, the valence electrons are significantly measured, being first of all compressed to a small volume of space called (Wigner Seitz Cell) which leads a reduction to the electron

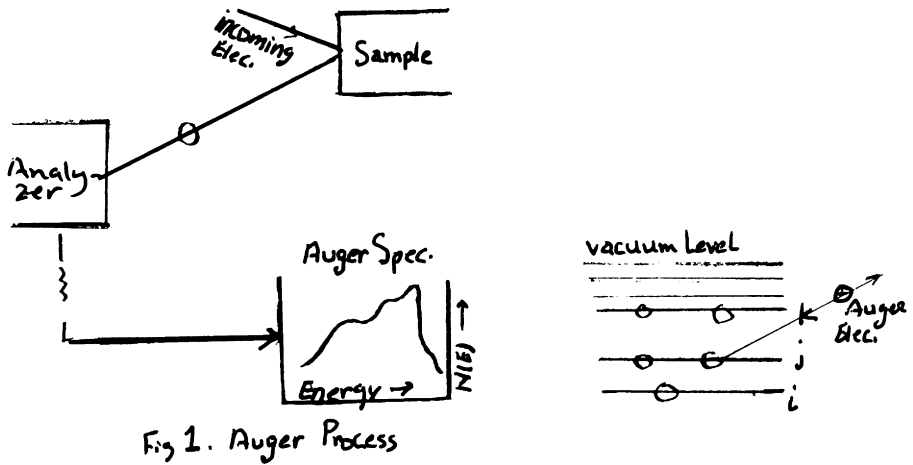


Fig 1. Auger Process

reported accompanied with more precision of site specificity of valence density of state (2).

In this review emphasis on electronic and chemical information for silicon surface during adsorption of oxygen obtained by AES are reported and compared to XPS? A study of  $\text{SiO}_2$  thin film by Auger electron energy shifts and its relation to chemical environment is discussed along with a study of line shape of Auger spectra (3,4).

#### AES ENERGY SHIFTS :

When two or more elements combined to form a compound, changes occurs in the electron binding energies caused by the change in effective charge on each atom. This will lead to change in the position of Auger spectra peaks. Predicting and explaining energy shifts is relatively complicated, however, it is more usual to use a fingerprint technique to identify compounds from Auger spectrum as in figure (2) in this figure examples of the changes in the peak position and peak shape observed in two metals on oxidation and in carbon from various carbides (5,6,7,8). Transitions involving core electrons and its relation to changes in peak shape and position are reported using high resolution analyzers, fig (3).

Chemically induced shifts of core level lines in XPS or the related shifts of core signals in AES are related to changes in core-level binding energy. Although a quantitative understanding of

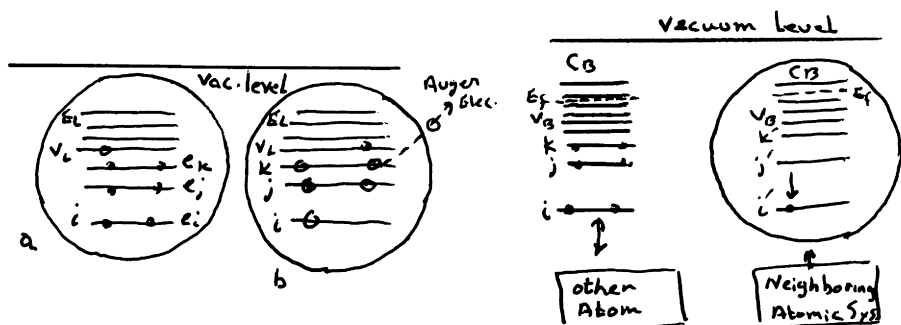
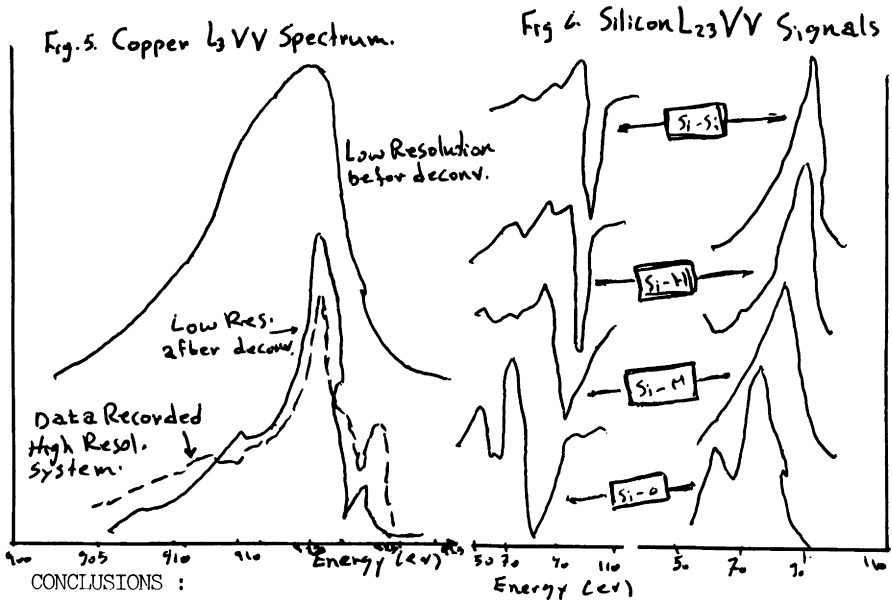


Fig. 4. Auger Electron Transition.

from the hole-hole interaction in the two hole final state configuration (17,18). It was found that these distortions have a bearing not only on the lineshape in c.v.v lines from metals but also on relative energy position of the components of c.v.v lines from gas phase molecules and on the decay probabilities involved in each electron and photon stimulated (ESD, PSD) respectively (19,20). Ramaker, White, and Murday (21,22) had proposed and quantified a model for Auger induced desorption from covalent (or ionic) system.

In the cases of material exhibiting band like c.v.v Auger lines, one can obtain valence band density of state change information from the changes in lineshapes of a series of Si-L<sub>23</sub>VV lines, fig.(6). The use of lineshape analysis in studies of gas phase molecules had demonstrated that AFS in a finger print mode, can be used identify the local chemical environment of an atom. Examples of such studies may be summarized in the following 1-To investigate the chemical and electronic properties of semiconductor materials (23,24,25) 2-Assessment of the surface chemical reaction relationship to the properties of the solid surface. 3-To study the passivation and corrosion of metals and metal alloys surface properties. 4-Depth profiling of thin films and crystalline materials (26, 27,28). 5-C-H bonding in tetrahedrally bonded carbon compounds (CH, C<sub>2</sub>H<sub>4</sub>, CH<sub>4</sub>,.....).





Auger electron spectroscopy is a truly surface analytical technique which is capable of providing chemical and electronic information for elements and compounds concerning the top few layers without damaging the surface with a great special resolution and good surface sensitivity. AFS is a probe of the local density of state about the Auger decay site and it is therefore; conceivable that the local valence electron distribution density of state at the bonding site may be obtained by combining AFS information and the data of XPS. The explanation as to when adsorption occurs following core-hole creation in a compound is tied-up with the concept of localization in the two hole final state of AES lineshape and electron energy position were closely related to the chemical and electronic information about the surface of the solids. Studies of this type are proving valuable in determining the causes of failures in materials, electronic properties of semiconductor materials and solid surface chemical reactions

#### REFERENCES

- 1 - David E. Ramaker, Springer Series in Chemical Physics (to be published).
- 2 - R. Graussner, Auger Effect and related topics, lecture notes, University Pierre et Marie Curie, Paris, France, 1974.
- 3 - C. Nordling, et al, Ark.F. Fysic, 13,483(1958).
- 4 - J.J. Lender, Phys, Rev.91.1382 (1953).
- 5 - W.D. Sevier, Low Energy Electron Spectroscopy, Interscience New York-

- (1974),
- 6 - A.V.Facrea, Surface Sci. 1,319, ( 1964).
  - 7 - R.H.Wild, Vacuum. 31,183, (1981).
  - 8 - F.Bauer, Vacuum, 22, 539 ( 1972 ),
  - 9 - G.C.Allen and R.H.Wild J.Electron Spectroscopy, 15,409 ( 1974).
  - 10- H.H.Madden, J.Vac.SCI. Technol, 18 April (1981).
  - 11- S.Oklunda and S.Leygraf, Surf.Sci,40,179,(1973).
  - 12- J.E.Houston, etal, Solid State Commun, 21,679,(1977).
  - 13- H.H, Madden and J.F.Housten, Solid state Commun,21,1080(1977).
  - 14- F.J,McGuire, Phys.Rev.A,16,2365, (1977).
  - 15- J.E.Housten, J.Vac.Sci?Technol. 12,225,(1975).
  - 16- D.E. Ramakerm etal,Phys.Rev. B19,5375 (1979).
  - 17- D.E.Ramaker, Phys,Rev. B21, 4608 (1980).
  - 18- M.L. Knotes and P.J. Feiblman?Surf. Sci.90,78(1979).
  - 19- D.E. Ramaker, etal, J.Vac. Sci. Technol. 18.748(1981).
  - 20- J.A,Tagle, etal, Surf.Sci.70.77.(1978).
  - 21- J,A,Appelbaum, etal,Surf,Sci. 70.654L1979).
  - 22- H,H,Madden,39<sup>th</sup>Conf,on Physical Electronics, College Park MD. 1979.  
Sci. 105(1981).
  - 23- T. Metsushema, etal, Surf. Sci,67,89(1977).
  - 24- M,De Crescenzi. etal. Phys. Rev. B.32,(1985).
  - 25- I,Sakata, and Y,Hayashi, Applied Phys.A, 37, 153 (1985).
  - 26- F.Demichelie, etal, solar Cells,14,149(1985).
  - 27- F,Haug, etal, Z,Physik, B,22,139,(1975).

## THE USE OF SOLAR CELLS UNDER 10X CONCENTRATION

\*A.J. CHIANUMBA, †R.W. BENTLEY, and †G.R. WHITFIELD

\*Department of Engineering, University of Reading,  
Reading, RG6 2AY, U.K.

†Department of Cybernetics, University of Reading,  
Reading, RG6 2AX, U.K.

### ABSTRACT

The major part of the cost of solar photovoltaic systems, such as water pumps, is the solar cells themselves. The paper reports on the measurement at intensities up to about  $10\text{KW/m}^2$  of prototype commercial technology solar cells,  $5\text{cm} \times 5\text{cm}$ , that incorporate a fine screen-printed front contact grid optimized for 10-sun performance. Comparison was made with commercial cells of the same technology with a conventionally spaced front grid. The results showed the efficiency of the 1-sun cells to fall from 13% at 1-sun to 7% at 10-sun illumination, while the efficiency of the 10-sun cells went from 10% to 9% under the same test conditions. The series resistance of the 1-sun cells was found to be about 0.07 ohms, and that of the 10-sun cells to be around 0.025 ohms.

A 51-cell string of the 10-sun cells used with a reflective parabolic solar concentrator gave an output of 88 watts at the maximum power point when the direct radiation was about  $800\text{ W/m}^2$ . This cell string was used to power a small motor/pump unit.

Initial calculations indicate that a simple concentrator system using these 10-sun cells would pump water at a cost significantly below that from a conventional flat PV array system.

### KEYWORDS

Solar water pumping; photovoltaics; concentration

### INTRODUCTION

While small energy needs, such as for water pumping, can be met by photovoltaics, particularly in developing countries with an abundance of sunshine, the cost of such systems still renders this option of limited popularity.

Of the components of a typical photovoltaic (PV) system, solar cells constitute the major cost. The cost of water pumped can be reduced by increasing the system efficiency, or by concentrating sunlight on the cells to increase their electrical output. This paper examines the testing and use of PV cells suitable for relatively low concentrations, in the order of 10 sun intensities. This level of concentration was chosen because it achieves most of the available reduction in cell area; because it is achievable with concentrators that do not require continuous tracking throughout the day; and because it is near the practicable limit for conventional screen printed grids.

#### 1-SUN AND 10-SUN CELLS

Normal commercially available 1-sun cells are between about 12% and 14% efficient at 1-sun illumination (1000 W/m<sup>2</sup> and 25°C standard cell temperature). However, their efficiency falls off at higher illumination levels due to the increasing power loss from cell internal resistance. This resistance contains contributions from the bulk of the material, the diffused layer, the contacts with the top metal grid, the grid itself, and finally the cell bus bars. Reducing grid finger spacing reduces the effect of diffused layer resistance and grid contact resistance; but it increases the power loss due to shadowing of part of the cell by the grid.

We were provided with information on contributions to cell resistance and minimum finger width by a commercial PV cell company (BP Solar Ltd., U.K) and carried out optimization calculations on finger width and spacing to achieve maximum output power at 10 suns. The cells so designed were kindly manufactured and provided to us by BP. The nominal cell size was 5 cm square.

#### TESTS

Two 1-sun commercial BP cells and three 10-sun cells (i.e. cells of the same 1-sun technology, but with the modified front grid) were tabbed and tested in our solar simulator. The simulator consists of a light source having 4 halogen bulbs, adjustable for setting the desired illumination uniformity, and a moveable base which could be set at approximately 1-sun and 10-suns illumination levels. The cells were mounted on a water cooled aluminium box fixed to the simulator base. The uniformity of the illumination over each test cell's surface was monitored using a 1 x 0.5 cm "small master" cell calibrated against a calibrated BP solar cell. The intensity was measured with a 10-sun "master" cell also calibrated against the calibrated BP cell.

The 4-point measurement technique was used to obtain the I-V characteristics of the cells which were plotted on an X-Y recorder and shown in Fig. 1. Cells A, B and C were 10-sun cells while D and E were 1-sun cells - though they were tested in the order A, D, B, C, E. Cell temperatures were monitored using thermocouples; they averaged 22°C at 1-sun and 35°C at 10-suns. The maximum power points,  $P_{mp}$ , were found by drawing constant power lines on an I-V axis and matching this with the cell characteristics. The efficiency of each cell was calculated as ((power output from the cell at  $P_{mp}$ /power input to the cell) x 100%). Table 1 shows the results.

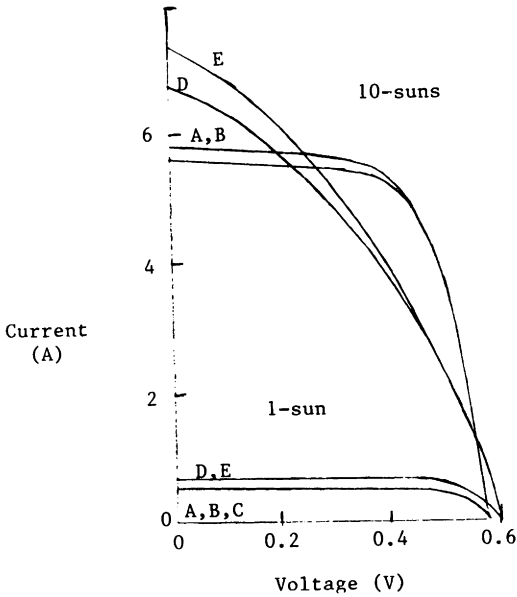


Fig. 1. I-V characteristics of single cells  
 A,B,C 10-sun cells  
 D,E 1-sun cells

Table 1. Summary of cell characteristics

Cell type and letter	1-sun test		10-sun test	
	Peak power (W)	Efficiency (%)	Peak power (W)	Efficiency (%)
10-sun A	.225	9.4	2.07	8.8
B	.241	10.2	2.04	8.8
C	.225	10.2	2.02	8.7
1-sun D	.305	13.4	1.57	7.0
E	.305	13.2	1.64	6.7

SERIES RESISTANCE

For measuring the series resistance, the I-V characteristics of the cells at the two light intensities were used. (Wolf and Rauschenbach, 1963) An interval  $\Delta I_1 = \Delta I_2$  from the short circuit currents  $I_{sc1}$  and  $I_{sc2}$  was chosen so as to obtain two points  $V_1, I_1$  and  $V_2, I_2$  on the characteristics near the maximum power points. The voltages were adjusted to the standard temperature of 25°C using the approximate relation  $\Delta V = -0.5\%/^{\circ}C$ . The corrected voltage was used to calculate the series resistance as

$$R_s = (V_1 - V_2)/(I_2 - I_1)$$

The 1-sun cells have a series resistance of 0.07 ohms while that of the 10-sun cells is 0.025 ohms.

## CELL STRING FORMATION

It was decided to test outdoors an assembly of the prototype 10-sun cells described above, using a reflective parabolic solar collector already available at the Department of Cybernetics, University of Reading. The collector has an aperture of 1.8 square metres and is mounted with the parabola's long axis transverse to a polar axis, so that it can track the sun through the day with just three manual re-positioning movements. The collector has a 5 cm x 5 cm square aluminium tube 1.52 m long placed at the focal line, with each of two faces of the tube receiving reflected light from half the parabola at a geometric concentration of 12 x. Cold water is passed through this tube to provide active cooling for cells mounted on the two faces.

Separate experiments (Chianumba, 1990) were conducted to find a suitable method of fixing cells to the faces of the aluminium tube to meet the requirements of good adhesion, electrical isolation, and high thermal conductance. The final method adopted consisted of the following: A thin layer of Chomerics 1641 (electrically isolating heat transfer adhesive) was applied to the aluminium tube and allowed to set. 10-sun cells were tabbed and stuck to this using a new thin layer of 1641, checking for each cell that no electrical contact was made to the underlying aluminium tube. The tabbed connections were then joined together giving a series string of 25 cells on one face of the tube, and a 26 cell string on the other face, and the strings were then encapsulated under 1 mm thick glass covers attached with Dow Corning RTV silicone. The best cells were used for the 25 cell string, and the rest for the 26 cell string.

## CELL STRING TESTING

String testing took place outdoors on a number of days under bright sun conditions. Global and direct radiation were measured before and after the I-V measurements, which themselves were carried out using the same controllable external power supply as used in the indoor solar simulator tests. Separately, approximate measurements were taken of the intensity distribution across selected cells along the string, and of the cell temperature (measured at the outer surface of the glass covers over the cells).

Results for the 25 and 26 cell strings, connected in series and parallel, are shown in Fig. 2. When the direct radiation was approximately 800 W/m<sup>2</sup> the series connection gave a maximum power output of 88 watts, about what would be expected from simply multiplying up the corresponding indoor one-cell performance. The cooling was remarkably effective, the cell temperature being only about 10°C above the cooling water temperature.

## TESTING WITH A REAL LOAD

To provide an illustration of the use of this system, it was connected to a small permanent magnet motor and centrifugal pump. Performance was reasonable considering the mismatch between string and pump and motor characteristics, and the low absolute value for efficiencies of the latter two components.

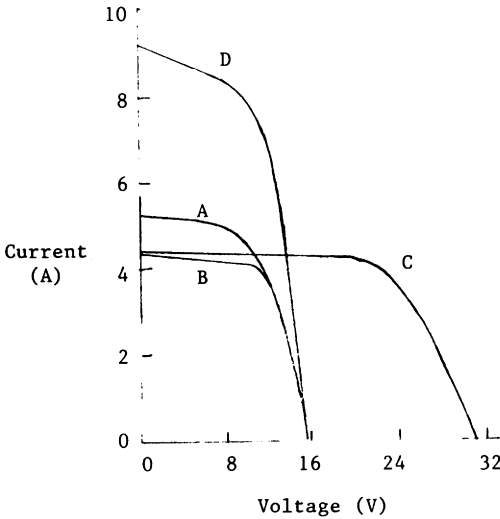


Fig. 2. I-V Characteristics of the cell strings in the concentrator.

- A 25 cell string (The best cells)
- B 26 cell string
- C Both strings in series
- D Both strings in parallel

SIMPLE ECONOMIC ANALYSIS

Here we compare the cost of a conventional PV array with that of a 12 x manually re-positioned concentrating system.

Previous work (Bentley, 1987) indicated that such a concentrator would need roughly twice the aperture of a PV array fixed at the latitude angle for it to have the same annual energy output. This is based on the following factors :

- i) Annual energy at aperture of the concentrator, vs. fixed PV array, at a typical site (New Delhi) 90%
- ii) Solar-grade glass mirror reflectivity 90%
- iii) Intercept and end-loss factors 75%
- iv) Cell cooling factor 85%

The construction cost, in small production runs in an end-use country, including labour and overheads, of a robust steel and marine-ply concentrator using steel-backed glass mirrors was estimated (Bentley, 1987) to be £100/m<sup>2</sup>, where this excludes the cost of cells. The life of such a collector should exceed 15 years.

The 10-sun cells described in this paper would incur, even in very limited production, costs not significantly different from that of conventional 1-sun cells. Taking the latter to cost either £4.50 or £2/Wp (representing small volume purchases at today's, and low-end estimates of medium term, prices) allows the costs of a 1 m<sup>2</sup> flat PV panel, and a 2 m<sup>2</sup> PV concentrator of equivalent annual output, to be compared (Table 2).

Table 2. Economic analysis

Cell costs	£4.50 / Wp		£2.00 / Wp	
	Flat	Conc	Flat	Conc
Collector type:	Flat	Conc	Flat	Conc
Area:	1 m <sup>2</sup>	2 m <sup>2</sup>	1 m <sup>2</sup>	2 m <sup>2</sup>
Cells (13% efficient)	585		260	
(9% efficient)		142		62
Collector	-	200	-	200
Total cost	£ 585	342	260	262

As can be seen, at today's small volume cell costs, the concentrator is a little over half the cost of the flat PV array; the costs only become equal when cell costs fall to £2/Wp.

#### CONCLUSIONS

The use of commercial one-sun cell technology (including screen printing of front surface contacts) to produce cells that give in the region of 9% efficiency under 10-sun concentration has been demonstrated. Such cells cost virtually the same, on an area basis, as 1-sun cells, and thus provide the prospect of significantly reducing the cost of PV power, provided they can be combined with a fairly inexpensive concentrating collector. A simply constructed manually re-positioned parabolic trough appears to be one candidate for such a collector, and a full-scale 1.8 m<sup>2</sup> aperture system using the prototype 10-sun cells coupled to a pump and motor unit has been demonstrated.

#### REFERENCES

- Bentley, R.W. (1987). A manually repositioned concentrating photovoltaic water pump, Ph. D. Thesis, Dept. of Eng., Univ. of Reading, U.K.  
 Chianumba, A.C. (1990). Investigating the performance of "10-sun" photovoltaic cells, M. Sc. Thesis, Dept. of Eng., Univ. of Reading, U.K.  
 Wolf, M. and Rauschenbach, H.S. (1963). Series resistance effects on solar cell measurements, Adv.En.Conv., 3, 455-479.



## EFFICIENCY OF HEAT PUMP APPLICATIONS OF RENEWABLE ENERGY SOURCES

R.Zakhidov, R.Mukhamedov, B.Inogamov  
M.Savochkin and R.Abdurakhmanov

Institute of Power Engineering and Automation  
Uzbek SSR Academy of Sciences  
700143, Tashkent, USSR

### ABSTRACT

This paper addresses itself to heat and cold generation processes using heat pumps, with solar energy and low-mineralized thermal waters serving as low-potential heat sources. It gives a general characteristic of the renewable energy sources of Uzbekistan whose territory is conventionally divided into six zones. The description of each zone includes data on the depth of occurrence, temperature and mineral content of underground waters. Given, also, are estimates of the forecast usable supplies of thermal waters in the republic.

### KEYWORDS

Thermal waters; heat pump; solar collector; heat flux; anomaly.

### INTRODUCTION

The development of the national, as well as world, economy is characterized by increased rates of production and consumption of fuel-energy resources. Therefore, it is of urgent necessity today to improve the fuel-energy balance structure, widely utilize renewable energy sources, and undertake effective energy conservation activity in all the spheres of economy.

In the USSR, heat-producing facilities of low efficiency (such as small boiler-houses, individual-purpose heat generators and stoves) are still in wide use. The principle of direct fuel burning to generate low-potential heat is, in itself, wasteful as part of the fuel energy that could be used in co-generation of heat and mechanical energy is just lost. Meanwhile, utilization of heat pumps with renewable heat sources (solar energy, thermal waters, soil, etc.) allows conversion of low-

potential heat flux into higher-temperature heat usable for heat supply.

#### SOLAR RADIATION. SOLAR-HEAT PUMP SYSTEM

According to the reported estimates, out of the  $1.5 \cdot 10^{21}$  W·h of solar energy radiated to the outer atmosphere about 47% reaches the earth (McVeig, 1981). This energy can be converted into other forms of energy daily used by mankind. In Soviet Central Asia, Uzbekistan in particular, the annual total radiation amounts to 4-5 GJ/m<sup>2</sup>, the annual average sunshine duration for Tashkent is 2500 hours.

The main difficulty in utilizing the solar radiation is associated with the variation of its intensity during the day. Utilization of solar energy requires special facilities to absorb this energy (solar collectors, solar plants, "solar ponds", etc.). The solar plant efficiency rises appreciably if a heat pump (HP) is incorporated in the heat supply system. Incorporation of the HP allows switchover of the solar collector in autumn-spring period to operation on lower-temperature solar energy potentials, further raised to the required levels in the HP. Experiments have shown that the solar plant efficiency in operation with the HP is 10-15% higher than alternatively (Darchia et al., 1982).

Since 1987 the Institute of Power Engineering and Automation has been conducting research activity on development of a solar-heat pump system (SHPS) for air-conditioning of apartment houses, drying agricultural products (summer operation mode), and for space heating and hot water supply (winter operation mode).

In summer the SHPS operates in the air-conditioning mode, the heat removed from the space used for drying agricultural products (apples, grapes, etc.). The high level of the solar radiation (up to 850 MJ/m<sup>2</sup> in July) permits heating water by the solar collector for daily needs. The excess heat can be stored up in a seasonal storage-tank or in the soil to be utilized later in winter time.

In winter the solar collector low-potential heat converted in the HP is used to provide space heating and hot water. At night and in cloudy days, with the solar collector out of operation, the system relies on the storage-tank as a low-potential heat source. At the end of the heating season the storage-tank temperature drops below 10°C, and this cold can be used at the beginning of the air-conditioning season.

The theoretical analyses have shown that combined use of the HP and the solar collector increases the HP conversion coefficient by a factor of 1.5-2, raises the solar energy application efficiency by a factor of 2-2.5, while reducing the organic fuel rate and, thus, improving the environment condition.

**GEOHERMAL RESOURCES: GENERAL CHARACTERISTIC  
AND PECULIARITIES**

In the USSR the geothermal resources developed so far constitute less than 2% of the forecast thermal water supplies estimated for the country to be 19750 thous. m<sup>3</sup>/day or 230 m<sup>3</sup>/s (Grebenshikova, 1976).

Soviet Central Asia is one of the promising regions of the USSR in terms of thermal water development for the national economy. The thermal waters of Uzbekistan can be used for space heating, hot water supply, in balneology and for extraction of minerals (Sr, B, etc.)

In spite of the general occurrence of thermal waters and their large supplies in the republic not all the districts have equal conditions for practical utilization of the deep-seated heat. Unfortunately the data on Uzbekistan's thermal waters vary greatly with different authors. Our group embarked on an investigation of its own, guided by the data obtained straight from geological and hydrogeological field studies.

We have investigated about 500 wells of different depth (ranging from 50 to 3500 m) possibly uniformly distributed over the republic's territory. The main parameters considered were the occurrence depth, temperature and mineral content of underground waters. Further on the piezometric level will be considered as well.

The territory of the republic was conventionally divided into 6 zones:

1. The territory adjoining the Aral Sea in the West (The Ustyurt Plateau)
2. The territory adjoining the Aral Sea in the South (Southern Kara-Kalpakia and Khorezm region)
3. The Kyzyl Kum desert artesian basins (Samarkand region)
4. The Bukhara-Karshi-Surkhandarya artesian basin
5. The near-Tashkent artesian basin (Samarkand, Sir-Darya and Tashkent regions)
6. The Fergana artesian basin (Fergana, Andijan and Namangan regions).

The territory of Kara-Kalpakia has been studied most thoroughly. From the data obtained from about 150 wells (out of the 1400 available here) it is seen that this artesian basin is practically an inexhaustible energy depository. Suffice it to say that 1 Gcal of supplied heat costs 2 roubles in this region, whereas the same, with conventional energy sources, costs 25 times as much, ranging in this autonomous republic between 50 and 60 roubles. It should be added that the water-bearing capacity of the near-Aral zones is very high and in the Southern territory it amounts, by our data, to 740 thous. m<sup>3</sup>/day, which at the average water temperature of 40°C gives a saving of 4200 tons of equivalent fuel per day or 1.5 mln. t.e.f. per year.

The Ustyurt Plateau is no less effective in terms of geothermal power engineering. Here the figure for the annual saving is 1.0-1.2 mln. t.e.f. per year.

The Central Kyzyl Kum zone of uplift is of special interest, geothermally, having some areas with anomalous thermal gradients (up to  $3.7^{\circ}\text{C}/100\text{m}$ ). The discharges in this zone range from 3 to 70 l/s, the mineral content reaching up to 10 g/l. The forecast usable supplies here amount to 450 mln  $\text{m}^3/\text{yr}$ . Thus, the Central Kyzyl Kum zone is comparable with the near-Aral zones in its reserves, while it seems to be more attractive by the characteristics of its underground waters.

The Bukhara-Karshi-Surkhandarya zone contains waters having a far more uniform temperature pattern and occurring at greater depths. About 170 wells have been investigated on the territory of these regions. The mineral content varies from 5 g/l to 120 g/l (Grebenshikova, 1976; Mavritski, 1971; Burak, 1968). The forecast usable supplies in the zone, on the basis of available data, is estimated to be 300-320 mln  $\text{m}^3/\text{yr}$ , which at the average temperature of  $38^{\circ}\text{C}$  gives an annual saving of about 1.7 mln t.e.f.

In the near-Tashkent artesian basin thermal waters occur mainly in three levels. The waters of the first aquifer are of excellent quality and successfully used in balneology and for water supply in the region. The two lower levels are widely used for irrigation of the tilled land and other agricultural needs. With some capital investment, the waters of these aquifers could be used for space heating and, after slight chemical treatment, for hot water supply of animal raising and industrial complexes.

The Fergana artesian basin has a small area but it is where the Adrasman-Chust anomaly, a most attractive object, occurs. The anomaly, discovered in 1968, extends over the territories of Uzbekistan and Tajikistan. Its length is 180 km from the North-West to the North-East along the Fergana valley margin. Here anomalous high temperatures have been recorded in 28 wells at depths ranging from 300 to 5400 m. At a depth of about 2000m rocks are heated to a temperature of  $100-160^{\circ}\text{C}$  and deeper at 5000 m a temperature of over  $200^{\circ}\text{C}$  has been recorded in oil prospecting wells.

The heat flux density within the Adrasman-Chust anomaly varies from 64 to  $207 \text{ mW}/\text{m}^2$ , while at the normal background in the Fergana depression it is  $62 \text{ mW}/\text{m}^2$ . Maximum heat flux density has been recorded in the Jarkamar area. Such high density of heat flux is characteristic of Earth heat deposits in Italy, Hungary, Mexico, and the USA. The aforesaid district has inflows of as much as 15 l/s with the temperature of up to  $50^{\circ}\text{C}$ , with the mouth pressure at 21-23 atm. (Balashov, 1960).

One of the significant features of thermal water is its constant initial temperature throughout the period of use. This is to no small degree important for round-the-year operation of the heat pump based on thermal water as a low-potential heat

source. The constant temperature of thermal water ensures stability for the main operation modes of the geothermal-heat pump system.

### CONCLUSION

None of the renewable energy sources is universal. Their application is determined by specific natural conditions and the needs of the community. Therefore, effective planning of renewable power engineering will require, firstly, systematic investigation of the environment and, secondly, survey of energy needs of a specific region for industrial, agricultural and domestic activities.

### REFERENCES

- Balashov, L.S. (1960). Surkhandarya Artesian Basin. Fan, Tashkent, Moscow.
- Burak, M.T. (1968). Kyzyl Kum Underground Water. Fan, Tashkent.
- Grebenshikova, T.V. (1976). Thermal Water in Eastern Regions of Turan Lowland in Sir-Darya-Amu-Darya Interfluve. Nedra, Moscow.
- Darchia, G.I., G.V. Ratiani, R.K. Khuntsaria and N.M. Ungiadze. Solar-Heat Pump System of Heat and Cold Supply. Kholodilnaya Tekhnika, 6, 43-46.
- Mavritski, B.F. (1971). Thermal Water in Folded and Platform Regions of the USSR. Nauka, Moscow.
- McVeig, D. (1981). Utilization of Solar Energy. Energoizdat, Moscow.

## REFRIGERANT FLOW CONTROLS FOR HEAT PUMPS

ROBERT W. COCHRAN, P.E.

ECR Technologies, Inc.  
P.O. Box 3271  
Lakeland, Florida 33802 USA

### ABSTRACT

New refrigerant flow controls replace conventional expansion devices and accumulators to regulate liquid and vapor refrigerant flow storage and charge control in heat pump and refrigeration systems, including direct expansion ground coupled units, to maintain optimum refrigerant charge under a wide range of operating conditions and increased efficiency. Superheating of vapor and subcooling of liquid are eliminated as are the blow-through of vapor from the condenser and the flow of unevaporated refrigerant vapor from the evaporator.

### KEYWORDS

Refrigerant flow controls; liquid flow controls; vapor flow control; refrigerant charge; superheating; subcooling; modulating control; ground coil; direct expansion ground coupled heat pump.

### REFRIGERANT FLOW CONTROLS

Improvements have been made in heat pump performance in recent years through the use of larger fan coils, improved compressors, multispeed fans and compressors which are electronically controlled. However, few improvements have been made in refrigerant flow controls.

Heat pumps with conventional controls such as thermal expansion valves (TXVs), electronic expansion valves (EXVs), fixed orifices, capillary tubes, accumulators, etc. share a common set of problems. These problems are the: (1) subcooling of liquid refrigerant in the condenser; (2) superheating of vaporized refrigerant in the evaporator; (3) varying refrigerant charge requirement of the system; (4) liquid refrigerant reaching the compressor inlet; (5) reduced volumetric efficiency of the compressor because of superheating the refrigerant vapor; and (6) blow-through of uncondensed vapor at the condenser outlet. Blow-through is the condition where a portion of the vapor pumped by the compressor is not

Copyright © 1989 ECR Technologies, Inc. Article prepared for presentation to International Energy Agency Heat Pump Conference, Tokyo, Japan, March, 1990.

condensed in the condenser and passes the condenser outlet and the expansion device.

Figure 1 illustrates the typical refrigeration circuit with the thermal expansion valve and the accumulator, two refrigerant controls which are very commonly used.

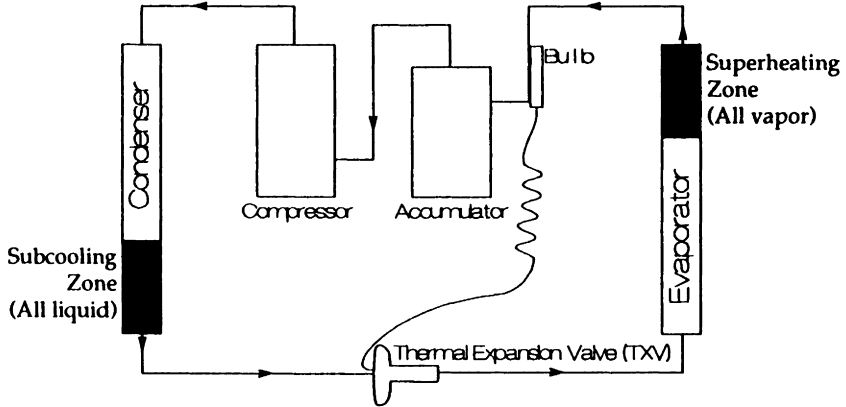


Fig. 1

### Typical Operation of Conventional Systems

**Subcooling of liquid refrigerant** occurs when the conventional system's refrigerant charge requirements are low, and the excess charge is stored as liquid in the lower portion of the condenser. With conventional controls it is necessary to allow subcooling during most of the operating cycle to prevent blow-through of uncondensed vapor at the condenser outlet when the system's charge requirements are high. If vapor were permitted to blow-through the TXV, it could not function properly to regulate the flow of liquid.

**Superheating of vapor in the evaporator** is intentionally maintained by the thermal expansion valve, to prevent the flow of unevaporated refrigerant from the evaporator to the compressor. Although the accumulator is located between the evaporator and the compressor, conventional accumulators do not fully accumulate liquid refrigerant. They "meter" any liquid refrigerant or compressor oil to the compressor, and only slow the passage of large quantities (slugs) of liquid.

**The varying refrigerant charge requirement** occurs as a result of temperature and pressure changes in the condenser, the evaporator, the compressor, the accumulator, etc. All parts of the system are involved in the varying refrigerant charge requirement. The optimum refrigerant charge at one extreme of temperatures and pressures is substantially different from the optimum charge at the opposite extreme. The application having perhaps the greatest range of optimum charge requirement is the direct expansion ground coupled heat pump.

**Liquid reaching the compressor inlet** can cause damage to, and the early failure of the

compressor. Even though the accumulator slows and meters the liquid to the compressor, “metering” can happen continuously with fixed orifices and capillary tubes; and intermittently with expansion valves that oscillate or hunt between the open and the closed positions.

**The volumetric efficiency of the compressor** is reduced as a result of superheating of refrigerant vapor in the evaporator. Superheating expands the vapor and therefore less refrigerant mass can be pumped with each revolution of the compressor. The compressor also runs hotter than it otherwise would without the superheating condition.

**Blow-through of vapor from the condenser** occurs when the refrigerant charge in the system is insufficient to maintain a liquid-only condition at the condenser outlet or may occur due to inappropriate action of the expansion device which allows vapor to pass through the expansion device. Blow-through results in a substantial loss of efficiency because vapor pumped by the compressor delivers very little energy to the condenser.

A significant additional problem with TXVs is that they are unstable in applications where long evaporators are used, as in direct expansion ground coupled heat pumps. In such applications, the TXV hunts almost continuously because of the long time lag between any correction made by the valve, and its detection of the result of that correction at the evaporator outlet where its sensor bulb is located. This hunting action (oscillating from too far closed to too far open) is very detrimental to the efficiency of the system in this application. Although fixed orifices and capillary tubes are stable in this application, they are efficient at only one specific set of temperature, pressure and refrigerant charge conditions. Therefore they have a low average efficiency in any system having a substantial range of operating temperatures and pressures.

A primary reason for the inefficiency of commonly used liquid flow controls is that none of them sense and adjust conditions in the condenser. A high-side float does prevent blow-through of unevaporated liquid, but it is unable to modulate the liquid flow rate, and generally moves back and forth from the fully closed to the fully open position.

One additional limitation of conventional refrigerant controls is their inability to achieve the start-up of direct expansion ground coupled heat pumps in the cooling mode.

### ECR's Approach to Refrigerant Control

The criteria which ECR has followed in developing its refrigerant controls are that they must be: (1) efficient; (2) mechanically simple; (3) reliable; (4) stable; and (5) must address all the operating requirements of the major components of the refrigerant system. The result has been the development of two simple devices, the Liquid Flow Control (LFC) and the Active Charge Control (ACC). Four U.S. patents have been issued and international patents are pending. The LFC has only one moving assembly and only one wear point—a simple hinge which is continuously lubricated with compressor oil so that it is not expected to show significant wear in 30 years of operation. The ACC has no moving parts and no points of wear.



Figure 2 illustrates the application of the LFC and ACC in a refrigerant circuit, wherein the LFC replaces the expansion device and the ACC replaces the accumulator.

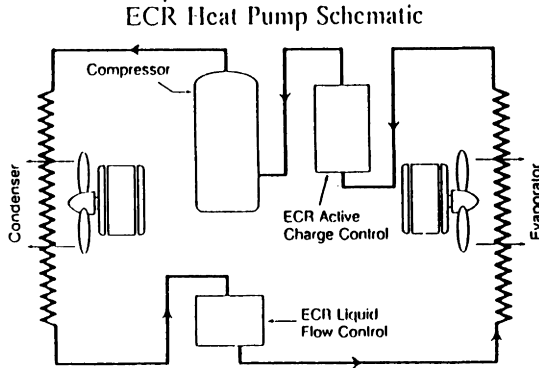


Fig. 2

With reference to Figure 3, the LFC consists of an enclosed liquid/vapor reservoir, with an enclosed hollow float, which is attached to a metering segment. A circular metering surface is in close proximity with a liquid metering orifice drilled in an outlet tube. During operation, the reservoir contains liquid refrigerant and refrigerant vapor.

The LFC receives its operating signals entirely from the condenser. When only liquid arrives at its inlet, as occurs during start-up, the float rises and the metering segment moves to uncover the metering orifice and allow maximum liquid flow. The liquid-only condition therefore signals the LFC that subcooling is occurring in the condenser and maximum flow is to be allowed.

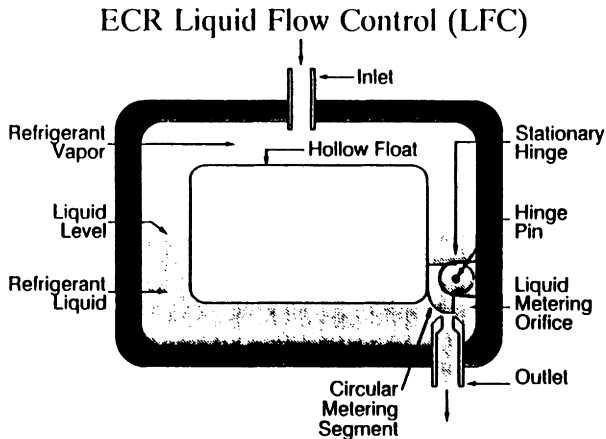


Fig. 3

When vapor begins to arrive at the LFC, the float is forced downward and the metering segment begins to obstruct the flow of liquid from the reservoir. Slowing the outflow of liquid causes the pressure within the LFC and in the condenser to increase. As vapor continues to arrive, the outflow is continuously reduced, and the pressure continues to increase in the condenser until nearly all of the vapor is being condensed in the condenser and a condition of equilibrium is reached.

In the operating condition of equilibrium, the LFC causes the pressure in the condenser to be just sufficient to condense all the vapor in the condenser except a very small amount of vapor that arrives continuously to provide the signal to the LFC, and is then condensed inside the LFC reservoir.

When any system condition reduces the flow of vapor arriving at the LFC such as cooling down of the heat sink at the condenser, the float will rise to increase the rate of liquid flow until equilibrium is restored. Conversely, when any system condition causes an increase in vapor flow to the LFC such as a warming of the heat sink at the condenser, the float will drop to decrease the rate of liquid flow until the equilibrium is restored.

Thus the LFC serves to assure that vapor is continuously present throughout the entire condenser (zero subcooling) and that no vapor blows-through from the condenser to the evaporator. Therefore the LFC passes liquid at the rate that it is being produced within the condenser, without storing liquid in the condenser.

With conventional controls, subcooling does have the effect of slightly increasing the BTU capacity of the heat pump system; however, the system's efficiency is decreased because the condensing surface is made effectively smaller, the condenser and compressor output pressures are increased, and the compressor's power consumption is increased.

As shown in Fig. 4, the ACC consists of a liquid/vapor reservoir enclosed in thermal insulation containing an evaporator tube wherein the incoming refrigerant is mixed with

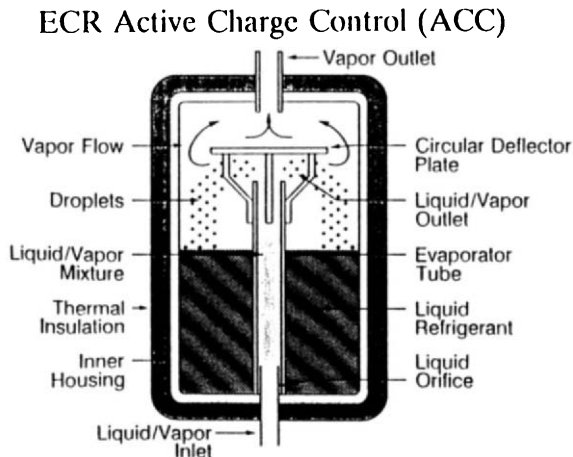


**Fig. 4**

liquid refrigerant continuously entering the evaporator tube through an orifice from the reserve of liquid stored in the reservoir. The turbulence of the liquid/vapor mix in the evaporator tube causes a foaming and misting of the usual compressor oil within the mix. A circular deflector plate above the evaporator tube outlet deflects the mixture radially and reduces the velocity of the mix as it approaches the interior wall of the reservoir.

All refrigerant vapor in the mix is drawn upward to exit at the vapor outlet. Likewise the oil mist and oil foam (tiny vapor and oil bubbles) are entrained in the vapor stream and exit at the vapor outlet. All liquid refrigerant droplets and any foam bubbles containing a significant amount of liquid refrigerant, are too heavy to be entrained in the vapor stream and therefore fall into the reservoir.

Any liquid arriving at the ACC inlet from the evaporator is deflected and trapped in the reservoir, and is added to the liquid stored and circulating in the ACC. No mechanism is provided for liquid refrigerant to exit the ACC and proceed to the compressor. Liquid must evaporate to leave the ACC. Liquid refrigerant arriving at the ACC indicates that the evaporator is flooded, and the system is overcharged (assuming an LFC is in the circuit to prevent the accumulation or back-up of the excess liquid refrigerant into the condenser). The ACC senses the overcharge and quickly traps and removes the excess refrigerant circulating in the system, thereby reducing the refrigerant actively circulating in the system.

Because the outlet of the ACC is coupled directly to the compressor inlet, the interior of the ACC maintains essentially the same pressure as the compressor's inlet (suction) pressure. The use of thermal insulation to totally encapsulate the ACC reservoir causes the liquid in the reservoir to maintain the "saturated vapor temperature" that corresponds to the suction pressure. Maintaining the stored liquid at the saturated suction temperature enables the ACC to sense any superheating of vapor in the evaporator, because the superheated vapor will be hotter than the stored liquid by the same number of degrees as the number of degrees of superheat.

Any vapor arriving at the ACC in a superheated condition will be hotter than the stored liquid in the ACC, and by contact with the stored liquid within the evaporator tube, will evaporate some of the liquid and place more refrigerant into active circulation within the system. This process of evaporating stored liquid continues until the evaporator is flooded and the superheat is reduced to, or near, zero.

Maintaining the condition of near zero superheat at the ACC inlet, the ACC outlet, and at the compressor inlet is the condition of operating equilibrium for the ACC. When any changing system condition causes the evaporator to be "overflooded" such as a cooling down of the evaporator's heat source, some amount of liquid refrigerant will exit the evaporator and be trapped by the ACC. This trapping of liquid will continue until the excess system charge is removed and equilibrium is restored.

Conversely when any changing system condition causes the evaporator to be less than fully flooded (meaning the system is undercharged and the evaporator is superheating the vapor), the ACC will evaporate and place more refrigerant into active circulation until the evaporator is again flooded and equilibrium is restored.

Thus the ACC serves to prevent liquid refrigerant from reaching the compressor inlet (while continuously passing the compressor oil); prevents superheating of vapor in the evaporator, supplies cool dense vapor to the compressor inlet; and continuously adjusts the amount of refrigerant charge in active circulation. The ACC maintains an optimum active charge through a wide range of system operating pressures and temperatures.

With conventional controls, the superheating of vapor in the evaporator increases the BTUs per pound of circulated refrigerant, however, it also reduces the mass flow of refrigerant circulated by the compressor per unit of time due to the reduced volumetric efficiency and reduced suction pressure. The reduced suction pressure is due to the reduction in active evaporator surface. The net result of superheating therefore is a substantially reduced system efficiency and a higher compressor operating temperature.

### Application of Controls

With the LFC and ACC coupled in a heat pump system as in Figure 2, all of the six problems identified above are effectively overcome. Each major component--the compressor, condenser and evaporator--are allowed to operate at maximum efficiency.

Manufacturers of conventional systems, knowing that a fixed refrigerant charge system will be most efficient (relative to the quantity of charge) at only one set of operating temperatures and pressures, must determine the "optimum charge" for that system. They generally recommend a charge of refrigerant to be placed in the system by the installer which will allow the system to be most efficient in the most frequently occurring band of temperatures and pressures in the region where the system is to be installed. The charge is a compromise which is intended to minimize subcooling at one extreme of conditions and limit blow-through at the other extreme. Even with the exact optimum charge recommended by the manufacturer, the charge is optimal at only one point in the system's operating range.

With the ECR controls, an optimum charge is maintained in circulation throughout the system's operating range, thereby resulting in optimum efficiency throughout that range. The amount of refrigerant placed in the system is not critical, because a sufficient amount of refrigerant is in reserve in the ACC to accommodate to all operating conditions and for any leakage that might occur in any system over a long period of time.

### The ECR Direct Expansion Ground Coupled Heat Pump

Heat pumps for heating or cooling space generally are more efficient when the heat source or heat sink has a temperature near the temperature to be maintained in the conditioned space. When the heat source or heat sink temperature varies to an extreme above or below the temperature of the conditioned space, as happens with an air source heat pump, the system efficiency drops dramatically. This is especially true in extreme cold weather when the outside air temperature reaches its greatest departure from the controlled temperature in the conditioned space.

Ground coupled heat pumps are generally more efficient than air source units because the earth's subsurface temperature is much more stable than the ambient air. Heat exchange

contact with the earth is more efficient, especially if the heat exchange contact can be made without the intermediate heat exchange equipment that is used in conventional ground coupled heat pumps.

The direct expansion ground coupled heat pump (dxgc) eliminates the intermediate fluid loop, its heat exchanger, the fluid pump, and the pumping power requirement. Therefore, the dxgc is a more efficient system. However, instability of the TXV and the problem of returning refrigerant from the ground coil to the compressor at the time of start-up in the cooling mode required totally new refrigerant controls for the dxgc system.

The LFC overcomes the stability problem by sensing only the conditions in the condenser, thereby eliminating the delayed response in the evaporator that causes the TXV to hunt between the opened and closed position. The difficulty of starting up a direct expansion ground coupled heat pump in the cooling mode arises when the earth may be cold from previous heat extraction in the heating mode. Most of the refrigerant is condensed and remains at the bottom of the ground coil. The problem is acute in northern areas where earth temperatures are much lower. A cold ground coil condenser will allow only a very low compressor discharge pressure to develop. The low discharge pressure is insufficient to overcome the downward pressure of the vertical column of liquid and raise the condensed (liquid) refrigerant upward in the liquid line of the ground coil.

ECR has overcome this problem by coordinating the design of the ground coil system with the design of the ACC. The liquid refrigerant reserve normally stored in the ACC is transferred to the ground coil during cooling cycle start-up. As a result, a large portion of the vertical column in the liquid line is offset by a vertical column of liquid in the vapor line of the coil, and the effective condensing surface of the condenser is substantially reduced, which increases the discharge pressure.

The system is essentially started-up with a small condenser, then as the earth coil warms up, the liquid is returned to storage in the ACC and the effective condensing surface increases to its normal full size.

The patented LFC and ACC have been used to improve the efficiency of ground coupled heat pumps, air source heat pumps and the standard commercial sized air conditioner. The first application was an ECR direct expansion earth coupled heat pump water heater which was the most efficient water heater ever tested at the Florida Solar Energy Center. The second application was in various ECR ground coupled heat pumps for space heating and cooling. Five electric utilities and one university have tested the systems in field demonstration projects in the far South and far North of the U.S. in residential and commercial buildings.

The direct expansion system eliminates the plastic pipe loop of the closed loop system, the pumping to circulate antifreeze, the intermediate heat transfer, and the transfer of heat between plastic pipes in the same bore hole.

This is accomplished with the use of three standard refrigeration tubes installed concentrically with a thermal barrier separating the liquid from the vapor line. The thermal barrier is established by drawing a vacuum in the space around the liquid line and by also using either a nylon liquid line, or a copper tube which has a thermally reflective surface coating.

These tubes have been successfully operated in vertical and diagonal installations for systems ranging from one to five tons of capacity. In Florida with undisturbed earth temperatures of approximately 76°F (24°C), in a 13 month electric utility monitored test of the ECR dxgc system for space heating and cooling, the heating season performance factor (HSPF) was 18.1 (COP=5.30), and the cooling season efficiency rating (SEER) was 13.6 (COP=3.99). The weather-sensitive winter peak demand reduction of the 2.5-ton ECR dxgc was 4.28 kW as compared to an air source heat pump using electric resistance heat strips at the winter peak.

In Michigan with undisturbed earth temperatures of approximately 48°F (9°C), and 6,400 heating degree days, the HSPF, as monitored by an electric utility, was 10.89 (COP=3.19). With an ambient temperature of 6°F (-15°C), the ECR system, even though intentionally undersized in design capacity for testing purposes, maintained the residence at a comfortable 74°F (23°C) without supplemental heating, and at an operating cost equal to that of a natural gas furnace in Michigan.

In comparison with the closed loop method, the ECR dxgc reduces the bore hole volume by 92%, reduces the trenching requirement by 90%, and by elimination of the plastic loop, it reduces the installed cost by at least US \$1,000 and achieves an efficiency gain of approximately 15%.

In an electric utility sponsored test by the University of Central Florida using two standard efficiency York<sup>™</sup> air source heat pumps for space heating and cooling, the unit which was retrofitted with ECR's controls, showed more than a 20% average efficiency gain over the unmodified unit after nine months of operation.

In a test of a 15-ton WeatherKing<sup>™</sup> air conditioner mounted on a supermarket roof operated with ECR's controls, the building owner and ECR are monitoring a greater energy efficiency gain in a side-by-side comparison with an identical unit operating with standard controls.

Although these efficiency gains are being achieved without the use of variable speed compressors, scroll compressors, multispeed compressor or desuperheaters, the addition of any of those features would further increase system efficiency.

## INVESTIGATIONS OF SOLAR WATER HEATING SYSTEMS

V. F. BOGACHKOV, Z. R. ZAKAR'YAEV and A. G. MOZGOVOY

Institute of High Temperature of the USSR Academy of  
Science, Izhor'skaya 13/19, Moscow 127412 USSR

### ABSTRACT

Two installations for solar collectors testings have been developed at IVTAN scientific stations—tested "Solntse". The design of the installations and the results of solar collectors testing are discussed.

### KEYWORDS

Solar furnace; solar collector; testing; thermosyphone; reverse circulation

At the IVTAN scientific station—tested "Solntse" the installations for solar water and space heating systems testings were developed. One of the important problems that can be solved by using of these installations is solar collectors testing and determinations of their performances (optical and thermal).

One of the installations that has been developed by IVTAN constructors is shown on Figure 1. This installation consists of solar collectors array, five heat store tanks (volume of the one is  $1.25 \text{ m}^3$ ): one is upper vertical and four are lower horizontal, pumps, pipe-lines with stop valves. The collectors are placed on supporting frame ( $9 \times 5 \text{ m}$ ), which is oriented towards equator and inclined at  $60^\circ$  to the horizon. The tanks are situated under collectors array so the installation can operate as thermosyphone solar water heater. During testings the horizontal heat store tanks can be used as a passive thermostat to maintain temperature of a heat transfer media at a constant

level with a high accuracy ( $0.2^{\circ}\text{C}$ ). The installation is equipped with diagnostic instrumentations: meteorostation, pyranometers, thermocouples (in 32 points), flow meters, water counters, pressure gauges, pressure transformer, automatic potentiometers and ohmmeters. At the first stage of the experimental studying the flat-plate collectors of "Spetsgeliomontazh" (Georgia, USSR) has been tested. The collectors consist of steel non selective radiators covered by one glass pane (0.04 m). Bottom of the collector is insulated by fiberglass (0.04). There is no side insulation. The radiator

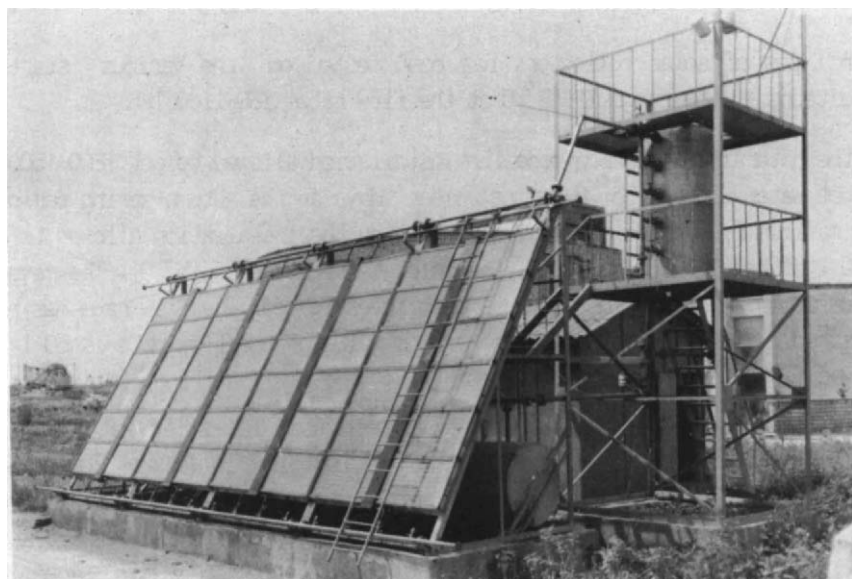


Fig. 1. The experimental thermohydraulic installation.

layes on metal part of collectors.

For the collectors testing the NBS procedure (ASHRAE Standart 93-77, 1977) has been used. Adopted procedure has been used to intensification of the testing procedure (Tabor J.G., 1978): the testings simultaneously has been carried out with series solar collectors array during two hours at the noon at the natural and forsed circulation modes. The result of the testings allowed to define the following collectors performances:  $F'(\tau\alpha) = 0.77$  and  $F'U_1 = 10.66 \text{ W}\cdot\text{m}^{-2}\cdot\text{K}^{-1}$ .

At the second stage of the investigation the improved (by "Solntse" team)



solar collectors have been tested. The one glassed collectors (fig.2) consist of the steel radiators ( $0.8 \text{ m}^2$ ) pointed by black varnish, which was mixed with soot (100:1). Radiators are situated in the cells of the wood frame. They are covered by one pane of the glass and hermetic (Gerlen-200) to prevent the radiators from dust and moisture. The radiators are separated from lower side of collector by thermal insulation. The frame has been made by cant ( $0.096 \times 0.05 \text{ m}$ ).

The test allowed to define the following collector's performances:

$$F'(\tau\alpha) = 0.78 \qquad F'U = 6.5 \text{ W} \cdot \text{m}^{-2} \cdot \text{K}^{-1}$$

Both types of solar collectors has been tested on the various starting conditions in the range  $11-48^\circ \text{C}$  at the flow rates 180-1100 l/h.

At the natural circulation mode the installation allowed to get 1200-1500 l of hot water with  $47-55^\circ \text{C}$  during clear days at the autumn-spring period. The maximum flow rate was 250 l/h. In winter the installation allowed to get 1100 l of hot water with  $41^\circ \text{C}$  (the inlet temperature is  $15^\circ \text{C}$ ). The reverse circulation in night time also has been investigated. The flow-rate has been measured by impeller counter. The maximum value of the flow-rate is 50 l/h. It was fixed three hours after sunset.

Above mentioned IVTAN's collectors have been used for solar water heating system which had been designed for market building in Manas (50 km near Solntse). Scheme of the hydraulic loop of the system is shown on Figure 2. The system consists of the collectors array (Fig. 2, position 1), heat store tank (position 2), pump (position 3), pipe-lines, stop valves, automatic equipment. The collectors array consists of seven solar collectors installed on the supporting frame, which is inclined at  $45^\circ$  to the horizon and is oriented towards the equator. The vapour-water heater is used as a heat store tank. The area of it's heat exchanger enlarge from  $1.93 \text{ m}^2$  to  $3.1 \text{ m}^2$ . The heat store tank and the heat exchanger can be rotated at  $180^\circ$  around the horizontal axis. The tank was insulated with glass mats (three layers).

The solar water heating system has two hydraulic loops. The tank is filled from the water pipe-line. To fill the water in the collector the pump is used. After filling it is switched out. To prevent undesirable drain of the water from the collector to the tank the check valve is used. After the filling of the collector the water level in the tank is reduced to "h" level and remain constant during a oill operation season. An air space in the tank

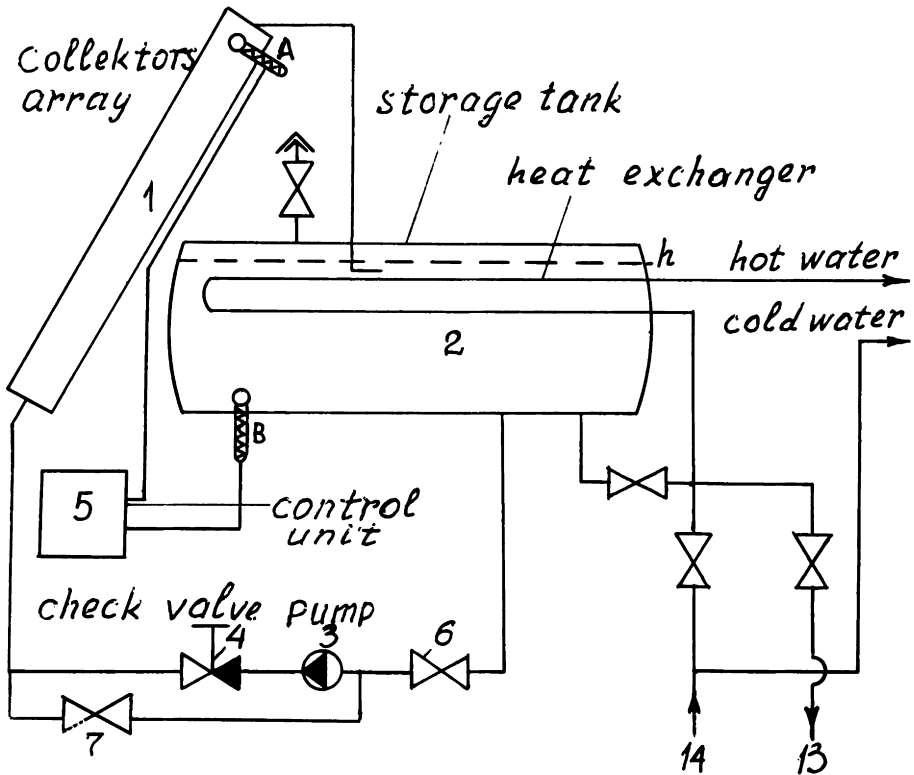


Fig. 2. The hydraulic scheme of installation for the solar water heating.

allows to reduce a heat losses from the upper hottest water layers. Due to closed loop scheme of collectors and water tank the corrosion is greatly reduced.

Under the influences of solar radiation the water in the collectors is heated to demanded temperature level (even to  $100^{\circ}\text{C}$ ). At summer-autumn months the maximum irradiance on the plane of the collectors is  $900\text{--}1000\text{ W/m}^2$ . When the signal from the thermocouple sensor, that installed on the outside of the upper radiator (point A), is appeared the pump is switched on. The hot water is forced out from the collectors into the tank by the water from the lower part of the tank. To prevent the mixing of the hot and cold water the pipe-line from collectors has horizontal terminal in storage tank. During the water forcing out process the temperature in collector is decreased and the control block switches out the pump. During the day there is a few cycles repetition. To prevent the froze damage the water from the

collectors drain out through the bypass line by opening the valve (position 7). The full draining is realized through the opening valves (positions 4, 6, 12) along the draining line.

Let's examine some operational performances of the system. In July clear day conditions the water temperature in the system arise from  $24^{\circ}\text{C}$  to  $60^{\circ}\text{C}$ . Through seven operation cycles. 1330 l of the hot water can be obtained. If the water is heated to  $75^{\circ}\text{C}$  then the number of operation cycles is five and 945 l of the hot water can be obtained. In the October 945 l of the water can be heated from  $12^{\circ}\text{C}$  to  $60^{\circ}\text{C}$  through five operational cycles. In summer at the forced circulation mode (340 l/h) 2000 l of the water in the tank can be heated from  $25^{\circ}\text{C}$  to  $61^{\circ}\text{C}$  through six hours. In autumn when flow rate is 260 l/h 1300 l of the water can be heated from  $15^{\circ}\text{C}$  to  $54^{\circ}\text{C}$  through five hours.

## RESULTS

1. The industrial collectors were tested on various inlet temperatures ( $11-48^{\circ}\text{C}$ ) and the flow rates ( $7.5 - 50 \text{ l}\cdot\text{h}^{-1}\text{m}^{-2}$ ) of water through NBS procedure using the experimental thermohydraulic installations.
2. The experimental solar module was tested in the inlet temperatures range  $17 - 40^{\circ}\text{C}$  and the flow rates range  $12.5 - 25 \text{ l}\cdot\text{h}^{-1}\text{m}^{-2}$ .
3. The unique active hot water installation, which includes solar modules was constructed.
4. The hot water productivities of both installations were obtained.

## REFERENCES

- Methods of Testing to Determine the Thermal Performance of Solar Collectors. (1977). ASHRAE Standart 93-77. ,N.Y.
- Tabor J.G. (1978). Testing of Solar Collectors. *Solar energy*, 20, N4, 293 - 303.

SOLAR GREENHOUSE OF AGRO-ENERGY APPLICATION  
WITH CONTROLLED SAILNESS

G.F. KUROCHKIN, G.M. VOROBEV  
AND L.V. POTOURAEVA

Department of Physics, State University,  
Dnepropetrovsk, Gagarin Avenue 72, 320625  
GSP, USSR

**ABSTRACT**

Hothouses structures utilizing redundant radiation which roofs are made in the form of parabolic-cylindrical surfaces from transparent film. To the lower side of the film light-transparent stiffening ribs are fixed integrated between each other along elements. The active dim-out device of the hothouses is a metal foil reeling on a rotating drum. The suggested hothouses structure allows to stop radiation access into the construction by metal foil unreeling at solar radiation redundant for plants. A parabolic-cylindrical mirror, formed as a result, focuses reflected solar rays on a pipe steam generator. Resulting from the heating of the latter steam is worked out in it which is directed towards turbo-generator to work out electric power. The hothouse roof and walls film structure as well as the possibility of their lowering to decrease sailness at a strong wind allows to reduce many times materials consumption in comparison with other plants (sets) for solar energy transformation and to create optimal conditions for hothouse plants life activity.

**KEYWORDS**

Solar energy, hothouse, parabolic-cylindrical roof, light-reflecting film.

**INTRODUCTION**

Yield capacity of agricultural crops in particular vegetables, in the hothouses is approximately ten times more than average yield capacity of the same crops on the open soil. Therefore expansion of the areas occupied by the hothouses is a matter of topical interest. The estimates show that for supplying the Soviet people with products of the hothouses the hothouses area should occupy up to 30000 hectares. For heating the area

mentioned above one should burn up natural gas up to  $5 \cdot 10^{10}$  cubic meters per year. Therefore the hothouses with gas heating annually need natural gas up to  $1 \cdot 6 \cdot 10^9$  cubic meters per hectare. For the most perfect hothouses one turns out well to keep an optimal artificial climate with the help of moistening soil, keeping the specific temperature and optimizing solar and artificial lighting. The proper solar lighting is achieved with the help of artificial dim-out of transparent surfaces of the hothouses during intensive solar glowing from 10 to 16 hours of day time. For this purpose the different methods are used including coating the transparent roof with lime, chalk and other opaque substances. When the hothouses are dimmed-out excess solar energy is not used. For the hothouse structure suggested here full regulation of artificial climate is provided when energy of solar radiation exceeds optimal demand of plants in solar rays and the excessive energy is used for production of electric energy. In the case of the approach mentioned above two consumers of solar energy agriculture and power industry which need large areas for the collectors of solar radiation are united for consumption of materials and soil areas. In this case profitableness of investment to such hothouses of double function increases sharply in comparison with the hothouses intended for solar-heat power industry only or for agriculture only. The air inflated roof of the solar hothouse suggested here with using excess solar energy simultaneously allows to solve partly food and energetic problems. This device does not use electric energy from outside, on the contrary, it generates it for its own need. Excess of generated energy goes to the power network of the complexes where it is erected. The hothouse for growing plants in cold climate is known (U.S. Patent N 4242833, 1981). Its structure contains reflecting-isolating panels located above the hothouse roof which act as regulators of solar energy arrived inside the hothouse through the water layer. The water layer located near the hothouse ceiling is necessary for heat accumulation of excess radiation. The shortcoming of the structure is that it does not allow to transform excess radiant energy into electric one during warm time of the year. Besides, keeping the water layer above the hothouse ceiling needs increased consumption of materials because of the large weight of the water. The hothouse with a removed transparent roof is known which allows to regulate amount of solar heat and light penetrating inside the hothouse (Japan Patent N 55-44567, 1980). However, this device has an essential shortcoming because it regulates arrival of solar energy only for its transformation into thermal one and then into electric one which can be used in the future for equalizing temperature inside the hothouse during the year. The suggested structure of the hothouse roof is made of transparent film and its parabolic-cylindrical shape is made with air inflated film cylindrical transparent stiffening ribs touching to each other located parallel to linear focus of parabolic-cylindrical surface and fastened behind the rear side with the main film breadth. During intensive solar radiation the parabolic-cylindrical surface of the hothouse transparent roof is covered by light reflecting film or metal foil. So the roof surface becomes as a parabolic-cylindrical reflector. The tube steam generator located in the focus of the reflector

is heated by solar rays. So water in the tube changes into superheated steam. The steam is carried to the turbine for transformation of steam kinetic energy into electric one and waste steam is carried into the air heater located inside the hothouse.

#### EXPERIMENTAL METHODS

The general view of the hothouse structure suggested is given in Fig. 1, where 1 - an inflated parabolic-cylindrical surface

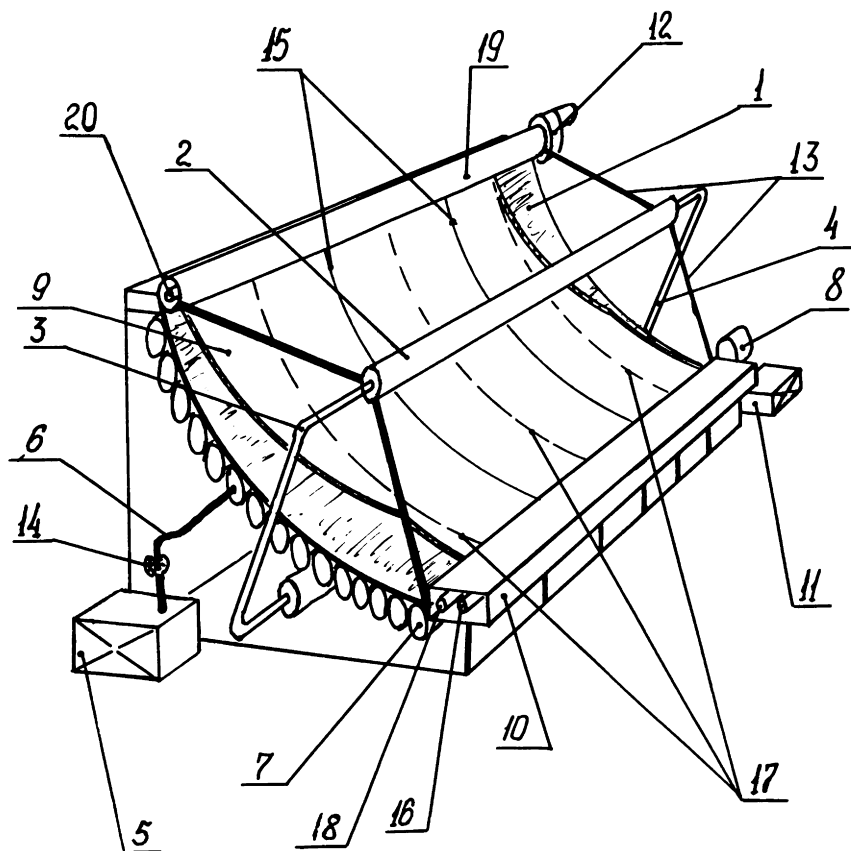


Fig. 1. Solar Hothouse

made of transparent film; 2 - a steam generator located in the focus of the parabolic-cylindrical surface; 3 - a tube for supply of water or other heat-transfer agent to the steam generator; 4 - tubes for removal of superheated steam to the turbine; 5 - a pump for building up proper pressure in the stiffening ribs of the film surface of the hothouse roof; 6 - a hose for air supply into the film cylindrical stiffening ribs; 7 - stiffening ribs of the film roof in the form of cylinders made of transparent film which allow to shape the parabolic-cylindrical inflated roof; 8 - a reverse electric motor for spreading and folding the film roof; 9 - a guiding cable for fastening the light-reflecting film; 10 - a box in which shaft 16 for reeling up ropes 17 spreading and folding the film roof of the hothouse is located when additional access of solar rays inside the hothouse is needed and also shaft 18 for reeling up the light reflecting film; 11 - a turbine for transformation of superheated steam energy into electric one; 12 - a reverse electric motor for spreading and folding the light reflecting film; 13 - rods for fastening the steam generator in the focus of the reflector; 14 - a pressure gauge; 15 - cross stiffening ribs of the inflated roof preventing its deflection under the influence of rain, snow and wind.

## RESULTS

The structure described above operates as follows. Firstly the command for switching on air pump 5 is given. During operation of pump 5 air is supplied to cylindrical stiffening ribs 7 of the hothouse film roof with the help of hose 6. When the desired air pressure displayed by pressure gauge 14 is achieved, the inflated roof takes a desired parabolic-cylindrical shape and pump 5 automatically is switched off. Then when reverse motor 8 is switched on ropes 17 reeling up on shaft 16 spread the film roof. When the film roof reaches the stop in the low part, the command for switching off the motor is automatically given. During intensive solar radiation the command is given to reverse motor 12. Guiding rope 9 spreads the light reflecting film up to stopper device 19. When the light reflecting film reaches stopper device 19, electric motor 12 automatically switches off. Spreading the light reflecting film on the inflated parabolic-cylindrical roof constructs a mirror reflector which concentrates excessive flow of radiant energy to steam generator 2 filled with water or other heat-transfer agent through pipe 3. The water inside the steam generator transforms into superheated steam and goes to turbine 11 through the pipe, where kinetic energy of the steam changes to electric one. If it is necessary to increase temperature inside the hothouse in cool days, the waste steam after the turbine goes to the air heater located in the hothouse. With sticking snow or icing the roof, warm air is supplied to the gaps between the toroid ribs in order to melt snow or ice and free the roof from the excessive load. Solar rays needed for progress of photosynthesis in plants penetrate to the hothouse through the side transparent wall parts. If lighting is not sufficient the light reflecting film will be reeled on the roll on shaft 18 with the help of reverse electric motor 12.

In case when intensity of solar radiation is so small that one can neglect absorption of solar rays with the hothouse roof, and weather conditions are not dangerous for plants located in the hothouse, the inflated film roof is removed with the help of ropes system 17. When electric motor 8 is switched on ropes 17 are reeled on shaft 20 and the air is simultaneously released out of the cylindrical stiffening ribs with the help of hose 6. As a result, the film roof is folded like a curtain near the upper end of the hothouse.

#### DISCUSSION

So the suggested structure of the solar hothouse with an inflated parabolic-cylindrical roof allows to save materials and decrease the weight of the structure with the help of changing metal and glass roof parts to air inflated film pieces and also to use excessive solar radiation spreading a light reflecting film above the roof during increased solar radiation. The light reflecting film taking a shape of the hothouse parabolic-cylindrical roof looks like a mirror reflector and concentrates solar rays on the steam generator located in the focus of the reflector. Excessive solar radiation concentrated on the steam generator transforms into kinetic energy of steam and then into energy of steam directed to the turbine and transforms into electric energy. Besides the suggested structure allows to solve two important problems simultaneously: autonomous supply of energy to structures like hothouses and increase in output of agricultural products by effective use of soil areas. Transformation of solar energy into electric one with the help of an inflated parabolic-cylindrical roof of the suggested hothouse allows to provide it with energy for heating during cool time of the year and send some excessive amount of energy for other purposes. So the suggested structure of the hothouse allows to use effectively solar rays of different intensity (average and weak) for agriculture and solar rays of high intensity which are harmful for plants may be used for energetic purposes saving materials because of using air inflated film structures.

#### REFERENCES

- U.S. Patent N 4242833. - Int.cl<sup>3</sup>. A 01 G 9/18. 1981  
Japan Patent N 55-44567. - Int.cl<sup>3</sup>. A 01 G 9/22, 13/00;  
E 06 B 9/24; B32B 27/20; C03C 17/32, 1980.



AN ANNUAL UTILIZABILITY METHOD FOR SOLAR COLLECTORS  
IN THE SWEDISH CLIMATE

Bengt Perers      and      Björn Karlsson  
Studsvik Energy      Älvkarlebylaboratory  
S-61182 Nyköping      S-81071 Älvkarleby  
Sweden                      Sweden

ABSTRACT

An annual utilizability method is presented that gives a very accurate estimation (within a few percent) of the yearly performance of a solar collector directly from instantaneous collector parameters. The model has been validated against long term outdoor measurements and detailed simulation as presented in this paper.

KEYWORDS

Annual Collector Performance; Simplified Model; Simulation; Incidence Angle Effects; Critical Radiation Level.

INTRODUCTION

A simplified expression for estimation of the annual heat production of a collector in the Swedish climate has been suggested (Karlsson 1988). The model which is based on a time integration of the collector equation for all hours of the year of irradiances exceeding 300 W/m<sup>2</sup> is of the form.

$$Q_{112} = (H_{100}_{op} F'(\tau\alpha) - F'U_L (T_{op} - T_{acp}) t_{op}) C \quad (1)$$

Where:

$H_{100}_{op}$  = yearly solar radiation >300 W/m<sup>2</sup> in the collector plane.

$F'(\tau\alpha)$  and  $F'U_L$  = standard collector test parameters based on average fluid temperature. [ - ] resp. [W/(m<sup>2</sup>\*K)]

$T_{op}$  = yearly average collector operating temperature  $(T_{in} + T_{out})/2$  [C]

$T_{acp}$  = yearly average ambient temperature during operating hours [C]

$t_{op}$  = yearly time with solar radiation in the collector plane >300 W/m<sup>2</sup>. [hours/m<sup>2</sup>]

$C$  = empirical correction factor based on comparison with long term and instantaneous performance measurements. [ - ]

Typical values for the middle of Sweden, Lat 59°, are given in table 1. These values are determined directly from hourly climate data. Given is also a value of C determined by comparison with measured longterm data.

The MINSUN simulation programme has been used to validate this simplified model as part of a simulation and evaluation project in Studsvik. The climate used was for Stockholm 1986.

The MINSUN simulation program has been developed from the well known TRNSYS programme within the IEA SH&C task VII for simulation and optimization of seasonal storage systems.

The weather data is obtained from the Swedish Meteorological and Hydrological Institute. The direct radiation is measured with pyrhelimeter. This means that the calculation of incident radiation onto the collector plane is more straight forward and accurate than when using horizontal global and diffuse radiation. This is especially important for Swedish conditions with low solar altitudes.

## RESULTS

The simple expression eq. (1) was compared with detailed simulation with the MINSUN programme for Stockholm 1986. The agreement was surprisngly good, see table 1. The collector tilt was 45° and the operating temperature  $T_{op}$  was 70°C.

Table 1. Comparison between the basic Karlsson model eq.(1) and detailed simulation with the MINSUN programme.

Parameters used was:  $H100_{op}=781$ ,  $T_{acp}=13^{\circ}\text{C}$ ,  $t_{op}=1370$  h,  $C=0.9$

COLLECTOR PARAMETERS		SIMPL.MODEL	MINSUN	DIFFERENCE
$F'(\tau\alpha)$ [-]	$F'U_L$ [W/(m <sup>2</sup> *K)]	[kWh/m <sup>2</sup> ]	[kWh/m <sup>2</sup> ]	[ % ]
0.75	3.5	281	288	-2.4
0.79	3.5	309	318	-2.8
0.81	3.35	334	344	-2.9
0.847	3.35	360	373	-3.5
0.847	2.6	415	439	-5.5

The basic model does not take incidence angle effects into account in an explicit form. The accuracy of the model can be improved by letting the C-value be effective only on the optical term  $H100 * F'(\tau\alpha)$ . This is equivalent to an effective yearly incidence angle modifier  $K_{\tau\alpha e}$ . In this case the model is changed to the following form:

$$Q_{112} = H100_{op} F'(\tau\alpha) K_{\tau\alpha e} - F'U_L (T_{op} - T_{acp}) t_{op} \quad (2)$$

$K_{\tau\alpha e}$  has been calculated as an energy weighted average during hours of operation. For the climate Stockholm 1986 and 45° collector tilt  $K_{\tau\alpha e}$  was 0.96 for a collector with  $b_0=0.1$  (The same equation  $K_{\tau\alpha e} = 1 - b_0 (1/\cos(\theta) - 1)$ , see (Duffey 1980 p.263), and  $b_0$  was used as in the MINSUN simulation). The discrepancy then was decreased to less than 0.5% for the four first collector options in table 1.

For the extreme future flat plate collector the simplified model underestimates the performance with 1.6% se table 2. The reason for this underestimation is that this collector has a much lower critical radiation level  $I_c=175 \text{ W/m}^2$  than the  $300 \text{ W/m}^2$  used to calculate the basic parameters.

Table 2. Comparison between the improved Karlsson model eq.(2) and detailed simulation with the MINSUN programme. The C-value is only effective on the optical term  $H100_{op}$ .

Parameters used was:  $H100_{op}=781$ ,  $T_{aop}=13^\circ\text{C}$ ,  $t_{op}=1370 \text{ h}$ ,  $C=K_{\tau\alpha e}=0.96$

COLLECTOR PARAMETERS		SIMPL.MODEL [kWh/m <sup>2</sup> ]	MINSUN [kWh/m <sup>2</sup> ]	DIFFERENCE [ % ]
F'( $\tau\alpha$ ) [-]	F'UL [W/(m <sup>2</sup> *K)]			
0.75	3.5	289	288	+0.3
0.79	3.5	319	318	+0.3
0.81	3.35	345	344	+0.5
0.847	3.35	373	373	+0.1
0.847	2.6	432	439	-1.6

DISCUSSION

To quantify the dependence of the critical radiation level a recalculation of the model parameters for different levels of  $I_c$  has been made. The result is shown in fig 1. It can be seen that both  $H100_{op}$  and  $t_{op}$  as can be expected increase with decreasing  $I_c$ .

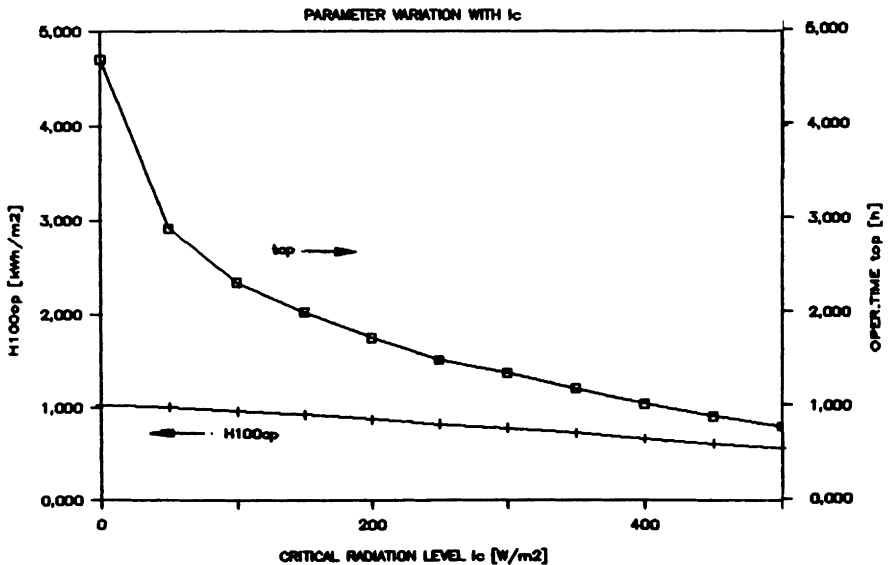


Fig 1. Dependence of the operating time  $t_{op}$  and yearly energy  $H100_{op}$  on the critical radiation level  $I_c$ . Climate Stockholm 1986.

The dependence on  $I_C$  is almost linear near 300 W/m<sup>2</sup> so the variation can be described with a linear equation with good accuracy for both parameters between 100 and 450 W/m<sup>2</sup>. The resulting equations derived by linear regression are:

$$t_{op} = 2608 - 3.980 \cdot I_C \quad (3)$$

$$H100_{op} = 1068 - 1.002 \cdot I_C \quad (4)$$

Where:

$$I_C = F'UL \cdot (T_{op} - T_{acc}) / F'(\tau\alpha) \quad (5)$$

By equation (3), (4) and (5) a more accurate value of  $t_{op}$  and  $H100_{op}$  can be calculated for collectors with low UL.

Theoretically  $T_{acc}$  also varies slightly with  $I_C$  but the influence on the final result is very small and can be neglected.

If equation (3), (4) and (5) are used instead the discrepancy for the best collector is reduced from -1.6% to +0.8% .

The value of  $K_{toe}$  can be determined by calculating the distribution of the incident direct radiation when the total incident radiation is greater than 300 W/m<sup>2</sup>. From this statistics an energy weighted yearly incidence angle modifier  $K_{toe} = 0.96$  can be calculated for the operating time. Figure 2 shows the amount of  $K_{toe}$  insolation within different 15° intervals of incidence angle to the collector. Also the duration time is given for each interval.

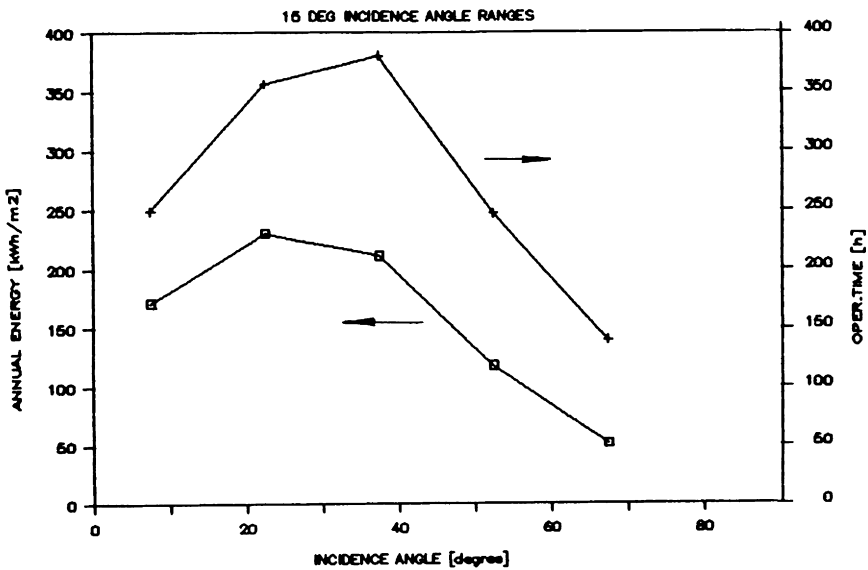


Fig 2. Yearly insolation within 15° ranges for the incidence angle to a collector with 45° tilt angle at latitude 59°. Also the operating time within each interval is shown for comparison. Climate Stockholm 1986.

The Karlsson model eq.(1) and (2) has also been compared with MINSUN simulations for other collector orientations than 45° south. The simplified model works just as accurate for a wide range of tilt angles and azimuthal directions provided that the parameters  $t_{op}$  and  $H_{100}$  are recalculated for the orientation in question. The operating<sup>op</sup> time ambient<sup>op</sup> temperature  $T_{aop}$  is almost constant within  $\pm 1.5^\circ\text{C}$  for all tilt angles from 0° to 90° and azimuth angles from 90° east to 90° west, see table 3.

The accuracy is reduced for both equations for the extreme orientations  $\pm 90^\circ$  and tilt 0° resp. 90°. This overestimation of the performance at extreme orientations is probably caused by incidence angle effects which become more important at these orientations since  $(K(\tau\alpha_e))$  has been kept constant in eq.(2)).

Table 3. Comparison between the Karlsson model and MINSUN for other azimuth and tilt angles. Collector parameters  $F'(\tau\alpha)=0.75$   $F'UL=3.5 \text{ W}/(\text{m}^2\text{K})$   $b_0=0.1$ . Climate Stockholm 1986.  $T_{op}=70^\circ\text{C}$ .

TILT	AZIMUTH	$H_{100}$ <sub>op</sub>	$t_{op}$	$T_{aop}$	Q112 MINSUN	Q112 eq(1)	REL. MINSUN	Q112 eq(2)	REL. MINSUN
deg	deg	kWh/m <sup>2</sup>	h	°C	kWh/m <sup>2</sup>	kWh/m <sup>2</sup>	-	kWh/m <sup>2</sup>	-
45	-90	543	1001	13,6	182	183	1,01	187	1,030
45	-60	670	1192	13,0	242	238	0,98	245	1,010
45	-45	717	1255	12,7	264	258	0,98	265	1,005
45	-30	754	1315	12,9	279	273	0,98	280	1,005
45	-15	774	1347	12,9	286	281	0,98	288	1,007
45	0	781	1370	13,0	288	281	0,98	289	1,005
45	15	755	1321	13,2	280	274	0,98	281	1,004
45	30	733	1313	13,6	267	262	0,98	269	1,007
45	45	682	1239	13,9	246	242	0,98	248	1,008
45	60	628	1176	14,7	221	219	0,99	225	1,017
45	90	484	975	15,9	157	161	1,02	164	1,039
0	0	621	1249	15,3	191	204	1,07	208	1,089
15	0	729	1353	14,2	249	254	1,02	261	1,045
30	0	778	1374	13,5	284	281	0,99	288	1,015
45	0	781	1370	13,0	288	281	0,98	289	1,005
60	0	711	1268	12,8	258	252	0,98	258	1,001
75	0	591	1106	12,5	201	199	0,99	203	1,008
90	0	433	891	11,6	124	128	1,03	130	1,042

From table 3 it can also be seen that eq.(1) systematically gives a lower annual performance than eq.(2) for collectors with low UL-values.

In this investigation the effect of thermal capacitance on the collector performance has been neglected. In (Klein 1973) it is shown that for flat plate collectors the introduction of thermal capacitance in collector models gives an almost insignificant improvement in accuracy. In [Perers et al 1990) it has been shown by detailed simulation with 1 min time step that when using a 1hr time step in a standard simulation program as MINSUN the reduction in performance due to thermal capacitance (compared to a collector with zero capacitance) is automatically taken into account to a large extent by using hourly mean values for the climate data. The early morning radiation below the critical radiation level  $I_c$  gives required heat for the collector to reach the operating temperature.

The basic climate data reduction in this method is similar to the well known utilizability method (Duffey 1980) but in this case the duration time and ambient temperature for each critical radiation level is also stored. This gives the possibility to have a similar equation for instantaneous and annual collector performance.

#### CONCLUSIONS

The basic Karlsson model can be used for predicting the annual collector performance directly from instantaneous collector parameters.

As a method for estimating the change in performance due to improved  $F'(\tau\alpha)$  or  $F'UL$  both eq.(1) and (2) show a very good agreement with detailed simulation.

By introducing an effective incidence angle modifier in the model the accuracy can be improved significantly.

The Karlsson model can be used for a wide range of azimuth and tilt angles.

For high performance collectors that can operate under very low irradiation levels two equations are given to calculate  $t_{op}$  and  $H100_{op}$ . This improves the accuracy significantly for these collectors.

#### ACKNOWLEDGEMENTS

This work has been financed by the Swedish Council for Building Research and the Swedish National Energy Administration.

#### REFERENCES

- KARLSSON, B. (1988). Potential Improvements of High Temperature Flat Plate Collectors, NORTH SUN Conference 1988.
- KLEIN, S A. (1973). The effects of Thermal Capacitance Upon The Performance of Flat Plate Solar Collectors. Msc Thesis, University of Wisconsin, 1973.
- PERERS, B, KARLSSON, B, WALLETUN, H. (1990). Simulation and Evaluation Methods for Solar Energy Systems. Application for New Collector Designs at High Latitudes. STUDSVIK AB, 1990. STUDSVIK REPORT/ED-90/4.
- DUFFIE, J A, BECKMAN, W A. (1980). Solar Engineering of Thermal Processes John Wiley & Sons, 1980.

SOLAR HEATED BUILDINGS FOR EXTREME  
ENVIRONMENT REGIONS OF HIGH LATITUDES

E.E.SHPILRAIN and A.S.SHEINSTEIN

Institute for High Temperatures USSR Academy of Sciences, Moscow, Izhor'skay 13/19,  
127412, USSR

ABSTRACT

Solar heated buildings design concept has been developed for extreme environment regions of high latitudes. "Adaptable" buildings design concept has been suggested.

KEYWORDS

Antarctica, extreme environment, solar heated buildings, passive solar architecture, "adaptable" buildings.

INTRODUCTION

Energy conservation is a key option to save costly fuel in isolated extreme environment regions. In Antarctica more than 50% of costly diesel fuel is used for space heating. At the inland regions of Antarctica annual heating degree-days reach 25,000. At the same time solar radiation intake is significant there (Shpilrain and Sheinstein, 1988). Thus there is a favorable potential for solar space heating systems using in Antarctica.

DESIGN OF SOLAR HEATED BUILDINGS

Design of solar heated buildings for extreme environment regions is shown on Fig.1-4. Some compacted passive solar heated buildings design for windy climate is shown on Fig.1,2. "Sandwich" panels, which widely are used in Antarctica for buildings constructions, can be used as a solar thermosyphone air collectors, Fig.2. For harsh environment regions which have long durnal cycles of continuously sunlight and no solar radiation intake, "adaptable" buildings design concept (it's our term) can be interesting. "Adaptable" building can be opened to use solar energy (during Austral Summer) and can be transformed to be "superinsulated" when there is no solar radiation, Fig.3,4.

## ACKNOWLEDGEMENT

The authors wish to express thanks to A.R.Asadov for his work

## REFERENCES

E.E.Shpilrain and A.S.Sheinstein (1988). Potential for solar energy in the Antarctic. In: Proceedings of "North Sun'88" (L.Broman and M.Ronnellid ed.), pp. 593-598. Swedish Council for Building Research, Borlange.

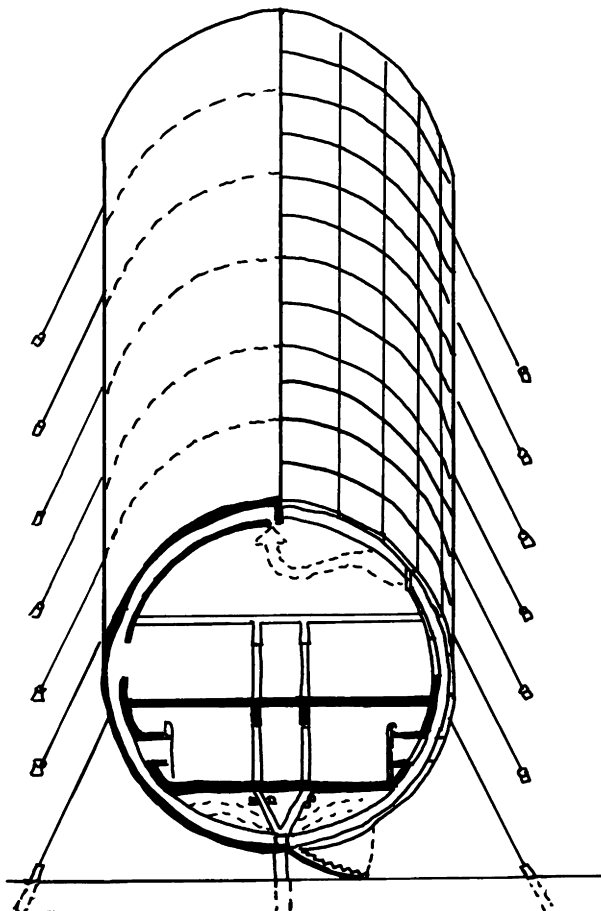


Fig. I. Passive solar building



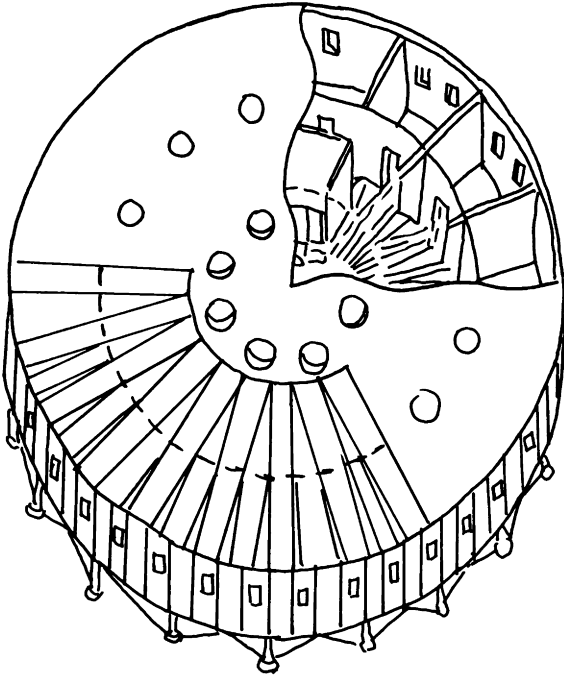
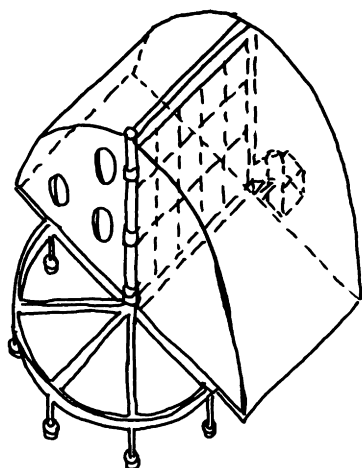
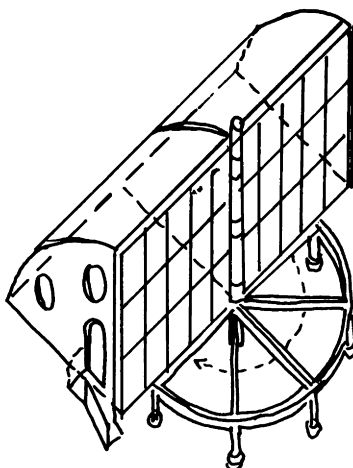


Fig.2. Passive solar building ("sandwich" panels construction)



b. "closed" position



a. "open" position

Fig. 3. Transformation scheme of the "adaptable" building

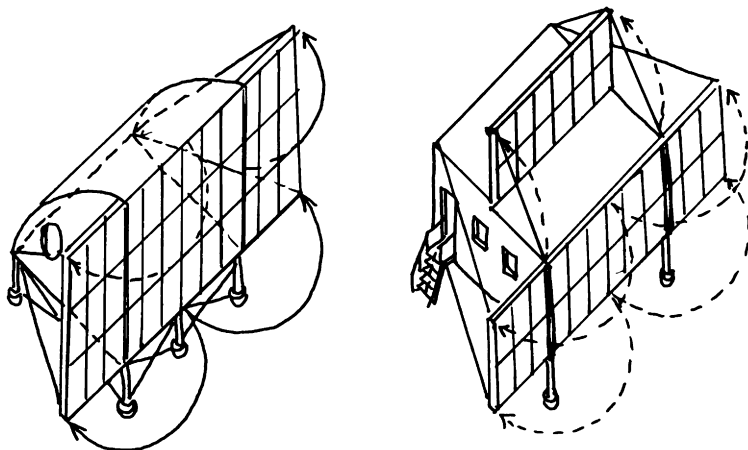


Fig. 4. "Adaptable" active solar building.

## SOLAR PROGRAMME OF THE FEDERAL REPUBLIC OF GERMANY

V. Lottner

Forschungszentrum Jülich GmbH, Projektträger  
Biologie, Energie, Ökologie, P.O. Box 1913, D-5170 Jülich, FRG

### ABSTRACT

The presentation summarizes objectives, current activities and accomplishments of the programme and in particular of active and passive solarthermal systems for hot water preparation and heating of buildings. These applications offer a great energy saving and substitution potential in the FRG of the order of 35% of the total end-use energy demand. The solar programme comprises R&D and demonstration of new innovative concepts, e.g. the application of transparent insulation in integrated solar collector storage systems as well as in building facades, monitoring programmes of solar low-energy houses, the long term test of the reliability and thermal performance of solar domestic hot water (DHW) systems and the development of new dynamic short term test procedures for DHW systems.

### KEYWORDS

Solar programme; active solar; passive solar; innovative concepts; transparent insulation; demonstration.

### INTRODUCTION

In 1990 the Federal Minister for Research and Technology (BMFT) established the 3rd Programme on Energy Research and Technology (BMFT, 1990). R&D on energy conservation and renewable energy sources has again been given a high priority. 15 years ago, after the first oil crisis, the main goal was directed towards guaranteeing a secure energy supply by substituting oil by other energy sources (coal, gas, nuclear, renewables) and energy conservation. Today the major impact is the protection of the environment and of the world climate which is believed to be changed as a result of greenhouse gases. Recently a Parliamentary Commission: "Protection of the world climate" requested enhanced efforts on R&D and implementation of renewable energies and energy conservation technologies in order to meet the growing energy demand of the world in an ecologically acceptable way in the future.

During the past 15 years a lot of different energy saving technologies have been developed and successfully implemented. The primary energy consumption has been kept constant in the FRG in spite of a 40% increase in the gross national product. There is still an enormous energy saving potential, in particular in buildings. This sector requires more than 35% of the total primary energy

demand for space heating and hot water preparation. Solar active and solar passive technologies as well as energy conservation can reduce the primary energy demand considerably.

PROGRAMME: RENEWABLES AND ENERGY CONSERVATION

This paper can only present a very concise review. Since 1974 more than 500 projects have been funded by BMFT with 2,500 million DM. Table 1 gives a breakdown of the main topics and the allocated budget. The annual funds have been increased considerably during the last few years. New priorities have been set. Many technologies are now ready for commercialization or have already been implemented successfully, e.g. high efficient burners and low temperature heating systems, district heating systems, heat pumps and solar domestic hot water systems.

Table 1. Renewables and Energy Conservation  
BMFT Expenditures in Million DM

	1974 - 89	87	88	89	90
Photovoltaics	567	60	70	97	95
Wind	252	18	16	34	27
Technologies for developing countries	551	31	36	42	35
Geothermal	173	5	3	12	15
Solar Thermal active/passive	238	11	12	11	16
Energy Storage	130	14	5	7	10
Hydrogen	113	8	10	21	18
Biological Energy Generation					20
Research Centres	268	22	24	24	29
<b>Total</b>	<b>2 507</b>	<b>181</b>	<b>198</b>	<b>255</b>	<b>309</b>

However, the market penetration of renewables and energy saving technologies is still hampered by high investment costs and long amortization times of the systems at the present energy prices. Therefore a major goal is to improve the cost-effectiveness, efficiency and durability of these technologies. To achieve this goal both long term R&D on new innovative concepts as well as demonstration programmes to implement advanced technologies are being carried out in the programme.

Photovoltaics have been given the highest priority (Table 1) with respect to the high technological potential and the increasing market. Both the development of new solar cell production technologies and new solar cell concepts,

e.g. thin film technologies, are expected to reduce the module costs from 15 DM/W to 5 DM/W in the next 10 years. Long term efforts include R&D on solar hydrogen as well as basic R&D in a recently started programme on photobiological production of hydrogen.

Another important subject of the programme is the development of renewables for application in developing countries (DC). Obviously the utilization of renewables can contribute to their rapidly growing energy demand. Renewable energy systems often fit very well into existing decentralized energy systems in DC. Several bilateral cooperation projects deal with the demonstration of new solar technologies under the specific climatic and social conditions of DC. The joint projects include photovoltaic powered systems, e.g. telecommunications and water pumps and solar thermal systems, such as low cost air heaters for drying, sea water desalination, cooling and power generation.

The implementation of renewable energy technologies in Germany is being supported by extended demonstration programmes. A 100 MW wind programme was initiated in 1989 and will be extended up to 200 MW in view of the great public response and interest in 1991. Recently the 1000 solar roof programme was announced by BMFT. In this programme grid connected photovoltaic systems with 1-5 KW capacity will be installed on roofs of houses. The installation costs will be shared between BMFT (50%), the States (20%) and the home owners. Surplus electricity can be fed into the grid at a favourable price. The field test and monitoring programme will provide broad experiences and reliable results for the optimization of the systems.

#### Solar Active Technologies

Solar domestic hot water systems (DHW) have been commercial for more than ten years. More than 300,000 m<sup>2</sup> solar collectors have been installed so far in the FRG. The efforts in the programme focused on the following topics:

- long term monitoring programmes on selected solar installations
- test programmes on solar DHW systems
- development of standardized system test methods (DIN, ISO)
- investigation of new innovative components and systems, e.g. new sputtered selective absorber surfaces, transparent insulation for high efficient collectors.

From 1979 - 1984 about 140 large solar-assisted DHW and heating systems were installed in public buildings (Peuser, 1990). As part of the CEC programme on solar heated outdoor swimming pools, 8 plants have been erected in Germany, the last two in 1988 consisting of low cost plastic absorbers. About 40 solar plants and 6 solar heated swimming pools have been monitored. Solar heated swimming pools have proved to be one of the most economic applications of solar energy in Germany. The substitution potential is large: there are more than 6,000 public outdoor swimming pools and 300,000 private pools.

The monitoring programme on selected solar installations detected many deficiencies and often a poor system efficiency. This was a result of incorrect planning and design of the plants, unfavourable control, installation mistakes and improper connection to the conventional back-up heating system. Meanwhile all the monitored systems have been repaired and show quite an improved efficiency.

These results confirm that active solar systems can contribute considerably to the energy demand even under the less favourable solar radiation conditions of

FRG provided the proper design and correct installation and maintenance of the installations are ensured. The active solar systems can provide  $250 \text{ KWh/m}^2$  with standard flat plate collectors and up to  $450 \text{ KWh/m}^2$  with high efficient collectors or in low temperature solar-assisted preheating systems.

The dissemination of the results, in particular to designers and architects is considered to be a key issue of the programme. Information on projects is provided by a special information center BINE as well as in seminars.

Recently an extensive test programme on 14 commercial solar DHW systems was completed (HöB, A. 1987). The project was carried out by TÜV Bayern e.V. to determine the thermal performance, reliability and economics of solar DHW systems. Data from the test programme have been used by companies to optimize systems and have been published to inform the public. The project started in 1985 with a long term outdoor monitoring programme. The solar systems had to provide 200 liters hot water of  $45^\circ \text{C}$  daily. The systems consist generally of  $6 - 8 \text{ m}^2$  solar collectors (flat plate, high efficient tubular collectors, pumped or thermosyphon systems) and a 200 - 500 liter hot water boiler. The components were tested in separate laboratory tests. The test programme was extended in 1987 for 5 selected systems which have been rebuilt. The improved systems show a good thermal performance, reliability and safety. System efficiencies vary between 19% and 47%. High efficient solar collectors delivered up to  $600 \text{ KWh/m}^2$  of useful solar energy to the consumer. Amortization times of 15 and 30 years were calculated with an energy price of 0.21 DM/KWh.

The development of standards for quality control is a very important prerequisite for the market implementation. A standard test procedure is being developed to allow the determination of the annual performance of the solar system within a few weeks. The investigations are being carried out in a cooperation of DIN e.V., TÜV Bayern e.V. and the Universities of Munich, Stuttgart and Aachen/Jülich. The results show that the proposed method of a short term dynamic test is able to determine the annual performance with an accuracy of about 5%. The method has been validated with several different small solar DHW systems (pumped, thermosyphon, flat plate and evacuated collectors, integrated storage collector systems). The method is being proposed as the German National Standard (DIN) and for the International Standard Organization (ISO). Future work will investigate the applicability of the method for in-situ measurements and plants of larger sizes.

### Solar Passive Technologies

This topic of the programme covers a very broad spectrum of R&D and demonstration projects dealing with different energy saving technologies and solar architecture. The efforts focus on the reduction of the space heating demand. The present standards set an upper specific limit of  $150 \text{ KWh/m}^2 \text{ a}$ . A new regulation under preparation reduces this upper limit by 30%. The results of the programme show that even much lower heating demands are technically feasible. This has been shown, for instance, in the project Landstuhl (Gruber et al., 1989) for single and two family houses. A summary of the results will be presented below. In a joint Swedish-German cooperation low energy terrace houses were built in Ingolstadt (FRG) and Halmstadt (Sweden). The space heating demand of these buildings in Ingolstadt could be reduced by 60% compared with conventional buildings. In the new houses, Swedish building and German heating technologies have been combined. Recently the project Heidenheim was started to show the great energy saving potential with presently available technologies integrated in well-designed heating systems.

In the programme new innovative concepts are also being investigated for the building of very low-energy or even energy autonomous houses. A part of these efforts is being included in the IEA-cooperation: Solar Advanced Buildings within the IEA Programme: Solar Heating and Cooling (Hestnes, 1989). A main effort of the Solar Passive Programme focuses on R&D on transparent insulation and the demonstration of its applicability in pilot projects. Further topics of the programme are thermal modelling of buildings and the development of simplified design tools which can be used by architects. Germany is participating in the CEC project PASSYS and in many other IEA projects. In the following only two projects can be reviewed briefly.

### Project Landstuhl

From 1984 to 1985, 22 solar houses and 3 reference houses were built in Landstuhl and at some other places in the FRG within this project. The houses were insulated very well. Between 1985 and 1987 an extensive monitoring programme was carried out to determine the thermal performance of the components and systems. The houses were designed as solar passive houses with large south oriented windows and winter gardens and temporary shadings. The houses were equipped with low temperature floor heating and air heating systems; in 13 houses solar domestic hot water systems were installed and 6 houses included space heating heat-pump systems. Summarizing, the results of the project show that the highest priority must be given to an extremely good insulation for the building. The behaviour of the inhabitants (closing the roller shutters, operation of the ventilation system) and the required comfort (indoor temperature) drastically influence the energy savings. The solar gains of the windows are to a large extent compensated for by the thermal losses of the windows with the usual standard of  $k = 2.8 \text{ W/m}^2 \text{ K}$  (double glazing). The evaluation of the monitoring programme shows that winter gardens reduce the heating demand only marginally by about 10% provided that these are not heated conventionally in winter. Today, winter gardens are very popular in Germany mainly in view of their high living comfort.

The solar domestic hot water systems showed typically system efficiencies of 40 - 55% for vacuum collector systems and of 30 - 40% for standard flat plate collectors. The solar DHW systems achieved a useful solar energy gain of up to 2 MWh/year. This value, however, depends strongly on the consumption. Low consumption leads to higher losses.

### Transparent Insulation

In close cooperation between several research institutes and companies was started in 1986 (Götzberger, A., 1989). Meanwhile a remarkable state of development has been attained which already allows the application of the materials in pilot and demonstration projects. Basic R&D addresses the development of new materials (e.g. aerogels) and the optimization of thermo-optical properties as well as the integration in systems (facades, windows with automatically driven roller blinds to prevent overheating in summer). A recent study (Lohr et al., 1989) has shown that the space heating demand can be reduced by 50% in conventionally insulated houses and up to 80% with transparent insulation. Transparently insulated facades can contribute to a space heating demand with 100 - 200 kWh/m<sup>2</sup> a. First houses have been equipped with the transparent insulation. Advanced systems have now been installed in a two-family house and a multifamily house, Sonnenackerweg in Freiburg and in one family terrace houses, Hellerhof in Düsseldorf. Interesting and architecturally acceptable concepts have been worked out.

## REFERENCES

- BMFT (1990). 3. Programm Energieforschung und Energietechnologie
- Götzberger, A. (1989). Transparent Insulation - A New Solar Energy Component, In: 2nd European Conference on Architecture, p. 234 - 238, T.C. Steemers and W. Palz, Kluwer Academic Publisher, Dordrecht, The Netherlands
- Gruber, E., H. Erhorn and J. Reichert (1989). Chancen und Risiken der Solararchitektur: Solarhäuser Landstuhl, TÜV Rheinland GmbH, Köln, Germany
- HöB, A., W. Kunz, H. Riemer and P. W. Wensierski (1987). Sonnenenergie zur Warmwasserbereitung, Fachinformationszentrum Karlsruhe, TÜV Rheinland GmbH, Köln, Germany
- Hestnes, A.G. (1989). Advanced Solar Low-Energy Buildings. In: Proceedings of the Workshop "On the Way to Zero-Energy Buildings" G. Taninger, Universitäres Forschungsinstitut für Fernstudien, Klagenfurt
- Lohr, A. and B. Weidlich (1989). Systemstudie - Lichtdurchlässige Wärmedämmung
- Peuser, F.A. and R. Croy (1990). Erfahrungen mit Solaranlagen zur Warmwasserbereitung, ZfS in der GFHK mbH, Hilden



## PERFORMANCE OF COLLECTORS WITH FLAT FILMS OR HONEYCOMBS

Bengt Hellström, Solid State Physics, Department of Technology, Uppsala University,  
Box 534, S-751 21 Uppsala, Sweden.

Björn Karlsson and Lars Svensson, Älvkarleby Laboratory, Swedish State Power Board,  
S-810 71 Älvkarleby, Sweden.

### ABSTRACT

Detailed comparative measurements have been performed on collectors with a Teflon film or a honeycomb structure as the secondary glazing. The results indicate that a replacement of the Teflon film by a 30 mm honeycomb in a large area flat collector in Sweden, operating at a temperature of around 70°C, will increase the performance by around 40-50 kWh/m<sup>2</sup> or 10-15% on an annual basis. This is estimated from laboratory optical transmittance measurements and hot-box heat loss measurements, and also confirmed by outdoor collector measurements of daily efficiency. The improved efficiency is a result of a strong reduction in the  $U_L$ -value of 0.7-1.1 W/m<sup>2</sup>°C, combined with only a small decrease in the solar transmittance of 1-2 %.

### KEYWORDS

Transparent insulation materials; honeycomb; flat plate collectors.

### INTRODUCTION

The collectors in the large Swedish solar systems, used for district heating, operate at a relatively high temperature (50-90°C). They are always equipped with one or two Teflon films between the absorber and the glass cover. However, at these high temperatures, there is a need for a more efficient transparent or translucent insulation material (TIM), which reduces the heat losses without losing significantly in solar transmittance.

The use of a translucent honeycomb structure as secondary glazing in high temperature collectors has been proposed by Rommel and Wittver (1987). In this paper a commercially available polycarbonate honeycomb (reg. trademark Arel) is investigated and compared with a flat Teflon film. The laboratory measurements were performed with several different thicknesses of the honeycomb, while in the outdoor collector measurements only the 30 mm was used.

## COLLECTOR MEASUREMENTS

### Test Collectors

Two identical solar collectors (Fig. 1) have been constructed at the Älvkarleby laboratory for the purpose of comparing the performance of collectors with different kinds of TIM's. The collectors are mounted side by side on a stage, which can be either tracking around a vertical axis or set in a static position. The slope could be adjusted freely between 0 and 90 degrees. The collectors are insulated with 100 mm polyurethane foam and furnished with 2,5 m<sup>2</sup> selective Sunstrip absorbers. Low iron glass is used for the covers.

The two collectors are fed with water from the same tank, to ensure equal inlet temperatures. Flow rates, inlet and outlet temperatures for both the collectors as well as the irradiance and the air temperature were measured, and from this the collector efficiency is derived. A data logger was installed to record at every half minute and to store average data for every ten minutes. It was important that the inlet water temperatures as well as the flow rates could be controlled and kept approximately constant.

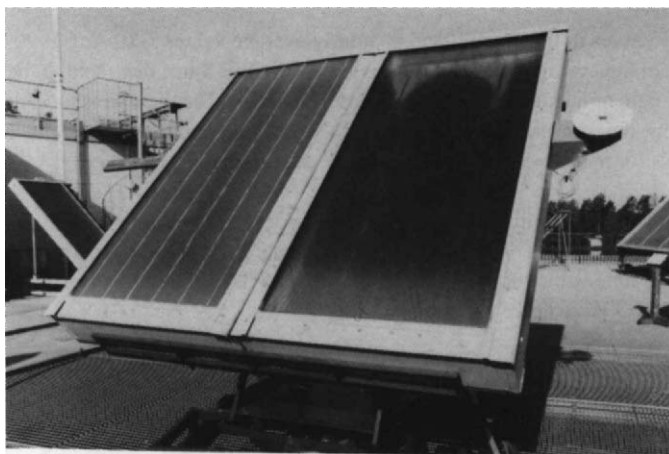


Fig. 1. The two test collectors, the left one equipped with 30 mm Arel honeycomb and the right one with a flat Teflon film.

### Measurements of Hourly Average Efficiency

The flow rates were kept constant at about 50 liters/m<sup>2</sup>h and the tracking mechanism was activated. At first a flat Teflon film was mounted in each collector. The distance between the film and the glass cover was about 30-35 mm. The measurements were used for calibration purposes.

Then, in one collector, the Teflon film was replaced by a 30 mm Arel polycarbonate honeycomb. The honeycomb was fastened to the glass by strings of silicone, as visible in Fig. 1.

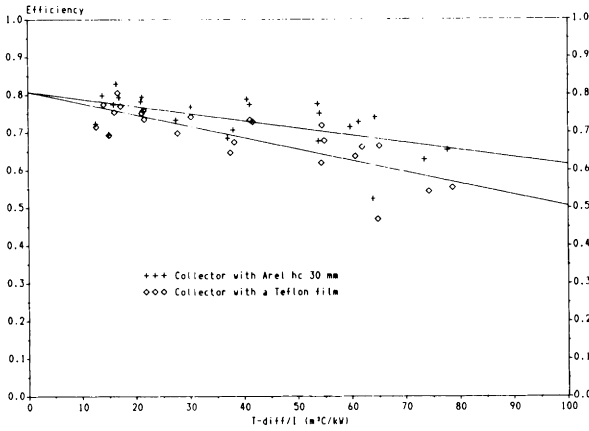


Fig. 2. Hourly average efficiency as a function of  $\Delta T / I$

The efficiency curves in Fig. 2 are based on hourly average values 3-10 Aug 1990 between 9.00 and 15.00, when the average irradiance exceeded  $300 \text{ W/m}^2$ . Since the tracking mechanism was activated the angle of incidence was always close to normal. The diagram shows that, because of dynamic effects, the measurement points are highly scattered, but that the simultaneously recorded points for the two collectors are strongly correlated.

In Fig. 3, which shows the difference in efficiency under the same conditions, the dynamic effects are almost eliminated. The measurements indicate that  $\eta_0$ , at an incidence close to normal, has the same value for both collectors, but that  $F'U_L$  is about  $1.1 \text{ W/m}^2\text{C}$  lower for the collector with the 30 mm hc.

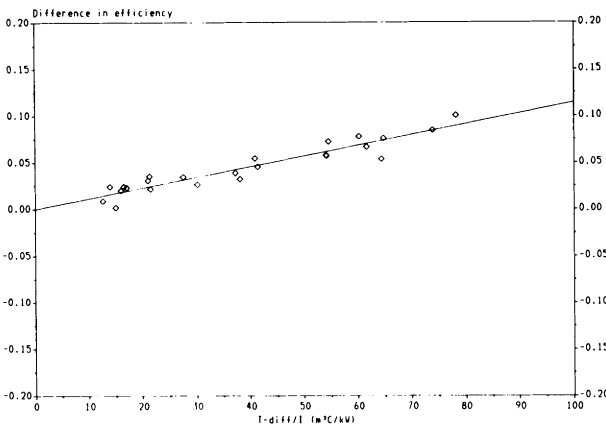


Fig. 3. Difference in hourly average efficiency between collectors with 30 mm Arel honeycomb and a flat Teflon film

### Measurements of Daily Efficiency

Measurements of daily efficiency were performed with the tracking mechanism deactivated, with the collectors tilted  $45^\circ$  and facing south. The inlet temperature was kept at about  $65\text{--}70^\circ\text{C}$ , while the ambient temperature was about  $10\text{--}20^\circ\text{C}$ . In Fig. 4 the daily efficiency is shown as a function of the daily irradiation for both collectors. The difference in efficiency between the two collectors was approximately 0.05, almost independently of the daily irradiation above  $1.5\text{ kWh/m}^2$ . The regression lines are put into the diagram only to stress this fact. From Brunström *et al.* (1986) it can be seen that the annual irradiation above  $2\text{ kWh/m}^2\text{day}$  in Älvkarleby 1985 (a normal year) is summarized to about  $950\text{ kWh/m}^2$ . This indicates that the annual improvement for a collector working at about  $70^\circ\text{C}$ , by replacing the Teflon film by a  $30\text{ mm hc}$ , is about  $45\text{--}50\text{ kWh/m}^2$ .

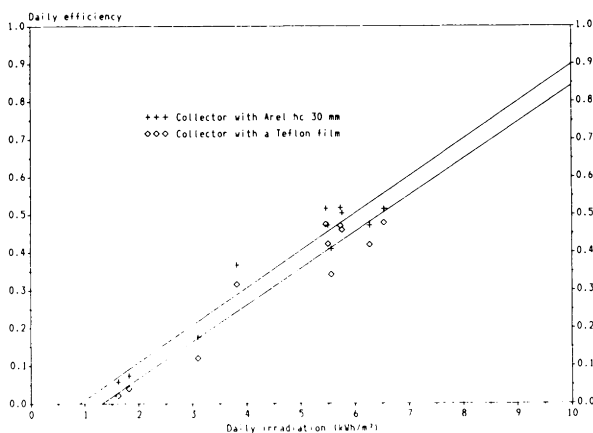


Fig. 4. Daily efficiency as a function of daily irradiation

## LABORATORY MEASUREMENTS

### Measurements of $U_L$ -values

An unguarded hot-box with a selective surface as the hot plate was used for comparative measurements of  $U_L$ -values. The hot-box can be described as a small and well insulated solar collector model with an electrically heated absorber ( $A \approx 0.53\text{ m}^2$ ). The  $U_L$ -values were derived from dividing the electrical input power at thermal equilibrium by the temperature difference between the absorber and the room and by the absorber area.

In this experiment a selective absorber surface ( $\epsilon \approx 0.23$ ) was used. Comparing the flat film with the  $30\text{ mm hc}$ , see Fig. 6, gives  $\Delta U_L \approx 0.6$  at  $\Delta T \approx 50\text{--}60^\circ\text{C}$ , which should be compared with  $\Delta U_L \approx 1.1$  that was derived from the outdoor efficiency measurements (if  $F' \approx 1$  is assumed). However, Brunström *et al.* (1987), have shown that the  $U_L$ -values obtained indoors should be recalculated in order to be valid outdoors, due to a difference in outer heat resistance between the

glazing and the surroundings. This means that the differences in  $U_L$ -values are expected to be larger outdoors than indoors. From measurements of the glass temperature, recalculations gave  $\Delta U_L \approx 0.7\text{-}0.8 \text{ W/m}^2\text{°C}$  at  $\Delta T \approx 50\text{-}60\text{°C}$ , depending on the assumptions for the corresponding resistance outside.

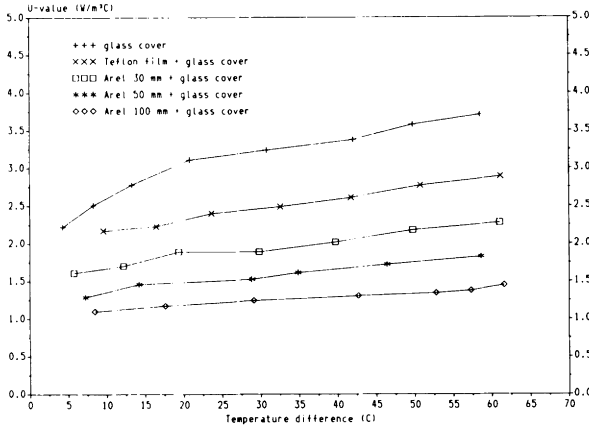


Fig. 5.  $U_L$ -values measured in an unguarded hot-box

Measurements of Solar Transmittance

An integrating sphere, 1 m in diameter, was used for measurements of solar transmittance at different angles of incidence. It has the ability to measure up to about 60°, but for thick and scattering samples the values at high angles of incidence tend to be too low, since some transmitted light is scattered outside the port of the sphere. Another problem is an irregularity in the sphere wall, which caused too high values at and around 20°. These points are therefore neglected in the transmittance curves in Fig. 6.

The measurements show that the 30 mm hc has a transmission that is 1-2% lower than the flat Teflon film for most angles of incidence, except at normal incidence, where the honeycomb is equally good or even better, which corresponds well with the outdoor measurements of  $\eta_0$ .

Annual Performance

A simple formula for calculations of annual performance of solar collectors in Sweden has been derived by Karlsson (1988) and modified by Karlsson and Perers (1990). From the laboratory measurements one can conclude that the gain in  $U_L$ -value is 0.7-0.8  $\text{W/m}^2\text{°C}$  and that the loss in transmittance is 0.01-0.02. This corresponds to an increase of the annual heat production by 40  $\text{kWh/m}^2$ .

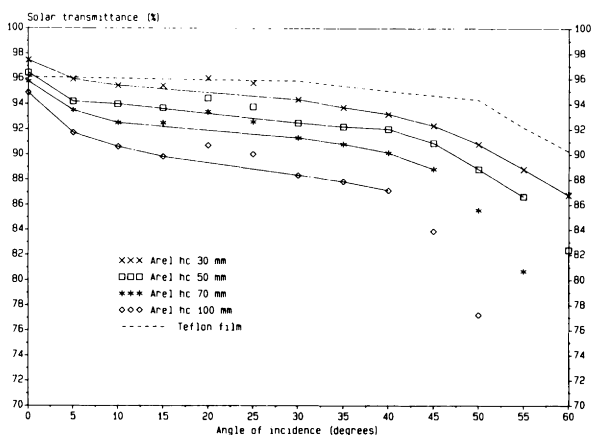


Fig. 6. Solar transmittance at different angles of incidence

## CONCLUSIONS

Calculations, based on laboratory measurements of solar transmittance and  $U_L$ -values, indicate that it is possible to gain  $40 \text{ kWh/m}^2$  annually for Swedish collectors, working at an average temperature of about  $70^\circ\text{C}$ , by replacing the flat Teflon film with a 30 mm polycarbonate honeycomb as secondary glazing. This conclusion was confirmed by outdoor measurements of daily efficiency, which indicated an even higher annual increase of  $45\text{-}50 \text{ kWh/m}^2$ . The gain is a result of a strong reduction in the  $U_L$ -value of  $0.7\text{-}1.1 \text{ W/m}^2\text{C}$ , combined with only a small decrease in the solar transmittance of 1-2%.

## ACKNOWLEDGEMENT

This work has been financially supported by the Swedish National Energy Administration.

## REFERENCES

- Brunström, C., B. Karlsson and M. Larsson (1986). Climatic limitations and collector performance in the middle of Sweden. *Proc. of North Sun '86*, 161-166.
- Karlsson B. (1988). Potential improvements of high temperature flat plate collectors. *Proc. of North Sun '88*, 419-422.
- Perers, B. and B. Karlsson (1990). An annual utilizability method for solar collectors in the Swedish climate. *Proc. of North Sun '90*, (this Volume).
- Rommel, M. and V. Wittwer (1987). Flat plate collector for process heat with honeycomb cover - an alternative to vacuum tube collectors. *Proc. of the Biennial Congress of ISES*, 641-645.

# REDUCING OUT-GASSING IN SOLAR COLLECTORS BY USING AIR COLUMNS

Peter Kjaerboe

Dept. of Heating and Ventilation, Royal Institute of Technology  
S-100 44 Stockholm, Sweden

## ABSTRACT

Some methods for reducing out-gassing are discussed. The use of air columns as insulation on the back of the collector seems to have advantages from other aspects it gives a collector with a quick thermal response to varying insulation.

## KEYWORDS

Solar collectors, insulation, air columns.

## INTRODUCTION

Solar collectors or the materials in them emit vapours when in use. This often leads to condensation. This is deposited in places with relatively low temperatures (low pressure), such as glass or pipes carrying the heat transfer medium. Some of the problems that can be caused here are:

- o reduced transmission, see e.g. Hsich (1977), Fig. 1
- o corrosion, see e.g. Wennerholm et al. (1979) and Rudnick et al. (1986).

One way of avoiding condensation is to ventilate. This should be done in such a way that the heat insulation is not compromised. Another way is to avoid vapourisation by reducing the working temperatures in insulation that is sensitive to relatively high temperatures. Examples of ways to prevent vapourisation are:

- o to select insulation material that can withstand the temperatures in question without vapourising, or without absorbing moisture that is then emitted with the temperature increase
- o to minimise the working temperature.

Both these solutions will be examined here.

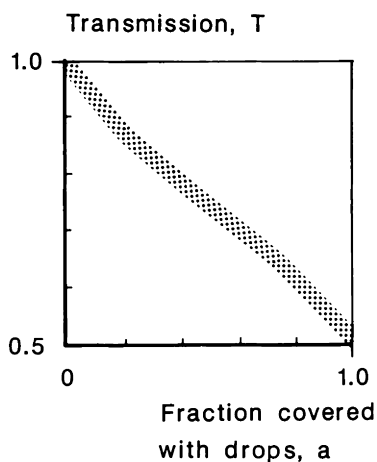


Fig. 1. Transmission, perpendicular radiation, for water drops on glass depend on the fraction covered. From Hsieh (1977).

The manageability during manufacture and erection is probably one of the reasons that plastic is used for the insulation. But the durability used to be reduced at the existing temperatures, see Fig. 2. It was also common that some parts melted and vapourised, and condensation occurred.

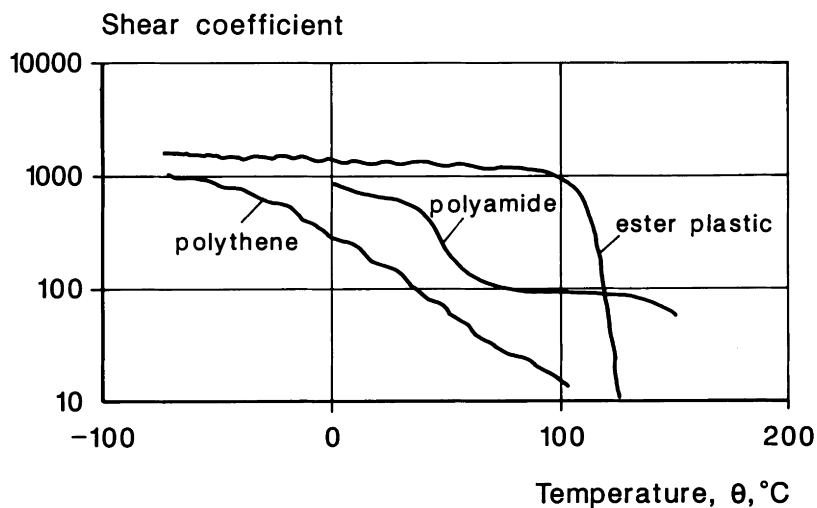


Fig. 2. Durability of some plastic materials at various temperatures.



Other materials such as mineral wool and glass wool are once again being used. However, some of the extra parts will vapourise/condense, so an air-tight layer has been installed between the insulation and absorber. This prevents gas from passing through. More recently, use has been made of air columns that can be formed on either side of the air-tight layer, see Fig. 3. This is analogous to the space in double-glazing.

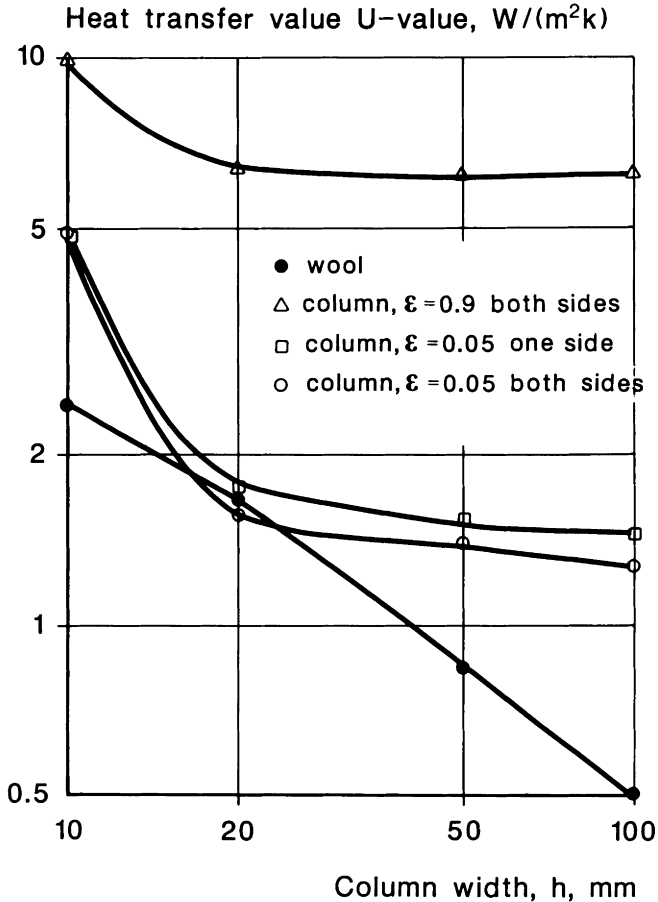


Fig. 3. Heat transmission for an air column of two surfaces with a low emission coefficient can be compared with a "normal" wool insulation.

In addition, the radiation part can be reduced by covering the layer with a surface having a low emission factor to provide an insulation. This will result in the temperature drop being large, and so simpler, cheaper insulation can be used.

The use of air columns also gives a collector with a thermally faster response to variations in radiation. With varying radiation, such as occurs with changing cloud cover, there is a higher mean temperature in the collector compared to a heavy collector. Table 1 shows that the thermal diffusivity is considerably lower for an insulation consisting of air columns than for one without.

Table 1. Some physical data for insulation materials.

Material	Thermal conductivity $\lambda$ W/(mK)	Density $\rho$ kg/m <sup>3</sup>	Specific heat $c_p$ Ws/(kgK)
Wood	0,15-0,35	500	2500
Mineral wool	0,05	100	800
Glass wool	0,06-0,07	35	2000
Cork	0,04-0,05	140-200	1700
Cellular plastic	0,04-0,05	20-240	1700
Air column	0,025-0,03	1,2-1	1000
Aluminium	220	2700	900

Material	Thermal diffusivity $\lambda$ W/(mK)	Thickness, $d$ , and mass, $m$ for $U$ -value of 0,5 W/(m <sup>2</sup> K)	$m$ kg/m <sup>2</sup>
Wood	0,1-0,3 · 10 <sup>-6</sup>	0,5	240
Mineral wool	0,6-0,3 · 10 <sup>-6</sup>	0,1	20
Glass wool	0,6-0,3 · 10 <sup>-6</sup>	0,12	19
Cork	1,7-0,3 · 10 <sup>-6</sup>	0,09	15
Cellular plastic	1,2-0,3 · 10 <sup>-6</sup>	0,09	2,6
Air column	20-0,3 · 10 <sup>-6</sup>	0,05	1,4
Aluminium	90-0,3 · 10 <sup>-6</sup>	0,05	1,4

The use of a steam or vapour-lift pump in the system, see e.g. Kjaerboe (1990), gives longer running times with an accompanying higher efficiency.

## CONCLUSION

Air columns as insulation can be built onto the back of a solar collector. They will be formed with layers having low emission coefficients for thermal radiation. Such a system results in a collector that is:

- o lighter and thus easier to assemble,
- o thermally faster, which gives a higher efficiency when clouds occur,
- o less inclined to have condensation, as less moisture is absorbed.

The smaller size, easier mounting, higher effectiveness and longer life give a more economic unit.

#### REFERENCES

- Hsieh, C.K., Rajvanshi, A.K. (1977). The effect of dropwise condensation on glass solar properties. *Solar Energy*, No. 19, p. 389.
- Kjaerboe, P. (1990). A vapour-lift pump for solar systems. Proc. North Sun 1990, Reading, UK.
- Lagerqvist, K.O., Wennerholm, H. (1983). Solfångares hållbarhet och tillförlitlighet. *T R S P 1983:41*, Borås.
- Rudnick, A., Kaplan, Y., Kudish, A.I., Wolf, D. (1986). A study of solar collector aging and material problems. *Solar Energy*, Vol. 36, No. 3.
- Wennerholm, H., Lagerqvist, K.O. (1979). Åldring och korrosion hos plana termiska solfångare. En studie baserad på litteratur och erfarenhetsutbyte. *T R S P 4*, Borås.
- Wennerholm, H., Andreasson, B. (1986). Besiktning av plana termiska solfångare 1984 och 1985. *SP 1986:02*, Borås.

## Author Index

- Abu-Ebid, M. 78  
Akhundov, S. Ya. 216, 392  
Al-Zuhair, M. 406  
Alessandro, S. 318  
Aliyev, I.M. 392  
Andersen, N.B. 119  
Bagachkov, V.F. 440  
Ballinger, J.A. 85  
Bentley, R.W. 420  
Berg, P. 357  
Bergmeijer, P.W. 266  
Bertolino, S. 60  
Bishena, N. S. 413  
Borde, I. 401  
Briheim, B. 260  
Broman, L. 249  
Broman, A. 301  
Bryn, I. 130  
Burton, S.H. 151  
Butera, F. 318  
Cannistraro, G. 60  
Carmi, Y. 401  
Casablanca, G. 109  
Chianumba, A.J. 420  
Chibuye, T. 177  
Clarke, D. 31  
Cochran, R.W. 431  
Cohen, R.R. 78, 140  
Cotana, F. 308  
Croome, D.J. 6, 125  
Dalenback, J. O. 205, 254, 260  
de Geus, A.C. 37  
de Schiller, S. 101, 109  
Doggart, J. 151  
Duckers, L.J. 243  
Efendieva, N.G. 216  
Elagoz, A. 146  
Esbensen, T. 169  
Evans, J.M. 101, 109  
Felli, M. 308  
Fisch, N. 237  
Forrest, R. 72  
Franzitta, G. 60  
Furbo, S. 351, 357  
Ghassemi, B. 369  
Gillett, W.B. 140  
Hahne, E. 237  
Hellstrom, B. 466  
Holmes, D. 48  
Inogamov, B. 426  
Isakson, P. 249  
Jacques, J.K. 395  
Jilar, T. 205, 211  
Karlsson, B. 177, 450, 466  
Kenisarin, M.M. 287, 323, 330  
Kjaerboe, P. 363, 471  
Knoll, S. 66  
Kolodziej, A. 221  
Konis, C.Y. 395  
Korin, E. 401  
Kubler, R. 237  
Kucukdogu, M. 146  
Kurochkin, G.F. 445  
Litvinenko, Y.M. 272  
Liu Qi-xian 374  
Liu Antian, 115  
Liu Yi, 115  
Lottner, V. 460  
MacGregor, K. 24  
Marinoff, A.M. 386  
Mazzarella, L. 237  
McCubbin, I. 140  
Mintah, I.K. 172  
Morck, O.C. 1, 130  
Morel, N. 130  
Mozgovoy, A.G. 440  
Mukhamedov, R. 426  
Mustafayev, I.I. 392  
Mustafayev, R.M. 392  
Myer, A. 31  
Nielsen, J.E. 283  
Nordell, B. 211  
Nordlander, S. 249  
Nowak, S. 221  
Olsen, L. 119  
Olseth, J.A. 193  
Pasichny, V.V. 272, 336  
Pedersen, P.V. 1  
Perers, B. 199, 450  
Pinter, J. 106  
Potouraeva, L.V. 445  
Prasad, D.K. 85  
Raza, K. 163  
Reyes, J. 101  
Rizzo, G. 60, 318  
Roaf, S.C. 56

Robertson, G. 43  
 Rockendorf, G. 294  
 Ronnelid, M. 249  
 Ruysevelt, P.A. 78, 140  
 Rzaev, P.F. 216,392  
 Saluja, G.S. 157  
 Sayigh, A.A.M. 90, 163, 406  
 Shafeev, A.I. 287  
 Shakhbazov, Sh.D. 216  
 Shaltout, M.A.M. 183  
 Sheinstein, A.S. 456  
 Shpilrain, E.E. 456  
 Silvestrini, G. 130, 318  
 Skartveit, A. 193  
 Snøj, M.V. 101  
 Stricker, R. 130  
 Sun Xiaoren 381  
 Svensson, L. 466  
 Tayeb, A.M. 277  
 Tkachenkova, N.P. 287, 323, 330  
 Tripanagnostopoulos, Y. 346  
 Tsilingiris, P.T. 232  
 Tunc, M. 134  
 Uysal, M. 341  
 van Dijk, H.A.L. 37  
 van Amerongen, G.A.H. 266  
 Vorobjev, G.M. 445  
 Wackelgard, E. 177  
 Walletun, H. 199  
 Welteke, U. 66  
 Wereko-Brobby, C.Y. 172  
 Whitfield G.R. 420  
 Wu Xiangsheng, 115  
 Yang Xiao-feng 374  
 Yianoulis, P. 346  
 Zakar'yaev, Z.R. 440  
 Zakhidov, R. 426  
 Zuhairy, A.A. 90